भौतिक अनुसंधान प्रयोगशाला, अहमदाबाद

Physical Research Laboratory, Ahmedabad

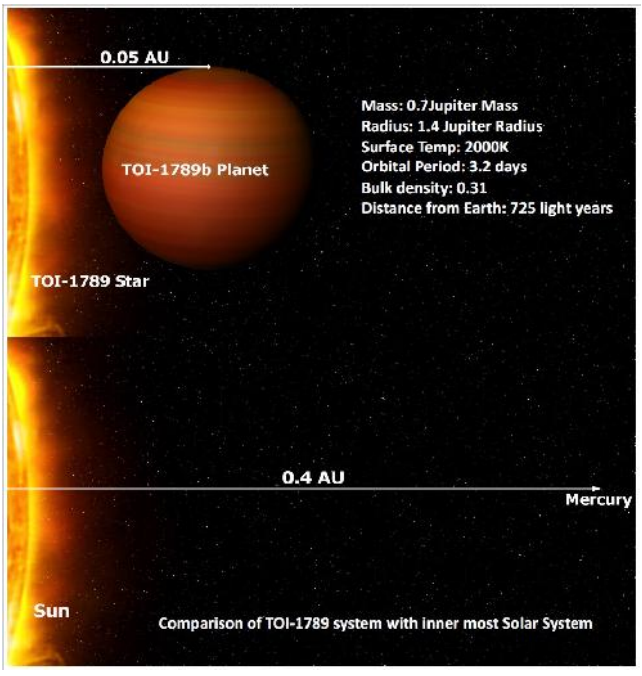

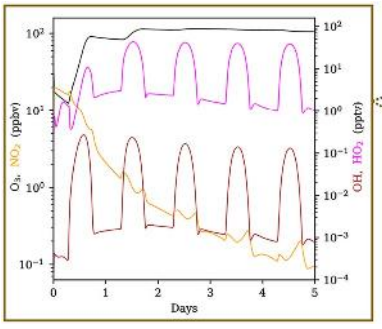

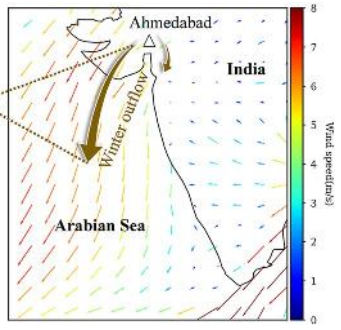

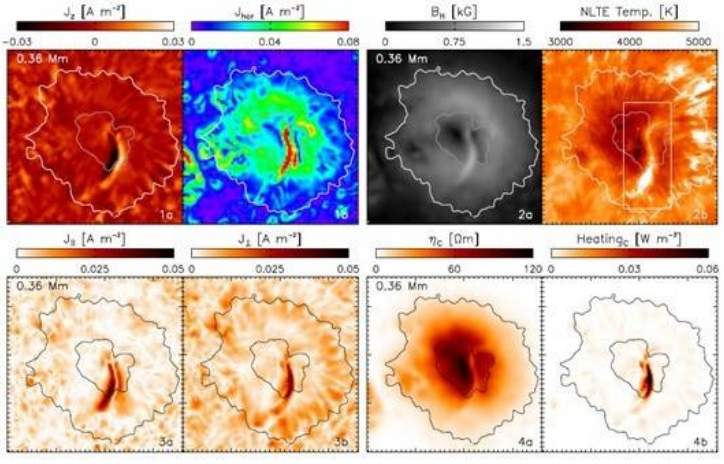

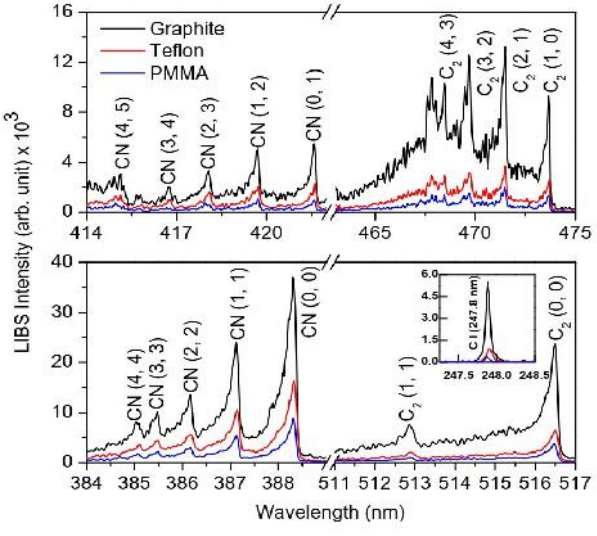

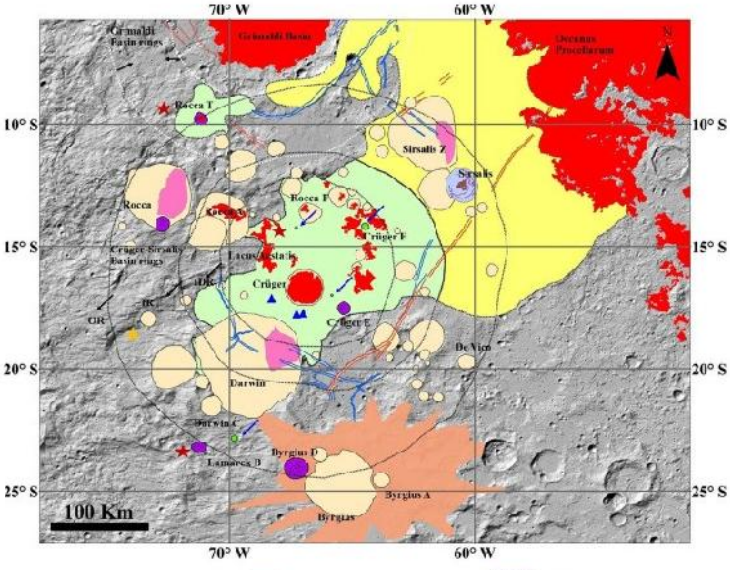

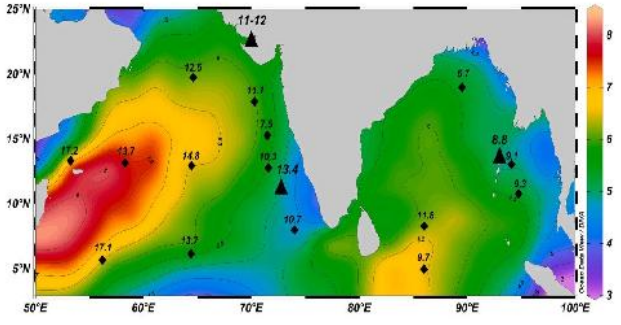

वार्षिक प्रतिवेदन

Annual Report

2021-2022

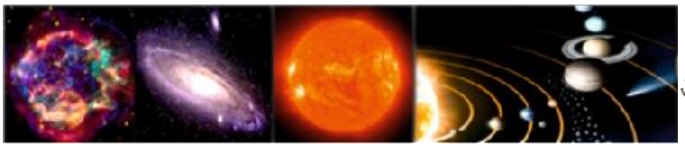

आज़ादी का अमृत महोत्सव

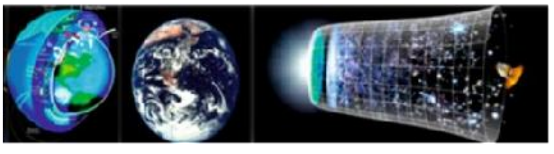

Front cover page:

Top Right Panel: Model simulated photochemical evolution of air in the downwind of Ahmedabad

Top Left Panel: Artistic impression of the TOI-1789 star-planet system, along with characteristics of planet

Center Right Panel: Physical parameters in leading sunspot in NOAA AR 12002 on 2014 March 13

Center Left Panel: The LIBS emission spectra of graphite, PMMA, and Teflon in air when interacting with an 800 nm Ti: Sapphire laser pulses of duration 29 fs

Bottom Left Panel: Air-sea CO_2 exchange rates in the northern Indian Ocean along with colour contours of average wind speed (m s^{-1})

Bottom right Panel: Geological map of the Cr*ii*ger-Sirsalis Basin overlapped on the hill-shade map derived from SLDEM 2015

Inside back cover pages: Events at PRL

Back cover page:

PRL campuses with official logo of PRL's platinum jubilee celebrations

Compilation and Layout by:
Office of the Dean, PRL.

Published by:
Physical Research Laboratory, Ahmedabad.

Contact:
Physical Research Laboratory
Navrangpura
Ahmedabad - 380 009, India
Phone: +91-79-2631 4000 / 4855
Fax: +91-79-2631 4900
Email: info@prl.res.in
Website: `https://www.prl.res.in/`
YouTube: `https://www.youtube.com/c/PRLAhmedabad_webinars`
Facebook: `https://www.facebook.com/PhysicalResearchLaboratory`
Twitter: `https://twitter.com/PRLAhmedabad`
KOO: `https://www.kooapp.com/profile/prlahmedabad`
Instagram: `https://www.instagram.com/prl1947/`
LinkedIn: `https://www.linkedin.com/in/prl-ahmedabad-89600122b`

Contact

Website

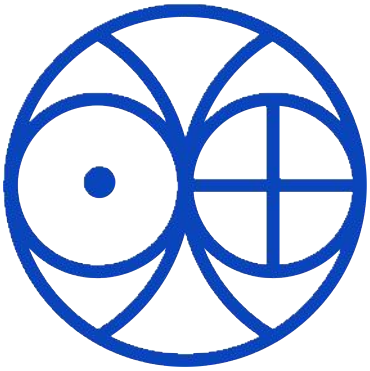

Annual Report

2021 – 2022

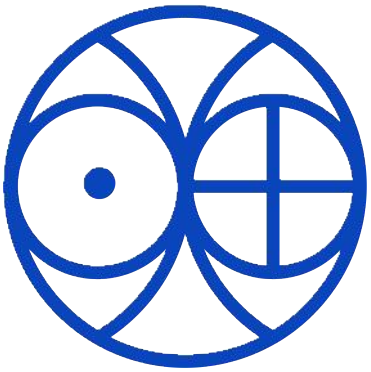

PRL research

encompasses

the Earth, the Sun

Immersed in the fields

and radiations

reaching from and to infinity,

all that man's curiosity

and intellect can reveal

PRL Council of Management

Three nominees of the Government of India

1. Shri A. S. Kiran Kumar Dr. Vikram A Sarabhai Professor, ISRO Antariksh Bhavan, New BEL Road Bengaluru-560231	Chairman
2 (i). Dr. K. Sivan, Secretary, Department of Space, Govt. of India Chairman, ISRO Antariksh Bhavan, New BEL Road Bengaluru-560231	Member (Up to 13.01.2022)
2 (ii). Shri. S. Somanath, Secretary, Department of Space, Govt. of India Chairman, ISRO Antariksh Bhavan, New BEL Road Bengaluru-560231	Member (From 14.01.2022)
3. Shri M. Maheshwar Rao, IAS Additional Secretary & FA Department of Space, Govt. of India Antariksh Bhavan, New BEL Road Bengaluru-560231	Member

A nominee of the Karmakshetra Education Foundation

4. Shri Kartikeya V. Sarabhai Director, Centre for Environment Education Ahmedabad-380054	Member

A nominee of the Ahmedabad Education Society

5. Shri Sanjay S. Lalbhai Chancellor & Chairman, Board of Governors, Ahmedabad University, Ahmedabad-380009	Member

A nominee of the Govt. of Gujarat, Gandhinagar

6. (i) Smt. Anju Sharma, IAS The Principal Secretary Education Dept. (Higher & Technical Education) Government of Gujarat, Gandhinagar	Member (Up to 18.06.2021)
6. (ii) Shri S.J. Haider, IAS The Principal Secretary Education Dept. (Higher & Technical Education) Government of Gujarat, Gandhinagar	Member (From 19.06.2021)

Physical Research Laboratory, Ahmedabad

7. Dr. Anil Bhardwaj, Director	Member (Ex-Officio)
8. Registrar	Member (Ex-Officio)

Areas of Scientific Research and Activities

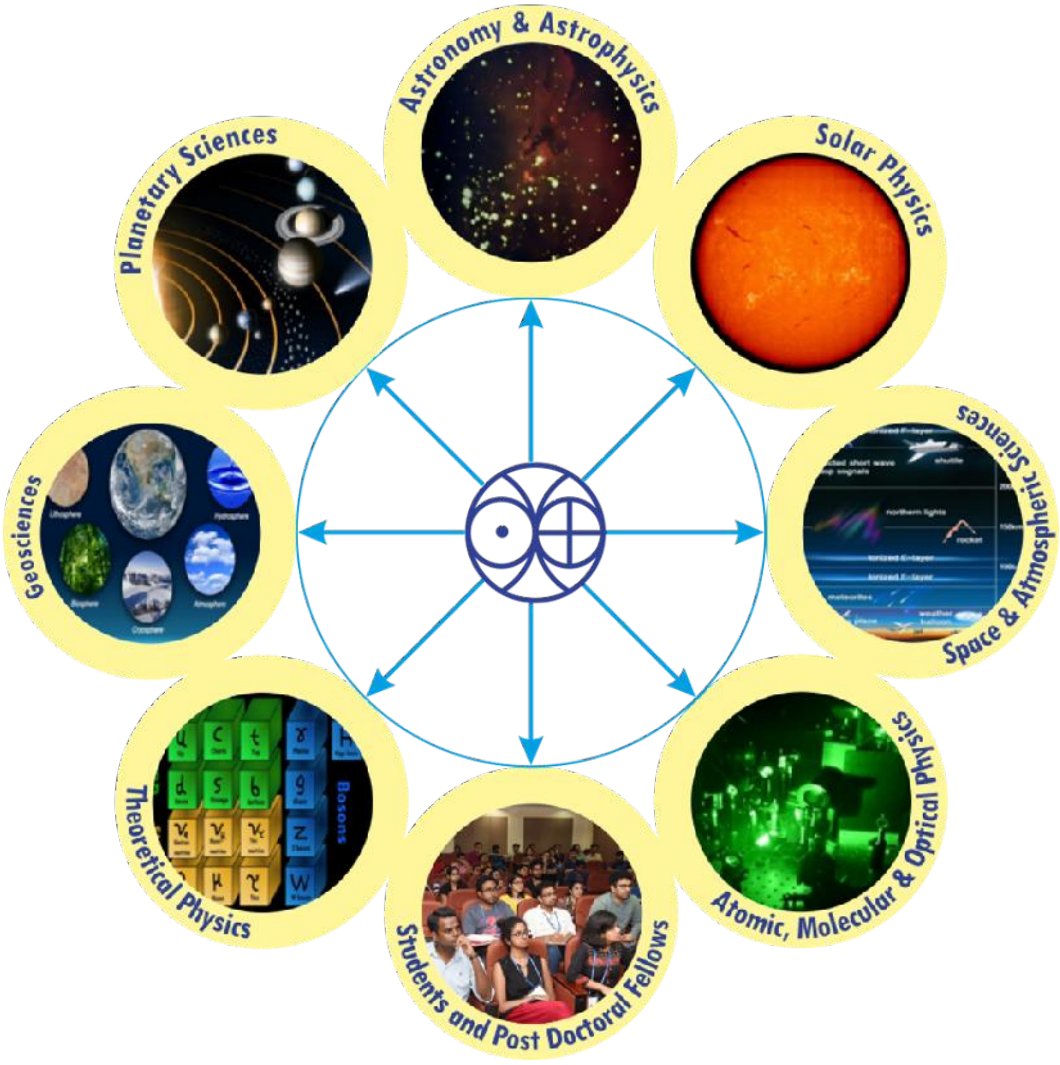

Contents

From The Director's Desk

The year 2021-2022 is exceptional as India is celebrating "Azadi Ka Amrit Mahotsav" (AKAM)-commemorating 75 years of independence and the glorious history of its people, culture, and achievements. This Mahotsav is dedicated to the people of India, who have been instrumental in bringing India thus far in its evolutionary journey and hold within them the power and potential fuelled by the spirit of Aatmanirbhar Bharat. Instituted in the year 1947, PRL is celebrating 75 years of its establishment. In keeping up with the spirit, in this platinum jubilee year, various programs and events are planned and organized to commemorate the splendid and rich legacy of PRL's journey thus far. The activities include, but not limited to, Science Popularization, Outreach Activities, Lectures, Webinars, Cultural and Sports Events, and Awareness Programs at all the four campuses of PRL, to ensure maximum public participation. One of the prominent events is the start of online webinar series called "PRL ka Amrut Vyakhyaan" (PKAV), on 4 August 2021. The PKAV series is aimed at conducting 75 Vyakhyaans to mark 75 years of PRL's formation. Till the end of March 2022, 35 Vyakhyaans have been delivered un-interreptedly on every Wednesday.

Excellence in science continues to be the hallmark of research at PRL. This includes robust training of young scientists through the vibrant and highly sought after Post-Doctoral and Research Fellowship programs. This year PRL's research resulted in 300 peer-reviewed scientific publications. Nine research fellows were awarded Ph.D. degrees, and several researchers have won best paper prizes in national and international conferences for their work that is being pursued during their doctoral careers. This year the list of coveted awards and recognitions span from national and international Academy Fellowships to the international Young Scientist and Early Career awards. Several colleagues received invitations to serve as the members of the editorial boards of national and international peer-reviewed journals, boards of studies in universities, science advisory committees, and governing council of research and academic institutes. Several colleagues were elected to leadership positions in committees of international bodies. This year too, two PRL faculty continue to be listed in the list of Top 2% of Scientists in the world in their respective fields published by Stanford University. Around 140 invitations were received by PRL faculty members to deliver plenary or invited talks in universities, institutes, and national and international conferences or symposia, demonstrating the leadership role PRL commands in different research fields, both internationally and nationally. PRL scientists have active collaborations with domain experts in reputed institutes and universities in both India and abroad. PRL scientists are also at the forefront of utilizing data from the global space missions of astrophysics, planetary and space sciences and are contributing to bringing out new, pathbreaking, and insightful results. A small sample of results from the diverse fields of research being pursued in PRL are given below, essentially to provide a flavor of the accomplishments made.

A Hot-Jupiter has been discovered, orbiting in very close proximity, at a period of 3.21 days, around an evolved F-type star, TOI-1789. It is one of the lowest density exoplanets known so far. TOI-1789b falls under a unique category of 10 exoplanets among all the known ones, which are orbiting the evolved stars in a very close orbit (within 0.05 AU). This is the second exoplanet discovery from PRL and India. Such discoveries help in understanding the physics of the formation of planets around stars and the physics of orbital dynamics.

Timing and spectral studies of Be/X-ray binary pulsar EXO2030+375 carried out using observations from the LAXPC and SXT of AstroSat at various phases of Type-I outbursts revealed the lowest luminosity of 2.5 $\times 10^{35}$ ergs^{-1} in 0.5-30 keV energy range with 41.3 s pulsations that were clearly detected in the X-ray light curves. This finding establishes the first firm detection of pulsations in EXO 2030+375 at an extremely low mass accretion rate to date.

Time-resolved X-ray spectroscopic analysis for the small B-class solar flares was carried out for the first time using observations from the XSM aboard Chandrayaan-2 mission. The results show that the evolution of temperature and emissions from the flaring plasma agree well with the standard flare model. This suggests that, like their bigger counterpart, the smaller flares also follow the standard flare model. The spectroscopic analysis further shows that the elemental abundances of low first ionization potential elements change from their coronal to photospheric values during the impulsive phases of the flares, which subsequently recover. This quick recovery also provides the first indirect evidence towards magnetic reconnection-driven Alfven waves, observations of which were long sought after.

Intense electric currents and strong chromospheric temperature

enhancements over a sunspot, which occur because of the large-scale magnetic flux emergence at the location of light bridge were studied using the Calcium ion emissions from the Dunn Solar Telescope and vector magnetic field measurements from the Helioseismic and Magnetic Imager. The temperature excess from the dissipation of currents is located in the lower chromosphere between 0.4 and 0.7 Mm and is possibly sustained over the whole passage of flux emergence lasting about 13 hr. This study combining the models of magnetic field topology and thermal inversions provides a direct evidence of lower chromospheric heating through Ohmic dissipation of electric currents in the sunspots.

The studies of DH type II bursts associated with CMEs are significant as they are primarily associated with the energetic and wider CMEs that frequently cause space-weather disturbance. Characteristic of DH type II radio bursts for the Solar Cycles 23 and 24 were explored. The results suggest that the initial speed of CME or flare energetics are partly related with the duration of type II bursts and the survival of CME-associated shock is determined by multiple factors related to CMEs, flares, and state of coronal and interplanetary medium.

The significance of the Hall effect on magnetic reconnection to understand the observed solar flare ribbon brightening is studied using the first-ever data-based Hall MHD simulation. Based on the numerical techniques to detect favorable topologies for reconnection, the investigations revealed the presence of 3D nulls, quasi-separatrix layers, and a magnetic flux rope. A comprehensive analysis of the magnetic field line dynamics associated with these topologies reveals faster and efficient reconnections during the Hall Magneto-Hydro-Dynamics (MHD) and an excellent Spatio-temporal agreement with the observed flare brightening, which is not captured in the standard MHD simulations.

A photochemical model for NO density distribution in the dayside of Martian upper atmosphere is developed using observations from NGIMS onboard MAVEN for 120 and 200 km altitudes. It is found that local CO_2 and N_2 density variations can lead to a change in NO density and consequently its dayglow intensity by a factor of 2 to 5.

Identifying the obscured impact basins and their spatio-temporal extension on the Moon is important. For the first time, deciphered geology of an obscured impact basin on the Moon is reported. The Crurger Sirsalis Basin (with $\sim$475 km diameter and location of 16^{o}S / 293^{o}E) of pre-Nectarian age uniquely showcases the volcanic history of the Moon.

An analysis of new carbonaceous chondrite Bukhara using noble gas mass spectrometer for isotopic ratios revealed that the cosmic ray exposure age is 22 Million years, indicating the ejection of this meteorite long ago from its parent body. Nitrogen isotopic signature indicates a heavier ratio than solar wind, showing the chondritic components inhibiting nitrogen from an evolved region of the proto-planetary disk.

An analysis of black carbon (BC) aerosols measured simultaneously over a source and a background region revealed distinct differences in the probable sources and source regions for BC, especially during postmonsoon and winter, when long-range transport of agricultural waste and biomass burning emissions from northwestern India and the Indo-Gangetic Plain reach the background region. The observation-model comparison reveals that the model significantly underestimates BC mass over the urban Ahmedabad, whereas, the agreement is good over the high-altitude background Gurushikhar, suggesting a need to improve aerosol emission inventories.

The photochemistry over a tropical urban environment (Ahmedabad) has been investigated by integrating state-of-the-art measurements with the Master Mechanism model. The results revealed a strong ozone build-up and numerous secondary organics in the outflow towards the Indian Ocean. Notably, the measurement-driven simulation has been used further to estimate the hydroxyl radical levels ($\sim$0.3 pptv in noontime) and to analyze its budget. The study is of paramount significance as the OH radical governs the atmosphere's self-cleaning capacity, but its direct measurements remain lacking in the tropical Indian region.

Large field-of-view optical measurements of oxygen 630.0 nm dayglow emission rates using in-house built daytime optical spectrographs from two latitudinal locations in Indian longitudes combinedly covered a large extent of 5°-18° magnetic latitudes. This enabled systematic investigations of the effect of the equatorial electric fields (as seen in the equatorial electrojet strengths) on the latitudinal electrodynamic behaviour of the thermosphere as seen in the dayglow emissions. The studies reveal that the effect of equatorial electric fields in the daytime are nearly non-varying at least until the equatorial ionization anomaly crest region, this has significant implications on our understanding of the equatorial electrodynamics.

Indian Summer Monsoon (ISM) played important role in the rise and collapse of ancient civilizations in the subcontinent. In the mid to late Holocene period, Indus Valley or Harappan Civilization flourished in the western part of India and collapsed around the beginning of the Meghalayan Age (4.2 kyr Before Present). It is believed that a prolonged drought condition or decrease in the ISM rainfall caused the decline in the Indus Civilization. Using proxy records and other available studies, PRL scientists showed that the ISM was significantly weak around the 4.2 kyr before present which probably caused the dispersion and migration of the Harappan Civilization.

A comparison between two radiometric dating methods demonstrate a significant difference in dating threshold and resolution. The study shows that the 10Be method very well mimics the radiocarbon method. The extrapolation of radiocarbon ages beyond its limit using a constant sedimentation rate may cause errors in age estimation. The meteoric 10Be method can be used as a potential tool to extrapolate radiocarbon ages beyond 50 kyr.

Recent results have shown a distinct decline in sea surface salinity in the south eastern Arabian Sea off Mangalore during 1990-2010. The results of the analysis of multiple datasets shows that the decrease of sea surface salinity is part of a regional decadal trend, which is due to increased transport of low-salinity water from the Bay of Bengal and intensified coastal currents in the winter months.

In this precision era of cosmology, dark matter remains one of the mystique objects measured as a dominant matter component of the Universe. Among the different paradigms, the feebly interacting massive particle provides one exciting possibility. Here, starting from its near-zero abundance in the early Universe, the amount of dark matter grows gradually from the annihilation or decay of the thermal bath particle when the Universe was hot. In this context, an exciting possibility has been developed wherein dark matter is produced because of the thermal effects through a channel that was not kinematically allowed in the first place.

Compact analytic expressions are derived for one-loop Higgs+4-parton helicity amplitudes, which reveal fascinating relationship between the scalar theory and fermion theory.

A new mechanism is proposed that connects the observed pattern of fermion masses with the anomaly cancellations in the theories with an extra spatial dimension. The hierarchical masses result from the specific localization of fermions in the extra dimension, which is determined by an abelian gauge symmetry and its stability under quantum corrections.

A new quantum key distribution (QKD) protocol, called Coincidence Detection protocol, was developed, and it was demonstrated to give a 70% higher secure key rate compared to the most popular QKD protocols, i.e., BB84 and decoy-state.

Molecular emission dynamics from a femtosecond filament-induced plasma plume have been investigated of molecular species such as CN and C_2. It is found that the molecular signal intensity strongly depends on the sample properties and position of the sample in the filament.

A technique was demonstrated to achieve an accuracy of measuring the displacement of around 2 μm over a longitudinal range of more than 2 mm using a single beam line and only two quadrant detectors.

PRL continued with zest its activities towards outreach and popularization of science at various levels and fora. PRL is committed towards spreading the scientific temper and spirit, not only at the highest level in terms of organizing the weekly colloquiua for the advancement of research in various fields of specialization in PRL, but also, very importantly, of education and outreach at the level of schools and colleges, and to the common public at large. Through various events from time to time, particular attention is given to students from rural backgrounds by encouraging them to visit PRL and get a chance to gain first hand and on many occasions, hands-on, experience of excitement in science. During the last year, in view of the continued pandemic conditions, PRL has been using the online platform for its outreach activities to the best possible extent. To take our efforts further in this direction, PRL has instituted a scholarship scheme exclusively for the students of economically weaker sections living in rural areas in the state of Gujarat, called the Vikram Sarabhai Protsahan Yojana "VIKAS." Many researchers from various institutes and universities have visited PRL this year on short visits (extending to about a month) to carry out collaborative experimental works, discussions and training by the experts that exists in PRL.

Undeterred by the challenges posed by the COVID-19 pandemic, the National Science Day celebrations saw significant participation of nearly 600 students from the state of Gujarat, of which 150 were selected for participation in the online program held on 26 February 2022. Five brilliant students were awarded the Aruna Lal Fellowship. Additionally, special efforts were made to popularize science among all students who participated in the screening test by inviting them to attend the online science day celebrations. PRL's unfettered and relentless capacity-building efforts continued this year with enhanced vigor. Around 40 students participated in the summer internship program during May-July 2021 and nearly 40 students carried out their four-month final project training with PRL faculty during January-April 2022 in ONLINE mode. The major online meetings and programs organized by PRL during this academic year include Conference on Condensed Matter Physics in August 2021, 1^{st} Venus Science Conference and 1^{st} Frontiers in Geosciences Research Conference in September 2021, 1^{st} Dr. Arvind Bhatnagar Memorial Lecture, 1^{st} "Meteoroids, Meteors and Meteorites: Messengers from Space" Symposium, and Students Conference in Optics and Photonics (SCOP) in November 2021, 1^{st} Indian Space Weather Conference in January 2022, 2^{nd} Dr. Bibha Chawdhuri Memorial Lecture and 4^{th} PRL-IAPT Dr. Vikram Sarabhai Lecture in February 2022, 3^{rd} Indian Planetary Science Conference (IPSC-2022) in March 2022. Early career researchers' webinar series was initiated in April 2021 wherein young scientists (Doctoral and post-doctoral fellows) working in the areas of Astrochemistry and Astrobiology from around the globe presented their work. So far 14 lectures have been held. PRL Platinum Planetary Seminar Series (PPP-SS) is being conducted where younger and seasoned scientists are delivering seminars, about two to three seminars every month on Thursdays, since September 2021.

The scientists from PRL take active role in collaborating with the researchers from institutions and universities in India through ISRO's RESPOND program, wherein they extend their expertise to have a capacity building and human resource development in highly specialized areas. PRL continues to impart knowledge in the area of Space and Atmospheric sciences to the participants of the Asia Pacific through the courses organized under the auspices of the CSSTEAP (Centre for Space Science and Technology Education in Asia and the Pacific, affiliated with the United Nations). The 12^{th} Post Graduate Course on Space and Atmospheric Science (SAS-12) was hosted online by PRL during 01 October 2021 – 31 March 2022, which will continue until June this year. In this course there are participants from Bangladesh, Ethiopia, Mongolia, Nepal, Uzbekistan and India.

PRL had the honour of playing host to several dignitaries who have visited all the PRL campuses. They include the Rajasthan Governor, Honourable Kalraj Mishra, Shri. Talleen Kumar, Member Finance and Member, Space Commission, Government of India, and Shri. Pawan Goenka, Secretary, InSpace, Government of India. We are delighted by their visit and humbled by the very appreciate remarks they have made on the high and excellent quality of work that is being pursued by PRL. The use of Hindi in all administration and official communications areas is ensured in PRL. Bilingual communication is encouraged in all administrative orders. The website of PRL is bilingual. The participation in Hindi Pakhwada celebrations continues to rise. PRL received the year's 2020-2021 Second Prize for best work in Hindi from the Town Official Language Implementation Committee, Ahmedabad.

In our endeavour to strive for excellence in scientific research, capacity building, human resource development and dissemination of knowledge, we are constantly encouraged and whole-heartedly supported by Shri. A. S. Kiran Kumar, Chairman, PRL Council of Management, Shri S. Somanath, Secretary, Department of Space, and all the members of the PRL Council of Management. I thank them for their astute advice, guidance, and steadfast faith in PRL.

Anil Bhardwaj

Director

PRL in News

1. “Indian Mars Orbiter Mission (MOM) used for Investigating the Solar Corona by ISRO Scientists. https://www.isro.gov.in/update/28-feb-2022/indian-mars-orbiter-mission-mom-used-investigating-solar-corona-isro-scientists
2. “Ahmedabad dust can muddy unhackable quantum communication, shows study. https://timesofindia.indiatimes.com/city/ahmedabad/abad-dust-can-muddy-unhackable-quantum-communication-shows-study/articleshow/89392585.cms
3. “Department of Space conducts breakthrough demonstration of hack-proof quantum communication. https://www.prl.res.in/prl-eng/sites/default/files/images/prl_in_news/prl-news-quantum.jpg
4. “Mars is alive! Indian scientists find unique movements on the surface. https://www.indiatoday.in/science/story/mars-boulder-movement-tracks-indian-scientists-physical-research-laboratory-nasa-isro-1904142-2022-01-25
5. “Swarnajayanti fellow exploring ways of enhancing ocean alkalinity for removing atmospheric carbon dioxide.” https://dst.gov.in/swarnajayanti-fellow-exploring-ways-enhancing-ocean-alkalinity-removing-atmospheric-carbon-dioxide
6. “Tidings from an exploding star make astronomers happy”. https://www.nature.com/articles/d41586-021-03508-0
7. “Unraveling the mysteries of the Solar Corona: New results from Chandrayaan-2 Solar X-ray Monitor”. https://www.isro.gov.in/update/22-jun-2021/unraveling-mysteries-of-solar-corona-new-results-chandrayaan-2-solar-x-ray
8. “Discovery of an Inflated Hot-Jupiter around a Sub-Giant Star by PRL Scientists”. https://www.isro.gov.in/update/15-nov-2021/discovery-of-inflated-hot-jupiter-around-sub-giant-star-prl-scientists
9. “How Young Massive Protostars Form”, Nature India Research Highlight: December 2021 https://doi.org/10.1038/d44151-021-00086-y
10. “Study on volcanic structures in an unnamed crater at Arabia Terra, Mars has become the cover page in the Issue of November 2021 in JGR-Planets”. https://agupubs.onlinelibrary.wiley.com/doi/epdf/10.1002/jgre.21394
11. “Natural selection in few milliseconds: Shock-induced formation of complex macroscale structures”. https://www.isro.gov.in/update/14-jun-2021/natural-selection-few-milliseconds-shock-induced-formation-of-complex-macroscale

Science Highlights

Astronomy and Astrophysics

- Time-resolved X-ray spectroscopic analysis for the small B-class solar flares was carried out for the first time using observations from the Chandrayaan-2/XSM. The results show that the evolution of temperature and emission measure of the flaring plasma agrees well with the standard flare model, suggesting that like their bigger counterpart, the smaller flares also follow the standard flare model. Our spectroscopic analysis further shows that the elemental abundances of low FIP (First Ionization Potential) elements change from their coronal to photospheric values during the impulsive phases of the flares. Nevertheless, the respective coronal values are quickly recovered during the decay phases of the flares. While the change of abundances from the corona to photospheric values was observed earlier for the bigger flares, their quick recovery is certainly observed for the first time. This quick recovery also provides the first indirect evidence towards magnetic reconnection-driven Alfven waves, observation of which was long sought.

- A Hot-Jupiter has been discovered which is orbiting in very close proximity, at a period of 3.21 days ($a \sim 0.05$AU), around an evolved F-type star, TOI-1789. This is the second exoplanet discovery from India. Such discoveries help in understanding the physics of formation of planets around stars and as well as the physics of orbital dynamics. Initially identified as an exoplanetary candidate using the TESS photometry data, pending for further necessary observations, the exoplanet was finally discovered using the follow-up ground-based transit data from PRLs 43cm Telescope and the mass measurements from the high-resolution spectrographs, PARAS at PRL, India and TCES at TLS, Germany. TOI-1789b found to be having a mass of $\mathrm{M_P} = 0.70 \pm 0.16\ \mathrm{M_J}$, a radius of $\mathrm{R_P} = 1.44^{+0.24}_{-0.14}\ \mathrm{R_J}$, and a bulk density of ρ_P = $0.28^{+0.14}_{-0.12}$ g cm^3. This makes it one of the lowest density exoplanets known so far. TOI-1789b falls under a very unique category of 10 exoplanets among all the known ones, which are orbiting the evolved stars in a very close orbit (within 0.05 AU). Due to such closeness to its parent star, the planet has high incidence flux and high surface temperature of $\sim$2000 K, which is the main reason behind the inflated radius of TOI-1789b.

- Massive OB stars (M $\gtrsim$ 8 $\mathrm{M_\odot}$) have a significant impact on the evolution of galaxies and the universe, in general, through their energetics. However, despite their importance, unraveling the exact formation mechanism of massive stars is one of the outstanding issues in massive star formation research. It is directly related to the understanding of the process of mass accumulation in massive star formation, which is also a key open research problem. In recent years, several multi-wavelength large-scale surveys reveal the common presence of hub-filament systems in massive star-forming regions. In such hub-filament systems, several parsec-scale filaments are directed to the central denser regions hosting massive stars. Hence, the study of massive star formation requires a careful investigation of the inner environments of the central hub in hub-filament systems. In this context, a massive star-forming region W42 has been observationally examined using a multi-scale and multi-wavelength approach. The findings discovered a disk-outflow system (extent $\sim$800 AU to 9000 AU) around the rare young massive O-type protostar W42-MME (mass $\sim$19 $\mathrm{M_\odot}$). Furthermore, it is found that the core forming the massive protostar and embedded protostar gain mass simultaneously.

- A comprehensive study of three large long-duration flares detected on an active M-dwarf binary EQ Peg is carried out using the Soft X-Ray Telescope of ISRO's AstroSat observatory. The peak X-ray luminosities of the flares in the 0.3-7-keV band are found to be within $\sim$5-10 $\times$ 10^{30} ergs^{-1}. The e-folding rise- and decay-times of the flares are derived to be in the range of 3.4-11 and 1.6-24 ks, respectively. Spectral analysis indicates the presence of three temperature corona wherein the first two plasma temperatures remain constant during all the flares and the post-flare observation at $\sim$3 and $\sim$9 MK. The peak emission measures are found to be 3.9-7.1 $\times$ 10^{53} cm^{-3} whereas, the abundances peaked at 0.16-0.26 times the solar abundances. The magnetic field for all three flares is estimated to be $<$ 100 G. The estimated energies of all three flares are $\gtrsim$ 10^{34}-10^{35} erg, putting them in a category of superflare. All three superflares are also found to be the longest duration flares ever observed on EQ Peg.

- Timing and spectral studies of Be/X-ray binary pulsar EXO 2030+375 are carried out using observations with the LAXPC and SXT of AstroSat, at various phases of its Type-I outbursts in 2016, 2018, and 2020. The pulsar was faint during these observations as compared to earlier observations. At the lowest luminosity of 2.5 $\times 10^{35}$ ergs^{-1} in 0.5-30 keV energy range, 41.3 s pulsations were clearly detected in the X-ray light curves. This finding establishes the first firm detection of pulsations in EXO 2030+375 at an extremely low mass accretion rate to date. The shape of the pulse profiles is complex due to the presence of several narrow dips. Though pulsations were detected up to $\sim$80 keV when the source was brighter, pulsations were limited up to $\sim$25 keV during one of the AstroSat observations at lowest source luminosity. Spectral analysis of the AstroSat data showed that the spectrum of the pulsar was steep with a power-law index of $\sim$2. The values of photon-indices at observed low luminosities follow the known pattern in sub-critical regime of the pulsar.

- The nature of the changing-look active galactic nucleus NGC 1566 during its 2018 June outburst is investigated using data from various X-ray observatories. During the outburst, the X-ray intensity of the source rises up to $\sim$25-30 times

compared to its quiescent state intensity. Timing and spectral analysis of the source are carried out during pre-outburst, outburst, and post-outburst epochs using semi-simultaneous observations with the XMM-Newton, NuSTAR, and Neil Gehrels Swift Observatories. The variance, normalized variance, and fractional rms amplitude are calculated in different energy bands to study the variability. The broad-band 0.5-70 keV spectra are fitted with phenomenological models, as well as physical models. A strong soft X-ray excess is detected in the spectra during the outburst. The soft-excess emission is found to be complex and could originate in the warm Comptonizing region in the inner accretion disc. It is found that the increase in the accretion rate is responsible for the sudden rise in luminosity. The results suggest that NGC 1566 most likely harbours a low-spinning black hole with the spin parameter a* $\sim$0.2.

- A detailed spectral and timing analysis of a Seyfert 1 galaxy Mrk 509 is carried out using data from the Neil Gehrels Swift observatory between 2006 and 2019. To study the variability properties from the optical/UV to X-ray emission, a total of 275 pointed observations were used in this work. The average spectrum over the entire duration exhibits a strong soft X-ray excess above the power law continuum. The soft X-ray excess is well described by two thermal components with temperatures of $\sim$120 eV and $\sim$460 eV. The warm thermal component is likely due to the presence of an optically thick and warm Comptonizing plasma in the inner accretion disk. The strength of the correlation within the UV and the optical bands (0.95-0.99) is found to be stronger than the correlation between the UV/optical and X-ray bands (0.40-0.53). These results clearly suggest that the emitting regions of the X-ray and UV/optical emission are likely distinct or partly interacting. Having removed the slow variations in the light curves, we find that the lag spectrum is well described by the 4/3 rule for the standard Shakura-Sunyaev accretion disk when we omit X-ray lags. All these results suggest that the real disk is complex, and the UV emission is likely reprocessed in the accretion disk to give X-ray and optical emission.

- A detailed timing and spectral studies of the black hole candidate MAXI J0637-430 is carried out during its 2019-2020 outburst using observations with the NICER and the Neil Gehrels Swift Observatory. It is found that the source evolves through the soft-intermediate, high-soft, hard-intermediate, and low-hard states during the outburst. Weak variability with fractional rms amplitude $<$5% is found in the softer spectral states. In the hard-intermediate and hard states, high variability with the fractional rms amplitude of $>$20% is observed. The 0.7-10 keV spectra with NICER are studied with a combined disc-black-body and nthcomp model along with the interstellar absorption. The temperature of the disc is estimated to be 0.6 keV in the rising phase and decreased slowly to 0.1 keV in the declining phase. The disc component was not detectable or absent during the low-hard state. From the state-transition luminosity and the inner edge of the accretion flow, we estimate the mass of the black hole to be in the range of 5-12 solar mass, assuming the source distance of d $<$ 10 kpc.

Solar Physics

- Coronal loops are basic building blocks of the solar atmosphere and are observed on various length scales. For a better insight into their formation, small-scale transients and subsequent formation of transient hot and cool loops were studied using spectroscopic and imaging observations. Energy estimates suggest that flux cancellation can easily power the hot transients but is insufficient for cool transients. Lifetime estimates and magnetic field extrapolation suggest the presence of small-scale and fine structures within these loops. Results provide crucial ingredients on the physics of loop formation and involved thermodynamics.

- Ohmic dissipation is one of the several processes that have been proposed to heat the solar chromosphere. However, there has been very little observational evidence to support this. Intense electric currents and strong chromospheric temperature enhancements over a sunspot, which occur because of the large-scale magnetic flux emergence at the location of light bridge were studied using observations. The temperature excess from the dissipation of currents is located in the lower chromosphere between 0.4 and 0.7 Mm and is possibly sustained over the whole passage of flux emergence lasting about 13 hr. A study, combining the models of magnetic field topology and thermal inversions provides direct evidence of lower chromospheric heating through Ohmic dissipation of electric currents in the sunspot.

- Possible reasons for the failed-eruptive M-class flare were investigated using multi-wavelength observations and nonlinear force-free field extrapolations of the coronal magnetic fields. The study suggests that magnetic decay index initially increased to the torus-unstable limits within the heights of the flux ropes and then decreased rapidly reaching to negative values, which is most likely responsible for the failed eruption.

- The studies of DH type II bursts associated with CMEs are significant as they are primarily associated with the energetic and wider CMEs that frequently cause space-weather disturbance. Characteristic of DH type II radio bursts for the Solar Cycles 23 and 24 were explored. The results suggest that CME initial speed or flare energetics are partly related with the duration of type II bursts and the survival of CME-associated shock is determined by multiple factors/parameters related to CMEs, flares, and state of coronal and interplanetary medium.

- Significance of the Hall effect on magnetic reconnection to understand the observed solar flare ribbon brightening is studied using the first ever data-based Hall MHD simulation. The investigations, based on the numerical techniques to detect favorable topologies for reconnection revealed the presence of 3D nulls, quasi-separatrix layers (QSLs), and a magnetic flux rope. A comprehensive analysis of the magnetic field lines dynamics associated with these topologies reveals the faster and efficient reconnections during the Hall MHD as well as an excellent spatio-temporal agreement with the observed flare brightening which is not captured in the standard MHD simulation.

Planetary Sciences

- For the first time, a consolidated map of the chemical provinces of Mars is derived, which demonstrates secular chemical trends and indicate complex processes related to partial melting within a highly differentiated mantle source. The result is distinct from that of the Hesperian lowland units and the methodology can also be applied to other planetary bodies.

- Identifying the obscured impact basins and their spatio-temporal extension on the Moon is important. For the first time, deciphered geology of an obscured impact basin on the Moon is reported. The C*ü*rgerSirsalis Basin (with $\sim$475 km diameter and location of 16.0°S/293.0°E) of pre-Nectarian age uniquely showcases the volcanic history of the Moon.

- An analysis of new carbonaceous chondrite Bukhara using noble gas mass spectrometer for isotopic ratios, revealed that the cosmic ray exposure age is 22 Ma, indicating ejection of this meteorite long ago from its parent body. Nitrogen isotopic signature indicates a heavier ratio than solar wind, showing the chondritic components inhibiting nitrogen from an evolved region of proto-planetary disk.

- Cosmogenic radionuclides measured in Mukundpura CM2.0 chondrite are dependent on the Solar cycle intensity. Absence of ^{60}Co constrains smaller pre-atmospheric size, while the cosmogenic stable isotopes of Ne, Ar, and combined Ne-Al systematics yield the exposure age of 6 Ma for Mukundpura. Also, solar wind noble gases are present in the meteorite, indicating regolithic exposure of the rock.

- Lobate Debris Apron in the Mars' mid-latitudes substantiate extensive glaciation during the Late Amazonian. Our morphological investigation of landforms in Erebus Montes region revealed evidence of the Lobate Debris Apron deposits consistent with typical down-gradient flow characteristics, and integrated flow patterns. The findings add a case to support the rapidly accumulating evidences for glacial land systems on Mars in the Late Amazonian geological history.

- High-resolution images of the same place on Mars, taken at different times, show that all new boulder fall ejecta. Our results revealed that it takes $\sim$2 to 4 Mars years for the boulder fall ejecta to disappear, whereas, the boulder fall ejecta on Earth are rarely preserved. We found that the Cerberus Fossae region adjacent to the landing site of InSight hosts $\sim$30 % of boulder fall ejecta, suggesting a currently active region.

- Modelling of observable Schumann Resonance and analysis of Martian Year 28 were carried out for Mars, considering an inverted cone-shaped of the dust devil. It is found that Schumann Resonance essentially depends on the shape of dust devil and does not depend much on the conductivity.

- A numerical study is carried out to evaluate the effect of lunar landing on the surface, surrounding environment and hardware. A quantitative estimation of the damage is estimated, suggesting various materials to be used for future lunar missions. DSMC code is used to evaluate the plume dynamics and its interaction with the lunar soil. The work has implications for science and engineering aspects of a mission when multiple landings are sought in the vicinity.

- Seasonal variability of ozone heating rates have been estimated. It is found that at low and mid latitudes, ozone heating rates increased until Ls $\sim$47.5°. Afterward, they decreased until Ls $\sim$127.5° and then they reached a minimum value between Ls $\sim$167.5° and 327.5°. These are the first reports of this kind.

- A photochemical model for NO density in the dayside of the Martian upper atmosphere is developed using observations from NGIMS on MAVEN for 120 and 200 km altitudes. It is found that local CO_2 and N_2 density variations can lead to a change in NO density and consequently its dayglow intensity by a factor of 2 to 5.

Space and Atmospheric Sciences

- An analysis of black carbon (BC) aerosols measured simultaneously over a source and a background region revealed distinct differences in the probable sources and source regions for BC, especially, during postmonsoon and winter, when long-range transport of agricultural waste and biomass burning emissions from northwestern India and the Indo-Gangetic Plain reach the background region. Observation-model comparison reveals that model significantly underestimates BC mass over the urban Ahmedabad, whereas, the agreement is good over the high-altitude, background Gurushikhar, suggesting a need to improve aerosol emission inventories.

- A comprehensive year-round analysis of black carbon (BC) mass concentration measured over an urban and an adjoining semi-urban environment using multi-wavelength aethalometer enabled quantification of the relative source strengths of vehicular and residential emissions, for the first time. Further, using the spectral dependence of BC mass concentration for different fuel types, region and fuel specific absorption Ångström exponent (α) was derived. The application of region and fuel specific α, and the resulting apportionment data (vehicular vs. residential) will be useful for planning future policies on air quality improvement.

- An analysis of satellite and ground-based observations over Asia along with simulations from climate models in Coupled Model Intercomparison Project Phase 6 (CMIP6) experiment with state-of-the-art treatment of aerosol chemistry, physics and meteorology, for the first time, revealed large inter-model differences in model estimates, and discrepancies between model simulations and observations as most models are not able to capture the recent observed magnitudes and trends in aerosols. These results on model-observations comparison need to be taken into account while examining projected/expected future climate impacts due to aerosols, and potential value of various mitigation measures.

- An analysis focusing on the climate benefits of energy transitions by making firsttime use of two decades of high quality observations of atmospheric loading of light-absorbing black carbon (BC) over Kanpur (South Asia) and Beijing (East Asia), and relating these observations to changing energy, emissions and economic trends in India and China, revealed that absorption aerosol optical depth due to BC has decreased substantially, by 40% over Kanpur and 60% over Beijing between 2001 and 2017. Our findings show additional benefits for climate (beyond benefits of CO_2 reduction), and for several other issues of sustainability over South and East Asia, provide motivation for ongoing cleaner energy production and consumption transitions, especially when they are associated with reduced emissions of air pollutants. Such an analysis connecting the trends in energy transitions and aerosol absorption loading, unavailable so far, is crucial for simulating the aerosol climate impacts over Asia which is quite uncertain.

- Biomass burning emissions from forest fires and agricultural residue burning can influence the physical and chemical properties of aerosols, air quality and climate. An analysis of the influence of biomass burning on aerosol characteristics and radiative forcing investigated over three locations in south (Kanpur and Gandhi College) and south east Asia (Singapore) which are influenced by biomass burning emissions revealed that the results remained the same for low and high fire count scenarios suggesting that the properties of aerosols and their radiative effects are governed more by the variations in the sources of aerosol emissions resulting in variations in their composition (chemical), and less by the amount of aerosol emissions (physical).

- The photochemistry over a tropical urban environment (Ahmedabad) has been investigated by integrating state-of-the-art measurements with the Master Mechanism model. The results revealed strong build-up of ozone and numerous secondary organics in the outflow towards the Indian Ocean. Notably, the measurement driven simulation has been used further to estimate the levels of the hydroxyl radical ($\sim$0.3 pptv in noontime) and to analyse its budget. The study is of paramount significance as the OH radical governs the self-cleaning capacity of the atmosphere, but its direct measurements still remain lacking in the tropical Indian region.

- Machine learning - a novel modeling approach has been applied to simulate the variations in urban ozone over Doon valley of the Himalaya. The model, trained with past variations in ozone and meteorology, successfully reproduced the independent ozone observations ($r^2 \sim 0.7$). The inclusion of precursors further enhanced the ability of the model to capture the outliers, which are crucial in the air quality assessments. The study suggests that machine learning can strongly complement the conventional models for unravelling the feedback between pollution and meteorology over fragile Himalayan ecosystem.

- Outbreaks of the COVID19 pandemic necessitated the implementation of a strict lockdown in India, which drastically decreased anthropogenic activities. The elevated levels of aromatic volatile organic compounds (VOCs) known as BTEX (benzene, toluene, ethylbenzene and xylenes) can adversely affect human health. We performed a thorough analysis of BTEX data measured continuously during the COVID-19 lockdown and our previous data (PTR-TOF-MS for years 2014-2015-2018) being used as a reference (representing business as usual (BAU) conditions). We conducted a comprehensive data analysis to attribute the changes to the reduction in emissions caused by the lockdown restrictions. During the lockdown, the meteorology-corrected BTEX concentrations reduced by 54-88% from the same period during the normal years (2014-2015-2018). In addition to reduced anthropogenic emissions, the balance between photochemical processes and evaporative emissions seems to control BTEX concentration and composition during the lockdown period. These significant reductions in BTEX concentrations are consistent with the change in peoples movement as inferred from mobility data during the lockdown. Although enforced, the decrease in ambient BTEX concentrations was a good change for air quality, as these compounds are primary pollutants and precursors for secondary pollutants. Further, this study suggests a need for more effective science-based policies that consider local and regional factors. This is the most comprehensive study investigating the impact of lockdown on ambient BTEX concentrations at an urban site in India.

- Plants have several defense mechanisms to deal with different environmental conditions, and the emission of VOCs is one of them. VOCs emitted from natural sources are known as biogenic VOCs (BVOCs). BVOCs emitted from the tropical forest comprise a significant fraction of global atmospheric VOC emissions. However, the measurements of BVOCs over tropical forests are very limited, especially over South Asian tropical forests. The ambient air concentrations of C2-C5 non-methane VOCs (NMVOCs) were measured at a remote forest site of the Bhagwan Mahaveer Sanctuary (BMS) located in the central Western Ghats of India. There is significant diversity in the forest vegetation of the Western Ghats covered by the tropical wet evergreen, tropical semi-evergreen, and tropical moist deciduous forests. The average percentage contributions of light alkenes (sum of ethene and propene) to the total measured NMVOCs were much higher of $\sim$65% at BMS compared to that at a typical urban site of India. This study suggests the need for the comprehensive measurements of VOCs and other reactive trace gases to understand the photochemistry leading to ozone and secondary aerosol formation in the remote forest regions of South Asia.

- The Atmospheric Boundary Layer (ABL) is the lowermost layer of the atmosphere in contact with the Earths surface and act as a packing volume of the atmospheric pollutants. ABL characteristics have been investigated using a Ceilometer Lidar over Ahmedabad and a stark winter-summer difference in is found. ABL has been found to collapse during monsoon and is often ambiguous due to the presence of thick clouds on the top of the ABL. The ABL is thicker during the onset of monsoon in contrast to active monsoon, rises again during the withdrawal of monsoon. Such quantitative (during winter $\sim$0.5 km, and summer $\sim$3.0 km) evaluation of ABL is formerly unavailable over this region, which can now be used to improve the representation in numerical models and thereby estimates of radiative and climate effects due to ABL dynamics.

- Planetary wave (PW) associated dynamical variability in the low-latitude middle atmosphere during a Southern hemisphere minor sudden stratospheric warming revealed a major involvement of the quasi-16-day and quasi-6-day waves. Significant wave driven latitudinal mixing is noted in the winter hemisphere along with mid to low-latitude propagation of PW.

- A prominent signature of mesospheric bore propagation is observed over a Himalayan location. Stable thermal structure possibly driven by dynamics/chemistry seems to favour spectacular bore propagation through suitable duct formation. Tropospheric weather conditions, e. g., front, jet streams are surmised to be the source of the mesospheric dynamical event.

- The cause of enhancement in post-sunset in the thermospheric OI 630.0 nm nightglow emissions has been found to be the northward turning of meridional wind (or cessation of equatorward winds). This feature of airglow could serve as a proxy for the existence of meridional winds during that time, the information on which is rather difficult to obtain.

- The latitudinal variation on the effect of equatorial electrodynamics has been investigated by two in-house built large field-of-view optical spectrographs that combinedly cover 5°-18° magnetic latitude. Latitudinal variation in the OI 630.0nm dayglow emissions was investigated as a function of the equatorial electrojet, which was used to represent the strength of equatorial electrodynamics. It was revealed that the effect of equatorial electrodynamics is nearly similar until the crest latitude of the equatorial ionization anomaly. This information has far reaching implications on the understanding of the equatorial electrodynamics in both the day and nighttimes.

Geosciences

- In recent years, the atmospheric radiocarbon values have become depleted relative to the northern Indian Ocean surface $\Delta^{14}C$ values. This indicates that major fraction of bomb radiocarbon has moved in to the ocean reservoir from the atmosphere.

- A comparison between two radiometric dating methods demonstrate a significant difference in dating threshold and resolution. The study shows that the ^{10}Be method very well mimics the radiocarbon method. The extrapolation of radiocarbon ages beyond its limit using a constant sedimentation rate may cause errors in age estimation. The meteoric ^{10}Be method can be used as a potential tool to extrapolate radiocarbon ages beyond 50 kyr.

- The ^{10}Be depositional flux determined from a sediment core from the central Indian Ocean shows changes in depositional flux and $^{10}Be/^{9}Be$ ratio during the last 43 ka, which demonstrates that local processes affect the ^{10}Be deposition into the sediment column. Reconstructed ^{10}Be fluxes indicates change in past geomagnetic field strength.

- Based on bomb radiocarbon records from corals of the Andaman and the Lakshadweep Islands in the northern Indian Ocean, estimates of air-sea CO_2 exchange rates in the region have been derived. The calculated net regional CO_2 flux from the Lakshadweep region shows it as a region of source of CO_2 from the ocean, whereas, northern Andaman acts as sink of CO_2.

- Studies based on isotopic composition has shown that the Lakshadweep corals can potentially provide information about both rainfall and sea Surface Temperature (SST) changes related to the monsoon. The Lakshadweep corals record monsoon-induced seasonal SST cooling in the region.

- Based on reconstruction of the redox conditions of the abyssal water mass (>3800 m) in the Arabian Sea for the last 39 kyr using paleoredox proxies, it has been shown that the increase in the supply of poorly oxygenated mNADW and stronger deep mixing in the Southern Ocean resulted in a decline in the oxic condition during the deglacial period.

- Using stable isotopic composition of black carbon in a Himalayan lake, the timeline of the natural to anthropogenic shift in the region was identified. Also, using the same data, fire events in the area were reconstructed; which was verified using the historical records from the region. This study further strengthened the potential of lake sediments as an efficient recorder of the changes in regional environment.

- Decadal changes in sea surface salinity act as a marker of changes in the hydrological cycle and/or ocean circulation. Evaporation, rainfall, continental runoff, and coastal currents regulate salinity in the eastern Arabian Sea. Recent results have shown a distinct decline in sea surface salinity in the southeastern Arabian Sea off Mangalore during 1990-2010. Our analysis of multiple datasets shows that the decrease of sea surface salinity is part of a regional decadal trend, which is due to increased transport of low-salinity water from the Bay of Bengal and intensified coastal currents in the winter months.

- Indian Summer Monsoon (ISM) plays important role in maintaining the socio-economic conditions of people living in the Indian subcontinent. The ISM played important roles in rise and collapse of ancient civilizations in the subcontinent. In the mid to late Holocene period, Indus Valley or Harappan Civilization flourished in the western part of India and collapsed around the beginning of the Meghalayan Age (4.2 kyr Before Present). It is believed that a prolonged drought condition or decrease in the ISM rainfall caused the decline in the Indus Civilization. PRL scientists using proxy records and other available studies showed that the ISM was significantly weak around the 4.2 kyr Before Present which probably caused the dispersion and migration of the Harappan Civilization.

- Molybdenum (M_0) is the most abundant transition metal in the ocean and plays important role in regulating several biogeochemical processes. In addition, because M_0 is actively linked with redox transformations, Mo isotopic composition ($\delta^{98}M_0$) can be efficiently used to understand past oceanic redox changes. The $\delta^{98}M_0$ of the present-day ocean water

shows consistent values, of $\sim$2.3, which can be taken as a tenet for M_0 isotopic geochemistry of the ocean. However, in contrast, our recent results from the northern coastal Bay of Bengal show significantly lighter $\delta^{98}M_0$ (average = 1.64 $\pm$0.42; 1σ) than the open ocean seawater. These results showed that the in-situ reduction and dissolution of Fe-Mn oxyhydroxide phases adsorbed on suspended particulate matter can explain the depleted/lighter Mo in these waters. It is also estimated that around 5-11% of leachable M_0 fraction adsorbed on Fe-Mn oxyhydroxide fraction is released under suboxic/anoxic conditions in these waters.

- Light-absorbing organic aerosols (termed as brown carbon, BrC) are shown to impact Earth's climate and air quality. Unlike black carbon that absorb uniformly across the wavelengths, the BrC absorb more towards UV region. Different BrC species exhibit different absorption at different wavelengths. Unique online measurements of BrC were performed over New Delhi using an assembled analytical system, which showed a large diurnal variability in absorption coefficient, mass absorption efficiency, and absorption angstrom exponent of BrC. Biomass burning derived BrC were most absorbing among all the sources. This work infers that BrC are a mixture of different species with variable optical properties.

Theoretical Physics

- The discovery of Gravitational Waves (GW) have opened a new window for astronomy. The computation of GW from macroscopic bodies like binary-pulsars was pioneered using the Feynman diagram techniques. This has provided a method for calculating radiation of other light particle like scalars and vector bosons (which can be the ultra-light dark matter of the universe) and testing modified gravity using the techniques of quantum field theory.

- A new mechanism is proposed that connects the observed pattern of fermion masses with the anomaly cancellations in the theories with an extra spatial dimension. The hierarchical masses are result of specific localization of fermions in the extra dimension which is determined by an abelian gauge symmetry and its stability under quantum corrections.

- Using the powerful self-consistent renormalization theory of spin fluctuations for the system $CaMn_2$-Al_{10} discovered in 2015, it is demonstrated that this system is a case of itinerant magnetism. The inverse static (paramagnetic) susceptibility has been calculated and have been compared it with the experimental data with very good agreement. The agreement is very good. Spin fluctuations have been calculated at various temperatures and have also estimated the strength of the electronic correlation i.e., (I=0.3136 eV) in the Hubbard Hamiltonian. Based on the quantitative explanation of the inverse static (paramagnetic) susceptibility data within the framework of SCR theory, it is decisively concluded that CaMn2Al10 exhibits the phenomena of itinerant magnetism. Further, our DFT and DFT+U calculations corroborate the strong Mn-Al hybridization which is the key behind the itinerant magnetism in this system.

- Predicting different observables at a particle physics experiment like the Large Hadron Collider requires a thorough knowledge of Quantum Chromodynamics. Any such observable must follow Infra-Red and Collinear (IRC) safety, i.e., any modification on constituents by a collinear splitting or the addition of a soft emission must keep all the observables in the event unchanged. Modern deep-learning algorithms provide a powerful mechanism that takes measured properties as input. However, they typically forgo such an IRC construction to become susceptible to long-distance physics. We devise a graph neural network algorithm that is IRC safe by design, making the network output less sensitive to low-energy effects. We find such a general but straightforward architecture to perform on par with other algorithms, which are IRC unsafe.

- In this precision era of cosmology, dark matter (DM) remains one of the mystique objects measured as a dominant matter component of the Universe. Among the different paradigms, the feebly interacting massive particle provides one exciting possibility. Here, starting from its near-zero abundance in the early Universe, the amount of dark matter grows gradually from the annihilation or decay of the thermal bath particle when the Universe was hot. In this context, an exciting possibility has been developed wherein dark matter is produced because of the thermal effects through a channel that was not kinematically allowed in the first place.

- The in-medium properties of axion i.e., its mass and self-coupling are estimated within a three flavor Polyakov loop extended NambuJona-Lasinio (PNJL) model with Kobayashi-Maskawa-tHooft determinant interaction. The topological susceptibility of strong interaction is also estimated within the same model. It is observed that (statistical) confinement effects simulated by Polyakov loop potential play an important role in the estimation of all these quantities, particularly, near the critical temperature. Both the mass and the self-coupling of the axion get correlated with the chiral and deconfinement transition. The results for all these quantities obtained within the PNJL model is compared with chiral perturbation theory, NambuJona-Lasinio (NJL) model and lattice QCD simulation results wherever available. The results for properties of axions at finite baryon densities are also presented.

Atomic, Molecular and Optical Physics

- A new quantum key distribution (QKD) protocol, called Coincidence Detection protocol was developed and it was demonstrated to give 70% higher secure key rate compared to the most popular QKD protocols i.e., BB84 and decoy-state.

- For quantum key distribution (QKD) the possible information leakage through side channel was calculated by evaluating mutual information between source and eavesdropper. Based on our experimental observations of cross correlation between parameter values for different laser diodes used for transmitting weak coherent pulses, methods were suggested to reduce information leakage to the eavesdropper.

- An improved calculation of the nuclear spin-independent parity violating electric dipole transition amplitude ($E1_{PV}$) or the 6S $\leftrightarrow$ 7S transition in ^{133}Cs was performed which in combination with the most accurate (0.3%) measurement yielded a new value for the nuclear weak charge Q_w = -73.71$(26)_{ex}(23)_{th}$ against the Standard Model (SM) prediction $Q^{SM}w$ = 73.23(1). The advances in the calculation was achieved by using a variant of the perturbed relativistic coupled-cluster theory, which treated the contributions of the core, valence, and excited states to $E1_{PV}$ on the same footing unlike the previous high-precision calculations. This approach resolved the earlier ongoing controversy regarding the sign of the core correlation effects. Implications of these results to different scenario of particle physics were discussed.

- Molecular emission dynamics from a femtosecond filament-induced plasma plume have been investigated using femtosecond laser and imaging techniques. The evolution dynamics of molecular species such as CN and C_2 from these samples in ambient conditions are studied. It is found that the molecular signal intensity strongly depends on the sample properties and the position of the sample in the filament.

- Strong-field ionization of CH_3Cl using femtosecond laser pulses and a home-built COLTRIMS (Cold Target Recoil Ion Momentum Spectrometer) setup was studied. The H^+ yield showed an enhancement with increasing intensity and pulse duration. The H_2^+ and H_3^+ yield, on the other hand, increased with intensity but showed a reduction for stretched pulses.

- Isoprene and its oligomers are expected to be present, along with other complex organic molecules, in the diverse environments of the Interstellar Medium (ISM) and in our solar system. To assist the detection and understanding the chemistry of these molecules in those regions, the vacuum ultraviolet (VUV) photoabsorption studies of pure molecular ices of isoprene and a few of its oligomers: limonene, α-pinene and β-pinene in such extreme astrochemical conditions have been carried out. The first low temperature (10K) VUV spectra of isoprene and its oligomers is reported. Isoprene absorption at the longer wavelength is found to be red shifted in comparison with the gas phase by nearly $\sim$20 nm which is unique as molecules in general, are expected to be blue shifted with lowering temperatures. This unique property of isoprene along with distinctive absorption at longer wavelengths supports its candidature for detection on icy bodies.

- Theoretical estimation and Monte Carlo simulation of distribution in radiation doses received by quartz in a sedimentary matrix was done. The results were used to explain the distribution in doses obtained from single grains of quartz. A methodology was proposed to obtain ages from such distributions in doses.

- A technique was demonstrated to achieve an accuracy of measuring displacement of around 2 μm over a longitudinal range of more than 2 mm using a single beam line and only two quadrant detectors.

Collaborations of PRL with national/international institutions/ universities

Astronomy and Astrophysics

- **Area of Collaborations:** AstroSat-CZTI data analysis, For the proposed Daksha mission, Future Broad-band X-ray Astronomy mission, scientific analysis and interpretation of Chandrayaan-2/XSM observations, AstroSat data of Galactic X-ray Binaries and Active Galactic Nuclei (AGNs), scientific analysis and interpretation of results from other space-based X-ray observatories such as NICER, Swift, NuSTAR

- **Collaborating Institutes/Universities:** ARIES, Nainital, Academia Sinica Institute of Astronomy and Astrophysics, Taipei, Taiwan Asiago Astronomical Observatory, Italy Atomic Astrophysics group at DAMTP, Cambridge University, UK, Cambridge University, Cambridge, United Kingdom Central University of Himachal Pradesh, Dharamshala, . Centre for Space Research (CSR), South Africa Dayananda Sagar University, Bengaluru, . Deen Dayal Upadhyaya Gorakhpur University, Gorakhpur, . Delhi University, New Delhi. Heliophysics group,GSFC,NASA, IIA Banglore, IISER, Mohali, IISER, Tirupati, IISST, Thiruvantapuram, IIT Bombay,Mumbai, IIT, Indore, IIT, Kanpur, INAF Astronomical Observatory of Padova, Italy IUCAA,Pune, Institute of Applied Physics of the Russian Academy of Sciences, Nizhny Novgorod, Russia, Instituto Nacional de Astrofsica, ptica y Electrnica (INAOE),Tonantzintla, Mexico, Instituto de Radioastronoma y Astrofsica, UNAM, Morelia, Mexico, Keele University, United Kingdom Laboratoire d'Astrophysique de Marseille, Marseille, France, Maharashtra Udayagiri Mahavidyalaya, Udgir, Malaviya National Institute of Technology, Jaipur, Monterey Institute for Research in Astronomy, California, USA, NCRA-TIFR Pune, National Astronomical Research Institute of Thailand, Chiangmai, Thailand, National Space Institute,Technical University of Denmark, Denmark, Nicolaus Copernicus Astronomical Center, Polish Academy of Sciences, Poland, Nucleo de Astronoma de la Facultad de Ingeniera, Santiago, Chile, Presidency University, Kolkata, RRI, Bangalore, S.N. Bose National Centre for Basic Sciences, Kolkata, SAG-URSC, Bangalore, STIX group Solar Orbiter mission, ESA, Solar physics group,SAG-URSC, Bangalore, Swami Ramanand Teerth Marathwada University, Nanded, TIFR, Mumbai, Thringer Landessternwarte Tautenburg, Tautenburg, Germany, URSC, Bengaluru, Univ. Grenoble Alpes, CNRS, IPAG , Grenoble, France, Universita di Torino, Torino, Italy, University of California, San Diego, USA, University of Groningen, Netherlands, University of Leicester, United Kingdom, University of Minnesota, Minneapolis, United States, Warsaw University Astronomical Observatory, Poland, Wuhan University, China.

Solar Physics

- **Area of Collaborations:** Global Oscillation Network Group (GONG) Program, Automatic detection of solar features such as sunspots, filaments and extraction of their attributes, Investigation of Solar eruptions using Sub-photospheric Dynamics and Magnetic Field Measurements of Active Regions.
- **Collaborating Institutes/Universities:** Arecibo Observatory, University of Central Florida, Arecibo, USA C. U. Shah University, Wadhwan, Gujarat CCSU, Meerut Center for Space Plasma and Aeronomic Research, The University of Alabama in Huntsville, USA, Department of Physics and Astronomy, California State University, Northridge, USA IIA, Bengaluru Instituto Ricerche Solari Locarno (IRSOL), Switzerland Korea Astronomy and Space Science Institute, Daejeon, Republic of Korea Max Planck Institute for Solar System Research, Germany NCRA, Pune NIT, Calicut. National Solar Observatory, Boulder, CO, USA, Rosseland Centre for Solar Physics, University of Oslo, Norway SERF, Ahmedabad. Univ of Graz, Austria University of Science and Technology, Daejeon, Republic of Korea. VIT, Chennai.

Planetary Sciences

- **Area of Collaborations:** Planetary Atmospheres; Laboratory analyses of Shocked Meteorites; Laboratory analyses of Martian meteorite and Planetary Analogue materials, Impact crater studies of Moon using Ch2 data, Meteorite Study, Astrobiological and Geological investigations on Mars, Geological investigations of glacial landforms, active processes on Mars, Martian gullies, Plasma environment on Moon, Experimental Simulation of Lightning and Development of Lightning Detection Antenna for Future Planetary Missions, ChaSTE Payload Development for Chandrayaan-3 Lander, Numerical Simulations of the effect of lunar Landing on the surface and surrounding hardware structures, Planetary Remote Sensing.
- **Collaborating Institutes/Universities:** Laboratoire de Mtorologie Dynamique LMD, France, IIT Kharagpur, IIT (ISM), Dhanbad, Presidency University, Kolkata, School of Environmental Sciences, Jawaharlal Nehru University, New Delhi, IIST, Thiruvananthapuram, Kerala, Centre National de Recherche Scientifique, LPG, University of Nantes, France, Department of Physical Geography, Utrecht University, Netherlands, Dept. of Applied Sciences, Gauhati University, Guwahati, Space Physics Laboratory, Vikram Sarabhai Space Centre, Thiruvananthapuram, CHARUSAT, Changa, SPL-VSSC, Thiruvananthapuram, LPSC, Valiamala, Kerala, Banasthali Vidyapith, Rajasthan, Geological Survey of

India, Kolkata, Uzbekistan Academy of Science, Tashkent, Uzbekistan, Jawaharlal Nehru University, University of Nantes France.

Space and Atmospheric Sciences

- **Area of Collaborations:** Daytime upper atmospheric dynamics, equatorial dynamics, equatorial dynamics in the nighttime, Ionospheric physics, Substorm and Radiation belt physics, Prompt penetration electric field, Medium Scale Traveling Ionospheric Disturbances (MSTID) physics, Ring current asymmetry, Solar wind and Heliospheric physics, Low latitude ionospheric electrodynamics, Geomagnetic storm, Equatorial F-layer vertical drift, Equatorial electrojet, GAGAN SBAS TEC, Air quality assessment techniques, Air pollution from informal electronic waste recycling and allied sectors in India, Investigate relationship between PM (particulate matter) and ozone over different urban environment in India, Carbonaceous Aerosol Emissions, Source apportionment & Climate impacts (NCAP-COALESCE), Metals in coarse ambient aerosol as markers for source apportionment, Chemical composition and radiative forcing of atmospheric aerosols over the high altitude western Himalayas of India, Effect of lockdown on pollutant levels in the Delhi Megacity: Role of local emission sources and chemical lifetime, Balloon borne observations of tropopause aerosol layer, Optical experiments for upper atmospheric studies, Space weather studies, Geomagnetic storm effects, Mesosphere-Thermosphere-Ionosphere studies, Photochemical ageing of primary VOCs, Effect of the sea and land breeze circulations in the levels and compositions of VOCs in the coastal environments, Air chemistry in Himalayan valley, Middle atmospheric wave and Tidal dynamics, Long-term variability in the lower and middle atmosphere, Meteor studies, Cloud characteristics and the dynamics of atmospheric boundary layer over various locations in India, middle atmospheric temperature and ozone.
- **Collaborating Institutes/Universities:** Airport Authority of India, New Delhi; Andhra University, Visakhapatnam; British Antarctic Survey, Cambridge, UK; CSIR-NIO, Goa; Department of Atmospheric Science, Central University of Rajasthan, Ajmer; Dibrugarh University, Dibrugarh; Environment and Sustainability Department, CSIR- Institute of Minerals and Materials Technology, Bhubaneswar; Environmental Pollution Assessment Laboratory, Doon University, Dehradun; Federal University of Campina Grande, Campina Grande, Brazil; GFZ German Research Center for Geosciences, Germany; IIT-Kanpur, Delhi, Indore, Bombay and, Chennai; IIG Navi Mumbai; Instituto Nacional de Pesquisas Espaciais, Sao Paulo, Brazil; Jawaharlal Nehru Technological University, Hyderabad; Laboratory for Atmospheric and Space Physics, USA; Leibniz Institute of Atmospheric Physics, Kuhlungsborn, Germany; Los Alamos National Laboratory, USA; Multi institute field campaign with NASA Langley Research Center, Hampton, VA, USA as lead institute; Nagoya University, Japan; Northumbria University, UK; Osmania University, Hyderabad; SRM Institute of Science and Technology, Chennai; SPL-VSSC, Trivandrum; Universidade do Vale do Paraiba, Brazil; University of Mumbai; University of Saskatchewan, Canada; Utah State University, USA; Istituto Nazionale di Geofisica e Vulcanologia, Rome, Italy; Aryabhatta Research Institute of Observational Sciences, Nainital; SAC, Ahmedabad; IIRS, Dehradun; NE-SAC, Shillong; ISTRAC Bangalore center at Lucknow; NARL, Gadanki; NRSC, Hyderabad; University of La-reunion, Reunion, France; NCMRWF (MoES), Delhi; IMD, Delhi; IIA Bangalore Leh Campus, Leh; JNU, Delhi; Delhi University, Delhi; Ahmedabad University, Ahmedabad; PPN Postgraduate College, Chathrapati Sahu ji Maharaj University, Kanpur.

Geosciences

- **Area of Collaborations:** Sources of aerosols over Delhi, Carbonaceous aerosols over Hyderabad, Jammu, and Kolkata, Composition of UTLS aerosols, BATAL Campaign, CO_2 inventories in the Atmosphere; Basin-scale N_2 fixation, Riverine trace gas dynamics, Lacustrine palaeo-biogeochemistry; Cambrian Stratigraphy; Arabian Sea Ecology; Mangrove Carbon Stock; Composition and deposition fluxes over marine and coastal region Stratigraphy of Phosphorite; Geochemical analysis of ophiolites; Climate and Civilization, Development and applications of Non-traditional stable isotope proxies, Holocene Climate Reconstruction, Sea Level Change, Paleoenvironmental Studies; Indian Summer Monsoon impact on vegetation in the Himalaya; Archaeology and Harappan Civilization; Hydroclimatic variability during Holocene; Arabian Sea Salinity; Carbon fixation in the ocean and CO_2; Uncertainty in paleosalinity measurements; Upwelling in the Indian Ocean; Indian Ocean Circulation; Breccia in mud volcano; Deltaic Environmental Change; Meltwater and groundwater recharge; Sources of river flow in the cold arid desert; Groundwater hydrology; Geochemistry of groundwater.
- **Collaborating Institutes/Universities:** IIT Kanpur, Kanpur; Hyderabad University; Central University of Jammu; Bose Institute; CNRS, France; NASA, USA; Mediterranean Institute of Oceanography, Marseille, France; Ewha Womans University, South Korea; IISER, Mohali; Wadia Institute of Himalayan Geology, Dehradun; National Centre of Earth Science Studies, Trivandrum; National Centre for Coastal Research, Chennai; Centre for Marine Living Resources and Ecology, Cochin; National Institute of Oceanography, Goa; Pondicherry University (Andaman and Nicobar Islands); PDPU, Gandhinagar; University of Ahvaz, Iran; Manipur Central University, Manipur; Academia Sinica, Taiwan; NGRI, Hyderabad; University of California, Riverside, USA; National Taiwan Ocean University, Taiwan; IIT, BHU; Birbal Sahni Institute of Paleosciences, Lucknow; IISER, Kolkata; IIT, Kharagpur; Deccan College, Pune; IISc, Bangalore; GEOMAR Helmholtz Center for Ocean Research, Kiel, Germany; University of Arizona, USA; University of Tasmania, Australia; Banaras Hindu University, Varanasi; University of Calcutta, Kolkata; University of Kashmir, Srinagar; CWRDM, Kozhikode, Kerala.

Theoretical Physics

- **Area of Collaborations:** High Energy Physics, Neutrino Physics, DUNE, Measuring Higgs interaction at LHC, Constructing infra-red and collinear safe graph neural network, Anomaly detection with convolutional Graph Neural Networks, QCD precision calculation, Development of tools

and techniques for precision calculation, Scattering amplitude, Neutrino oscillation in curved spacetime, Leptogenesis in Grand Unified Theories, Condensed Matter Physics, Quark-Gluon Plasma.

- **Collaborating Institutes/Universities:** Imperial College London, UK; Campinas State University, Brazil; Assam Don Bosco University, Sonapur, Assam; Royal Inst Tech, Stockholm; Stockholm University, OKC; IISER, Kolkata; HRI, Allahabad; Institute for Particle Physics Phenomenology, Durham, United Kingdom; School of Physics and Astronomy, University of Glasgow, Glasgow, United Kingdom; University of Durham, UK; Freiburg University, Germany; Fermilab, USA; Indian Institute of Science Educationa dn Research, Mohali; National Institute of Technology, Tiruchirapalli; Harvard University, USA; Uppsala University, Sweden; Institute of Nuclear Physics, Krakow, Poland.

Atomic, Molecular and Optical Physics

- **Area of Collaboration:** Luminescence dating, Ultrafast Atomic and Molecular Physics, Photoionization of molecules of astrochemical relevance, Plasmonics, Light-matter interaction, Raman scattering, Quantum Optics, Nonlinear optics, and structured optical beams, Vacuum ultraviolet spectroscopy of astrochemical ices, hypervelocity impacts on solar system ices, ion irradiation of astrochemical ices, reflectance spectroscopy of astrochemical ices and astromaterials, far infrared spectroscopy of astrochemical ices, Atomic Physics.
- **Collaborating Institutes/Universities:** M. S. University, Baroda, IIT Gandhinagar, IITRAM Ahmedabad, NPL Delhi, Central University of Jharkhand, IIT Madras Chennai, Weizmann Institute of Science, Israel, TIFR Hyderabad, IISc Bangalore, IISER Kolkata, The Institute of Photonic Sciences Barcelona, University of the Witwatersrand, South Africa, Tecnolgico de Monterrey, Mexico, Ahmedabad University, Ahmedabad, RRCAT Indore, TIFR, Mumbai, and IUAC, New Delhi, University of Kent UK, Atomki Hungary, Aarhus University Denmark, National Synchrotron Radiation Research Center Taiwan, Planetary Spectroscopy Laboratory DLR-Berlin Germany, University of Grenoble Alpes France, Free Electron Lasers for Infrared eXperiments FELIX Nijmegen, Netherlands, Department of Physics, Guru Nanak Dev University, Amritsar 143005, Punjab, India; Department of Physics, IIT Delhi, India; Department of Physics & Center for Atomic, Molecular and Optical Sciences and Technologies, IIT Tirupati; Centre for Quantum Engineering, Research and Education, TCG CREST, Kolkata; Physics Department, Universidade Federal de Santa Catarina, Brazil; Department of Physics, University of Jyvskyl, Finland; Institute for Particle Physics and Astrophysics, Switzerland; Massachusetts Institute of Technology, USA; Department of Chemistry, Graduate School of Science, Hiroshima University, Japan; Center for Nuclear Study, The University of Tokyo, Japan; Institute of Physics, Graduate School of Arts and Sciences, The University of Tokyo, Japan; Institut de Physique de Nice, Universit Cte dAzur, CNRS, France; Beijing National Laboratory for Condensed Matter Physics, Institute of Physics, Chinese Academy of Sciences, Beijing, China; Fritz-Haber-Institut der Max-Planck-Gesellschaft, Berlin, Germany; Department of Physics, Pennsylvania State University University, USA.

Externally Funded Projects in PRL

Sr. No.	Funding agency	PI	Status	Duration	Broad Area
1.	DST	R P Singh	Active	2019-2022	Quantum I.T Photonic Devices
2.	DST/SERB	Brajesh Kumar	Active	2020-2022	Solar Dynamics and Space Weather
3.	Indo Uzbek SWC	Nandita Srivastava	Active	2021-2024	Space Weather
4.	Indo-U.S. Science and Technology Forum	Nandita Srivastava	Active	2021-2024	Space Weather
5.	DST CEFIPRA	Kuljeet Kaur Marhas	Active	2021-2024	Study of Chondrites
6.	Europlanet 2024	Kuljeet Kaur Marhas	Active	2021-2022	Study of Chondrites
7.	DST CEFIPRA	Neeraj Rastogi	Active	2021-2023	Exploring the Asian pollution signature
8.	ISRO-NASA (Co-PI)	Neeraj Rastogi	Active	2021-2024	Investigation of the Stratospheric Aerosols
9.	DST	Arvind Singh	Active	2022-2026	Biogeochemical Cycling
10.	DST CEFIPRA	Arvind Singh	Active	2020-2023	Dinitrogen Fixation in the Indian Ocean
11.	MoES	Arvind Singh	Active	2022-2025	Biogeochemical Processes in Marine Carbon
12.	CARS	Goutam K Samanta	Active	2021-2023	Photonics
13.	SERB (MATRICS)	Ketan Patel	Active	2022-2025	Baryogenesis in Grand Unified Theories
14.	DST (INSPIRE)	Ketan Patel	Active	2015-2021	Standard Model Flavour Puzzle in Higher Dimension
15.	Europlanet grant	B. Sivaraman	Active	2021-2022	Astrochemistry
16.	The Royal Soc. Int. Exchange Grant with Uni. of Kent, UK	B. Sivaraman	Active	2020-2022	Astro chemical ices
17.	Europlanet grant to visit DLR, Berlin (Germany)	B. Sivaraman	Active	2022	Spectroscopy of shock processed planetary analogues
18.	Beamtime grants, NSRRC, Taiwan	B. Sivaraman	Active	2021-2023	VUV Spectroscopy of Astrochemical ices

Sr. No.	Funding agency	PI	Status	Duration	Broad Area
19.	DAAD-Research Internships in Science and Engineering Worldwide (Germany)	B. Sivaraman	Active	2022	Research Internships in Science and Engineering
20.	Europlanet Transnational access grants [Fast track]	Surendra Vikram Singh	Active	2022	Identifying the biosignatures on icy moons

Field work/Campagins/Observations Conducted

Atmosphere

1. Effect on atmospheric constituents due to biomass combustion of aerosols, and sea and land breeze on the Volatile organic compounds were studied based on the gases collected from urban, and coastal areas different seasons.

2. Studies of carbonaceous aerosols and microplastics in different regions of the country were carried out wherein aerosol samples were collected in the field and their chemical properties analyzed in PRL.

Ocean-atmosphere interactions

3. Measurements of sulfur and volatile organic compound in marine air over the Bay of Bengal and Arabian Sea during post-monsoon season were conducted based on ship cruise campaign over Sagar Kanya.

4. An oceanographic expedition was conducted on board ORV Sagar Kanya (SK-374) in the Arabian Sea (during Oct. -Nov. 2021) for studies of distribution of trace elements, primary productivity, nitrogen fixation, cell abundances, variation in Redfield ratio, atmospheric inputs to surface ocean, marine black carbon, Be-10 distribution, radio carbon, paleooceanographic features, microplastics, and atmospheric volatile organic compounds.

5. A team led by PRL scientists and consisting of scientists from various institutes, such as, NCESS Trivandrum, BHU Varanasi, CUSAT Kochi, IISER Pune and Pondicherry University carried out experiments on board ORV Sagar Kanya in the Andaman Sea (during Sep. - Oct. 2021) to conduct studies of geological and ocean-atmospheric evolution of the sea, wherein data were collected from rock samples from the ocean water using dredge, sediment cores using gravity corer, water samples using CTD rosette sampler and several atmospheric trace gases and aerosol samples.

Marine Geochemistry

6. Studies of Petro-geochemistry and Sr-Nd isotopes of Padhar mafic-ultramafic complex from Betul Belt, Central India, were carried out wherein rock samples were collected.

Biogeochemical cycling

7. The collection of soil samples was done to estimate the carbon sequestration potential of mangrove soils of the Andaman Islands (March to April 2021).

8. Sampling along the Jhelum River for carbon and nitrogen assessment and estimating GHGs fluxes were carried out.

Solid Earth Geochemistry

9. Fieldworks were carried out in the Nubra valley, Northwestern Himalaya, to collect samples of eroded bedrocks from the Nubra valley and Gangalas valley to study the reconstruction of the chronology of quaternary glaciation.

Awards and Honors

Faculty

Anil Bhardwaj

1. Prof. M. G. K. Menon Lecture Award of the National Academy of Sciences, India, 2021
2. Elected Fellow, Astronautical Society of India, Bangalore, 2021
3. Elected Council Member, The National Academy of Sciences, India, Allahabad, 2022
4. Member of the Senate, National Institute of Design (Autonomous institution under the aegis of the Ministry of Commerce and Industry, Government of India), Ahmedabad, 2021-2023

S. A. Haider

5. Elected: Chair of Sub-Commission C3 in 44th COSPAR Assembly to be held in Athens, Greece during 16-24 July, 2022

Manmohan. M. Sarin

6. Co-chair, United Nations/GESAMP Working Group on "Climate Change and Greenhouse Gas Related Impacts on Contaminants in the Ocean" sponsored by IAEA (Monaco) as lead agency. GESAMP is an interagency advisory body of the United Nations.
7. Member, CSIR Expert/Monitoring Committee for research projects under 'Ecology, Environment, Earth, and Ocean Science & Water' (E3OW)
8. Member, Research Council of CSIR-National Institute of Oceanography, Goa.

Subhendra Mohanty

9. Elected as Fellow, The National Science Academy of India, 2021

Duggirala Pallamraju

10. Elected as Vice-Chair of Scientific Commission (SC-C) in COSPAR for the duration 2021-2024

S. Ramachandran

11. Associate Editor, Frontiers in Environmental Science
12. Top 2% of Scientists in the world in their respective fields (Atmospheric and Climate Science) published by Stanford University
13. Affiliate Scholar, Institute for Advanced Sustainability Studies, Potsdam, Germany

Nandita Srivastava

14. Nominated as National Coordinator, International Space Weather Initiative (ISWI)
15. Invited as an Associate Editor, on the Editorial Board of Stellar and Solar Physics (specialty section of Frontiers in Astronomy and Space Sciences and Frontiers in Physics)

Varun Sheel

16. Nominated as Member, Programme Interphase Committee of IPSTRA (IARSc Programme on Science, Technology, Research and Applications); IARSc-Institute for Advanced Research in Science, Bangalore, January 2021
17. Nominated Chairman, IPSTRA Panel for Planetary Sciences & Exploration, May 2021
18. Nominated as Member, Advisory Committee for PARAM SHAVAK HPC system at School of Engineering and Applied Science, Ahmedabad University, March 2021

Bijaya K. Sahoo

19. Listed among Top 2% of Scientists in the world in the respective research fields published in 2021 by Stanford university

Debabrata Banerjee

20. Member, Technical Advisory Committee for Science, Technology and Innovation (STI) Policy Funds, GUJCOST

Ravi Bhushan

21. Member, Research Advisory Council, Birbal Sahni Institute of Paleosciences (2021-2024).
22. Associate Editor, Radiocarbon Journal
23. Associate Editor, Frontiers in Marine Sciences (Marine Biogeochemistry section)
24. Member, Editorial Board: Journal of Paleosciences

Kuljeet Kaur Marhas

25. SERB-POWER Fellow, Science and Engineering Research Board-Promoting Opportunities for Women in Exploratory Research (DST), 2021
26. Continued Council member, (2^{nd} term) The Meteoritical society 2018-2022

Neeraj Rastogi

27. Editorial Advisory Board, Asian Journal of Atmospheric Environment, since 2020 to Present
28. Nodal Faculty for Gujarat, the National Clean Air Programme (NCAP), Ministry of Environment, Forest & Climate Change, since 2019 to Present
29. Member, Board of Studies Committee for the Space and Atmospheric Science, Centre for Space Science and Technology Education in Asia and the Pacific, (CSSTEAP), United Nations, since 2021.

Som Kumar Sharma

30. Associate Editor of the "Journal of Indian Society of Remote Sensing".

Goutam. K. Samanta

31. Served as the technical committee of the IEEE Photonics Conference (IPC) 2021 for last three years
32. Editorial Board Member, Journal of Optics, IOP
33. Guest Editor, Special Issue on Advances in Optics in India

Jayesh P. Pabari

34. Member of the Doctoral Research Committee for several disciplines at GTU, Ahmedabad
35. Member of the Board of Studies at CSPIT, CHARUSAT, Changa, Nadiad

Neeraj Srivastava

36. Member, IPSTRA Panel for Planetary Sciences & Exploration, May 2022

Arvind Singh

37. DST-Swarnajayanti Fellowship (2021).
38. Editor: JGR: Oceans (an AGU journal) (July 2021 - present)
39. Scientific Steering Committee member of SOLAS (Surface Ocean Lower Atmosphere Study) (2022-2024)
40. EGU's Blog of the Year (2021) Award

Narendra Ojha

41. Selected for the International Centre for Theoretical Physics (ICTP) Prize - 2021

Sourita Saha

42. First Prize in oral presentation at International Conference on Space Science and Technology (ICSST), Ahmedabad, 5-7 April 2021

Research Scholars

Nidhi Tripathi

43. Humboldt Research Fellowship by the Alexander von Humboldt Foundation, Germany

Yogesh

44. Early Career Scientist Award in the First Indian Space Weather Conference - 2022 (ISWC-2022) hosted by PRL during January 11-12, 2022

Bijoy Dalal

45. Best poster award for the poster titled "Comparison of suprathermal particles between the last two solar cycles: Insights" in Plenary Session 3: Solar and planetary sciences of the 21^{st} National Space Science Symposium, IISER Kolkata, 31 January to 4 February, 2022

Recognition, Best paper & Thesis awards

Faculty

Anil Bhardwaj

1. Member, Governing Council, Indian Institute Astrophysics, Bangalore
2. Member, Sunanda & Satimay Basu International Early Career Award Committee of American Geophysical Union, 2021
3. Member, Governing Council, Indian Institute of Geomagnetism, Mumbai
4. Member, AOGS Publication Committee, 2020-2022
5. Chairman, INSA-International Science Council Joint Committee for COSPAR, URSI and SCOSTEP
6. Member, National Advisory Committee for the IAGA-IASPEI Joint Scientific Assembly, 21-27 July, 2021, Hyderabad
7. President, Indian Committee of URSI-International Union of Radio Sciences, 2020-2023
8. Member, State Audit Advisory Board (SAAB) for Gujarat, 2020-2021
9. Member, Projects Advisory Committee (PAC) for the International Cooperation Programmes of DST in the area of Physics, Astrophysics and Laser. (Chairman: Prof. A. K. Raychaudhuri, SERB Distinguished Fellow at CSIR-CGCRI Kolkata and former Director SN Bose National Centre for Basic Sciences.), Feb. 2020-Present
10. Nominated as Member of Advisory Committee for the Ahmedabad / Gandhinagar City Knowledge and Innovation Cluster (CKIC), by Department of Science & Technology, Govt of Gujarat, April, 2021
11. Advisory Board Member of Book Series: Advances in Planetary Science, World Scientific, since 2015
12. Member, SS Bhatnagar Award Committee, 2021
13. Chairman, Search-cum-Selection Committee of Scientist/technologist for the position of Scientist 'H'/Outstanding Scientist, CSIR-Human Resource Development Group (CSIR-HRDG), CSIR, 2021 Oct.
14. Panel Member, US-India Space Exploration Dialogue on Space Radiation, online ARIES, Jan. 27, 2022
15. Member, Advisory Committee, Cosmic Ray Laboratory of TFIR, Ooty, 2022
16. Member, Indian Academy of Sciences Sectional Committee for Earth and Planetary Sciences, 20222024
17. Moderator and Panel Member, in Panel Discussion on "Journey of Indian Space Program - Past, Present, and Future", jointly organized by Regional Science Centre of National Council of Science Museum and Master Control Facility, ISRO, Bhopal, as part of World Space Week (Theme: Women in Space), October 8, 2021
18. Co-Convener, Session ST-22-PS03, "Future and Current Space Missions and Instrumentation for Space and Planetary Science", AOGS Virtual 18th Annual Meeting, Singapore, 1-6 August, 2021
19. Chief Guest at space-tech fest, "National Students' Space Challenge", Indian Institute of Technology, Kharagpur, Dec. 10, 2021
20. Chief Guest, AARUSH-21, the National Level Techno-Management fest of SRM-IST, Chennai, 16 Sept., 2021
21. Chief Guest, PhD Orientation Program, Indus University, Ahmedabad, 22 Jan., 2022
22. Guest of Honour, at National Seminar to celebrate National Science Day, National Institute of Homoeopathy, Kolkata, with Bharatiya Shikshan Mandal - Dakshinbanga Prant, 28 February, 2022
23. Guest of Honour, at Celebration of National Science Day, Indus University, Ahmedabad, 2 March, 2022
24. Chief Guest, Valedictory Ceremony, National Science Week, VIT, Bhopal, 3 March 2022

S. A. Haider

25. Extended J.C. Bose National Fellowship for 2^{nd} Term (2022-2026)
26. Main Scientific Organizer (MSO) of C3.2 event to be held in 44^{th} COSPAR Scientific Assembly, Athens, Greece during 16-24 July, 2022

Srubabati Goswami

27. Member,C11 commission of IUPAP (2022-2025)
28. Member, Programme Advisory Committee, Physics II, SERB, Since November 2021
29. Member of screening committee SUPRA, SERB, Since June 2021.
30. Co-opted member, Expert Committee on Physical and Mathematical Sciences, SERB, Since July 2021.
31. Member, Science Education panel, Indian Academy of Sciences , Since February 2022.
32. Member, Pottipuram Research Centre Management Board, DAE, (2021-)
33. Team leader, Country team of India, ICWIP 2021 held in Melbourne (online)
34. Guest Editor, Special issue of Physics News on Dr. Bibha Chowdhuri
35. Member, International Advisory Committee, TAUP 2021, held online in September 2021, Valencia

36. Member, International Advisory Committee, Neutrino 2022, to be held in May-June 2022, Seoul Korea
37. Member, International Advisory Committee, NOW 2022 , to be held in September 2022, Otranto, Italy
38. Member, National Advisory Committee, DAE-HEP symposium, to be held in December 2022, ISER, Mohali, India

Duggirala Pallamraju

39. Member, Local Organizing Committee for the IAGA-IASPEI meeting held during 21-27 August 2021.
40. Member, National Advisory Committee, One day National conference on, "Advances in Materials Science: Challenges and Opportunities (AMSCO-2021)", 21 September 2021, Department of Physics, Maharaja Krishnakumarsinhji Bhavnagar University, Gujarat, India.
41. Chair, Session 6: IDP, Upper Atmosphere and SW InteractionVenus Science Conference 2021, Online Conference 23 - 24 September 2021.
42. Chair, Scientific Organization Committee, First Indian Space Weather Conference 11 - 12 January 2022.
43. Member, Scientific Organizing Committee, SCOSTEP 15^{th} Quadrennial Solar-Terrestrial Physics Symposium (STP-15), February 21-25, 2022, Alibag, India.
44. Co-Chair, Local Organizing Committee, SCOSTEP 15^{th} Quadrennial Solar-Terrestrial Physics Symposium (STP-15), February 21-25, 2022, Alibag, India.
45. Convener, Session 3 on PRESTO Pillar 2: Space Weather and Atmosphere, in SCOSTEP 15^{th} Quadrennial Solar-Terrestrial Physics Symposium (STP-15), February 21-25, 2022, Alibag, India.
46. Chair for 4 scientific sessions, S3-PRESTO Pillar 2, Space Weather and Earth's Atmosphere, SCOSTEP 15^{th} Quadrennial Solar-Terrestrial Physics Symposium (STP-15), February 21-25, 2022, Alibag, India.
47. Chair for a scientific sessions, S7-New ground- and space-based initiatives for Solar Terrestrial Physics, SCOSTEP 15^{th} Quadrennial Solar-Terrestrial Physic Symposium (STP-15), February 21-25, 2022, Alibag, India.
48. Member, Scientific Organizing Committee, 16^{th} International Symposium on Equatorial Aeronomy (ISEA-16) to be held in Kyoto, Japan, September 12 - 16, 2022.
49. Expert Member, RESPOND Review Committee.

Nandita Srivastava

50. SOC member, First Indian Space Weather Conference, Physical Research Laboratory, Ahmedabad during January 11–12, 2022.
51. Co-chair, SOC, 40^{th} Meeting of the Astronomical Society of India, IIT Roorkee during March 25–29, 2022.
52. Member, SOC and Member LOC, 15^{th} Quadrennial Solar-Terrestrial Physics Symposium (STP-15), organized at IIG, Mumbai, February 21–25, 2022.
53. Session Chair in three sessions at 15^{th} Quadrennial Solar-Terrestrial Physics Symposium (STP-15), organized at IIG, Mumbai, February 21–25, 2022 (Online)
54. Member, Convener, COSPAR 2022 Session E2.2 on "Catalyzing progress in our understanding of the physics of solar and stellar eruptions via data-driven simulations" during June, 2022
55. Research paper co-authored in Palmerio et al. 2021 has been highlighted as press releases:
    - `https://blog.frontiersin.org/2021/07/21/astronomy-space-sciences-predicting-stealth-coronal-mass-ejections/`
    - `https://frontiers.altmetric.com/details/107638162/news`
    - `https://www.brusselstimes.com/belgium/178921/belgian-scientists-help-develop-new-method-to-predict-hidden-solar-storms/`
    - `https://www.issibern.ch/spotting-hard-to-detect-coronal-mass-ejections-from-the-sun/`
56. Research paper co-authored in Mishra et al. 2021 highlighted by Department of Science and Technology, as "Study probes how ejections from Sun's corona influence space weather predictions crucial for monitoring satellites" `https://pib.gov.in/PressReleasePage.aspx?PRID=175671`
57. Research paper co-authored in Mishra et al 2021 highlighted by Department of Science and Technology, as "Smaller solar storms in the last decade baffles scientists" `https://pib.gov.in/PressReleseDetail.aspx?PRID=1781703`
58. Ph.D. thesis examiner at Department of Astronomy, Astrophysics and Space Engineering, Indian Institute of Technology, Indore

Varun Sheel

59. Main convener of PS-04, Science and Exploration of Terrestrial Worlds, 18th Annual Meeting of the AOGS, 01-06 August 2021, Online
60. Convenor of the 3^{rd} Indian Planetary Science Conference (IPSC-2022), ONLINE, 14-16 March 2022, PRL, Ahmedabad
61. Co-convenor of "Impact of space weather on the Earths magnetosphere, ionosphere, and thermosphere", ISWC-2022, January 11-12, 2022
62. Chaired Sessions, ISWC-2022, Online, 11-12 January 2022
63. Chaired Session, Venus-SC-2021, Online, 23-24 September 2021
64. Chaired Session, MetMeSS-2021, Online, 29-30 November 2021
65. Member-SOC, of the First Indian Space Weather Conference (ISWC-2022), January 11-12, 2022
66. Member-SOC, Venus Science Conference (Venus-SC-2021), Organised Online by PRL, 23-24 September 2021
67. Member-SOC, Symposium on Meteoroids, Meteors and Meteorites: Messengers from Space (MetMeSS-2021), Organised Online by PRL, 29-30 November 2021

Santosh Vadawale

68. Invited to chair a session on Small Bodies, Exoplanets and Solar System Processes in the Indian Planetary Science Conference 2022 held during 14-16 March 2022.
69. Invited as National Convener for the Astronomy & Astrophysics session of the 21st National Space Science Symposium organized by IISER, Kolkata during 31st January to 4th February 2022.

Debabrata Banerjee

70. LOC Member, 3rd Indian Planetary Science Conference, PRL, Ahmedabad, 14-16, March, 2022

Dibyendu Chakrabarty

71. Member, COSPAR Task Group on International Geospace Systems Program (TGIGSP), 2021-2025.
72. Member, AGU SPA Fellows committee (SPAFC), 2022.
73. Member, National Advisory Committee, Plasma Science and Applications, 20-21 December, 2021 (PSA-2021), organized by the Department of Physics, Sardar Vallabhbhai National Institute of Technology, Surat. Also invited to be jury member for the ORAL session (session chair) and the Emerging Scientist award presentations.
74. Chair of one session in S3 PRESTO Pillar 2: Space weather and Earth's atmosphere, STP-15, 21-25 February, 2022.
75. Nominated by ISRO for the COSPAR-2022 Organizing Committee in Venus Science and Exploration category, 2021.
76. Member, Board of Studies of the Space and Atmospheric Science Course, Centre for Space Science and Technology Education in Asia and the Pacific (CSSTEAP), 2021.
77. Member, Scientific Organizing Committee (SOC), Workshop -1 (25 March 2022) on "Planetary space weather" in ASI-2022 meeting, 25-29 March 2022.
78. Member, RESPOND Review Committee.
79. Chair, Panel of Experts on Solar-Terrestrial Physics, IARSc Programme on Science, Technology, Research and Applications (IPSTRA), Institute for Advanced Research in Science (IARSc), 2021.
80. Co-author in the Best Poster Award (Comparison of suprathermal particles between the last two solar cycles: Insights) in the National Space Science Symposium, 2022 hosted by IISER-Kolkata during 31 January - 04 February, 2022.
81. Co-author in the Early career Scientist Award paper (Investigation on variation in solar wind Helium abundance during the last four solar cycles) in the First Indian Space Weather Conference - 2022 (ISWC-2022) hosted by PRL during January 11-12, 2022.
82. Member, Scientific Organizing Committee (SOC), Indian Space Weather Conference (ISWC-2022), PRL, 11-12 January, 2022. Also, convener of one session.
83. Member, Local Organizing Committee (LOC), 3rd Indian Planetary Science Conference (IPSC-2022), PRL, 2022.
84. Member, Scientific Organizing Committee (SOC), Venus Science Conference (Venus-SC-2021), PRL, 23-24 September, 2021. Also chaired one of the sessions on "Radio and Ionospheric Science".

S. Naik

85. Member, Science Advisory Committee: Aryabhatta Research Institute of Observational Sciences, Nainital.
86. Guest Editor of Journal of Astrophysics and Astronomy.
87. Member, National Organizing Committee : Conference on Astrophysical Jets and Observational Facilities : National Perspective : April 05-09, 2021, ARIES, Nainital
88. External examiner for Ph.D. thesis submitted to (i) Indian Institute of Technology (IIT), Kanpur, (ii) Pondicherry University, Puducherry, (iii) University of Delhi, New Delhi, (iv) North Bengal University, West Bengal, (v) Tata Institute of Fundamental Research, Mumbai.
89. Session Chair in the National Conference on Astrophysical Jets and Observational Facilities : National Perspective : April 05-09, 2021, ARIES, Nainital

Som Kumar Sharma

90. Member of Board of Studies (BoS) for the Space and Atmospheric Science (SAS) course, under CSSTEAP (affiliated to UN).
91. Member of Board of Studies (BoS) for the Satellite Meteorology (SATMET) course, under CSSTEAP (affiliated to UN).
92. Expert member of the Recruitment committee of Sci./Eng. -SC in DOS/ISRO centre.
93. Expert member of the review panel of the NSA postdoctoral Programme (NPP)-2021-2022.
94. Expert member of Departmental Promotion Committee (DPC) in DOS/ISRO centres.
95. On review panel of the Indo-French Centre for the Promotion of Advanced Research (IFCPAR/CEFIPRA) projects.
96. Elected as Joint Secretary of the Executive Council of the Indian Society of Remote Sensing.
97. On the review panel of the scientific projects submitted to various funding schemes/agencies such as, DST-INSPIRE, NPDF, MoES.
98. An Expert Member of the BEL (DRDO) Electronics vocabulary augmentation board under CSTT (Ministry of HRD).

Neeraj Rastogi

99. Session Chair,"Aerosols, Air Quality and Ocean-Atmosphere Coupling" in the national conference 'Frontiers in Geosciences Research Conference (FGRC)', online, at Ahmedabad, India, September 27-28, 2021.

Shashikiran Ganesh

100. External examiner for PhD thesis submitted to Sam Higginbottom University, Prayagraj, January 2022.

Bhuwan Joshi

101. Co-chair in PS-3 (Solar and planetary sciences) at 21st National Space Science Symposium-2022 (NSSS-2022), IISER-Kolkata during January 31–February 4, 2022

Brajesh Kumar

102. Judge for the best poster paper in "Sun and the Solar System" category during 40^{th} Annual Meeting of the Astronomical Society of India, IIT Roorkee, Roorkee, March 26–29, 2022

Jayesh P. Pabari

103. Convener, Venus Science Conference (Venus-SC-2021), PRL, Ahmedabad, 23-24 September 2021
104. LOC Member, 3^{rd} Indian Planetary Science Conference, PRL, Ahmedabad, 14-16, March, 2022
105. Life Member of Indian Society for Technical Education, New Delhi
106. Life Member of Indian Society of Remote Sensing, Dehradun

Bhalamurugan Sivaraman

107. Co-Chair, National Space Science Symposium-2022 hosted by IISER Kolkata, 31st Jan - 4th Feb, 2022 (online).

    2. Chair for the session Astrochemistry, Astrobiology and ISM, Indian Planetary science conference - 2022, PRL, Ahmedabad, 14th - 16th March, 2022 (online).

    3. Member, SSPO committee, ISRO for microgravity science experiments.

Kinsuk Acharyya

108. Session Chair, Venus Science Conference (Venus-SC-2021), 23-24 September 2021, PRL Ahmedabad
109. LOC Member, Indian Planetary Conference-2022. 14-16 March 2022, PRL, Ahmedabad

Neeraj Srivastava

110. Session Chair, IPSC 2022, 14-17 March 2022, PRL
111. Session Chair, Venus Science Conference, 2021, 23-24 Sept. 2021, PRL
112. Convener, BDR Committee, Planetary Rock Sampling Technology, MyVision 2030, ISRO

Amit Basu Sarbadhikari

113. Cover page appearance of the paper Evidence of regionally distributed tectono-volcanism in a floor fractured crater of North-Central Arabia Terra, Mars on Journal of Geophysical Research: Planets (https://doi.org/10.1002/jgre.21394)
114. Session Chair, Meteoroids, Meteors and Meteorites: Messengers from Space Symposium (MetMeSS-2021). 22-23 November 2021, PRL, Ahmedabad
115. Session Chair, Indian Planetary Science Conference (IPSC-2022). 14-16 March 2022, PRL, Ahmedabad
116. Section (Mineralogy, Petrology and Geochemistry of the surface of the Moon) Editor for Encyclopedia of Lunar Science, Springer Publishing

Veeresh Singh

117. Served as a reviewer for M.Phil. thesis submitted to Tata Institute of Fundamental Research (TIFR) Mumbai, Jan 2022.

Girjesh R. Gupta

118. Lead Investigator on "Waves and Oscillations in Sunspots with SUIT/Aditya-L1"
119. External Examiner for JRF and PDF reviews at JAP/IISc and ARIES, respectively.

Megha Bhatt

120. Session Chair, IPSC 2022, 14-17 March 2022, PRL
121. Session Chair, NSSS 2022, 31st Jan-4th Feb 2022, IISER Kolkata

K. Venkatesh

122. Convener, First Indian Space Weather Conference (ISWC-2022), PRL, Ahmedabad, 11-12 January 2022.

Atul Ashok Manke

123. Member, Local Organizing Committee (LOC), First Indian Space Weather Conference (ISWC-2022), PRL, 11-12 January, 2022. Also, designed and developed the web portal for first ISWC2022 (https://www.prl.res.in/iswc2022) having some key features like Online registration of participants, Abstract Submission and some MIS reports.

Research Scholars

Hema Kharayat

124. Second prize for oral presentation, International Conference on Space Science and Technology (ICSST-2021) organized by Space Education and Research Foundation (SERF), Ahmedabad during April 5–7, 2021.

Prabir K Mitra

125. Member of the team for summarizing the conference sessions during First Indian Space Weather Conference (ISWC-2022), Physical Research Laboratory, Ahmedabad, January 11–12, 2022.

Sana Ahmed

126. Won third prize for Young Scientist Award in MetMeSS-2021, 22-23 November 2021, PRL, Ahmedabad

Shanwlee Sow Mondal

127. Understanding the Particle Acceleration in ICME shocks Early Career Scientist Award, First Indian Space Weather Conference (ISWC- 2022), PRL, 11-12 January, 2022

Archita Rai

128. K.D. Abhyankar Best Thesis Presentation Honourable Mention Award for the PhD thesis presentation Infrared Astronomical Instrumentation and Polarisation Studies, at the 40th meeting of the Astronomical Society of India, March, 2022 held at IIT, Roorkee).

Human Resource Development

Human Resource Development at PRL PRL has a strong Human Resource Development (HRD) component with Doctoral, Post-Doctoral and Visiting Scientist programs. In addition, we have an Associate program for university teachers and project training for graduate and post graduate students in both science and engineering. PRL organizes project training as a part of the curriculum for students of undergraduate and post graduate levels from Science and Engineering disciplines. The purpose is to provide the students with an insight into current research activities being pursued at PRL which they can continue even after returning to their colleges. It is also aimed at motivating them to take up research in basic sciences in their higher studies and career. Brief details of scientific output and staff in numbers during the reporting year are provided here. This year due to the continued pandemic situations the training programmes were conducted only via virtual mode in view of the safety of students and in complete adherence with various advisories issued from time to time by the State and Central Governments.

Research Programmes

One of the important aims of the laboratory is to serve as a post-graduate and post-doctoral study centre in physics, earth & planetary sciences and chemistry to train research students in various aspects of experimental and theoretical physics. With this in view, PRL offers a graduate programme through Research Fellowship leading to Ph. D. degree. PRL provides opportunities for carrying out post-doctoral research. The strength of fellows under these programmes are presented in figure 1.

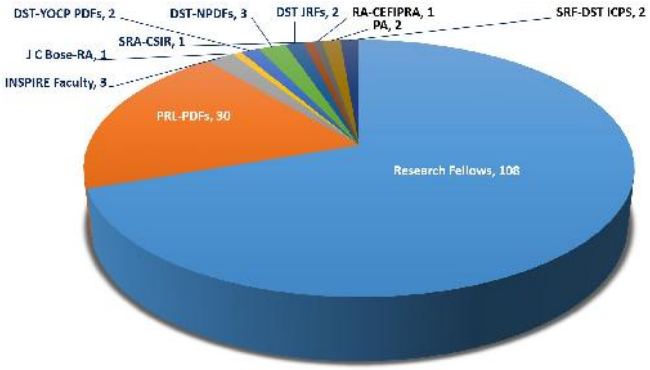

Figure 1: Research Programmes.

Research Programmes through Externally funded schemes

PRL encourages candidates with external funding from Government agencies such as DST, CSIR, NBHM, UGC, ISRO RESPOND, etc., to carry out their research in all campuses of PRL. Such candidates will be governed by fellowship rules of the concerned funding agencies as applicable from time to time. Such candidates will have an option to register for a Ph.D. degree in any of the institutes/universities with which PRL has an MoU with, subject to their fulfilling the required eligibility criteria and course work requirement of the concerned university/Institute. Following table summarize the ongoing externally funded projects in PRL and figure 1 give statistics of the Research Scholars/PDFs/RAs in PRL including the ones employed through the externally funded projects.

Training Opportunities

PRL provides project training in engineering disciplines like computer engineering, electronics & communication, instrumentation & control, information technology to graduate/post-graduate students. Details of the same are presented in figure 2.

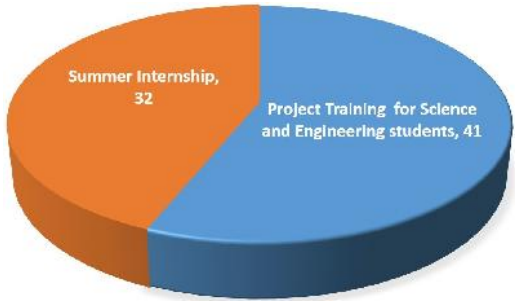

Figure 2: Internship Training Programmes.

PRL also offers training programmes in computers, electronics, library science, engineering and administrative services (Fig. 3).

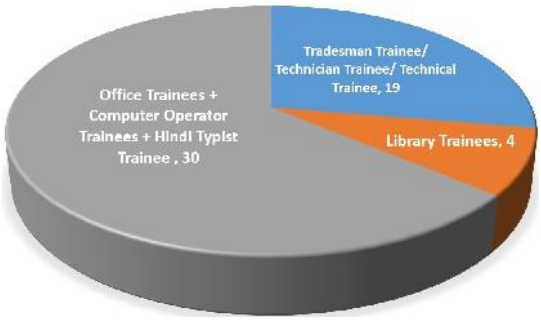

Figure 3: Training Programmes in technical and administrative areas.

Research Contributions

The research work carried out by PRL scientists are published in reputed and peer reviewed national and international journals. Few of our scientists are also invited to write review articles in the field of their specialization. Some of our scientists have also edited books.

Many of our scientists attend conferences and symposia at home and abroad where they present the results of their research investigations. Some of them are invited to present review talks. Few of them serve as chairpersons and Members of scientific committees for organizing national and International conferences and symposia. They are also invited to Convene and Chair sessions during symposia and meetings. The research output during the AY 2021-22 is shown in figure 4. All these activities were held in ONLINE mode only due to the prevailing COVID-19 situation.

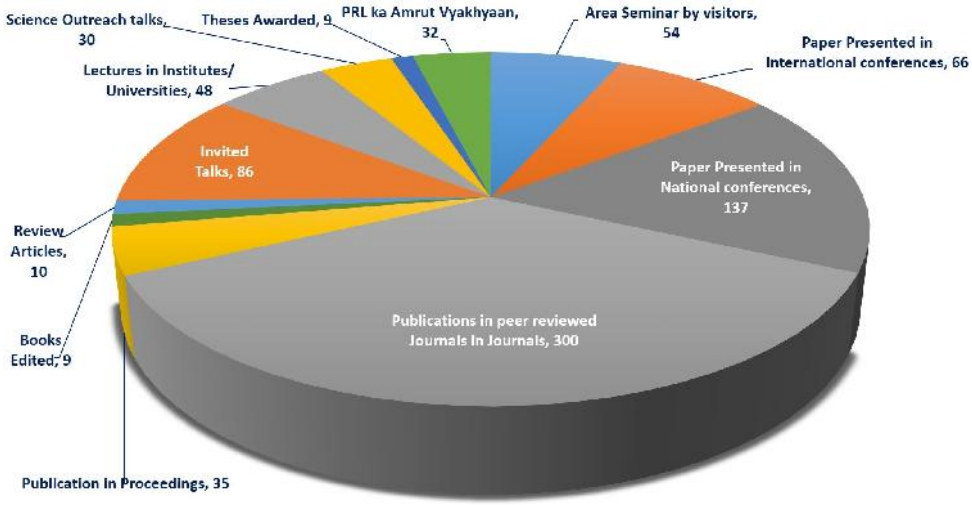

Figure 4: Research Contributions.

Administrative Support

Behind the scientific achievements of PRL is the able and efficient support given by the administrative and the technical staff. The administrative section of our laboratory continues to play an important role in providing an excellent management support to carry out our scientific activities. In addition, it also provides management support to the Solar Observatory at Udaipur and the Infrared Observatory al Mt. Abu. The staff structure of PRL is shown in figure 5.

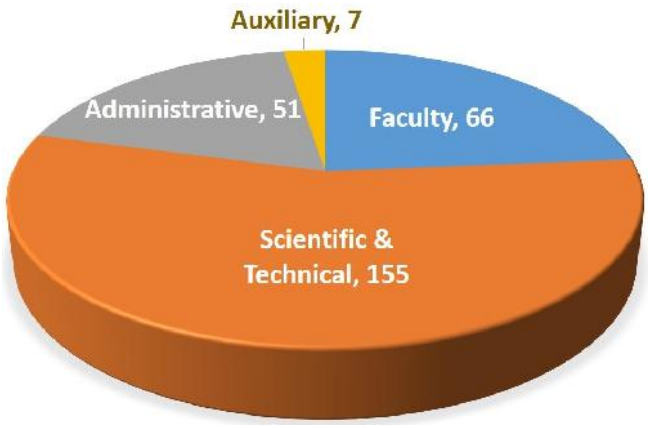

Figure 5: The distribution of PRL staff.

Status of Scheduled Caste/ Scheduled Tribe Personnel as on 31/03/2021

Centre/ Unit	Total Strength of Employees 2020-21	Strength of SC Employees	Strength of ST Employees	Strength of OBC Employees
PRL	279	12	07	53

Status of Differently Abled persons as on 31/03/2021

Centre/ Unit	Total Strength of Employees	Strength of Differently Abled Persons	Classification of employees with Disabilities			
			Deaf and Dumb	Blind	Partially Blind	Orthopedically Handicapped
PRL	279	5	1	0	0	4

Research Fellowship Programme and Pre-PhD courses

PRL offers Junior Research Fellowships (JRFs) leading to a Ph.D. degree in the broad areas of ongoing research activities in PRL. Since inception of PRL around 460 research scholars have obtained their Ph.D. degree. PRL alumni have played a key role in the development of institutions and programmes in India and abroad. The Indian Space Research Organization (ISRO) was nucleated in PRL in the early seventies and two of the past ISRO Chairmen, Prof. U.R. Rao and Prof. K. Kasturirangan - are distinguished alumni of PRL. After admission to PRL, each JRF needs to undergo a prescribed pre-Ph.D. course work prior to joining the research. In consideration of the requirements of (a) various Universities / IIT, where PRL research scholars register for their Ph.D. degree, and (b) University Grants Commission guidelines, two semesters of rigorous course work is offered to JRFs. In addition, JRFs are also required to do four projects as a part of their course work. In the year 2021-22, 19 new JRFs have joined PRL and 09 SRFs have been awarded Ph.D. degree. Following is the list of courses that were offered to the Junior Research Fellows of 2021 batch. Each course is of four credits and 40 hours of teaching.

Following is the list of courses offered to Junior Research Fellow of 2021 batch. Each course is of four credits and 40 hours of teaching.

Semester 1 courses

1. Fundamentals of Astronomy & Astrophysics [Instructors: Dr. Mudit Kumar Srivastava & Dr. Vishal Joshi]
2. Light-matter interaction [Instructors: Dr. R P Singh and Dr. Rajesh Kushwaha]
3. Stable Isotopes in Nature [Instructors: Dr. Amzad Hussain Laskar]
4. Isotope Geochemistry [Instructors: Dr. Vineet Goswami]
5. Planetary Atmospheres and Environment [Instructors: Dr. Jayesh Pabari, Dr. Durga Prasad & Prof. Varun Sheel]
6. Planetary Geology [Instructors: Dr. S. Vijayan & Dr. Neeraj Srivastava]
7. Physics of the Earths Lower and Middle Atmosphere [Instructors: Prof. S. Ramachandran & Prof. Som Kumar Sharma]
8. Physics and Diagnostics of Near Earth Space [Instructors: Dr. Ravindra Pratap Singh & Dr. Dibyendu Chakrabarty]
9. Basics of Solar Physics [Instructors: Dr. Brajesh Kumar]
10. Basic Cosmochemistry [Instructors: Prof. D. Banerjee & Dr. K. K. Marhas]
11. Planetary Geochemistry & Cosmochemistry, [Instructors: Prof. Kuljeet Marhas & Dr. Amit Basu Sarbadhikari]

Semester 2 courses

12. Planetary Remote Sensing Geology [Instructors: Dr. Neeraj Srivastava & Mr. Rishitosh Sinha]
13. Palaeoclimate and Paleoceanography [Instructors: Prof. MG Yadava & Prof. Ravi Bhushan]
14. Solid Earth and Geochemical Methods [Instructors: Prof. Anil D. Shukla]
15. Surface Ocean and Lower Atmosphere Studies (SOLAS) [Instructors: Dr. A K Sudheer]
16. Instrumentation and Data Handling in Geosciences Research [Instructors: Mr. Akash Ganguly & Mr. A. Shivam]
17. Advanced Electrodynamics [Instructors: Prof. Srubabati Goswami]
18. Introduction to Quantum Field Theory [Instructors: Dr. Satyajit Seth]
19. Statistical Mechanics [Instructors: Prof. Navinder Singh]
20. General Relativity and Cosmology [Instructors: Dr. Ketan M. Patel]
21. Solar internal structure, dynamics and Magnetohydrodynamics [Instructors: Dr. K. Venkatesh]
22. The active Sun and space weather [Instructors: Dr. T. A. Rajesh & Dr. H. Gadhavi]
23. Aerosols, trace gases, and radiative effects [Instructors: Prof. L. K. Sahu & Prof. S. Ramachandran]
24. Dynamical, chemical, and coupling processes in the Earth's atmosphere [Instructors: Dr. A. Guharay & Dr. S. K. Sharma]
25. Star formation and Star Clusters [Instructors: Dr. Lokesh Dewangan & Dr. Manash R. Samal]
26. Galactic and Extragalactic Astronomy [Instructors: Dr. S. Naik & Dr. Veeresh Singh]
27. Astronomical Instrumentation [Instructors: Dr. Santosh Vadawale & Dr. Mudit Srivastava]
28. Solar internal structure, dynamics and Magnetohydrodynamics [Instructors: Dr. Brajesh Kumar & Prof. Ramit Bhattacharyya]

29. The active Sun and space weather [Instructors: Dr. Bhuwan Joshi & Prof. Nandita Srivastava]
30. UV and X-ray Sun [Instructors: Dr. Girjesh Gupta & Dr. A. Raja Bayanna]
31. Instrumentation [Instructors: Dr. Rohan Eugene Louis]
32. Quantum Optics and Nanophotonics [Instructors: Dr. Shashi Prabhakar Dr Satyendra Nath Gupta]
33. Atomic and Molecular Spectroscopy [Instructors: Dr. Rajesh Kushawaha & Dr. Bhalamurugan Sivaraman]

List of projects done by JRF of 2021 batch are as follows:

Chahat Kaushik

1. "Generation and Characterization of Orbital Angular Momentum States of Light", Semester 1 project, from 03 August 2021 to 23 Nov 2021, [Supervisior: Prof. R P Singh, Division: Atomic, Molecular and Optical Physics].
2. "Supercontinuum Generation of structured beam", Semester 1 project, from 04 January 2022 to 25 April 2022, [Supervisior: Dr. G K Samanta, Division: Deanś Office].

Akash Sundriyal

3. "Pre-Main Sequence Evolution of Young Stellar Objects in the Cepheus Cloud", Semester 1 project, from 03 August 2021 to 23 Nov 2021, [Supervisior: Dr. Manash Samal, Division: Astronomy and Astrophysics].
4. "Cataclysmic Variable RW Tri and its Optical Spectroscopic Data Reduction", Semester 2 project, from 04 January 2022 to 25 April 2022, [Supervisior: Dr. Vishal Joshi, Division: Astronomy and Astrophysics].

Varsha M Nair

5. "Shocked Feldspar and Maskelynites from Lonar Impact Crater, India and Martian Shergottite: Insights into Formation Process and Comparative Planetology", Semester 1 project, from 03 August 2021 to 23 Nov 2021, [Supervisior: Dr. Dwijesh Ray, Division: Planetary Sciences].
6. "Study on the geological features in juvantae dorsa region, Mars", Semester 2 project, from 04 January 2022 to 25 April 2022, [Supervisior: Dr. Vijayan S, Division: Planetary Sciences].

Narendranath Layek

7. "Understanding the accretion dynamics of x-ray banaries", Semester 1 project, from 03 August 2021 to 23 Nov 2021, [Supervisior: Prof. Sachindra Naik, Division: Astronomy and Astrophysics].
8. "The Standard Model of Disc Accretion", Semester 2 project, from 04 January 2022 to 25 April 2022, [Supervisior: Prof. Sachindra Naik, Division: Astronomy and Astrophysics].

Harithasree S

9. "Analysis of Cloud Base Height measurements from Ceilometer CL31 over Ahmedabad", Semester 1 project, from 03 August 2021 to 23 Nov 2021, [Supervisior: Dr. Som Kumar Sharma, Division: Space, Atmospheric, Molecular and Laser Physics].
10. "Assessment of aerosols and associated radiative effectsfollowing a major dust storm in the Middle East usingground-based observations: Implications", Semester 2 project, from 04 January 2022 to 25 April 2022, [Supervisior: Prof. S Ramachandran, Division: Space, Atmospheric, Molecular and Laser Physics].

Vaishnavi Parihar

11. "Elemental behaviour within Suptal Lake Sediments, Chamoli, Uttrakhand", Semester 1 project, from 03 August 2021 to 23 Nov 2021, [Supervisior: Prof. A D Shukla, Division: Geosciences].

Rahul Kumar Agarwal

12. "Assessment of black carbon in Mangrove sediments of Andaman and Nicobar Islands.", Semester 1 project, from 03 August 2021 to 23 Nov 2021, [Supervisior: Prof. Sanjeev Kumar, Division: Geosciences].
13. "Radiocarbon and stable carbon isotope ratio measurements in dissolved inorganic carbon in groundwater: implications to groundwater dynamics", Semester 2 project, from 04 January 2022 to 25 April 2022, [Supervisior: Dr. Amzad Hussain Laskar, Division: Geosciences].

Shreya Mehta

14. "87Sr/86Sr and Sr concentrations in the catchment of west-flowing Ambika River basin draining the Deccan Traps: Implication to Silicate erosion rate and CO2 drawdown", Semester 1 project, from 03 August 2021 to 23 Nov 2021, [Supervisior: Dr. Vinit Goswami, Division: Geosciences].
15. "Radiocarbon and stable isotope ratios in two speleothems from Kashmir for dating and paleomonsoon reconstruction", Semester 2 project, from 04 January 2022 to 25 April 2022, [Supervisior: Dr. Amzad Hussain Laskar, Division: Geosciences].

Indrajit Kabiraj

16. "Generation of Spatial Structured Optical Beams", Semester 1 project, from 03 August 2021 to 23 Nov 2021, [Supervisior: Dr. G K Samanta, Division: Deanś Office].
17. "A Study on Femtosecond Laser Filamentation", Semester 2 project, from 04 January 2022 to 25 April 2022, [Supervisior: Dr. Rajesh Kumar Kushwaha, Division: Atomic, Molecular and Optical Physics].

Kiran

18. “Increasing Trends of Heatwave over India”, Semester 1 project, from 03 August 2021 to 23 Nov 2021, [Supervisior: Dr. Narendra Ojha, Division: Space, Atmospheric, Molecular and Laser Physics].
19. “Gas Chromatography and its application”, Semester 1 project, from 03 August 2021 to 23 Nov 2021, [Supervisior: Prof. L K Sahoo, Division: Space, Atmospheric, Molecular and Laser Physics].

Godly Ahuja

20. “Study of embedded filaments at Galactic longitude of [224°, 233°]”, Semester 1 project, from 03 August 2021 to 23 Nov 2021, [Supervisior: Dr. Lokesh Kumar Dewangan, Division: Deanś Office].
21. “A Toy - Model of the Solar Surface Flux Transport”, Semester 2 project, from 03 August 2021 to 23 Nov 2021, [Supervisior: Dr. Aveek Sarkar, Division: Astronomy and Astrophysics].

Sandeep Kumar Dubey

22. “Sheath accumulation propagation model of CME”, Semester 1 project, from 03 August 2021 to 23 Nov 2021, [Supervisior: Prof. Nandita Srivastava, Division: Solar Physics].
23. “Mast data reduction”, Semester 2 project, from 04 January 2022 to 25 April 2022, [Supervisior: Prof. Shibu K Mathew, Division: Deanś Office].

Ravi Chaurasiya

24. “Analysis of super-penumbral fibriuls in sunspots using mast observations”, Semester 1 project, from 03 August 2021 to 23 Nov 2021, [Supervisior: Dr. Rohan Eugene louis, Division: Deanś Office].
25. “Comparing the parameters of ICMEs for solar cycle-23 & 24”, Semester 2 project, from 04 January 2022 to 25 April 2022, [Supervisior: Prof. Nandita Srivastava, Division: Solar Physics].

Arijit Maiti

26. “Study of metallicity of Milky Way stars using APOGEE survey”, Semester 2 project, from 04 January 2022 to 25 April 2022, [Supervisior: Dr. Shashi Kiran Ganesh, Division: Astronomy and Astrophysics].

Dhiman Biswas

27. “A brief review of the state of the art experiments to build quantum random number generator”, Semester 2 project, from 04 January 2022 to 25 April 2022, [Supervisior: Dr. G K Samanta, Division: Atomic, Molecular and Optical Physics].

Neeraj Kumar Tiwari

28. “Solar Wind Power Spectrum”, Semester 1 project, from 04 January 2022 to 25 April 2022, [Supervisior: Dr. Aveek Sarkar, Division: Astronomy and Astrophysics].
29. “SED Modeling of a Star: Deriving the Spectral type”, Semester 2 project, from 04 January 2022 to 25 April 2022, [Supervisior: Dr. Vishal Joshi, Division: Astronomy and Astrophysics].

Ashis Kumar Mandal

30. “Flickering study of a symbiotic system using UVIT”, Semester 2 project, from 04 January 2022 to 25 April 2022, [Supervisior: Mudit Kumar Srivastava, Division: Astronomy and Astrophysics].

Joel M Sunil

31. “Helicity sorter for the OAM states of light”, Semester 2 project, from 04 January 2022 to 25 April 2022, [Supervisior: Prof. R P Singh, Division: Atomic, Molecular and Optical Physics].
32. “Helicity sorter for the OAM states of light”, Semester 2 project, from 04 January 2022 to 25 April 2022, [Supervisior: Dr. Shashi Prabhakar, Division: Atomic, Molecular and Optical Physics].

Writasree

33. “Dark Matter Detection and Phenomenology”, Semester 2 project, from 03 August 2021 to 23 Nov 2021, [Supervisior: Prof. Partha Konar, Division: Theoretical Physics].

Arjun Krishnan U M

34. “Continuous variable quantum key distribution with Gaussian modulation”, Semester 2 project, from 04 January 2022 to 25 April 2022, [Supervisior: Dr. Mudit K Srivastava, Division: Astronomy and Astrophysics].

Dipanshu Srivastava

35. “Primordial Black Holes as Dark Matter Candidate”, Semester 2 project, from 03 August 2021 to 23 Nov 2021, [Supervisior: Prof. Partha Konar, Division: Theoretical Physics].

Ph.D. Awarded

[PRL students/project associates/employees]

Subir Mandal

1. “Daytime thermospheric neutral wave dynamics over low- and equatorial-latitudes”, IIT Gandhinagar, 01-06-2021, [Supervisor: Duggirala Pallamraju].

Rahul Kumar Kushwaha

2. “Infrared and Vacuum Ultraviolet Spectroscopy of Interstellar Icy Mantles”, Mohanlal Sukhadia University, Udaipur, 06-07-2021, [Supervisor: Janardhan Padmanabhan & Bhalamurugan Sivaraman].

Archita Rai

3. “Infrared Astronomical Instrumentation and Polarisation Studies”, Indian Institute of Technology, Gandhinagar, 29-08-2021, [Supervisor: Shashikiran Ganesh].

Harish

4. “Insights into the Geological History of Mars through Impact Craters”, IIT Gandhinagar, 20-09-2021, [Supervisor: S. Vijayan].

Sushree S. Nayak

5. “Magnetic field and Electric current in the Solar atmosphere”, IIT Gandhinagar, Gandhinagar, 22-09-2021, [Supervisor: Ramit Bhattacharyya].

Priyank Parashari

6. “Probing New Physics with Cosmological Observations”, Indian Institute of Technology, Gandhinagar, 12-10-2021, [Supervisor: Subhendra Mohanty].

Sandeep K. Rout

7. “Various manifestations of accretion onto stellar-mass black holes”, Indian Institute of Technology, Gandhinagar, 21-10-2021, [Supervisor: Santosh Vadawale].

Surendra Vikram Singh

8. “An experimental investigation of biomolecules under impact induced shock”, IIT Gandhinagar, 29-11-2021, [Supervisor: Bhalamurugan Sivaraman].

Deepika Sahoo

9. “Non-Redfieldian C:N:P ratios in the inorganic and organic pools of the northern Indian Ocean”, IIT - Gandhinagar, 31-01-2022, [Supervisor: Arvind Singh].

PRL ka Amrut Vyakhyaan

1. **Harold C. Connolly Jr.**
   Rowan University, NJ, USA
   OSIRIS-REX: Sample Science And The Geologic Context For The Return Regolith From Active Asteroid Bennu
   04 August 2021

2. **S. Somanath**
   Vikram Sarabhai Space Centre (VSSC), ISRO, Thiruvananthapuram
   Reaching the Sky : Indian Launch Vehicles
   11 August 2021

3. **Prabal K Maiti**
   Indian Institute of Science, Bangalore
   Confined Water: Many Surprises
   18 August 2021

4. **Chandrima Shaha**
   Indian National Science Academy, New Delhi
   Our immunity and emerging diseases
   25 August 2021

5. **P P Mujumdar**
   Indian Institute of Science, Bangalore
   Floods in a Changing Climate
   01 September 2021

6. **Alok Dhawan**
   Centre of Bio-Medical Research, Lucknow, India
   Safety of nanomaterials: A journey from research to policy
   08 September 2021

7. **Purnima Jalihal**
   National Institute of Ocean Technology, Chennai, India.
   Green Energy and Clean Water from the Oceans
   15 September 2021

8. **Valentin Martinez Pillet**
   National Solar Observatory (NSO) Boulder, USA.
   Prospects in Solar Physics for the Next Decade: a Multimessenger Era
   22 September 2021

9. **Kazuo Shiokawa**
   Institute for Space-Earth Environmental Research, Nagoya University, Japan.
   Dynamics of aurora and airglow in the upper atmosphere and space around the Earth
   29 September 2021

10. **Madhulika Guhathakurta**
    NASA, USA
    A Song for the SOL
    06 October 2021

11. **Ralph Lorenz**
    Johns Hopkins Applied Physics Lab, Maryland, USA.
    The Mystery of Venus Lightning
    13 October 2021

12. **M. Rajeevan**
    Ministry of Earth Sciences, Govt. of India
    Earth System Science for Socio-Economic Benefits
    20 October 2021

13. **Jonathan Tennyson**
    University College London (UCL), Chief Scientist, Quantemol Ltd, UCL.
    What are exoplanets made of? Molecular line lists to aid the characterisation of exoplanets
    27 October 2021

14. **V. Adimurthy**
    Vikram Sarabhai Space Centre, Thiruvananthapuram
    Opportunities and Challenges beyond Mangalyaan in Interplanetary Missions and Planetary Protection Measures
    03 November 2021

15. **Sanjay Lalbhai**
    Chairman and Managing Director, Arvind Ltd., Ahmedabad
    Business Journey and Learnings on the Way
    10 November 2021

    1st Dr. Arvind Bhatnagar Memorial Lecture

16. **Sami K. Solanki**
    Max Planck Institute for Solar System Research, MPS, Gttingen, Germany.
    The Sun's Magnetic Field and Global Climate Change
    17 November 2021

17. **Andrew Bowie**
    Institute for Marine and Antarctic Studies (IMAS), University of Tasmania, Hobart, Tasmania
    GEOTRACES and Southern Ocean iron biogeochemistry - where have we come?
    24 November 2021

18. **Paul Ho**
    James Clerk Maxwell Telescope, East Asia Observatory, Mauna Kea Hawaii, USA
    The Development of the East Asian Observatory
    01 December 2021

19. **Rohini Godbole**
Indian Institute of Science, Bangalore.
Shedding light on the Dark Matter in the Universe
08 December 2021

20. **Sreerup Raychaudhuri**
Tata Institute of Fundamental Research, Mumbai
Future Colliders
15 December 2021

21. **Dipankar Saha**
Chair Professor, Manav Rachna International Institute for Research and Studies, Faridabad. Former Member, CGWB
Sustainable groundwater resource use in India- Achievable or a mirage?
22 December 2021

22. **V. Chandrasekhar**
Indian Institute of Technology Kanpur, Kanpur
From P. C. Ray to the present: Chemistry in Action
29 December 2021

23. **Sun Kwok**
The University of Hong Kong, Hong Kong and University of British Columbia, Vancouver, Canada
Organic Matter in the Universe
05 January 2022

24. **Daniel N. Baker**
aboratory for Atmospheric and Space Physics, University of Colorado, Boulder, Colorado
Societal and Economic Impacts of Space Weather
12 January 2022

25. **Girish S. Agarwal**
Institute for Quantum Science and Engineering, Departments of Biological and Agricultural Engineering, and Physics and Astronomy, Texas A&M University, USA
Squeezed light from abstraction to real-life applications: sensing and imaging well beyond standard quantum limit
19 January 2022

26. **Brigadier (Retd.) P. Ganesham**
President, Innovation Diffusion Center, Palle Srujana, Sainikpuri, Secunderabad
Grassroots Innovations: Mining the Minds of Masses
26 January 2022

27. **Derek Vance**
Department of Earth Science, ETH Zrich, Switzerland
The oceanic geochemistry of the transition metals: tools to quantify the history of the oxygenation of the surface Earth
02 February 2022

2nd Dr. Bibha Chowdhuri Memorial Lecture

28. **Gagandeep Kang**
Division of Gastrointestinal Sciences, Christian Medical College, Vellore, India
Prevention is Health, and Wealth
09 February 2022

29. **V. R. Lalithambika**
Indian Space Research Organization, Bangalore
Human Space Program - challenges and strategies
16 February 2022

30. **Mallika Sarabhai**
Darpana Academy of Performing Arts, Ahmedabad
Realising A Dream: Vikram Sarabhai and Television for Change
23 February 2022

31. **Annapurni Subramaniam**
Indian Institute of Astrophysics, Bangalore
Ultra-violet Imaging Telescope and beyond
02 March 2022

32. **Ashwini Nachappa**
Olympian, Arjuna Awardee Founder, Ashwini's Sports Foundation Managing Trustee, KALS
Sport - An Integral component of Nation building
09 March 2022

33. **Uta Grothkopf**
Head, Library and Information Centre ESO - European Southern Observatory, Germany
Open Access in Astronomy
16 March 2022

34. **Bedangadas Mohanty**
National Institute of Science Education and Research (NISER), Bhubaneswar
Quark-Gluon Plasma: the perfect and most vortical fluid
23 March 2022

35. **Subir Sachdev**
Harvard University, Cambridge
Quantum entanglement at all distances
30 March 2022

Conference/Symposium/Workshop organized by PRL

Solar Physics

1. "One day workshop on "Long-term Study of the Solar Activity"", during 40^{th} Astronomical Society of India (ASI) Meeting (ASI-2022) at IIT Roorkee jointly with members of IIT BHU and ARIES on March 25, 2022.

Planetary Sciences

2. "Venus Science Conference (Venus-SC-2021)", PRL, Ahmedabad, 23-24 September, 2021.
3. "Meteoroids, Meteors and Meteorites: Messengers from Space Symposium (MetMeSS-2021)", PRL, Ahmedabad, 22-23 November 2021.
4. "3^{rd} Indian Planetary Science Conference (IPSC-2022)", PRL, Ahmedabad, 14-16 March 2022.

Space and Atmospheric Sciences

5. "First Indian Space Weather Conference (ISWC-2022)", PRL, 11-12 January 2022.

Geosciences

6. "The first conference of the series 'Frontiers in Geosciences Research Conference' (FGRC-2021)", Spetember 27-28, 2021.
7. "International Faculty Development Program" on 'Emerging Trends in Nano Technology (ETNT-2021)' in association with Vishnu Institute of Technology, Bhimavaram, November 9-13, 2021.

Theoretical Physics

8. "PRL conference in Condensed Matter Physics (PRLCCMP-2021)", At PRL, Aug 16–18, 2021.
9. "Young Physicists Meet 2022", Physical Research Laboratory, Feb., 23-25, 2022.

Atomic, Molecular and Optical Physics

10. "SCOP-the Students conference in optics and photonics", PRL Ahmedabad, 24-26 November 2021.

4^{th} PRL-IAPT Dr. Vikram Sarabhai Lecture-2022

11. Abhijit Chakraborty, Physical Research Laboratory, Ahmedabad
    "Challenges and limitations of detecting exoplanets"
    11 February 2022

Invited Talks at Conference / Symposia / Workshops

Astronomy and Astrophysics

Abhijit Chakraborty

1. "The PRL 2.5m telescope", Astrophysical jets and observational facilities: National perspective, ARIES, Nainital, 05-09 April 2021.

Santosh Vadawale

2. "Galactic black hole binaries: An observational perspective", 40th Annual Meeting of the Astronomical Society of India, IIT Roorkee and ARIES Nainital, 25-29 March, 2022.
3. "Hard X-ray Polarimetry with AstroSat-CZTI and Beyond", 2nd Indo-China work- shop on High Energy Astrophysics, China, 6 10 December, 2021.
4. "Chandrayaan-2 XSM Data Analysis and Results", Lunar Science Workshop, ISRO HQ, Banglore, 6 7 September, 2021.
5. "AstroSat-CZTI", IUCAA Advanced AstroSat Data Analysis Workshop, Organized by IRSO and IUCAA, 21 30 June, 2021.

Lokesh Kumar Dewangan

6. "How do massive O-type stars form", 40th Annual Meeting of the Astronomical Society of India (ASI), IIT Roorkee, 26 March, 2022.

Vishal Joshi

7. "A glimpse of Astrophysical research to participants of Gujarat Vigyan Sammelan (GVS-2022)", Indian Institute of Teacher Education (IITE), Gandhinagar, Gandhinagar, Gujarat, 2 February, 2022.

Shanwlee Sow Mondal

8. "MHD-PIC: A novel approach to study particle acceleration in CME shocks", PLUTO Symposimum, Universita di Torino, Torino, Italy, 28-29 June, 2021.

Solar Physics

Nandita Srivastava

9. "Observing solar activity from ground and space", National Space Science Symposium-2022 (NSSS-2022), IISER, Kolkata, 31 Jan – 4 Feb, 2022.
10. "ISRO-RESPOND basket projects of Space Sciences", ISRO-Academia Day, ISRO, Bangalore, 15 Mar, 2022.

Ramit Bhattacharyya

11. "Simulating source region dynamics of solar coronal transients: progress and challenges", 40^{th} Astronomical Society of India (ASI) Meeting (ASI-2022), IIT Roorkee, Roorkee, 25–29 Mar, 2022.

Brajesh Kumar

12. "Can major flares excite global waves in the Sun?", International Conference on Space Science and Technology, Space Education and Research Foundation, Ahmedabad, 5–7 Apr, 2021.

Bhuwan Joshi

13. "Application of 2D and 3D magnetic reconnection in solar flares: A perspective", 36^{th} meeting of Plasma Science Society of India (PSSI), Birla Institute of Technology, Mesra, Jaipur Campus, 13–15 Dec, 2021.
14. "Solar Source Regions of Space Weather Events", The International Space Weather Initiative (ISWI) Workshop on Space Weather: Science and Applications, The United Nations office for Outer Space affairs and the Vikram Sarabhai Space Centre (ISRO/VSSC), 2–3 Nov, 2021.
15. "Multi-wavelength view of solar activity: Space and ground-based observations", Faculty Development Program (e-FDP) on Theoretical and Practical Aspects in Applied Physics (TAPAAP-2021), Radha Govind Group of Institutions, Meerut, U.P., Sponsored by AICTE, New Delhi, 24–28 Sept, 2021.
16. "Observations of solar transients and their signatures at low-frequency radio emission by Udaipur-CALLISTO", International Conference on Space Science and Technology, Space Education and Research Foundation, Ahmedabad, 5–7 Apr, 2021.

Planetary Sciences

Anil Bhardwaj

17. "Indian Lunar Program", ESA's Lunar Communications and Navigation Services (LCNS) User Engagement Workshop, European Space Agency, 01 June 2021.
18. "Interaction of Solar Wind with Moon: Results from Chandryaan-1 and Implications", Lunar Science Workshop, ISRO HQ, Bangalore, 06 Sept 2021.
19. "Overview on Venus", Venus Science Conference-2021, PRL, Ahmedabad, 23 Sept 2021.
20. "Venus and its Facets", IIST-ISAC-SUPERO Joint Student Project Meeting, IIST, Trivandrum, 11 Oct 2021.

21. "Moon-Sun Interactions: Results from Indian Lunar Missions Chandrayaan-1 and Chandrayaan-2", IEEE India Geoscience and Remote Sensing Symposium (InGRASS-2021), The Institute of Electrical and Electronics Engineers Geoscience and Remote Sensing Society, 07 Dec 2021.
22. "Science from the Chandrayaan-2 and Mars Orbiter Missions", National Space Science Symposium 2022, ISSER Kolkata, 01 Feb 2022.
23. "g. Saturn X-rays, in Towards Solar System X-rays Astronomy", GEO-X workshop, Tokyo Metropolitan University, Japan, 16 Feb 2022.
24. "Indian Planetary Missions", 3^{rd} Indian Planetary Science Conference, PRL, Ahmedabad, 14 March 2022.

S. A. Haider

25. "Characteristics of Venus and Mars Ionopauses: Modeling and Observations", 3^{rd} Indian Planetary Science (IPSC-2022), PRL, Ahmedabad, 14-16 March 2022.
26. "Do we understand the ionospheres of Venus and Mars?", Venus Science Conference (Venus-SC-2021), PRL, Ahmedabad, 23-24 Sept 2021.

Kuljeet Kaur Marhas

27. "Nascent Sun and Super flares", Invited Talk at Seminar, Academia Sinica Institute of Astronomy and Astrophysics, Taiwan, 04 Nov 2021.

Jayesh P. Pabari

28. "Interplanetary dust flux at Venus and its effect on atmosphere", Venus Science Conference (Venus-SC-2021), PRL, Ahmedabad, 23-24 Sept 2021.

Neeraj Srivastava

29. "A Scientific expedition to the Moon", National Science Day - 2022, Chandigarh University in collaboration with Indian Society of Remote Sensing, IIT Ropar, Punjab State Council for Science & Technology, 28 Feb 2022.

K. Durga Prasad

30. "Simulating the Moon in the Laboratory Opportunities and Challenges", Geoconfluence: 2021, Dept. of Applied Geophysics, IIT (ISM) Dhanbad, 20-21 Aug 2021.

Rishitosh Kumar Sinha

31. "Application of Remote Sensing Techniques in Investigating Recent Flow of Water on Mars", National Science Day - 2022, Chandigarh University in collaboration with Indian Society of Remote Sensing, IIT Ropar, Punjab State Council for Science & Technology, 28 Feb 2022.

Space and Atmospheric Sciences

Duggirala Pallamraju

32. "Materials in Space Research", Advances in Materials Science: Challenges and Opportunities, Department of Physics, Maharaja Krishnakumarsinhji Bhavnagar University, 21 Sept, 2021.
33. "Space Weather: Science and Applications", 12^{th} UN-CSSTEAP Post Graduate Course on Satellite Meteorology and Global Climate and 12^{th} UN-CSSTEAP Space and Atmospheric Science Joint Session of SATMET-12 and SAS-12 courses 2021, Space Applications Centre, Ahmedabad and Physical Research Laboratory, Ahmedabad, 4 Oct, 2021.
34. "Space Weather Research from Space-based Platforms, PS2", 21^{st} National Space Science Symposium, IISER, Kolkata, 31 Jan - 4 Feb, 2022.
35. "Space weather effects on the ionosphere-thermosphere system: Science and Applications", Solar Terrestrial Physics for Students and Young Scientist (STEPSYS), a Solar Terrestrial Physics School for International Students, IIG Mumbai (Online), 19-20 Feb, 2022.
36. "New Results on the Latitudinal Variations in Equatorial Phenomena Over Indian Longitudes as Obtained Using Night and Daytime Optical Airglow Emissions", Asia Oceania Geosciences Assembly Annual Meeting, (ST-21-A009), 01-06 Aug, 2021 (Online).

S. Ramachandran

37. "Aerosols, Radiation and Chemistry-Climate Interaction", UN-CSSTEAP Online Course on "Use of Space Technology for Weather and Climate Studies", Space Applications Centre, Ahmedabad, 17-31 May, 2021.
38. "Ozone: Past, Present and Future", International Ozone Day, Vidya Mandir Estancia, Chennai, 13 Sept, 2021.
39. "Aerosols and Climate Impacts", UN-CSSTEAP Online Course on "Satellite Meteorology and Global Climate (SATMET)", Space Applications Centre, and "Space and Atmospheric Sciences", Physical Research Laboratory, Ahmedabad, 6 Oct, 2021.
40. "Climate Change: Issues and Challenges", I.A. Shrestha Visiting Professor Scheme, Inaugural Lecture, Sardar Patel University, Vallabh Vidyanagar, 13 Oct, 2021.
41. "Keynote Address", 2^{nd} Winter School on "Contemporary Environmental Issues", Madurai Kamaraj University, Madurai, 18-31 Oct, 2021.
42. "Climate Change: Issues and Challenges", 2^{nd} Winter School on Contemporary Environmental Issues, Madurai Kamaraj University, Madurai, 18-31 Oct, 2021.
43. "Ozone: Past, Present and Future", 2^{nd} Winter School on Contemporary Environmental Issues, Madurai Kamaraj University, Madurai, 18-31 Oct, 2021.
44. "Air Pollution and Climate Change: Challenges", International Webinar on "Air Pollution and Climate Change Challenges and Mitigation", Koneru Lakshmaiah Education Foundation (KLEF), Guntur, 26 Nov, 2021.
45. "Air & Climate Change", in "Session IX In the Wind", Anant National University, Ahmedabad, 1 Dec, 2021.

46. "Keynote Address", Refresher Course on "Environmental Issues and Energy Management", Madurai Kamaraj University, Madurai, 8-21 Dec, 2021.
47. "Climate Change: Issues and Challenges", Refresher Course on "Environmental Issues and Energy Management", Madurai Kamaraj University, Madurai, 8-21 Dec, 2021.
48. "Air Pollution and Climate Change: Challenges with References to COP26", UGC-STRIDE International Symposium on "Outcomes of the Conference of the Parties 26 (COP26)", Madurai Kamaraj University, Madurai, 11-12 Dec, 2021.
49. "Ground Level Ozone: Issues and Challenges", Discussion Meeting on "Ground Level Ozone Current Understanding and Future Prospects", CSIR-NIScPR, New Delhi, 16 Dec, 2021.
50. "Air Pollution and Climate Change", Guest Lecture, Data Visualization Coarse, Anant National University, Ahmedabad, 15 Feb, 2022.

Dibyendu Chakrabarty

51. "Long term variation of solar wind helium and suprathermal population", in the 40^{th} Meeting of, ASI, IIT-Roorkee and ARIES, Nainital (Virtual), 25-29 Mar, 2022..
52. "Understanding the prompt electric field disturbances over low-equatorial latitude ionosphere A paradigm shift", S3 PRESTO Pillar 2: Space weather and Earth's atmosphere, STP-15, IIG Mumbai, 21-25 Feb, 2022.
53. "Space weather and probing the solar wind plasma from the first Lagrangian point of the Sun-Earth system", in Plasma Science and Applications (PSA-2021), organized by the, Department of Physics, Sardar Vallabhbhai National Institute of Technology, Surat, 20-21 Dec, 2021.
54. "Air & Space", at the, Ananth National University, Ahmedabad, 20 Nov, 2021.
55. "Penetration Electric Fields: Meaning, Nature, Importance and Complexities", in the International Space Weather Initiative (ISWI-2021) Workshop on Space Weather: Science and Applications jointly organized by the, United Nations Office for Outer Space Affairs (UNOOSA) and the Vikram Sarabhai Space Centre (VSSC) of the Indian Space Research Organization (ISRO), India, 2 - 3 Nov, 2021.
56. "Potential of atomic oxygen airglow diagnostics to probe Venusian upper atmosphere", Venus Science Conference, 2021 (Venus-SC-2021), Physical Research Laboratory, Ahmedabad, 23-24 Sept, 2021.
57. "Aditya Solar wind Particle EXperiment (ASPEX) on-board Aditya-L1 Mission of India", delivered on 23 August, 2021 in the session 4.1(5) - Advances and Upcoming Developments in Solar and Heliospheric Physics of the Joint Scientific Assembly of IAGA-IASPEI-2021, CSIR-NGRI, 21-27 Aug, 2021 (Virtual).

Lokesh Kumar Sahu

58. "Observing atmospheric trace gases and VOCs: Basics, Instruments, knowns and unknowns over India", AICTE Virtual School on Atmospheric Pollutants and Their Impact, IIT Madras, India, 07-12 Mar, 2022.
59. "Measurements of Trace Gases in the Atmosphere: Study of Climate and Environment", THEORETICAL AND PRACTICAL ASPECTS IN APPLIED PHYSICS (TAPAAP 2021), Radha Govind Group of Institutions Meerut, India, 24-28 Sept, 2021.

Som Kumar Sharma

60. "Inaugural Speech and talk on "Lower and Middle Atmospheric Studies"", in Hindi Fortnight Inaugural Function-2021 at, National Centre for Earth Science Studies, MoES, Thiruvananthapuram, 14 Sept, 2021.
61. "Atmospheric Exploration Tools and Techniques", in 12^{th} CSSTEAP Course on Satellite Meteorology and Global Climate (SATMET-12), SAC (ISRO) Ahmedabad, 11 Oct, 2021.
62. "Earth's Lower and Middle Atmospheric Processes", 12^{th} CSSTEAP Course on Satellite Meteorology and Global Climate (SATMET-12), SAC (ISRO) Ahmedabad, 12 Oct, 2021.
63. "Physics Glossary and New Education Policy 2020", Commission of Scientific and Technical Terminology (CSTT), Ministry of HRD, New Delhi, 12 Nov, 2021.
64. "Changing Earth's Climate: Observations by Lidar and Satellites", International Conference on Climate Change-An Imminent Global Emergency-2021 (ICCCIEG-2021), Delhi University, New Delhi, 17 Dec, 2021.

Narendra Ojha

65. "Atmospheric modeling over India: Challenges and opportunities", to the participants of the Training on chemistry-climate modeling, Department of Environmental Science and Engineering, IIT (ISM) Dhanbad, 16 Aug, 2021.

Geosciences

R.D. Deshpande

66. "Importance of Groundwater in Earth-Atmosphere System: Frontiers of Fundamental and Applied Research", in 'GROUNDWATER QUALITY MONITORING AND ASSESSMENT' a CSIR Integrated Skill Initiative, NGRI, Hyderabad, 14-25 February, 2022.
67. "Plenary talk 'Frontiers in hydrology Research'", in Frontiers in Geosciences Research Conference (FGRC-2021), PRL, Ahmedabad, 27-28 Spetember, 2021.

M.G. Yadava

68. "Paleoclimate: need potential applications and technological options", to the participants of Institution of Geoscientists, Odisha, Bhubaneshwar, 11 December, 2021.

Neeraj Rastogi

69. "Organic & Brown Carbon Aerosols: Insights from Real-time Measurements", workshop on 'Concepts in Measurement, Laboratory Experiment and Modelling of Atmospheric Aerosols', IIT-Madras, 7-12 March, 2021.

Theoretical Physics

Subhendra Mohanty

70. "Tests of Lorentz violation in gravitational waves from binary pulsars", To the participants of Fourth Summer School and Workshop on the Lorentz- and CPT-violating Standard-Model Extension, Indiana University, Bloomington, USA, 20-30 May, 2021.

V.K.B. Kota

71. "Multiple multi-j pairing SO(5) and seniority $Sp(2\Omega)$ algebras with isospin in nuclei", Multiple multi-j pairing SO(5) and seniority $Sp(2\Omega)$ algebras with isospin in nuclei, Sofia (Bulgaria), 16-18 September, 2021.

Srubabati Goswami

72. "Neutrino physics: Developments and challenges to the participants in the Lecture Workshop challenges in Theoretical and Computational Physics,", To the participants in the Lecture Workshop challenges in Theoretical and Computational Physics, Indian Institute of Technology, Bombay, 25.10. 2021.
73. "Neutrino Oscillation: Current status and future prospects", To the participants High-end workshop (Karyashala) on Software Tools and Techniques used in EHEP and its Applications, Malaviya National Institute of Technology, Jaipur, 25.6.2021.
74. "The Panorama of a Nu-World", To the participants of 3rd Research Conclave 2021, National Institute of Technology, Meghalaya, 28.2.2022.

Hiranmaya Mishra

75. "Unmasking hybrid stars", Current trends in high energy Physics and condensed matter physics-21, Center of excellence in high energy and condensed matter Physics, Physics Department, Utkal University, Vani Vihar, Bhubaneshwar, Dec. 20-21, 2021.
76. "G-modes in hybrid stars", Current trends in non-equillibrium physics 21 (CTNEP-21), School of Physics, Jawaharlal Nehru University (JNU), New Delhi, Nov. 22-25, 2021.

Ketan M. Patel

77. "Some phenomenological aspects of 6D SUSY SO(10) model with magnetic flux", To the participants of conference on Supersymmetry and Unification of Fundamental Interaction (SUSY 2021), Beijing, China, 25 August, 2021.

Atomic, Molecular and Optical Physics

R. P. Singh

78. "Free-space quantum communication: Effect of atmospheric aerosols", International Conference on Quantum Information and Foundations (ICQIF-2022), Physics and Applied Mathematics Unit, Indian Statistical Institute, Kolkata, India., 14-24 February, 2022.
79. "Free space quantum communication: Experiments at PRL", Quantum Information and Computation: From Foundations to Applications -2021 (QFA-2021), Indian Institute of Technology, Jodhpur., 18-23 October 2021.

B. K. Sahoo

80. "Parity nonconservation in atomic systems", INT Workshop on Hadronic Parity Nonconservation II, Institute of Nuclear Theory, University of Washington, USA, 24 - 27 January,2022.

G. K. Samanta

81. "Satellite Based Quantum Science & Experiments", DTDI Technology Conclave, Indian Space Research Organization (ISRO), Bangalore, 22-26 November, 2021.
82. "Development of entangled photon sources for future space-based experiments", 44th Annual Symposium of the Optical Society of India, Frontiers in Optics and Photonics (FOP21), Indian Institute of Technology, Delhi., 24-27 September, 2021.
83. "Nonlinear effects of structured beams in classical and quantum optics experiments", Weekly webinar arranged by SPIE, OSA and OSI student chapters in association with the Department of Applied Optics and Photonics, University of Calcutta, Calcutta., 12 September 2021.
84. "Structured beam optical parametric oscillator based mid-IR sources", Student Conference on Photonics and Quantum Technology (SCPQT), National Institute of Science Education and Research, Bhubaneswar., 24-26 February, 2021.

Prashant Kumar

85. "Synthetic spectrum method for laser induced breakdown spectroscopy", XII Biennial National Conference of Physics Academy of North East (PANE 2021), Department of Physics, Tripura University, 15-17 December, 2021.

Bhalamurugan Sivaraman

86. "Need for CFD in planetary and space science", Workshop on Computational Fluid Dynamics, Hindustan University, Chennai, May 29,2021.

Lectures at Universities / Institutions

Astronomy and Astrophysics

Shashikiran Ganesh

1. "Comets - The Majestic Visitors", Public Outreach and Education Committee of the Astronomical Society of India, August 14. 2021

Lokesh Kumar Dewangan

2. "Probing the physical processes involved in forming massive stars", Department of Astrophysics & Cosmology, SNBNCBS, Kolkata, March 04, 2021

Veeresh Singh

3. "Radio galaxies after the active phase", 75th years of Indias Independence: Azadi ka Amrit Mahotsav at ARIES Nainital, August 10, 2021

Prachi Prajapati

4. "A Voyage into Astronomy: History and the Modern Times", Anna University, Tamilnadu, India, September 29, 2021

Solar Physics

Nandita Srivastava

5. "Coronal Studies & coronagraphs", Online lecture for graduate students of Physics and Astronomy at Samarkand State University Uzbekistan, as Principal-Investigator of Indo-Uzbek Collaborative project., December 7, 2022
6. "Coronal mass ejections: properties & associated phenomena", Online lecture for graduate students of Physics and Astronomy at Samarkand State University Uzbekistan, as Principal-Investigator of Indo-Uzbek Collaborative project., December 14, 2022

Bhuwan Joshi

7. "Sun and Space", Invited talk as a Resource Speaker: Workshop for government teachers of Science and Maths under Rashtriya Avishkar Abhiyan, organized by the District Institute of Education and Training (DIET), Govt. of Rajasthan, Udaipur, January 6, 2022
8. "Sun: The ultimate Driver of Space Weather", Keynote lecture during National Science Day celebrations by Department of Education, Mohanlal Sukhadia University (MLSU), Udaipur, February 28, 2022

Rohan E Louis

9. "The Structure of the Sun", Two online lectures for graduate students of Physics and Astronomy at Samarkand State University Uzbekistan, as Co-Investigator of Indo-Uzbek Collaborative project, October 26, 2021 & November 02, 2021
10. "Inferring Physical Conditions in the Solar Atmosphere", Two online lectures for graduate students of Physics and Astronomy at Samarkand State University Uzbekistan, as Co-Investigator of Indo-Uzbek Collaborative project, November 16, 2021 & November 23, 2021

Planetary Sciences

Anil Bhardwaj

11. "Indian Planetary and Space Missions", Independence Day Colloquium, Aryabhatta Research Institute of Observational Sciences (ARIES), August 17, 2021
12. "Challenges and Science of Indian Planetary Missions", Distinguished Talk, Achievements in Science and Technology of India in Applied Sciences, on the occasion of 75th years of Independence - Half-day Virtual Webinar, Amity Institute of Applied Sciences, Amity University, August 25, 2021
13. "Overview of Astronomy and Space Sciences", Commemorative Lecture, Tribute to Prof. Thanu Padmanabhan - Commemorative Webinar Series, KSCSTE, Trivandrum, September 30, 2021
14. "Inaugural Chief Guest Lecture", AARUSH-21, the National Level Techno-Management fest of SRM-IST, Chennai, September 16, 2021
15. "Indian Planetary Missions", Live TV Webinar Series: Listening to Learn of the Department of Education in Science and Mathematics, National Council of Educational Research and Training (NCERT), New Delhi, November 16, 2021

Space and Atmospheric Sciences

Duggirala Pallamraju

16. "Recent results in the upper atmospheric dynamics over low-latitudes", University of Massachusetts, Lowell, MA, USA, 22 April 2021
17. "Effects of Societal Applications from Space weather", Department of Physics, Osmania University, 25 March 2022

Lokesh Kumar Sahu

18. "12^{th} Post Graduate Course in Space and Atmospheric Sciences of CSSTEAP, affiliated to the United Nations.", 5-Lectures on "Dynamics of Earth's Atmosphere", [Mode: ONLINE]

Narendra Ojha

19. "Trace gases pollution and modeling", on the World Environment Day, Department of Physics, KLEF deemed to be University, Vijayawada, Mode: ONLINE., 5 June 2021

Som Kumar Sharma

20. "Study of Earth's Atmosphere using Ground and Satellite based Observations", in TAPAAP- 2021 (Theoretical and Practical Aspects in Applied Physics), Radha Govind Group of Institutes, Meerut, 27 September 2021
21. "Study of the Earth's Lower and Middle Atmosphere: Importance and Challenges", organized by Marwadi University and SERF (Space Education and Research Foundation), Rajkot, 5 March 2022

Harish Chandra

22. "52 lectures on space science course and 1 lecture in the common module", lectures to UN course, Mode: Online

Geosciences

Ravi Bhushan

23. "Role of Cosmogenic Radionuclides in Oceanography", Invited talk given at the National Institute of Oceanography, December 02, 2021

M.G. Yadava

24. "Paleoclimate", Lecture delivered at Centre for Space Science and Technology Education in Asia and the Pacific (CSSTEAP), SAC, Ahmedabad., February 25, 2022
25. "Paleoclimate", Lecture delivered at Centre for Space Science and Technology Education in Asia and the Pacific (CSSTEAP), SAC, Ahmedabad., February 28, 2022
26. "Paleoclimate", Lecture delivered at Centre for Space Science and Technology Education in Asia and the Pacific (CSSTEAP), SAC, Ahmedabad., March 01, 2022

Sanjeev Kumar

27. "Carbon and nitrogen dynamics in the Indian estuaries", Lecture delievered at Hamburg University, Germany, January 18, 2022

A D Shukla

28. "The fragility of Himalayan ecosystem and response to the climate change", invited talk given in a UGC sponsored Refresher Course for teachers organized by JNV University, Jodhpur., November 26, 2021

Arvind Singh

29. "Ocean Science: Climate Science Perspective", lecture delievered at Pandit Deendayal Energy University, Gandhinagar, India, March 25, 2022
30. "Effect of Ocean acidification marine nitrogen fixation", Invited talk organized by NANO-DOAP Global Project, October 29, 2021
31. "Indian Ocean research by early careers", invited talk organized by IIOE-2, April 13, 2021
32. "'Climate action, Life below water, Life on the water'", deleivered six lectures at UGC-HRDC at Pondicherry University by Pondicherry University (ONLINE), 16 August, and 22 October 2021, and 24 February 2022.
33. "'Sustainable forest management'", Course lectures (8 lectures) to the III semester M.Sc. students at Gujarat University, Ahmedabad, June-August 2021.
34. "'Palaeoclimate'", Course lectures (8 lectures) to the I semester M.Sc. students at Gujarat University, Ahmedabad, Jan-March 2022.
35. "'Sustainable forest management'", Course lectures (8 lectures) to the III semester M.Sc. students at Gujarat University, Ahmedabad, June-August 2022.

Vineet Goswami

36. "'Application of isotopes in earth science studies'", lecture deleivered at CSIR-Institute of Himalayan Bioresource Technology, Palampur, Himachal Pradesh, March 4, 2022

Theoretical Physics

Srubabati Goswami

37. ""Neutrino mass models" at the Virtual School on Flavor Structure of the Standard Model", "Neutrino mass models" at the Virtual School on Flavor Structure of the Standard Model, IIT Kanpur, 4th and 5th September, 2021

Hiranmaya Mishra

38. "Matter under extreme conditions", "Matter under extreme conditions", Talk presented at Government Womens college, Sambalpur, Dec 17, 2021
39. "Unmasking hybrid star", "Unmasking hybrid stars", Seminar given at Institute of Physics Bhubaneswar, October 28, 2021
40. "Lectures on Color superconductivity", "Lectures on Color superconductivity", Four lectures given to High energy nuclear theory group at VECC Kolkata, April-May 2021

Navinder Singh

41. “A crash course on magnetism”, A crash course on magnetism, MS university, Vododara, 10th to 12th Jan 2022

Ketan M. Patel

42. “”Flavour structure from gauge interaction in higher dimensions”, given at the Virtual School on Flavor Structure of the Standard Model”, ”Flavour structure from gauge interaction in higher dimensions”, given at the Virtual School on Flavor Structure of the Standard Model, IIT Kanpur, India, September 08, 2021

Atomic, Molecular and Optical Physics

R. P. Singh

43. “Free space quantum communication”, Colloquium at Indian Institute of Science, Bengaluru., November 17,2021
44. “Satellite-based quantum communication 1 & 2”, VSSC Thiruvananthapuram, ISRO, November 18,2021

Bhalamurugan Sivaraman

45. “It is shocking to realize the Origin of Life”, Engineers day talk, Society for Shock Wave Research and Department of Aerospace Engineering,IISc, Bangalore, Mode: ONLINE, September 15,2021

Naveen Chauhan

46. “Basics of luminescence and its relevance to Diamond Industry”, Gemmological Institute of India, Mumbai on, March 15,2021

Jaya Krishna Meka

47. “I need some space”, Department of Electronics and Communication Engineering, AAA College of Engineering and Technology, Sivakasi, Tamilnadu, September 28,2021

Dean’s Office

Bhushit G Vaishnav

48. “Science as a Career: Framing the Roadmap,” Vanita Vishram Women’s University, Surat, 04 September 2021 (online).

Computer Centre

Jigar Raval

49. “Cyber Security and Prevention”, Delivered an expert talk on “Cyber Security and Prevention” at Zydus School for Excellence, Godhavi, Ahmedabad on February 11, 2022., February 11, 2022

Science Outreach Talks by PRL Scientists

Astronomy and Astrophysics

Abhijit Chakraborty

1. “Challenges and limitations of detecting exoplanets”, 4th PRL-IAPT Vikram Sarabhai Lecture, on 11-02-2022

Vishal Joshi

2. “Black Holes: mistery in the dark”, Big bang astronomy club, O. V. Sheth Regional Community Science Center, Rajkot, on 15-04-2022
3. “Exoplanets: A search for a new home”, NASI-DDUC Science Promotion Activities for school students, on 15-09-2021

Mithun N. P. S

4. “Observing the Sky from Earth and Space”, Promotion of Excellence among Gifted Children - Kerala, Irinjalakkuda Educational District, on 13-02-2022
5. “An Introduction to Space Science and Technology”, Sastrarangam club inauguration, T.H.S. Puthenchira, Kerala, on 31-07-2021

Solar Physics

Nandita Srivastava

6. “Sun and Space Weather”, at Department of Aerospace Engineering-SRMIST, SRM University, Chennai during World Space week with theme “Women in Space”, on 07-10-2021

Bhuwan Joshi

7. “Sun, Heliosphere and Space Weather”, Dr. Abdul Kalam Jayanti Celebrations at at Vidya Bhawan Sr. Sec. School, on 21-10-2021

Planetary Sciences

Anil Bhardwaj

8. “Overview of Astronomy and Space Science”, Space Technology & Applications, Target Participants - School Teachers (TGT & PGT), IIRS, Dehradun, on 21-06-2021
9. “Vigyan Utsav”, webinar of the State Science & Technology Program (SSTP), DST, Govt. of Gujarat, to mark the celebration of ”Azadi Ka Amrit Mahotsav”, on 03-09-2021
10. “Introduction to PRL”, IETE Varodara Webinar on ”Let’s Know Our Institutions”, on 18-09-2021
11. “Indian Planetary and Space Missions”, New Zealand India Research Institute Talk, on 26-10-2021
12. “Indian Planetary Missions”, Talk at CSIR-JIGYASA program webinar series called ’Demystifying Science” under the CSIR-JIGYASA-ATL (Atal Tinkering Labs of NITI AAYOG), on 18-11-2021
13. “Indian Planetary Missions”, Talk at Parsec - Astronomy Club, IISER, Trivandrum, on 14-12-2021
14. “Indian Planetary Missions”, Expert Talk and interaction at 29th National Children Science Congress (NCSC-2022) in ’Meet the Scientist’ Program of Gujarat Council on Science and Technology, on 17-02-2022
15. “Planetary and Space Missions of India”, Talk at National Seminar to Celebrate National Science Day, National Institute of Homoeopathy, Kolkata, on 28-02-2022
16. “Indian Planetary Mission”, Talk at Celebration of National Science Week, VIT, Bhopal, on 03-03-2022

Space and Atmospheric Sciences

Lokesh Kumar Sahu

17. “Past, Present and Future Scenarios of Ozone in the Earth’s Atmosphere”, World Ozone Day 2021, Gujarat Science City, Ahmedabad, India [Mode: OFFLINE]., on 16-09-2021

Theoretical Physics

Subhendra Mohanty

18. “S. P. Pandya Memorial Lecture on “Wave Dark Matter””, Indian Physics Association, on 21-09-2021

Srubabati Goswami

19. “Gender Parity in Physics Profession in India: data, surveys and best practice”, Invited talk in Working Group, International Conference on Women in Physics, Melbourne, on 11-07-2021
20. “Gender Equity in Physics Profession in India: Status, interventions and outcomes”, Invited talk in Association of Asia Pacific Physical Societies (AAPPS) Workshop, International Conference on Women in Physics, online, Melbourne, on 16-07-2021

21. “The Neutrino Story: From Impossible Dreams to Unreachable Stars”, Delivered in “Kuriosity during Kuarantine” outreach programme organized by International Centre for Theoretical Physics, Bangalore talk, on 21-05-2021
22. “Diversity and Inclusion in Astroparticle Physics”, Panelist in the session ”Diversity and Inclusion in Astroparticle Physics” held in XV11 International Conference on Topics in Astroparticle and Under ground Physics held in Valencia, on 03-09-2021
23. “A star from another sky”, SN Bose Centre for basic Sciences, Kolkata, on 28-01-2022
24. “Dr. Bibha Chowdhuri : A star from another sky”, “Dr.Bibha Chowdhuri: A star from another sky”, Indian Institutes of Technology, Gandhinagar, on 19-02-2022
25. “Women in Science: Breaking Barriers”, Women in Science: Breaking Barriers, Aryabhatta Research Institute of Observational Sciences, Nainital, on 10-02-2022
26. “Women in Science: Challenges and way forward”, Women in Science: Challenges and way forward ,Department of Physics, Jamia Millia Islamia, on 11-03-2022
27. “Women in Science: Breaking the Barriers”, Public lecture as a part of a special lecture series in Vigyan Vidushi 2021,Tata Institute of Fundamental Research, on 19-06-2021

Namit Mahajan

28. ““Outreach @ PRL”, a Vigyan Utsava webinar on a Science Communication & Popularisation (under the State Science & Technology Programme (SSTP)”, Department Of Science & Technology, India, on 02-02-2022

Atomic, Molecular and Optical Physics

Bhalamurugan Sivaraman

29. “Biography of molecules beyond Earth”, NASI-DDUC Science Promotion Activity, Mode: Online, on 20-09-2021
30. “Biography of molecules beyond Earth”, A Webinar delievered in Astro Club, Bangalore, on 11-12-2021

Area Seminar by visitors

Somnath Dutta

1. “Jets and outflows properties of extremely Young Stellar Objects”, Institute of Astronomy and Astrophysics, Academia Sinica (ASIAA), Taiwan, on 25-02-2022

Rolf Schlichenmaier

2. “The Secrets of Sunspot Penumbra and a Status Description of the European Solar Telescope”, Leibniz-Institut für Sonnenphysik (KIS), Freiburg Germany, on 27-07-2021

Michal Sobotka

3. “Heating of the solar chromosphere by acoustic waves”, Astronomical Institute of the Czech Academy of Sciences, Ondřejov, Czech Republic, on 20-08-2021

Christian Beck

4. “The Inverse Evershed Flow - Data, Analysis Methods, Results, Physics, Model”, National Solar Observatory (NSO), USA, on 16-09-2021

Manolo Collados

5. “The European Solar Telescope: A telescope for the XXI century”, Instituto de Astrofísica de Canarias, Tenerife Spain, on 22-10-2021

Markus Roth

6. “Probing Solar and Stellar Physics by Helio- and Asteroseismology”, Leibniz-Institut für Sonnenphysik (KIS), Freiburg Germany, on 12-11-2021

Bernhard Kliem

7. “Initiation and Driving of Solar Eruptions”, Institute of Physics and Astronomy, University of Potsdam Germany, on 10-12-2021

Toshifumi Shimizu

8. “Energy releases and transfer in the solar atmosphere”, Institute of Space and Astronautical Science, Japan Aerospace Exploration Agency, and The University of Tokyo, Japan, on 31-01-2022

Lucie Green

9. “The Suns Twisted Magnetic Mysteries”, Mullard Space Science Laboratory, University College London, UK, on 18-02-2022

Sandeep Sahijpal

10. “Origin of the solar system”, Punjab University, Punjab, on 12-08-2021

Queenie Chan

11. “Organics on Itokawa asteroid via analyses of Hayabusa samples”, Royal Holloway, University of London, UK, on 26-08-2021

N G Rudraswami

12. “Micrometeorites on the Earth surface: Understanding their origin and properties”, National Institute of Oceanography (NIO) Goa, on 02-09-2021

Maitrayee Bose

13. “Water, Asteroid and Planet formation: The connections”, Arizona State University, USA, on 09-09-2021

Sujoy Ghosh

14. “Shock-induced incongruent melting of olivine and formation of natural Fe-bearing aluminous bridgmanite in ordinary chondrites”, Indian Institute of Technology, Kanpur, on 16-09-2021

Nan Liu

15. “^{26}Al in AGB grains”, Washington University St. Louis, USA, on 23-09-2021

Lionel Vacher

16. “Sulfur isotope anomalies in Acfer 094 inherited from the Irradiation of the Protosolar Molecular Cloud by Massive Nearby Stars”, Washington University St. Louis, USA, on 30-09-2021

Manavi Jhadav

17. “Isotopic and elemental studies of presolar graphite grains and what they tell us about their parent stars”, University of Louisiana, USA, on 06-10-2021

Smail Mostefaoui

18. "Minor and trace element concentrations in adjacent kamacite and taenite in the Krymka chondrite", Muséum National d'Histoire Naturelle, Paris, France, on 14-10-2021

Ritesh Mishra

19. "Nascent Sun & repetitive Super flares", Application Engineer, Cameca, India, on 21-10-2021

Frank Gyngard

20. "Entering an Unseen World: Biology vs. Science - Who sees further?", Harvard Medical School, USA, on 28-10-2021

Rita Parai

21. "Heterogeneous accretion of volatiles to Earth's mantle reservoirs", Washington University, USA, on 12-11-2021

Pierre Haenecour

22. "Constraining thermal processing of dust grains in space and on the surface of airless bodies through in-situ laboratory experiments", University of Arizona, Tucson, USA, on 18-11-2021

Alik Sundar Majumdar

23. "Serpentinization of iron-rich olivine and its potential for abiotic methane synthesis in planetary bodies", Indian Institute of Technology, Dhanbad Jharkhand, India, on 25-11-2021

Christian Vollmer

24. "The Origins of Organic Matter and Amorphous Silicates in Meteorites Clues from Nanoscale Investigations", Institute for Mineralogy WWU Munster, Germany, on 09-12-2021

Yves Marrocchi

25. "Isotopic constraints on the conditions of chondrule formation in carbonaceous chondrites", CRPG,Centre national de la recherche scientifique, France, on 16-12-2021

Prajkta Mane

26. "First Formed Solids: Records of the Earliest Times of the Solar System", Lunar and Planetary Institute (USRA), NASA Johnson Space Center, Houston, USA, on 23-12-2021

Yogita Kadlag

27. "Chondrites and the early solar system", University of Bern, Switzerland, on 30-12-2021

Nikitha Susan Saji

28. "Nucleosynthetic heterogeneity in the early solar system: insights from Nd isotopes", Centre for Star and Planet Formation Globe Institute, University of Copenhagen, Denmark, on 06-01-2022

Thomas Burbine

29. "How well can we link meteorites to asteroids", Mount Holyoke College, USA, on 13-01-2022

Evelyn Furi

30. "Origin and evolution of nitrogen on planetary bodies in the inner solar system", Centre de Recherches Petrographiques et Geochimiques, France, on 20-01-2022

Maria Eugenia Varela

31. "Chondrule formation: A controversial issue among different models", ICATE-CONICET, San Juan, Argentina, on 27-01-2022

Susanne P. Schwenzer

32. "Volatiles on Mars - from meteorites to sample return", The Open University, Milton Keynes, U. K., on 10-02-2022

Daisuke Nakashima

33. "Oxygen isotope systematics of chondrules: regional heterogeneity of oxygen isotope reservoirs in the solar nebula", Tohoku University, Japan, on 17-02-2022

Jangmi Han

34. "Atomic-Scale Structure and Non-Stoichiometry of Meteoritic Hibonite", University of Houston, USA, on 24-02-2022

Ryan Ogliore

35. "Condensation and Radial Transport of Filamentary Enstatite Crystals from Interplanetary Dust", Washington University St. Louis, USA, on 03-03-2022

Reto Trappitsch

36. "Hands-on Astrophysics: Analysis of Presolar Stardust Grains to decipher Stellar Nucleosynthesis", Brandeis University, Waltham, MA, USA, on 10-03-2022

Imran Girach

37. "Tropospheric carbon monoxide over India and adjoining oceanic region", Space Physics Laboratory, Vikram Sarabhai Space Centre, Thiruvananthapuram, India, on 05-04-2021

Surendra Dhaka

38. "Thermal structure and climatic insights in the range of 1-40 km altitude of Earth's atmosphere: Updates from COSMIC/Formosat-3 observations", Rajdhani College, University of Delhi, New Delhi, India, on 12-04-2021

Ashik Paul

39. "Multi-scale size ionospheric irregularities impacting signal-in-space performance of satellite-based communication and navigation links", University of Calcutta, Kolkata, India, on 19-04-2021

Vijay Kanawade

40. "Observations of new particle formation and growth: Indian perspective", University of Hyderabad, Hyderabad, India, on 26-04-2021

Soumik Ghosh

41. "Inter-annual and intra-seasonal variability of the Indian summer monsoon: A regional climate modeling approach", Department of Earth and Planetary Sciences, Weizmann Institute of Science, Israel, on 24-05-2021

K. N. Uma

42. "Dynamics and microphysics of tropical mesoscale convective systems", Space Physics Laboratory, Vikram Sarabhai Space Centre, Thiruvananthapuram, India, on 13-12-2021

Manish K. Joshi

43. "Climate variability and its teleconnection with Indian summer monsoon", Genesis Ray Energy Pvt. Ltd., India, on 17-01-2022

Rajesh Kumar

44. "MAP-AQ: An international system for monitoring, analysis, and prediction of air quality", National Center for Atmospheric Research, Boulder, USA, on 21-02-2022

Bhargav Vaidya

45. "Developing a space weather modeling framework in the era of Aditya-L1", Indian Institute of Technology Indore, India, on 21-03-2022

K.S. Mishra

46. "Comparative study of Climatic Changes and Volcanism on Earth and Extraterrestrial Bodies", (Former) Additional Director General, Geological Survey of India, Dehradun, on 25-03-2022

Bivin Geo George

47. "A geochemical outlook on sedimentary basins of India", Scientist, NCESS Thiruvananthapuram, on 08-02-2022

Maguni Mahakhud

48. "Higher order precision calculations in QCD and N=4 SYM", Indian Institutes of Science Education and Research, Mohali, India, on 26-07-2021

Rinku Maji

49. "Grand Unification: Proton Lifetime, Topological Defects, Inflation and Gravity Waves", Indian Institutes of Technology, Kanpur, India, on 26-08-2021

Animesh Chatterjee

50. "Synergy of Neutrino and Dark matter at the advanced particle detector", University of Pittsburgh, USA, on 16-09-2021

Bruce Mellado

51. "The anatomy of the multi-lepton anomalies at the LHC and a candidate for a singlet scalar", University of the Witwatersrand, Johannesburg, South Africa, on 20-09-2021

Shireen Gangal

52. "Precision Prediction of Higgs cross section and New Physics signals in B-decays", Laboratoire d'Annecy-le-Vieux de Physique Thorique ,Annecy, France, on 06-01-2022

Raghunath Ghara

53. "Probing the First Billion Years of our Universe with 21-cm radiation from neutral hydrogen", Technion, Israel, on 24-03-2022

Santanu Mondal

54. "Lower moments of nucleon parton distribution functions (PDFs) in lattice QCD", Michigan State University, USA, on 31-03-2022

Student Training

Solar Physics

1. Asha Lakshmi, St. Sacred Heart College, Kochi, “Methods for estimating the Image quality of solar observations”, from May 2021 to July 2021, [Supervisor: A. Raja Bayanna].
2. Kshitij Dave, Institute of Advanced Research, Gandhinagar, “Algorithms for Deconvolution of absorption spectra”, from May 2021 to July 2021, [Supervisor: A. Raja Bayanna].
3. Bhavna Agarwal, St. Xaviers College, Mumbai, “Influence of fast solar wind in the propagation of coronal mass ejections”, from Jan 2021 to Apr 2021, [Supervisor: Nandita Srivastava].
4. Urmi Doshi, M. P. Birla Institute of Fundamental Research. Bangalore, “Statistical Study of ICMEs in solar cycle 23 & 24”, from Jan 2021 to July 2021, [Supervisor: Nandita Srivastava].
5. Stephen Dsouza, St. Stephen’s College, New Delhi, “Forecasting the Arrival of Interplanetary Coronal Mass ejections using a Drag Based Model”, from Sep 2021 to Dec 2021, [Supervisor: Nandita Srivastava].
6. Sandeep Kumar, PRL, Ahmedabad, “Coronal Cavities”, from Apr 2021 to Jun 2021, [Supervisor: Nandita Srivastava].
7. Sandeep Dubey, PRL, Ahmedabad, “Sheath Accumulation Propagation Model of CME”, from Aug 2021 to Nov 2021, [Supervisor: Nandita Srivastava].
8. Sandeep Kumar, PRL, Ahmedabad, “Parametric Study of Empirical Modeling of Solar Wind”, from Aug 2021 to Nov 2021, [Supervisor: Nandita Srivastava].

Planetary Sciences

9. Riya Singh, Banasthali Vidyapith, Banasthali, “Mineralogical Observation by Curiosity at Gale Crater of Mars”, from May 2021 to July 2021, [Supervisor: Amit Basu Sarbadhikari].
10. Kishalaya Singh, Pondicherry University, “Chemical Observations by Curiosity at Gale Crater, Mars”, from May 2021 to July 2021, [Supervisor: Amit Basu Sarbadhikari].
11. Sangeeta Koner, National Institute of Technology, Durgapur, “Understanding The Role of Initial Mass Flux, Partition Coefficient and Oxygen Fugacity In The Homogenous Accretion Scenario.”, from May 2021 to July 2021, [Supervisor: Amit Basu Sarbadhikari].
12. Francis Gracy Arockiaraj, Madurai Kamaraj University, Madurai, “Core Growth and Mantle Formation During Accretion In Terrestrial Planets”, from May 2021 to July 2021, [Supervisor: Amit Basu Sarbadhikari].
13. Ritwick Sen, Indian Institute of Technology, Kharagpur, “Comparison of Martian and Continental flood basalt: A geochemical approach”, from May 2021 to July 2021, [Supervisor: Dwijesh Ray].
14. Ruchi Yadav, University of Delhi, Delhi, “Watery, Early Mars: Evidences from Minerals”, from May 2021 to July 2021, [Supervisor: Dwijesh Ray].
15. Manisha Chandel, Himachal Pradesh University, Shimla, “Study of lightning generated whistlers”, from May 2021 to July 2021, [Supervisor: Jayesh P. Pabari].
16. Rosanna K. Anto, University of Calicut, Tenhipalam, “Understanding dust ring around Venus”, from May 2021 to July 2021, [Supervisor: Jayesh P. Pabari].
17. Virti Shah, Indus University, Ahmedabad, “Dynamical Evolution of Interplanetary Dust Particle (IDP) in the Solar System”, from Jan 2022 to April 2022, [Supervisor: Jayesh P. Pabari].
18. Zeel P. Patel, Hemchandracharya North Gujarat University, Patan, “Venus Lightning: Study of Meteor Showers during LADEE Observation Time”, from Nov 2021 to Feb 2022, [Supervisor: Jayesh P. Pabari].
19. Aditi Sharma, Banasthali Vidyapith, “Modelling and analysis of Schumann Resonance due to lightning”, from Feb 2021 to June 2021, [Supervisor: Jayesh P. Pabari].
20. Tanu Garg, Banasthali Vidyapith, Banasthali, “Modelling and analysis of Schumann Resonance due to lightning”, from Feb 2021 to June 2021, [Supervisor: Jayesh P. Pabari].
21. Srishti Iyer, M. S. University, Vadodara, “Study of interplanetary dust around Earth and Venus”, from Feb 2021 to April 2021, [Supervisor: Jayesh P. Pabari].
22. Sonal Mashram, IEHE, Bhopal, “Group velocity and wave propagation in ionosphere”, from Feb 2021 to July 2021, [Supervisor: Jayesh P. Pabari].
23. Vishnupriya Pradeep, Cochin University of Science and Technology, “Thermal analysis of specific sites on the Moon using remote sensing datasets”, from Feb 2021 to Aug 2021, [Supervisor: K. Durga Prasad].
24. Anirudh Kumar, Cochin University of Science and Technology, “Seismic and gravity data analysis of potential sites on the Moon”, from Feb 2021 to Aug 2021, [Supervisor: K. Durga Prasad].
25. Varsha Natarajan, Pondicherry University, “Thermophysical Analysis of distinct sites on Mars using remote sensing data”, from Feb 2021 to Oct 2021, [Supervisor: K. Durga Prasad].
26. Mrittika Ghosh, West Bengal State University, “Investigation of Deuterium to Hydrogen Ratio in the Universe”, from May 2021 to July 2021, [Supervisor: Kinsuk Acharyya].
27. Viswakannan, R. K., Dwaraka Doss Goverdhan Doss Vaishnav College, Chennai, “Formation of Stars and Planets and Minimum Mass Solar Nebula”, from May 2021 to July 2021, [Supervisor: Kinsuk Acharyya].
28. Sathiya Sundar, The American College, Madurai Kamaraj University, Madurai, Tamilnadu, “Study of Exoplanet Atmosphere”, from May 2021 to July 2021, [Supervisor: Kinsuk Acharyya].

29. Malika Singal, Physical Research Laboratory, “TL property of refractory minerals from primitive meteorites”, from Aug 2021 to Dec 2021, [Supervisor: Kuljeet Kaur Marhas].
30. Advait Uninthan, St. Xaviers, “GCR interaction with silicate presolar grains in ISM”, from Dec 2020 to June 2021, [Supervisor: Kuljeet Kaur Marhas].
31. Sourajit Sahoo, IISER Pune, “Carbon diffusion in IAB Iron meteorite”, from July 2021 to June 2022, [Supervisor: Kuljeet Kaur Marhas].
32. Jeel, Institute of Advanced Research, Gandhinagar, “Sulphur isotopes in Novae”, from May 2021 to July 2021, [Supervisor: Kuljeet Kaur Marhas].
33. Rajvee Sheth, Gujarat University, “Machine Learning based Hydroxyl signature detection utilizing M3 data from Chandrayan-1”, from Feb 2022 to June 2022, [Supervisor: Megha Bhatt].
34. Roshni Ramnani, Gujarat University, “Machine Learning based Hydroxyl signature detection utilizing M3 data from Chandrayan-1”, from Feb 2022 to June 2022, [Supervisor: Megha Bhatt].
35. Lad Virangkumar, St. Xaviers College, Ahmedabad, “Reflectance spectroscopy of Moon analogues under simulated conditions”, from Jan 2022 to June 2022, [Supervisor: Neeraj Srivastava].
36. Sarangu. S., Earth System Science, IIST Trivandrum, “Geological investigation of Cerulli crater, Mars: Insights into the history of glacial processes”, from July 2021 to May 2022, [Supervisor: Rishitosh Kumar Sinha].
37. Sharini, College of Engineering, Anna University, Chennai, “Mars Imbrium age estimation”, from April 2021 to April 2022, [Supervisor: S. Vijayan].
38. Tuhi Saumya, College of Engineering, Anna University, Chennai, “Impact craters and its role in Mars evolution”, from April 2021 to April 2022, [Supervisor: S. Vijayan].
39. Manish Kumar Singh, Amity University, Noida, “Dust Influence on Planetary Plasma Environment, Subtitle: Exploring the possibility of ultralow frequency DA wave excitations in dusty ionosphere of Mars”, from Jan 2021 to May 2021, [Supervisor: Sanjay K. Mishra].
40. Mishal Mehta, St. Xaviers College, Ahmedabad, “MAVEN-NGIMS & MOM-MENCA data analysis”, from Jan 2022 to Sept 2022, [Supervisor: Shiv Kumar Goyal].
41. Debayan Rakshit, Pandit Deendayal Energy University, Gandhinagar, “Python based data processing for particle detectors”, from Jan 2022 to May 2022, [Supervisor: Shiv Kumar Goyal].
42. Sakshi Jagani, Indus university, Ahmedabad, “Python based data processing for particle detectors”, from Jan 2022 to May 2022, [Supervisor: Shiv Kumar Goyal].

Space and Atmospheric Sciences

43. Kelvy P Dalsania, St. Xaviers College, Ahmedabad, “Performance evolution of F-layer peak height models in IRI-2016 over the Indian equatorial and low latitudes”, from January 2022 to June 2022, [Supervisor: K. Venkatesh].
44. Yashraj Nagraj Upase, National Institute of Technology, Surathkal, Karnataka, “Tropospheric Ozone and CO Variation in Hyderabad Region”, from 27 May 2021 to 31 July 2021, [Supervisor: Lokesh Kumar Sahu].
45. Jyoti Verma, Indian Institute Of Technology, Jodhpur, “Ozone variation in troposphere”, from 27 May 2021 to 31 July 2021, [Supervisor: Lokesh Kumar Sahu].
46. Ashish Ojha, Banaras Hindu University, Varanasi, “Hydroxyl Radical in the Atmosphere”, from 27 May 2021 to 31 July 2021, [Supervisor: Lokesh Kumar Sahu].
47. Easwaran C. E., NSS Hindu College, Changanacherry, Mahatma Gandhi University, Kerala, “Investigations of Wave and Clouds using ground based LIDAR and Satellite observations”, from May 2021 to August 2021, [Supervisor: Som Kumar Sharma].
48. Aditya Mishra, University Institute of Engineering and Technology, Babasaheb Bhimrao Ambedkar University, Lucknow, UP, “Atmospheric Clouds and Atmospheric Boundary Layer”, from May 2021 to August 2021, [Supervisor: Som Kumar Sharma].
49. Mittal Parmar, Sardar Vallabhbhai National Institute of Technology, Surat, Gujarat, “Investigations of Wave-Cloud Interactions using Satellite Observations”, from May 2021 to August 2021, [Supervisor: Som Kumar Sharma].
50. K. Mallikarjun, CSSTEAP student (Space Science Course) and employee at NRSC (ISRO), Hyderabad., “Study of regional variation of Greenhouse Gas concentrations and the effect of Land use/ Land Cover Change on its variation over Indian region using long term satellite observations”, September 2021. [Supervisor: Som Kumar Sharma].
51. Chandrima Shaw, PRL, “Distribution of trace gases over the Indian Subcontinent”, from August 2021 to December 2021, [Supervisor: Narendra Ojha].
52. Kiran, PRL, “Increasing trends of heatwave over India”, from August 2021 to December 2021, [Supervisor: Narendra Ojha].
53. Ankush G. K., BITS Pilani, “Analysis of surface ozone variation using machine learning”, from May 2021 to July 2021, [Supervisor: Narendra Ojha].
54. Ishita Tanna, S. P. University, “Climate change and heatwaves”, from August 2021 to December 2021, [Supervisor: Narendra Ojha].
55. Sanket Karkathala, Gujarat University, “Atmospheric modeling”, from May 2021 to July 2021, [Supervisor: Narendra Ojha].
56. Nancy Abraham, Pandit Deendayal Energy University, Gandhinagar, “Derivation of Gravity Wave Parameters using Spectral analysis of Nightglow Emission Brightness and Temperatures”, from Dec 2021 to March 2022, [Supervisor: Ravindra Pratap Singh].
57. Devanshi Shukla, St. Xaviers College, Ahmedabad, “High Latitude Mesospheric Temperatures during Sudden Stratospheric Warming events”, from Jan 2022 to May 2022, [Supervisor: Ravindra Pratap Singh].
58. Kinjal Jayantkumar Patel, St. Xaviers College, Ahmedabad, “Characteristics of Sudden Stratospheric Warming events over last 20 years”, from Jan 2022 to June 2022, [Supervisor: Ravindra Pratap Singh].

Geosciences

59. Emansi Yadav, Miranda House, University of Delhi, New Delhi, “Inhaled aerosols: Lung deposition, hazards and applications”, from May 2021 to July 2021, [Supervisor: Neeraj Rastogi].
60. Mansi Gupta, Physical Research Laboratry, Ahmedabad, “Optical properties of brown carbon in Water-soluble Organic Carbon”, from June 2021 to July 2021, [Supervisor: Neeraj Rastogi].
61. Akanksha, Physical Research Laboratory, Ahmedabad, “Brown carbon and their characteristic optical properties: a summary”, from August 2021 to December 2021, [Supervisor: Neeraj Rastogi].
62. Kamran Ansari, Physical Research Laboratory, Ahmedabad, “Study of atmospheric aerosols: Secondary formation of inorganic and organic aerosols”, from August 2021 to December 2021, [Supervisor: Neeraj Rastogi].
63. Anuj Kumar Singh, IIT - Bombay, “Effect of cyclone on water isotopic composition”, from May 2021 to July 2021, [Supervisor: Arvind Singh].
64. Akansha Verma, Gujarat University, “Geochemistry of foraminefera”, from January 2022 to March 2022, [Supervisor: Arvind Singh].
65. Shalini Singh, Banaras Hindu University, Varanasi, “Spatial and seasonal variations of stable isotope ratios of Indian rivers”, from January 2021 to December 2021, [Supervisor: Amzad H. Laskar].
66. Shikhar Dubey, Physical Research Laboratory, Ahmedabad, “Estimation of the fossil fuel component in atmospheric CO_2 in Ahmadabad based on radiocarbon measurements”, from January 2021 to May 2021, [Supervisor: Amzad H. Laskar].
67. Sudhanshu Singh, Physical Research Laboratory, Ahmedabad, “Estimating the contributions of CO_2 from different sources in air in Ahmedabad using stable carbon and oxygen isotope ratios”, from January 2021 to May 2021, [Supervisor: Amzad H. Laskar].
68. Uddalak Chakraborty, Banaras Hindu University, Varanasi, “Mixing ratios and stable isotopes in CO_2 and N_2O in a coastal station of a western pacific island: quantification of influences from regional and long range transported sources”, from May 2021 to July 2021, [Supervisor: Amzad H. Laskar].
69. Ananya Srivastava, Babasaheb Bhimrao Ambedkar University, Lucknow, “Role of climate on human civilization and vegetation in the north and north-western India”, from August 2021 to October 2021, [Supervisor: Amzad H. Laskar].
70. Aditya Das, Physical Research Laboratory, Ahmedabad, “Groundwater Situation in the Indo-Gangetic Plain”, from October 2021 to December 2021, [Supervisor: Amzad H. Laskar].
71. Shreya Mehta, Physical Research Laboratory, Ahmedabad, “$^{87}Sr/^{86}Sr$ and Sr concentrations in the catchment of west-flowing Ambika River basin draining the Deccan Traps: Implication to Silicate erosion rate and CO_2 drawdown”, from August 2021 to December 2021, [Supervisor: Vineet Goswami].

Theoretical Physics

72. Drona Vatsyayan, University of Delhi, “Possibility of low scale Leptogenesis in Type-III seesaw scenarios”, from 12/7/2021 to 11/8/2021, [Supervisor: Srubabati Goswami].
73. Prashant Sheladiya, Institution MS University, Baroda, “Low earth altitude variation of muon flux using GM counter”, from 10/01/2022 to 7/05/2022, [Supervisor: Navinder Singh].
74. Writasree Maitra, Physical Research Laboratory, “Dark matter phenomenology”, from 01/01/2022 to 30/04/2022, [Supervisor: Partha Konar].
75. Deepanshu Srivastava, Physical Research Laboratory, “Primordial Black Hole as Dark matter”, from 01/01/2022 to 30/04/2022, [Supervisor: Partha Konar].
76. Gurucharan Mohanta, Physical Research Laboratory, “Inclusive Higgs production at the LHC”, from 10/05/2021 to 09/07/2021, [Supervisor: Satyajit Seth].
77. Debashis Pachhar, Physical Research Laboratory, “First order QCD corrections to the Drell-Yan process”, from 10/05/2021 to 09/07/2021, [Supervisor: Satyajit Seth].

Atomic, Molecular and Optical Physics

78. Anil Devara, SRF, Maharaja Sayajirao University, Baroda, “Luminescence dating of archaeological palaeolithic samples”, from Nov 1,2021 to Nov 20,2021, [Supervisor: Naveen Chauhan].
79. Dr. Ravi Kant, PDF, IIT Gandhinagar, “Luminescence dating of lake sediment deposits in Rajasthan”, from March 15, 2022 to June 15, 2022, [Supervisor: Naveen Chauhan].
80. Dr.Saptarishi Dey, Inspire Faculty, IIT Gandhinagar, “Luminescence dating for Himalayan Samples”, from July 5, 2021 to July 9, 2021, [Supervisor: Naveen Chauhan].
81. Varsha M Vijay, Mahatma Gandhi University, Kottayam, “MATLAB based code for Dose Rate Estimation in Luminescence Dating”, from 27 May 2021 to 23 July 2021, [Supervisor: Naveen Chauhan].
82. Manasa VS, Pondicherry University,Puducherry, “Exploring Dosimeters suitable for radiation Dosimetry for high let radiation fields in space”, from 27 May 2021 to 23 July 2021, [Supervisor: Naveen Chauhan].
83. M Vyshak Menon, Lovely Professional University,Phagwara, “Effect of sensitization on Luminescence Parameters”, from 27 May 2021 to 23 July 2021, [Supervisor: Naveen Chauhan].

Information Technology

84. Krittika Iyer, Institute of Technology, Nirma University, Ahmedabad, “Online Application Management System”, from 01 June 2021 to 29 June 2021, [Supervisor: Dinesh Mehta].

Division Visitors

Astronomy and Astrophysics

1. Somnath Dutta, Institute of Astronomy and Astrophysics, Academia Sinica (ASIAA), Taiwan, “Collaborative Work”, from 20-02-2022 to 27-02-2022,[Seminar: “Jets and outflows properties of extremely Young Stellar Objects”].

Planetary Sciences

2. Dr. Alik S. Majumder, Indian Institute of Technology (Indian School of Mines), Dhanbad, “Abiotic synthesis of methane at the recess of Martian crust and prospect of microbial life in the Noachian Mars - Constraints from experimental and meteorite studies.”, from 14-03-2022 to 19-03-2022.

Space and Atmospheric Sciences

3. Dr. Bhargav Vaidya, Assistant Professor, IIT-Indore, “Scientific discussions”, from 19-03-2022 to 25-03-2022,[Seminar: “Developing a space weather modeling framework in the era of Aditya-L1”].

Geosciences

4. Dr Shubha Anand, National Insitute of Oceanography (NIO), Goa, “for scientific analysis”, from 04-01-2022 to 31-03-2022.
5. Ms. Garima Shukla, CSIR-National Insitute of Oceanography, Goa, “To perform experimental work.”, from 08-02-2022 to 22-02-2022.
6. Dr. Mar Benavides, Scientific Researcher (tenured), French National Research Institute for Sustainable Development (IRD), Mediterranean Institute of Oceanography (MIO), France, “for collaborative work under DST sponsered project”, from 15-03-2022 to 24-03-2022.

Astronomy and Astrophysics

Acceleration of Solar Energetic Particles by the Shock of Interplanetary Coronal Mass Ejection

Solar Energetic Particles (SEP) are highly energetic particles emanating from the Sun. They are detected soon after solar flares or when the heliospheric particle detectors encounter Interplanetary Coronal Mass Ejections (ICMEs). Intense SEP events may become hazardous for humans in space and can also damage the electronics of space instruments. The detailed energization mechanisms of these particles are still enigmatic. However, observations suggest that they either get energized at magnetic reconnection sites or by the ICME shocks. We simulate (see Figure 1) such particle energization in ICME shocks with a sophisticated Magnetohydrodynamic-Particles in Cell code. We find that the energization process depends on the angle between the shock normal and the upstream magnetic field. The Mach number of the shock also plays a vital role in energizing the particles. Our simulations suggest that when the shock normal is roughly along the upstream magnetic field, the energetic particles generate turbulence by means of instability in the shock upstream. Through these simulations, we suggest ways to further explore the observation data that may confirm various physical processes occurring around ICME shocks.

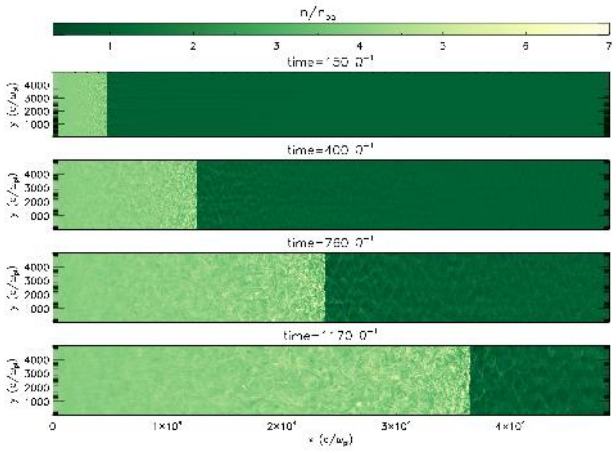

Figure no. 1: Time evolution of particle density around the shock. The shock is moving from left to right. Irregularities in density are because of the turbulence created by the energetic particles.

This work was done in collaboration with B. Vaidya of Indian Institute of Technology, Indore, India and A. Mignone of Universita di Torino, Torino, Italy.

doi : https://doi.org/10.3847/1538-4357/ac2c7a

(S. Sow Mondal and A. Sarkar)

Evolution of Elemental Abundances During B-Class Solar Flares: Soft X-ray Spectral Measurements with Chandrayaan-2 XSM

Determining elemental abundances at different layers of the Sun is crucial for understanding the mass and energy outflow from the star. It has been observed that abundances of certain elements whose First Ionization Potential (FIP) is lower than 10eV are 2-4 times more abundant in the atmosphere of the magnetically active regions of the Sun than that of the solar surface. The phenomenon is popularly known as the FIP bias of the Sun. This has been studied extensively in the past decades. However, the time evolution study of elemental abundances during the transient events, e.g., the solar flare was limited due to instrumental limitation.

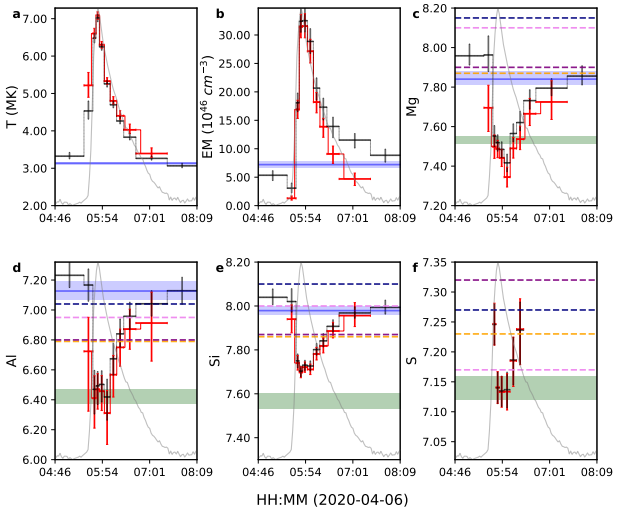

Figure no. 2: The six panels show the results of the time-resolved X-ray spectroscopy of a B-class flare using XSM observations. Panels (a-b) show the variation of the temperature and emission measure, respectively, while, panels (c-f) show the variation of the elemental abundances during the flare. The gray curve in the background shows the temporal profile of the flare. The violet and green bands represent the range of coronal and photospheric abundances.

The Solar X-ray Spectrometer (XSM) onboard the Chandrayaan-2 orbiter, measures the soft X-ray of the Sun at every second in the energy range of 1 - 15 keV. Its high energy resolution (180 eV at 5.9 keV), high sensitivity and high time cadence is ideal for the time-resolved spectroscopy to study the abundance evolution during impulsive events like solar flares. During the period from 2019 September to 2020 May, covering the minimum of Solar Cycle 24, the XSM observed nine B-class flares ranging from B1.3 to B4.5. Using time-resolved spectroscopic analysis during these flares, we examined the evolution of temperature, emission measure, and absolute elemental abundances of four elements-Mg, Al, Si, and S.

These are the first measurements of absolute abundances during such small flares and this study offers a unique insight into the evolution of absolute abundances as the flares evolve. Our results (Figure 2) demonstrate that the abundances of these four elements decrease toward their photospheric values during the peak phase of the flares. During the decay phase, the abundances are observed to quickly return to their preflare coronal values. The depletion of elemental abundances during the flares is consistent with the standard flare model, suggesting the injection of fresh material into coronal loops as a result of chromospheric evaporation. The observation of quick recovery to the coronal abundance values is a totally new, and can not be explained in terms of conventional model. This observation shows that any process giving rise to such fractionation must be occurring on a time scale of few tens of minutes. To explain the quick recovery of the FIP bias, two scenarios are proposed based on the Ponderomotive force model. One of the scenarios suggests the presence of the long sought after, alfven waves induced by magnetic reconnection, in the flaring loops.

This work was done in collaboration with G. Del Zanna and H. E. Meson of Cambridge University, UK; and S. Narendranath of SAG, URSC.

doi : https://doi.org/10.3847/1538-4357/ac14c1

(B. Mondal, A. Sarkar, S. Vadawale, N. P. S. Mithun and P. Janardhan)

The disk-outflow system around the rare young O-type protostar W42-MME

Unraveling the exact formation mechanism of massive OB-type stars ($M \gtrsim 8\ M_\odot$) is one of the outstanding issues in massive star formation research. It is directly related to the understanding of the process of mass accumulation in massive star formation, which is also a key open research problem. Both theoretical and observational studies of the birth process of massive stars have been extensively performed, and face serious difficulties. In this context, the inner circumstellar environment (1000–10000 AU scales) of the O-type protostar (W42-MME; distance ∼3.8 kpc) has been examined using the multi-scale and multi-wavelength continuum and line data sets (resolutions ∼0.3 arcsec – 3.5 arcsec). These data sets have been analyzed to examine in detail the morphological and kinematical structure of the molecular gas immediately associated with and surrounding the rare jet-outflow system near the O-type protostar. The ALMA 1.35 mm continuum map (resolution ∼1 arcsec) shows that W42-MME is embedded in one of the cores (i.e., MM1) located within a thermally supercritical filament-like feature (extent ∼0.15 pc) containing three cores (mass ∼1–4.4 $M_\odot$). Several dense/hot gas tracers are detected toward MM1, suggesting the presence of a hot molecular core with the gas temperature of ∼38–220 K. The ALMA 865 m continuum map (resolution ∼0.3 arcsec) reveals at least five continuum sources/peaks ("A-E") within a dusty envelope (extent ∼9000 AU) toward MM1, where shocks are traced in the SiO(8-7) emission. The source "A associated with W42-MME is seen almost at the center of the dusty envelope, and is surrounded by other continuum peaks. The ALMA CO(3-2) and SiO(8-7) line observations show the bipolar outflow extended below 10000 AU, which is driven by the source "A (see Figures 3a and 3b). The ALMA data hint the episodic ejections from W42-MME. A disk-like feature (extent ∼2000 AU; mass ∼1 $M_\odot$; see Figure 3a) with velocity gradients is investigated in the source "A (dynamical mass ∼9 $M_\odot$) using the ALMA $H^{13}CO^+$ emission, and is perpendicular to the CO outflow. Furthermore, it is found that the core forming the massive protostar does not accumulate all the mass before core collapse, but instead, the core and embedded protostar gain mass simultaneously. Overall, W42-MME appears to gain mass from its disk and the dusty envelope.

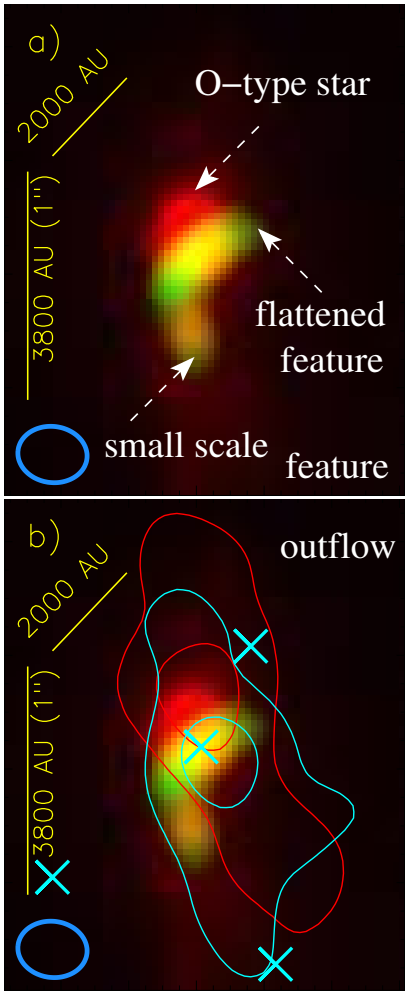

Figure no. 3: A zoomed-in view of the core hosting the O-type protostar (W42-MME). a) The panel shows a two color-composite map (VLT/NACO L' band/3.8 μm image (red) + ALMA $H^{13}CO^+$ map (green)). b) The panel is the same as the left-panel but overlaid with the CO outflow lobes. Multiplication symbols indicate the positions of the continuum sources.

This work was done in collaboration with I. I. Zinchenko (IAP RAS, Russia), P. M. Zemlyanukha (IAP RAS, Russia), S.-Y. Liu (ASIAA, Taiwan), Y.-N. Su (ASIAA, Taiwan), S. E. Kurtz (IRyA UNAM, México), D. K. Ojha (TIFR, India), A. G. Pazukhin (IAP RAS, Russia), and Y. D. Mayya (INAOE, México).

doi: https://doi.org/10.3847/1538-4357/ac36dd

(L. K. Dewangan)

Probing gas kinematics and PDR structure around O-type stars in Sh 2-305 HII region

Massive OB-type stars ($M_* > 8\ M_\odot$) drive powerful energetics, which allow them to control the physical state of the interstellar medium (ISM). The extreme ultraviolet (EUV; $h\nu \geq 13.6$ eV) photons from such massive stars ionize the hydrogen atoms and create HII regions. Due to the thermal pressure difference between the ionized region and the surrounding neutral/molecular gas, an HII region continues to grow in size, and may trigger star formation in numerous ways.

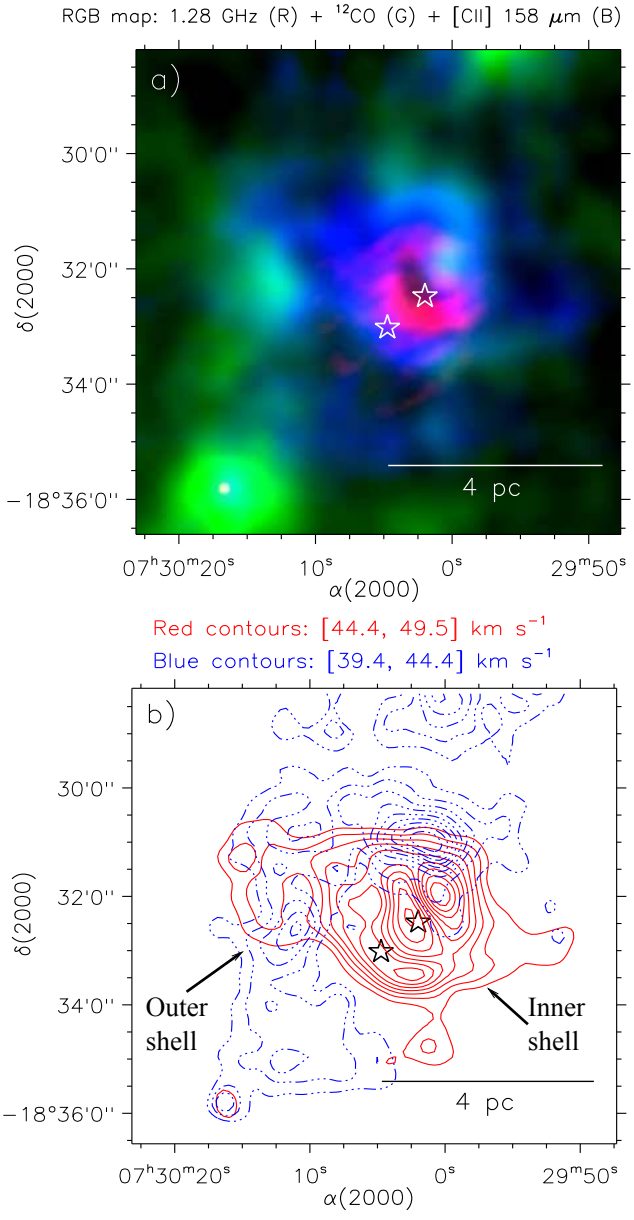

Figure no. 4: (a) Three-color (Red: GMRT 1.28 GHz, Green: FUGIN ^{12}CO(1-0), Blue: SOFIA [CII] 158 μm) composite map of S305. (b) The [CII] emission contours for the inner (in red) and outer (in blue) shell structures. The red contour levels range from 23.34 to 93.36 K km/s in steps of 7.78 K km/s, while the blue contour levels range from 19.57 to 65.24 K km/s in steps of 5.07 K km/s. The stars are the positions of previously known massive O-type stars. A scale bar referring to 4 pc (at a distance of 3.7 kpc) is also displayed.

However, the study of the interaction of massive stars with their surrounding environment is still an open research topic in astrophysics. In this relation, we carried out an analysis of the [CII] 158 μm line data of the Galactic HII region Sh 2-305/S305 (distance ∼3.7 kpc), which has enabled us to examine the gas dynamics and structure of photodissociation regions. The integrated [CII] emission map at [39.4, 49.5] km/s spatially traces two shell-like structures (i.e., inner and outer neutral shells; see Figures 4a and 4b) having a total mass of ∼565 $M_\odot$. The inner neutral shell encompasses an O9.5V star at its centre and has a compact ring-like appearance. However, the outer shell is seen with more extended and diffuse [CII] emission, hosting an O8.5V star at its centre and surrounds the inner neutral shell. The velocity channel maps and position-velocity diagrams confirm the presence of a compact [CII] shell embedded in the diffuse outer shell, and both the shells seem to expand with vexp ∼1.3 km/s. The outer shell appears to be older than the inner shell, hinting that these shells are formed sequentially. The [CII] profiles are examined toward S305, which are either double-peaked or blue-skewed and have the brighter redshifted component. The redshifted and blueshifted components spatially trace the inner and outer neutral shell geometry, respectively. The ionized, neutral, and molecular zones in S305 are seen adjacent to one another around the O-type stars (see Figure 4a). The regularly spaced dense molecular and dust clumps (mass ∼10–10^3 $M_\odot$) are investigated around the neutral shells, which might have originated due to gravitational instability in the shell of collected materials.

This work was done in collaboration with P. M. Zemlyanukha (IAP RAS, Russia), D. K. Ojha (TIFR, India), I. I. Zinchenko (IAP RAS, Russia), and Saurabh Sharma (ARIES, India).

doi : https://doi.org/10.3847/1538-4357/ac2a44

(N. K. Bhadari and L. K. Dewangan)

Lynds Bright Nebulae: Sites of possible twisted filaments and ongoing star formation

In the last decade, the study of infrared (IR) and sub-millimeter (sub-mm) observations revealed that filaments are common structures in low-mass and high-mass star-forming regions and their role in the star formation processes has been evident. In this context, one can study the signatures of the convergence of filaments toward the compact and dense hub, the intersection/merging of filaments, and the collisions of filaments, which can explain the ongoing physical processes in star-forming regions. In such events/scenarios, the highest column density can be observed in the interaction zones of filaments. Additionally, a filament braid, where continuous multiple filaments are twisted, could also be considered as one of the interesting star-forming sites. In such configuration, multiple common zones with high column densities are expected. However, in the literature, we do not find any promising star-forming sites where the twisting of filaments is investigated. In this relation, this work is focused on two Lynds Bright Nebulae (LBN), LBN 140.07+01.64 and LBN 140.77−1.42 (distance ∼2 kpc). The 1420 MHz continuum map reveals an extended Y-shaped feature (linear extent ∼3.7 degree), which consists of a linear part and a V-like structure. The sites LBN 140.07+01.64 and AFGL 437 are located toward the opposite sides of the V-like structure, and LBN 140.77−1.42 is spatially seen toward the linear part. Infrared-excess sources are traced toward the entire Y-feature, suggesting star formation activities. Infrared and

sub-millimeter images show the presence of at least two large-scale dust filaments extended toward the LBN sources. The Herschel maps, which are available only toward the northern and central parts of the Y-feature, display the presence of higher column density ($\geq 2.4 \times 10^{21}$ cm^{-2}) of materials toward the filaments (see Figures 5a and 5b toward the northern part of the Y-feature). Using the ^{12}CO(1-0) line data, the distribution of molecular gas at [−42.7, −34.4] km/s traces the cloud associated with the Y-feature, and confirms the existence of filaments (see Figures 5c and 5d). The large-scale filaments appear to be possibly spatially twisted. There is a hint of an oscillatory-like velocity pattern along both the filaments, favouring their proposed twisted nature. It is the first study showing the possible twisting of filaments, which is more prominent in the northern and central parts of the Y-feature. This possible twisting/coupling of the large-scale filaments appears to be responsible for the observed star formation (including known OB-stars). The proposed physical process and the energetics of OB-stars together seem to explain the origin of the ionized Y-feature.

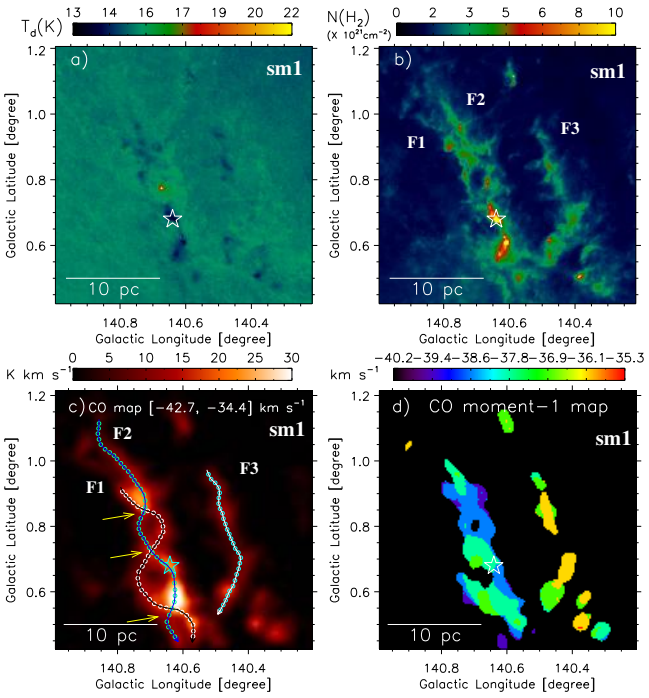

Figure no. 5: a) Herschel temperature map of the subregion "sm1, which is located northern part of the Y-feature. b) Herschel column density map of "sm1. c) The ^{12}CO(1-0) emission (moment-0) map of "sm1. Three Filaments (i.e., F1, F2, and F3) are highlighted by curves. Several small open circles (radii = 20 arcsec) are also marked along each filament. Arrows highlight the common zones of the filaments F1 and F2. d) The ^{12}CO(1-0) moment-1 map of "sm1. In each panel, a star symbol indicates the location of a previously known star-forming region, and the scale bar referring to 10 pc (at a distance of 2.0 kpc) is shown.

This work was done in collaboration with J. S. Dhanya (MNIT, India), D. K. Ojha (TIFR, India), and T. Baug (SNBNCBS, India).

doi : https://doi.org/10.1093/mnras/stab2137

(L. K. Dewangan and N. K. Bhadari)

A Comprehensive Study of the Young Cluster IRAS 05100+3723: Properties, Surrounding Interstellar Matter, and Associated Star Formation

Formation of massive young clusters is unknown. In this work, we present a comprehensive multi-wavelength investigation of a likely massive young cluster "IRAS 05100+3723" and its environment with the aim to understand its formation history and feedback effects. We find that IRAS 05100+3723 is a distant (∼3.2 kpc), moderate-mass (∼500 M$_\odot$), young (∼3 Myr) cluster with its most massive star being an O8.5V type. From spectral modelling, we estimate the effective temperature and log g of the star to be ∼33,000 K and ∼3.8, respectively. Modelling to radio continuum observation emission reveals that the star has ionised its environment, forming an H II region of size ∼2.7 pc, temperature ∼5700 K, and electron density ∼165 cm^{-3} (See Figure 6). However, our large-scale dust maps reveal that it has heated the dust up to several parsecs (∼10 pc) in the range 17–28 K and the morphology of warm dust emission resembles a bipolar H II region. From dust and CO gas analyses, we find evidence that the formation of the H II region has occurred at the very end of a long filamentary cloud around 3 Myr ago, likely due to edge collapse of the filament. We show that the H II region is currently compressing a clump of mass ∼2700 M$_\odot$ at its western outskirts, at the junction of the H II region and filament. We observe several 70 μm point sources of intermediate mass and class 0 nature within the clump. We attribute these sources as the second-generation stars of the complex. We propose that the star formation in the clump is either induced or being facilitated by the compression of the expanding H II region onto the inflowing filamentary material.

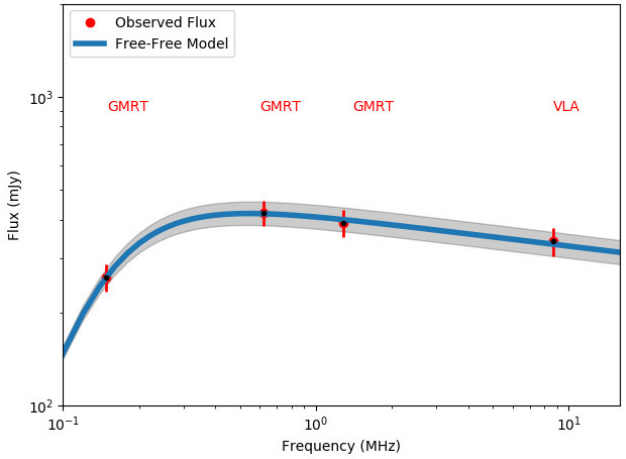

Figure no. 6: Free-Free emission modelling to the radio continuum observations of the H II region.

This work has been done in collaboration with Ramkesh Yadav, E. Semenko (NARIT, Thailand), A. Zavagno (LAM, France) and other collaborators from various national and inter-national institutes/organizations

doi : https://doi.org/10.3847/1538-4357/ac3a78

(Manash Samal and Prachi Prajapati)

Subaru Hyper Suprime-Cam Survey of Cygnus OB2 Complex – I: Introduction, Photometry and Source Catalog

Low mass star formation inside massive clusters is crucial to understand the effect of cluster environment on processes like circumstellar disk evolution, planet and brown dwarf formation. The young massive association of Cygnus OB2, with strong feedback from massive stars, is an ideal target to study the effect of extreme environmental conditions on its extensive low-mass population. We aim to perform deep multi-wavelength studies to understand the role of stellar feedback on the IMF, brown dwarf fraction and circumstellar disk properties in the region. We introduce here, the deepest and widest optical photometry of 1.5 degrees diameter region centered at Cygnus OB2 in r2, i2, z and Y-filters using Subaru Hyper Suprime-Cam (HSC). This work presents the data reduction, source catalog generation, data quality checks and preliminary results about the pre-main sequence sources. We obtain 713,529 sources in total, with detection down to $\sim$28 mag, 27 mag, 25.5 mag and 24.5 mag in r2, i2, z and Y-band respectively, which is $\sim$3 - 5 mag deeper than the existing Pan-STARRS and GTC/OSIRIS photometry. We confirm the presence of a distinct pre-main sequence branch by statistical field subtraction of the central 18$'$ region. We find the median age of the region as $\sim$5 $\pm$ 2 Myrs with an average disk fraction of $\sim$9%. At this age, combined with AV $\sim$6 - 8 mag, we detect sources down to a mass range $\sim$0.01 - 0.17 $M_{\odot}$. The deep HSC catalog will serve as the groundwork for further studies on this prominent active young cluster.

This work has been done in collaboration with Saumya Gupta, Jessy Jose (IISER Tirupati), Surhud More (IUCCA) and other collaborators from various national and international institutes/organizations.

doi : https://doi.org/10.1093/mnras/stab2751

(Manash Samal)

Testing the role of environmental effects on the initial mass function of low-mass stars

In the star-formation process, the vital impact of environmental factors such as feedback from massive stars and stellar density on the form of the initial mass function (IMF) at the low-mass end is yet to be understood.

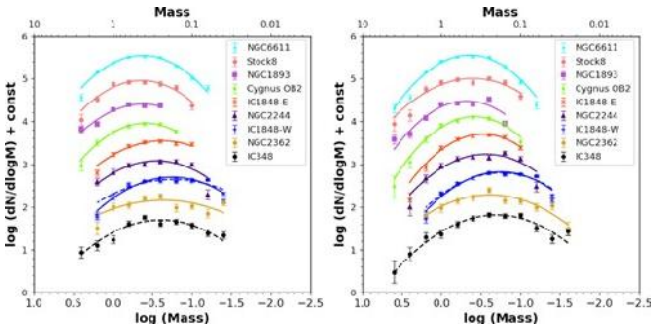

Figure no. 7: The IMF derived from the J band (left) and K band (right) for all the clusters. Error bars denote the Poisson error on each data point. The curves are the lognormal fits to the individual cluster IMF. The blue dotted curve shows the IMF estimated by applying the extinction correction to individual sources of the IC 1848-West cluster.

Hence, a systematic highly sensitive observational analysis of a sample of regions under diverse environmental conditions is essential. We analyse the IMF of eight young clusters (<5 Myr), namely IC 1848-West, IC 1848-East, NGC 1893, NGC 2244, NGC 2362, NGC 6611, Stock 8, and Cygnus OB2, which are located at the Galactocentric distance (Rg) range $\sim$6-12 kpc along with the nearby cluster IC 348 using deep near-IR photometry and Gaia DR2. These clusters are embedded in massive stellar environments of radiation strength log(LFUV/$L_{\odot}$) $\sim$2.6-6.8, log(LEUV) $\sim$42.2-50.85 photon s^{-1}, with stellar density in the range of $\sim$170-1220 star pc^{-2}. After structural analysis and field decontamination we obtain an unbiased uniformly sensitive sample of per-main-sequence members of the clusters down to the brown-dwarf regime. The log-normal fit, shown in Figure 7, to the IMF of nine clusters gives the mean characteristic mass (mc) and σ of 0.32 $\pm$ 0.02 $M_{\odot}$ and 0.47 $\pm$ 0.02, respectively. We compare the IMF with that of low- and high-mass clusters across the Milky Way. We also check for any systematic variation with respect to the radiation field strength and the stellar density as well with Rg. We conclude that there is no strong evidence for an environmental effect in the underlying form of the IMF of these clusters.

This work has been done in collaboration with Damian Belinda, Jessy Jose (IISER Tirupati), Moraux Estelle (France) and other collaborators from various national and inter-national institutes/organizations.

doi : https://doi.org/10.1093/mnras/stab194

(Manash Samal)

Discovery of TOI-1789b, an Inflated Hot-Jupiter around Sub-Giant Star

PRL has discovered a Hot-Jupiter orbiting in a short orbit, at a period of 3.208664 ± 0.000015 days around TOI-1789 (TESS_{mag} = 9.1). This is the second exoplanet discovery from India. This is also a very unique discovery as there are less than 10 such kinds of planets known so far existing around the evolved stars. Such discoveries help us understand the physics of formation of planets around stars and as well as the physics of orbital dynamics.

Initially identified as an exoplanetary candidate using the TESS photometry data, pending for further necessary observations, the exoplanet was finally discovered using the follow-up ground-based transit data from PRLs 43cm Telescope and the mass measurements from the high-resolution spectrographs, PARAS at PRL, India and TCES at TLS, Germany. TOI-1789 is an evolved metal rich late F-type star, with a radius of $R_* = 2.168^{+0.036}_{-0.034}$ $R_{\odot}$ located at a distance of $223.53^{+0.91}_{-0.90}$ pc. The global modelling of the all the datasets (multiple light curves and the RV datasets; see Figure 8) of TOI-1789 reveals that TOI-1789b has a mass of $M_P = 0.70 \pm 0.16$ M_J, a radius of $R_P = 1.44^{+0.24}_{-0.14}$ R_J, and a bulk density of ρ_P = $0.28^{+0.14}_{-0.12}$ g cm^{-3} with an orbital separation of $a = 0.04882^{+0.00063}_{-0.0016}$ AU. This makes it one of the lowest density exoplanets known so far. TOI-1789b falls under a very unique category of 10 exoplanets among all the known ones, which are orbiting the evolved or ageing stars in a very close orbit (within 0.05 AU). Due to such closeness to its parent star, the planet has high incidence flux and high surface temperature of $\sim$2000 K, which is the main reason behind the inflated radius of TOI-1789b.

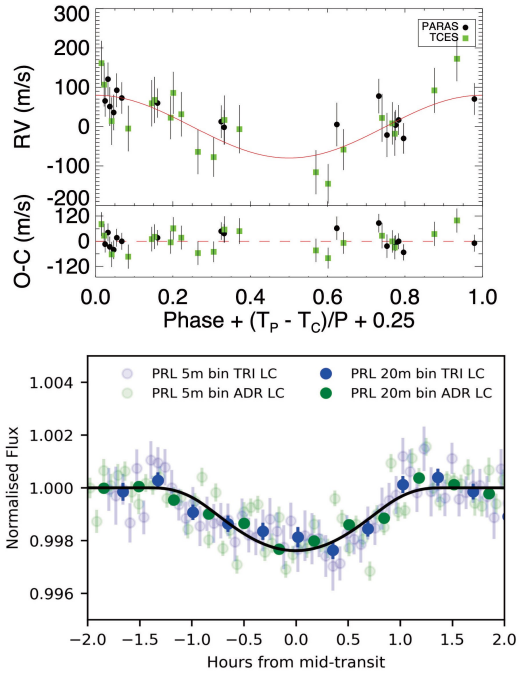

Figure no. 8: Top Panel is showing the phased RV data points along with the best fit orbital model, while the bottom panel shows the ground-based transit data acquired using PRLs 43 cm telescope. Overlaid is the best fit transit model from global modelling. TRI and AND stands for TRIUS CCD and ANDOR CCD, respectively.

This work has been done in collaboration with Dr. Priyanka Chaturvedi of Thuringer Landessternwarte Tautenburg, Germany.

doi : `https://academic.oup.com/mnras/advance-article/doi/10.1093/mnras/stab2970/6409152`

(Akanksha Khandelwal, Abhijit Chakraborty, Rishikesh Sharma, Neelam J S S V Prasad, Ashirbad Nayak and Dishendra)

Optical and near-infrared spectroscopy of Nova V2891 Cygni: evidence for shock-induced dust formation

Nova outbursts are caused by thermonuclear runaway events on the surface of a degenerate white dwarf, which has accreted gas from the Roche-lobe overflow of a secondary star in a close binary system. Nova V2981 Cyg was discovered in September 2019 and later classified as a slow nova of Fe II class. Nova V2891 Cyg had been followed in optical wavelengths with indigenously developed MFOSC-P instrument on PRL 1.2m Mt. Abu telescope and other worldwide facilities for its multi-wavelength evolution for nearly 15 months since its discovery. The photometric monitoring of the object revealed it to be a very slow nova (one of the slowest novae recorded in recent times) with a rather unusual, nearly flat, light curve. The evidence that the current outburst of V2891 Cyg has undergone several distinct episodes of mass ejection is seen through time-varying P Cygni profiles of the O I 7773Å line (Figure 9). Such episodes of mass ejection provided the most suitable environment for the shocks. It is proposed that these shock-induced conditions gave rise to the high-excitation coronal lines emissions during the nova evolution. A short period of dust formation also occurred, which coincided with the appearance of these coronal emission lines. The simultaneous occurrence of the dust and coronal lines (with varying velocity shifts) supports the possibility that dust formation was also shock-induced. Such a route for dust formation has not previously been seen in a nova, and these phenomena are rare in the evolution of novae. Thus, the data set of this observational campaign and our associated analysis would be of interest to the community to explore the physics of the nova phenomenon.

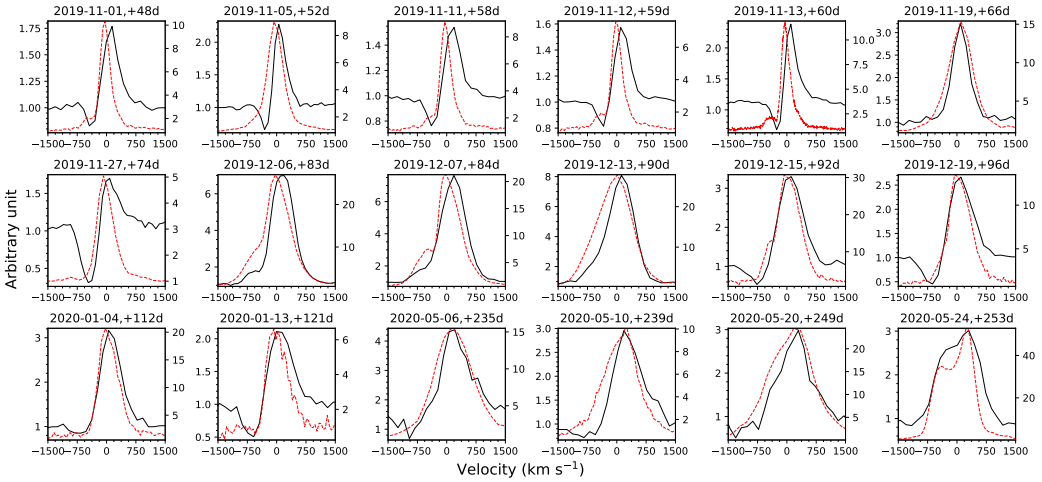

Figure no. 9: The line profile variation seen in the O I 7773Å (solid black) and Hα (dashed red) lines during 2019 Nov - 2020 May for the Nova V2891 Cyg. The relative flux for O I 7773Åand Hα are given on the left and right axes for each of the sub-plots respectively. The appearance and disappearance of P Cygni features is evident. These profile variations are the indicators of multiples episodes of periodic mass ejections in the nova outbursts.

This work has been done in collaboration with C. E. Woodward (University of Minnesota, USA), Ulisse Munari (INAF Astronomical Observatory of Padova, Italy), Aneurin Evans (Keele University,UK), Sergio Dallaporta (Asiago Astronomical Observatory, Italy), and Kim L. Page (University of Leicester,UK).

doi : https://doi.org/10.1093/mnras/stab3772

(Vipin Kumar, Mudit K. Srivastava, Dipankar P.K. Banerjee and Vishal Joshi)

V838 Monocerotis: A remnant of a binary merger in a triple system

The eruptive variable star V838 Mon was thought to be a classical nova when it went into eruption in 2002. However, it became the prototype of a new type of stellar eruption known today as the (luminous) red nova. Red nova outbursts are thought to be caused by stellar mergers. In the case of V838 Mon the eruption occurs as a result of the merger that took place in a triple or higher system involving two B-type stars. In order to characterize the merger remnant $\sim$17 yr after the eruption we mapped the merger site with ALMA at a resolution of $\sim$25 mas, or 148 AU for a distance of 5.9 kpc, in continuum dust emission and in rotational lines of simple molecules, including CO, SiO, SO, SO2, AlOH, and H2S. We reproduced the architecture of the remnant at the epoch of the ALMA observations using radiative transfer calculations. We also make use of optical spectroscopy data obtained mainly with VLT/X-shooter and SALT/HRS. For the first time, we identify the position of the B-type companion relative to the outbursting component of V838 Mon. The stellar remnant is surrounded by a clumpy wind with characteristics similar to those of the winds of red supergiants. The merger product is also associated with an elongated structure of 17.6 $\times$ 7.6 mas (104 $\times$ 45 AU) seen in continuum emission, and which we interpret as a disk seen at a moderate inclination. Maps of continuum and molecular emission also show a complex region of interaction between the B-type star (its gravity, radiation, and wind) and the flow of matter ejected in 2002. The remnant's molecular mass is about 0.1 $M_\odot$ and the dust mass is 8.3 $\times$ 10^{-3} $M_\odot$. The B-type star not only deflects the merger ejecta but also changes its molecular composition with an involvement of circumstellar shocks. ALMA maps show us an extreme form of interaction between the merger ejecta and the distant ($\sim$250 AU) companion. This interaction is similar to that known from the Anteres AB system but at a much higher mass loss rate. This study of V838 Mon offers the best images of a merger site so far.

This work has been done in collaboration with Tomek Kamiski (Nicolaus Copernicus Astronomical Center, Polish Academy of Sciences, Poland), Romuald Tylenda (Warsaw University Astronomical Observatory, Poland) and Carl Melis (University of California, San Diego, USA).

doi : https://doi.org/10.1051/0004-6361/202141526

(Vishal Joshi)

Spectral and timing evolution of MAXI J1631-479 during the 201819 outburst with NICER

The phenomenology of low-mass X-ray binaries during outbursts is fairly well understood thanks to the continuous, near daily, monitoring of the sources.

Such observations and the resulting spectral and timing studies have helped us in understanding the systems and also at the same time presented us with a myriad of challenges. One such X-ray binary, namely MAXI J1631$-$479, went into an outburst on 21 December 2018 and was observed by many observatories. In this work we report the results of our analysis using data from the NICER observatory. We carried out a comprehensive analysis of the source and traced the evolution of the various spectral and timing properties through the outburst. We also examine spectral-timing correlations to understand the origin of the quasi-periodic oscillations (QPOs) detected during the hard/intermediate state.

The NICER observations did not span the entire outburst as the initial observations were curtailed due to sun-angle restriction of the instrument. When the observations started the source was already in the high/soft state. This was characterised by a disk dominated spectrum and a very low fractional variability ($<$ 5%). Then the source underwent a hard excursion for about two months where it remained formally in a hard/intermediate state. This state was characterised by powerlaw-dominated energy spectrum with the spectral index lying around 3. The broadband variability was $\sim$10% and the power spectra consisted of Type-C QPOs which were often accompanied by a second harmonic component. After this state the source went back to the high/soft state and remained there along with decreasing flux till a point where the source became dominated by background emission.

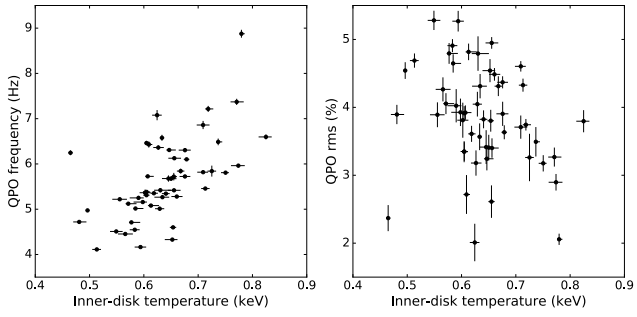

Figure no. 10: The dependence of QPO frequency (LEFT) and fractional rms (RIGHT) with the inner-disk temperature.

We attempted to understand the origin of QPOs by studying spectral and timing correlations. NICER provides a unique opportunity to study the variation of QPO frequency and rms with the inner disk temperature. Figure 10 shows the variation of QPO frequency and fractional rms with the best-fit inner disk temperature. The frequency shows a positive correlation while rms shows a negative correlation with disk temperature. These results support those models of QPOs that assumes a truncated disk geometry and in which the frequency originates from the inner radius of the thin disk. The geometrical models based on the Lense-Thirring precession of a torus or a hot blob of gas are able to qualitatively explain the observations. The disk emission is known to be less variable than the Coronal emission. Therefore the increase in disk temperature that is associated with the

decrease in the disk radius leads to an increase in QPO frequency. Consequently, the increase in disk temperature leading from an increase in disk contribution results in a decrease in QPO variability.

This work was done in collaboration with M. Mendez of University of Groningen, Netherlands and T. Belloni of INAF, Italy.

doi : https://doi.org/10.1093/mnras/stab1341

(S. K. Rout and S. Vadawale)

Detection of X-ray pulsations at the lowest observed luminosity of Be/X-ray binary pulsar EXO 2030+375 with AstroSat

EXO 2030+375 is one of the well studied Be/X-ray binary pulsars associated with regular Type-I outbursts during almost every periastron passage. This transient accreting X-ray pulsar was discovered in 1985 with EXOSAT during a giant outburst. The associated optical counterpart of EXO 2030+375 is a highly reddened B0 Ve star showing infrared excess and Hα in emission. The regular Type-I X-ray outbursts have been extensively monitored with the X-ray instruments onboard RXTE, INTEGRAL, XMM-Newton, Suzaku and Swift/BAT observatories to understand the characteristic properties of the pulsar. A detailed and comprehensive study of EXO 2030+375 was carried out by using extensive RXTE pointed observations during many Type-I and 2006 Type-II outbursts starting from 1995 till 2011. Timing and spectral studies of the pulsar were carried out from observations during the entire duration of RXTE campaign. Timing studies of more than 600 RXTE pointings revealed the evolution of pulse profiles of the pulsar with luminosity - a main peak and a minor peak at low luminosity evolved into a two-peaked profile along with minor dips at high luminosity. Since the discovery in 1985, the pulsar had been showing regular X-ray outbursts for about 25 years. Since early 2015, however, the Type-I outbursts appeared to be of decreasing intensity and eventually vanished from the light curve towards the end of 2015 or early 2016. The Type-I X-ray outburst activity commenced again in early 2016 and still continuing, though with much fainter peak luminosity than the usual ones. As the pulsar is still showing Type-I X-ray outbursts with fainter peak luminosity, it is interesting to carry out timing and spectral studies with AstroSat to explore whether the pulsar has gone into the propeller regime or still undergoing accretion. We present the results obtained from timing and spectral studies of Be/X-ray binary pulsar EXO 2030+375 using observations with the Large Area Xenon Proportional Counters and Soft X-ray Telescope of AstroSat, at various phases of its Type-I outbursts in 2016, 2018, and 2020. The pulsar was faint during these observations as compared to earlier observations with other observatories. At the lowest luminosity of 2.5 $\times$ 10^{35} erg/s in 0.5-30 keV energy range, $\sim$41.3 s pulsations were clearly detected in the X-ray light curves. This finding establishes the first firm detection of pulsations in EXO 2030+375 at an extremely low mass accretion rate to date. The shape of the pulse profiles is complex due to the presence of several narrow dips. Though pulsations were detected up to $\sim$80 keV when the source was brighter, pulsations were limited up to $\sim$25 keV during the third AstroSat observation at lowest source luminosity. Spectral analysis of the AstroSat data showed that the spectrum of the pulsar was steep with a power-law index of $\sim$2. The values of photon-indices at observed low luminosities follow the known pattern in sub-critical regime of the pulsar.

This work was done in collaboration with Gaurava K. Jaisawal of National Space Institute, Denmark, Prahlad Epili of Wuhan University, China and P. C. Agrawal of TIFR, Mumbai.

doi : https://doi.org/10.1007/s12036-021-09699-2

(Neeraj Kumari, Birendra Chhotaray, Shivangi Gupta, Arghajit Jana and Sachindra Naik)

AstroSat Observations of Eclipsing High Mass X-ray Binary Pulsar OAO 1657-415

OAO 1657$-$415 is an accreting high mass X-ray binary pulsar, discovered with the Copernicus satellite in 1978. The X-ray pulsations from the neutron star were detected at 38.2 s. Later, the system was identified as an eclipsing binary by using 1991 and 1992 observations with BATSE onboard Compton Gamma Ray Observatory. This study also revealed the orbital period of the system to be Porb = 10.4 days along with the eclipse duration of about 1.7 days. Being located at a low galactic latitude, OAO 1657$-$415 is highly absorbed with a column density of 10^{23} cm^{-2}. The energy spectrum of the pulsar can be described by a power law continuum with an exponential high energy cutoff along with a soft excess and prominent emission lines at 6.4, 6.7, and 7.1 keV. Suzaku observation of the source in September 2011, covering 0.12–0.34 orbital phase range, revealed flaring activities in the soft and hard X-ray light curves. Detailed time-resolved spectroscopy of the Suzaku data suggested the accretion of clumpy material as the cause of flare-like episodes during the observation. Using BeppoSAX observation, a presence of a cyclotron absorption line was suggested at 36 keV. However, later studies with INTEGRAL and Suzaku did not confirm the feature. We present the results obtained from analysis of two AstroSat observations of the high mass X-ray binary pulsar OAO 1657$-$415. The observations covered 0.681-0.818 and 0.808-0.968 phases of the $\sim$10.4 day orbital period of the system, in March and July 2019, respectively. Despite being outside the eclipsing regime, the power density spectrum from the first observation lacks any signature of pulsation or quasi-periodic oscillations. However, during July observation, X-ray pulsations at a period of 37.0375 s were clearly detected in the light curves. The pulse profiles from the second observation consist of a broad single peak with a dip-like structure in the middle across the observed energy range. We explored the evolution of the pulse profile in narrow time and energy segments. We detected pulsations in the light curves obtained from 0.808-0.92 orbital phase range, which is absent in the remaining part of the observation. The spectrum of OAO 1657$-$415 can be described by an absorbed power-law model along with an iron fluorescent emission line and a blackbody component for out-of-eclipse phase of the observation. Our findings are discussed in the frame of stellar wind accretion and accretion wake at late orbital phases of the binary.

This work was done in collaboration with Gaurava K. Jaisawal of National Space Institute, Denmark, Prahlad Epili of Wuhan University, China and P. C. Agrawal of TIFR, Mumbai.

doi : https://doi.org/10.1007/s12036-021-09701-x

(Birendra Chhotaray, Arghajit Jana and Sachindra Naik)

AstroSat observations of long-duration X-ray superflares on active M-dwarf binary EQ Peg

Flares on the Sun and stars are the most extreme evidence of magnetic activity in solar/stellar atmospheres. Flares occur in close proximity to the active regions. Magnetic loops from these active regions extend into the stellar corona. As the footpoints of these loops are jostled by the convective motions in the stars, they are twisted and distorted until magnetic reconnection occurs near the loop tops. The reconnection process drives a rapid and transient release of magnetic energy in coronal layers, which is also associated with the electromagnetic radiation from radio waves to γ-rays. Typically the solar flares emit the energy of $10^{29}-10^{32}$ erg within the flare duration of several minutes to hours. Stellar flares on solar-type stars with energies $10^{33}-10^{38}$ erg are generally termed as 'superflares'. Although there are thousands of superflares, have been observed to date in optical and UV bands, but X-ray superflares are still very few. It is to be noted that most of the host stars of the X-ray superflares are either an M-dwarf or a binary or multiple systems with an M-dwarf component. Moreover, M-dwarfs show a higher level of magnetic activities than other solar-type stars. This makes them very interesting objects to study. The active M-dwarf binary EQ Peg has a record of frequent and large flaring activities across the electromagnetic spectrum. The visual binary system EQ Peg consists of an M3.5 primary and an M4.5 secondary, separated by an angular separation of 5.8 arcsec. With V magnitudes of 10.35 and 12.4, both the primary and secondary components are well known optical flare stars. The EQ Peg system is a strong X-ray and extreme ultraviolet source with a number of recorded flares. The first X-ray observation that allowed an unambiguous spectral separation of the two binary components was done with Chandra/HETG. Using the Soft X-ray Telescope (SXT) of AstroSat, the first Indian multi-wavelength space observatory, we have observed and investigated three superflares that occurred on the M-dwarf binary EQ Peg. All three flares are remarkable in their flare duration and the X-ray energies. The peak X-ray luminosities of the flares in the 0.3–7 keV band are found to be within 5-10 $\times$ 10^{30} erg/s. The e-folding rise- and decay-times of the flares are derived to be in the range of 3.4–11 and 1.6–24 ks, respectively. Spectral analysis indicates the presence of three temperature corona with the first two plasma temperatures remain constant during all the flares and the post-flare observation at $\sim$3 and $\sim$9 MK. The flare temperature peaked at 26, 16, and 17 MK, which are 2, 1.3, and 1.4 times more than the minimum value, respectively. The peak emission measures are found to be 3.9–7.1 $\times$ 10^{53} cm^{-3}, whereas the abundances peaked at 0.16–0.26 times the solar abundances. The magnetic field for all three flares is estimated to be $<$100 G. The estimated energies of all three flares are greater than 10^{34}–10^{35} erg, putting them in a category of superflare. All three superflares are also found to be the longest duration flares ever observed on EQ Peg.

This work was done in collaboration with J, C, Pandey of ARIES, Nainital.

doi : https://doi.org/10.1093/mnras/stab3099

(Subhajit Karmakar and Sachindra Naik)

NICER observations of the black hole candidate MAXI J0637-430 during the 2019-2020 outburst

An X-ray binary (XRB) consists of a normal star and a compact object. The compact object can be a black hole (BH), or a neutron star (NS). A transient XRB spends most of the time in the quiescent state during which the compact object is marginally detectable or even non-detectable with the current generation X-ray detectors. The transient XRBs occasionally show X-ray outbursts that last for several weeks to months. During the outburst, the X-ray luminosity of the source increases by several orders of magnitude compared to the quiescent state. A spectrum of a black hole X-ray binary (BHXRB) can be approximated with a soft thermal multicolour black-body component and a non-thermal power-law component. The multicolour black-body component originates from a standard thin accretion disc. In contrast, the power-law component originates in a Compton cloud located close to the BH. The soft X-ray photons originated from the standard accretion disc undergo inverse-Comptonization in the Compton cloud and produce the hard power-law component. An outbursting BHXRB shows rapid variation and fluctuation in spectral and timing properties. A correlation between the spectral and timing properties of the source can be seen in the hardness–intensity diagram, accretion rate–intensity diagram, rms–intensity diagram, or hardness–rms diagram. In general, an outbursting BHXRB exhibits four different spectral states, viz. low-hard state (LHS), hard-intermediate state (HIMS), soft-intermediate state (SIMS), and high-soft state (HSS). A BHXRB also shows low-frequency quasi-periodic oscillations (LFQPOs) in the power-density spectra (PDS) observed in a range of 0.1–20 Hz.

The black hole candidate MAXI J0637-430 was discovered with MAXI/GSC on 2019 November 2 during the onset of the 2019–2020 X-ray outburst. The outburst continued for $\sim$6 months. Several X-ray satellites such as NICER, AstroSat and NuSTAR also reported the primary timing and spectral analysis of the source. We present detailed timing and spectral studies of the black hole candidate MAXI J0637-430 during its 2019-2020 outburst using observations with the NICER and the Neil Gehrels Swift Observatory. We find that the source evolves through the soft-intermediate, high-soft, hard-intermediate, and low-hard states during the outburst. No evidence of quasi-periodic oscillations is found in the power-density spectra of the source. Weak variability with fractional rms amplitude $<$5% is found in the softer spectral states. In the hard-intermediate and hard states, high variability with the fractional rms amplitude of $>$20% is observed. The 0.7-10 keV spectra with NICER are studied with a combined disc-black-body and nthcomp model along with the interstellar absorption. The temperature of the disc is estimated to be 0.6 keV in the rising phase and decreased slowly to 0.1 keV in the declining phase. The disc component was not detectable or absent during the low-hard state. From the state-transition luminosity and the inner edge of the accretion flow, we estimate the mass of the black hole to be in the range of 5-12 $M_{\odot}$, assuming the source distance of d $<$ 10 kpc.

This work was done in collaboration with Gaurava K. Jaisawal of National Space Institute, Technical University of Denmark, Denmark.

doi : https://doi.org/10.1093/mnras/stab1231

(Arghajit Jana, Neeraj Kumari, Birendra Chhotaray and Sachindra Naik)

NuSTAR and Swift Observations of the Extragalactic Black Hole X-ray Binaries

Among the known population of over 100 stellar mass BHXBs, only five BHXBs, namely, LMC X−1, LMC X−3, IC 10 X−1, M33 X−7, and NGC 300 X−1 have an extra-galactic origin. Of these five sources, LMC X−1 and LMC X−3 are nearby sources and are located at a distance of ∼48.1 kpc in the Large Magellanic Cloud (LMC), a satellite galaxy of Milky Way. LMC X−1 and LMC X−3 are the second and third black holes discovered after Cygnus X−1. LMC X−1 is the first extra-galactic X-ray source discovered by UHURU. It is a persistent X-ray source in a high mass BHXB. The black hole (BH) mass in this binary system is found to be 10.91 $\pm$ 1.41 solar mass. The BH is found to be rapidly rotating with a spin parameter of $\geq$ 0.92. LMC X−1 does not show any long-term variability, though short-term variabilities have been reported. Consistent with the long-term light curve, the source is always found to be in the thermal dominated spectral state. LMC X−3 is a persistent high mass BHXB consisting of a BH of mass 6.98 $\pm$ 0.56 $M_{\odot}$. The spin of the BH in LMC X−3 is reported to be low. LMC X−3 is found to spend most of the time in thermal dominated state with occasional transition to the LHS. Occasionally, LMC X−3 is observed to be in an anomalous low/hard state.

We present the results obtained from detailed spectral and timing studies of extragalactic black hole X-ray binaries LMC X−1 and LMC X−3, using simultaneous observations with Nuclear Spectroscopic Telescope Array (NuSTAR) and Neil Gehrels Swift observatories. The combined spectra in the 0.5−30 keV energy range, obtained between 2014 and 2019, are investigated for both sources. We do not find any noticeable variability in 0.5−30 keV light curves, with 0.1−10 Hz fractional rms estimated to be <2 per cent. No evidence of quasi-periodic oscillations is found in the power density spectra. The sources are found to be in the high soft state during the observations with disc temperature $T_{in} \sim 1$ keV, photon index, $\Gamma > 2.5$ and thermal emission fraction, $f_{disc} > 80$ per cent. An Fe K_{α} emission line is detected in the spectra of LMC X−1, though no such feature is observed in the spectra of LMC X-3. From the spectral modeling, the spins of the black holes in LMC X−1 and LMC X−3 are estimated to be in the range of 0.92-0.95 and 0.19-0.29, respectively. The accretion efficiency is found to be, ∼0.13 and $\eta \sim 0.04$ for LMC X−1 and LMC X−3, respectively.

This work was done in collaboration with Gaurava K. Jaisawal of National Space Institute, Technical University of Denmark, Denmark and D. Chatterjee of IIA, Bangalore.

doi : https://doi.org/10.1093/mnras/stab2448

(Arghajit Jana and Sachindra Naik)

Multi-wavelength study of the galactic black-hole binary GRS 1716−249

The origins of X-ray and radio emission from an X-ray binary are relatively better understood than those in the ultraviolet (UV), optical, and infrared (IR) wavelengths. This is because, while X-rays and radio are exclusively emitted from the inner accretion disk and jet respectively, the mid energy range is dominated by multiple competing sources such as outer accretion disk, secondary star, synchrotron jet etc. Over the years various techniques have been developed to decipher the true emission mechanism for the UV, optical and IR bands. These include studying rapid variability, correlations with other wave bands, fitting the broadband SED etc. In this work we attempt to discern the origin of the near IR (NIR), optical and UV emission from a galactic X-ray binary GRS 1716−249 by modelling the broadband SED. GRS 1716−249 went into an outburst on 18 December 2016 after more than 20 years of quiescence. We monitored the source in optical and NIR bands from the Mt Abu Infrared Observatory on 24 nights spanned across 3 months. It was also observed with AstroSat as a Target of Opportunity on 3 epochs. Finally, we secured the UV data from the extensive monitoring program of the Swift observatory. Using quasi-simultaneous data from all these wavebands we modelled the SED by an absorbed irradiated accretion disk model. The spectrum along with the best fit model is depicted in Figure 11. As can be seen from figure, emission from the irradiated disk is able to adequately explain the UV and optical points, whereas the NIR points show a significant excess. We verified that this excess is unlikely due to the secondary star as the object was not detected in the 2MASS catalogue during the quiescence phase indicating it to be too faint. Neither was the source detected in the WISE catalogue, thus, ruling out the possibility of a dust cloud engulfing the binary that could emit in far IR. Thus, the most plausible source for the NIR excess is Synchrotron emission from a jet. This is confirmed by the fact that the source was bright in radio wavelengths throughout the outburst duration. Fixing the Synchrotron break at the Ks band, we find that the radio spectrum is steeply inverted which suggests the possibility of a flaring jet geometry.

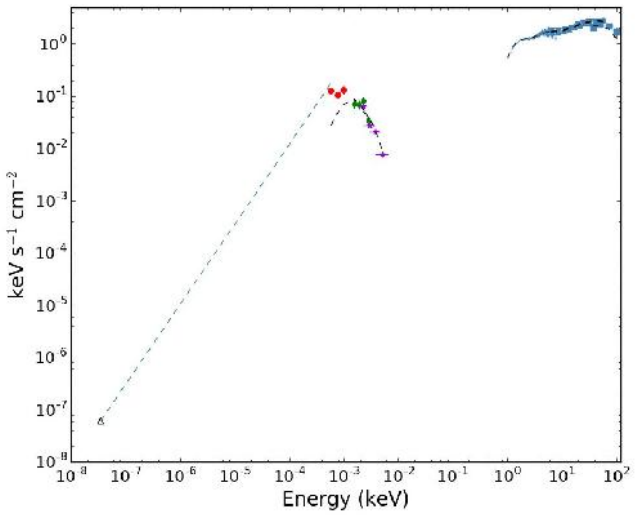

Figure no.11: Broadband SED of GRS 1716−−249 after fitting an absorbed irradiated disk model. The X-ray spectrum, shown in steelblue color, is unfolded and rebinned. The SXT, LAXPC10, LAXPC20 and CZTI points are represented by dots, up-triangles, down-triangles and squares respectively. In lower energies, the NIR spectrum is represented with red circles, optical points with green diamonds, and UV points with violet stars. The black dashed line represents the best-fit model. The radio observation is shown with an open triangle and the grey dashed line joining it with the Ks band is just for representation and not a fitted model.

This work was done in collaboration with R. Misra and J. Roy of IUCAA and J. S. Yadav of IIT Kanpur.

doi : https://doi.org/10.1007/s12036-021-09696-5

(S. K. Rout, S. Vadawale, E. Aarthy, S. K. Ganesh, and V. Joshi)

Our peculiar motion from Mid Infra Red AGNs and the discordance seen with the cosmological principle

In the last one decade, Solar peculiar motion values inferred from the number counts and sky brightness observed in large samples of distant radio galaxies and quasars have yielded peculiar velocity amplitudes many times larger than the value, 370 km/s, determined from Cosmic Microwave Background Radiation (CMBR), though in all cases the directions matched with the CMBR dipole along RA=168°, Dec=−7°. Now the solar peculiar motion has been determined from a sample of 0.28 million Mid Infra Red AGNs, which is more than five times the CMBR value, although the direction seems to be within 2σ of the CMBR dipole (see Figure 12). A genuine value of the solar peculiar velocity should be the same irrespective of the data or technique employed. Such discordant dipole amplitudes might mean that the explanation for these dipoles, including that of the CMBR, might in fact be something else. It might instead suggest a preferred direction in the Universe, implying a genuine anisotropy, which would violate the Cosmological Principle, the core of modern cosmology.

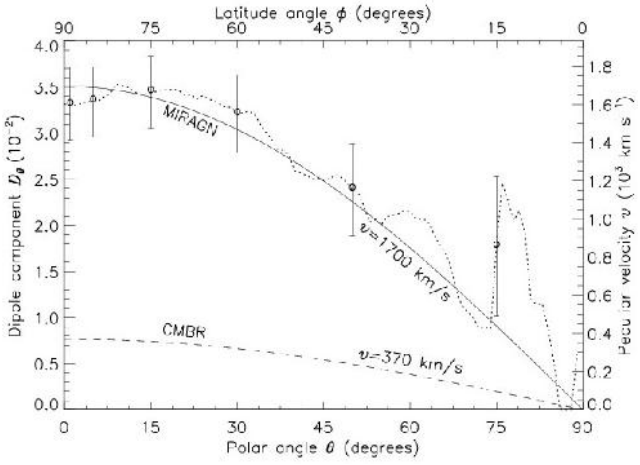

Figure no.12: A plot of the dipole components and the equivalent peculiar velocity component, computed for various zones of the sky between the great circle and a parallel circle at the angle θ with respect to the dipole direction. The latitude angle ϕ=(90° - θ) is measured from the great circle. For a comparison, the expectation for the CMBR value is shown by a dashed curve, which lies way below the values observed for the MIRAGNs.

doi : https://doi.org/10.3390/universe7040107

(Ashok K. Singal)

X-Ray observations of 1ES 1959+650 in its high-activity state in 2016-2017

The blazar 1ES 1959+650 was observed with a number of instruments at multiple wavelengths from radio to gamma rays. Among these, we carried out photometric optical observations with the CCD instrument mounted on the 1.2 m telescope of Mount Abu IR Observatory. This blazar was observed in B, V, R bands (Johnson-Cousins filters) during MJD 57690 to 57697 (2015 December to 2017 December). The data was reduced (including bias subtraction, flat-fielding, and cosmic-ray correction) and analyzed using standard photometry packages from Image Reduction and Analysis Facility (IRAF). For each image the PSF value was measured and aperture photometry was carried out. The high quality X-ray data using AstroSat allowed for high-cadence monitoring during 20162017. The data enables us to establish a detailed description of X-ray flares in 1ES 1959+650. The synchrotron peak shifts significantly between different flux states, in a manner consistent with a geometric (changing Doppler factor) interpretation. A time-dependent leptonic diffusive shock acceleration and radiation transfer model is used to reproduce the spectral energy distributions and X-ray light curves, to provide insight into the particle acceleration during the major activity periods observed in 2016 and 2017. The extensive data of Swift-XRT from 2015 December to 2021 February reveals a positive correlation between flux and peak position. We are working further to investigate the statistical properties and interpretation of long-term variations seen in this blazar.

This work was done in collaboration with S. Chandra (CSR, South Africa).

doi : https://doi.org/10.3847/1538-4357/ac01d1

(S. Ganesh)

Imaging and photometric studies of NGC 1316 (Fornax A) using Astrosat/UVIT

NGC 1316 (Fornax A) is a nearby (z=0.00587) giant peculiar S0 galaxy hosting numerous tidal tails, shells, unusual dust patches all embedded within a much larger outer envelop of stars and a prominent dust lane oriented along its optical minor axis. In addition to the intricate dust patches and shells, NGC 1316 also hosts filamentary, nebular emission features, ripples, arcs and several complex filamentary loops of other phases of interstellar medium (ISM). The faint tidal tails wisps and shells of stars evident around the galaxy suggest that they have been torn from their original locations and flung into intergalactic space through complex gravitational effects. The presence of a compact disk of gas near its center that has different orientation and much faster rotation relative to the stars, has also been reported. All of these signs of complex dust features, shells, loops and other sub-structures evident in NGC 1316 collectively point to its violent past built-up through the merger of several smaller dust rich galaxies in the distant past. Based on the expansion time of the outer stellar loops and the spread in the ages of globular clusters demonstrate that the mergers might have happened between 1 to 3 Gyr ago and then NGC 1316 has continued accretion of smaller satellite galaxies. We present imaging and photometric studies of the radio galaxy NGC 1316 (Fornax A) using high spatial resolution near-ultraviolet (NUV) and far-ultraviolet (FUV) imaging telescopes of the first Indian multi-wavelength space observatory AstroSat. The residual maps of UV emission obtained from the subtraction of smooth models witness peculiar features within the central few kpc (1-2 kpc) region. The spatial correspondence between the radio emission maps and FUV imaging study reveal that the UV emitting sources are displaced away from the centre by the AGN outburst (radio jet). The presence of rims and clumpy structures in the outskirts of this galaxy delineate that the galaxy has acquired a large fraction of gas through merger-like events and is still in the process of settling. The estimates of the star formation rates (SFR) using FUV and NUV luminosities are found to be 0.15 $M_\odot$/yr and 0.36 $M_\odot$/ yr, respectively, and provide the lower limit due to the screen effect. The estimated lower rates of SFR

in this galaxy probably represent its quenching due to the AGN driven outflows emanating from the central engine of NGC 1316.

This work was done in collaboration with Nilkanth Vagshette of Maharashtra Udayagiri Mahavidyalaya, Udgir and M. K. Patil of Swami Ramanand Teerth Marathwada University, Nanded Maharashtra.

doi : https://doi.org/10.1007/s12036-021-09708-4

(Neeraj Kumari and Sachindra Naik)

Accretion Properties of MAXI J1813-095 during its failed outburst in 2018

MAXI/GSC. Follow up observations with the Swift/XRT localized the source at RA = 18h 13m 34.0s , Dec = -09° 31′ 59″.0. The GROUND observation of the above location detected the optical counterpart of the source. From the multi-wavelength observations, We present the results obtained from detailed timing and spectral studies of a black hole candidate MAXI J1813-095 using Swift, NICER, and NuSTAR observations during its 2018 outburst. The timing behavior of the source is mainly studied by examining NICER light curves in the 0.5-10 keV range. We did not find any signature of quasi-periodic oscillations in the power density spectra of the source. We carry out spectral analysis with a combined disk blackbody & power law model, and physical two-component advective flow (TCAF) model. From the combined disk blackbody & power-law model, we extracted thermal and non-thermal fluxes, photon index and inner disk temperature. We also find evidence for weak reflection in the spectra. We have tested the physical TCAF model on a broadband spectrum from NuSTAR and Swift/XRT. The parameters like mass accretion rates, the size of Compton clouds and the shock strength are extracted. Our result affirms that the source remained in the hard state during the entire outburst which indicates a "failed" outburst. We estimate the mass of the black hole as 7.4 $\pm$ 1.5 $M_{\odot}$ from the spectral study with the TCAF model. We apply the LAOR model for the Fe K_{α} line emission. From this, the spin parameter of the black hole is ascertained as $a^{\star} > 0.76$. The inclination angle of the system is estimated to be in the range of $28^{\circ} - 45^{\circ}$ from the reflection model. We find the source distance to be $\sim$6 kpc.

This work was done in collaboration with Gaurava K. Jaisawal of National Space Institute, Technical University of Denmark, Denmark.

doi : https://doi.org/10.1088/1674-4527/21/5/125

(Arghajit Jana, Neeraj Kumari and Sachindra Naik)

Complex optical/UV and X-ray variability in Seyfert 1 galaxy Mrk 509

Active galactic nuclei (AGNs) are strongly believed to be fuelled by accreting matter from the surrounding medium around the supermassive black hole at the center. This has been recently confirmed through the observations of a nearby radio-galaxy M87 with the Event Horizon Telescope (EHT). Imaging the central black hole and the accretion disk at the center of other galaxies that are farther away is impossible even with EHT. There are, however, other indirect methods that are used to derive the physical structure and size of these objects. Continuum reverberation mapping technique is one such method in which the estimated time lag between the continuum emission in shorter and longer wavelength ranges has been used to derive the size of the broad-line region (BLR) and hence the black hole virial mass in several AGNs. Understanding of the emission mechanism in AGNs has been a topic of intense research for several decades. However, the origin of emission in different wavelength ranges of the electromagnetic spectrum and correlation between them remain ambiguous to date. The general picture is that the low energy photons in ultraviolet (UV) and optical bands are believed to be originated from the accretion disk and the broad-line region (BLR). These photons get inverse Compton scattered in the hot electron plasma (corona), causing X-ray emission from the AGNs.

The origin of the UV/optical and X-ray variabilities and correlation between them have been one of the most intriguing questions in the studies of the physical size and structure of AGNs. In Seyfert galaxies, the energy spectrum is dominated by UV radiation which is believed to be originated from a multi-colour blackbody disk. The X-ray/UV/optical emission from the accretion disk shows variabilities over timescales ranging from a few hours to years in the AGNs. We performed a detailed spectral and timing analysis of a Seyfert 1 galaxy Mrk 509 using data from the Neil Gehrels Swift observatory that spanned over 13 years between 2006 and 2019. To study the variability properties from the optical/UV to X-ray emission, we used a total of 275 pointed observations in this work. The average spectrum over the entire duration exhibits a strong soft X-ray excess above the power law continuum. The soft X-ray excess is well described by two thermal components with temperatures of 120 eV and 460 eV. The warm thermal component is likely due to the presence of an optically thick and warm Comptonizing plasma in the inner accretion disk. The fractional variability amplitude is found to be decreasing with increasing wavelength, i.e., from the soft X-ray to UV/optical emission. However, the hard X-ray (2–8 keV) emission shows very low variability. The strength of the correlation within the UV and the optical bands (0.95–0.99) is found to be stronger than the correlation between the UV/optical and X-ray bands (0.40–0.53). These results clearly suggest that the emitting regions of the X-ray and UV/optical emission are likely distinct or partly interacting. Having removed the slow variations in the light curves, we find that the lag spectrum is well described by the 4/3 rule for the standard ShakuraSunyaev accretion disk when we omit X-ray lags. All these results suggest that the real disk is complex, and the UV emission is likely reprocessed in the accretion disk to give X-ray and optical emission.

This work was done in collaboration with Main Pal of Delhi University and P. Kushwaha of ARIES, Nainital.

doi : https://doi.org/10.1017/pasa.2021.41

(Neeraj Kumari, Arghajit Jana, and Sachindra Naik)

Broad-band X-ray observations of the 2018 outburst of the changing-look active galactic nucleus NGC 1566

Active galactic nuclei (AGNs) are classified as type-1 or type-2, depending on the presence or absence of broad optical emission lines. The existence of different classes of AGNs can be explained

by the unified model, which is based on the orientation of the optically thick torus with respect to our line-of-sight. Recently, a new sub-class of AGNs, known as changing look AGNs (CLAGNs), has been identified by optical observations. These objects display the appearance or disappearance of the broad optical emission lines, transitioning from type-1 to type-2 and vice versa. In the X-rays, a different type of changing-look events have been observed, with AGN switching between Compton-thin (line-of sight column density $< 1.5 \times 10^{24} cm^{-2}$) and Compton-thick (line-of sight column density $> 10^{24} cm^{-2}$)) states, These X-ray changing-look events have been observed in many AGNs, namely, NGC 1365, NGC 4388, NGC 7582, NGC 4395, IC 751, NGC 4507, NGC 6300. The origin of the CL events is still unclear. The X-ray changing look events could be explained by variability of the line-of-sight column density associated with the clumpiness of the BLR or of the circumnuclear molecular torus. NGC 1566 is a nearby (z=0.005), face-on spiral galaxy, classified as a type SAB(s)bc. The AGN was intensively studied over the last 70 years and is one of the first galaxies where variability was detected. In the 1970s and 1980s, NGC 1566 was observed to be in the low state with weak H emission. Over the years, it was observed to change its type again from Seyfert 1.9-1.8 to Seyfert 1.5-1.2, with two optical outbursts in 1962 and 1992. We study the nature of the changing-look active galactic nucleus NGC 1566 during its 2018 June outburst. During the outburst, the X-ray intensity of the source rises up to $\sim$ 25-30 times compared to its quiescent state intensity. We perform timing and spectral analysis of the source during pre-outburst, outburst, and post-outburst epochs using semi-simultaneous observations with the XMM-Newton, Nuclear Spectroscopic Telescope Array(NuSTAR), and Neil Gehrels Swift Observatories. We calculate variance, normalized variance, and fractional rms amplitude in different energy bands to study the variability. The broad-band 0.5-70 keV spectra are fitted with phenomenological models, as well as physical models. A strong soft X-ray excess is detected in the spectra during the outburst. The soft-excess emission is found to be complex and could originate in the warm Comptonizing region in the inner accretion disc. We find that the increase in the accretion rate is responsible for the sudden rise in luminosity. This is supported by the 'q'-shape of the hardness-intensity diagram that is generally found in outbursting black hole X-ray binaries. From our analysis, we find that NGC 1566 most likely harbours a low-spinning black hole with the spin parameter $a^{\star} \sim 0.2$. We also discuss a scenario where the central core of NGC 1566 could be a merging supermassive black hole.

This work was done in collaboration with Gaurava K. Jaisawal of National Space Institute, Technical University of Denmark, Denmark and C. Ricci of Ncleo de Astronoma de la Facultad de Ingeniera, Santiago, Chile.

doi : https://doi.org/10.1093/mnras/stab2155

(Arghajit Jana, Neeraj Kumari , Prantik Nandi and Sachindra Naik)

Blazar OJ 287 after First VHE Activity: Tracking the Reemergence of the HBL-like Component in 2020

Blazars are the most prominent and persistent nonthermal emitters with a continuum powered by a relativistic jet roughly aligned with our line of sight. The continuum shows variations on all accessible timescales and spread across the entire accessible electromagnetic (EM) spectrum. Detailed multiwavelength (MW) studies have revealed that the variability is pervasive – seen in all the observables : flux, spectra, and polarization with changes in one often accompanied by changes in others. These studies have also firmly established or confirmed many phenomenological features, e.g., the variations are stochastic and the broadband emission shows a characteristic bimodal spectral energy distribution (SED) with one peak in between infrared and UV/X-ray energies and the other at MeV/GeV energies. The broadband SED of all blazars can be categorized into three different spectral subclasses: low-energy-peaked, intermediate-energy-peaked, and high-energy-peaked, based on the location of the low-energy hump. A remarkable property of each spectral subclass is the stability of the location of the two peaks despite huge variations in flux and often spectral shape. In OJ 287, a shift in the location of only the high-energy peak was observed during the 2015–2016 activity, while in 2016–2017 a new broadband emission component overwhelmed the overall emission, appearing as an overall shift in both the peaks.

A detailed exploration of spectro-temporal evolution and spectral changes of OJ 287, from optical to LAT gamma-ray energies between 2017 May 27 and 2020 June 10 and compare the behaviors with the 2017 activity that was also driven by the soft X-ray spectrum, has been carried out. The period covered here corresponds to the end phase of the first VHE activity and the highest recorded X-ray flux state to the end of the second-highest reported X-ray flux. This allows a continuous access to the flux and spectral behavior of the source and, in turn, to the evolutionary track of the new broadband emission component that was responsible for the 2017 activity and its revival, resulting in the 2020 activity. We report the reemergence of a new broadband emission through a detailed and systematic study of the multiwavelength spectral and temporal behavior of OJ 287 after its first-ever reported very high energy activity in 2017 to date, which includes the second-highest X-ray flux of the source. The source shows high optical to X-ray flux variations, accompanied mainly by strong spectral changes. The optical to X-ray flux variations are correlated and simultaneous except for two durations when they are anticorrelated. The flux variations, however, are anticorrelated with the X-ray spectral state while correlated with optical–UV. Weekly binned Fermi-LAT data around the duration of the highest X-ray activity show a few detections with a log-parabola model but none with a power law, yet the extracted LAT spectral energy distribution of the high-activity duration for both the models is similar and shows a hardening above 1 GeV. Further, near-infrared data indicate strong spectral change, resembling a thermal component. Overall, the combined optical to gamma-ray broadband spectrum establishes the observed variations to a new high-energy-peaked broadband emission component, similar to the one seen during the highest reported X-ray flux state of the source in 2017. The observed activities indicate some peculiar features that seem to be characteristic of this emission component, while its appearance a few years around the claimed $\sim$12 yr optical outbursts strongly indicates a connection between the two.

This work was done in collaboration with P. Kushwaha and A. C. Gupta of ARIES, Nainital, and Main Pal of Delhi University.

doi : https://doi.org/10.3847/1538-4357/ac19b8

(Neeraj Kumari and Sachindra Naik)

X-ray confirmation of the intermediate polar IGR J16547-1916

Using X-ray observations from the NuSTAR and Swift satellites, we carried out temporal and spectral studies of an intermediate polar (IP) IGR J16547-1916. A persistent X-ray period at ∼546 s confirming the optical spin period obtained from previous observations is detected. The detection of a strong X-ray spin pulse reinforces the classification of this system as an intermediate polar. The lack of orbital or side-band periodicities in the X-rays implies that the system is accreting predominantly via a disk. A variable covering absorber appears to be responsible for the spin pulsations in the low energy range. In the high energy band, the pulsations are likely due to the self occultation of tall shocks above the white dwarf surface. The observed double-humped X-ray spin pulse profile indicates two-pole accretion geometry with tall accretion regions in short rotating IP IGR J16547-1916. We present the variation of the spin pulse profile over an orbital phase to account for the effects of orbital motion on the spin pulsation. X-ray spectra obtained from the contemporaneous observations of Swift and NuSTAR in the 0.5-78.0 keV energy band are modeled with a maximum temperature of 31 keV and a blackbody temperature of 64 eV, along with a common column density of 1.8 $\times$ 10^{23} cm^{-2} and a power-law index of -0.22 for the covering fraction. An additional Gaussian component and a reflection component are needed to account for a fluorescent emission line at 6.4 keV and the occurrence of X-ray reflection in the system. We also present the spin phase-resolved spectral variations of IGR J16547-1916 in the 0.5-78.0 keV energy band and find dependencies in the X-ray spectral parameters during the rotation of the white dwarf.

This work was done in collaboration with Arti Joshi and W. Wei of Wuhan University, China, J.C. Pandey or ARIES, Nainital, and K.P. Singh of IISER, Mohali.

doi : https://doi.org/10.1051/0004-6361/202142193

(Sachindra Naik)

Unravelling the foretime of GRS 1915+105 using AstroSat observations: Wide-band spectral and temporal characteristics

We carried out a comprehensive study of GRS 1915+105 in wide energy band ($0.5-60$ keV) using AstroSat - *SXT* and *LAXPC* observations during the period of 2016−2019. %using *SXT* ($0.5-7$ keV) and *LAXPC* ($3-60$ keV).

The *MAXI* X-ray light curve of the source shows rise and decay profiles similar to canonical outbursting black holes. However, the source does not follow the exemplary 'q'-diagram in the Hardness-Intensity Diagram (HID). Model independent analysis of light curves suggests that GRS 1915+105 displays various types of variability classes (δ, χ, ρ, κ, ω and γ). We also report possible transitions from one class to another ($\chi \rightarrow \rho$, $\rho \rightarrow \kappa$ via an 'unknown' class and $\omega \rightarrow \gamma \rightarrow \omega + \gamma$) within a few hours duration. The rising phase of the light curve witnesses the evolution of the source through the classes $\chi \rightarrow \rho \rightarrow \kappa \rightarrow \omega \rightarrow \gamma \rightarrow \delta$ and the descent follows the transition from δ to χ. Broadband energy spectra are well modeled with multi-coloured disc blackbody and Comptonised components. We explore the 'spectro-temporal' features of the source in the different variability classes, transitions between classes, and evolution during the three year period considered. Detailed analysis indicates a gradual increase in the photon index (Γ) from 1.83 to 3.8, disc temperature (kT_{in}) from 1.33 to 2.67 keV, and Quasi-periodic Oscillation (QPO) frequency (ν) from 4 to 5.64 Hz during the rise, while the parameters decrease to $\Gamma \sim$1.18, $kT_{in} \sim$1.18 keV, and $\nu \sim$1.38 Hz respectively in the decline phase. Our findings confirm that QPO rms amplitude increases with frequency (ν) till ∼2.4 Hz beyond which an anti-correlation exists between the two. The source shows maximum bolometric luminosity (L_{bol}) during the peak at ∼36% of Eddington luminosity (L_{EDD}), and a minimum of ∼2.4% of L_{EDD} during the decay phase. Further evolution of the source towards an obscured low-luminosity (L_{bol} of ∼ 1% L_{EDD}) phase, with a decrease in the intrinsic bolometric luminosity of the source due to obscuration, has also been indicated from our analysis. The implication of our results are discussed in the context of accretion disc dynamics around the black hole.

This work was done in collaboration with Athulya M. P. and Radhika D. of Dayananda Sagar University, Bengaluru, V. K. Agrawal , Ravishankar B. T. and Anuj Nandi of U R Rao Satellite Centre, Bengaluru, Samir Mandal of IIST, Thiruvantapuram.

doi : https://doi.org/10.1093/mnras/stab3614

(Sachindra Naik)

Spectro-timing analysis of a highly variable narrow-line Seyfert 1 galaxy NGC 4748 with AstroSat and XMM-Newton

We carried out a detailed timing and spectral study of an extremely variable narrow-line Seyfert 1 galaxy NGC 4748 using observations in the year 2017 and 2014 performed with AstroSat and XMM-Newton, respectively. Both observations show extremely variable soft and hard X-ray emission that are correlated with each other. In the 2014 data set, the source retains its general behaviour of "softer when brighter" while the 2017 observation exhibits a "harder when brighter" nature. Such changing behaviour is rare in AGNs and is usually observed in the black hole binary systems. The "harder when brighter" is confirmed with the anti-correlation between the photon index and the 0.3-10 keV power-law flux. This suggests a possible change in the accretion mode from standard to the advection-dominated flow. Additionally, both the observations show soft X-ray excess below 2 keV over the power-law continuum. This excess was fitted with a single or multiple blackbody component(s). The origin of soft excess during the 2017 observation is likely due to the cool Comptonization as the photon index changes with time. On the other hand, the broad iron line and delayed UV emission during the 2014 observation strongly suggest that X-ray illumination onto the accretion disk and reflection and reprocessing play a significant role in this AGN.

This work was done in collaboration with Main Pal (Delhi University), P. Kushwaha and A. C. Gupta of ARIES, Nainital, K. P. Singh of IISER, Mohali, G.C. Dewangan and P. Tripathi of IUCAA, Pune.

doi : https://doi.org/10.1007/s12036-021-09719-1

(Neeraj Kumari and Sachindra Naik)

Short-timescale variability of the blazar Mrk 421 from AstroSat and simultaneous multi-wavelength observations

We study the multi-wavelength variability of the blazar Mrk 421 at minutes to days timescales using simultaneous data at gamma-rays from Fermi, 0.7-20 keV energies from AstroSat, and optical and near infrared (NIR) wavelengths from ground based observatories. We compute the shortest variability timescales at all of the above wave bands and find its value to be $\sim$1.1 ks at the hard X-ray energies and increasingly longer at soft X-rays, optical and NIR wavelengths as well as at the GeV energies. We estimate the value of the magnetic field to be 0.5 Gauss and the maximum Lorentz factor of the emitting electrons $\sim 1.6 \times 10^5$ assuming that synchrotron radiation cooling drives the shortest variability timescale. Blazars vary at a large range of timescales often from minutes to years. These results, as obtained here from the very short end of the range of variability timescales of blazars, are a confirmation of the leptonic scenario and in particular the synchrotron origin of the X-ray emission from Mrk 421 by relativistic electrons of Lorentz factor as high as 10^5. This particular mode of confirmation has been possible using minutes to days timescale variability data obtained from AstroSat and simultaneous multi-wavelength observations.

This work was done in collaboration with R. Chatterjee of Presidency University, Kolkata.

doi : https://doi.org/10.1007/s12036-021-09709-3

(Neeraj Kumari and Sachindra Naik)

Remnant radio galaxy candidates of small angular sizes

Remnant radio galaxies (RRGs), characterized by the cessation of AGN activity, represent a short-lived last phase of radio galaxy's life-cycle.

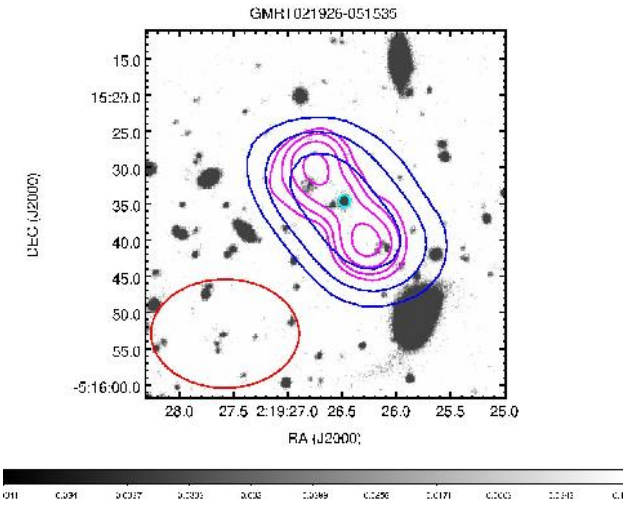

Figure no.13: Image of a remnant showing 325 MHz GMRT radio contours (in Blue) and 1.4 GHz JVLA radio contours (in Magenta) overlaid on the corresponding *i* band Subaru optical image. The potential host galaxy is marked with a small circle (in Cyan) around it. The 325 MHz GMRT synthesized beam of $10''.7 \times 7''.9$ is shown by an ellipse (in Red) in the bottom left corner.

Hitherto, searches for RRGs, mainly based on the morphological criteria, have identified sources of large angular sizes, which in turn, result into a bias towards the remnants of powerful radio galaxies. In this study we make the first attempt to perform a systematic search for RRGs of small angular sizes ($< 30''$) in the XMM$-$LSS deep extragalactic field. We discover 48 RRGs exhibiting strong spectral curvature i.e., $\alpha_{\rm low}$ - $\alpha_{\rm low} \geq$0.5. The spectral characteristics at higher frequency regime ($>$ 1.4 GHz) indicate that some of our remnant candidates can depict recurrent AGN activity with an active core. Figure 13 shows radio contours overlaid on the optical image for a RRG found in our study. Considering the full sample of radio galaxies we place an upper limit on the remnant fraction to be 5.4 per cent above flux density cutoff limit of 10 mJy at 150 MHz. We find that our small$-$size ($<$ 200 kpc) RRGs are often found to reside in less dense environments and at higher redshifts (z $>$ 1.0). We suggest that a relatively shorter active phase and/or low jet power can give rise RRGs of small sizes. This work has been done in collaboration with Prof. Yogesh Wadadekar and Prof. Ishwara-Chandra from NCRA-TIFR Pune, India.

doi : https://doi.org/10.3390/galaxies9040121

(Veeresh Singh and Sushant Dutta)

A comparative study of the physical properties for a representative sample of Narrow and Broad-line Seyfert galaxies

We present a comparative study of the physical properties of a homogeneous sample of 144 Narrow line Seyfert 1 (NLSy1) and 117 Broad-line Seyfert 1 (BLSy1) galaxies.

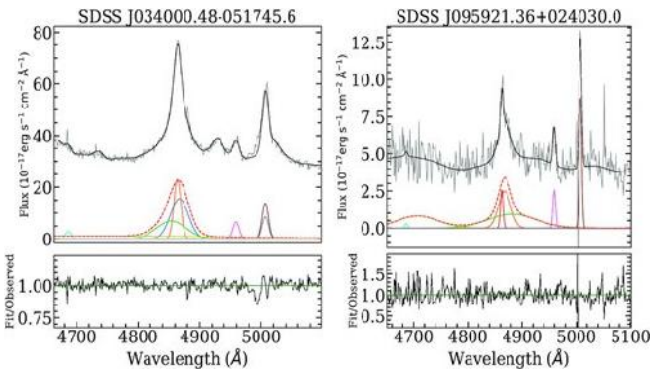

Figure no.14: Demonstration of asymmetric Hβ emission profiles. The multiple Gaussian profiles used to fit the Hβ emission line are also shown. The combination of broad components used to estimate asymmetry index is shown as a dashed red line. An example of a blue asymmetric profile having a negative asymmetry index of -0.152 is shown in left panel, while the right panel shows an example of red asymmetric profile having a positive asymmetry index of +0.227.

These two samples are matched in luminosity and redshift range. We performed direct correlation analysis (DCA) and principal component analysis (PCA) to compare the observational and physical parameters of optical and X-ray spectra of the two samples of Seyfert galaxies. We confirm that the correlations for the general quasar population hold for both types of galaxies despite significant differences in their physical properties. We also characterize the sample galaxies by using the line shape parameters namely the asymmetry and kurtosis indices (see

Figure 14). The PCA shows that NLSy1 and BLSy1 galaxies occupy different parameter spaces. Further, the fraction of NLSy1 galaxies showing outflow signatures, characterized by blue asymmetries, is higher by a factor of about 3 than that for BLSy1 galaxies. We suggest that the presence of high iron content in the broad-line region of NLSy1 galaxies in conjunction with higher Eddington ratios can be the possible reason behind this phenomenon. Hence, our results show intrinsic differences between NLSy1 and BLSy1 galaxies.

This work has been done in collaboration with Mr. Vivek Kumar Jha, Dr. Amitesh Omar from ARIES Nainital, Prof. Hum Chand from Central University of Himachal Pradesh, Dharamshala, and Shantanu Rastogi from Deen Dayal Upadhyaya Gorakhpur University, Gorakhpur, India.

doi : https://doi.org/10.1093/mnras/stab3700

(Vineet Ojha)

Intra-night optical variability study of a non-jetted narrow-line Seyfert 1 galaxy: SDSS J163401.94+480940.1

The nature of radio jet in Narrow-Line Seyfert 1 galaxies (NLS1s) is not well understood due to their relative weakness in radio wavelengths. Intra-night optical variability can be used as a tool to probe the existence of outflowing jets. In our recent study we performed optical monitoring of SDSS J163401.94+480940.2, a non-jetted radio-loud narrow-line Seyfert 1 (NLSy1) galaxy, using 3.6-m Devasthal optical telescope.

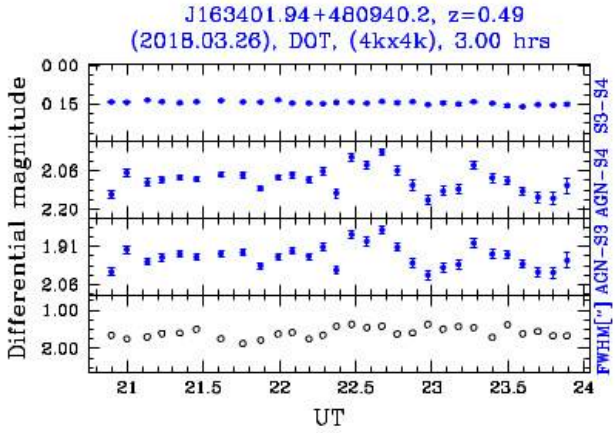

Figure no. 15: Intranight differential light curve (DLC) of SDSS J163401.94+480940.2 monitored on 2018.03.26. The upper DLC is derived using the chosen two (non-varying) comparison stars, while the lower two DLCs are the 'RLNLSy1-star' DLCs, as defined in the labels on the right side. The bottom panel displays the variations of the seeing disc (FWHM) during the monitoring session.

Using two sessions each of >3.0 hours we investigated intra-night optical variability (INOV) in this NLS1 for the first time. We detected a remarkable flare showing rapid brightening phase implying an extremely fast minute-scale variability which is similar to that observed in blazar PKS 1222+21 (see Figure 15). The detection of micro-variability in this NLS1 suggests the existence of relativistic jets with a small viewing angle. We highlight that this source represents an interesting case in which relativistic jets remained undetected in the Very Long Baseline Array (VLBA) radio observations.

doi : https://doi.org/10.1007/s12036-022-09814-x

(Vineet Ojha)

Exploring sub-MeV sensitivity of AstroSat-CZTI for on-axis bright sources

The Cadmium Zinc Telluride Imager (CZTI) onboard AstroSat is designed for hard X-ray imaging and spectroscopy in the energy range of 20 - 100 keV. The CZT detectors are of 5 mm thickness and hence have good efficiency for Compton interactions beyond 100 keV. The polarisation analysis using CZTI relies on such Compton events and has been verified experimentally. The same Compton events can also be used to extend the spectroscopy up to 380 keV. Further, it has been observed that about 20% of pixels of the CZTI detector plane have low gain, and they are excluded from the primary spectroscopy. If these pixels are included, then the spectroscopic capability of CZTI can be extended up to 500 keV and further up to 700 keV with a better gain calibration in the future. We explored the possibility of using the Compton events as well as the low gain pixels to extend the spectroscopic energy range of CZTI for ON-axis bright X-ray sources. We demonstrate this technique using Crab observations and explore its sensitivity.

We have outlined a methodology of sub-MeV spectroscopy using Crab observations. For this purpose, we have used the single-pixel mask-weighted spectral data in the 30 – 100 keV energy range, 2-pixel Compton events including low gain pixels in the 100 – 500 keV energy range, and the single-pixel events including low gain pixels in the 100 – 700 keV energy range. For the background subtraction, we have used the phase match method for the exposure correction since the background and source observations are of different times and exposure. The spectral fits using bknpower law in XSPEC show sufficient flux sensitivity of CZTI to carry out spectroscopy for ON-axis bright sources up to 500 keV. In the future, we plan to develop better background subtraction methods and investigate the gain of the low gain pixels in more detail to establish the Compton spectroscopy for ON-axis sources using the Astrosat-CZTI.

This work was done in collaboration with T. Chattopadhyay, A. R. Rao, S. Gupta, V. Bhalerao and D. Bhattacharya of AstroSat-CZTI team.

doi : https://doi.org/10.1007/s12036-021-09711-9

(A. Kumar, S. Vadawale and N. P. S. Mithun)

PRL 2.5m Telescope

The PRL 2.5m telescope project is a state-of-the-art technological development taken up at Physical Research Laboratory (PRL) in collaboration with Advanced Mechanical and Optical Systems (AMOS), Belgium. First in the country, the telescope is equipped with the highly advanced active optics and with first order seeing corrections using a tip/tilt unit working at a frequency of 20Hz. The design of the main tube of

the telescope is a Ritchey-Chretien (RC) configuration, i.e. a hyperbolic concave primary mirror (M1) and a hyperbolic convex secondary mirror (M2) sharing a common conical focus.

Figure no 16a: PRL 2.5m observatory at Gurushikhar, Mount Abu, India

The plate scale of the telescope is 10.313″/mm. The effective focal ratio of the telescope is f/8 with the operational waveband between 370-4000 nm. The size of the M1 mirror is 2.56m supported over 42 axial and 18 peripheral pneumatic actuators which are part of the active optics systems. The secondary mirror M2 is mounted over a hexapod and has five degrees of freedom (tip, tilt and focus) to correct for the optical aberrations. The telescope has an un-vignetted Field-of-View (FOV) of 25′ diameter at the main port. Two side ports are designed for FOV of 10′ diameter. There are two M3 mirrors mounted over rack and pinion support systems to direct the central light to two side ports respectively. The pointing accuracy of the telescope is 2″ rms absolute and 0.5 arcsec rms differential. The tracking accuracy of the telescope is 0.1 - 0.2 arcsec rms in close loop with the auto-guider unit. The telescope arrived at the site (Gurushikhar, Mount Abu, India) in the first week of February, 2021. Thereafter, due to the second wave of COVID pandemic in India and the monsoon season, the telescope installation started in the first week of October, 2021. The entire telescope installation is expected to be over by May 2022, subject to advancement of the monsoon season in 2022.

The first light instruments that will get attached to the telescope for science are a) the CCD imager or Faint Object Camera (FOC), b) the PARAS-2, which is a fiber-fed optical high resolution optical spectrograph, and c) the Speckle Imager. Figure 16 shows the whole facility constructed at Gurushikhar, Mt. Abu, India, along with the fully assembled telescope.

Figure no 16b: Fully assembled Telescope installed at the main telescope site

(Abhijit Chakraborty, Kapil Kumar, Neelam JSSV Prasad, Kevikumar Lad, Ashirbad Nayak, Vivek Kumar Mishra, Vishal Joshi, Mudit K. Srivastava and Nafees Ahmed)

Faint Object Camera (FOC)

Faint Object Camera (FOC) comprises 4k X 4k ANDOR CCD with a set of SDSS (Sloan Digital Sky Survey) *u, g, r, i, z* photometric band filters. CCD Imager will mainly be used for carrying out photometry studies of various astronomical objects using the aforesaid filters. The FOV of the CCD imager is $10' \times 10'$. It will be attached to the main port of the 2.5m telescope. Two numbers of filter wheels (diameter approx. 360mm) have been realised for mounting the filters. The position of each filter wheel is controlled by an independent stepper motor and interruption sensor. The controller for filter wheels is designed and developed entirely in-house. Custom-build software has been developed in-house for the operations of the instrument (see Figure 17). Provision has also been kept for carrying out photometry study with a neutral density filter, which is controlled by servo motor. The neutral density filter will help us to image bright sources, without getting the detector saturated. The FOC will be sensitive enough to detect faint sources with the sky background limit of 21 magnitude in the *SDSS i- band*, and will be helpful for extragalactic astronomy and GRB observations.

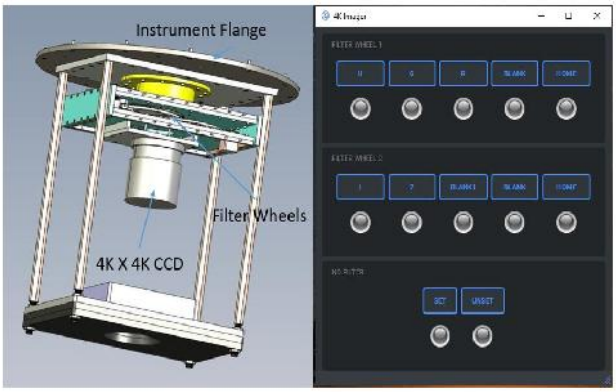

Figure no. 17: Left panel shows the mechanical 3D model of the FOC, while right panel shows the filter wheel control software.

(Abhijit Chakraborty, Kevikumar Lad, Neelam JSSV Prasad, Kapil Kumar, Ashirbad Nayak and Vishal Joshi)

PARAS-2

PARAS-2 (PRL Advanced Radial-velocity Abu-sky Search) is an optical fiber-fed, high-resolution spectrograph aimed to detect super-Earths around bright G & K dwarf stars.

Figure no. 18: The PARAS-2 spectrograph installed at the 2.5m Telescope facility, Gurushikhar Observatory, Mt Abu is shown in the left panel, while the right panel is showing the 3D- model of the PARAS-2 Cassegrain Unit.

This is the highest-resolution spectrograph in the country and Asia with a median Resolution of 110,000, in the wavelength range of 380-690 nm. It consists of optical elements like, R4 Echelle grating, M1 & M2 off-axis parabolic mirrors, Grism as cross disperser, Camera lens barrel and a 6K X 6K CCD detector, and have an overall efficiency of 23% - 28%. A combination of octagonal and circular fibers along with the double scrambler is used for achieving the RV precision of $50cm\ s^{-1}$ or better. The whole spectrograph is kept inside a thermally controlled vacuum chamber (Figure-18, left), in which temperature and pressure are maintained at $22.5 \pm 0.0007°$C and $0.001 \pm 0.0005\ mbar$, respectively. With such precise thermal control, the spectrograph has shown a relative fiber drift of 34 cm s^{-1} (see Figure 19) for the time interval of approximately 6 hours, which is the evidence of the spectrograph's capability to be able to go down to sub-m s-1 precision with stars. Figure 20 shows the Uranium-Argon (UAr) spectra taken from PARAS-2 at 110,000 resolution. The Cassegrain unit of the spectrograph, which will be attached with the telescope side port to collect the star light, is also designed and developed within the PRL (see Figure 18, right). The Cassegrain unit contains a focal reducer (f/8 to f/4), calibration unit and two PI actuator motors, to move the star fiber and other for the calibration fiber. The Atmospheric Dispersion Corrector (ADC) unit designed in PRL will be placed between parallel beams of focal reducer to correct for atmospheric dispersions.

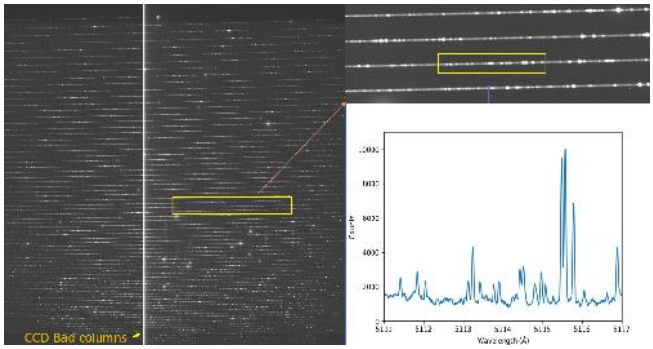

Figure no. 19: PARAS-2 Echellogram is shown here with single fiber illuminated by Uranium-Argon (UAr) hollow cathode lamp . A small zoomed part of the echellogram along with the wavelength calibrated extracted spectra is also shown.

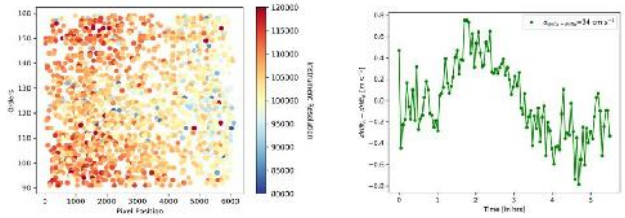

Figure no. 20: The spectrographs resolution map is shown in left. We measured the median resolution to be ∼1,10000 for PARAS-2. In right, the plot is showing the inter-fiber drift (A-B) for 6 hours and its dispersion is 34 cm s^{-1}.

(Abhijit Chakraborty, Kapil Kumar, Neelam JSSV Prasad, Kevikumar Lad, Ashirbad Nayak and Rishikesh Sharma)

Speckle Imager

Speckle Imaging / Lucky Imaging is one of the ways to image and resolve, very close to the diffraction limit of the telescope. Due to the presence of the earth atmosphere and air turbulence stars twinkle, as a result their images are blurred, with an angular diameter of 1-3", which is known as the seeing parameter of a particular astronomical site. However, if one takes very short exposures with timescales of 2-10 ms, during which the atmosphere is partially frozen, and hence the atmospheric turbulence effect is reduced. So in principle, this technique of cumulative short exposures and co-adding them can produce near diffraction limited images of stars, with FWHM of 0.1-0.3". Thus, the speckle imager for the 2.5m telescope will be used to image the close binary systems. The speckle imager will have a

FOV of $1.5' \times 2.0'$, and will have capability to give exposure times of 2-50 ms. It will have a fixed V-band and neutral density filter. The speckle imager is expected to resolve stars as close as 0.3 to 0.4 arcsec.

(Abhijit Chakraborty, Kapil Kumar, Neelam JSSV Prasad, Kevikumar Lad, Ashirbad Nayak, Rishikesh Sharma and Nikitha K. Jithendran)

Refurbishment of EMPOL: an EMCCD based optical imaging polarimeter

EMPOL is an EMCCD based Optical Imaging Polarimeter for the PRL 1.2m Cassegrain-type telescope situated at Gurushikhar, Mt. Abu. This instrument is a product of a fully inhouse development at PRL. EMPOL uses an Andor iXon 1K $\times$ 1K EMCCD detector (with 4 $\times$ 4 binning). The original old optical design of EMPOL consisted of a rotating half-wave plate along with a Glan-Taylor prism as an analyzer. Total number of steps per rotation of the half-wave plate is 48. Recently, we have refurbished the design and now this prism has been replaced with a wire-grid polarizer as the analyzer in a combination of a half-wave plate as polarization optical elements. This allowed a shorter instrument length and a relatively larger useful field of view. EMPOL covers a 3 arcmin $\times$ 3 arcmin field of view. EMPOL has negligible instrumental polarization. A new frame structure was designed and fabricated at the PRL-Thaltej workshop to hold the optical barrel as well as the associated electronics and the control PC in one unit. A compact box was designed and built for housing the electronics of EMPOL. All the wiring was redone to ensure stable operation in the box. The box was mounted on the optical barrel. After assembling all the parts and fixing them in the frame, the functionality of EMPOL was checked by acquiring test images with EMCCD at Ahmedabad. EMPOL was then sent to Mt Abu for regular observations. Now the entire instrument is a single unit with just power and network cable to be connected at the time of mounting the instrument to the Cassegrain plate of the 1.2 m telescope (see Figure 21). This allows for routine remote observations with the instrument.

Figure no 21: EMPOL at 1.2 m telescope of Mount Abu Observatory.

(Alka, Prachi Prajapati and Shashikiran Ganesh)

Adaptive Optics (AO) System Development

Design of an AO assisted near-infrared (NIR) camera for upcoming PRL 2.5m telescope

Adaptive optics (AO) technique is used in astronomy to enhance the imaging quality of optical/near-infrared (NIR) telescopes by compensating for the effects of wavefront distortions, which are caused by the turbulent atmosphere of the Earth. We have started a project for developing an Adaptive Optics (AO) based instrument for the upcoming PRL 2.5m telescope. The proposed system is being designed for a 30 arc-sec field of view and would be able to work with both Natural Guide Star (NGS) as well as with artificial Laser Guide Star (LGS). The instrument will have two science detectors, one in the Visible range (0.39μ to 1.0μ) and other will cover NIR J, H & K bands. Optical relay consists of several custom-designed Off-axis parabolas to avoid any chromatic aberration. The system is going to employ a Tip-tilt Mirror (TTM) operating at 100Hz for lower order corrections and a Deformable mirror (DM) for correcting higher orders at 1KHz rate. There will be a Shack-Hartmann Wavefront Sensor(SHWFS) for measuring the distortion in the wavefront, operating in the visible waveband. During LGS operation, tip-tilt measurement will be separately carried out on a nearby field star using one of the science detectors (either visible or NIR camera). Provisions have been made to search a bigger field using field steering mirror. In case of NGS operation, a field stop and a steering mirror will enable light only from the guide star to fall on the wavefront sensor. Figure 22 shows the optical design of the proposed instrument which is currently undergoing optimization.

In the NIR arm, a focal reducer type camera has been planned using custom-designed lenses. The pupil plane will have a cold stop and a filter wheel assembly. In order to avoid thermally generated noise, the entire NIR assembly would be kept in vaccuum cryogenic dewar at a low temperature.

Atmospheric dispersion is another destructive effect apart from the astronomical seeing, in degrading the image quality. Due to differential refractive index of air for different wavelengths, an elongated image of the object is obtained on the camera thus defeating the purpose of AO correction. Atmospheric Dispersion Corrector (ADC) is a device which corrects for the atmospheric dispersion. We have designed and simulated a rotating double Amici prism based ADC and suitable placed it in the instrument optical design.

Development of real-time closed loop control for the AO System

In an AO instrument, a control system is used to extract the SHWFS signals and compute the signals that are to be sent to the deformable-mirror (DM) and tip-tilt mirror (TTM). This is a compute intensive task, as the new DM feedback signal is computed from the raw SHWFS frame data typically at 1KHz rate. A general purpose CPU running on the Linux operating system, is not a strict real-time system and often causes time jitter due to its default Completely Fair Scheduler(CFS)s scheduling policies. However the scheduling policies can be adjusted to suit the needs of real-time applications. We developed an arduino based AO emulator (Figure 23) to test the scheduling policies.

The key hardware components of AO controller i.e. SHWFS, DM and

TTM are simulated using Arduino Atmega 2560.The firmware for the simulator is written in Embedded C. The software is developed on Linux-Centos Operating system in C language. Various functionalities for device detection, serial port detection, listing the device Id and mapping the serial ports with devices have been implemented. Preliminary command structure and protocol for PC to Arduino communication is also implemented. Communication over COM port using USB has been successfully established between PC and device simulators. Continuous loop algorithm for communication between SHWFS and DM is based on status flag check methodology. This loop can be terminated via user command. Also there is provision of terminating the loop from hardware end by the user, by switching the Arduino pin.

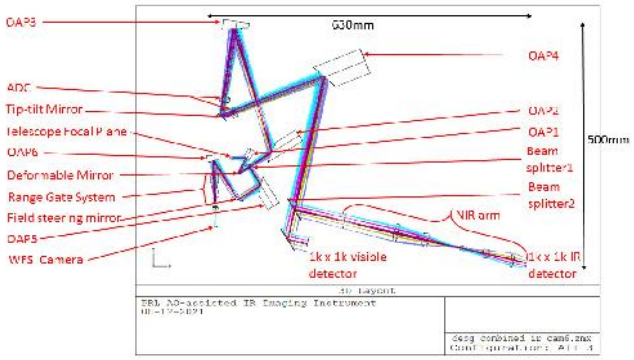

Figure no. 22: Optical design of the AO Assisted Near-Infrared (NIR) Camera for Upcoming PRL 2.5m Telescope.

For the actual AO control system implementation, we are using a 2 PC approach. For convenience purpose we are calling them 1) Compute PC and 2) User PC. Compute PC would be used for running real-time control software while the user PC would provide a user interface and functionalities to execute other instrument related tasks like operations of science camera, ADC, filter wheels, field steering mirrors etc. Socket programming based interprocess communication(IPC) is being used for PC-PC communication between User and Compute PC over ethernet. Figure 24 shows the details of the architecture we have adopted for the implementation.

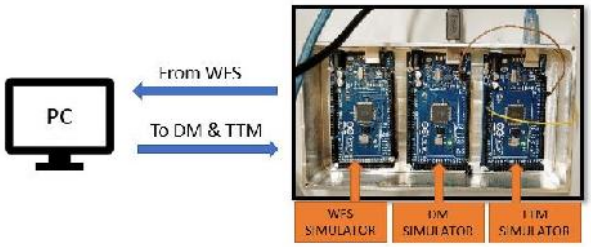

Figure no. 23: Arduino based simulator for the AO system.

PC-PC communication algorithm is designed with three simultaneous data communication channels where the first channel will execute routine commands, the second channel will be exploited for data transfer and the third channel will be used for monitoring the status of various processes and variables. Both the User PC and Compute PC have multi-threading model to execute tasks in parallel. Scheduling will ensure that data telemetry from compute PC to User PC will have minimal effect on the performance of Compute PC. We have developed and tested codes for the communication architecture. Individual AO subsystems will be tested for their hardware performance with the control system in the next phase.

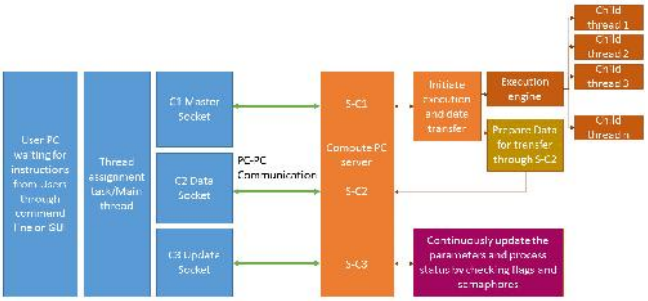

Figure no. 24: The socket programming architecture for the AO control system

(Vaibhav Dixit, Ankita Patel and Mudit K. Srivastava)

Mt. Abu Faint Object Spectrograph and Camera - Echelle Polarimeter (MFOSC-EP) for PRL 2.5m Telescope

Mt. Abu Faint Object Spectrograph and camera Echelle Polarimeter (MFOSC-EP) is being designed for the upcoming PRL 2.5m telescope. MFOSC-EP would work in the visible regime (3900-9900Å) and would provide the functionalities of a seeing limited filter-based imaging, low-resolution spectroscopy using grisms, and intermediate resolution spectro-polarimetry. The system would utilize a common collimator optics to couple the low-resolution module and spectro-polarimeter module using a movable fold mirror. The low-resolution module would provide the spectral resolution of $\sim$500-800 over $\sim$3800-9900Å spectral range with two custom designed grisms. This module will also be used for filter-based seeing limited imaging in SDSS u,g,i,r and z filters. 1K$\times$1K EMCCD camera of this module would also enable the fast timing studies of variety of astrophysical systems. The spectro-polarimeter module would use half-waveplate + Wollaston prism to separate o and e-rays of the incoming beam and would feed into an echelle spectrometer. The echelle spectrometer would use a higher order echelle grating along with two plane reflection gratings as the cross-disperser elements. The multi-order spectra for o and e-rays would be recorded on a 2K$\times$2K CCD detector. The spectral resolution of $\sim$15000 would be achieved for 1 arc-second slit (sampled by 4.5 pixels).

The complete system architecture and optical designs of each of the modules were described in previous years annual reports. These designs were again re-optimized and has now been completed (after couple of re-iterations) based on the manufacturing feasibility of the optical elements. The complete optical layout of the instrument is shown in Figure 25. The base specification of the instrument are given in Table 1.

Parameters	Values
Low Resolution Mode	
Imaging Wavelength range	390-990 nm
Imaging field of view	$\sim 5.52' \times 5.52'$ arc-minute square
Imaging pixel scale	3.1 pixels/arc-sec
Imaging mode quality requirement	80% EE diameter should be within 1 pixel (13 μm)
Magnification in LRA mode	$\times$0.416
Camera f/#	3.325
CCD Detector	1K X 1K EMCCD with 13μm pixel size
Broad-band filters	SDSS u,g,i,r,z filters
Spectral coverage of grisms	380-990 nm using two different grisms
Spectral resolution	$\sim$500-800
Pupil diameter	$\sim$ 35mm
Spectro-Polarimeter Mode	
Imaging Wavelength range	390-990 nm
Polarimeter Optics: Magnification	$\times$1
Polarimeter Optics: Pupil diameter	$\sim$ 35 mm
Polarimeter Optics: Field of View	$\sim$ 1 X 1 arc-minute square
Polarimeter Optics: Half wave plate	Material: PMMA Retardance- 180 degree Required Clear Aperture: 37.4mm (1'X1' field)
Polarimeter Optics: Polarizer	Type- Wollaston prism Material: MgF2 Prism Cut angle: 4.5 degree Deviation angle:$\sim$0.106 degree Required CA: 36.8mm X 36.8mm (1'X1' field)
Separation between o-ray and e-ray at polarimeter focal plane	$\sim$ 514 μm ($\sim$5 arc-seconds)
Echelle-Sepctrometer: Pupil size	$\sim$50.8mm
Echelle-Spectrometer: input f/#	8
Echelle-Spectrometer: output f/#	4.428
Echelle-Spectrometer: Magnification	$\times$0.55
Echelle grating specification	52.67lp/mm
Blaze, Alpha and Beta angles for Echelle grating	63.5 degree
Gamma angle for Echelle grating	6.5 degree
Blue cross disperser grating	600lp/mm, λ_b=500nm
Alpha and Beta values	36.75 and 18.25 degree
Order range (Wavelength range)	60-87(382nm-570nm)
Red cross disperser grating	235lp/mm,λ_b=750nm
Alpha and Beta values	33.5 and 21.5 degree
Order range (Wavelength range)	34-59 (564nm-1000nm)
Detector	2Kx2K CCD (13.5 μm pixel size)
Minimum separation between two order	$\sim$41 pixel
Separation between o & e-ray at detector	$\sim$ 21 pixels
Spectral-Resolution 650nm	$\sim$15000

Table 1: Specification for various modes of MFOSC-EP

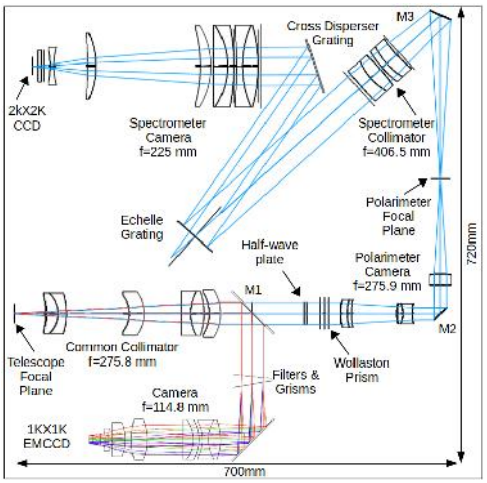

Figure no. 25: The complete optical design layout of MFOSC-EP instrument. Fold mirrors are used to fold the design within the constraints of the mechanical dimensions.

(Mudit K. Srivastava, Vipin Kumar, Vaibhav Dixit, Ankita Patel and Bhaveshkumar Mistry)

Design and development of ProtoPol : A Prototype Spectro-polarimeter

As a precursor of MFOSC-EP, a prototype spectro-polarimeter (named ProtoPol) is currently being developed. ProtoPol has been designed with commercially available off-the-shelf optical components. This feature makes the design cost-effective and helping in faster development timescales. ProtoPol has been designed to cover 3820-9660Å on an 1K$\times$1K CCD at resolutions of $\sim$6000-7000 with 1.0 arc-second slit-width. Commercially available optical elements (one-inch optics) are used in the collimator and polarimeter optical modules. Wollaston prism and Half-wave plate are also chosen from the existing catalogue of the commercial manufacturers. The echelle spectrometer module of ProtoPol has been designed with an off-axis parabola as the collimator, a commercial Canon 200mm, f/2 lens system as the camera optics and ANDOR 1K$\times$1K off-the-shelf CCD camera as the detector. Similar to MFOSC-EP instrument, it also works on the concept of an echelle grating and two plane reflection gratings as the cross-dispersers. This prototype instrument can be used on the existing 1.2m PRL telescope as well as on the upcoming 2.5m PRL telescope with suitable mechanical interfaces. Figure 26 shows the optical and mechanical design models of the instrument. The mechanical parts of ProtoPol are currently being manufactured in-house while the optical parts are being procured.

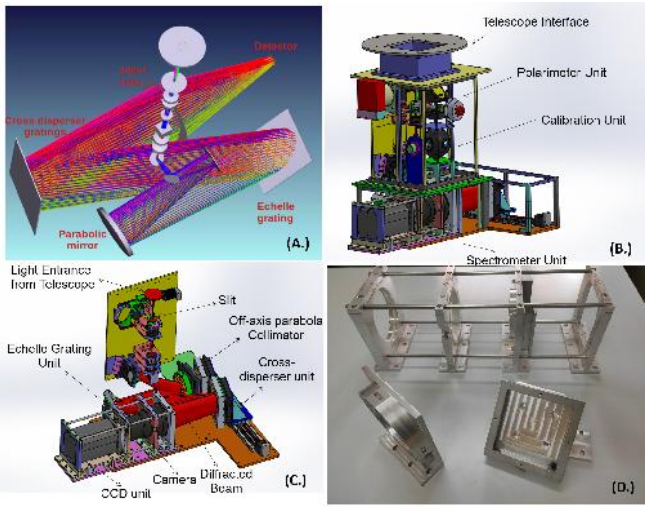

Figure no. 26: (A.) The optical design layout of the ProtoPol instrument (B.) The complete mechanical design layout of the ProtoPol instrument. The height of the instrument is $\sim$700mm. (C.) CAD schematics for the internal model of ProtoPol (D.) Some of the mechanical components of ProtoPol which have been manufactured in-house.

(Mudit K. Srivastava, Vipin Kumar, Vaibhav Dixit, Ankita Patel, Bhaveshkumar Mistry and Kevikumar Lad)

Solar X-ray Observations with Chandrayaan-2 XSM: POC Operations, Data Processing and Release, and Website

Solar X-ray Monitor (XSM) on-board Chandrayaan-2 mission has been operational in-orbit for more than two and half years providing soft X-ray spectra of the Sun during quiescent periods to large solar flares. Data from the spacecraft downloaded at the ground stations

during each playback undergo pre-processing at ISSDC and XSM data along with required auxillary information are made available to the Payload Operations Center (POC) at PRL where higher levels of data processing happen. Data downloaded during mutliple passes are combined to generate the complete raw data set for each day of observation and then further processing is carried out on these data sets where various aspects of calibration are incorporated. When the complete data for a given day of observation is available, after a minimum wait period of 15 days, the data gets automatically posted to ISSDC and released publicaly on PRADAN. The entire processing chain at POC is fully automated with provisions for email notifications. We have also developed a website that allows interactive plotting of solar X-ray flux obtained with XSM, a screenshot of which is shown in Figure 27. The website shows the X-ray flux obtained by integrating the spectra over 1-8Å or 1-15 keV, which is updated as and when data becomes available. The website is basically a python-based web application made using flask module. The home page of the website has option for the users to select start and end dates and then it generates plot of XSM light curve for the selected duration. The plot widget has a tool box that allows reformatting the plot such as zoom, pan, hover etc. at client side. The website also includes information on the instrument, observations as well as provide detailed guides for analysis of XSM data.

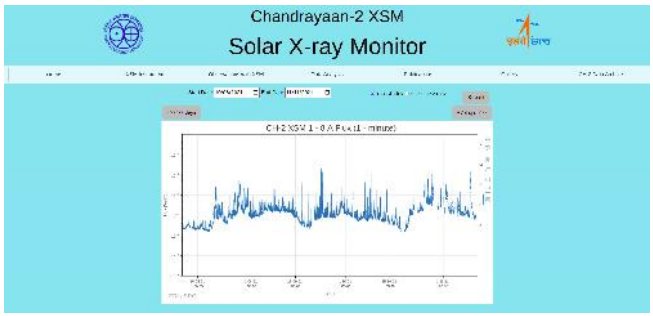

Figure no. 27: Screenshot of the website for interactive plotting of solar X-ray flux light curves obtained from XSM observations

(N. P. S. Mithun, C. S. Vaishnav and S. Vadawale)

An experimental setup for validation of off-axis polarimetry with CZT detectors of AstroSat CZTI and proposed Daksha mission

Pixellated Cadmium Zinc Telluride (CZT) detectors capable of hard X-ray spectral measurements in $\sim$ 20 – 200 keV have been used in the CZT-Imager instrument of AstroSat mission and are also planned as the primay detectors for the proposed Daksha mission aimed at discovery and characterization of electromagnetic counterparts to gravitational wave sources as well as Gamma Ray Bursts (GRBs). In addition to spectroscopy, the same CZT detectors can be used for measurement of X-ray polarization using the principle of Compton scattering. This technique has been verifed experimentally and was used to obtain new results for Crab pulsar using observations with AstroSat CZTI. It also has been extended to carry out polarimetry of GRBs that are incident at off-axis angles; however, polarimetric capability of off-axis source has not been demonstrated experimentally. In this context, we have developed a novel experimental setup to invetsigate the off-axis polarimetric capability of CZT detectors to strengthen the GRB polarimetry with AstroSat CZTI and Daksha mission. Figure 28 shows a photograph of the realized experimental setup. The aluminium box mounted on rotational and translational stages houses the CZT detector and in-house developed read out electronics. The FPGA-based readout electronics controls the ASIC within the CZT detector module and reads out the pixel number and pulse height of each X-ray event interaction. The events are time-tagged, packetized, and transmitted to the labview based data acquisition system and stored in the computer for further analysis. The detector box mount has two angular degrees of freedom: one angle can be changed by the rotational stage and the other can be varied by mounting the detector box at specific angles on the bracket. This allows the detector to be placed at different polar and azimuthal incidence angles with respect to the X-rays from the source placed on the platform at the top. To characterize the response of detector to unpolarized source, the detector can be shined with emission from laboratory radioactive sources. For carrying out experiments with partially polarized beam, we have developed the setup shown in lower panels of Figure 28. X-rays from a radioactive source are collimated and allowed to undergo Compton scattering in an aluminium cylinder. The scattered X-rays are allowed to exit the assembly in one direction through a slit providing highly polarized beam. Polarization angle can be varied by placing the partially polarized source at different angles on the top platform. The experimental setup is being used to demonstrate the off-axis polarization capabilities of CZT detectors. The same will also be used in future to refine and improve the polarimetric analysis techniques to be used in Daksha mission.

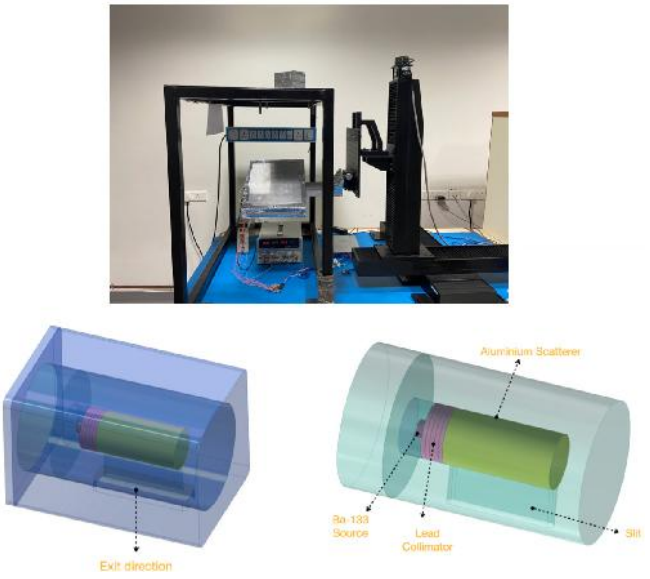

Figure no. 28: Top: Photograph of experimental setup for validation of off-axis polarimetric capabilities of CZT detectors. Bottom: CAD design of the setup to generate a partially polarized X-ray beam by Compton scattering.

(C. S. Vaishnav, N. P. S. Mithun, A. R. Patel, N. K. Tiwari, H. K. Adalja and S. V. Vadawale)

Proof-of-concept demonstration of X-ray concentrator optics

We have initiated development of X-ray focusing optics for future Indian astronomical missions. As part of this several instrument configurations are being worked out consid- ering the requirements to meet various science goals. One such configuration involves use of modular X-ray flux concentrators with non-imaging focal plane detectors to carry out wide band (1-30 keV) spectroscopy with high sensitivity. The modular design of this optics with relatively short focal lengths allows to design instruments with large effective area using an array of individual modules. The X-ray concentrators for this proposed configu- ration have a design that is based on KirkpatrickBaez (K-B) optics. However, unlike K-B optics, this concept uses flat mirror foils. The X-rays are first reflected by a set of foils arranged in vertical direction followed by the mirror foils that are placed in orthogonal direction so that they get focusses onto a single point (see Zeemax simulation in Figure 29). The designed concentrator module is realized using an in-house fabricated mirror module with precisely machined grooves to assemble the flat mirror foils as shown in Figure 29.As a first step, we have assembled flat mirror foils without any coating which is required for reflection of X-rays. To demonstrate the flux concentration by the module and to compare the geometrical optical properties of the system with simulations, we have carried out an experiment by illuminating it with a plane parallel laser beam. As the beam diameter was limited, different parts of the mirror module were illuminated. The last panel of Figure 29 shows the image at the focal plane showing the beam concentrated at the focal plane. Images due to reflection from only one set of foils can also be seen. With this initial proof-of-concept, we now plan to demonstrate focusing of X-rays where the mirror foils have appropriate single multi-layer coating. The modular design of this optics with relatively short focal lengths allows to design instruments with large effective area using an array of individual modules.

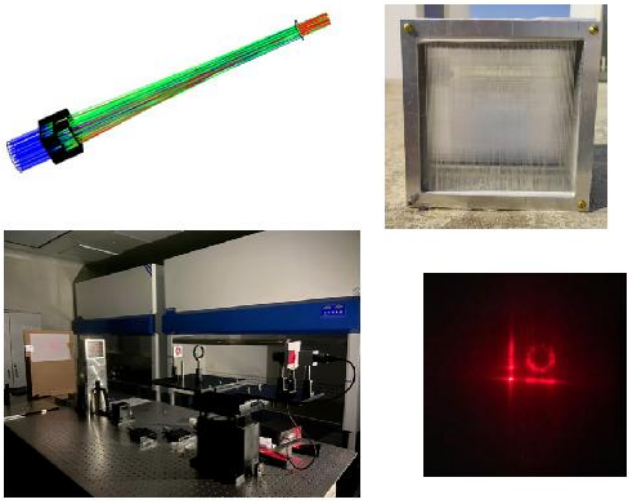

Figure no. 29: Top left: Zeemax implementation of mirror assembly. Top right: The optics module assembled with uncoated mirrors. Bottom left: optics setup for demonstrating the proof of concept. Bottom right: The image obtained on the focal plane

(C. S. Vaishnav, B. Mondal, N. P. S. Mithun, N. K. Tiwari, H. K. Adalja and S. V. Vadawale)

Solar Physics

Two-Stage Evolution of an Extended C-Class Eruptive Flaring Activity from Sigmoid Active Region NOAA 12734: SDO and Udaipur-CALLISTO Observations

We present a multi-wavelength investigation of a C-class flaring activity (Figure 1(a)) that occurred in the active region NOAA 12734 (Figure 2(a)) on 8 March 2019.

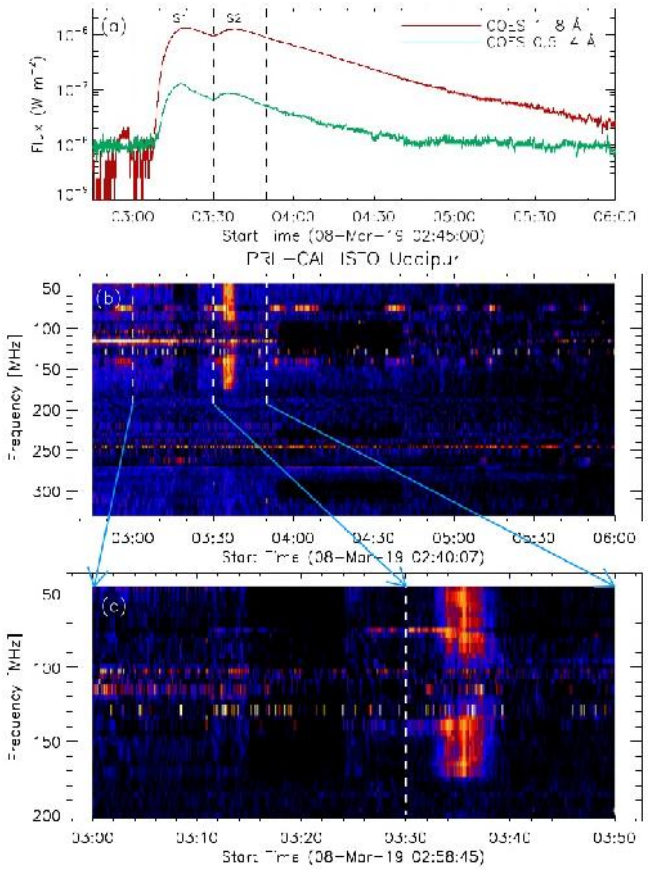

Figure 1.: Panel (a): GOES light curves showing the evolution of the extended C-class flaring activity in active NOAA 12734. The red and green lines indicate X-ray flux in 1-8Å and 0.5-4Å wavelength bands which correspond to disk-integrated X-ray emission in 1.5-12.5 keV and 3-25 keV energy range, respectively. GOES profiles reveal two distinct episodes of energy release (marked as S1 and S2) that peak at 03:19 and 03:38 UT, respectively, implying two-step process of energy release. Panel (b): Radio emission observed by PRL-CALLISTO Udaipur between the frequency range ≈50-180 MHz during the stage II of the flaring activity (S2). Panel (c): Zoomed view of the CALLISTO dynamic radio spectrum. Note that the horizontal void at ≈90-125 MHz is due to the filtering of radio emission by the FM rejection filter and therefore should not be interpreted as the absence of solar radio emission at these frequencies.

The investigation utilizes data from the Atmospheric Imaging Assembly (AIA) and the Helioseismic Magnetic Imager (HMI) on board the Solar Dynamics Observatory (SDO) and the Udaipur-CALLISTO solar radio spectrograph of the Physical Research Laboratory. This low intensity C1.3 event (Figure 1(a)) is characterized by typical features of a long-duration event (LDE), viz. extended flare arcade, large-scale two-ribbon structures and twin coronal dimmings.

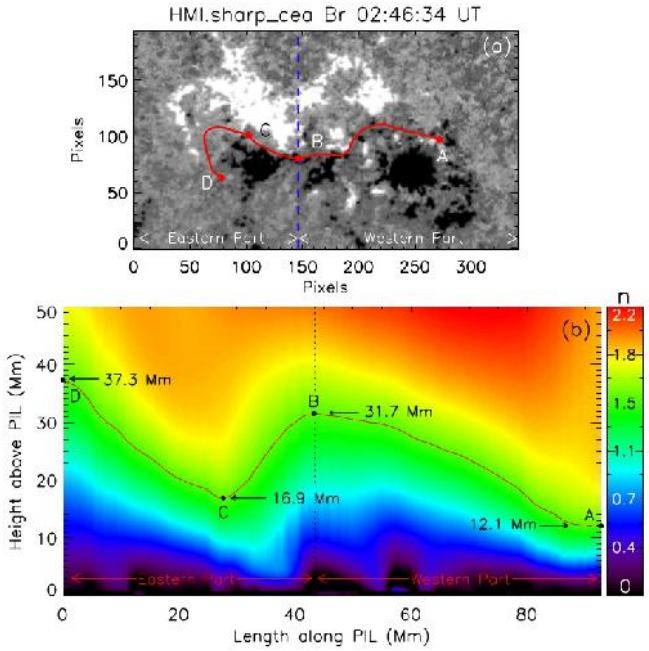

Figure 2.: Panel (a): HMI LOS magnetogram showing the photospheric configuration of the AR NOAA 12734 prior to the flaring activity. The approximate polarity inversion line (PIL) is shown by red curve (ABCD). Panel (b): Distribution of magnetic decay index (n) above the PIL. The red curve refers to the contour of n = 1.5

The eruptive event occurred in a coronal sigmoid and displayed two distinct stages of energy release, manifested in terms of temporal and spatial evolution. The formations of the twin-dimming regions are consistent with the eruption of a large flux rope with footpoints lying in the western and eastern edges of the coronal sigmoid. The metric radio observations obtained from Udaipur-CALLISTO reveals a broad-band (≈50–180 MHz), stationary plasma emission for ≈7 min during the second stage of the flaring activity that resemble a type IV radio burst (Figures 1(b)–(c)). A type III decametre-hectometre radio bursts with starting frequency of ≈2.5 MHz precedes the stationary type IV burst observed by Udaipur-CALLISTO by ≈5 min. The synthesis of multi-wavelength observations and non-linear force-free field (NLFFF) coronal modeling together with magnetic decay index analysis (Figure 2(b)) suggest that the sigmoid flux rope underwent a zipping-like uprooting from its western to eastern footpoints in response to the overlying asymmetric magnetic field confinement. The asymmetrical eruption of the flux rope also accounts for the observed large-scale structures viz. apparent eastward shift of flare ribbons and post-flare loops along the polarity inversion line (PIL), and provides

evidence for lateral progression of magnetic reconnection site as the eruption proceeds.

This work was done in collaboration with Divya Oberoi (NCRA, Pune), K. Sasikumar Raja (IIAP, Bangalore) and Christian Monstein (Istituto Ricerche Solari Locarno (IRSOL), Switzerland).

doi : https://doi.org/10.1007/s11207-021-01820-6

(B. Joshi, P. K. Mitra, R. Bhattacharyya and K. Upadhyay)

Multiwavelength Signatures of Episodic Null-point Reconnection in a Quadrupolar Magnetic Configuration and the Cause of Failed Flux Rope Eruption

We present the multiwavelength observations of triggering a failed-eruptive M-class flare from active region NOAA 11302 and investigate the possible reasons for the failed eruption.

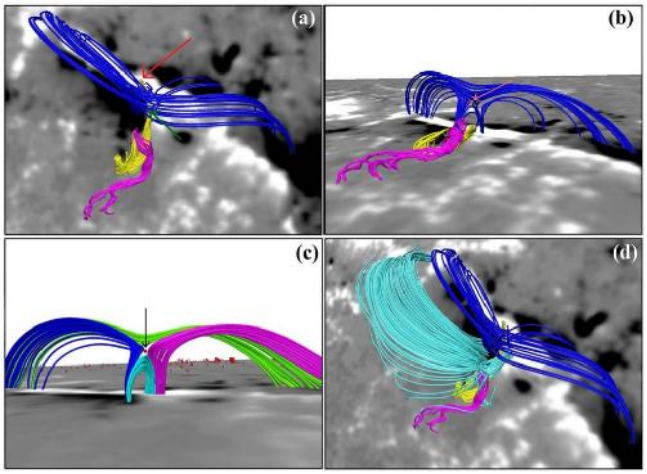

Figure 3.: Modeled coronal configuration involved in the preflare activities and the M-class flare including the two flux ropes (shown in bright yellow and pink color) and the low-coronal closed loops connecting the multipolar photospheric configuration (shown in blue color). The northern leg of the yellow-colored flux rope is indicated by the red arrows in panels (a). The red-colored patch within the blue lines (also indicated by the orange arrow in panel (b)) is characterized by log(Q) = 8.5 which represents a coronal nullpoint. The green arrow in panel (a) indicates the approximate location of the nullpoint. In panel (c), only the representative magnetic lines involved in the nullpoint configuration are shown. For a better representation, the four domains of magnetic field lines are shown in different colors. The black arrow indicates the nullpoint. The sky-colored lines in panel (d) represent the set of coronal loops that intensified during the gradual phase of the flare.

Photospheric observations and coronal magnetic field obtained through nonlinear force-free field extrapolation revealed that the flaring region had a complex quadrupolar configuration (Figure 3) with a pre-existing coronal nullpoint (indicated by the black arrow in Figure 3(c)) situated above the core field. Prior to the onset of the M-class flare, multiple small-scale flux enhancements are observed around the nullpoint, evidenced in the soft X-ray passbands of GOES and RHESSI. The preflare configuration and evolution reported here are similar to the configurations presented in the breakout model, but at much lower coronal heights. The core of the flaring region was characterized by the presence of two flux ropes in a double-decker configuration (shown by yellow and pink colors in Figures 3(a), (b) and (d)). During the impulsive phase of the flare, one of the two flux ropes initially started erupting, but resulted in a failed eruption. Calculation of the magnetic decay index revealed a saddle-like profile (Figure 4) where the decay index initially increased to the torus-unstable limits within the heights of the flux ropes, but then decreased rapidly and reached negative values, which was most likely responsible for the failed eruption of the initially torus-unstable flux rope.

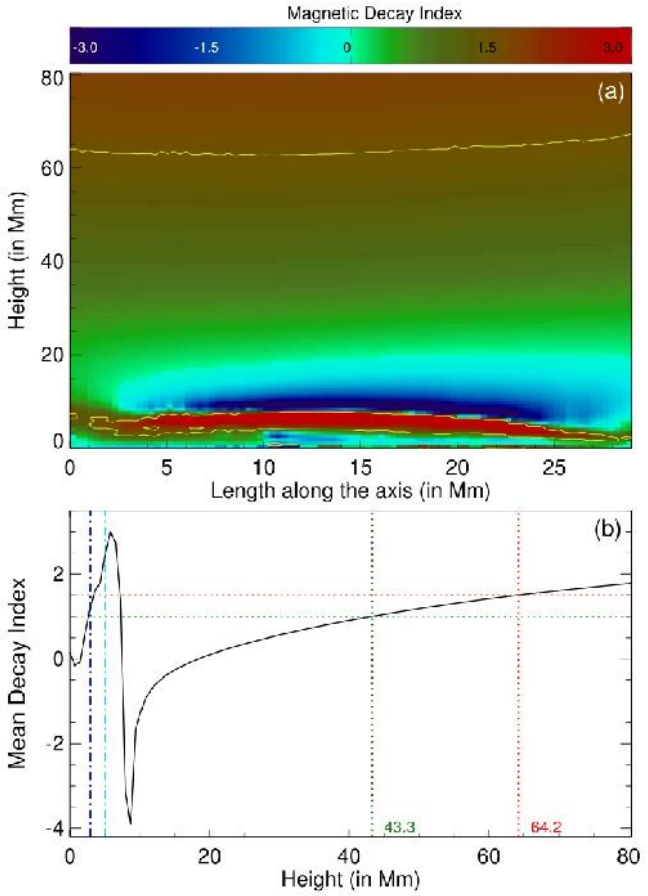

Figure 4.: (a): Distribution of magnetic decay index with height along the vertical surface above the axis of the yellow flux. The yellow curves refer to n=1.5. The variation in decay index with height, averaged over the flux rope axis, is shown in panel (b). The dotted green and red lines indicate the critical heights corresponding to n=1.0 and n=1.5, respectively. The dash-dotted blue and teal lines indicate the maximum heights of the yellow and pink flux ropes, respectively (see Figure 3).

This work was done in collaboration with Astrid M. Veronig (Univ. of Graz, Austria) and Thomas Wiegelmann (Max-Planck Institute, Germany).

doi : https://doi.org/10.3847/1538-4357/ac4756

(P. K. Mitra and B. Joshi)

DH Type II Radio Bursts During Solar Cycles 23 and 24: Frequency-Dependent Classification and Their Flare-CME Associations

Coronal mass ejections (CMEs) are the most energetic and large scale phenomena associated with the eruption of plasma and magnetic field from the Sun into the heliosphere. It is well established that the Earth-directed CMEs are the primary cause of severe geomagnetic

storms. A fraction of CMEs can produce the magnetohydrodynamic shock, subsequently giving rise to type II radio bursts. In this context, it is worth mentioning that the decameter-hectometer (DH: 30 MHz $\leq$ f $\leq$ 300 kHz) type II radio bursts driven by a CME indicate powerful MHD shocks leaving the inner corona entering the interplanetary medium. Therefore, the study of DH type II bursts associated CMEs becomes significant as they are primarily associated with the energetic and wider CMEs that frequently cause space-weather manifestations.

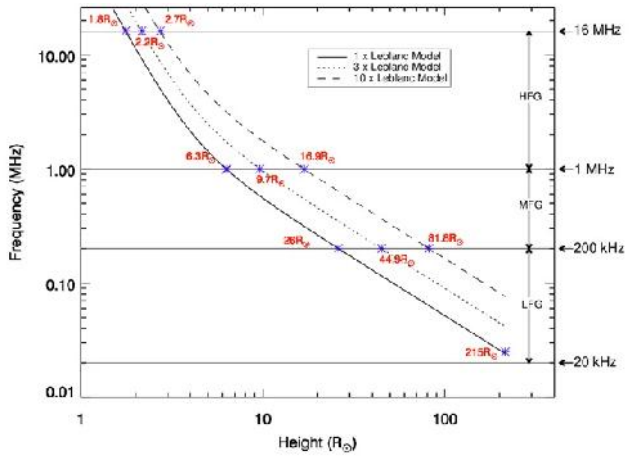

Figure 5.: Variation of heliocentric burst height ($R_\odot$) with plasma frequency estimated from Leblanc electron density distribution model. Solid, dotted, and dashed lines represent one-fold, three-fold, and ten-fold models, respectively. We consider three groups of DH type II radio bursts, depending upon their end frequency in the ranges of 1–16 MHz, 200 kHz–1 MHz, and 20 kHz–200 kHz, which are denoted as High-Frequency Group (HFG), Medium-Frequency Group (MFG), and Low-Frequency Group (LFG), respectively.

We explore the characteristics of DH type II bursts for the Solar Cycles 23 and 24. In Figure 5, we present the frequency–height relationship inferred from the atmoshpheric density model given by Leblanc. In Figure 5 the solid, dotted, and dashed lines illustrate the one-, three-, and ten-fold Leblanc models. The frequency–height relationship suggests that the observing window of 16 MHz–20 kHz essentially represents a large heliocentric distance from $\approx 2R_\odot$ to 1 AU. Therefore, to explore the characteristic of DH type II radio bursts, we divide this vast frequency range into three groups: Low Frequency Group (LFG; 20 kHz $\leq$ f $\leq$ 200 kHz), Medium Frequency Group (MFG; 200 kHz $\leq$ f $\leq$1 MHz), and High Frequency Group (HFG; 1 MHz $\leq$ f $\leq$ 16 MHz). Since end frequency of a type II burst provides a quantitative estimation on the distance up to which a shock can survive, we have classified the events into three groups based on their end frequencies. We find that the sources for LFG, MFG, and HFG events are homogeneously distributed over the active region belt. Our analysis shows a drastic reduction of the DH type II events during Solar Cycle 24 which includes only 35% of the total events (i.e., 179 out of 514). Despite having smaller number of DH type II events in the Solar Cycle 24, it contains a significantly higher fraction of LFG events compared to the previous cycle (32% vs 24%). However, within the LFG group the cycle 23 exhibits significant dominance of type II bursts that extend below 50 kHz, suggesting rich population of powerful CMEs traveling beyond half of the Sun-Earth distance. The events of LFG group display strongest association with faster and wider (more than 82% events are halo) CMEs while at the source location they predominantly trigger large M/X class flares (in more than 83% cases). Our analysis also indicates that CME initial speed or flare energetics are partly related with the duration of type II burst and that survival of CME associated shock is determined by multiple factors/parameters related to CMEs, flares, and state of coronal and interplanetary medium. The profiles relating CME heights with respect to the end frequencies of DH type II bursts suggest that for HFG and MFG categories, the location for majority of CMEs (≈65%-70%) is in well compliance with ten-fold Leblanc coronal density model, while for LFG events a lower value of density multiplier (≈3) seems to be compatible.

This work was done in collaboration with Dr. Kyung-Suk Cho (Korea Astronomy and Space Science Institute, Daejeon, Republic of Korea) and Dr. Rok-Soon Kim (University of Science and Technology, Daejeon, Republic of Korea).

doi : https://doi.org/10.1007/s11207-021-01890-6

(B. D. Patel and B. Joshi)

Comparison of the Hall Magnetohydrodynamics and Magnetohydrodynamics Evolution of a Flaring Solar Active Region

Solar coronal plasma, having a large magnetic Reynolds number ($\sim 10^{12}$), exhibits explosive behavior in form of flares, coronal mass ejections and jets. The fundamental process causing such phenomena is magnetic reconnection, which in turn occurs due to the generation of small length scales in consequence of large scale ($\sim 10^6$ m) magnetic field dynamics. A back-of-the-envelope calculation based on observed impulsive rise time of hard X-ray emission ($\sim$ few minutes) during the solar flares, suggests that reconnection length scale is of the order of few tens of meters. A straightforward order analysis of the induction equation at reconnection scale length indicates the significance of Hall effects during diffusive processes or magnetic reconnection on the Sun. Hall MHD supports the faster reconnection while also capturing the effects of small-scale processes over large length scales. The data-constrained Hall MHD and MHD models are employed to simulate a flaring solar active region as a test bed. Comparison between the observed flare brightening and the evolution of modelled magnetic fields reveals the Hall MHD model as more convincing tool to explain the observed phenomena. Simulations use the line tied boundary condition at the bottom of the computational domain whereas all other boundaries are open for the magnetic field. For the plasma flow, all boundaries are kept open. In this work, the SDO/AIA data in the multiple wavelength channels has been analyzed to explore the spatio-temporal development of the flare ribbon brightening. Subsequently, to explore the magnetic field line morphologies over the active region, the non-force-free extrapolation is carried out by utilizing the photospheric vector magnetogram data from SDO/HMI instrument. Our investigation, based on the numerical techniques to detect 3D nulls and quasi-separatrix layers (QSLs), revealed the presence of favorable topologies for magnetic reconnection. Notably, a magnetic flux rope with QSLs as overlying field lines is found at the location of flare saturation in the SDO/AIA images. Evolution of the aforementioned magnetic structures is examined to explore the magnetic reconnection in the two simulations. The highlights of the work, which emphasize the significance of the Hall effects on magnetic reconnection to understand the solar transient phenomena are:

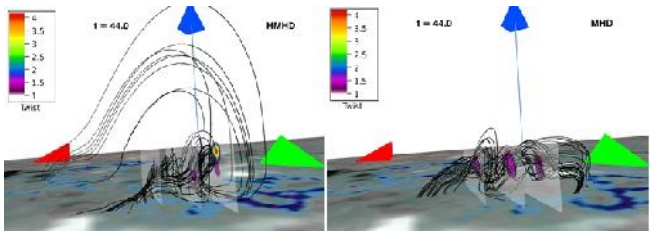

Figure 6.: Snapshots of the flux rope evolution at t=44 from the HMHD (left) and MHD (right) simulations. Earlier and higher rise of the flux rope during the HMHD simulation is evident from this figure.

(a) Contrary to the MHD simulation, the Hall MHD simulation shows a higher and faster ascend of the magnetic flux rope along with the overlying QSL, which further reconnects with the another QSL located higher upin the corona. The rope evolves through a series of slipping reconnections at the anchored footpoints. Such mechanism of flux rope eruption is not widely documented in the literature (Figure 6).

(b) Additionally, there is a remarkable spatial as well as temporal agreement of rotating magnetic field lines (Figure 7) with the observed plasma motion in circular pattern (as spotted in the SDO/AIA images and can be seen in the published paper whose link is given below).

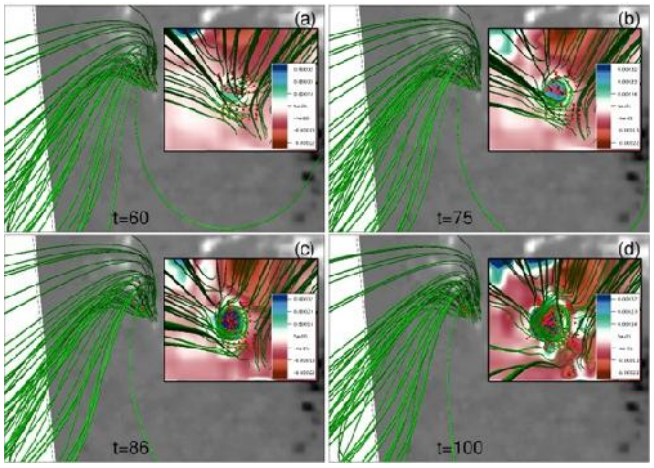

Figure 7.: Spatial and temporal development of the circular motion of magnetic field line at the location of observed plasma rotation. The color bars in all the inset images show the z-component of flow ranging from -0.00022 to 0.00032 in code units.

This work has been done in collaboration with Avijeet Prasad (Rosseland Centre for Solar Physics, University of Oslo, Norway), and Qiang Hu (Center for Space Plasma & Aeronomic Research, The University of Alabama, Huntsville.

doi : https://doi.org/10.3847/1538-4357/ac3bce

(K. Bora, R. Bhattacharyya and B. Joshi)

A Transient Coronal Sigmoid in Active Region NOAA 11909: Build-up Phase, M-class Eruptive Flare, and Associated Fast Coronal Mass Ejection

Coronal Mass Ejection (CME)–productive active regions exhibit some interesting features such as coronal sigmoids, filaments (or prominences), filament channels, and extreme ultraviolet (EUV) hot channels during the pre-eruption phase. In this work, we investigate the formation and disruption of a coronal sigmoid from the active region NOAA 11909 on 07 December 2013, by analyzing multi-wavelength and multi-instrument observations.

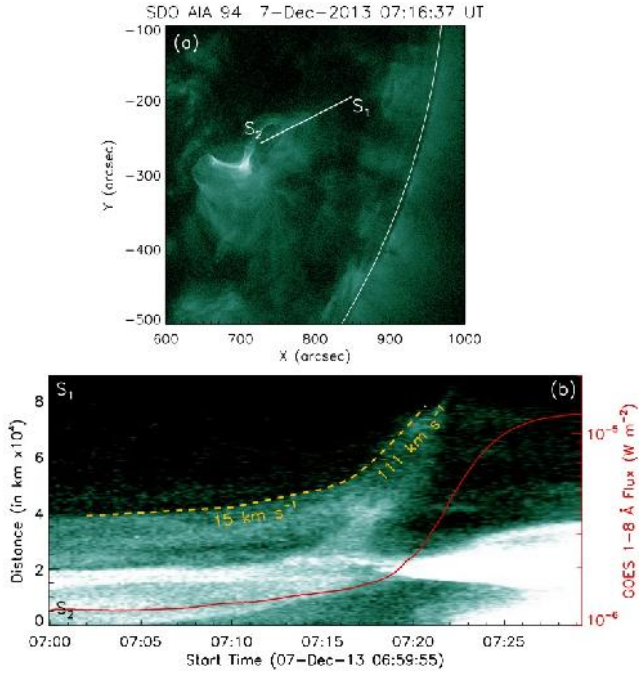

Figure 8.: (a) An AIA 94Å image on 07 December 2013 at 07:16 UT with a straight line S_2S_1 along which we have constructed a time-slice diagram. (b) Time-slice diagram showing the eruption of the flux rope during 07:00 UT to 07:29 UT. Red curve shows the temporal variation of the GOES SXR flux for the same time interval. In the precursor phase, we have observed a slow rise of the flux rope with linear speed 15 km/s. As the flare entered into the impulsive phase, the flux rope eruption accelerated to high linear speed of ≈110 km/s.

Our analysis suggests that the formation of the sigmoid initiated ≈1 hour before its eruption through a coupling between two twisted coronal loop systems. This sigmoid can be well regarded as of 'transient' class due to its short lifetime as the eruptive activities started just after ≈20 min of its formation. A comparison between the coronal and photospheric images suggests that the coronal sigmoid was formed over a simple β–type AR which also possessed dispersed magnetic field structure in the photosphere. The line-of-sight photospheric magnetograms also reveal moving magnetic features, small-scale flux cancellation events near the polarity inversion line, and overall flux cancellation during the extended pre-eruption phase which suggest the role of tether-cutting reconnection toward the build-up of the flux rope. The disruption of the sigmoid proceeded with a two-ribbon eruptive M1.2 flare (SOL2013-12-07T07:29). In radio frequencies, we observe type III and type II bursts in meter wavelengths during the impulsive phase of the flare. The successful eruption of the flux rope leads to a fast CME (with a linear speed of ≈

1085 km/s) in SOHO/LASCO field-of-view. During the evolution of the flare, we clearly observe typical “sigmoid-to-arcade” transformation. Prior to the onset of the impulsive phase of the flare, flux rope undergoes a slow rise (≈ 15 km/s) which subsequently transitions into a fast eruption (≈110 km/s) (see Figure 8). The two-phase evolution of the flux rope shows temporal associations with the soft X-ray precursor and impulsive phase emissions of the M-class flare, respectively, thus pointing toward a feedback relationship between magnetic reconnection and early CME dynamics.

This work was done in collaboration with P.K. Manoharan and Christian Monstein of Arecibo Observatory, University of Central Florida, Arecibo, USA and Istituto Ricerche Solari Locarno (IRSOL), Switzerland, respectively.

doi : https://doi.org/10.1007/s11207-021-01830-4

(H. Kharayat, B. Joshi and P.K. Mitra)

Imaging and spectroscopic observations of hot and cool transient loops

Coronal loops are basic building blocks of solar atmosphere and are observed on various length scales. However, their formation mechanism is still unclear. Solar atmosphere is also highly inhomogeneous and shows several small-scale transient energy release events. These events provide hot mass supply to the coronal loops. In this project, we carried out spectroscopic and imaging observations of small-scale transients and subsequent formation of transient loops. For the purpose, we have utilized multi-wavelength observations recorded by Atmospheric Imaging Assembly (AIA) and Interface Region Imaging Spectrometer (IRIS) SlitJaw-Imager (SJI), along with spectroscopic measurements provided by IRIS. For the photospheric magnetic field data, we obtained line-of-sight magnetogram provided by Helioseismic and Magnetic Imager (HMI). Different images from multi-wavelength observations can be find in different panels of Figure 9. Small-scale transients are simultaneously observed with several EUV and UV passbands of AIA and IRIS-SJI. Observations of these transients in several AIA and IRIS passbands indicate their multi-thermal nature. HMI magnetogram provides evidence of negative flux cancellations beneath these transients. Differential Emission Measure (DEM) analysis showed that one of the transients attains temperature up to 8 MK whereas another one reaches only up to 0.4 MK and thus termed as hot and cool transients respectively. These transients further led to the formation of small-scale loops which also showed similar temperature distributions. Therefore, only the hot loop was observed with AIA 94Åpassband whereas both the loops were clearly visible in cooler IRIS passbands. IRIS spectroscopic slit was rastering the region and provided spectroscopic measurements of both transients and associated loops. Average electron densities along the hot and cool loop were found to be 1011.2 and 1010.8 cm^{-3}, respectively from density sensitive O IV λ1399/λ1401 line ratio. Energy estimates suggest that flux cancellation can easily power the hot transient whereas is insufficient for cool transient. Life time estimates and magnetic field extrapolation suggest presence of small-scale and fine structures within these loops which were observed with high resolution IRIS images. Further observations and numerical experiments will be crucial for understanding physics behind formation of hot and cool transient loops and their role in global coronal heating processes.

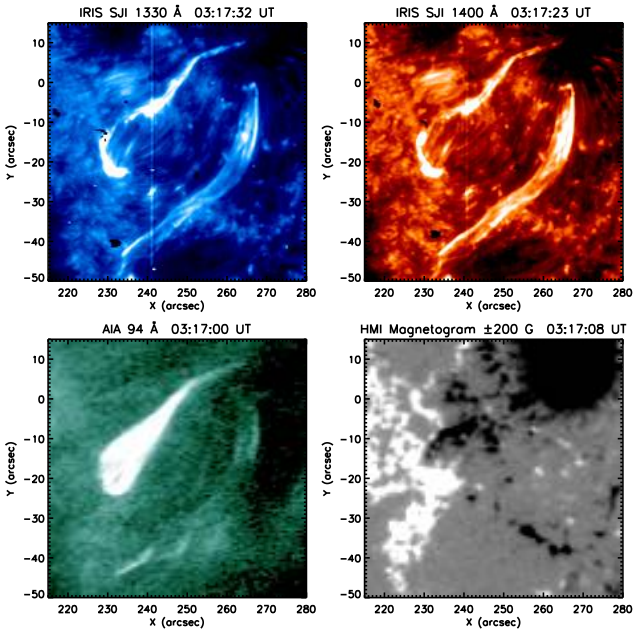

Figure 9.: Multi-wavelength images recorded on 15 August 2016 showing location of two transient loops. Images are from IRIS-SJI 1330Å (top left panel), IRIS-SJI 1400Å (top right panel), AIA 94Å (bottom left panel) passbands, and underlying HMI line-of-sight magnetogram (bottom right panel) scaled between ±200 G as labeled.

doi : https://doi.org/10.1093/mnras/stac657

(G. R. Gupta and S. S. Nayak)

Heating of the solar chromosphere in a sunspot light bridge by electric currents

The chromosphere is an important region of the solar atmosphere which couples the dense, 6000 K photosphere to the tenuous, million-degree corona. Owing to its complex magnetic structure, where the plasma beta changes dramatically, ascertaining the processes that maintain the thermal structure of the solar atmosphere is considered one of the fundamental problems in solar physics. While a number of mechanisms have been proposed for the energy transfer in the chromosphere, resistive Ohmic dissipation has been cited as one candidate process. Ohmic dissipation plays an important role in various dynamic phenomena in the chromosphere where the heating is a result of current sheets forming at discontinuities in the three-dimensional magnetic field. However, estimates of the current density are typically confined to the solar photosphere and only provide the vertical component of the current (Jz), while earlier studies found only a weak correlation between currents and chromospheric heating.

In this study we combined high-resolution spectroscopic CaII data from the 76 cm Dunn Solar Telescope and vector magnetic field observations from the Helioseismic and Magnetic Imager to investigate thermal enhancements in a sunspot light bridge. We found that the light bridge was a site of strong electric currents as shown in Figure 10, which extended to about 0.7 Mm while decreasing

monotonically with height. These currents produced a chromospheric temperature excess of about 600800 K relative to the umbra. Only the light bridge, showed a spatial coincidence of thermal enhancements and electric currents. These electric currents formed as a result of the emergence of a highly inclined magnetic structure characterized by conspicuous blue-shifts all along its length. The temperature enhancements and the Ohmic heating were primarily confined to a height range of 0.40.7 Mm above the light bridge. Our results provided direct evidence for currents heating the lower solar chromosphere through Ohmic dissipation.

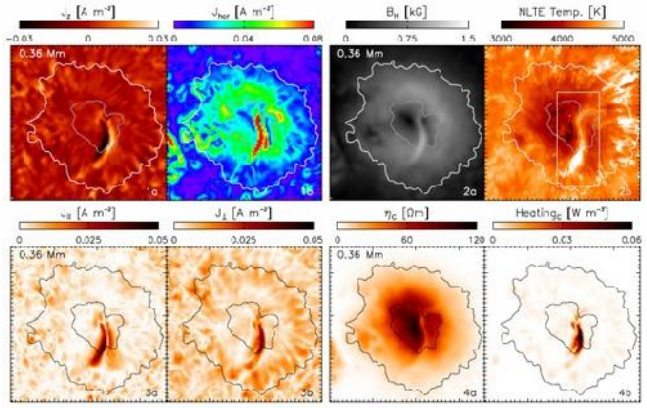

Figure 10.: Physical parameters in leading sunspot in NOAA AR 12002 on 2014 March 13. Top row, from left to right: Vertical and horizontal components of electric current density, horizontal component of magnetic field, and NLTE temperature at a height of 360 km. Bottom row, from left to right: Parallel and perpendicular components of electric current density to the magnetic field, Cowling resistivity, and Joule heating. The rectangle in panel2b indicates the light bridge field-of-view where the Ohmic dissipation by strong electric currents is observed

This work was done in collaboration with A. Prasad, Yalim, M. S. (Center for Space Plasma and Aeronomic Research, The University of Alabama in Huntsville, USA), C. Beck (National Solar Observatory, USA), D. Choudhary (Department of Physics and Astronomy, California State University, Northridge, USA)

doi : https://doi.org/10.1051/0004-6361/202141456

(R. E. Louis)

Does solar transition region rotate differentially?

The solar transition region is a thin but highly erratic region sandwiched between chromosphere and corona. To date, it is unclear whether the solar transition region also rotates differentially. We have studied the variability of the latitudinal rotational profile of solar transition region for the period from 2008 to 2018 covering the Solar Cycle 24, using the solar full-disk observations at 30.4 nm wavelength recorded by the Extreme Ultraviolet Imager instrument onboard STEREO space mission. Sixteen continuous rectangular bands with intervals of 10 degree latitude are made on full-disk images to extract a time series of extreme ultraviolet (EUV) flux. Our investigation shows that time average of sidereal rotation rate (from 2008 to 2018) of the equatorial region (-5 to +5 deg) is quite high (14.7deg/day) and drops to $\sim$13.6 deg/day towards the poles (both in the Northern and Southern hemispheres). The band from -20 to +20 degree rotates almost with the same rate (14.5 deg/day) during 2008 to 2018. Differentiality as a function of latitude is low during the high solar activity period (rotation rate varies from 14.5 to 14 deg/day). During the ascending and descending phases of 24th solar activity cycle, the differentiality is more (rotation rate varies from 14.5 to $\sim$12.5deg/day). Interestingly, the average sidereal rotation rate follows the trend of solar activity (c.f., Figure 11) i.e., it has maximum value as 14.97 deg/day during solar maximum in 2014 and slowly decreases up to 13.98 and 13.84 deg/day, respectively, during the solar minima in ascending (2008) and descending (2018) phases of the cycle. We also conclude that on an average the solar transition region rotates less differentially as compared to the corona. This is the first investigation on the latitudinal rotational profile of the solar transition region as well as its relationship with the solar activity.

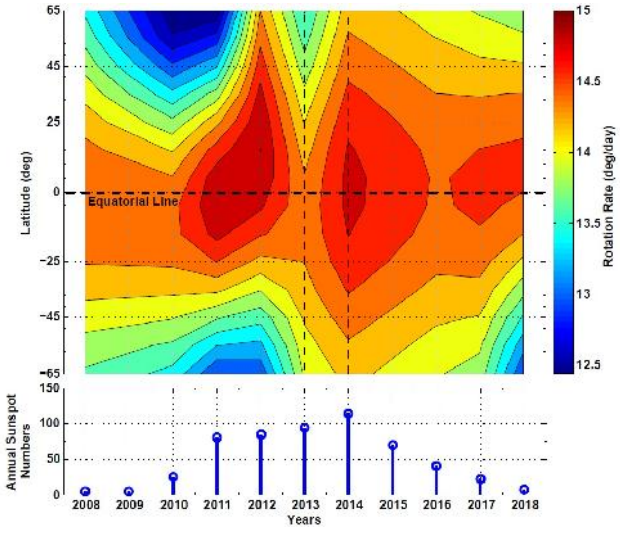

Figure 11: The contour plot (top panel) shows temporal (along the horizontal axis) and latitudinal (along the vertical axis) variation of the rotation rate (color coded) of the solar transition region in deg. day^{-1}. The bottom panel shows the temporal variation of annual sunspot numbers for the period from 20082018.

This work has been done in collaboration with Jaidev Sharma and Anil Malik of CCSU, Meerut and Hari Om Vats of SERF, Ahmedabad.

doi : https://doi.org/10.1093/mnras/stab1959

(B. Kumar)

Multipoint remote and in situ observations of ICME structures during 2011 and associated geomagnetic storms

Multipoint remote and in situ observations of interplanetary coronal mass ejection (ICME) structures during the year 2011 were studied. The selected ICMEs arrived at Earth on 2011 March 11 and 2011 August 6, and led to geomagnetic storms. The associated CMEs from the Sun, were observed by the coronagraphs onboard STEREO-A and-B and SOHO which enabled the CMEs to be imaged from three longitudinally separated viewpoints. We attempted to identify the in situ plasma and magnetic parameters of the ICME structures at multiple locations, for example at both STEREO spacecraft and also

at the ACE/ Wind spacecraft near Lagrangian point (L1), to investigate the global configuration, interplanetary propagation, arrival times and geomagnetic response of the ICMEs. Both these events of March 11 and August 6 were formed as a result of the interaction of two successive CMEs in the inner corona on March 7 and on August 3–4 respectively.

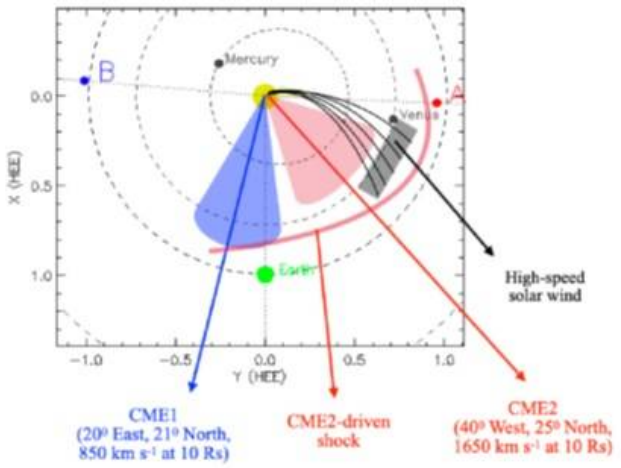

Figure 12.: The schematic of Earth- arriving August 6 ICMEs with the location of the Sun, STEREO, Mercury, and Earth. The preceding CME of August 3 (CME1) and its driven shock (blue), as well as the following CME of August 4 (CME2) and its driven shock (red), are shown.

Our multipoint in situ analysis study suggests that the structures associated with interacting CMEs including the shocks, possibly as a result of deflection or large sizes, may reach to even larger longitudinally separated locations in the heliosphere. Similarly, multiple cuts through the same ejecta/complex ejecta, formed as a result of CME–CME interaction, are found to have inhomogeneous properties. The study highlights the difficulties in connecting the local observations of an ICME from a single in situ spacecraft to its global structures.

This work has been done in collaboration with Wageesh Mishra (IIAP, Bangalore), Kunjal Dave (C. U. Shah University, Wadhwan, Gujarat) and Luca Teriaca (Max Planck Institute for Solar System Research, Germany)

doi : https://doi.org/10.1093/mnras/stab1721

(Nandita Srivastava)

Planetary Sciences

Modelling of Planetary Atmosphere, Simulations and Interstellar Medium

Estimation of charge and dimensions of regions for initiation of Venusian Lightning

The occurrence of Venusian lightning must be preceded by electrification of particles in Venusian clouds and separation of these charged particles to form distinct charged regions. We have carried out modelling of the minimum required charge and the dimensions of these charge regions in order for lightning to occur on Venus. The geometry of uniformly charged cylindrical regions in the Venusian clouds is shown in Figure 1. The expected streamer speed in Venusian middle clouds is on the order of 10^5-10^6 m/s. The charged region in the middle Venusian clouds has been approximated as uniformly charged cylinders. The radius, thickness, and charge density of the charged region have been estimated to be about 1-20 km, 1-3 km, and 1-28 nC/m^3, respectively. A typical profile of effective electric fields in the Venusian clouds is depicted in Figure 2. The electrostatic potential energy stored within the charge configuration is on the order of $\sim 10^{11}$ J, a large portion of which is distributed to RF and optical energies of the discharge.

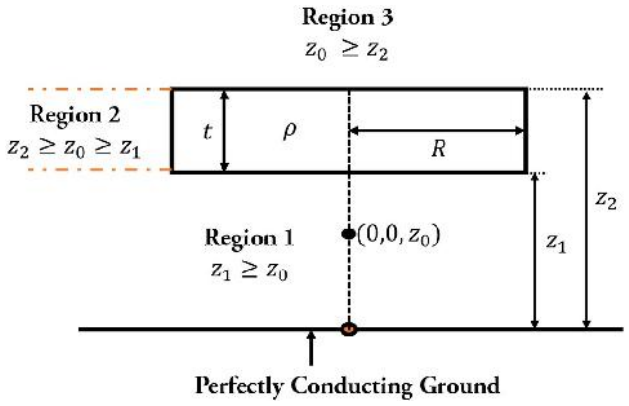

Figure 1: Geometry of uniformly charged cylindrical regions in the Venusian clouds. The dot on the plane of perfectly conducting ground corresponds to the origin.

In addition, the lack of global magnetic fields on Venus has resulted in the formation of weak induced magnetic fields that give unrestricted access to Galactic Cosmic Rays (GCR). We have carried out parametric sweep of the radii and thickness of uniformly charged cylinder, whose results are shown in Figure 3. The ionization of the lower atmosphere of Venus due to GCR has been a subject of many earlier studies, and it has been considered a source for cloud electrification on Venus. However. It is found that the fields produced by the GCR-induced ionization do not exceed breakdown fields. It is inferred that the GCR induced ionization cannot be the prime driving mechanism for Venus Lightning. Further, it is found that the required levels of charge density could be produced by collisional charging and hence, it is the dominating source on Venus.

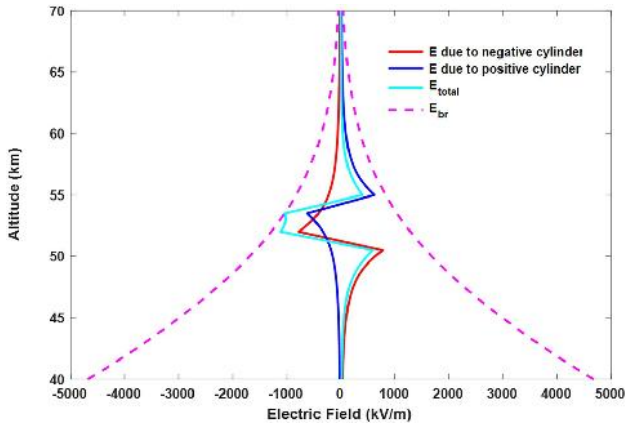

Figure 2: Typical profile of effective electric fields in the Venusian clouds. The total electric potential is found to be on the order of 109 V and the capacitance of the configuration is $\sim$166 nF. The electrostatic potential energy stored within this charge configuration is on the order of $\sim 10^{11}$ J, a large portion of which is distributed to RF and optical energies of the discharge.

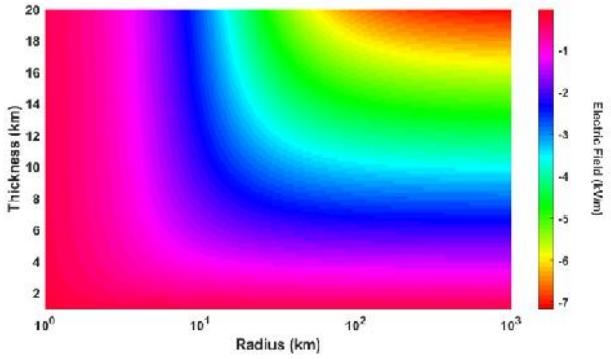

Figure 3: Parametric sweep of radii and thickness of uniformly charged cylinder with charge density of 6.4 pC/m^3 (corresponding to maximum electron concentration) to identify the source of lightning on Venus. GCR is not a source of lightning on Venus due to limited electric fields, not exceeding breakdown fields in the Venusian clouds. On the other hand, collisional charging is found to be a dominating source on Venus.

This work was done in collaboration with V. R. Dinesh Kumar, BITS, Hyderabad and C. T. Russell, UCLA, USA.

doi : https://doi.org/10.1016/j.icarus.2021.114473

(J. P. Pabari and K. Acharyya)

Numerical evaluation of the effect of Lunar Landing on its surface, surrounding environment and hardware

A numerical evaluation study has been carried out to evaluate the effect of lunar landing on the surface, surrounding environment and hardware. Quantitative estimation of the damage that would be caused to the surrounding structure/hardware due to another landing in the vicinity has also been estimated.

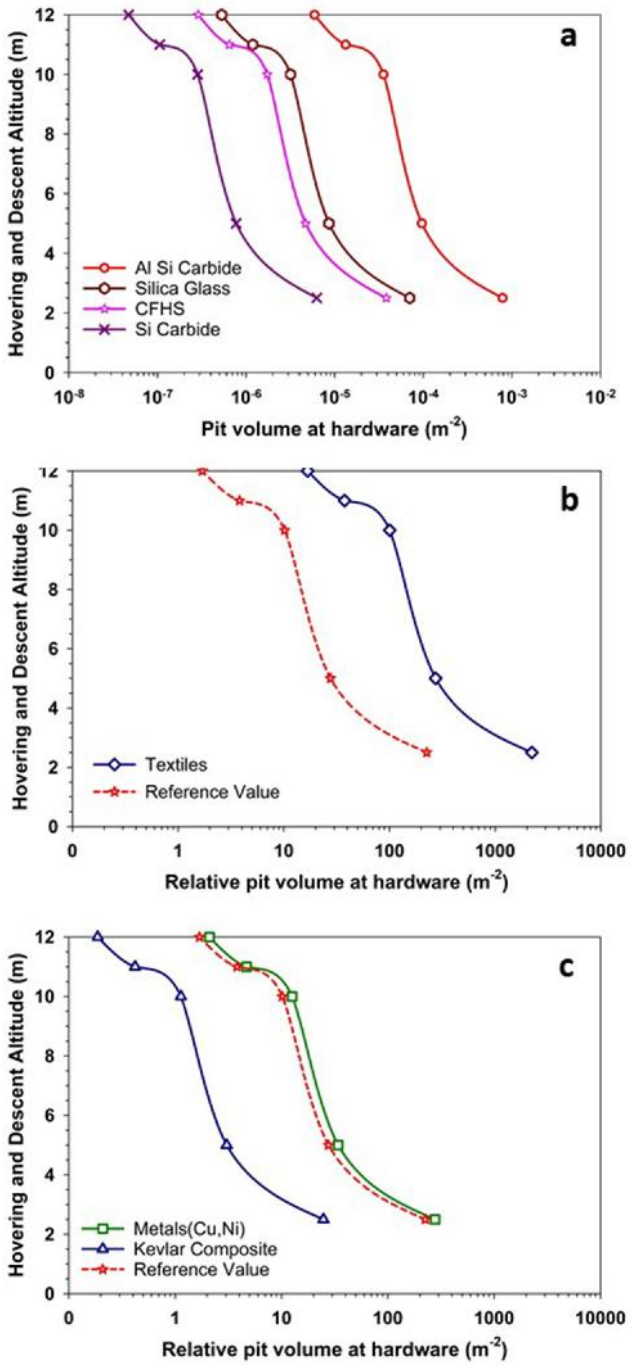

Figure 4: Overall damage at a distance of 100m from the landing site (assuming hardware is surrounding the whole landing site). (a) Quantified damage caused to brittle/hardened materials (b) and (c) Estimated damage to textiles and metals/composite w.r.t. a reference damage value.

Recommendations were given for various materials to be used in future lunar missions to mitigate the effects caused by other close-by landing. This work has implications for both science and engineering aspects of a mission, particularly when multiple landings are sought in vicinity of one another in view of human outpost and ISRU activities. A damage model in conjunction with plume dynamics and its interaction with the lunar surface is used to arrive at the estimates. A Direct Simulation Monte Carlo (DSMC) solver is used for the analysis of plume dynamics and gaseous interactions of the plume with the in-situ lunar soil. The output of the DSMC solver is employed to quantify the ejecta parameters such as eject velocity, mass flux rate, and ejecta kinematics, which are used to estimate the expected damage to a lunar outpost or hardware present in its vicinity. Estimates are made on the total amount of damage (defined as the amount of lunar regolith ejected from the surface into the surrounding environment) at different stages of landing, ejecta kinematics, and overall volume of pit/dent formed on the surface of surrounding hardware due to the high-velocity ejecta particles. The study considers a typical test case using a landing trajectory of a small class lander mission for these calculations and presents a picture of surface disturbance, ejecta profile, and damage that could happen to the surroundings up to a few 100s of meters as shown in Figure 4. An ejecta amount of 7.5 kg beneath the lander and damage of 1500 mm^3 to the surrounding hardware (situated at 100m from the landing site) is estimated from the configuration considered in the present study. Although the disturbance and damage caused due to small class landers seem to be minimal, large class landers and landing in close vicinity of an earlier landing would cause a significant threat to the existing hardware which needs to be mitigated for all future lunar ISRU/outpost activities.

This work was done in collaboration with LPSC, Valiamala Team.

doi : https://doi.org/10.1016/j.pss.2021.105398

(S. K. Mishra, K. Durga Prasad and Anil Bhardwaj)

Moon: Static equilibrium dust levitation may not exist

The composite system of the charged lunar surface, electron, and plasma cloud, and the charged dust create the dusty plasma over the Moon. This plasma environment is maintained by the interaction between the lunar surface and the solar photon radiation and solar wind/ magnetotail plasma. Photons in the extreme ultraviolet (UV) range primarily generate photoelectrons over the sunlit locations. In addition to that, solar wind electrons and ions are accreted to the lunar surface. The cumulative effect of these three creates a positively charged lunar surface on the dayside emitted photoelectrons near the surface form a dusty photoelectron sheath over the lunar surface.

The dust particles within the photoelectron sheath get electrically charged due to various dust charging currents these charging currents undergo natural random fluctuations. Due to natural randomization of the dust charging currents, the anisotropy in sheath photoelectron population and electric field/potential, and half FermiDirac velocity distribution of the emitted photoelectrons, the charge on the floating dust particles is found to be distributed over a wide range ($\sim$100 e). Alteration of static equilibrium of the floating dust particles due to this natural charge fluctuation gives rise to the altitudinal fluctuation ($\sim$10 %) about its mean position within the sheath. The concept and results suggest that the natural fluctuation of the dust charge

could be a reason that the strict dust levitation under static force equilibrium is less likely to exhibit over the sunlit lunar surfaces. This effect of dust charge and subsequent altitudinal fluctuations have been found pronounced at larger latitudes (near the terminator region) and higher lunar altitudes. The predictions based on natural dust charge fluctuations may be of practical significance in preparing test experiments for future lunar exploration campaigns.

doi : https://doi.org/10.1093/mnras/stab2862

(S. K. Mishra and T. Sana)

Possible dust acoustic wave excitations within dusty photoelectron sheath over Moon

The photoelectron sheath and floating fine positively charged dust particles constitute two-component dusty plasma in the sunlit lunar regolith's vicinity. By including the charge fluctuation into photoelectron-dust dynamics, the lunar exospheric plasma is proposed to support the propagation of long-wavelength small-amplitude linear and nonlinear dust acoustic (DA) modes. Physically, in a linear regime, the nonadiabatic dust charge variation modifies the usual DA wave dispersion and excites the ultralow frequency modes that propagate with sufficiently low phase speed. Such modes are anticipated to be pronounced near the sunlit lunar surface (within a couple of meters of vertical extent and parallel to the regolith), where the photoelectron/ dust density is sufficient to produce significant restoration force and coupling effects. The quantitative estimates suggest that the nominal exospheric plasma may exhibit DA waves propagating with frequencies of the order of unity.

In a nonlinear regime, the dust charge variation induces collisionless dissipation, which damps amplitude and reduces the velocity of propagating DA waves. Under typical solar irradiation conditions, the sunlit lunar dusty plasma might support DA solitary, and DA shock wave structures of both rarefied and compressive nature; the dominance of the dispersion and dissipation effects in the fluid dynamics are shown to exhibit oscillatory and monotonic shock waves, respectively. The passage of these nonlinear DA structures/ excitations might energize the ambient charged dust and photoelectrons locally and could be an important mechanism for energy/ particle transport in the vicinity of the sunlit locations over the Moon practical realization of such modes is of fundamental importance in understanding the dynamics and stability of sunlit lunar dusty plasma environment. These propagating DA structures are practically very similar to those observed in the dusty plasma laboratory experiments and can be detected within the sunlit lunar plasma environment by using a similar technique and appropriate camera setup. Another possible detection may be the measurement of the photoelectron density perturbation locally during the passage of nonlinear DA excitations using a suitably configured Langmuir probe setup.

doi : https://doi.org/10.1093/mnras/stab495

(S. K. Mishra)

Argon-40 in Lunar Exosphere: Observations from CHACE-2 on Chandrayaan-2 Orbiter

We report the first observation of Argon-40 (Ar-40) in the mid latitude regions (-60 to +60) of the lunar exosphere from CHandras Atmospheric Composition Explorer-2 (CHACE-2) experiment aboard Chandrayaan-2 orbiter as shown in Figure 5. The number density of Ar-40 shows pre-sunrise, sunrise and sunset peaks as well as nightside minima, typical of a condensable gas, which is similar to the features seen at the low latitudes in previous observations. The CHACE-2 observed number densities of Ar-40 and its diurnal variation at low latitudes (-30 to +30) are consistent with LACE/Apollo observations. CHACE-2 observations show Ar-40 enhancements over certain longitude sectors. In addition to KREEP region, Ar-40 bulges are observed at other longitudes, including the South Pole Aitken (SPA) terrain. The global distribution of Ar-40 shows that the sunrise peak is observed at the same local time over highlands and mare regions. These observations call for a deeper understanding of the surface-exosphere interactions and source distribution.

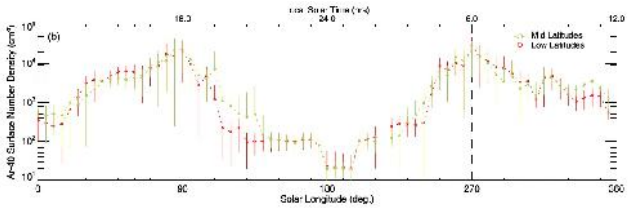

Figure 5: Number density of Ar-40 at the lunar surface for the mid latitude region (30 to 60 and -30 to -60 degree) measured by CHACE-2 (green). The curve for the low latitude region (within 30 degree) is also over plotted (red) for comparison. The top x-axis represents the local solar time.

This work was done in collaboration with M. B. Dhanya, Smitha V Thampi, Tirtha Pratim Das, R. Satheesh Thampi et al. of Space Physics Laboratory, VSSC, Trivandrum.

doi : https://doi.org/10.1029/2021GL094970

(Anil Bhardwaj)

Model for Nitric oxide and its dayglow emission in the Martian upper atmosphere using NGIMS/MAVEN measured neutral and ion densities

The in-situ NO density measurements are difficult to make in the Martian upper atmosphere because of its low abundance (more than three orders of magnitude compared to CO_2) and also highly reactive in nature. Moreover, the thermal recombination of atomic nitrogen and atomic oxygen inside the mass spectrometer also inhibits the accurate determination of NO density. Measurement of NO density from the remote dayglow observations is also difficult since its strongest ultraviolet emission feature, i.e., (1,0) gamma band, is severely obscured by the intense CO Cameron band (50 times higher in magnitude). We have developed a photochemical model to study the NO density in the dayside of Martian upper atmosphere by accounting for various production and loss mechanisms. By utilizing the Neutral Gas and Ion Mass Spectrometer (NGIMS) on board

Mars Atmosphere and Volatile Evolution (MAVEN) mission measured neutral and ion densities during deep dip 8 and 9 campaigns, we modelled NO number density in the Martian sunlit upper atmosphere for the altitudes between 120 and 200 km (Figure 6). The modelled NO densities are employed to calculate NO (1,0) γ band emission intensity profiles in the dayside upper atmosphere of Mars. The calculated NO density and its γ band intensity profiles are found to be consistent with Imaging Ultraviolet Spectrograph (IUVS) onboard MAVEN observations and also with other modelling studies. We found that the local CO_2 and N_2 density variations can lead to a change in NO density and consequently its dayglow intensity by a factor of 2 to 5. Since NO is a trace constituent and also its dayglow emissions are strongly obscured by CO Cameron band emissions, we suggest that the derivation of NO number density based on our approach can constrain its abundance in the dayside upper atmosphere of Mars. More observations of (1-0) γ band emission along with modelling will help to study the global distribution of NO in the Martian atmosphere.

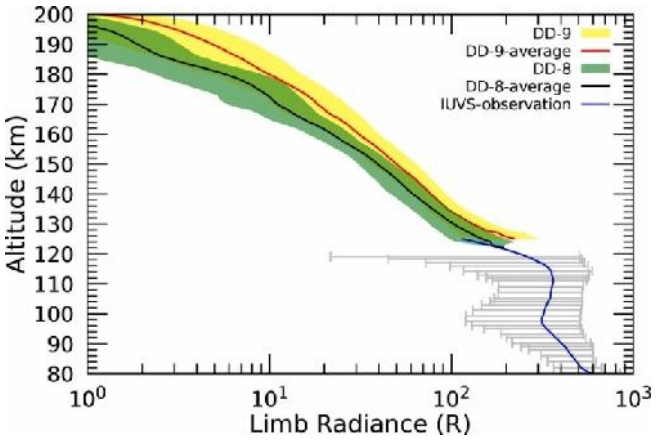

Figure 6: Comparison between the modelled and the IUVS/MAVEN observed NO (1,0) band limb intensity profiles. The black and red curves represent the calculated average NO (1,0) band limb intensity for MAVEN deep dip 8 and 9 observations, respectively. Blue curve and grey errors bars represents the observed average IUVS/MAVEN dayglow profile and 1-sigma uncertainty associated with observation, respectively. Green and yellow shaded areas represent the variability in the calculated NO (1,0) band limb intensity for deep dip 8 and 9 observations, respectively.

doi : https://doi.org/10.1016/j.icarus.2022.115010

(S. Raghuram, Anil Bhardwaj and M. Dharwan)

Impact of the 2018 Mars Global Dust Storm on the Ionospheric Peak: A Study Using a Photochemical Model

We report the impact of the 2018 Mars global dust storm on the ionosphere, in particular, its peak altitude during the onset and growth phases of the event (Figure 7). A one-dimensional photochemical model is applied to estimate the ionospheric electron densities below 200 km using the measurements of in situ neutral densities and ionizing solar radiation by the Mars Atmosphere and Volatile EvolutioN (MAVEN) mission. Our model results show that while the peak density of the ionosphere on the dawn side during the dust storm is hardly impacted, the altitude of the peak layer may be lifted by $\sim$10 km. The simulation results support the MAVEN radio occultation observations that there is a time delay in the response of the ionospheric peak altitude in the southern hemisphere (SH), compared with the northern hemisphere (NH) during the dust storm development. Although the 2018 global dust storm developed in the northern Martian mid-latitudes on 1 June and developed into a global dust event on 17 June, our study suggests that the impact on the ionospheric peak altitude near the equatorial and southern mid-latitudes became important only after 22 June. This suggests that there was a time-lag of about 3 weeks in the response of the Martian upper atmosphere of the SH to the dust storm that originated in the NH.

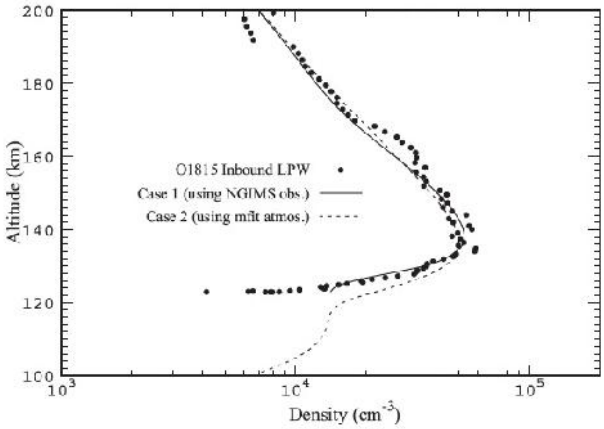

Figure 7: Electron density profiles of MAVEN orbit O1815. The symbols are the LPW-measured electron density during the inbound leg of O1815. The solid curve shows the simulated electron density profile using the NGIMS-measured neutral densities (Case 1) and the dashed curve is the one obtained using the multi-component fit atmosphere (Case 2). Both Case 1 and Case 2 profiles are in good agreement with the observations and thus validate both our model and the multi-component fit method used for extrapolating neutral densities to lower altitudes. LPW, Langmuir Probe and Waves; NGIMS, Neutral Gas and Ion Mass Spectrometer.

This work was done in collaboration with Vrinda Mukundan, NCESS, Thiruvananthapuram; Smitha V. Thampi, SPL, VSSC, Trivandrum; and Xiaohua Fang, ASP, UCB, Boulder, CO, USA.

doi : https://doi.org/10.1029/2021JE006823

(Anil Bhardwaj)

Ionospheric plasma energization at Mars during the September 2017 ICME event

During September 2017, the Solar Active Region (AR) 12673 produced several flares and Coronal Mass Ejections (CMEs). On 10 September 2017, a stronger and wider CME erupted from AR 12673, which was Marsdirected (Vsw $\sim$840 km/s near 1.5 au). This ICME caused a major space weather event at Mars on 1213 September. We investigated the impact of this event on Martian topside ionosphere by using the observations made by Langmuir Probe and Waves (LPW) and Suprathermal and Thermal Ion Composition (STATIC) instruments on board Mars Atmosphere and Volatile EvolutioN (MAVEN). LPW observed the ionopause feature at lower altitudes during the event period. This topside ionospheric compression and depletion observed by LPW was associated with enhanced electron temperatures.

STATIC observed significant energization of ionospheric heavy ions such as O^+ and O^{2+} to energies above 10 eV up to hundreds of eV below 300 km altitude. Intense solar wind (lighter ions such as H^+) penetration to lower altitudes was also observed. The increased energies for heavy ions and increased spread in energy for the lighter species are found at lower altitudes such as ∼300 km, suggesting that significant heating and acceleration process is acting even at these altitudes during severe solar events.

This work was done in collaboration with C. Krishnaprasad, Smitha V. Thampi, Tarun K. Pant, and R. Satheesh Thampi, SPL, VSSC, Thiruvananthapuram.

doi : https://doi.org/10.1016/j.pss.2021.105291

(Anil Bhardwaj)

A study on the solar coronal dynamics during the post-maxima phase of the solar cycle 24 using S-band radio signals from the Indian Mars Orbiter Mission

Radio signals from Indias Mars Orbiter Mission (MOM) have been used to study turbulence in the solar plasma during the post-maximum phase of solar cycle 24. S-band (2.29 GHz) radio carrier downlink signals from MOM were received at the Indian Deep Space Network (IDSN), Bangalore, and frequency residuals were spectrally analysed to obtain coronal turbulence spectra at heliocentric distances ranging between 4 and 20 R_{Sun}, corresponding to coronal regions where the solar wind is primarily accelerated. The frequency fluctuation spectrum relates to the turbulence regime in the near-Sun region. The turbulence power spectrum (the temporal spectrum of frequency fluctuations) at smaller heliocentric distances ($<$ 10 R_{Sun}) reveals flattening in lower-frequency regions, with a spectral index αf ∼0.3 0.5, which corresponds to the solar wind acceleration region. As shown in Figure 8, for larger heliocentric distances ($>$ 10 R_{Sun}), the curve steepens with a spectral index αf ∼0.7 0.8, a value close to 2/3 and indicative of a developed Kolmogorov-type turbulence spectrum. The findings are consistent with earlier results. Plausible explanations to support the theory of coronal heating by magnetohydrodynamic waves and the acceleration of the solar wind are presented. An insight into the feeble maximum of solar cycle 24 is obtained.

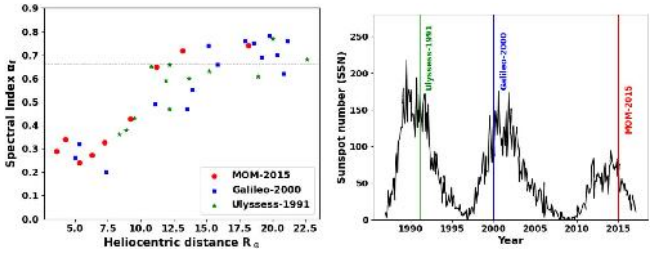

Figure 8: Left-hand panel: spectral index (αf) of the frequency fluctuation spectrum from spacecraft radio signals at various heliocentric distance R_{Sun} during the coronal radio sounding experiments of (a) Ulysses , (b) Galileo, and (c) MOM (Indian Mars Orbiter Mission). Right-hand panel: average sunspot numbers over the years 19872016, spanning three solar cycles. Vertical lines mark the period when radio-sounding experiments were conducted by the three spacecrafts.

This work was done in collaboration with Richa N. Jain, R. K. Choudhary, SPL, VSSC, Trivandrum; and Umang Parikh, Bijoy K. Dai, and Roopa M. V, ISTRAC, Bengaluru.

doi : https://doi.org/10.1093/mnras/stac056

(Anil Bhardwaj)

Characteristics of convective vortices and dust devils on Mars

Convective vortices are ubiquitous on Mars. If these vortices are strong enough, they can lift dust and are subsequently called dust devils. They are believed to be an efficient mechanism for dust entrainment in the Martian atmosphere. Such vortices can be identified in-situ by landers or rovers by the reduced surface pressure when they pass by the instrument.

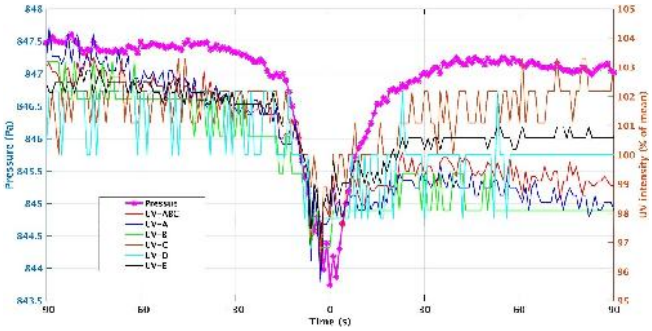

Figure 9: REMS measurement of ultraviolet radiation intensities during a vortex event on mission sol 1546 at 14:37 local time.

We analyse data from the Rover Environmental Monitoring Station (REMS) on-board the Mars Science Laboratory (MSL) rover Curiosity during mission sols 1019 to 1686 (corresponding to Martian Year (MY) 33). We identified 611 short pressure drops that likely indicate the passage of convective vortices in vicinity of the rover. The cumulative power-law analysis of the detected pressure drops suggests a low abundance of stronger pressure drop events at the MSL site as compared to the Pathfinder and Phoenix sites. The reason for this can be attributed to the smaller boundary layer height at Gale crater. The power-law slope is smaller for MY 33 as compared to previous years, suggesting that the dust devil activity also increased inside the Gale crater with the progressing year.

Among all vortices detected, 63 vortices (∼10%) also show a simultaneous drop in ultraviolet intensity, which signifies obscuration of sunlight by the dust-laden vortices (Figure 9). A seasonal study for dust devils occurrences based on UV flux data shows an increase in their frequency during the local southern summer season. A majority of our estimated tangential wind velocities are well below the Martian dust lifting threshold. This indicates that either the vortices passed far from the measuring instrument or that the threshold being used is higher than the actual threshold on Mars. We provide a comparison of the seasonal variation of dust lifting vortices and the dust devil activity as calculated by MarsWRF model. We predict that vortices in Gale crater are less capable of lifting dust as compared to its Earth counterpart.

This work was done in collaboration with Claire Newman, Aeolis Research, USA

doi : http://dx.doi.org/10.1016/j.pss.2022.105430

(V. Sheel and S. Uttam)

Simulation of Dust Lifting and Distribution within a Dust Devil

Dust devils, are a source of dust injection into the atmosphere. But its quantitative contribution to the total dust loading in the atmosphere and relative dust loading within the dust devil, are not well understood. We have developed a comprehensive numerical model to study the spatial distribution of dust within a steady state dust devil for the first time, by using equations of motion for dust particles and Navier Stokes equations. Later, we use continuity equation to determine the dust loading within that vortex. We consider an initial wind profile, which is dependent on the circulation strength (Γ) of the vortex and viscosity of the air (ν). Our simulations indicate a maximum concentration of $\sim 10^3$ particles/cc near the surface inside the dust devil, which falls exponentially as we move in the vertical direction. We also find a major particle load at the boundary of the core. Our analysis shows that higher circulation strength (Γ) leads to a high loading of dust inside the steady state dust devil, whereas a change in the air viscosity (ν) does not lead to any significant change in dust loading. We also estimate a dust flux of $\sim 310^{-3}$ kgm^{-2}s^{-1}, which lies in the estimated range of dust fluxes from dust devils at the Mars Pathfinder site varying between $\sim 610^{-4}$ kgm^{-2}s^{-1} to $\sim$510-3 kgm^{-2}s^{-1}. The larger-sized dust particles are more concentrated toward the ground whereas, the smaller-sized dust particles can reach up to dust devil heights. This has the potential to create large electric fields and consequently lightning, within the dust devils.

doi : http://dx.doi.org/10.1029/2021JE006835

(V. Sheel, S. Uttam and S. Mishra)

Simulation of limb intensity of CO ($a^3\pi$) Cameron band in the Martian thermosphere: Comparisons with (1) SPICAM and IUVS observations and (2) other model results

Using Analytical Yield Spectrum (AYS) method, we have calculated limb intensity of CO ($a^3\pi$) Cameron band between altitudes 90 km and 200 km. In Figure 10 (a-b) we have compared this result with the other model calculation of Gêrard et al. (2019) and the dayglow observations carried out by the Spectroscopy for Investigation of the Characteristics of the Atmosphere of Mars (SPICAM) and Imaging Ultraviolet Spectrograph (IUVS) onboard Mars Express (MEX) and Mars Atmosphere and Volatile EvolutioN (MAVEN) respectively. SPICAM observations were carried out during two orbits # 3301 and # 8488 that occurred on 4 August 2006 and 20 August 2010 respectively. IUVS observations were also made during two orbits # 9960 and # 10974 that occurred on 22 September 2019 and 25 January 2020 respectively. SPICAM and IUVS instruments measured the limb intensities of CO ($a^3\pi$) bands at nearly same aerophysical conditions. The Figures 10a and 10b represent the observations and modeling of CO ($a^3\pi$) Cameron band limb intensities in northern and southern hemispheres respectively. The IUVS and SPICAM instruments observed the peak intensity of CO ($a^3\pi$) band at 120 km and 110 km, respectively. The increase in the peak height of IUVS observations can be attributed to Solar Zenith Angle (SZA) because IUVS observations were carried out at high SZA$\sim$66°-72° in comparison to that observed by SPICAM at low SZA$\sim$29°-40°. Below the peak height Cameron band intensity observed by IUVS is lowered by a factor of $\sim$2 than that observed by SPICAM. Our results have shown reasonable agreement with both observations within the uncertainties of the measurements. In Figure 10a, we have also compared our estimated CO Cameron band dayglow intensity with the model calculation of Gêrard et al. (2019). Gêrard et al. (2019) used Boltzmann kinetic model. They used larger cross section by a factor of 2 than that used by us. Therefore, we have divided the limb intensity of Gêrard et al. (2019) by a factor of 2 to get a close agreement between two different model calculations.

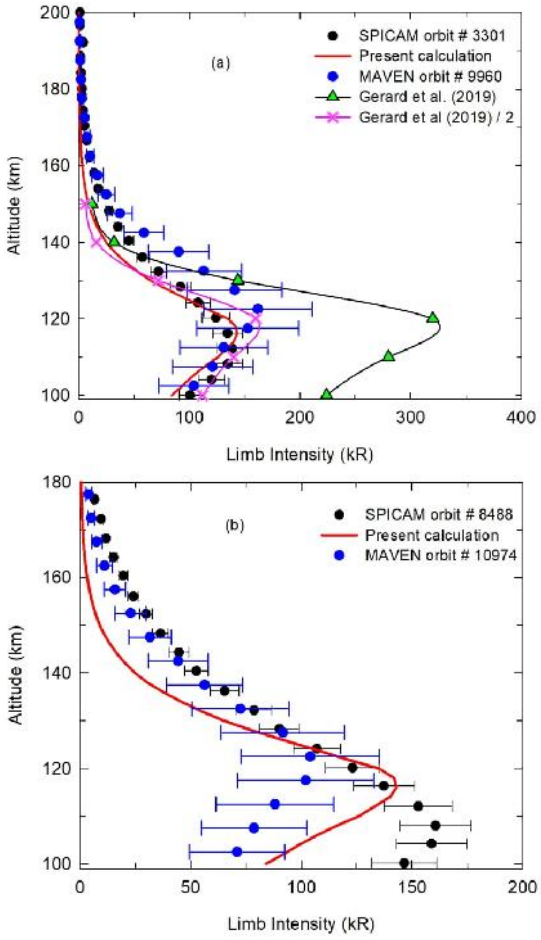

Figure 10: (a) Comparison of present calculation of limb intensity of CO ($a^3\pi$) bands with the observations carried out by SPICAM and IUVS in northern hemisphere during orbits # 3301 and # 9960, respectively. The present calculation is also compared with the model of Gêrard et al. (2019). 10 (b) Comparison of present calculation of limb intensity of CO ($a^3\pi$) bands with the observations carried out by SPICAM and IUVS in southern hemisphere during orbits # 8488 and # 10974, respectively.

doi : https://doi.org/10.1007/s12040-022-01822-3

(S. A. Haider, P. Thirupathaiah and J. Masoom)

Annual variability of ozone and dust opacity in the Martian atmosphere: SPICAM observations

We have used SPICAM observations of column ozone and dust opacity to study their annual variability at low latitudes (10°-30° N-S), mid-latitudes (30°-50° N-S) and high latitudes (50°-70° N-S) for four Martian Years (MY27-MY30).

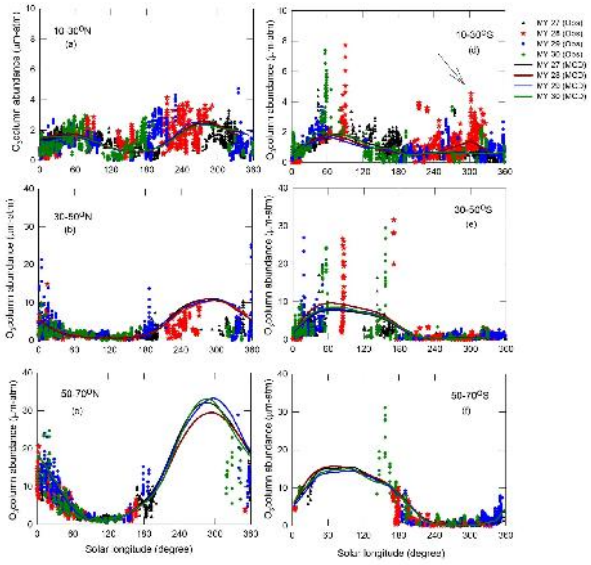

Figure 11: The annual variability of zonally averaged column ozone at (a) 10°-30°N, (b) 30°-50°N, (c) 50°-70°N, (d) 10°-30°S, (e) 30°-50°S, (f) 50°-70°S observed by SPICAM and modeled by MCD between M27and M30. The effect of dust storm on column ozone at latitude 10°-30°S is shown by an arrow.

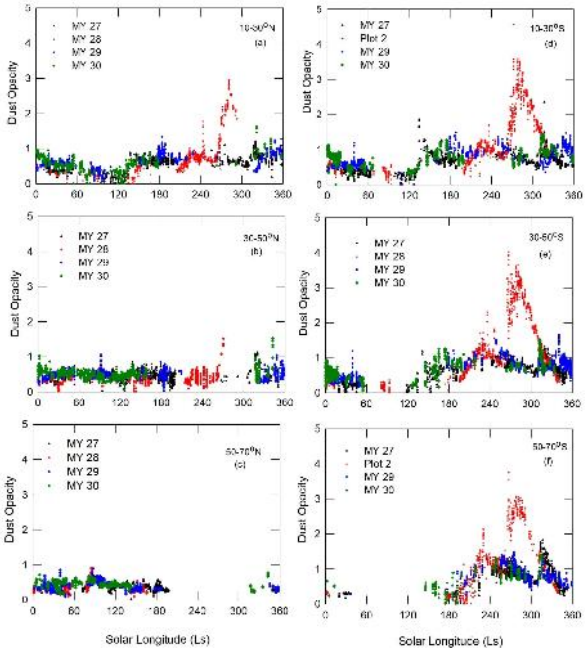

Figure 12: The annual variability of zonally averaged dust opacity at (a) 10°-30°N, (b) 30°-50°N, (c) 50°-70°N, (d) 10°-30°S, (e) 30°-50°S, (f) 50°-70°S observed by SPICAM between MY27-MY30.

In Figure 11 (a-f) the observed column abundances of ozone are compared with the Mars Climate Database (MCD, version 5.3). The comparison of year to year annual variability of estimated column ozone shows a strong similarity by the SPICAM observations. At low latitudes (10°-30° N-S) the estimated peak of annual column ozone profile for MY27 to MY30 is lower than the measurements by a factor of ∼1.5. This difference between model and observations at low latitude may be due to transportation of excess water vapor from Tharsis and Arabia Terra, which can reduce column ozone in the model. Another reason may be due to errors of 10%-30% in the SPICAM observations. In Figure 12 (a-f), the column dust opacity observed by SPICAM are shown in presence and absence of dust storm. The Figures 12 (d-f) show that column dust opacity increases by a factor of ∼4 at southern latitudes during global dust storm, which occurred in MY 28 between Ls ∼270° to 310°. Afterward the dust storm moved to the north at low latitudes and then almost disappeared at mid-latitudes.

This work was done in collaboration with T. Kuroda, Tohoku University, Japan.

doi : https://doi.org/10.1016/j.pss.2022.105424

(S. A. Haider and Y. S. Siddhi, J. Masoom and Varun Sheel)

Dependence of Martian Schumann resonance on the shape of dust devil

Dust Devils (DDs) prevail near the Martian surface during the Southern hemisphere summer. Their whirlpool effect gives rise to smaller particles in the atmosphere, which subsequently affects optical depth and decreases ion concentration.

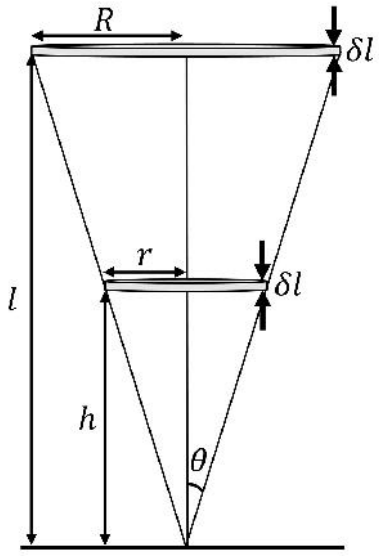

Figure 13: Inverse cone shaped DD with slices in vertical direction.

Presence of dust affects atmospheric conductivity and permittivity, which in turn affect electromagnetic wave propagation. An understanding of the underlying physics of electrical discharges due to dust is critical for future missions. Low atmospheric pressure and arid, windy environment suggest that dust is more susceptible

to triboelectric charging. The work presents a study of Schumann Resonance (SR) on Mars, whose presence indicates a possibility of the lightning. The modelling includes variable dust mixing in the DD. A random dust mixing is chosen and finally, an inverted cone-shaped DD is considered as shown in Figure 13, for the effective permittivity. Figure 14 shows fundamental, observable SR during Martian year 28 for conical dust distribution. It is found that SR modes essentially depend on the shape of DD, which consequently determines the effective permittivity of the medium. Also, SR does not depend much on the conductivity. At present, InSight magnetometer is searching for the presence of SR on Mars. Our results could be useful for future missions to carry out in situ measurements of SR, the most promising detection related to electrical activity on Mars.

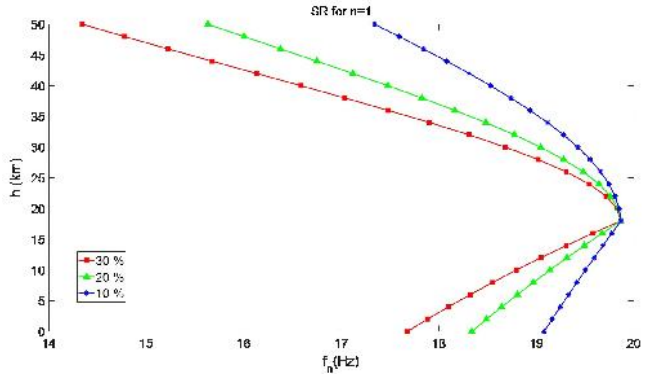

Figure 14: Fundamental, observable SR during Martian year 28 for conical (shape dependent) dust distribution.

doi : https://doi.org/10.18520/cs/v121/i6/769-774

(J. P. Pabari and T. Sana)

Interstellar Comet 2I/Borisov: Chemical and dynamical evolution of its atmosphere

Comets are the intriguing objects in the night sky that have captured the attention of the human mind since time immoral due to their distinct shape and sudden appearance. They are of the very few objects that survive the protoplanetary disk and provide the history of the formation of the planets. Recently Interstellar comet 2I/Borisov visited our solar system from an unknown planetary system. Its unique CO rich environment was a notable exception compared to the solar system comets. We have studied its atmosphere using a state-of-the-art multi-fluid chemical-hydrodynamical model built in-house PRL. We have treated neutral, ions, and electrons as three separate fluids and considered energy exchange between them due to elastic and inelastic scattering. The chemical network used for the simulation contains more than 400 chemical species connected by about 4500 reactions. We found that due to the presence of a large amount of CO in comet 2I/Borisov, a significant amount of CO^+ and HCO^+ ions are produced. These two ions substantially affect the formation and destruction rates of other major ions such as H_2O^+, H_3O^+, N-bearing ions, and large organic ions. We also find that the high presence of CO leads to a higher abundance of organic ions and neutrals such as $CH_3OH_2^+$, $CH_3OCH_4^+$ and CH_3OCH_3, as compared to a typical H_2O-rich Solar System comet. Finally, the study of the interstellar comet is very insightful since it provides information regarding the chemical inventory of comet 2Is natal disk and physical conditions prevailing in its host planetary system during its formation and our model output provided an understanding of its composition in its atmosphere.

doi : https://doi.org/10.1038/d44151-022-00005-9

(S. Ahmed and K. Acharyya)

Remote Sensing and Data Analysis

The Cr*ü*ger-Sirsais Basin: A window into the volcanic history of the Moon

Unravelling and mapping the geology of an obscured impact basin on the Moon for the first time, we have deciphered the geological history of the pre-Nectarian Cr*ü*ger-Sirsais Basin (∼475 km in diameter and centered at 16.0°S, 293.0°E) and have prepared a geological map of the region (Figure 15) using data from Chandrayaan-1, LRO, SELENE, and GRAIL.

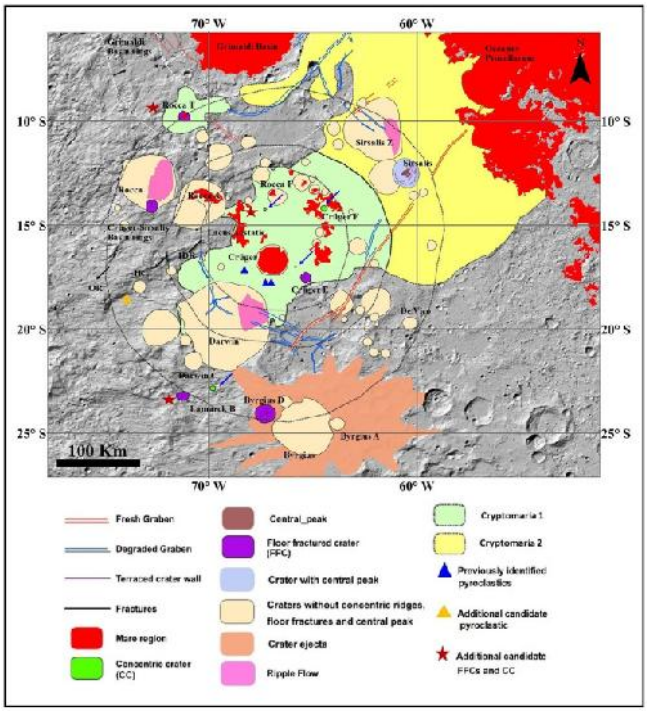

Figure 15: Geological map of the Cr*ü*ger-Sirsalis Basin overlapped on the hill-shade map derived from SLDEM 2015.

We have found evidence for the presence of an inner depression ring (IDR) for the first time and provide several geological shreds of evidence for the existence of largely obliterated inner and outer rings of diameters ∼243 km and ∼425 km, respectively. Further, we have found evidence of recent volcanism (up to ∼1.4 Ga) and Copernican aged tectonism in the region and compositionally two different types

of cryptomaria. Thus, in this study, we establish that the small isolated mare patches in the region are geologically related to the currently obscured and largely obliterated Cr*ü*ger-Sirsalis Basin. Also, from being host to cryptomaria that would have formed before ∼3.9 Ga, the main phase volcanism, and emplacement of the late phase basalts (∼2.0 Ga to ∼1.4 Ga), the small-sized Cr*ü*ger-Sirsalis Basin uniquely showcases the volcanic history of the Moon.

doi : https://doi.org/10.1016/j.icarus.2021.114875

(T. Singh, N. Srivastava, M. Bhatt and Anil Bhardwaj)

Boulder Fall Ejecta: Present Day Activity on Mars

Boulder falls are archives of recent surface activity on Mars. However, determining how recently they fell remains elusive. Our multitemporal HiRISE image analysis shows that new tracks are characterized by a herringbone-like ejecta pattern at each boulder bounce that we call boulder fall ejecta (BFE) (Figure 16).

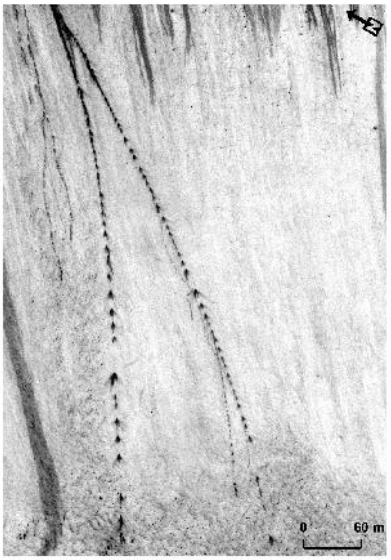

Figure 16: Boulder Fall Ejecta (BFE). Formation of boulder track with ejecta along the track. Boulder fall ejecta with a diverse spread of ejecta along the track. The ejecta spread along the track varies. The spacing between the bounces and ejecta spatial spread varies and small sub-tracks from some boulder bounces.

First systematic survey of BFE revealed ∼4,500 tracks whose total integrated track length is ∼900 km. Our BFE longevity analysis reveals that these tracks likely formed in the last few decades. From a few examples we also observed slope streaks originating from BFE tracks, providing additional evidence favoring a dry origin theory. BFE fade in as little as ∼2 to 4 Mars years, whereas, others can persist >6 Mars years suggesting differential weathering. Nearly 30% of BFE are observed in the Cerberus Fossae region, which suggests it is one of the most seismically active regions. Thus, BFE can be used to recognize very recent surface processes on planetary surfaces.

This work was done in collaboration with Susan Conway, Laboratoire de Plan*é*tologie et G*é*odynamique, Nantes, CNRS; Vigneshwaran, Govt. college of Salem and Tuhi S., Anna University, Chennai.

doi : https://doi.org/10.1029/2021GL096808

(Vijayan S., Harish, Kimi K. B., Sinha R. K., Bhalamurugan S. and Anil Bhardwaj)

Evidence of Regionally Distributed Tectono-Volcanism in a Floor Fractured Crater of North-Central Arabia Terra, Mars

Arabia Terra's is one of the oldest regions of Mars consists of highly cratered and heavily eroded plains, which is situated at a critical geologic division between the Martian highlands and lowlands. Previously, plain-style caldera complexes that resemble to terrestrial supervolcanic calderas have been reported in Northern Arabia Terra. However, the geomorphic extent of volcanism in Arabia Terra is not constrained. In this context, we discuss previously unrecognized evidence of an intrusive igneous process at the center of a floor-fractured crater (FFC) in North-Central Arabia Terra. We consider whether the observed geomorphic features are related to impact cratering or regional intrusive activity during the late Noachian - early Hesperian time. Our study reveals the existence of volcanic cones and dikes within the central floor of the crater. We also observe a preferred orientation of the igneous features, which shows a parallel alignment to regional linear tectonic features. We suggest that the igneous intrusions within the FFC were controlled preferably along the pre-existing weak planes (i.e., faults) in response to the regional tectonism, while the FFC-forming impact event primarily triggered the magmatism. These findings shed new light on the regionally distributed magmatic systems within Arabia Terra during the late Noachian and early Hesperian.

This work was done in collaboration with S Karunatillake, G Komatsu and A Bates, Louisiana State University - USA, and International Research School of Planetary Sciences, Italy.

doi : https://doi.org/10.1029/2020JE006748

(A. Rani, A. B. Sarbadhikari, and R. K. Sinha)

Extensive glaciation in the Erebus Montes region of Mars

Lobate debris apron (LDA) in the Mars' mid-latitudes substantiate extensive glaciation during the Late Amazonian. Detailed investigation of these landforms is imperative because different areas distributed at different latitudes, distinct geologic settings and varied regional topography may have responded to climate in different ways. In this study, mapping of LDA deposits in Erebus Montes region in the flat, low-lying plains of the northern mid-latitudes has been undertaken and examined at a detail previously not attempted to infer new insights on the history of extensive glaciation. LDA deposits show convex-up, steep terminus profiles consistent with typical down-gradient flow characteristics, and integrated flow patterns akin to the glacial landforms reported along the dichotomy boundary. Evidence for a broad piedmont-like lobe (Figure 17a), down-gradient flow within a possible oblique-impact crater, and infilled craters, suggest focused localized flow and glaciation. Lobate flows emanating from small alcoves and superposed on the main LDA are not observed (Figure 17b), which likely suggests that there is a lack of multi-stage glaciation facilitated by the alcove microclimatic conditions in the region. Linear-curvilinear ridges on the LDA deposits could be the

remnant of the internal flow lineations, and are most likely produced by the sublimation of debris-rich ice. Brain-terrain textures, polygonal cracks and ring-mold craters are ubiquitous on the upper surface of LDA deposits (Figures 17c-d), which provides the morphological evidence for the past accumulation of latitude dependent mantle (LDM) in the region. Hitherto, radar-based investigations do not provide substantial evidence for the presence of extant water ice beneath LDA deposits. We find that the LDA deposits examined here are consistent with the cold-based glacial behavior - morphological observations and supports existence of the sublimation process in the region. We suggest that the derived best-fit age of ∼30 Ma for the LDA deposits indicates age of the debris apron that has been mantled and the mapped LDA deposits in our study should be better represented by a broad age range of ∼10100 Ma. Together, our findings add another well-documented case to support the rapidly accumulating evidences for widespread extensive debris-covered glacial landsystems in the northern mid-latitudes of Mars in the Late Amazonian geological history.

doi : https://doi.org/10.1016/j.icarus.2021.114557

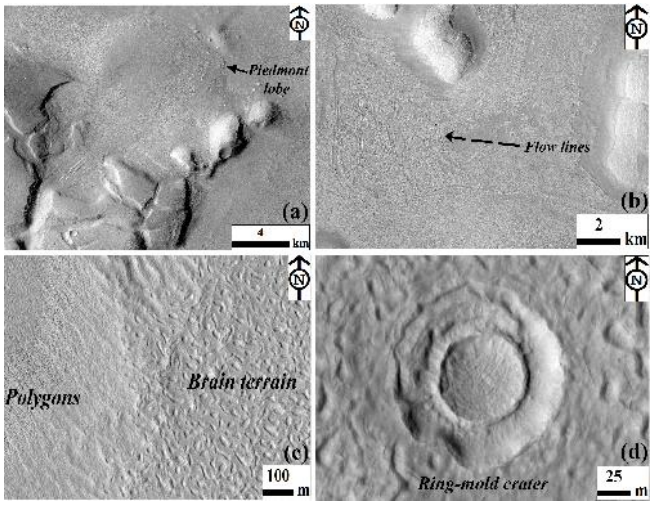

Figure 17: Examples of landforms observed within the study region. (a): Close-up view of a broad piedmont-like lobe (arrow). (b) LDA compressing, bending, looping, and coalescing to emerge as a large flow unit (arrow indicates the downslope direction of the flow lines). Note the absence of superposed flow units. (c) Brain-terrain texture and polygonal cracks are diagnostic signature of past accumulation of latitude dependent mantle (LDM) in the region. (d) Ring-mold craters are formed as a result of cyclic deposition of LDM inside the crater and their subsequent degradation.

(R. K. Sinha and D. Ray)

Astrobiological potential of Fe/Mg smectites with special emphasis on Jezero crater, Mars 2020 landing site

Life is known to adapt in accordance with its surrounding environment and life-sustaining sources available to it. Since harsh conditions would have precluded any possible aerobic evolution of life at the martian surface, it is plausible that martian life, should it exist, would have evolved in such a way as to derive energy from more optimum resources. Iron is one of the most abundant elements present in the martian crust and occurs at about twice the amount present on Earth. Clay minerals also contribute to about half of the iron found in soils and sediments. On Earth, clay acts as an electron donor as well as an acceptor in the carbon cycles and thereby supports a wide variety of metabolic reactions. In this context, we consider the potential of Fe/Mg smectites, one of the most widely reported hydrated minerals on Mars, for preservation of macro- and microscopic biosignatures. We proceed by considering the environmental conditions at the time smectites typically form and various microbes and metabolic processes associated with them as indicated in Earth-based studies. We also explore the possibility of biosignatures and their identification within the Mars 2020 landing site (Jezero crater) by using the astrobiological payloads on board the Perseverance rover.

This work was done in collaboration with D. Singh, P. Singh, N. Roy, S. Mukherjee, Jawahar Lal Nehru University, New Delhi.

doi : https://doi.org/10.1089/ast.2021.0013

(R. K. Sinha)

SHARAD detection of sedimentary infilling within an unnamed crater near Mangala Fossa region, Mars

We present the first Shallow Radar (SHARAD) based observations of subsurface reflections within an unnamed crater centered at 21.0° S, 150.6° W (Figure 18).

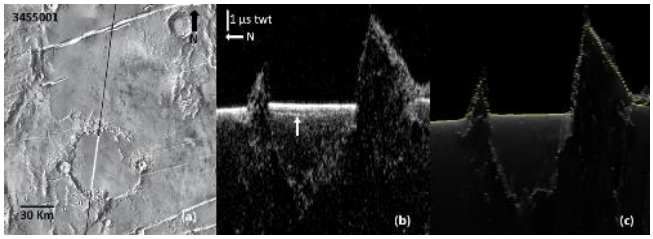

Figure 18: Subsurface reflections at Mangala crater: a) the daytime THEMIS images with the SHARAD ground tracks 3455001. The white patch indicates the extent of a subsurface detection in (b). b) SHARAD radargrams 3455001 shown in two way time (twt) delay; the vertical white arrow indicates the subsurface reflection. c) Simulated radargrams displaying off-nadir topographical clutter echoes. No clutter is found inside the crater, so we interpret the reflector to indicate a subsurface interface.

It is situated south of the Mangala Fossa and Mangala Valles, a major fluvial outflow channel system. We informally name the crater Mangala crater for this paper. In contrast with adjacent Tharsis lava flow, our analysis of radar propagation in the Mangala crater reveals a low loss tangent (0.0080.009) and lower dielectric subsurface material (average 5.6) for a subsurface unit that is ∼40m thick. These values are unexpected in this region. Lava flows dominate the surface and surrounding region, and SHARAD investigations of lava flows in the Tharsis region have detected higher values, creating a discrepancy that we discuss. Based on observed stratigraphy, and subsurface geophysical properties, we propose that the crater infilling is composed of moderate density sedimentary material buried by a layer of lava in the eastern portion of Mangala crater but left exposed in the west. Our measurements are also supported by previously done geologic mapping. We identify two subsurface reflections that provide details to determine one of the layers is sediment rather than lava. Detection of multiple reflections also indicates that infilling occurred in at least four successive events. These results are significant

because it adds more context to this highly studied region and provides compelling evidence that water moved large volumes of sediment into this basin.

This work was done in collaboration with Isaac B. Smith, Planetary Science Institute, Lakewood, CO, USA and Shital H Shukla, Gujarat University, Ahmedabad.

doi : https://10.1016/j.icarus.2021.114713

(R. R. Bharti, S. K. Mishra and N. Srivastava)

Meteorite, Analogue and Laboratory Studies

Chronology of coastal dune ridges in Vaigai Prodelta region, South Eastern Tamil Nadu, India

The Quaternary period is of great interest to the geoscientist for inferring the ecological, environmental and climatic changes. Although several global studies have been carried out on coastal dunes, the southern part of the indian penninsula has not been largely investigated in respect of geochronology. The Tamil Nadu coastline has extensive dunes which can be used for inferring quaternary paleoclimates. Teri sands, i.e., weathered red dunes occur inland, whereas white dunes are prevalent along the present shoreline. Dune reddenning has been previously suggested to be post-depositional, and due to in-situ weathering of feldspar grains. Earlier chronological studies have suggested that near coastal dunes aggraded at ∼5.6 ka, and coastal teri dune deposition occurred before ∼11.4 ka. The present study aimed at determination of new chronology of dunes in Vaigai prodelta region along the south-eastern coastline of India. Optically stimulated luminescence ages for the elevated beach ridge samples SANK-5, SANK-4, SANK-3, SANK-2 and SANK-1 are estimated to be 0.9±0.1, 1.1±0.1, 1.8±0.2, 5.3±0.4, and 27±2.3 ka respectively from top to the bottom of the section. The first four phases of aeolian activation occurred in marine oxygen isotope stage 1, whereas the ∼27 ka age suggests that sediment deposition occurred in marine oxygen isotope stage 3 (MIS 3). The luminescence ages are in stratigraphic order, and represent the first dates of aeolian activation in the Vaigai region. It is significant that periods of monsoon intensification during the late Holocene (∼6 ka and ∼1-2 ka) are coincidental with periods of aeolian activity in the Vaigai region. Furthermore, during the early Holocene, dune building activity may have stopped due to reduced sand supply in the region. Aggradation is more prevalent during lower sea-level stands, when part of the continental shelf was exposed providing available sand for aeolian reworking and is perhaps related to large scale aggradations during LGM in the river sequences along the west coast of India.

This work was done in collabration wth S. Sathyaseelan, Department of Remote Sensing, Bharathidasan University, Tiruchirappalli.

doi : https://doi.org/10.18520/cs/v120/i2/382-388

(D. K. Panda, D. Banerjee and A. D. Shukla)

Probing the proto-planetary disk isotopic composition from CV3 chondrite Bukhara

Carbonaceous chondrites preserved the records of gas composition of the proto-planetary disk and various processes that occurred in the early solar system. Chondrites are un-melted material and hence are the only rocks available for getting insights into the isotopic composition of gas from the proto-planetary disk. Bukhara meteorite, witness as fall on July 9th 2001 in Uzbekistan, classified as carbonaceous chondrite (CV3) is studied for isotopic composition of noble gases and nitrogen. The gases were extracted in step-wise heating method using resistance furnace and measured in noble gas mass spectrometer. Isotopic and elemental ratios of noble gases revealed that gas in this chondrite is a mixture of Q-type and solar wind as shown in Figure 19 Using cosmogenic $^{21}Ne_c$, the cosmic ray exposure age is determined as 22.6 ± 4.0 Ma, indicating the ejection of this meteorite long ago from its parent body.

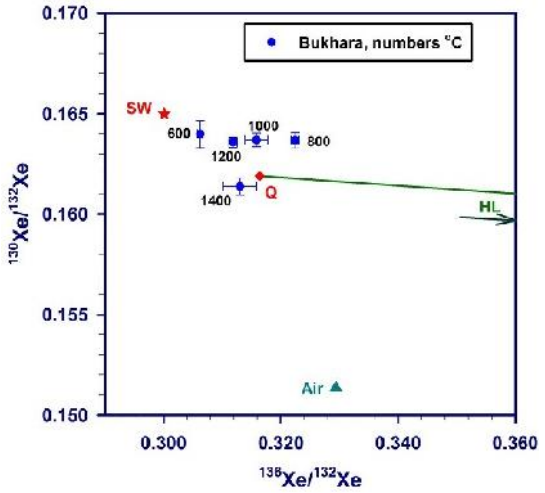

Figure 19: Xenon three isotope plot for Bukhara CV3 chondrite

The cosmogenic ratio ($^{82}Kr/^{83}Kr$)c of 1.34 ± 0.13 constrain the pre-atmospheric size of the meteoroid > 22 cm. Isotopic ratio of trapped nitrogen in bulk sample analysis of Bukhara is, $\delta^{15}N$ of +10.9±1.6 ‰, distinct from solar wind and Q-phase. Both, solar wind and Q-phase has lighter nitrogen isotopic signature. This provides an important constraint that the individual constituents of this chondrite sampled nitrogen from the reservoir other than that of Sun and Q-phase. This chondrite contains radiogenic isotopes of Xe and Ar. The ratio of $^{129}Xe/^{132}Xe$ in stepwise analysis is 1.34 at 1000°C temperature, and 1.26 for total, due to decay of ^{129}I (half-life of 15.6 Ma) to ^{129}Xe providing evidence of retention of gases. However, lower gas retention ages derived from ^{4}He and ^{40}Ar suggest thermal metamorphism at low temperature that could have occurred in late history of the meteorite.

This work was done in collaboration with S. A. Ehgamberdiev, Uzbekistan Academy of Science, Tashkent, Uzbekistan.

doi : https://doi.org/10.1016/j.pss.2021.105334

(R. R. Mahajan and S. Naik)

Achondritic neon composition to constraints on the evolution of differentiated asteroidal and terrestrial volatiles

The isotopic composition of noble gases in differentiated meteorites have the potential to yield stringent constraints on the evolution of matter in the solar system. For this purpose, neon abundance and isotopic composition in achondritic meteorites, eucrites and diogenites were studied. Eucrites, which are mafic basaltic rocks and diogenites, which are cumulates represent lower crust and mantle of asteroid Vesta. The stepwise heating data from eucrites are used to infer trapped neon, while bulk extraction data from eucrites and diogenites are used for quantitative estimates. It is found that all the eucrites and diogenites are enriched with cosmogenic noble gases.

This provides the constrain on the samples measured and pre-atmospheric sizes of the meteoroids. The average $^{20}Ne_t$ in eucrites and diogenites are 8.02 x 10^{-9} cm^3STP/g and 1.02 x 10^{-8} cm^3STP/g, respectively. The concentration of trapped ^{20}Ne in Earths mantle and Martian mantle are comparable to eucrites and diogenites. The trapped ^{20}Ne in all differentiated reservoirs are depleted with respect to chondritic material. This indicates that the differentiated bodies lost their gases irrespective of size, precursors and closure timing. Investigation of noble gas isotopic ratio and quantitative estimates of trapped gases in eucrites and diogenites have provided crucial constraints of the extent of outgassing during the melting/differentiation of asteroid Vesta.

This work was done in collaboration with S. Jaiswal and M. Ngangom, Banasthali Vidyapith, Rajasthan.

doi : https://doi.org/10.1016/j.jaesx.2022.100084

(R. R. Mahajan)

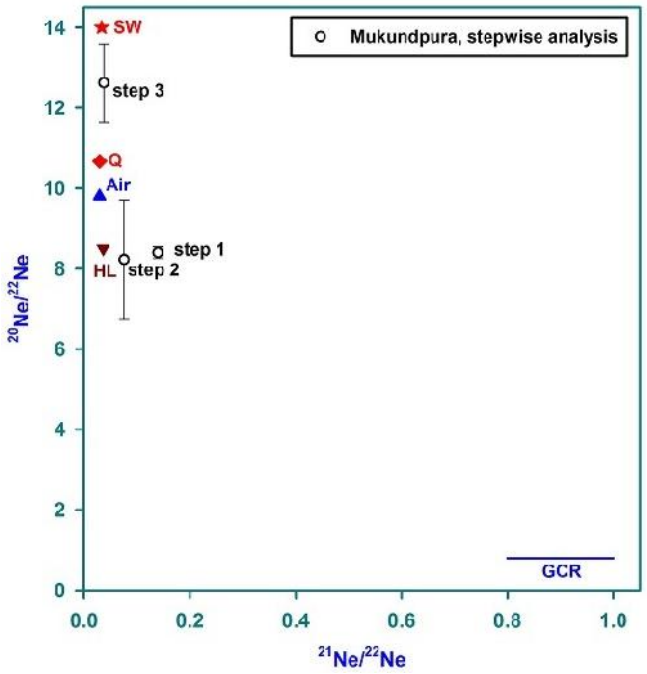

Figure 20: Neon three isotope plot for Mukundpura CM2.0 chondrite showing trapped components

This work was done in collaboration with D. Raychaudhuri and A. Dutta, GSI, Kolkatta.

doi : https://doi.org/10.1016/j.pss.2022.105465

(R. R. Mahajan and A. D. Shukla)

Cosmogenic records in Mukundpura CM2.0 carbonaceous chondrite

Mukundpura carbonaceous chondrite is a recent fall, provides unique opportunity to investigate cosmogenic records using radioactive and stable isotopes. The activities of cosmogenic radionuclides ^{22}Na, ^{54}Mn, and ^{26}Al were measured in ultra-low background level hyper pure germanium (HPGE) γ-ray detector. The activities of ^{22}Na, ^{54}Mn are lower in Mukundpura, which has fallen close to minima of solar cycle 24, compared to other chondrites. The observed differences in activities in similar circumstances/time of fall with respect to Solar cycles may be related to its intensity. There is absence of thermal neutron produced ^{60}Co isotope ($<$0.5 dpm/kg) supports the small size of the meteoroid. Noble gases were measured in a fragment using noble gas mass spectrometer to determine the exposure age. The trapped noble gases were found to be mixture of two sources, solar wind and Q-phase as shown in Figure 20 for neon three isotopes.

The concentration of cosmogenic ^{21}Ne and ^{38}Ar yields the exposure age of 6.54 $\pm$ 1.34 Ma for Mukundpura. This indicates longer irradiation of the meteorite. The ^{26}Al concentration of around 35 dpm/kg confirms it. The exposure age revealed that this meteorite belongs to one of the major ejection events from the CM parent body.

Microstructural and Chemical Investigations of Presolar Silicates from Asymptotic Giant Branch Stars and Type-II Supernova Explosions

Tiny dust grains formed in the stellar envelopes of massive stars such as red giant branch (RGB) and asymptotic giant branch (AGB) stars and in exploding stellar objects such as novae and supernovae before the formation of our solar system are known as presolar grains. Of different presolar phases, silicates are the most abundant presolar phase with abundances reaching upto 1.5% in the interplanetary dust particles (IDPs). More interestingly, presolar silicates studied in laboratory condensed in a range of stellar environments such as RGB and AGB stars, novae and supernovae explosions and also J type C-stars. Hence, the structural and chemical compositions of presolar silicates provide insights into the physiochemical conditions of the parent stars, stellar environments at the time of grain formation and various alteration processes that take place in the interstellar medium and on the meteorite parent body. The present study discusses the formation environments of silicate dust grains and the possible alteration mechanism that may have played a role in shaping the present structure and chemical compositions of the grains in this study.

Our study compared putative AGB silicate grains with the silicates

from supernovae using microstructural and chemical compositions of grains. Presolar silicates analysed in this study show a wide range of microstructural and chemical compositions. Both the AGB stars and supernovae reveal equilibrium and non-equilibrium grain formation conditions. Microstructural composition of the three out of nine grains indicate that these grains formed as crystalline olivine or forsterite, and later altered structurally and chemically either in the interstellar medium or the meteorite parent body. An indication of the terrestrial weathering of the meteorite is also found in a grain with relatively high Fe composition and very low $Fe^{3+}/\Sigma Fe$ ratio (Figure 21). A unique compound grain was also identified with the oldhamite phase incorporated within the enstatite. It is likely the case where oldhamite grain acted as a seed nucleus for presolar enstatite grain formation. This study highlights the complexity of the formation and alteration histories of presolar silicates.

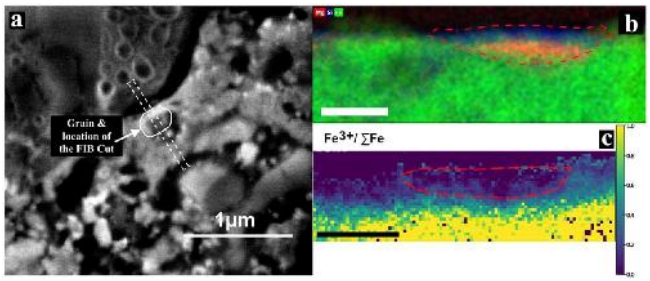

Figure 21: (a) SE image and location of the FIB section for the grain NWA 801_21. (b) Chemical maps derived from STEM EDS corresponding to Mg (red), Fe (green), and Si (blue); the white square bar represents 50 nm. (c) $Fe^{3+}/\Sigma Fe$ chemical map. The outer boundary of the grain is shown as a red dashed line. The black square bar represents 50 nm.

This work was done in collaboration with Luc Lajaunie, Universidad de Cádiz: Cadiz, ES and M. Bizzaro, University of Copenhagen: Copenhagen, DK.

doi : https://doi.org/10.3847/1538-4357/ac3332

(M. Sanghani and K. K. Marhas)

The iron oxidation record and progressive aqueous alteration in Mukundpura CM2: Implications for water-rich primitive asteroid

The CM (Mighei type) chondrites, one of the primitive members of Carbonaceous Chondrites, comprise mainly of hydrated mineral phases ($\geq$70 vol% phyllosilicate) and record unambiguous records of the action of water. The CMs also include the most abundant group and represent $\sim$25% of carbonaceous chondrite fall (The Meteoritical Bulletin 2021). Based on the C-H-O isotopic systematics of CM chondrites, it is generally assumed that their volatile-rich parent bodies were formed in the outer solar system and later migrated to the current position. The matrices of CM chondrites are fine-grained and have undergone different degrees of aqueous alteration. Based on mineral chemical composition of matrix phyllosilicate of Mukundpura CM2, the evidence of progressive aqueous alteration is understood and also reflected in gradual changes in S/SiO_2 and FeO/SiO_2 ratios. Further, we performed X-ray absorption near-edge spectroscopy at the Fe K-edge to explain the redox state of the phyllosilicate (Figure 22). The Iron Oxidation Index of Mukundpura yields 2.423 and the Fe^{3+}/Fe^{2+} ratio is 0.733. The Fe speciation in phyllosilicate is also sensitive to the degree of aqueous activity. Our data are consistent with the presence of Cronstedtite and Tochilinite-Cronstedtite intergrowths in the matrix suggested for different extent of alteration and recorded history of pervasive aqueous alteration in the asteroidal parent body. The VNIR absorption occurs around 0.70.8 μm due to the presence of Fe^{2+}-Fe^{3+} charge transfer, while 0.91.0 μm spectral range is induced by crystal field transition of Fe within Fe^{2+} bearing phyllosilicate. Presence of both absorption spectra and their relative intensities further testifies to the fact that Mukundpura CM2 phyllosilicate matrix is an ensemble of Fe serpentine (Cronstedtite) and Mg-serpentine (Antigorite) and slight dominance of Mg-type resulted due to progressive alteration.

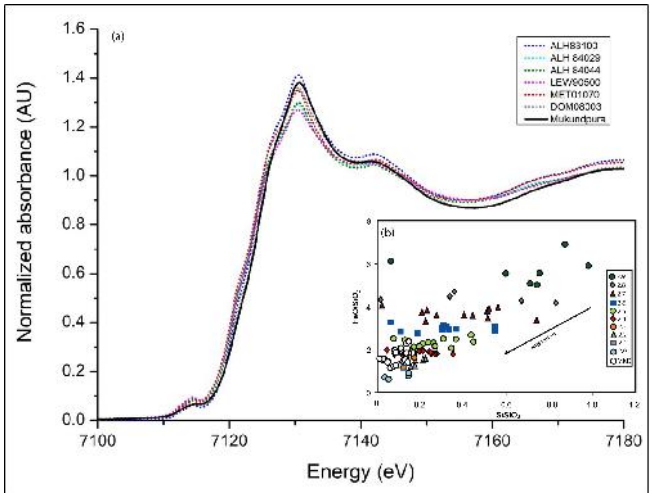

Figure 22: (a) Normalised XANES spectra of Mukundpura and other matrix-rich CM2 samples. Data source: GHOSST/SSHADE database, https://www.sshade.eu/db/ghosst. (b) Inset showing FeO/SiO_2 versus S/SiO_2 of matrices clasts of CM chondrite with subtype ranging 2.0 to 2.9 including the Mukundpura (MKD).

This work was done in with collaboration with C. Nayak, BARC and RRCAT, Indore

doi : https://doi.org/10.1016/j.asr.2021.06.009

(D. Ray and S. Baliyan)

Petrochemistry and Oxygen Isotope of Karimati (L5) Chondrite, a 2009 Fall in Uttar Pradesh, India

Karimati, a single stone, weighing $\sim$1 kg, fell on the mid-day of May 28, 2009, in Karimati village of Tahsil Hamirpur in Uttar Pradesh, India. Based on textures and mineralogy, Karimati is classified as brecciated, L5 (S2), ordinary chondrite. Petrologically, the chemical group, L has been assigned based on the typical mean compositions of olivine (Fa:25.5) and low-Ca pyroxene (Fs:21.6). The bulk chemical composition also resembles L chondrite as Mg/Si ratio $\sim$0.82. Finally, the oxygen isotopic ratios of bulk meteorite sample yielded $\Delta^{17}O$ (+3.78 and +4.07) and $\Delta^{18}O$ (+4.95 and +5.52), respectively, further confirming Karimati as L-chondrite (Figure 23). The Karimati appears to have been subjected to single fragmentation

in the atmospheric flight and it is evident from similar characteristics of all the lateral faces except the base of the pyramid in terms of its uniform colour, homogeneous fusion crust and shallow regmaglypts. The metamorphic equilibration temperature for Karimati chondrite using two different thermometers (olivine-chromite and two pyroxene thermometry) has been estimated and ranges 655°C and 770°C, respectively with a mean value of ∼710°C and corresponds to the Type 5 thermal equilibration event.

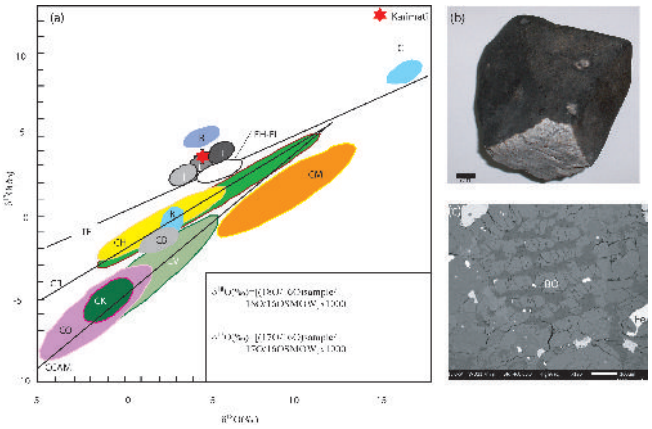

Figure 23: (a) Schematic representation of location and ranges of whole-rock oxygen isotopic composition of major chondritic classes. The Terrestrial Fractionation (TF) line and Carbonaceous chondrite anhydrous minerals (CCAM) are shown for reference (after Clayton, 2003). (b) Hand specimen of Karimati chondrite and (c) BSE image of Barred Olivine (BO) chondrule-one of the early forming objects in Solar System.

This work was done in collaboration with S. Chakrabarti, University of California, San Diego, USA

doi : https://doi.org/10.1007/s12594-022-1983-4

(D. Ray, D. K. Panda and G. Arora)

Developmental Work

VODEX Development

Smaller size ($> \sim 0.1\ \mu$m) Interplanetary Dust Particles (IDPs) travel inward toward Sun and can encounter various planets during their travel. The IDP flux is known at the Earth. However, it is not measured at Venus, except existence of a few measurements of IDP at larger distances from Venus. Since the IDP is ablated in the Venusian atmosphere, its study is crucial to understand the third meteor ion layer in the electron density profile. A Venus Orbit Dust Experiment (VODEX) is proposed for future Venus orbiter to study flux and distribution of high-altitude dust at and around Venus and also between Earth and Venus. The operating principle of VODEX is shown in Figure 24, where the impacting dust particle produces plasma in the detector space. The plasma is collected by the biased electrodes and processed in the electronics chain depicted in Figure 25. The Engineering Model (EM) of VODEX is under assembly, after optimization of flux, size and payload mass. Both, the front-end electronics and processing electronics were developed and tested in the laboratory. Its further testing and optimization are underway. A photograph of the EM model of detector is depicted in Figure 26, during a testing.

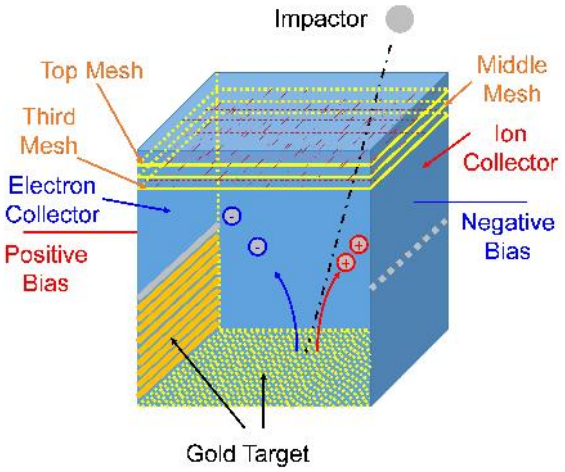

Figure 24: Working principle of VODEX.

The dust detector is tested inside a vacuum chamber at IPR and a pulse laser is fired to obtain the impact plasma in the detector space. These plasma species are collected to study the further parameters. In order to find equivalence between the dust impact energy and laser energy, explained in Figure 27, an experiment was performed. A photogram of the experimental set up is depicted in Figure 28. When a pulse laser shot is incident on the target plate of detector, plasma is generated. Charged ions and electrons are collected by voltage biased collector plates of the detector. Based on the signal peak, number of charge carriers and further the energy utilized in generation of charge carriers is derived. This energy is then compared to the fraction of dust particle energy which is utilized for ionization and a relation is derived. This experiment was carried out at a laser energy of 7 mJ and to further refine the equation, the experiment has to be repeated at multiple laser energy levels. Results show that the pulse energy is at higher level at present and needs to be reduced. Further work on lower energy testing is underway.

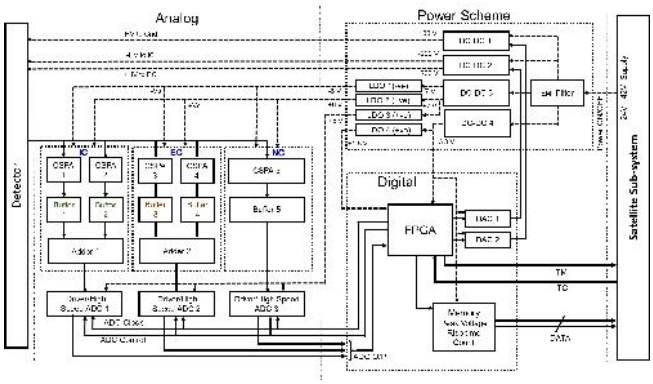

Figure 25: Analog electronics, digital electronics and power scheme of VODEX.

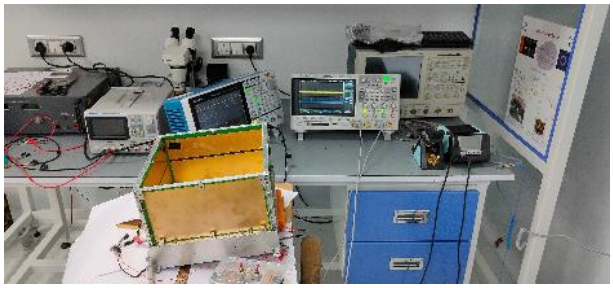

Figure 26: Photograph of EM (underway) of VODEX during a testing in laboratory.

In addition, the expected impact rate of the IDP at Venus has been studied using available observations and models. It is found that the expected rate is about 12-15 per day in the normal conditions and may rise to higher levels during the meteor shower period. The IDP is ablated in the Venusian atmosphere and leave a metal ion layer. A model of ablation process is under development for the dust ablation in planetary atmosphere. Based on the modelling and simulation, the ablation parameters in the Venusian atmosphere were estimated to show the application aspects of VODEX. The results are shown in Figure 29 for the IDP mass, speed and temperature, respectively.

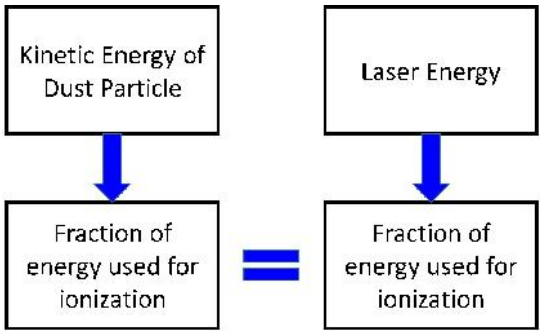

Figure 27: Block diagram of experiment to understand dust equivalence of pulse laser energy.

Figure 28: Experimental set up for dust detector testing at IPR.

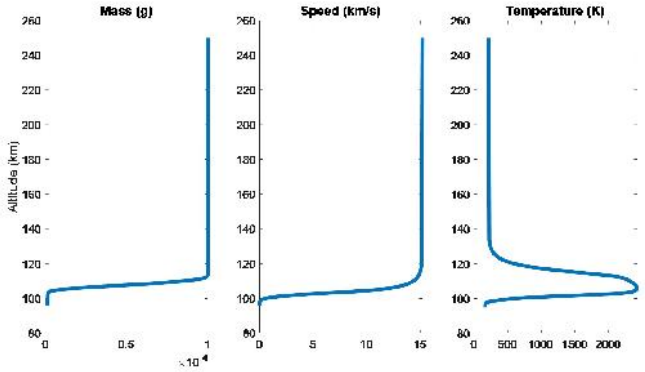

Figure 29: Application of IDP observation is explained through the ablation. The mass, speed and temperature profile on ablation of a particle with mass 10^{-4} g entering at 15.2 km/s speed in Venus atmosphere.

(J. P. Pabari, S. Nambiar, S. Jitarwal, Rashmi, K. Acharyya, V. Sheel, R. Mahajan, Anil Bhardwaj, S. M. K. Praneeth, B. Shah, J. Rami, V. Singh, R. Singh, S. A. Haider and Team)

Bias Optimization of VODEX and Plasma Capture Efficiency

To capture the impact plasma in electron and ion channels, the detector needs to be biased appropriately using high voltage. Also, to minimized the resources on satellite, the optimization is essential. SIMION software was utilized to understand the collection efficiency of detector. SIMION is a software package used to simulate electric fields and the trajectories of charged particles in those fields.

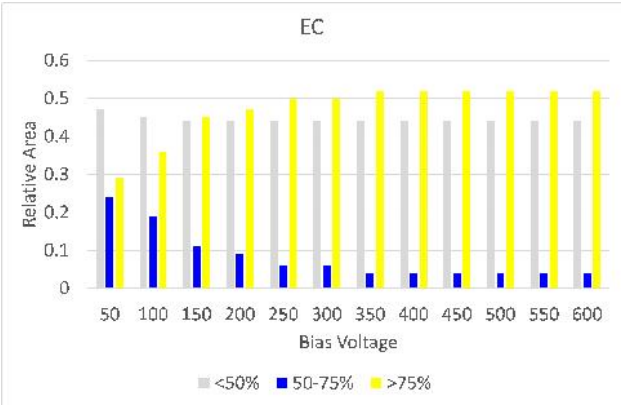

Figure 30: Relative area covered giving collection efficiency up to 50 %, between 50-75 % and more than 75 % at varying detector bias for EC

The geometry of detector is given as an input in the software and then appropriate potentials are defined. The trajectories of impact generated charge are then analyzed for the given electrostatic field. The simulation gives information about the collection efficiency of the detector. The charge carriers are initiated using SIMION from various positions on the target plate. The electrons and ions then follow electrostatic field lines and get collected at the collector plates. It is simplified due to the inherent symmetry involved in the detector

geometry. The bias voltage was varied from 50-600 V, with a 50 V interval for optimizing the detector performance for ion and electron capture. Some of the ions are attracted by the mesh placed on top of detector, which is negatively biased to repel low energy electrons in solar wind. Extensive simulation was carried out to obtain the optimum bias and find the detector capture efficiency. The area dependent results are shown in Figure 30 and Figure 31 for Electron Channel (EC) and Ion Channel (IC), respectively.

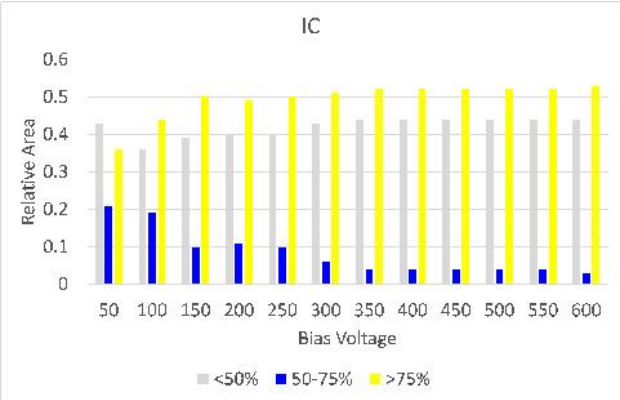

Figure 31: Relative area covered giving collection efficiency up to 50 %, between 50-75 % and more than 75 % at varying detector bias for IC (with negative polarity).

(J. P. Pabari, S. Nambiar, S. Jitarwal, Rashmi, K. Acharyya, V. Sheel, Anil Bhardwaj, R. K. Singh, K. A. Lad, J. M. Jakhariya and Team)

LIVE Development

A Lightning Instrument for VEnus (LIVE) is being developed at PRL for detection of lightning on Venus. A block diagram of LIVE is shown in Figure 32 where lightning signals are detected by an electrically short antenna and the signal is processed in the electronics. The development of Engineering Model (EM) of LIVE is initiated.

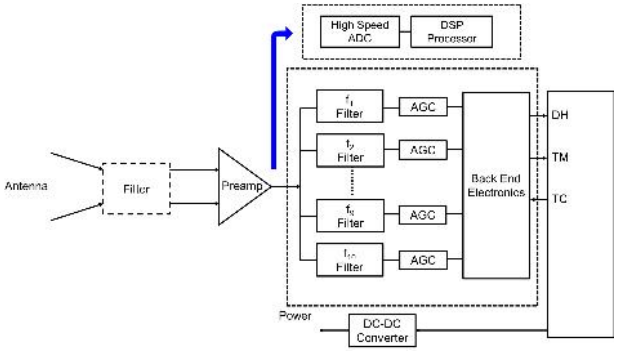

Figure 32: Design blocks of LIVE

The front-end electronics of LIVE was tested in laboratory, whose photograph is depicted in Figure 33 (left). The front-end electronics consists of preamplifier, followed by gain stages. Figure 33 (right) shows testing results of AD524 and 20 dB gain stages for the analogue electronics of LIVE. Further testing an optimization is underway. Further, a study on spectral comparison of natural lightning vs artificial source of lightning was carried out to understand the spectral similarity. Van-De-Graaff generator was utilized as an artificial source of lightning, while the natural lightning was captured on 7 October 2021 at PRL Thaltej campus. The first row of Figure 34 shows LIVE prototype set to measure the natural lightning. The results are shown in Figure 34 on the second and third rows for the artificial and natural sources, respectively, where the signals captured are typical ones. It can be seen from Figure 34 that typically, the natural lightning on Earth carries frequency components up to ∼10 kHz, while the artificial source of lightning gives sharp rise time causing the frequency components as high as ∼50 kHz. Further investigation is ongoing in this direction.

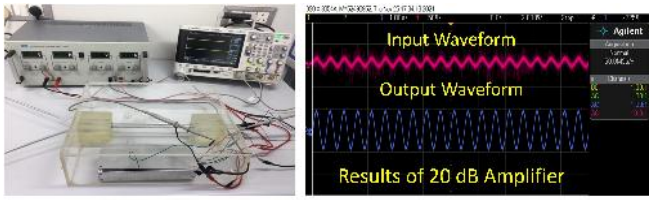

Figure 33: Testing of LIVE FE (on left) and results of preamplifier along with 20 dB gain stages (on right).

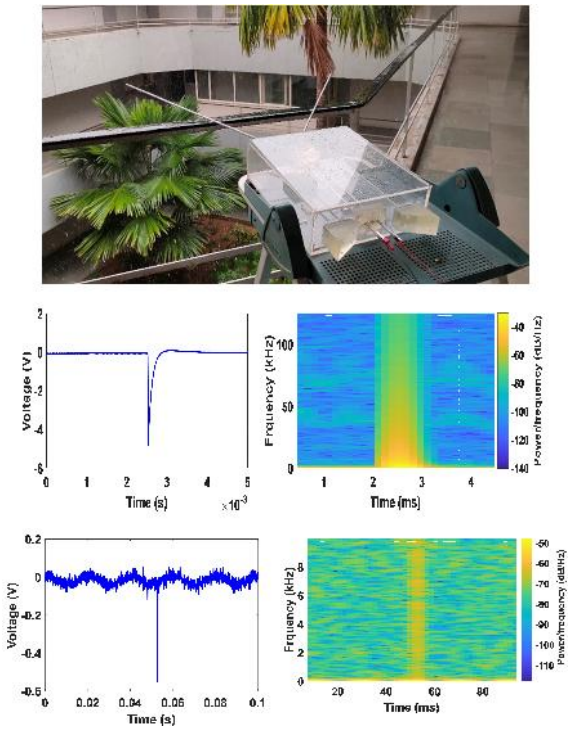

Figure 34: Comparison of lightning spectrum from artificial and natural lightning sources. First row gives lightning signal from artificial source of lightning (i.e., Van-De-Graaff generator) and its time-frequency localization. The second row shows lightning signal from natural lightning captured on 7 October 2021 at PRL Thaltej campus and its time-frequency localization.

In addition, sensitivity analysis test was carried out for the LIVE antenna with (i) 75 cm length and 60° angle between two arms (PVO OEFD antenna configuration) and (ii) 150 cm length and 120° angle

between the arms. Typical results are depicted in Figure 35 with yellow color for shorter antenna and green color for longer (150 cm) antenna. It is observed that ∼3 times larger voltage is induced in the longer antenna, indicating improved performance of longer antenna due to its increased length as well as the larger angle between the antenna arms. Further work is ongoing.

Figure 35: Results of time domain pulses for (i) 75 cm length and 60° angle (yellow) between two arms (PVO OEFD antenna configuration) and (ii) 150 cm length and 120° angle (green) between the arms. The later shows ∼3 times larger signal due to increased length as well as angle.

(J. P. Pabari, S. Jitarwal, S. Nambiar, Rashmi, K. Acharyya, V. Sheel, Anil Bhardwaj and Team)

Neutral & Ion Mass Spectrometer for the study of planetary atmospheres

Neutral & Ion Mass Spectrometer (NIMS) is based on the concept of quadrupole mass spectrometer (Mass range: 2 200 amu and mass resolution $\{M/\Delta M\}$ >10). The incoming sample of gaseous species is filtered based on the ratio of their mass to their charge (m/q). NIMS works in two different modes viz. a) The Neutral Mode, which is used to measure neutral species by passing them through an ionizer, and b) The Ion mode, which is used to measure the positively-charged ambient ions. NIMS can be programmed to either sweep across a range of (m/q) ratios or allow only a species of interest to pass, by tuning the instrument to a fixed (m/q).

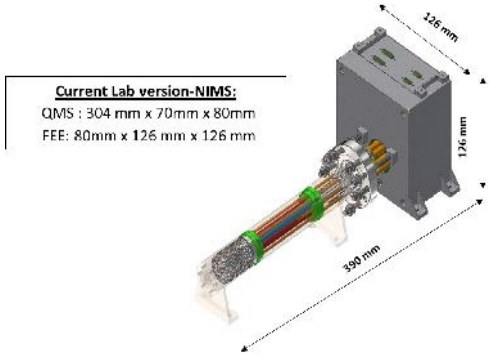

Figure 36: Orbiter variant for NIMS

It can be optimized for an orbiter mission as well as an atmospheric flight (atmospheric entry on board a nano-sat or balloon). NIMS can effectively characterize the neutral gases and ambient ions by measuring the isotopic and molecular compositions of the planetary upper atmosphere and ionosphere. NIMS Mechanical assembly has been realized in two separate variants. First of which is developed for future Orbiter missions (as Figure 36 shows). Other variant being designed for Ballooning or Nano-sat Mission (Figure 37), in which additional pumps (Turbo + Scroll) and Micro-Valves have been introduced. These additional parts are being operated using additional circuitry, that can be controlled using In-house developed electronics for it. For CEM Biasing operation, an optimized circuit has been designed to control CEM Gain (upto 10^7) and its External Biasing, based on Test Requirements.

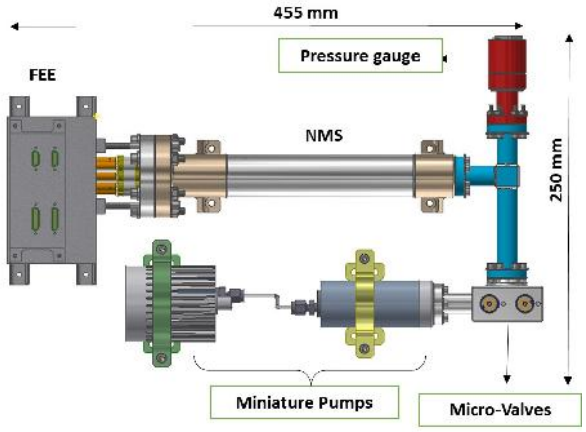

Figure 37: Ballooning Variant for NIMS

(P. Sharma, S. K. Goyal, R.R. Mahajan, Nirbhay Upadhyay, Abhishek Verma and A. Auknoor)

Characterization of Silicon Pin Detector and its readout electronics for the future Venus Mission

The silicon pin detectors and scintillators are widely used in high energy particle measurements. In one of the instruments proposed for the upcoming Venus Orbiter mission, it is proposed to use a stack of Si PIN detectors and a scintillator detector to measure the particle in the wide energy range. In this direction, we have developed the readout electronics for Si PIN detectors and characterized the detectors along with the electronics for the various parameters (Figure 38).

We have procured the Si PIN detectors with various thickness ranging from 50 μm to 1500 μm in order to study their suitability in detecting the particles in the energy range of 20 keV to 100 MeV. Each detector has the active area diameter of 17mm. We have characterized these detectors individually for the parameters such as leakage current, performance measurement with temperature and the energy resolution in order to evaluate their suitability to use in Venus Radiation environment monitor experiment proposed for the Venus orbiter mission. These parameters were tested using X-ray and alpha sources at different energies. The leakage current was measured and found to be in the range of ∼0.8 nA to 50 nA for detectors with thickness ranging from 50 μm to 1500 μm (Figure 39).

Table: The Energy resolution and other characteristics are also listed in the table below.				
	50μm	100μm	300μm	1500μm
Active Area Diameter	17 mm			
Full Depletion Voltage, VFD (V)	11	7	66	250
Leakage Current @ VFD	1.26	0.8	1.44	50.06
Detector Capacitance (pF)	467	233	78	47
Max. Operating Voltage (V)	(VFD + 30)V			
Energy Resolution @ 5.486 MeV	116.7 keV	98.2 keV	39.8 keV	30.23 keV

Figure 38: Laboratory Setup for Si PIN detector readout electronics.

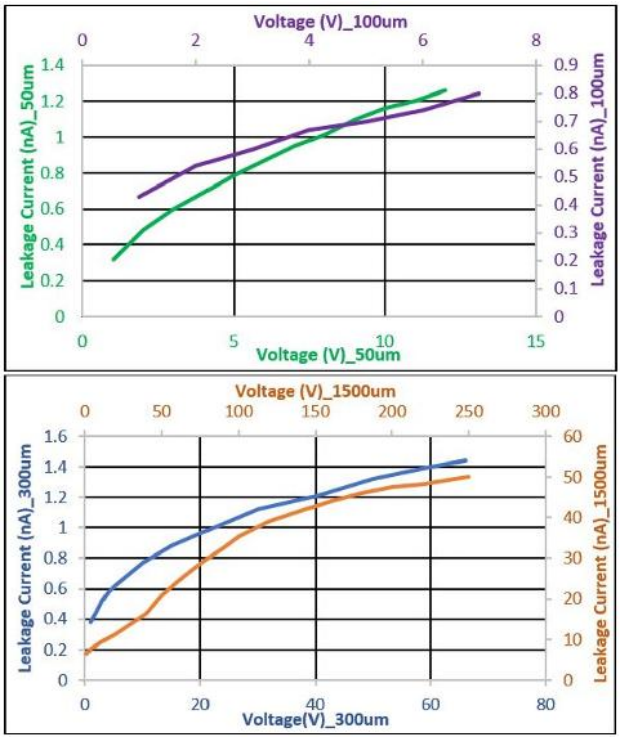

Figure 39: Leakage current of Si PIN detectors of different thicknesses

(Sushil Kumar, M. Shanmugam, A. Patel and T. Ladiya)

Characterization of Si Photomultipliers (SiPM) for upcoming Venus Orbiter Mission

In the recent development of detectors for High Energy Physics and Astrophysics, a new type of silicon detector known as Silicon Photomultipliers (SiPM) has been developed to replace the traditional vacuum-based photo detectors, photomultiplier tubes (PMT). The Silicon Photomultipliers (SiPM) consist of a high-density (up to 100 per mm^2) array of small, independent single-photon avalanche diodes (SPAD) sensors, working in a Geiger Mode to achieve gain at a level of $\sim 10^6$. It offers high Photon Detection Efficiency (PDE) up to 40%, low-voltage operation, insensitivity to magnetic fields, mechanical robustness, and excellent uniformity of response, which makes it an attractive alternative to the PMTs for space applications.

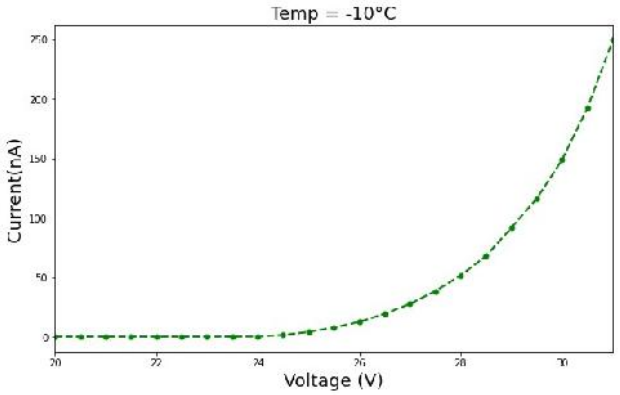

Figure 40: Dark Current vs Voltage for 3mm sensor at -10°C

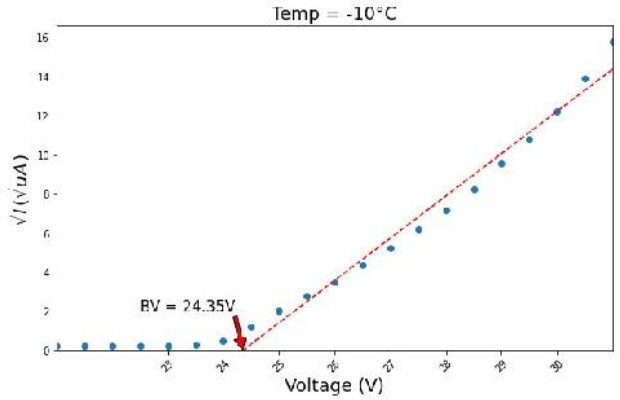

Figure 41: Breakdown voltage is determined from the intercept of a Linear fit to the $\sqrt{I}$ vs V.

We have studied the On-Semiconductor made Micro C series SiPM (30035) having a surface area of 3mmX3mm and 35μm microcell size. We have carried out the Current-Voltage (I-V) Characteristics (Figure 40) at a temperature ranging from -30°C

to 70°C, and measured the breakdown voltage at different operating temperatures (Figure 41 and 42), and the temperature coefficient of breakdown voltage. We are also working on the photons readout from the Plastic BC-408 and Thallium doped Cesium Iodide CsI(Tl) scintillators using the SiPM for radiation measurement purposes on the upcoming Venus orbiter mission.

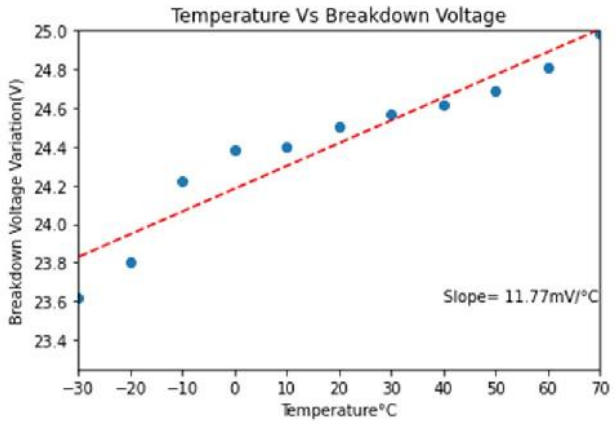

Figure 42: The Impact of Temperature Change on the Breakdown Voltage. The temperature coefficient is 11.77mV/°C

(D. K. Painkra, T. Ladiya and M. Shanmugam)

Supra Thermal & Energetic Particle Spectrometer (STEPS) - Subsystem of ASPEX payload

STEPS is one of the independent subsystems of Aditya Solar wind Particle EXperiment (ASPEX), which is going to be flown on Aditya - L1 mission. The spacecraft is going to be placed in a halo orbit around the Sun-Earth L1 Lagrangian point. ASPEX will measure the slow and fast solar wind, supra-thermal particles and solar energetic particles using its two subsystems: SWIS (Solar Wind Ion Spectrometer) and STEPS.

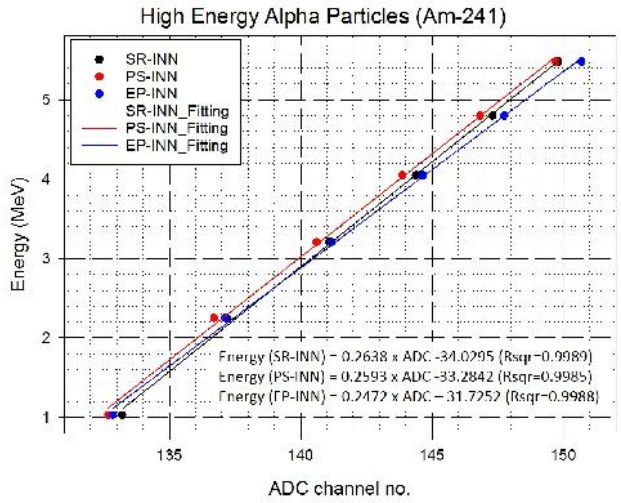

Figure 43: Conversion of ADC channels to Energy values for inner detectors of STEPS-FM.

STEPS covers the high-energy spectrum of the particles i.e. in the range of 20 keV/n to 5 MeV/n from six directions i.e. Sun-Radial (SR), Parker Spiral (PS), Earth Pointing (EP), Intermediate to SR and PS, and North & South of the Sun-Earth ecliptic plane. The STEPS subsystem has been configured into three packages in order to cover the six directional measurements i.e. STEPS-1, STEPS-2A & STEPS-2B. STEPS-1 package houses four detector units (SR, IM, PS and NP) and their front-end electronics (FEE). STEPS-2A package has one detector unit (EP) and FEE for EP and SP (STEPS-2B) detector units. ASPEX-PE is a processing electronics package, common for both SWIS and STEPS.

Flight models (FM) of the STEPS and ASPEX-PE have been developed and tested. Test & Evaluation (T&E) tests for STEPS-FM have been successfully completed. Calibration activities of STEPS-FM have also been over. Figure 43 shows the plots of conversion of ADC channels to energies for the inner detectors of STEPS. For this experiment, ^{241}Am source is used which emits 5.48 MeV alpha particles. The other energies of alpha particles are achieved using Ti foil attenuator. The energy vs ADC channel are fitted linearity and plotted along with experimental values. Similar exercises have been done for the rest of detectors. Qualification models (QM) of STEPS are undergoing T&E where Burn-In test, Storage tests, Vibration test, EMI/EMC and Thermo-vacuum tests have been completed. Mechanical shock and ESD tests are planned to be conducted in near future. Some part of calibration activities of QM is also completed. Figure 44 shows the photographs of the STEPS-QM models during 24 hours humidity storage tests (R.H. ∼95% at T=40 °C). STEPS instrument provides data of particle measurements in CDF format in three levels: Level0, Level1 and Level2. Level0 is the raw data from the instrument. Level1 is derived from Level0, which provides direction wise separated particle counts vs ADC channel. Level 2 is the energy-calibrated data, derived from Level1. The software for the same has been developed and is in final stage.

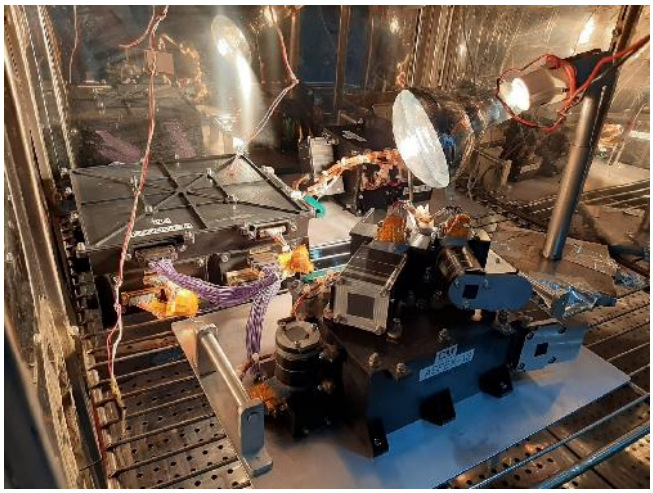

Figure 44: Humidity storage test of QM models of STEPS

(S. K. Goyal, A. R. Patel, N. K. Tiwari, P. Sharma, A. Auknoor, B. Dalal, A. Sarada, J. Sebastian, D. Painkra, S. Kumar, N. Singh, T. Ladiya, M. Shanmugam, S. V. Vadawale, D. Chakrabarty, P. Janardhan, and ASPEX Team)

Planetary Rock Sampling Technology Project

The project Planetary Rock Sampling Technology has made significant progress with respect to scientific and technological aspects of the drilling system design. The project will be executed in two phases. The first phase will target the design and development of a drilling system for sample acquisition from lunar subsurface for in-situ analysis mission. The second phase will target the development of drilling systems for sample acquisition from Martian subsurface for in-situ analysis and a core sample return mission from the Moon. The baseline design report has been finalized, which highlights some of the important scientific and technological advancements that have been with respect to design of the drilling system. These are as follows:

- In the first phase the depth of drilling is decided to be 1.5 m to acquire powdered samples from the lunar regolith with 10-15 cm interval of depths in each shot of drilling.
- Bite sampling approach has been adopted as the method to acquire powdered samples from the lunar regolith due to its advantages over other sampling methods.
- The conceptual and baseline design of a lander-based drilling system has been finalised and documented.

This work was done in collaboration with Tanmay Singhal, Aasik V., Manu V. Unnithan and U. A. Subramanian, VSSC.

(A. J. Verma, N. Upadhyay, N. Srivastava, R. R. Mahajan, K. Durga Prasad, V. Sheel and Anil Bhardwaj)

Integration and testing of Chandrayaan-3 ChaSTE Flight Model

Chandras Surface Thermophysical Experiment (ChaSTE) is one of the payloads to be flown onboard Chandrayaan-3 lander, which is developed jointly by the Physical Research Laboratory, Ahmedabad and Space Physics Laboratory (SPL) in collaboration with the various entities of VSSC. The objective of the experiment is in-situ investigation of thermal behaviour of outermost 100 mm layer of the lunar surface by deploying a thermal probe. ChaSTE aims to study the thermophysical properties of Lunar subsurface by deploying a 10 cm thermal probe consisting of a series of temperature sensors and a heater. The experiment for Chandrayaan-3 is similar to the one developed for the Vikram lander on Chandryaan-2 mission. After QC clearance for further activity by TEG/SRA, SAC, the flight package of ChaSTE Front-End (FE) Electronics was delivered to SPL/VSSC, Trivandrum, for integration with the processing electronics, probe and deployment mechanism. After QC inspection and acceptance at SPL/VSSC, the ChaSTE FE FM card was first tested independently from laboratory power. The functionality test was done using 1K calibration resistors. The performance was found to be as expected. The FE FM card was then integrated to Processing Electronics card and DC-DC connector and functional verification tests in dis-assembled mode (Figure 45) followed by fully integrated/assembled mode were conducted which were found to be acceptable. The functionality of the FM card was successfully verified in terms of output voltage as a function of temperature. Stability of the output voltages was also monitored. Motors and Heater functionality was also successfully verified. The integrated electronics were also successfully tested for several switch on and off cycles. After successful completion of all qualification tests, ChaSTE electronics was further integrated to the probe and deployment mechanism all functional and qualification tests were carried out on the Flight payload before delivering it to URSC for integration with Chandrayaan-3 Lander and further clean room activities.

This work was done in collaboration with ChaSTE Team, SPL/VSSC

Figure 45: Dis-assembled mode functional test verification of Chandrayaan-3 ChaSTE FM electronics

(K. Durga Prasad, Chandan Kumar, S. Mishra, P. K. S. Reddy, T. Ladiya, A.Patel, M. Shanmugam, N. P. S. Mithun and Anil Bhardwaj)

Development of PRATHIMA instrument onboard ISRO-JAXA LUPEX Mission for scouting of Water-ice at a polar site on the Moon

The possibility of the presence of water ice deposits in the polar regions of the moon has drawn a lot of attention in the recent past and continues to be of great interest. Evidences for the existence of water/ice on the moon provided by various missions require to be further augmented by confirmative in-situ measurements. Although the observations carried out so far gave a clear indication of lunar water/ice, in-situ investigations are necessary not only to understand its nature, distribution and process of formation/accumulation but also for its quantification for future in-situ resource utilisation. Presence, distribution and quantification of water-ice can be done by means of in-situ dielectric measurements of the lunar surface and subsurface. To accomplish these objectives, an experiment called Permittivity and Thermophysical Instrument for Moons Aquatic Scout (PRATHIMA) has been proposed and selected to be flown on ISRO-JAXA LUPEX (Lunar Polar Exploration) mission. The main objective of the proposed experiment is in-situ detection and quantification of water-ice mixed with lunar surface and sub-surface soil using a rover and lander platform. The proposed experiment will contain three parts: a permittivity probe (to be inserted into lunar surface) that will be deployed into $\sim$30 cm of the lunar surface, an electronics box

(on rover/ lander) and a deployment mechanism. PRATHIMA instrument uses the technique of dielectric permittivity for detection and quantification of water-ice in the lunar soil. Dielectric permittivity is an electrical property that has a unique signature for water-ice, particularly at low frequencies, that allows unambiguous identification of its presence among other materials, even when present in low quantities. As shown in the Figure 46, PRATHIMA probe contains a set of electrodes for measurement of in-situ dielectric permittivity and a series of temperature sensors. The probe will be initially kept in a stowed condition on a rover during flight. After landing on the lunar surface, the probe will be deployed to ∼30 cm into the lunar soil through a deployment mechanism. The probe will be connected to the probe electronics (on lander/rover) through harness. Using the set of transmitter and receiver electrodes on the probe, a sinusoidal current is injected into lunar soil and the resultant potential difference between two potential electrodes is measured. Design verification models of the probe and electronics have been realized and tested (Figure 47).

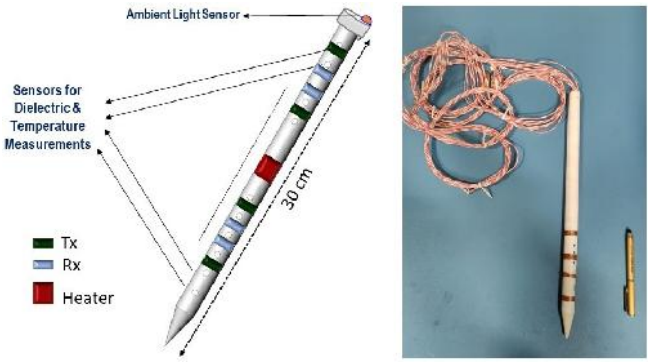

Figure 46: Schematic of PRATHIMA Probe and fabricated prototype probe

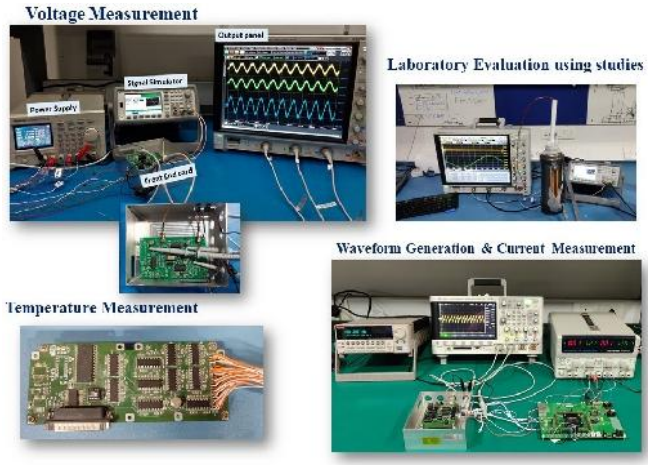

Figure 47: Design Verification model evaluation of PRATHIMA Electronics

(K. Durga Prasad, Chandan Kumar, S. K. Mishra, P. K. S. Reddy, Janmejay Kumar, T. Ladiya, N. Srivastava, M. Bhatt, M. Shanmugam, V. Sheel and Anil Bhardwaj)

Multi-purpose experimental setup for reflectance spectroscopic studies of planetary analogue soils and ices under simulated environment

We are in the process of setting up a versatile simulation planetary environmental test chamber (PETC) that operates under representative planetary surface conditions. One of the several objectives of this project is to setup a multi-purpose facility to carryout reflectance spectroscopic studies in the range UV-VIS-NIR of analogous soil and ice samples under representative environments of the Moon and Mars. As a first step, we tested the VIS-NIR spectrometers to study planetary analog samples. We considered powdered samples of different grain sizes from Sittampundi Anorthosite and basalts collected from Kutch. The test setup is shown in Figure 48. The reflectance spectra in the NIR wavelength range are shown in right pane of Figure 48. We found that the spectral characteristics of Kutch basalt matches to JSC-1A (mare) lunar analogues in general. Both the samples show spectral signature typical of a basalt with prominent 1 μ m absorption feature. However, deviation in the spectral shape below 1.1 μm is observed which will be further studied in detail by varying the grain sizes and by comparing them to Apollo returned samples. We also measured reflectance spectra of Anorthosite collected from Kutch with the Sittampundi Anorthosite. The absorption feature at 1.42 μm is common for both the sets of Anorthosites indicative of high plagioclase content. Both the reflectance spectra show high albedo. Further systematic studies under simulated Moon and Mars environments are underway.

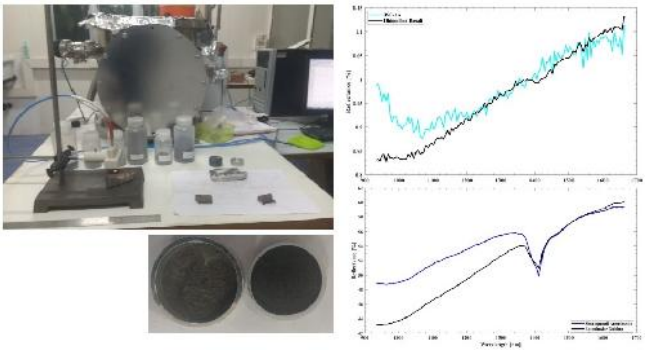

Figure 48: Experiment test setup for reflectance measurements outside vacuum chamber. The powdered samples can also be seen in the picture. Plots show reflectance spectra of lunar analog basalts and anorthosites obtained from the setup

(M. Bhatt, Janmejay Kumar, K. Durga Prasad)

Distinctive water-ice signature and its detection limit using permittivity technique for LUPEX PRATHIMA Payload

Dielectric permittivity has a unique signature for water-ice that allows unambiguous identification of its presence among other materials, even when present in low quantities. We have carried out a well-controlled laboratory experiments to measure dielectric permittivity of uniformly mixed lunar analogous soil and water-ice. The basic aim of the experiment was to arrive at the minimum detectable content of water-ice mixed with the soil that can be inferred from

observing the variation in the bulk dielectric permittivity. Terrestrial anorthosite (from Sittampundi, TN, India), a representative of lunar highland soil, is used for conducting the experiment. Custom-designed sensor having a two electrodes configuration is used to measure the bulk capacitance and thereby the dielectric permittivity of the soil sample. Around 0.5 kg of soil sample is taken, baked overnight and cooled in a desiccator. Initially, the dielectric permittivity of the dry sample is measured followed by which Milli-Q water is added in small (0.1 10 wt%) quantities, thoroughly mixed and frozen. Once completely frozen, the permittivity of the frozen soil is measured at different frequencies in a temperature/moisture controlled environment. The experiment is repeated for mixtures of different soil and water-ice percentage by weight. The variation of dielectric permittivity as a function of frequency for different water-ice and soil mixtures is obtained.

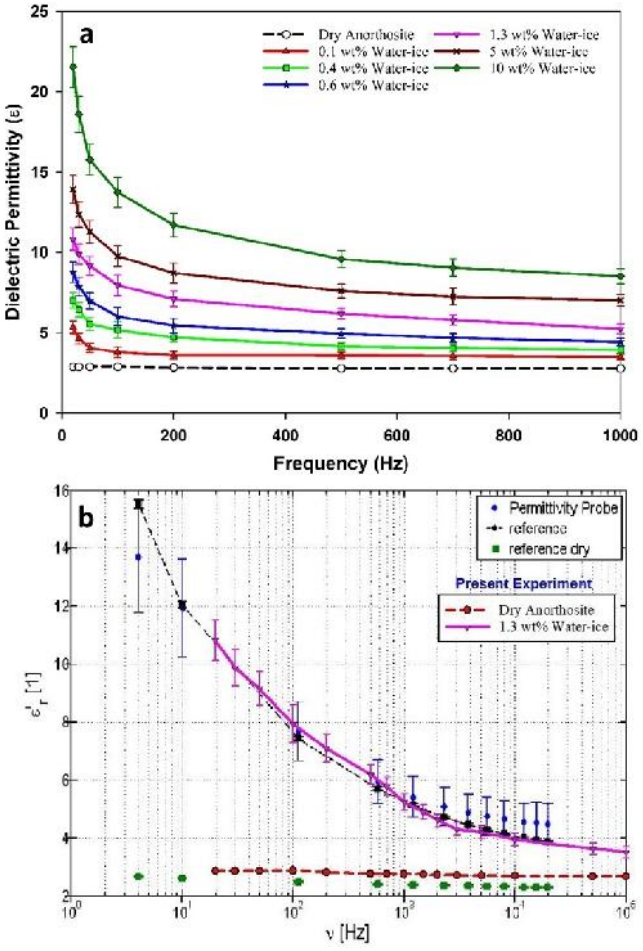

Figure 49: (a) Experimentally determined dielectric permittivity of various water-ice contents mixed with lunar analogous soil in the frequency range 0.1-1 KHz (b) Comparison of our experimental results (for 1.3 wt% water-ice mixed with soil sample) with published data. Pink curve shows the data for 1.3 wt% water-ice in sample and red plot is the data for dry sample obtained from our experiment.

Figure 49(a) shows the experimentally determined dielectric permittivity of various water-ice contents mixed with lunar analogous soil in the frequency range 0.1-1 KHz. It is evident from Figure 49 that the presence of water-ice (even in small quantities) shows a distinguishable variation in dielectric permittivity in comparison with that of a dry sample (black dotted-line). Experiments were also conducted with soil and different ice mixtures (water-ice and CO_2 ice) and the results are shown in Figure 50. A significant variation in the low frequency dielectric permittivity due to even a small quantity of water-ice can be seen. Figure 50 shows a comparison of the result obtained from the present experiment with that of a published data for 1.3 wt% water ice. A good agreement as seen in Figure 50 validates our experiment.

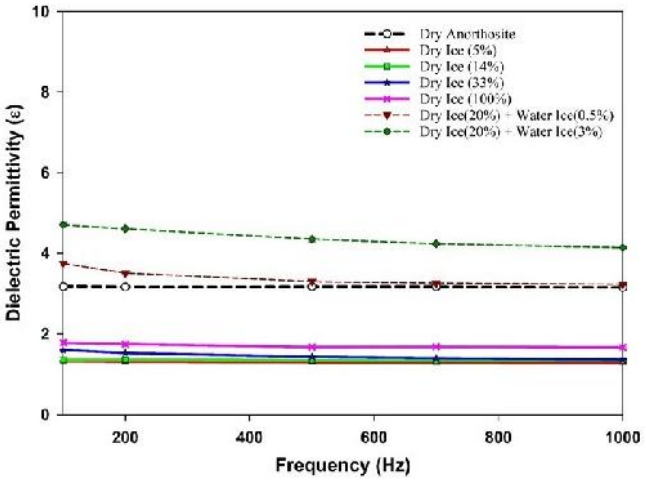

Figure 50: Plot showing experimentally derived permittivity signature of Water-ice in CO_2 ice + Soil mixture

(K. Durga Prasad, S. K. Mishra, Chandan Kumar, P. K. Reddy, Janmejay Kumar, V.Sheel and Anil Bhardwaj)

Innovative experimental setup for carrying out extended experimental studies of thermophysical properties on lunar analogue samples

The lunar simulation chamber developed and reported earlier has now been further upgraded to carry out science and engineering experiments on soil strata of ∼20 cm (Figure 51). With this enhancement, the chamber can now be used to measure thermophysical properties and their inter-dependence, on an analogous soil strata under simulated lunar environment. To account for radiative and conduction components in porous media, temperature dependent thermal conductivity and specific heat to be considered in all numerical studies. Current understanding from Apollo data suggest that these parameters are not constant and are inter-dependent. However, no systematic measurements exist. Therefore, we have devised an innovative experimental setup to carry out experiments to determine thermophysical properties of lunar analogues (under simulated lunar conditions as a function of multiple parameters and systematically understand their inter-dependence. Several experiments were conducted using terrestrial analogues of lunar basalt and anorthosite rocks. The experiments were conducted on powdered samples of various grain sizes prepared out of these rocks. Experiments were conducted at different pressure/vacuum levels from atmosphere to $\sim$1x10^{-5} Torr. Temperature profile, thermal diffusivity and thermal conductivity were obtained from the experimental data to study the dependence of thermophysical behaviour on vacuum and the role of interstitial gases/fluids. Under

high vacuum conditions ($>10^{-3}$ Torr), the heat flow was extremely sluggish while the same happened to be dominant in the case of ambient/low vacuum conditions. Under vacuum conditions, grain size had a direct dependence on the heat flow where smaller grain size exhibiting more heat flow and vice-versa. Results also indicate a significant dependence of thermal conductivity on temperature of the sample and becomes more prominent as the pressure decreases. Such data forms an invaluable input for estimation of realistic thermophysical behaviour/heat flow of the Moon. This is also essential in interpreting the post-flight data received from ChaSTE experiment of Chandrayaan-3.

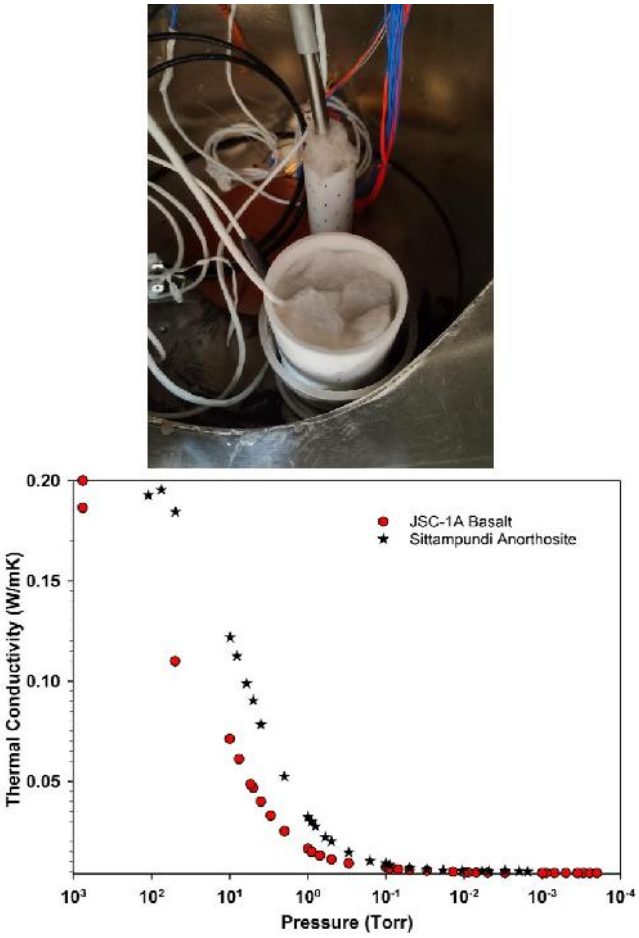

Figure 51: Experimetal setup and plot showing the dependence of vacuum and role of interstitial poregases on the thermal conductivity of lunar analogues

(K. Durga Prasad, P. K. Reddy and Janmejay Kumar)

Development of a SDD based Large Area X-ray Spectrometer with ASIC readout for future planetary mission

Silicon detector-based X-ray spectroscopy has been employed for applications varying from solar studies, XRF experiments, X-ray imaging to various astronomical observations. We have already developed a single-channel X-ray spectrometer with discrete components- Solar X-ray Monitor, flown on Chandrayaan-2 orbiter. We propose developing a multi-detector large area X-ray spectrometer using Silicon Drift Detectors (SDD) for future space and astronomical observations. Use of discrete components will lead to a bulky system and hence miniaturized system is desirable for space applications. In this direction, we propose to develop the spectrometer using Application Specific Integrated Circuit (ASIC) based readout which can process the signal from multiple detectors simultaneously. In this application, we use VERDI ASIC which can process the signal from 8 detector and allows us to have required numbers of detectors for the given applications. It is planned to use each SDD with 150 mm^2 area.

VERDI ASIC is 3.5 mm x 3.5 mm with multi-channel readout electronics from 8 independent analog inputs from an external charge-sensitive preamplifier. Each channel has a preamplifier, a shaper with adjustable shaping times from 0.25 μs to 8 μs, a peak stretcher with a stable baseline holder for leakage current of 0.1 pA to 11 nA. The system enables to stack multiple SDD modules in a compact assembly with excellent energy resolution in the range of 500 eV to 15 keV with fast readout (Figure 52). We have characterized the ASIC using different signals, replicating the detector, to understand the effect of various parameters such as channel threshold, shaping time, and dynamic range of the ASIC. With the ASIC based readout, we have achieved a resolution of 136 eV @ 5.9 KeV for the detector operating temperature of $\sim$ -35°C at an optimum shaping time of 2 μs (Figure 53). This translates to a system noise of $\sim$8 electrons at 2 μs shaping time and varies up to 43 electrons at 0.25 μs shaping time.

Figure 52: Experimental Setup

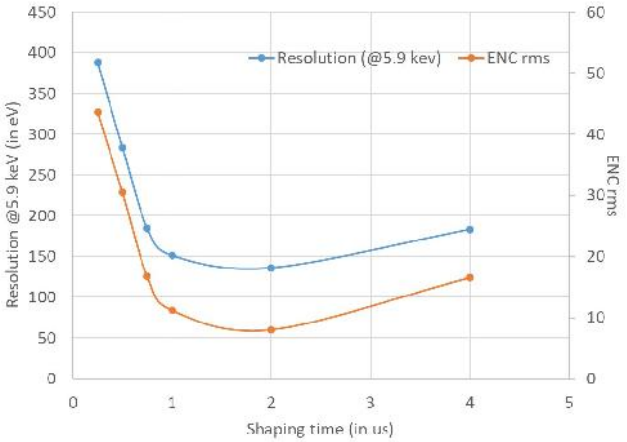

Figure 53: Variation in resolution and ENC with shaping time

(N. Singh, M. Shanmugam, A. Patel, T. Ladiya, and S. Vadawale)

Design and development of new sample chamber for noble gas mass spectrometer

New copper holder with blind holes is designed and developed inhouse for facilitating loading of various samples, as shown in Figure 54. The new holder has holes 6.1 mm in diameter and depth 5 mm. This allows to load multiple grains in one slot and single chips of diameter abound 6 mm. The sample holder consists of 27 locations for loading the samples at a time. The typical sample weight can be sub milligram to 10 mg. The new sample holder is tested for blank contributions in the vacuum system, which are low and this configuration found suitable for noble gas measurements using laser microprobe.

Figure 54: Sample chamber for Laser microprobe

(Avadh Kumar and R. R. Mahajan)

Design and development of the Catalogue of extra-terrestrial samples at PRL Repository

Extra-terrestrial samples are important proxies for understanding origin and evolution of solar system. The detailed chemical and isotopic sample studies are essential for complementing the remote and in-situ mission data and vice-versa. The extra-terrestrial samples include returned samples and meteorites. This requires to develop a catalogue of the samples under study at PRL. This will help to design new experiments for future scientific requirements. A new catalogue is designed for providing updated information about the extra-terrestrial samples, front page Figure 55. All previous results and new projections are documented.

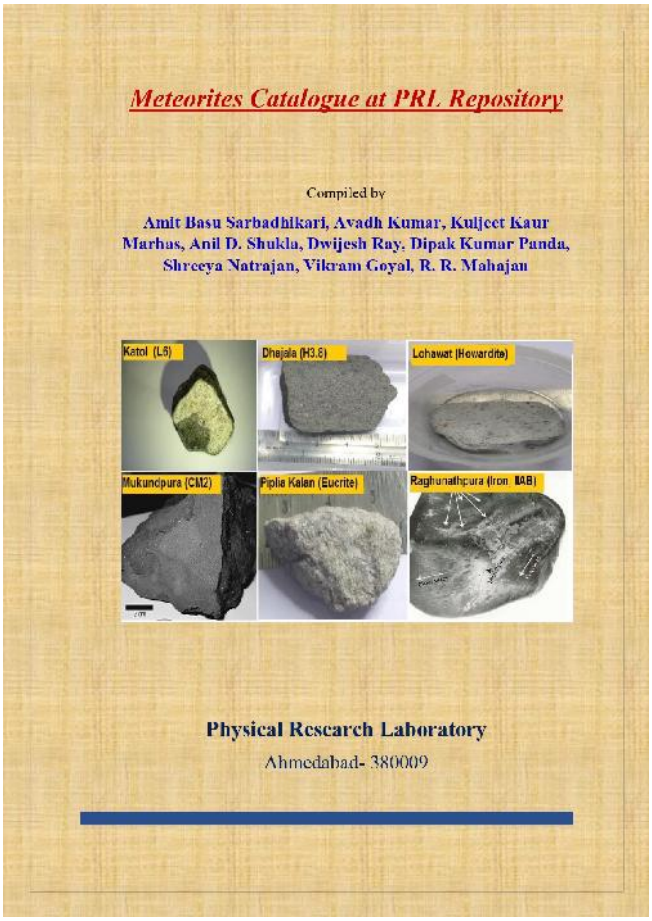

Figure 55: Meteorite catalogue

(A. B. Sarbadhikari, Avadh Kumar, K. K. Marhas, A. D. Shukla, D. Ray, D. K. Panda, S. Natrajan, V. Goyal and R. R. Mahajan)

Radio Occultation (RO) Experiment

The radio science experiment provides atmospheric profiles from the retrieved parameters of the signal, received at ground station, in the transmitting mode. While is receiver mode, the signal is received at the satellite and processed on board. A double heterodyne RO

receiver was designed and tested at PRL, whose block diagram is shown in Figure 56. An RF signal is received by the antenna and mixed with a local oscillator signal in the first down conversion stage. The local signal is generated from a stable source to maintain the required level of stability. The first intermediate frequency signal is then again down converted in the second stage to obtain in-phase (I) and quadrature (Q) signals. The second local oscillator frequency is used for this purpose. For the other option, an RO transmitter was designed and tested, which is depicted in the block diagram in Figure 57. The transmitter consists of a chain of multipliers and band pass filters to obtain the necessary frequency from a stable oscillator source. Both the receiver and transmitter were tested and found working satisfactorily. Further, based on optimization, the transmitter option is selected for future Mars orbiter mission. Figure 58 shows the testing set up for the receiver (top) and also the results of transmitter (bottom).

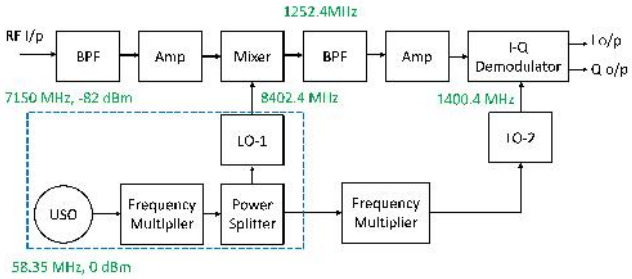

Figure 56: Design diagram of double heterodyne RO receiver for future Mars orbiter mission.

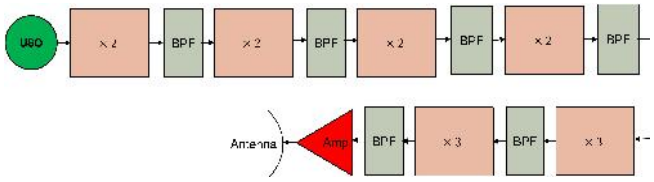

Figure 57: Design diagram of multiplier-based RO transmitter for future Mars orbiter mission.

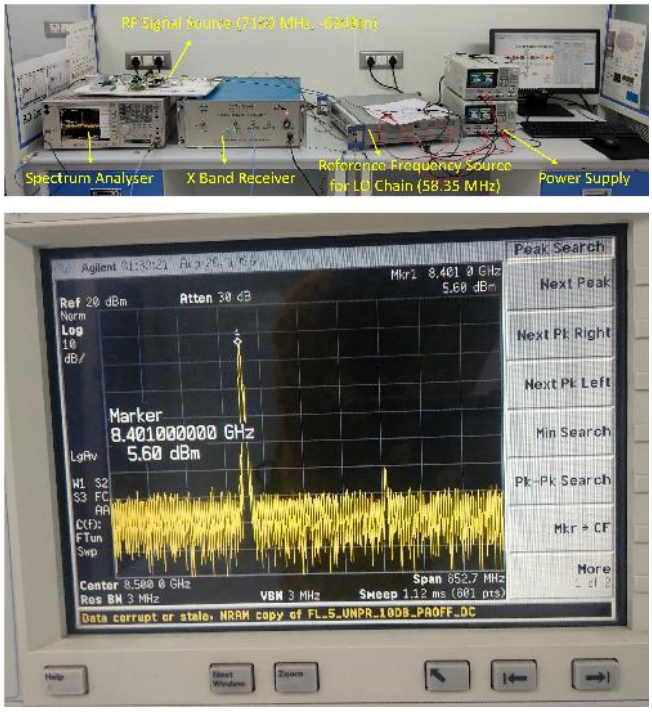

Figure 58: Experimental set up to test the microwave receiver (top) and testing results of transmitter.

(J. P. Pabari, V. Sheel, S. Jitarwal, S. Nambiar, Rashmi, S. A. Haider and Team)

Space and Atmospheric Sciences

Black carbon aerosols over a source and a background region: Atmospheric boundary layer influence, potential source regions, and model comparison

Black carbon (BC) aerosols measured simultaneously over a source (Ahmedabad, urban) and background (Gurushikhar, high-altitude) region are analysed. The influence of atmospheric boundary layer (ABL), and potential source regions for BC were examined, and compared with model, for the first time. BC mass in Ahmedabad was significantly higher (2 to 5 times) than Gurushikhar. BC mass concentrations in Ahmedabad peak during morning and evening hours when ABL is shallow and anthropogenic emissions are high.

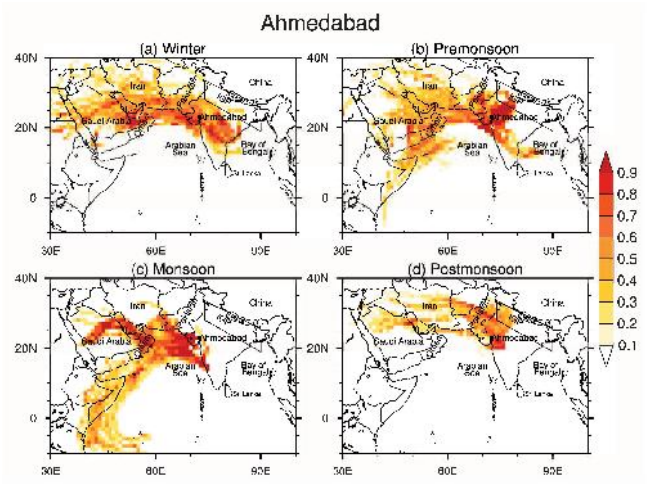

Figure no.1: Probable source regions for black carbon aerosols measured over Ahmedabad (urban location) deduced using Total Potential Source Contribution Function (TPSCF) analysis during (a) winter, (b) premonsoon, (c) monsoon and (d) postmonsoon.

In contrast over Gurushikhar BC emissions were higher in afternoon due to a fully evolved ABL and upward transport of pollutants from the valley/foothills during winter when Gurushikhar is within ABL. During other seasons the ABL is higher and diurnal variation is suppressed. BC_{max} over Gurushikhar is close to BC_{min} over Ahmedabad, which occurs during afternoon hours when ABL is fully evolved and anthropogenic sources are negligible over Ahmedabad while emissions get transported from foothills surrounding Gurushikhar. Potential source contribution function (PSCF) analysis reveals that probable source regions for BC in these two locations are distinctly different (Figures 1, 2), especially, during postmonsoon and winter, long range transport from northwestern India and the Indo-Gangetic Plain (IGP) are the probable source regions (agricultural waste and biomass burning) to the BC over the high-altitude location. Regional transport of BC emitted from urban areas of Ahmedabad to high-altitude Gurushikhar is evident in premonsoon from PSCF analysis (Figures 1, 2).

Observation-model comparison reveals that model significantly underestimates BC mass over Ahmedabad, whereas the agreement is good over Gurushikhar, suggesting a need to improve aerosol emission inventories. Such quantitative evaluation of BC aerosols over a source and a background region due to the influence of ABL, and potential source regions are hitherto unavailable over tropics which can be used to improve the representation of aerosols in models and thereby estimates of radiative and climate effects due to aerosols.

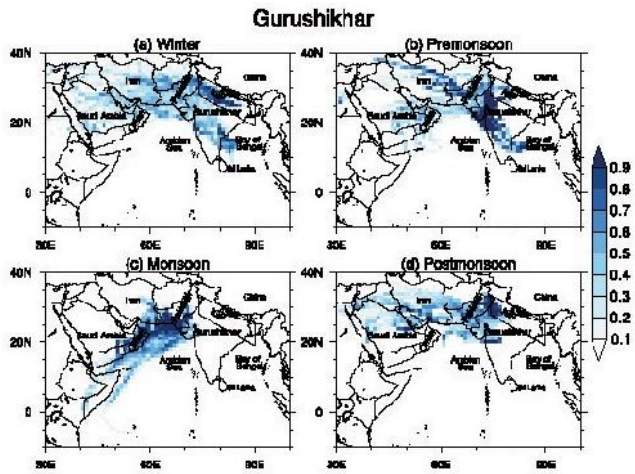

Figure no. 2: Probable source regions derived from TPSCF analysis for the BC mass concentrations measured over the high-altitude Gurushikhar (background location) for (a) winter, (b) premonsoon, (c) monsoon and (d) postmonsoon.

This work was done in collaboration with Ribu Cherian, University of Leipzig, Leipzig, Germany.

doi : https://doi.org/10.1016/j.atmosres.2021.105573

(S. Ramachandran, and T. A. Rajesh)

Black carbon aerosols: Relative source strengths of vehicular emissions and residential/open wood burning over an urban and a semi-urban environment

A comprehensive year-round investigation of black carbon (BC) mass concentration was conducted over an urban (Ahmedabad) and an adjoining semi-urban (Anand) environment using multi-wavelength aethalometer, with an objective to quantify the relative source strengths of vehicular and residential emissions, for the first time. The contributions of fossil fuel (BC_{ff}) and wood burning (BC_{wb}) emissions to total BC were quantified using the aethalometer model. The spectral properties of BC were obtained from the burning experiments conducted for different types of wood fuels used in the region. The absorption Ångström exponent (α_{wb}) values varied in the 1.67 to 2.18 range for different wood fuels (Figure 3).

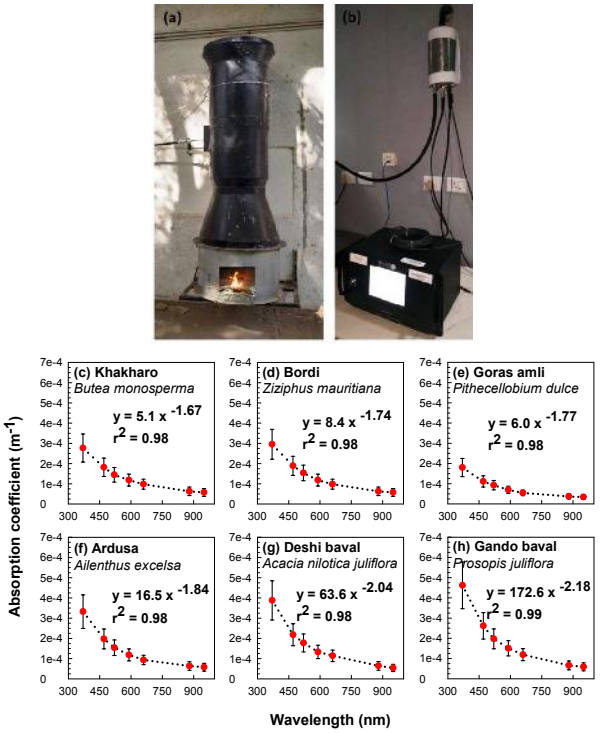

Figure no. 3: PRL aerosol chamber experiment (PACE) setup used to measure the equivalent black carbon aerosols produced by burning different wood fuels (a) chamber setup and (b) manifold with aethalometer AE33. Spectral variation of aerosol absorption coefficient (m^{-1}) obtained for different wood fuels (c-h) that are used for domestic burning in the study region. Vertical bars indicate $\pm 1\sigma$ variation from the mean obtained from 06 datasets. Botanical names of different wood fuels are listed (in italics in brown) in each figure.

The mean α_{wb} for wood burning emerged to be 1.87, lower than the commonly used value of 2.0. The lower α_{wb} contributes to a 14% decrease in the contribution of BC_{wb} to total BC. The BC_{ff} (86%) dominates the total BC throughout the year over Ahmedabad, whereas the contributions of BC_{ff} (55%) and BC_{wb} (45%) to total BC were comparable over Anand. The study highlights the observed heterogeneity in BC emission sources over an urban and an adjoining semi-urban environment with comparable total BC mass concentrations. The application of region specific α_{wb} and the resulting apportionment data will be useful in planning mitigation strategies, and for planning future policies on air quality improvement.

doi : https://doi.org/10.1016/j.apr.2021.101060

(T. A. Rajesh, S. Ramachandran and Vishnu K. Dhaker)

Recent aerosol trends over Asia analyzed from observations and model simulations

Aerosols continue to contribute the largest uncertainty in climate change. Over Asia, a global aerosol hotspot, spatial patterns of aerosol emissions are changing mainly because of changes in anthropogenic emissions, producing a dipole in atmospheric aerosol loading between East (decrease in emissions) and South Asia (increase in emissions).

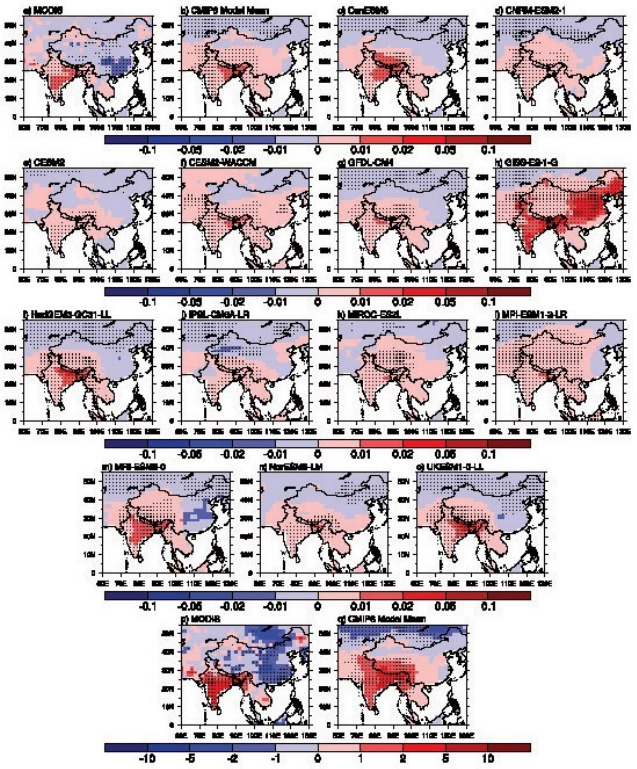

Figure no. 4 : Trends in aerosol optical depth (AOD) over South Asia and East Asia: Linear trends between 2002 and 2018 for the Asian region ($year^{-1}$) for AOD at 0.55 μm (a) in satellite observations (MODIS), (b) multi-model mean of CMIP6 model simulations, and the trends obtained for each model in CMIP6, in particular for (c) CanESM5, (d) CMRM-ESM2-1, (e) CESM2, (f) CESM2-WACCM, (g) GFDL-CM4, (h) GISS-E2-1-G, (i) HadGEM3-GC31-LL, (j) IPSI-CM6A-IR, (k) MIROC-ES2L, (l) MPI-ESM1-2-LR, (m) MRI-ESM2-0, (n) NorESM2-LM and (o) UKESM1-0-LL. Black dots correspond to points where the trend is significant at the 95% confidence level.

The resultant aerosol radiative effects are expected to be different as compared to the last decades of the 20^{th} century because of this emerging Asian aerosol dipole. The projection and assessments of radiative and climate impacts of aerosols rely on simulating accurately the aerosol properties, thus, making it imperative that current climate models involved in climate assessments including the Intergovernmental Panel on Climate Change Assessment (IPCC) Report, simulate well the magnitude and trends in changing aerosol properties. For the first time, we analyzed satellite and ground-based observations, and simulations from climate models in

Coupled Model Intercomparison Project Phase 6 (CMIP6) experiment with state-of-the-art treatment of aerosol chemistry, physics and meteorology. The results revealed large inter-model differences in model estimates, and discrepancies between model simulations and observations as most models are not able to capture the recent observed magnitudes and trends in aerosol optical depth (AOD) (Figure 4) and single scattering albedo (SSA) (Figure 5) over Asia.

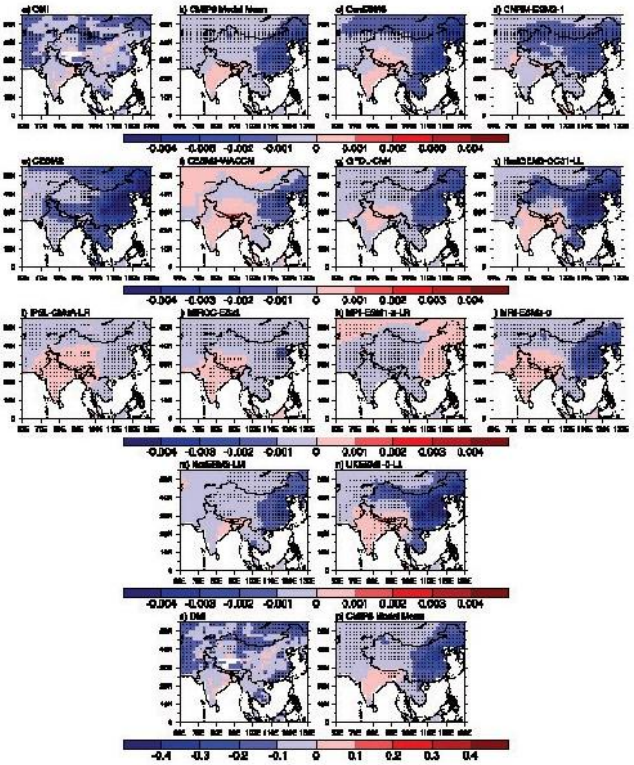

Figure 5: Trends in single scattering albedo (SSA) over South and East Asia: Linear trends between 2005 and 2018 for the Asian region (year^{-1}) for SSA (a) in satellite observations (OMI), (b) multi-model mean of CMIP6 model simulations, and in each CMIP6 model the outputs of which are used in the study, namely, (c) CanESM5, (d) CMRM-ESM2-1, (e) CESM2, (f) CESM2-WACCM, (g) GFDL-CM4, (h) HadGEM3-GC31-LL, (i) IPSI-CM6A-IR, (j) MIROC-ES2L, (k) MPI-ESM1-2-LR, (l) MRI-ESM2-0, (m) NorESM2-LM and (n) UKESM1-0-LL. OMI SSA corresponds to 0.388 μm and multi-model mean SSA corresponds to 0.55 μm. Black dots correspond to points where the trend is significant at the 95% confidence level.

The absolute trends (positive and/or negative) in AOD are significantly higher than the trends in SSA (Figures 4, 5). The aerosol-induced effective radiative forcing within the atmosphere simulated with three CMIP6 models show a positive (increasing) trend over Asia. A positive trend in atmospheric heating in model simulations is consistent with model simulated trends in AOD (positive) and SSA (negative) (Figure 6).

These results on model-observations comparison need to be taken into account while examining projected/expected future climate impacts due to aerosols, and potential value of various mitigation measures, in particular on regional and decadal climate change in Asia which is largely uncertain.

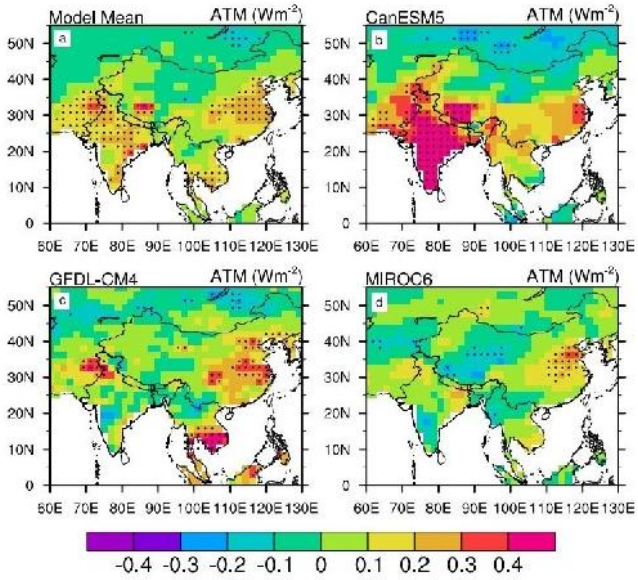

Figure no.6: Trends in aerosol radiative forcing over South and East Asia: Linear trend of aerosol-induced effective radiative forcing (ERF, Wm^{-2}) in the atmosphere (ATM) (ERF$_{\mathrm{ATM}}$) (= ERF at the top of the atmosphere ERF at the surface) over the Asian region (year^{-1}) between 2002 and 2018 in (a) multi-model mean of CMIP6 model simulations, (b) CanESM5, (c) GFDL-CM4 and (d) MIROC6. Black dots correspond to points where the trend is significant at the 95% confidence level.

This work was done in collaboration with Maheswar Rupakheti, Institute for Advanced Sustainability Studies, Potsdam, Germany, and with Ribu Cherian, University of Leipzig, Leipzig, Germany.

doi : https://doi.org/10.1016/j.scitotenv.2021.150756

(S. Ramachandran)

Climate benefits of cleaner energy transitions in East and South Asia through the reduction of black carbon aerosols

The state of air pollution has historically been tightly linked to how we produce and use energy. Air pollutant emissions over Asia are now changing rapidly due to cleaner energy transitions, however, magnitudes of benefits for climate and air quality remain poorly quantified. The associated risks involve adverse health impacts, reduced agricultural yields, reduced freshwater availability, contributions to climate change, and economic costs. We focus particularly on climate benefits of energy transitions by making firsttime use of two decades of high quality observations of atmospheric loading of light-absorbing black carbon (BC) over Kanpur (South Asia) and Beijing (East Asia), and relating these observations to changing energy, emissions and economic trends in India and China. Our analysis revealed that absorption aerosol optical depth (AAOD) due to BC has decreased substantially, by 40% over Kanpur and 60% over Beijing between 2001 and 2017, and thus became decoupled from regional economic growth (Figure 7).

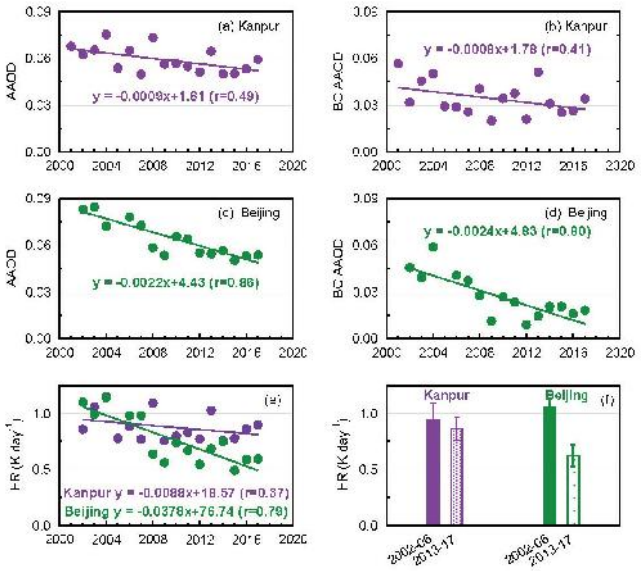

Figure no.7: Aerosol absorption and atmospheric heating rate induced by aerosols over Kanpur and Beijing during 2002-2017: Annual-mean absorption aerosol optical depth (AAOD) and black carbon absorption aerosol optical depth (BC AAOD) over (a, b) Kanpur in the Indo-Gangetic Plain (IGP) and (c, d) Beijing in the North China Plain (NCP), and (e) annual mean atmospheric heating rate due to aerosols (HR) over Kanpur and Beijing during 2002-2017. The ρ-values at the 99% confidence level for 2002-17 period are (a) 0.05, (b) 0.10, (c) 0.00001, (d) 0.0004, and (e) 0.10 (Kanpur), 0.0007 (Beijing), respectively. (f) HR for Kanpur and Beijing averaged for the two 5-year periods of 2002-2006 and 2013-2017. Vertical bars indicate $\pm 1\sigma$ (standard deviation) from the mean.

The aerosol-induced heating rate (HR) averaged over the two periods (Figure 7) the first period represents the first 5-year period of the analysis (2002-2006) and the second period corresponds to the last 5-year period of the analysis (2013-2017), which was done to quantify the change in HR due to BC reduction on a half-decadal scale in a more robust and quantitative manner. The 5-year period was selected so that the effect of interannual variations is smoothened out. Also, the year 2013 marks the beginning of the implementation of Clean Air Action Plan in China. The HR averaged over the periods 2002-2006 and 2013-2017 decreases from 1.05 to 0.62 K day^{-1} over Beijing, and from 0.94 to 0.86 K day^{-1} over Kanpur, i.e., a decrease of 41% over Beijing versus only 9% over Kanpur. Our observation-based results clearly provide evidence for the de-coupled trend between cleaner energy transitions and aerosol-induced atmospheric heating over India and China (Figure 8), as opposed to the more typical coupling between increasing energy use, economic growth, and CO_2 emissions. Further, the resultant decrease in BC emissions and BC AAOD over Asia is regionally coherent and occurs primarily due to transitions into cleaner energies (both renewables and fossil fuels), and not due to decrease in primary energy supply or decrease in use of fossil use and biofuels and waste (Figure 8). Model simulations show that BC aerosols alone contribute about half of the surface temperature change (warming) of the total forcing due to greenhouse gases, natural and internal variability, and aerosols), thus clearly revealing the climate benefits due to a reduction in BC emissions, which would significantly reduce global warming. However, this modelling study excludes responses from natural variability, circulation, and sea ice responses, which cause relatively strong temperature fluctuations that may mask signals from BC aerosols. Our findings show additional benefits for climate (beyond benefits of CO_2 reduction), and for several other issues of sustainability over South and East Asia, provide motivation for ongoing cleaner energy production and consumption transitions, especially when they are associated with reduced emissions of air pollutants. Such an analysis connecting the trends in energy transitions and aerosol absorption loading, unavailable so far, is crucial for simulating the aerosol climate impacts over Asia which is quite uncertain.

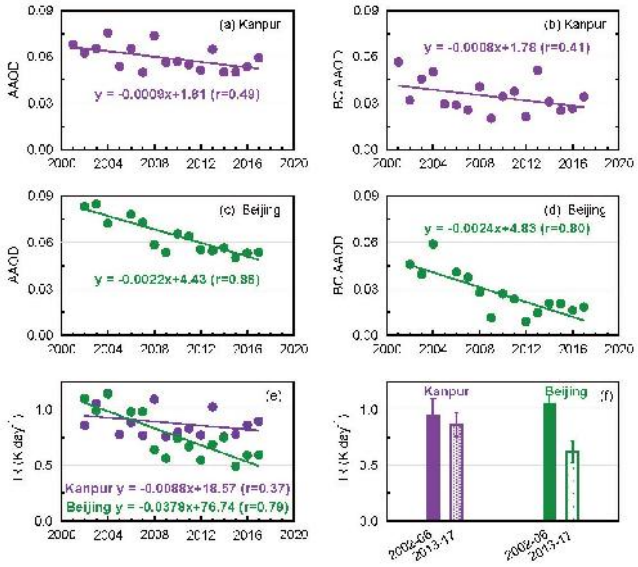

Figure no.8: Annual primary energy supply (PES), gross domestic product (GDP), and CO2 and BC emissions for India and China during 2000-2017: PES (in megatons oil-equivalent (Mtoe)) from different sources (a, b) and their total (sum of all PES from different sources shown in figures a and b) (c) for India and from different sources (d, e) and their total (sum of all PES sources drawn in figures d and e) (f) for China, along with GDP, and CO_2 and BC emissions for (g) India and (h) China.

This work was done in collaboration with Maheswar Rupakheti and Mark Lawrence, Institute for Advanced Sustainability Studies, Potsdam, Germany, and with Ribu Cherian, University of Leipzig, Leipzig, Germany.

doi : https://doi.org/10.3389/fenvs.2022.842319

(S. Ramachandran)

Biomass Burning and Impacts on Aerosols: Optical properties and Radiative effects

Biomass burning emissions from forest fires and agricultural residue burning can influence the physical and chemical properties of aerosols, air quality and climate. The influence of biomass burning on aerosol characteristics and radiative forcing are investigated over three locations in south (Kanpur and Gandhi College) and south east Asia (Singapore) which are influenced by biomass burning emissions. Kanpur and Gandhi College are influenced by agro-residue burning (manmade) emissions and Singapore is influenced by emissions from forest and peat fires (natural). Spectral aerosol optical depths (AODs) are higher over Kanpur and Gandhi College, and single scattering albedo (SSA) values are lower confirming an increase

in the abundance of absorbing aerosols due to biomass burning. In Singapore aerosol optical depths do not vary much, however, single scattering albedo values are lower. In all the locations the mid-visible AODs are greater than 0.3 during normal and biomass burning influenced scenarios indicating that all the sites are highly polluted. SSA in Singapore is higher than that of Kanpur and Gandhi College suggesting that the amount of scattering aerosols in the size distribution is higher. The Angstrom wavelength exponent is lower for Kanpur and Gandhi College when aerosols are influenced by biomass burning emissions and transport of mineral dust (pre-monsoon), while the values are the same for Singapore, suggesting that aerosols in fine mode always dominate the atmosphere of Singapore as it is an urban station. Analysis of aerosol types revealed that aerosols over Kanpur and Gandhi College originate from biomass burning, urban/industrial and dust emissions, while in Singapore the emissions were dominated more by urban/industrial and biomass burning sources. The aerosol radiative forcing at the surface (SFC), and in the atmosphere (ATM) is significantly higher ($\sim$25 Wm^{-2}) when aerosol characteristics are influenced by biomass burning over Kanpur and Gandhi College. In Singapore the aerosol radiative forcing is higher during non-biomass burning period which could be due to less significant variations in SSA. The aerosol radiative forcing efficiency (aerosol radiative forcing per unit AOD) at the surface and in the atmosphere are also higher. The radiative forcing and efficiency in the atmosphere are significantly higher (at least by about 25 Wm^{-2}) when compared to other locations in Asia. The high forcing values suggest that the biomass burning aerosols in this region could be a major contributor to the global mean aerosol radiative forcing. The results remained the same for low and high fire count scenarios suggesting that the properties of aerosols and their radiative effects are governed more by the variations in the sources of aerosol emissions resulting in variations in their composition (chemical), and less by the amount of aerosol emissions (physical).

This work was done in collaboration with Priyadarshini B., Bennett University, Greater Noida, India.

doi : https://www.routledge.com/Biomass-Burning-in-South-and-Southeast-Asia-Impacts-on-the-Biosphere-Volum

(S. Ramachandran)

Photochemistry over a tropical urban environment in India: A model-based study

The photochemical processes over tropical Indian region has significant impact on the global atmospheric composition and climate. Nevertheless, studies remain lacking in this part of the world especially on the chemistry of radicals and organics. In this direction, we combined state-of-the-art measurements with the Master Mechanism model to simulate the air chemistry in the downwind of Ahmedabad. Model predicts a strong ozone build up ($\sim$115 ppbv) in the outflow from Ahmedabad before a gradual decline over downwind region. In addition, substantial amounts of secondary inorganics (e.g., nitric acid $\sim$17 ppbv) and organics (e.g., ketones $\sim$11 ppbv) are produced. The peak concentrations of the hydroxyl (OH) and hydroperoxyl (HO_2) radicals are estimated as 0.3 and 44 pptv, respectively. Simulated chemistry combined with air trajectories shows the transport of ozone-rich air towards the northern Indian Ocean (Figure 9), in agreement with observations and global model. While the volatile organic compounds are the major OH sink on day 1, the contribution of CO is greater on subsequent days (Figure 10). Our findings highlight the intense photochemistry in the downwind of urban environments in the tropical Indian region. More observations of organics and radicals covering also the remote oceanic regions are essential to further improve the understanding of air chemistry in the tropics.

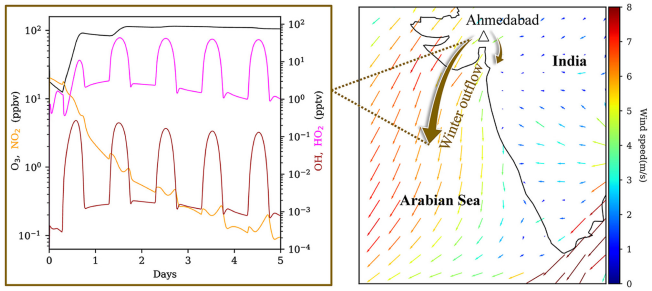

Figure no.9: Model simulated photochemical evolution of air in the downwind of Ahmedabad.

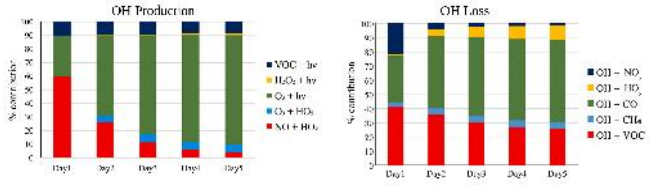

Figure no.10: The contributions of different reactions into noontime production and loss of OH.

This work is done in collaboration with Imran Girach of SPL, VSSC, Thiruvananthapuram, India.

doi : https://doi.org/10.1016/j.chemosphere.2022.134070

(Meghna Soni, Lokesh K. Sahu, and Narendra Ojha)

Exploring the potential of machine learning for simulations of urban ozone variability

Machine learning (ML) has emerged as a powerful modeling technique, nevertheless, its potential to simulate complex atmospheric chemistry remained largely unexplored. In this direction, we applied ML to simulate variations in urban ozone over Doon valley of the Himalaya. The model, trained with past variations in ozone and meteorology, successfully reproduced the independent ozone observations ($r^2\sim$0.7). The inclusion of precursors in the model further improved the performance and the outliers were also captured (Figure 11). The r^2 value is seen to increase from about 0.6 to 0.9 and RMSE shows reduction from11 to 6 ppbv with increase in the training data fraction. This highlights the need of long-term data from observations and validated chemistry-climate simulations to exploit the potential offered by ML approach. The series of simulations conducted here would serve as a reference for further applications of artificial

intelligence to complement conventional Earth system models. Future studies may extend the scope to additional climate-forcing pollutants and to unravel feedback between pollution and meteorology causing calamities in the fragile ecosystem of the Himalaya.

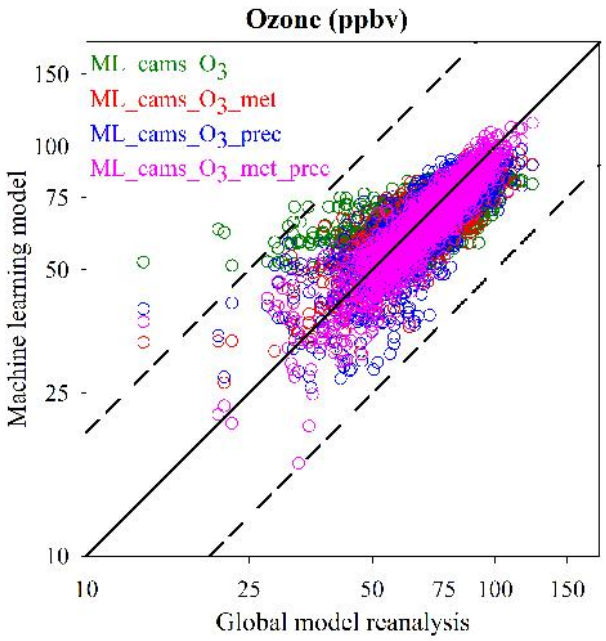

Figure no.11: Correlation between machine learning based simulations and result from a global model (CAMS reanalysis).

This work is done in collaboration with I. Girach of SPL VSSC Thiruvananthapuram, K. Sharma of Graphic Era Dehradun, A. Sharma of IIT Jodhpur, N. Singh of ARIES Nainital, and S. Gunthe of IIT Madras.

doi : https://doi.org/10.1038/s41598-021-01824-z

(Narendra Ojha)

Impact of COVID-19 Pandemic Lockdown in Ambient Concentrations of Aromatic Volatile Organic Compounds in a Metropolitan City of Western India

The real-time concentrations of Benzene, Toluene, Ethylbenzene, and Xylenes (BTEX) were measured in Ahmedabad city, India during January-May of 2020, and 2014-2015-2018 to assess the impact of emission reduction during the COVID-19 lockdown. The total BTEX (ΣBTEX) concentrations were 11.5 $\pm$ 9.0, 15.7 $\pm$ 16, 5.3 $\pm$ 5.0, 2.9 $\pm$ 2.0, and 0.93 $\pm$ 1.2 ppbv in January-May 2020, respectively. The evening rush hour peaks of BTEX during lockdown decreased by 4-5 times from the same period of years 2014-2015-2018. As shown in Figure 12, a significant decline in background concentrations suggests a regional-scale reduction in anthropogenic emissions. The contributions of ΣTEX compounds to ΣBTEX increased from 42% to 59% in winter to 64%$-$75% during the lockdown under hot summer conditions. While emission reductions dominated during the lockdown period, the meteorological and photochemical factors may also have contributed. Meteorological influence on actual observed BTEX data was removed by normalizing with ventilation coefficient (VC). The actual ambient air reductions of 85%-90% and VC-normalized reductions of 54%-88% of the BTEX concentrations during lockdown were estimated compared to those during the same period of 2014-2015-2018. The estimated changes using nighttime data, which take into account BTEX photooxidation removal, are $\sim$8% lower than the VC-normalized estimates using all data. These significant reductions in BTEX concentrations are consistent with the change in people's movement as inferred from mobility data during the lockdown. Although enforced, the significant decline in ambient BTEX levels during lockdown was a good change for the air quality. The study suggests a need for more effective science-based policies that consider local and regional factors.

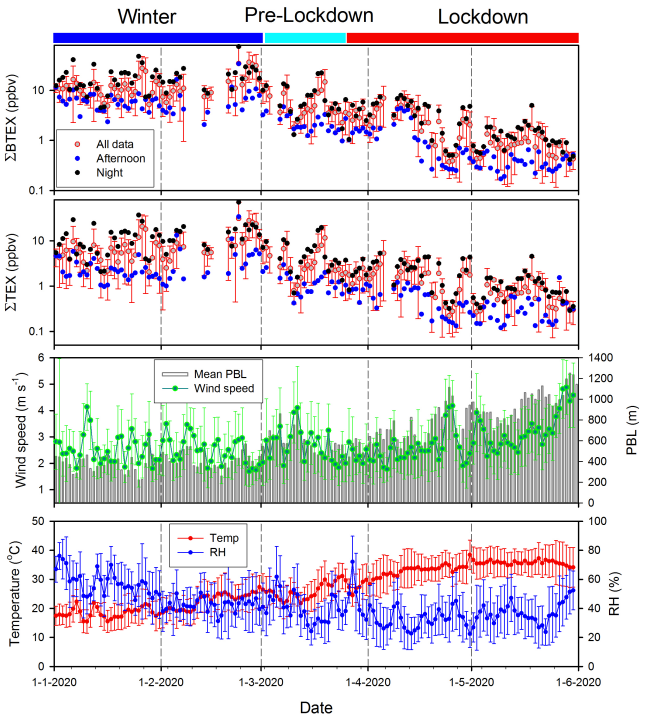

Figure no.12: The time series variations of the daily mean ($\pm 1\sigma$) (all data), afternoon, and night-time ambient air mixing ratios of ΣBTEX, ΣTEX, PBL and meteorological parameters at the urban site of Ahmedabad, India from 01 January to 31 May 2020.

This work is done in collaboration with Dr. Vikas Singh from National Atmospheric Research Laboratory (NARL), Gadanki and Dr. Ravi Yadav from Indian Institute of Tropical Meteorology (IITM), Pune.

doi : https://doi.org/10.1029/2022JD036628

(L. K. Sahu, Nidhi Tripathi, Mansi Gupta and Kashyap Patel)

Ambient air characteristics of biogenic volatile organic compounds at a tropical evergreen forest site in Central Western Ghats of India

Non-methane volatile organic compounds (NMVOCs) play key roles in local and regional atmospheric chemistry as precursors for the production of ozone and secondary organic aerosols. Plants are very sensitive to environmental conditions. They release a

wide range of volatile organic compounds (VOCs) in response to different biotic and abiotic stresses (Figure 13). Ambient air C_2-C_5 NMVOCs were measured at a tropical forest site in the central Western Ghats and urban site of Udaipur in India during the late monsoon period of 2016-17 and 2015, respectively. In the Western Ghats, air samples were collected from the protected Bhagwan Mahaveer Sanctuary. Ethene, propene, and isoprene were the dominant biogenic compounds with mean concentrations of 4.8$\pm$2, 1.6$\pm$0.66 and 1.05$\pm$0.43 ppb, respectively. The concentrations of anthropogenic compounds such as propane and pentane were significantly lower than those of light alkenes. The contributions of ethene and propene among different NMVOCs were $\sim$44 and 14%, respectively. However, the contributions of isoprene were highly variable of 3-22%. The tight correlation (r^2=0.90) between the mixing ratios of ethene and propene and their ratio indicates their common formation and emission mechanisms. The molar emission ratio of ethene/propene (2.9$\pm$0.17 ppb ppb^{-1}) was comparable to those measured at other biogenic sites of Asia while higher than those reported for mid-latitude sites. The concentrations of light alkenes and isoprene at the Western Ghats were 4-5 times higher than those measured in an urban environment in the same season. The higher ozone formation potentials and Propylene-Equivalent concentrations of alkenes and isoprene than those of other NMVOCs indicate important implications of biogenic emissions on ozone photochemistry in the forest regions of India.

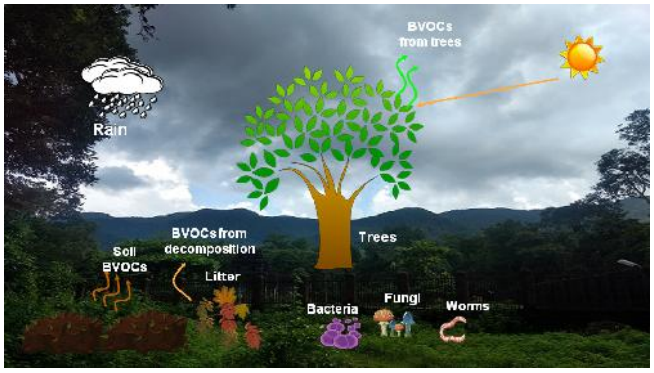

Figure no.13: Plant are very sensitive to environmental conditions. They release a wide range of biogenic volatile organic compounds (BVOCs) in response to different biotic and abiotic stresses.

This work is done in collaboration with Dr. Ashwini Kumar from CSIR-National Institute of Oceanography, Dona Paula, Goa and Dr. Ravi Yadav from Indian Institute of Tropical Meteorology (IITM), Pune.

doi : https://doi.org/10.1007/s10874-021-09415-y

(Nidhi Tripathi, L. K. Sahu and Kashyap Patel)

Vertical profiles of trace gases in the troposphere over South Asia

Most of the South Asia regions are experiencing prolonged air pollution episodes due to rapid urbanization and an unprecedented ever-increasing number of vehicles. The regulations to control ambient air pollutants over the Indian subcontinent involve understanding the complexities due to the vast geography, different climatic zones, and emissions from a variety of natural and anthropogenic sources.

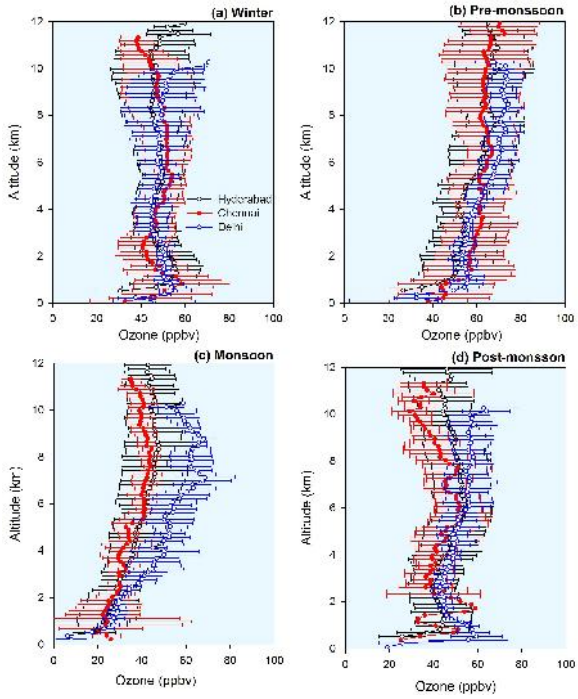

Figure no.14: The seasonal mean MOZAIC vertical profiles of ozone in the troposphere over Hyderabad, Chennai and New Delhi, India.

The ground-based in situ monitoring of various air pollutants provides detailed temporal features to assess the exposure related to human health. However, such ground-based measurements of pollutants remain applicable to address the local emissions and environmental issues but are important only as a supplementary for the regional projections. Therefore, a comprehensive plan must integrate the networks of both ground-based and vertical observations of various pollutants. Such programs will be particularly important over the South Asia region due to strong emissions of various pollutants and their transport and distribution in the downwind and remote regions. During the past decades, significant improvements and progress have been achieved in terms of the quality and spatiotemporal coverage related to the monitoring of various air pollutants over the South Asia region. However, among gaseous pollutants, information on vertical distributions of pollutants over the South Asia region remains limited and reported only for a few species but mainly of ozone (O_3) and carbon monoxide (CO). This study presents an overview of the studies reported on the tropospheric vertical profile measurements and model simulations of trace gases over the Indian subcontinent and surrounding oceanic regions. The combined study using balloon, aircraft, and remote sensing measurements of vertical distributions of O_3 (Figure 14) and CO provide important understanding on factors controlling their variations in the troposphere.

This work is done in collaboration Dr. P.R. Sinha from Indian Institute of Space Science Technology (IIST), Thiruvananthapuram, India.

doi : https://doi.org/10.1016/B978-0-12-816693-2.00009-3

(L. K. Sahu)

Passive Air Sampling of PCDD/Fs, PCBs, PAEs, DEHA, and PAHs from Informal Electronic Waste Recycling and Allied Sectors in Indian Megacities

Xenobiotic chemical emissions from the informal electronic waste recycling (EW) sector are emerging problem for developing countries, with scale and impacts that are yet to be evaluated. An intensive polyurethane foam disk passive air sampling was carried out in four mega-cities of India to investigate atmospheric organic pollutants. Intraurban emission sources were estimated and attributed by trajectory modeling and positive matrix factorization (PMF). EW contributed 45% of total polychlorinated biphenyls (PCB) concentrations. The dominance of dioxing-like PCBs (dl-PCBs) reflect combustion as the possible primary emission source. For both youth and adult, the highest estimated inhalation risks for dl-PCBs and plasticizers were seen at the EW transect in Bangalore, followed by Chennai and New Delhi.

This work was done in collaboration with Prof. Paromita Chakraborty of (SRM Research Institute and Department of Civil Engineering, SRM Institute of Science and Technology, Kancheepuram District, Tamil Nadu 603203, India) and others. doi : `https://doi.org/10.1021/acs.est.1c01460`

(Harish Gadhavi)

Metals in coarse ambient aerosol as markers for source apportionment and their health risk assessment over an eastern coastal urban atmosphere in India

Ambient PM_{10} (particulate matter with aerodynamic diameter $\leq$ 10 μm) samples were collected at Bhubaneswar, India for a period of one year and analysed for 19 different elements including heavy metals. Principal component analysis (PCA) revealed that crustal sources, industrial activities and vehicular emission were significant contributer. The predominant contribution of local/regional emission sources to the metallic components in coarse PM_{10} mass is evident from studies carried out using a Lagrangian Particle Dispersion Model (LPDM) FLEXPART, and also corroborated by the wind pattern polar plots. Further, carcinogenic and non-carcinogenic health risk assessments of the measured elements that find their way into the human body through different exposure pathways have been calculated using United State Environmental Protection Agency (USEPA) standards. The carcinogenic risk of most of the elements was insignificant.

This work was done in collaboration with Dr. Trupti Das of (Environment and Sustainability Department, CSIR-Institute of Minerals and Materials Technology, Bhubaneswar, 751013, India) and others. doi: `https://doi.org/10.1007/s10661-021-09057-3`

(Harish Gadhavi)

Effect of Lockdown on Pollutant Levels in the Delhi Megacity: Role of Local Emission Sources and Chemical Lifetimes

The COVID-19 pandemic resulted in changed emission regimes all over the world. India also imposed complete lockdown on all modes of travel and industrial activities for about 2 months from 25-March-2020 and later unlocked these activities in a phased manner. We studied signatures of emissions changes on levels of atmospheric trace gases and aerosols contributing to air pollution over multiple sites in Indias capital Delhi covering various lockdown and unlock phases using satellite data and in-situ observations. The resulting changes in the levels of these species were compared with respect to their average of 2015-2019 to attribute for year to year and seasonal changes. A clear impact of lockdown was observed for AOD (aerosol optical depth), PM (particulate matter), NO_2, CO, and SO_2 as a result of emission changes, while changed precursor levels led to an increase in O_3 because of changes in chemical regimes impacting its concentrations. A detailed analysis of FLEXPART trajectories revealed increased PM levels over Delhi in north-westerly air masses sourced to Punjab region all the way up to Pakistan. Changes in aerosols and NO_2 were not only restricted to the surface but transcended the total tropospheric column. While surface level aerosols and NO_2 showed significant and almost similar changes, AOD showed much lower decrease than tropospheric column NO_2. The tropospheric column NO_2 concentrations decreased by 56.9%, 53%, and 32.4% in April, May, and June, the AOD values decreased only by 25.3%, -22.5% and -7.1% with respect to the 5 years average. This could be due to the fact that loss of aerosols through deposition occurs near the Earths surface but NO_2 can be photochemically dissociated at higher heights too. Although biogenic emissions constitute a major source of CO, large changes in CO similar to other anthropogenic markers e.g., SO_2 indicate overwhelming anthropogenic components in Delhi.

This work was done in collaboration with Dr. Chinmay Mallik of (Department of Atmospheric Science, Central University of Rajasthan, Ajmer, India) and others. doi : `https://doi.org/10.3389/fenvs.2021.743894`

(Harish Gadhavi and Shyam Lal)

Chemical composition and radiative forcing of atmospheric aerosols over the high-altitude Western Himalayas of India

Atmospheric aerosols can travel to long distances and can act as short lived climate forcing agents in climatically sensitive zones such as Himalayas. However, very little information is available about types of aerosols and their impact in the Himalayas. Aerosol samples were collected from two sites in western Indian Himalayas which are Gangotri Glacier ($\sim$2600 m a.s.l) and Uttarkashi ($\sim$1400 m a.s.l) in two different seasons and analysed for their chemical composition. The chemical composition was used to model their optical properties and the optical properties used to estimate shortwave radiative forcing by aerosols over Himalayas. The clear-sky radiative forcing estimates varied from small (-0.1 W m^{-2}) negative radiative forcing to significant (+1.6 W m^{-2}) positive radiative forcing. The result indicate aerosol have potential to cause localised warming in Himalayas and to contribute melting of glaciers. A systematic monitoring of aerosols in Himalayas is essential.

This work was done in collaboration with Dr. Vijay Shridhar of (Environmental Pollution Assessment Laboratory, School of Environment and Natural Resources, Doon University, Dehradun, 248001, India) and others. doi : `https://doi.org/10.1007/s11356-021-15609-4`

(Harish Gadhavi)

Investigation of Atmospheric Boundary Layer characteristics using Ceilometer Lidar, COSMIC GPS RO satellite, Radiosonde and ERA-5 reanalysis dataset over Western Indian Region

The Atmospheric Boundary Layer (ABL) is the lowermost layer of the atmosphere in contact with the Earths surface. ABL is very crucial as it helps in the exchange of heat and momentum from the surface to the free atmosphere and vice versa, and helps in vertical mixing of the near-surface pollutants. In this study, the ABL characteristics have been investigated using a Ceilometer Lidar over Ahmedabad, a semi-arid urban region in western India. Strong diurnal variations of the ABL have been observed during 2019, the observation period. There is a stark winter-summer difference in ABL, with summer Boundary Layer Height (BLH) exceeding winter BLH by 1-1.5 km.

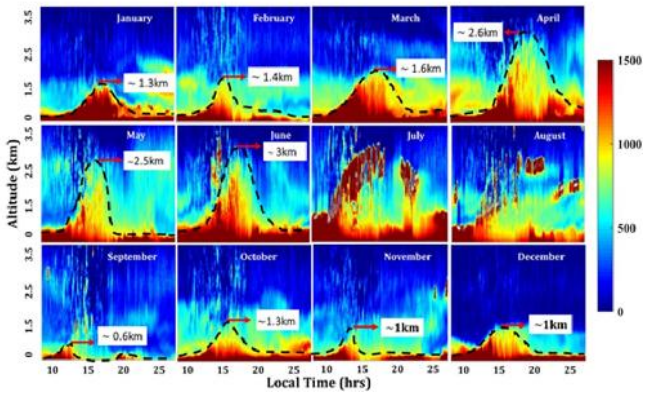

Figure no.15: Monthly variations of Atmospheric Boundary Layer (ABL) over a Western Indian station, Ahmedabad during 2019.

ABL has been found to collapse during monsoon and is often equivocal due to the presence of thick clouds on top of ABL. The ABL is thicker during the onset of monsoon in contrast to active monsoon, rises again during the withdrawal of monsoon. Ground lidar observed ABL has been compared with satellite, radiosonde, and European Centre for Medium-Range Weather Forecasts (ECMWF) Reanalysis (ERA5) dataset. ERA5 shows good agreement with differences within 500 m; radiosonde observations have under-estimated ground-based measurements, especially during summer. Satellite observations highly overestimated BLH. This comparative study reveals the importance of ground-based lidars in continuous monitoring of ABL at high vertical and temporal resolution because radiosonde, satellite, and reanalysis datasets have coarser resolutions and sparse observations. Such quantitative evaluation of ABL is formerly unavailable over this region, which can now be used to improve the representation in numerical models and thereby estimates of radiative and climate effects due to ABL.

This work was done in collaboration with Kondapalli Niranjan Kumar and Prashant Kumar of NCMRWF, MoES, Delhi, and SAC, ISRO, respectively.

doi : https://doi.org/10.1016/j.atmosres.2021.105999

(Sourita Saha, Som Sharma, Shyam Lal, and Dharmendra Kamat)

Impact of dust storm on the atmospheric boundary layer: a case study from western India

The present study focuses on investigating the impacts of a sudden dust storm on the atmospheric boundary layer (ABL) over Ahmedabad (23.02°N, 72.57°E), an urban site located in the western region of India. The accumulation of dust particles in the atmosphere during the dust storm, originating from the Thar Desert in Rajasthan, led to the decrease in surface temperature as a consequence of dust-radiation interaction. Ambient particulate matter data obtained from Air Quality (AQ) station at Ahmedabad showed a spike of 118.5% and 44.5% in PM10 and PM2.5 concentrations, respectively, during the event in comparison with the previous control day. Sudden exposure to an anomalous increase in the particulate matter may cause severe impacts on human health. These surface forcings have been reflected in the stable nocturnal ABL. Backscatter signals recorded by ground-based Ceilometer Lidar at Physical Research Laboratory (PRL) showed that ABL was shallow and collapsed during the dust storm episode. Turbulence has been detected in the ABL during the event which further assisted in the vertical mixing of dust particles in the ABL. These dust particles got trapped within the residual layer, preventing further percolation in the free atmosphere. Such sub-grid scale changes in the ABL during the dust storm were not reflected in the boundary layer height (BLH) obtained from the ERA-5 reanalysis dataset. A significant association between the ABL and the local radiative budget has been found. Coupled OceanAtmosphere Radiative Transfer Model (COART) simulations substantiated or showed a cooling event of the surface during the dust storm. This study is important as it can be taken as feedback to improve local climate models with respect to dust storm meteorology.

This work was done in collaboration with Kondapalli Niranjan Kumar (NCMRWF, MoES, Delhi) and Abha Chhabra and Prashant Kumar (SAC, ISRO, Ahmedabad).

doi : https://link.springer.com/article/10.1007/s11069-022-05293-z

(Sourita Saha, Som Sharma, Dharmendra Kamat, and Shyam Lal)

A case study on the vertical distribution and characteristics of aerosols using ground-based Raman lidar, satellite and model over Western India

Ahmedabad is an urban site in western region of India. Dust loading and its variability are very high over this semi-arid location. A state-of-the-art ground-based Raman lidar has been used for the study of day-to-day variability in vertical distribution of aerosol loading over Ahmedabad (23.02° N, 72.57° E) from 8 to 11 May 2018. We have done a comprehensive study about vertical profiles of aerosols across two wavelengths recorded simultaneously, namely, 355 nm and 532 nm, over this location. An interesting hump feature has been noted on 9 May at around 18 h (Local Time), with an additional peak at 19 h on 10 May. The loading over this region has more fine-mode aerosols than coarse-mode particles. Further, findings from ground-based lidar have been compared with MACC-II model simulations and Cloud-Aerosol Lidar with Orthogonal Polarization on-board Cloud-Aerosol Lidar and Infrared Pathfinder Satellite Observational. Back-trajectory analysis showed majority of the influx came from middle-east, carrying mineral dust and traces

of marine aerosols from Arabian Sea, except for 11 May, where low-level dust carrying trajectories and also coarser dust particles were not seen. This type of manifestation has also been observed while classifying aerosols over Ahmedabad using Lidar Depolarization Ratio and Lidar Ratio obtained from Raman Lidar. Fine mode aerosols have been characterized as industrial, vehicular and marine, while coarser as mineral dust and biomass burning. This study focuses on local variation and classification of aerosols based on size and type, which will further help in better estimation of radiative budget and other impacts of aerosols.

This work was done in collaboration with Kondapalli Niranjan Kumar (NCMRWF, MoES, Delhi), Prashant Kumar (SAC, ISRO) and Vaidehi Joshi (Johannes Gutenberg-Universitt Mainz, Germany).

doi : https://doi.org/10.1080/01431161.2021.1938737

(Sourita Saha, Som Sharma, and Shyam Lal)

Longitudinal differences in the ionospheric response over the South American sector during intense space weather conditions

Storm time response of Equatorial Ionization Anomaly (EIA) over the South American Sector and its longitudinal differences during an intense space weather event occurred between 27 and 29 May 2017 is investigated. Vertical Total Electron Content (VTEC) observations from a network of 120 Global Positioning System (GPS) receivers and magnetometer observations over two low latitude locations are used for this study. Variations of VTEC during the storm main phase inferred that the prompt penetration electric fields are not effective in this region since the storm occurred during local night time period. Correlation and periodicity analysis between Sym-H and magnetic field observations at low latitudes indicated that the H-component of the geomagnetic field at different latitudes are in phase under the influence of same eastward ionospheric current during the storm period. Strong positive storm effect is observed during the recovery phase of the storm on 28 May 2017, which is stronger over the anomaly crest locations compared to that at the equator. The EIA is intensified during the recovery phase of the storm and exhibit strong hemispheric asymmetry due to the storm induced wind disturbances. The strength of the EIA crest show significant differences between east and west Brazilian sectors within the 10° longitudinal separation. These longitudinal differences are possibly due to the combination of storm induced wind effects and geomagnetic field geometry where-in, over the east Brazilian sector, the field lines are more inclined with respect to the geographic equator.

This work is done in collaboration with A.J. de Abreu, E. Correia, C.M. Denardini, R. de Jesus, at INPE Brazil; M. Roberto, R. Abalde at ITA, Brazil; P.R. Fagundes at UNIVAP, Brazil; M.J.A. Bolzan at UFJ, Brazil and M. Gende at UNLP, Argentina.

doi : https://doi.org/10.1016/j.jastp.2021.105801

(K. Venkatesh)

On the cause of nocturnal OI 630nm airglow variability over low-latitude thermosphere

Ionosphere-thermosphere system is controlled by the electrodynamics and neutral winds. Airglow emissions act as tracer of these dynamics that take place at the altitudes from where they originate. OI 630 nm nightglow emissions that emanate from altitudes centered around 250 km have been investigated. Over 140 nights of data corresponding to the months of January, February, and March in the years 2013, 2014, and 2016, obtained from Gurushikhar, Mt. Abu (24.6°N, 72.7°E, 16°N Mag. Lat.), India, a low-latitude location, are used.

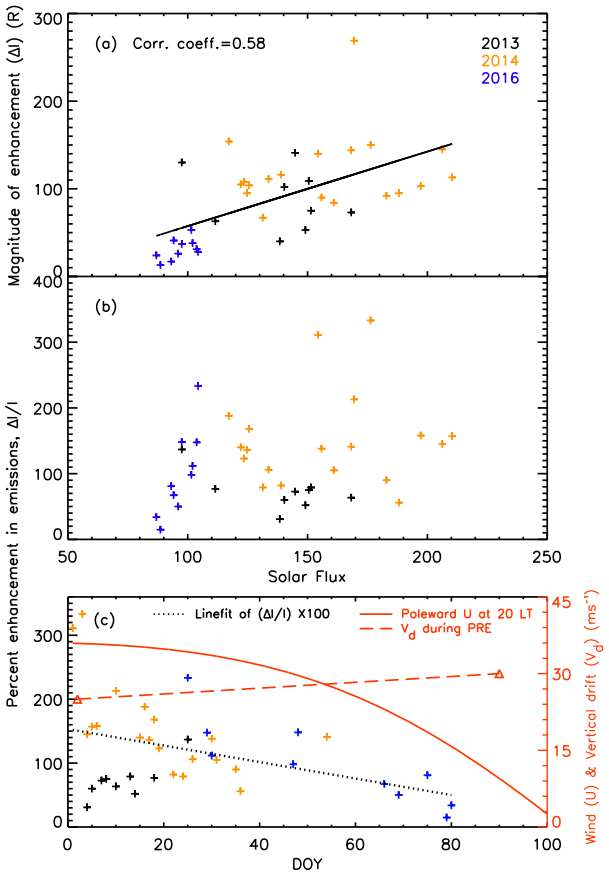

Figure no.16: The variation of magnitude of enhancement (ΔI) and percentage enhancement in emissions [(ΔI/I) 100] with solar fluxes are shown in top two panels, respectively. Panel c shows the percentage variation in (ΔI/I) with day of year for three different years.

These are compared with the column integrated emission rates calculated using the measured electron density as inputs. These electron density profiles have been obtained from a Digisonde at Ahmedabad (23.0°N, 72.6°E, 15°N Mag. Lat.). After sunset, the ionization stops, but the recombination continues to take place and as a consequence, the airglow emissions, which are proportional to the electron densities, decrease monotonically. On several occasions, enhancement in emissions has been observed with peaks at around 20-21 LT. The cause for this enhancement has been investigated by assessing the roles of equatorial electrodynamics and neutral winds. It is found that the meridional (north-south) winds, as obtained using digisondes at two locations (Ahmedabad and Trivandrum), show almost a very good correlation between a poleward directed wind or the cessation of equatorward winds over Ahmedabad and the observed enhancements in airglow emission during the post-sunset time. The magnitude of enhancement (ΔI) has been calculated

for 38 clear nights which show significant enhancement during the post-sunset time. Understandably, the variation in ΔI follows a linear relation with the solar flux (fig.16a) as the increasing solar flux produce larger number densities of ions in the ionosphere, an important reactant for the production of OI 630.0 nm airglow. To remove the bias imposed by varying solar flux levels in these epochs, percentage enhancement of the relative enhancement ((ΔI/I) 100) has been calculated which does not show any variation with the solar flux variation (fig.16b). However, this variation shows a decrease in magnitudes from January to March. This has a broad similarity with the decrease in the model (HWM-14) climatological meridional wind magnitudes in the same duration. In contrast to this the other potent factor that can cause such enhancement, namely the strength of PRE, shows an increase in magnitude from winter solstice to equinox (fig.16c). Based on the data spanning over different years, it is inferred that, during geomagnetic quiet periods, the post-sunset enhancement in the OI 630nm emissions over tropical latitudes is due to the variation in the neutral wind.

This work was done in collaboration with Tarun K. Pant of Space Physics Laboratory, Thiruvananthapuram, India and Supriya Chakrabarti of University of Massachusetts, Lowell, MA, USA.

doi : https://doi.org/10.1029/2021JA029146

(Sovan Saha and Duggirala Pallamraju)

On the Latitudinal Variation in OI 630.0 Dayglow Emissions in response to the Equatorial Electrodynamic Processes and Neutral Winds

In the Earth's upper atmosphere over the equatorial and low-latitudinal region during the daytime, various coupled phenomena e.g., the equatorial electrojet (EEJ), the equatorial plasma fountain effect or the equatorial ionization anomaly, the equatorial temperature and wind anomaly, are generated. The causes of these phenomena are the eastward electric field over the magnetic equatorial region and neutral winds. The thermospheric meridional winds can alter the plasma distributions and modulate the effect of the equatorial electrodynamics. To investigate the dynamics due to these two forces in the daytime, OI 630.0 nm dayglow emissions (that emanate from altitudes around 230 km) has been used as a tracer.

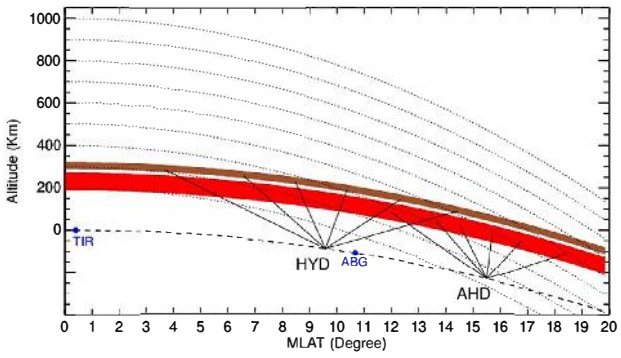

Figure no.17a: Schematic showing the regions of OI 630.0 nm dayglow emissions over different MLAT in red colour. The field-of-view of MISE is shown by black solid lines from HYD and AHD. The geomagnetic field lines are represented by dotted black line. TIR and ABG indicate the locations of geomagnetic measurements.

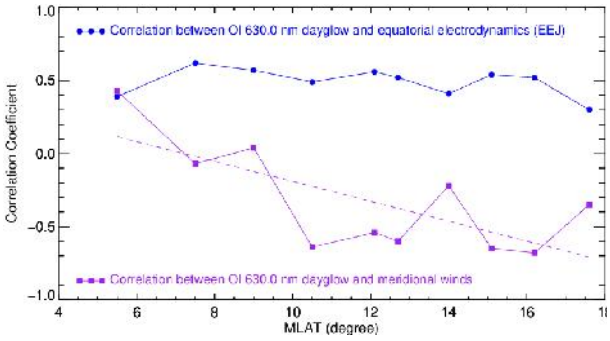

Figure no.17b: Values of correlation coefficients of OI 630.0 nm dayglow emission with EEJ and meridional winds are shown along with MLAT in blue and purple coloured lines, respectively. The linear fit between the correlation coefficients of the OI 630.0 nm averaged dayglow emission intensities with meridional wind and MLAT is shown in the dashed purple colour.

For these measurements, two In-house built multi-wavelength imaging echelle spectrographs, MISE, have been used. MISE is capable of measuring dayglow emissions over a large field-of-view which helps in the study of the upper atmospheric dynamics over large spatial extents. Simultaneous measurements of OI 630.0 nm dayglow emissions from Hyderabad and Ahmedabad in Indian longitude cover 5°-18° magnetic latitude (MLAT) (Figure 17a). To investigate the latitudinal variation of the upper atmosphere, the combined fields-of-view is divided into 10 independent spatial regions which are associated with different latitudes. The duration of January-February 2020 has been chosen when the variation in the Solar flux was negligible and all the days were geomagnetic quiet days (Ap $<$ 16). Thus, variations in the OI 630.0 nm dayglow emissions at different latitudes have been analyzed to with a view to investigate the contribution of equatorial electrodynamics and/ or the meridional winds over different latitudes. For the equatorial electrodynamics, EEJ is considered as a proxy. Linear regression analyses have been carried out in each of the view directions for the daily averaged dayglow emissions with respect to the EEJ and meridional winds and the correlations between them have been obtained. It is shown that for this solar epoch and winter season, the effect of the equatorial electrodynamics in the OI 630.0 nm dayglow emissions shows only a small variation with latitude, whereas, the effect of the meridional winds has a greater role to play in the OI 630.0 nm dayglow emissions with latitude. Due to meridional winds, the variation in the OI 630.0 nm dayglow emission intensities over 5°- 18° MLAT varied from that of positive correlation closer to the dip equator to that of negative as one moves away from the dip equator (Figure 17b). This has been interpreted to be due to more number densities of electron densities being brought-in/taken-away from the peak altitude region of the OI 630.0 nm dayglow, which is latitude dependent, as also verified by independent satellite measurements.

This work was done in collaboration with Tatiparti Vijayalakshmi of Jawaharlal Nehru Technological University, Hyderabad and Gopi K. Seemala of Indian Institute of Geomagnetism, Navi Mumbai.

doi : https://doi.org/10.1016/j.asr.2021.10.034

(Sunil Kumar, Duggirala Pallamraju, and Pradip Suryawanshi)

Signature of a mesospheric bore in 557.7 nm airglow emission using all-sky imager at Hanle (32.7°N, 78.9°E)

A prominent signature of dark bore front in the mesospheric O(1S) airglow emission is observed on a night in the late winter at Hanle (32.7°N, 78.9°E) located in the western Himalaya.

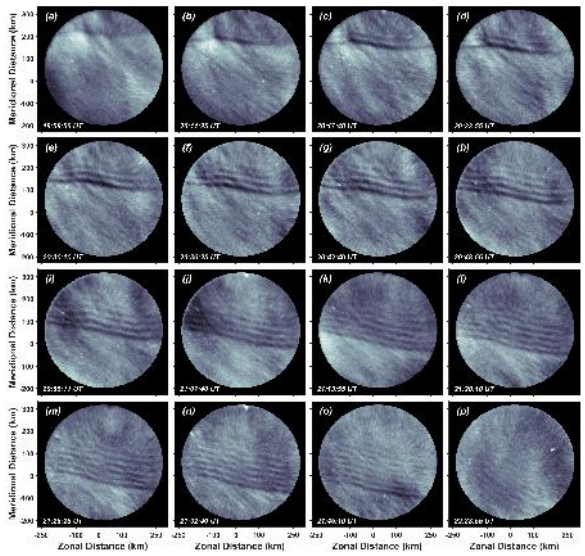

Figure no.18. Sequence of O(^{1}S) 557.7 nm airglow images on 02 February 2020. A dark front structure appears in the extreme north side of the image around 19:58:55 UT, and it propagates SW direction in the consecutive images followed by the trailing waves. Additionally, ripples (instability signature) are also evident in few images (h, i, and j) in the S, SW direction.

The leading front was followed by a series of evident trailing waves and the event lasts for more than two hours. The characteristic features of the bore indicate it to be linear undular type. Instantaneous temperature profile shows presence of stable region through formation of thermal duct in the upper mesosphere possibly supported by chemistry and/or dynamics. With time, the bore fronts became faint in presence of ripples as they reached other side of imager field of view (FOV). During the initial period around 3-4 waves h^{-1} appear to enter the imager FOV. The observed average phase speed, period and horizontal wavelength are found to be 40 m/s, 12 min and 29 km, respectively. The bore fronts exhibit a clockwise rotation at a rate of around 5° h^{-1}. The front edge perpendicular to the direction of propagation shows small-amplitude undulation indicating nonuniform duct structure. The tropospheric meteorological conditions may indicate plausible contribution from jet stream, weather front (linked with the Himalayan orography), and nonmigrating tides to excite and sustain the mesospheric bore event although further investigations in this direction are being sought to understand the actual underlying physical processes (Figure 18).

This research work was done in collaboration with S. Sarkhel, Indian Institute of Technology, Roorkee, India, M. Sivakandan, Leibniz Institute of Atmospheric Physics, Kühlungsborn, Germany and M. V. Sunil Krishna, Indian Institute of Technology, Roorkee, India.

doi : https://doi.org/10.1016/j.asr.2021.12.006

(A. Guharay and S. Mondal)

Impact of the September 2019 minor sudden stratospheric warming on the low-latitude middle atmospheric planetary wave dynamics

Planetary wave (PW) associated dynamical variability in the equatorial and extratropical middle atmosphere during the September 2019 Southern hemisphere minor sudden stratospheric warming (SSW) is investigated utilizing meteor radar wind observations from São João do Cariri (7.4°S, 36.5°W) and Cachoeira Paulista (22.7°S, 45°W) and reanalysis data.

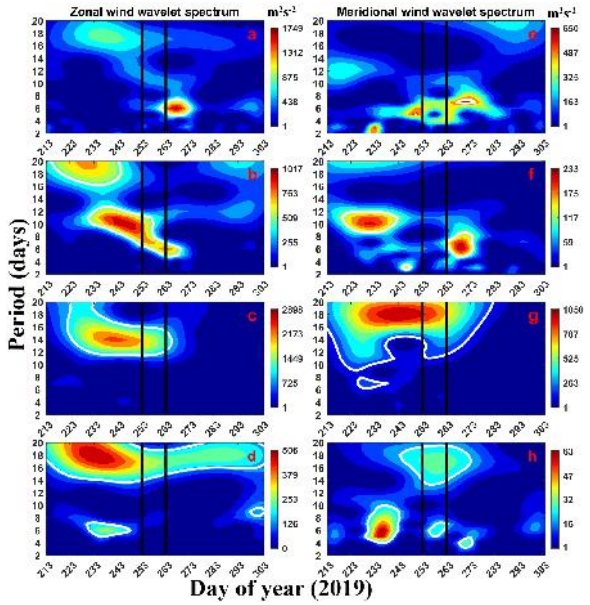

Figure no.19. Wavelet power spectra at 90 km for (a) zonal wind, (e) meridional wind using meteor radar. Wavelet spectra in the zonal wind at (b) 0.02 hPa, (c) 1 hPa, (d) 10 hPa and meridional wind at (f) 0.02 hPa, (g) 1 hPa, (h) 10 hPa at CP using ERA5. Bold white curves in each plot represent 95% confidence level. Please note the change of scale in the colorbars corresponding to each subplot while comparing

Signature of the mesospheric warming in conjunction with the stratospheric cooling is found at low latitudes. The strong westerly wind at low latitudes decelerates notably near 65 km at the onset of the warming episode, although no wind reversal is observed. The wind spectra reveal a prevalent quasi-16-day wave (Q16DW) prior to the SSW and existence of a quasi-6-day wave (Q6DW) after the warming event. Possible existence of barotropic/baroclinic instability in the low and mid latitude middle atmosphere may be responsible for exciting the Q6DW. Both traveling and stationary waves exhibit notable activities during the warming event. Although involvement of both zonal wavenumbers 1 and 2 PWs are found in the event, PW with zonal wavenumber 1 seems to play a vital role in preconditioning the same. Furthermore, significant latitudinal mixing of airmass between the tropics and high latitudes is evident in the potential vorticity map. The Eliassen-Palm flux diagnosis shows the propagation of the Q6DW and Q16DW from mid to low latitudes during the warming event (Figure 19).

This research work was done in collaboration with P. P. Batista, National Institute for Space Research, So Jos dos Campos, So Paulo, Brazil, and R. A. Buriti, Federal University of Campina Grande, Campina Grande, Paraiba, Brazil.

doi : https://doi.org/10.1029/2021JD035538

(G. Mitra and A. Guharay)

Evidence for the in-situ generation of plasma depletion structures over the transition region of geomagnetic low-mid latitude over the Indian sector

In general, the plasma depletion structures over either geomagnetic low or middle latitudes are widely investigated to understand the processes responsible for their generation and evolution.

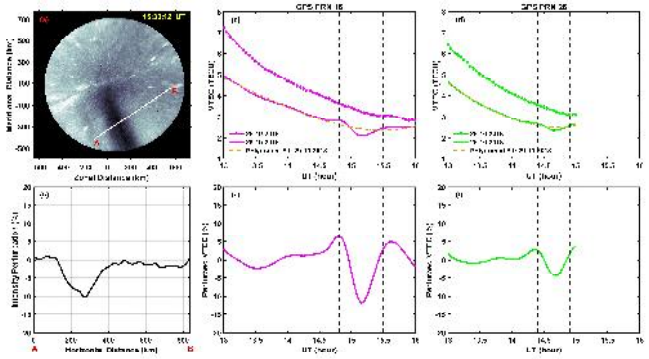

Figure no.20: In situ generated plasma depleted structure over Hanle, Leh Ladakh, a geomagnetic low-mid latitude transition region, and its associated perturbation in 630.0 nm airglow intensity & TEC. (a) and (b) depict the depleted plasma structure observed in the 630.0 nm airglow imager and its intensity perturbation (in %). (c) and (d) show the vertical total electron content (VTEC) variation on the control (October 28, 2018) and event (October 29, 2018) day. (e) and (f) indicates the perturbed VTEC (in %) on the event day.

However, characterization of plasma depletion structures over the transition region of geomagnetic low-mid latitudes has not received critical attention so far. This is important as these structures can affect communication and navigational applications. In this work, we show the in-situ generation of a plasma depletion structure (Figure 20) based on an all-sky imaging observations operating at 630.0 nm from Hanle, Leh Ladakh on a geomagnetically quiet night (October 29, 2018). The plasma depletion structure is also confirmed by the simultaneous GPS-TEC and ionosonde observations over New Delhi. We show that the growth time of the plasma depletion is $\sim$2 h if one considers only the Perkins instability mechanism. However, in the present case, the plasma depletion structure developed within $\sim$25 min. We show that by invoking possible Es layer instabilities and associated E-F region coupling, the growth rate can be increased roughly by an order of magnitude. This strongly suggests that the Cosgrove and Tsunoda mechanisms may be simultaneously operational in this case. Furthermore, it is also suggested that reduced F region flux-tube integrated conductivity over the low latitude region created conducive background conditions for the growth of the plasma depletion on this night.

This work is done in collaboration with M. Sivakandan [Leibniz Institute of Atmospheric Physics at the University of Rostock, Khlungsborn, Germany], S. Mondal, S. Sarkhel and M. V. Sunil Krishna [Indian Institute of Technology, Roorkee], A. K. Upadhayaya [CSIR National Physical Laboratory, New Delhi], A. Shinbori and T. Sori [Institute for Space-Earth Environment Research, Nagoya University, Nagoya, Japan], S. Kannaujiya and P. K. Champati Ray [Indian Institute of Remote Sensing, ISRO, Dehradun, India].

doi : https://doi.org/10.1029/2020JA028837

(D. Chakrabarty)

Daytime conjugate hemispheric asymmetry of low latitude ionosphere along 100°E

The hemispherical asymmetry of the low latitude ionosphere along 100°E $\pm$ 5°E is investigated for the year 2015 at magnetically conjugate points on seasonal and intra-seasonal time scales. It is found that the equatorial ionization anomaly (EIA) at the conjugate stations is highly asymmetric even during the equinoctial months of March and October, whereas it is nearly symmetric during April. During June/July, the morning time hemispheric asymmetry (larger on the winter side) temporarily reduces in the midday period and then reverses sign (larger in summer) in the afternoon. Based on detailed NmF2, hmF2 observations, theoretical (SAMI3/SAMI2) and empirical model (IRI) simulations and GIM-TEC maps, it is shown that hemispheric asymmetry at seasonal and intra-seasonal time scales are intricately connected to the meridional wind arising out of the relative position of the sub-solar point with respect to the field line geometry. This work brings out the importance of the location of the sub-solar point in assessing the hemispherical asymmetry of EIA.

This work is done in collaboration with B.R. Kalita, P.K. Bhuyan, S.J. Nath and M.C. Choudhury [Dibrugarh University, Dibrugarh], K. Wang [Space Weather Services, Bureau of Meteorology, Surry Hills, New South Wales, Australia], K. Hozumi [National Institute of Information and Communications Technology, Japan], P. Supnithi [King Mongkuts Institute of Technology Ladkrabang, Bangkok, Thailand], T. Komolmis [Chiang Mai University, Chiang Mai,Thailand], C. Y. Yatini [Indonesian National Institute of Aeronautics and Space, Indonesia], and M. Le Huy [Institute of Geophysics, Vietnamese Academy of Science and Technology, Hanoi, Vietnam]. doi : https://doi.org/10.1016/j.asr.2022.02.058

(D. Chakrabarty)

Properties of recovery phase of extreme storms

Understanding the properties of recovery phase of a geomagnetic storm is important as this phase can last for several days and the magnetosphere during the recovery phase is still far from the quiet time equilibrium condition. From a space weather perspective, it is therefore, important to understand the magnetospheric dynamics during the recovery phase of geomagnetic storm. Based on 31 extreme geomagnetic storms that occurred from 1990 to 2020, we show that each storm demonstrates two distinct features of the recovery phase - initially fast and later, slow rate of recovery. During the fast recovery phase captured by SYM-H, the rate of recovery has been characterized by either linear or non-linear (exponential or hyperbolic) decay function in SYM-H in various studies reported

earlier. In our study, we show that the hyperbolic function explains the complete recovery phase of only 11 extreme events. Furthermore, both exponential and hyperbolic decay functions fail to explain the late recovery phase of storms. We have found that the rate of recovery during the slow phase is independent of SYM-H. Our work also suggests that the rate of recovery during the late phase is proportional to the intensity of the storm.

This work is done in collaboration with Komal Choraghe, Anil Raghav, S. Kasthurirangan, and N. Bijewar [University of Mumbai, Mumbai, India.]

doi : https://doi.org/10.1029/2020JA028685

(D. Chakrabarty)

Development of automated sky scanner for PRL Airglow Infrared spectrograph (PAIRS)

In order to derive spatial information (zonal, meridional, and vertical wavelengths) of the mesospheric gravity waves (GWs) using PRL Airglow InfraRed Spectrograph (PAIRS), we have developed an automated sky scanner that has been coupled with PAIRS. The periodicities and the horizontal wavelength of the GWs can be derived from the time series obtained from the scanning PAIRS. The vertical wavelengths can be calculated using the dispersion relation of low and medium frequency GWs and information on horizontal winds.

The sky scanner consists of two mirrors of 50 mm diameter mounted on the centre of the hypotenuse of two right angles isosceles triangle-shaped body in which one is movable and one is fixed (Figure 21a). The incident light is allowed to fall onto the input mirror that is attached to a geared pulley fixed in a ball bearing and is driven by a motor using a belt drive. This arrangement enables rotation along the horizontal axis that provides the scanning of the sky at different elevation angles (Figure 21b). The reflected light from the input mirror falls onto the fixed output mirror, this two-mirror arrangement reflects the incoming light by 180 degrees and allowed it to fall onto the instrument aperture of 25 mm in length (Figure 21c). The mechanical structure of the mirror assembly are designed and fabricated in-house using 3-d printing and PLA material that make it light weight (1.1 kg including mirrors and motor mass).

We have used NEMA-17 motor to actuate the mechanism and automated it to record the spectral images by integrating it with a single GUI to operate the PAIRS. Communication between Arduino uno and GUI has been made via data and acknowledgement read on serial port of the device in use. The flow chart showing the steps that have been followed in order to integrate and automate the sky scanner with PAIRS is shown in Figure 21(d). The scanner is being operated to scan $\pm$60 degrees of the sky from a zenith view with the accuracy of $\pm$0.5 degrees. We have integrated the sky scanner with PAIRS (Figure 21c) and is being operated from optical aeronomy observatory, Thaltej Campus. Further work towards development of data analysis methods and optimization of scanning PAIRS is under progress.

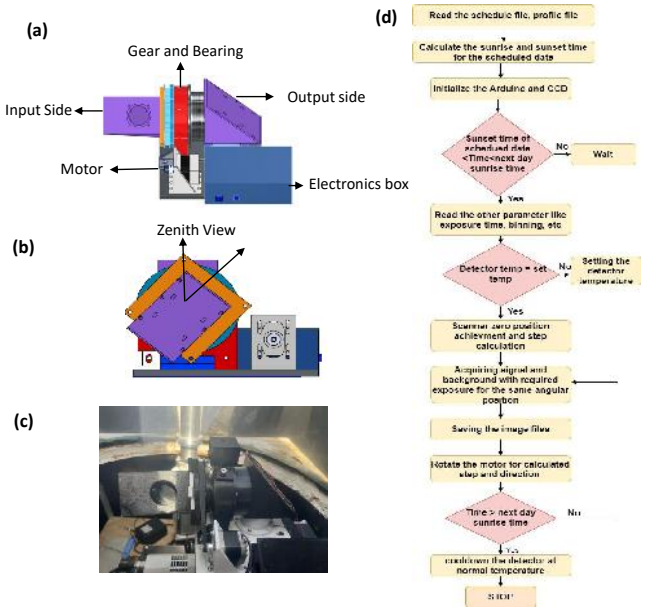

Figure no.21: (a) CAD of sky scanner (b) Showing angular position of scanner (c) Photograph of the sky scanner integrated with PAIRS (d) Flow chart for sky scanner automation and data acquisition.

(Mohit K. Soni, Shashank Urmalia, Pankaj K. Kushwaha, and Ravindra P. Singh)

Geosciences

Impact of Indian summer monsoon in westerly dominated water resources of western Himalayas

Stable water isotopes of oxygen and hydrogen were used to identify and estimate the seasonal contribution of precipitation from the two wind systems, namely, the WD and ISM, to the regional hydrology of Sindh and Rambiara catchments of western Himalayas. The two-component hydrograph separation based on d-excess suggests that the western disturbances (WD) contribute dominantly (76±4%) to the regional hydrology, compared to Indian summer monsoon (ISM) rainfall (24±4%). A comparison of d-excess values of WD and ISM indicates the groundwater consists of 90±3% WD sources and 10±2% ISM sources, signifying distinct seasonal variations in groundwater recharge sources. The sine wave model results showed that the annual mean residence time (MRT) of groundwater for the Sindh catchment (5.8±0.6 months) is greater than the Rambiara groundwater (3.6±0.5 months). The lower isotope values observed in the river water than in the precipitation suggest its origin from the snowmelt. This study provides valuable insights into the hydrological processes operating in the high altitude Himalayan catchments to facilitate the improved understanding of runoff generation mechanisms and water resource management in future climate change scenarios.

This study was done in collaboration with Dr. Gh. Jeelani, Kashmir University.

doi : https://doi.org/10.1080/10256016.2021.2011725

(V. Padhya and R.D. Deshpande)

Investigating hydrometeorology of the Western Himalayas: Insights from stable isotopes of water and meteorological parameters

The Himalayas govern the hydrometeorology of the entire Indian subcontinent and feed 19 major rivers on which a large population is dependent. Despite its vast socio-economic relevance, there exist knowledge gaps in the detailed understanding of Himalayan hydrometeorology. The present study attempts to understand subtle hydrometeorological processes concerning precipitation in Western Himalaya (WH), which is quite complex due to several mountain ranges in addition to the Great Himalaya and varied land cover. In this backdrop, oxygen and hydrogen isotopic analyses of daily precipitation samples collected from Jammu was done. Major processes and features identified are: (1) Raindrop re-evaporation is dominant, indicated by lower δ^{18}O - δD regression slope (6.6 ± 0.2). (2) Maximum raindrop re-evaporation occurs during Western Disturbances (WD), evident from the low d-excess (<10‰) and high δ^{18}O (>0‰) with low rainfall. (3) Contrary to expectations, negligible moisture is derived from the Mediterranean region (MR) through WD. In contrast, maximum moisture (∼97%) is derived from local terrestrial sources, estimated through backward wind trajectories and confirmed by vertical wind velocity (ω) and OLR.

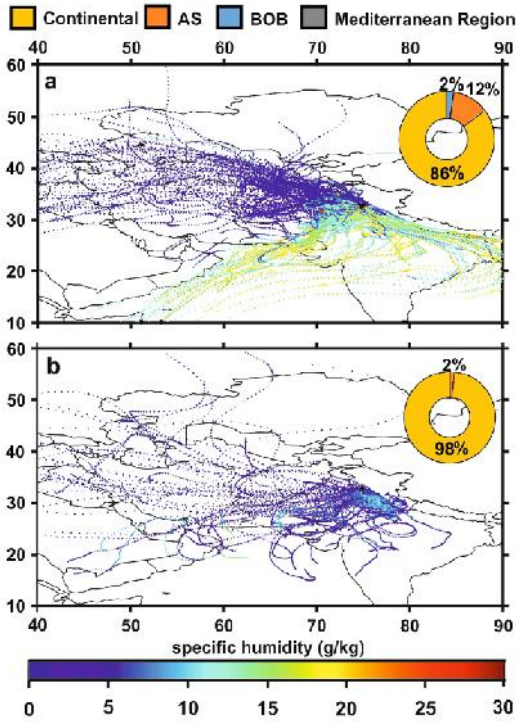

Figure 1: Map showing ensembles of four 120 h. backward trajectories at six hourly intervals for each rainy day, starting from Jammu at an altitude of maximum Cloud Liquid Water Content (CLWCmax) during monsoon (a) and WD period (b). The colour code indicates specific humidity in g/kg. The inset doughnut chart represents the relative contribution of each moisture source.

(4) The Arabian Sea (AS) moisture contributes more (∼11%) compared to the Bay of Bengal (BOB) moisture (∼8%) during the monsoon. (5) Isotopically, the most depleted precipitation during July-Aug is associated with continental recycling from the Indo-Gangetic plains and not with the BOB moisture. (6) Isotopic enrichment in precipitation towards end of monsoon is attributed to raindrop re-evaporation, lesser rainout fraction and moisture derived from enriched local sources. (7) Annually, 87% of the moisture for precipitation is derived through continental recycling, and only 13% of the moisture is derived through marine sources (11% from AS and 2% from BOB). Moisture from MR (<0.1%) is negligible.

doi : https://doi.org/10.1016/j.atmosres.2021.105997

(H. Oza, V. Padhya, A. Ganguly & R.D. Deshpande)

Meltwaters dominate groundwater recharge in cold arid desert of Upper Indus River Basin (UIRB), western Himalayas.

Groundwater resources play a key role in sustaining irrigated agriculture and providing domestic water supplies in the trans-boundary Upper Indus River Basin. Understanding groundwater recharge and flow pathways in Upper Indus Basin is critical to good groundwater management, yet groundwater recharge sources remain poorly quantified. In this study, stable oxygen and hydrogen isotope compositions and geochemical tracers of rain (n=110), groundwater (n=140), glacier melt (n=56) and snowmelt (n=46) have been analysed to investigate the spatio-temporal variation of δ^{18}O and δ^{2}H in source waters and groundwater and to quantify and estimate the sources of recharging water. Microclimate in sub-basins is dominantly controlling stable water isotopic composition of source waters and groundwater. It is shown that meltwaters supply up to 83% of groundwater recharge, emphasizing the importance of the cryosphere in sustaining groundwater resources in the Upper Indus River Basin. Meltwater-derived recharge is split evenly among glacial meltwaters (44% of annual recharge) and snowmelt (39%); by contrast, rainfall contributes only 17% of annual recharge. Our data highlight the dependence of groundwater recharge on meltwaters derived from glaciers and snowpacks, suggesting that changes to the pattern, form, timing and amount of precipitation as well as glacial retreat may have disproportionate impacts on groundwater recharge, with potential to alter water supplies and affect local and regional economies.

This work was carried out in in collaboration with Abhijit Mukherjee, IIT Kharagpur and Gh. Jeelani, Kashmir University.

doi : https://doi.org/10.1016/j.scitotenv.2021.147514

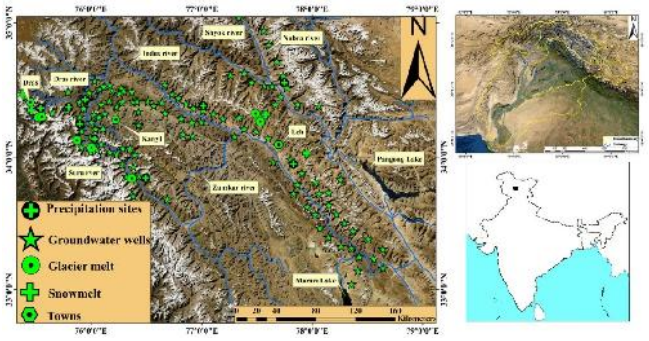

Figure 2: (a) Study area map of Upper Indus River Basin, Ladakh showing sampling sites on Landsat satellite image from Earth Explorer. (b) The map of drainage network of the Indus River basin. (c) Location of study area in India

(R.D. Deshpande)

Identifying and estimating the sources of river flow in the cold arid desert environment of Upper Indus River Basin (UIRB), western Himalayas

A reliable water supply in different Himalayan River basins is increasingly important for domestic, agriculture, and hydropower generation. These water resources are under serious threat due to climate change, with the potential to alter the economic stability of 237 million people living in the Indus River Basin alone. In the present study, we used new stable water isotope data set to identify and estimate the different sources of streamflow and their controlling factors in the Upper Indus River Basin (UIRB), India. The data set presented wide spatial and temporal variability without the distinct isotopic signature of various sources of river flow. However, variable but distinct signatures of sources of river/stream flow exist at the sub-basin or catchment scale. These variabilities are ascribed to changing physiographical, meteorological, and local climatic conditions. Further, the distinct microclimatic conditions including altitudinal variability, aspect slope, etc. govern the spatio-temporal variability of sources and streamflow, hence different lapse rates at sub-basin/catchment scale. The study suggested that the contribution of snowmelt and glacier melt to river flow varies spatially and temporally. The Bayesian mixing model results suggested that snowmelt contribution is higher in Indus (63$\pm$1.2%) and Shyok (58$\pm$1.7%) while as, glacier melt contribution is higher in Nubra 64$\pm$2.3% and Suru 60$\pm$2.7% sub-basins/catchments. The groundwater contribution (baseflow) sustains and regulates the flow in rivers/streams during winter and spring, which is very vital for the local water supply. The study suggests that the spatially diverse rugged topography and microclimate in UIRB dominantly control the differential contribution from various sources of river flow. The warming climate, which has resulted in a decrease in solid precipitation, continuous glacier mass loss, early melting of snow cover, etc., would have an inconsistent impact on the perennial flow of rivers with the potential to alter the economic and political stability in the region.

This work was carried out in in collaboration with Dr. Gh. Jeelani, Kashmir University.

doi : https://doi.org/10.1016/j.scitotenv.2022.154964

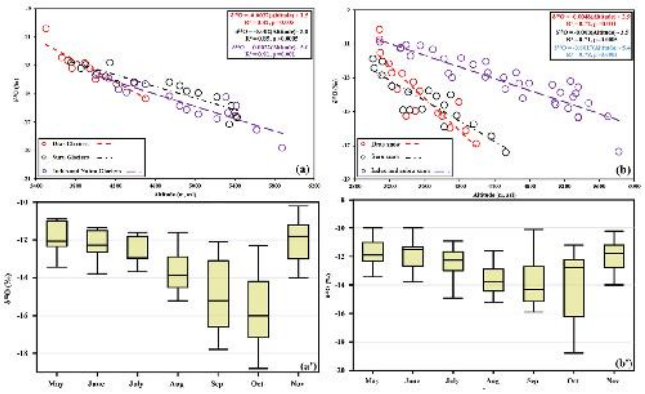

Figure 3: (a and b) Scatter plots showing the relationship of δ^{18}O values of glacier melt and snowmelt with sampling site elevation. The lower and higher δ^{18}O values tend to characterize the glacier melt and snowmelt collected respectively from higher and lower elevations. (a' and b') Box and whisker plots show the temporal variation of δ^{18}O values among the glacier and snowmelt samples. δ^{18}O values of glacier melt and snowmelt tend to be higher in May than September.

(V. Padhya and R.D. Deshpande)

Isotopic analysis to quantify the role of the Indian monsoon on water resources of selected river basins in the Himalayas

Western disturbances (WDs) and Indian summer monsoon (ISM) led precipitation play a central role in the Himalayan water budget. Estimating their contributions to water resource is although a challenging but essential for hydrologic understanding and effective water resource management. In this study, we used stable water isotope data of precipitation and surface waters to estimate the contribution of ISM and WDs to the water resources in three mountainous river basins-Indus, Bhagirathi and Teesta river basins of western, central and Eastern Himalayas.

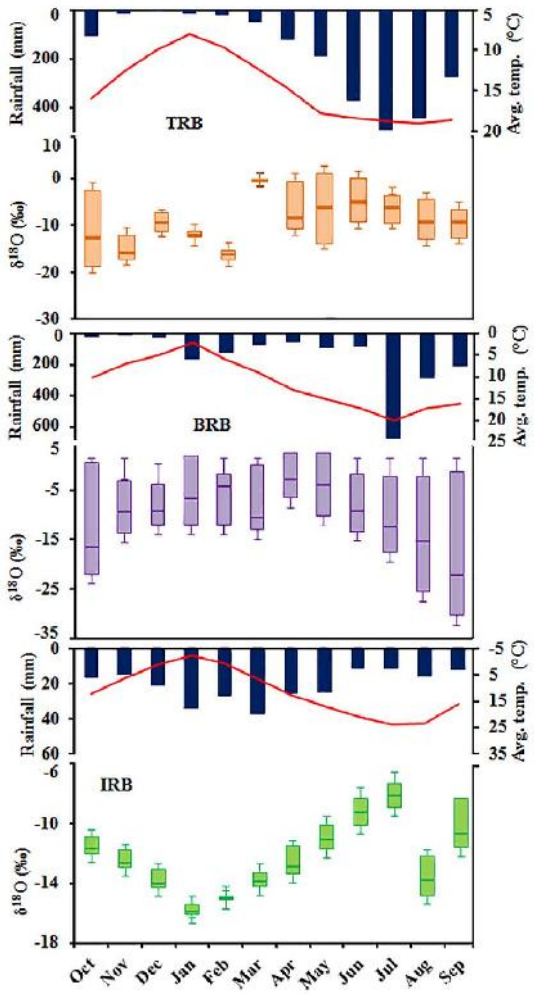

Figure 4: Box and whisker plots δ^{18}O of precipitation depicting spatio-temporal variation in the isotopic characteristics, and their relationship with air temperature and rainfall in three river basins. [TRB: Teesta River Basin; BRB: Bhagirathi River Basin; IRB: Indus River Basin.]

The study reveals distinct seasonality in isotope characteristics of precipitation and surface waters in each river basin is due to changes in moisture source, hydrometeorology and relief. The two-component end-member mixing method using d-excess as tracer suggest that the influence of the ISM on the water resources is high ($>$72% to annual river flow) in Teesta river basin (eastern Himalayas), while as the WDs led precipitation is dominantly contributing ($>$70% average annual river flow) to the surface waters in the Indus river basin (western Himalayas). The contribution of ISM and WD led precipitation in Bhagirathi river basin is 60% and 40%, respectively. The findings demonstrate that the unusual changes in the ISM and WD moisture dynamics have the potential to affect the economy and food security of the region, which is dependent on the availability of water resources. The obtained results are of assistance to policy makers/mangers to make use of the information for better understanding hydrologic response amid unusual behavior of the dual monsoon system over the region.

This work was carries out in collaboration with Dr. Gh.Jeelani, Kashmir University.

doi : https://doi.org/10.1002/hyp.14406

(R.D. Deshpande)

Isotopic differentiation of groundwater recharge processes in a semi-arid region of southern India.

Ensuring the availability of adequate quantity and quality of water to meet demands of domestic sector has become the prime objective for the developing countries like India. The coastal and the nearby inland region are the places of intense human activity due to urbanization and industrialization leading to the depletion and degradation of environmental resources.

Figure 5: Seasonal variation in δ^{18}O of the groundwater from bore wells in the Tuticorin coastal belt, which is an Ecologically Sensitive Zone in the Gulf of Mannar Biosphere Reserve and consists of highly productive ecosystems of great biological diversity.

This investigation on the coastal and inland aquifers of Tuticorin, Gulf of Mannar, Tamil Nadu was undertaken to better understand the recharge characteristics, factors controlling recharge, effect of weather parameters on recharge, source of recharge water, differences between inland and coastal recharge processes and climatic signature in groundwater isotopic composition from the hydrochemical and stable isotope data. Different mechanisms of salinization in the coastal aquifers were deduced as direct influence of the sea water and concentrations of ions by evaporation. The dissolution or leaching from the aquifer material is also imparting salinity to groundwater in this area.

This work was carried out in collaboration with Girish Gopinath, Centre for Water Resources Development and Management, Kerala.

doi : https://doi.org/10.1007/s12665-021-09816-y

(R.D. Deshpande)

Constraining ages of deltaic sediments from Sundarbans

The paleoenvironment of delta regions can be reconstructed using representative remains of the past vegetation. Pollen assemblage is a robust proxy of land vegetation evolution. However, frequent dry and wet conditions due to tidal activities in the coastal regions limit the preservation of microfossils and pollens. Phytoliths, which are silica deposits found in plants, have shapes characterizing the vegetation and survive well in the soils and sediments. The study of Sunderbans sediments from different deltaic environments was carried out to establish the potential of phytoliths as a proxy of surface environments. Radiocarbon dating of bulk sediments, in this regard, has helped to reveal a mangrove environment between 13.6 and 3.9 ka, absence between 3.9 to 2.2 ka and reappearance of it during 2.2 to 0.8 ka. These changes were driven due to past variations in the sea levels.

This work was done in collaboration with Prof. Subir Bera, University of Calcutta.

doi : https://doi.org/10.1177/09596836211041736

(M.G.Yadava)

Spatial and temporal changes in bomb radiocarbon in the northern Indian Ocean

For improved understanding of ocean circulation in the northern Indian Ocean region, long term continuous record of radiocarbon measurement is required. Limited radiocarbon records from the region demands investigations of natural archives.

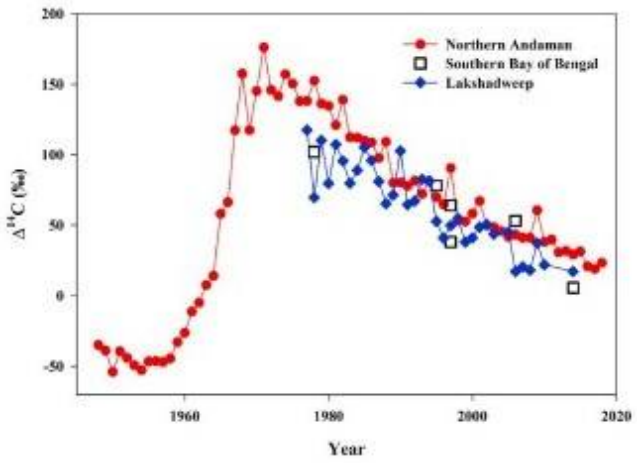

Figure 6: Δ^{14}C values from the northern Andaman coral, Lakshadweep coral and southern Bay of Bengal surface seawater (near 8.5°N 86°E; Stuiver and Ostlund, 1983; Key and Quay 2002; Dutta et al., 2010, Dutta and Bhushan 2012, and Gao et al., 2020) in the northern Indian Ocean. Note, overlapping values of surface seawater of southern Bay of Bengal and Lakshadweep coral.

Coral core records along with some literature data were analysed to study the temporal changes in ^{14}C values over the northern Indian Ocean. The major fraction of the bomb radiocarbon appears to have transferred in to the ocean, as recent records from the surface seawater Δ^{14}C values show comparable or even higher than the atmospheric Δ^{14}C values. The northern Andaman region showed higher Δ^{14}C decline rate between 1978 and 2014 compared to the southern Bay of Bengal and the Lakshadweep region. The comparable southern Bay of Bengal and the Lakshadweep Δ^{14}C values could be due to transfer of Arabian Sea waters to the southern Bay of Bengal. The southern Andaman region shows lower Δ^{14}C values compared to the northern Andaman region, suggesting the influence of ^{14}C depleted waters in the region.

doi : https://doi.org/10.1016/j.jenvrad.2021.106680

(H. Raj and R. Bhushan)

Production rate variation and changes in sedimentation rate of marine core dated with meteoric ^{10}Be and ^{14}C

The first measurement of meteoric beryllium-10 (^{10}Be) using Accelerator Mass Spectrometer (AMS) is reported from PRL-AURiS (Physical Research Laboratory-Accelerator Unit for Radioisotope Studies).

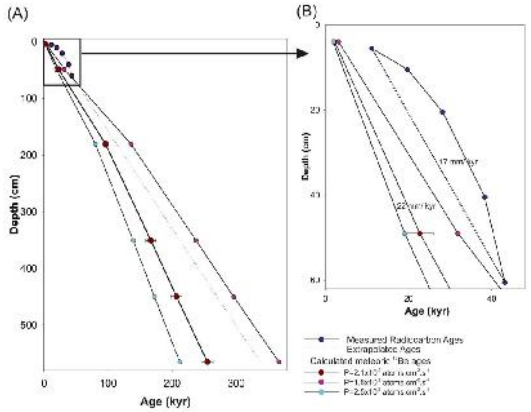

Figure 7: A comparison between the ages derived from Radiocarbon and meteoric beryllium-10 method. (A) shows the variation in ages with changing production rate along with the extrapolated radiocarbon ages. Error is only shown for 2.1×10^{-2} atoms.cm^{-2}.s^{-1}. (B) The radiocarbon and meteoric ^{10}Be results within 50 kyr show a continuous offset in ages. The radiocarbon ages are constantly older than the meteoric ^{10}Be ages.

Strategically, the meteoric ^{10}Be dating method can date events as old as 10 Myr, and its accuracy while dating marine sediment cores has been well tested with magnetic methods. An attempt is made for a comparative study between radiocarbon (^{14}C) and meteoric ^{10}Be dating methods from a 6 m long sediment core collected from the equatorial Indian Ocean. The core was dated using both radiocarbon and meteoric ^{10}Be and results showed remarkable similarity for both methods in terms of the sedimentation rate. A continuous age offset observed within 50 kyr could be due to a continuous influx of sediment with low ^{10}Be content and that may have caused the meteoric ^{10}Be ages to be younger. The sedimentation rate calculated by changing the ^{10}Be depositional flux rate from 1.5 to 2.5×10^{-2} atoms.cm^{-2}.s^{-1} shows large variation, indicating the choice of appropriate ^{10}Be depositional flux rate for the region. Additionally, being the first meteoric beryllium-10 measurements using AURiS, we have also

discussed and reported the laboratory protocols and efficiency based on repeat standard and blank measurements.

doi : https://doi.org/10.1016/j.jenvrad.2021.106678

(P.S. Jena, R. Bhushan, A. Shivam, R. Nambiar & N. Bharti)

^{10}Be depositional flux variation in the central Indian Ocean during the last 43 ka

The advent of Accelerator Mass Spectrometer (AMS) enhanced the application of meteoric ^{10}Be (half-life of 1.39 Ma) as a tracer for understanding earth surface processes on thousand to million-year time scales. However, for the majority of applications, an adequate understanding of the ^{10}Be depositional flux is a prerequisite. A number of efforts have been made to understand both spatial and temporal variation of ^{10}Be depositional flux. Yet, due to the limited globally distributed dataset and modulation of the ^{10}Be signal by local processes, a significant offset is observed between model-derived and measured deposition rates of ^{10}Be.

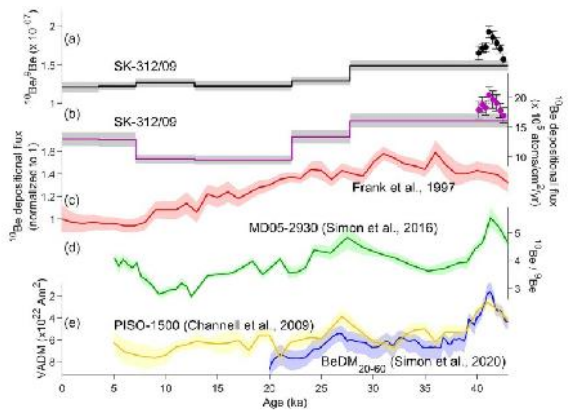

Figure 8: The temporal variation in (a) ^{10}Be/^{9}Be ratio in core SK-312/09 and (b) ^{10}Be depositional flux in core SK-312/09 (obtained using method 1; corrected for leaching yield), (c) highly resolved global average ^{10}Be depositional flux (normalized to 1) by (Frank et al., 1997), (d) ^{10}Be depositional flux variation obtained from MD05-2930 (Simon et al., 2016b), and (e) virtual axial dipole moment (VADM) record (Channell et al., 2009; Simon et al., 2020).

In this study, an attempt has been made to determine the ^{10}Be depositional flux from a marine sediment core from the central Indian Ocean chronologically constrained with the AMS radiocarbon dating and ^{10}Be concentration measured with AMS. The ^{10}Be depositional flux estimates using weak leaching method are found to be nearly 44% lower compared to the strong leaching method. The calculated ^{10}Be depositional flux during the Holocene varies between 9.63 and 13.01$\times$10^{5} atoms/cm^{2}/yr, which is 2-28% lower compared to the modelled depositional flux for the region. The difference observed in ^{10}Be depositional flux could be due to the local processes (such as boundary scavenging, changing rate of sediment deposition at the location) affecting ^{10}Be deposition into the sediment column or offset associated with the model estimations. The changes in ^{10}Be depositional flux and the ^{10}Be/^{9}Be ratio have been reconstructed up to 43 ka. An increase in the ^{10}Be/^{9}Be ratio during 28 to 43 ka is observed due to the lower geomagnetic field intensity during the period. A high-resolution ^{10}Be/^{9}Be ratio reconstruction shows a peak at 41.2 ka, which can be attributed to the Laschamp event.

doi : https://doi.org/10.1016/j.scitotenv.2021.149808

(P.S. Jena, R. Bhushan, A. Shivam, N. Bharti & A.K. Sudheer)

Air-sea CO_2 exchange rate in the northern Indian Ocean based on coral radiocarbon records

Corals growing in shallow oceanic regions record the radiocarbon variations in ocean surface waters. Tracing bomb radiocarbon in various carbon reservoirs, can help understand the pathways and rates of carbon exchange between the different reservoirs. The northern Indian Ocean comprising two adjoining basins (the Arabian Sea and the Bay of Bengal) demonstrates contrasting behaviour both in its hydrological condition and CO_2 sequestration. In this study, coral based bomb radiocarbon records from the Lakshadweep Islands and the Andaman Islands in the northern Indian Ocean have been analysed. The estimates of air-sea CO_2 exchange rate based on bomb radiocarbon for the Lakshadweep is 13.4$\pm$2.1 mol m^{-2} yr^{-1} and for the northern Andaman is 8.8$\pm$1.3 mol m^{-2} yr^{-1}. The bomb radiocarbon based air-sea CO_2 exchange over the Indian Ocean follow the trend of empirical relationship with wind speed. Using the air-sea CO_2 exchange rates, the net regional CO_2 fluxes over the Lakshadweep and the northern Andaman region has been determined.

doi : https://doi.org/10.1016/j.apgeochem.2022.105208

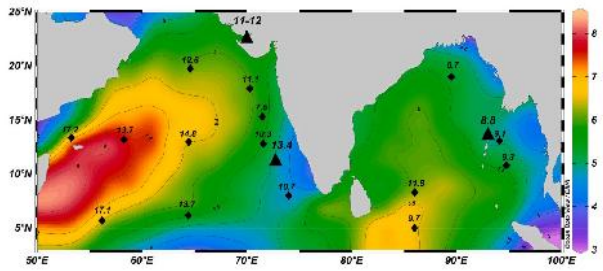

Figure 9: Air-sea CO_2 exchange rates in the northern Indian Ocean along with colour contours of average wind speed (m s^{-1}) (COADS, Slutz et al., 1985). ▲ represents coral based air-sea CO_2 exchange rates (mol m^{-2} yr^{-1}) from this study and Chakraborty et al. (1994). ▲ represents air-sea CO_2 exchange rates (mol m^{-2} yr^{-1}) estimated by Dutta and Bhushan (2012). Air-sea CO_2 exchange rates are denoted by bold numbers. This figure was created using Ocean Data View software Schlitzer, Reiner, Ocean Data View, https://odv.awi.de, 2020) (For interpretation of the references to colour in this figure legend, the reader is referred to the Web version of this article.).

(H. Raj, R. Bhushan, U.S. Banerji, M. Muruganantham, C. Shah, R. Nambiar & A.J. Dabhi)

Paleoredox condition of bottom waters in the northern Indian Ocean since 39 ka

Ocean circulation has undergone signifcant changes during the glacial and interglacial periods. The redox condition at the sediment-water interface is mainly regulated by export productivity and ventilation of abyssal water mass. The changes in the redox condition associated with bottom water circulation in the Indian Ocean are still unclear. The present study assessed multi redox proxies (Mn/Ti, Mo/Ti, U/Ti, V/Ti, Ni/Ca, Cu/Ca, MnEF, UEF, and VEF) and Corg in the sediment core collected from the Arabian Sea (NW Indian Ocean) to investigate the past variations in bottom water redox condition. The bottom water in the Arabian Sea is presently bathed with the Lower Circumpolar Deep Water (LCDW), consisting of a fraction of both North Atlantic Deep Water (NADW) and Antarctic Bottom Waters (AABW).Our results show signifcant changes in oxygenation conditions in response to changes in ocean circulation. The present study revealed that bottom water in the northern Indian Ocean was more oxic during Last Glacial Maximum (LGM) than the deglacial period. We interpret the variability in the contribution of NADW and AABW influenced the redox condition at the study location. Comparing the current study results with previously reported Nd isotopes suggests that the contribution of AABW to the Indian Ocean increased during LGM, resulting in a higher oxic condition in LCDW.

doi : https://doi.org/10.1016/j.palaeo.2021.110766

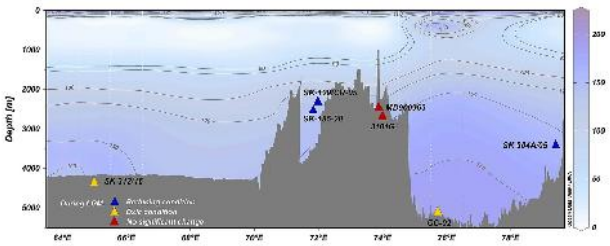

Figure 10: Compilation of redox condition during LGM in the northern Indian Ocean derived from trace element proxies. SK 312/16 (This study) and GC-02 (Pattan et al., 2005) lies in the lower circumpolar deep water (LCDW); SK-129/CR-05 (Pattan and Pearce, 2009), SK-185-20 (Sarkar et al., 1993), 3101G (Agnihotri et al., 2003), MD900963 (Pailler et al., 2002) and SK304A/05 (Chandana et al., 2017) lies in the upper circumpolar deep water (UCDW). The contour lines shows the modern oxygen concentration (μmol/kg) from World Ocean Atlas 2018 (Garcia et al., 2019).

(R. Bhushan, R. Nambiar & H. Raj)

Monsoon signature in corals from the northern Indian Ocean

The Indian monsoon signifcantly influences the sea surface conditions in the northern Indian Ocean. Corals growing in shallow waters record such monsoon-induced surface water changes. The record of monsoon signatures in the stable isotopic composition of the Porites coral skeleton from the Lakshadweep Islands, off the coast of South-western India, has been investigated. Corals record enhanced rainfall periods on the inter-annual scale along with seasonal changes in the sea surface temperature (SST) in their stable oxygen isotopic composition (δ^{18}O). Inter-colony variability observed in the δ^{18}O of the Lakshadweep corals was studied to decipher the δ^{18}O-SST relation of the region. The carbon isotopic (δ^{13}C) values for the coral show change during the monsoon period. The observed variations in the coral δ^{13}C values are modulated by other processes, along with its photosynthetic activity. The stable isotopic variation from the Lakshadweep coral demonstrated seasonal and inter-annual scales variability induced by monsoon activity. Thus, past monsoonal variations can be deciphered from long-term coral records from the Lakshadweep region.

doi : https://doi.org/10.1016/j.jmarsys.2021.103664

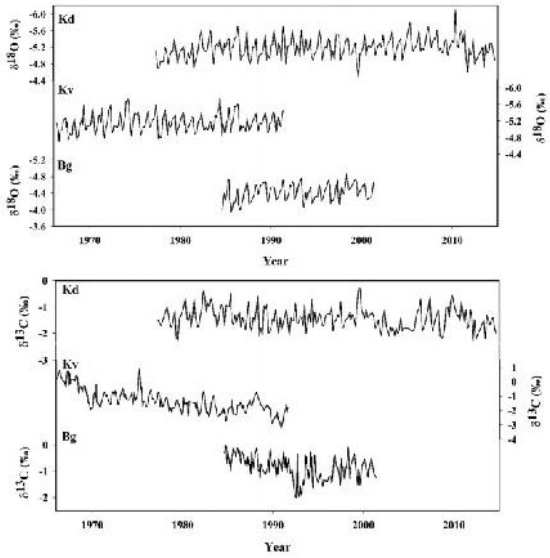

Figure 11: Stable isotopic (δ^{18}O and δ^{13}C) variation of the Kd coral (this study) and its comparison with Kv coral (Chakraborty and Ramesh, 1997), and Bg coral (Ahmad et al., 2011) from the Lakshadweep region.

(H. Raj, R. Bhushan, S. Kumar, U.S. Banerji, C. Shah & S. Verma)

Evidence of poorly ventilated deep Central Indian Ocean during the last glaciation

The Indian Ocean accounts for over 20% of the global ocean volume, nearly at par with the Atlantic, and possesses a unique hydrography characterized by turn-over entirely through exchange with the Southern Ocean, Pacific and Atlantic. Despite its volumetric and hydrographic importance, the role of the Indian Ocean in glacial-interglacial carbon cycle dynamics remains poorly constrained. Radiocarbon dates on foraminifera from two marine sediment cores have been used to decipher past changes in the 'radiocarbon ventilation age' of deep waters from the Central Indian Ocean (CIO) basin. Time-series spanning the last 37 ka show coherent variations in both sediment cores, and indicate greatly enhanced ocean-atmosphere radiocarbon disequilibrium in the region during the last glaciation, with peak ocean atmosphere radiocarbon age offsets occurring during Heinrich Stadial-1 (HS-1) and Heinrich Stadial-2 (HS-2). Uniquely, as compared to the bulk of existing radiocarbon data for the last deglaciation, CIO radiocarbon ventilation ages only approach modern values during

the Holocene, with Benthic-Atmosphere (B-Atm) offsets remaining $>3000^{14}$C yrs during the Bøolling-Allerøod period $\sim$15 ka BP. The more gradual rejuvenation of the CIO is supported by parallel oxygenation indicators, as well as existing stable isotope data and Nd isotope trends. Together, the data suggest that the CIO was isolated from well-ventilated North Atlantic sourced deep waters during the last glacial, and particularly during Heinrich stadials 2 and 1. These findings underline the important role played by the Indian Ocean in deglacial carbon cycle change, particularly in the latter half of the last deglaciation.

This work was done in collaboration with Prof. Luke Skinner from University of Cambridge, UK.

doi : https://doi.org/10.1016/j.epsl.2022.117438

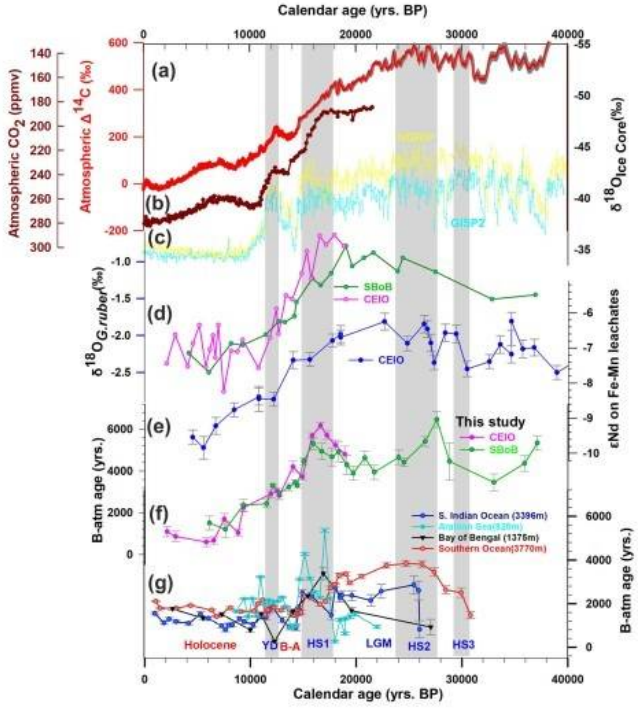

Figure 13: Paleo radiocarbon ventilation age estimates in the Indian Ocean & the Southern Ocean and its possible linkage with the atmospheric CO_2, atmospheric ^{14}, εNd and δ^{18}O (colored): (a) INTCAL20 atmospheric ^{14} in per mil (red) with ^{14} uncertainty in shaded gray (*Reimer et al., 2020*) (b) EPICA Dome C Ice core $_2$ data in ppmv (Brown) (*Monnin et al., 2004*) (c) NGRIP ice core 50 yr mean δ^{18}O record (yellow) and GISP2 ice core 50 yr mean δ^{18}O record (sky blue), placed on GICC05 timescale (*Rasmussen et al., 2014*; *Seierstad et al., 2014*). (d) δ^{18}O of G. ruber in CEIO (pink circle) & δ^{18}O of G. ruber in SBoB (green circle) (e) εNd in CEIO (SK129CR2; blue circle;*Piotrowski et al., 2009*) (f) Paleo-radiocarbon ventilation age or B-Atm age in CEIO (pink circle; this study), SBoB (green circle; this study) (g) Paleo-radiocarbon ventilation age or B-Atm age (water depth shown in the legend details) in the Southern Indian Ocean (blue circle; *Gottschalk et al., 2020*) Southern Ocean (red circle; *Skinner et al., 2010*), Arabian Sea (cyan square; *Bryan et al., 2010*) and Bay of Bengal (black circle; *Ma et al., 2019*). Light gray bands represent the major climatic event for the last 40 ka with events mentioned in the middle of the plot, red color represents the warm event and blue color represents the cold event. Calendar age in the x-axis is Bchron age of planktic foraminifera.

(N. Bharti, R. Bhushan, M. Muruganantham, P.S. Jena, A. Dabhi & A. Shivam)

Holocene monsoon and sea-level variability from coastal lowlands of Kerala, SW India

The widespread Early Holocene sea-level rise observed along the global coastal realms reinvigorated the need to decipher sea-level variability on a local and regional scale, yet limited attempts were made on simultaneously addressing sea-level and climate variability. The southwest coast of India is endowed with several geomorphic features providing cues on the paleosea-level and climate variability engrossed with its sedimentary sequence in the lowlands. In view of this, the present study aims to decipher the Holocene sea-level and climate variability based on geochemical and palynological proxies supported by 10 AMS radiocarbon ages on a 32m long sediment core (L7) raised from Upper Kuttanad Kole wetlands (Kuttoor), Kerala, Southwest India. The study demonstrated high sea-level along with warm and wet climate due to Indian summer monsoon (ISM) intensifcation during 9.69-7.56 ka corroborating with the Holocene Climate Optimum (HCO). However, a break in the sediment deposition is observed between 7.56 and 3.51 ka, the reason for which is yet to be fully understood. During 3.51-2.55 ka, the gradual weakening of ISM has been invoked with an intermittent monsoon spell during 3.20-3.40 ka. After 2.55 ka the sediment core records occurrence of coarser clastics indicating sediment deposition by the migrating distributary channel of the Pamba-Manimala rivers. The high sea level during HCO attests that the core location plausibly represented the southward extension of the Vembanad lagoon which transformed into part of the terrestrial system due to the gradual sea regression during the mid-late Holocene period followed by deposition of alluvial sediments from the hinterland rivers.

This work is primarily by J. Shaji, U. Banerjee, K. Maya, K.B. Joshi, and D. Padmalal from NCESS, Trivandrum and done in collaboration. PRL provided chronology of the core from the coastal lowlands of Kerala with AMS Radiocarbon dates.

doi : https://doi.org/10.1016/j.quaint.2022.03.005

(A.J. Dabhi, N. Bharti & R. Bhushan)

Holocene variability in chemical weathering and ocean redox state: A reconstruction using sediment geochemistry of the Arabian Sea

Major and trace elemental geochemistry of a sediment core (SSK40/GC10; water depth $\sim$50 m) from the eastern Arabian Sea have been investigated to reconstruct the continental weathering pattern and ocean redox state between 7.2 and 0.8 kyr BP (kyr, hereafter). The covariations of Fe/Al with K/Al and Ti/Al ratios indicate that the western-flowing Indian rivers (e.g., Narmada, Tapi, and Mahi) and eolian supply from the Thar regions are the major sediment suppliers to this location. Factor analysis of the geochemical dataset identifies four major factors explaining about 80% of the total variance. Down-core profiles of several detrital proxies (Fe/Al, Ti/Al, V/Al, and Co/Al) show that the sediment sources were nearly uniform until 2.6 kyr. In contrast, changes in provenance indices, K/Al ratios, and CIA* (modifed Chemical Index of Alteration) have been observed in the upper part of the core. The period of these weathering changes (2.6-1.6 kyr) mostly overlaps with the Roman Warm Period, indicating a weathering-climate linkage. Variations in the Ba/Al ratios and enrichment factors of U (EF-U) and Mo (EF-Mo), along with TOC/Al,

and S/Al trends, indicate a punctuating oceanic (bottom water) redox state during the studied period. These trends point to a shift from oxic to anoxic bottom water condition since ∼4.2 kyr. The timing of this change is synchronous to the earlier reported drought phase at the beginning of the Meghalayan stage, underscoring climatic control on the bottom water redox state.

This work was primarily from IISER, Pune of Gyana Ranjan Tripathy and Anupam Samanta, in collaboration with Dr. B. Nagendra Nath from NIO, Goa, and with Dr. Rajani Panchang from Pune University and Dr. Ankush Shrivastava from Mohanlal Sukhadia University, Udaipur. PRL provided chronology of the core from the Arabian Sea with AMS Radiocarbon dates.

doi : https://doi.org/10.1016/j.jseaes.2021.105029

(R. Bhushan and N. Bharti)

Historical variations in autochthonous and allochthonous sediment supplies to the largest freshwater lake in Central India

Lacustrine sediment preserves high-resolution biogeochemical records of past variations in watershed processes controlling lake sedimentation.The current study explores historical variations in autochthonous and allochthonous sediment supplies to a large tropical freshwater lake system (Upper Lake, Bhopal) protected under the international Ramsar Convention of 2002 against anthropogenic pressures. For this purpose, multi-proxy biogeochemical data are presented for organic matter (total organic carbon, total nitrogen, phosphorous, and loss on ignition [LOI] at 550^0C), carbonate (LOI at 950^0C), lithic sediment (aluminum, titanium, iron, calcium, magnesium, sodium, potassium, manganese, zirconium, niobium, hafnium, tantalum, thorium, uranium, and rare earth elements), and anthropogenic inputs (lead) measured in a 38 cm long sediment core retrieved from the lake. In addition to the lacustrine sediment core, the samples of catchment bedrock, surface soils, major stream sediment, and eolian dust collected from the lake periphery also are analyzed. The systematic biogeochemical excursions in the upper core section (top ∼8 cm) indicate increased anthropogenic inputs, watershed denudation by agricultural activities, artificially reduced fluvial sediment supply, relatively increased dust inputs and lake eutrophication in the last few decades. The current study underscores the roles of anthropogenic land-use and wetland conservation practices in the rapid alteration of autochthonous and allochthonous sediment supplies to open aquatic ecosystems. Further, rising lake eutrophication levels despite a managed reduction in allochthonous sediment supplies seem challenging to control due to dissolved nutrient supply from urban sewage discharge and runoff from agricultural land in the watershed.

This work is primarily by. Nafees Ahmad, Satinder Pal Singh, Aasif Mohmad Lone and Abul Qasim from IISER, Bhopal done in collaboration with Gyna Ranjan Tripathy from ISER, Pune. PRL provided chronology for the lake section using ^{210}Pb.

doi : https://doi.org/10.1016/j.ijsrc.2022.02.008

(R. Bhushan and C. Shah)

Diurnal Variability in the Spectral Characteristics and Sources of Water-Soluble Brown Carbon Aerosols over Delhi

It is well established that light-absorbing organic aerosols (commonly known as brown carbon, BrC) impact climate. However, uncertainties remain as their contributions to absorption at different wavelengths are often ignored in climate models. Further, BrC exhibits differences in absorption at different wavelengths due to the variable composition including varying sources and meteorological conditions. However, diurnal variability in the spectral characteristics of water-soluble BrC (hereafter BrC) is not yet reported.

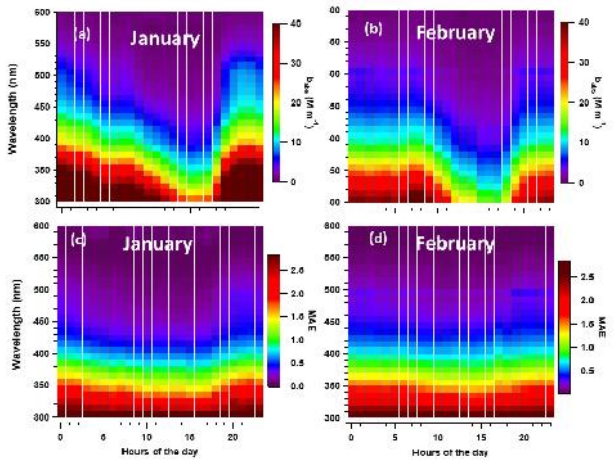

Figure 14: Diurnal variability in (a) BrC spectra during January and (b) BrC spectra during February, and in (c) MAE during January and (d) MAE during February

This study presents unique measurement hitherto lacking in the literature. Online measurements of BrC were performed using an assembled system including a particle-into-liquid sampler, portable UV-Visible spectrophotometer, and total carbon analyzer (PILS-LWCC-TOC). This system measured the absorption of ambient aerosol extracts at the wavelengths ranging from 300 to 600 nm with 2 min integration time and water-soluble organic carbon (WSOC) with 4 min integration time over a polluted megacity, New Delhi. Black carbon, carbon monoxide (CO), nitrogen oxides (NOx), and the chemical composition of non-refractory submicron aerosols were also measured in parallel. Diurnal variability in absorption coefficient (0.05 to 65 Mm^{-1}), mass absorption efficiency (MAE, 0.01 to 3.4 m^{-2} gC^{-1}) at 365 nm, and absorption angstrom exponent (AAE) of BrC for different wavelength range (AAE300-400: 4.2-5.8; AAE400-600: 5.5-8.0; and AAE300-600: 5.3-7.3) is discussed. BrC chromophores absorbing at any wavelength showed minimum absorption during afternoon hours, suggesting the effects of boundary layer expansion and their photo-sensitive/volatile nature. On certain days, a considerable presence of BrC absorbing at 490 nm was observed during nighttime that disappears during the daytime. It appeared to be associated with secondary BrC. Observations also infer that BrC species emitted from the biomass and coal burning are more absorbing among all sources. A fraction of BrC is likely associated with trash burning, as inferred from the spectral characteristics of Factor-3 from the PMF analysis of BrC spectra. Such studies are essential in understanding the BrC characteristics and their further utilization in climate models.

This study was led by PRL and carried out in collaboration with researchers from IIT-Kanpur, IIT-Delhi, and Paul Scherrer Institute, Switzerland.)

doi : https://doi.org/10.1016/j.scitotenv.2021.148589

(N. Rastogi, R. Satish & A.Singh)

Remarkably High Oxidative Potential of Atmospheric $PM_{2.5}$ Coming from a Large-Scale Paddy-Residue Burning over the Northwestern Indo-Gangetic Plain

High $PM_{2.5}$ (particulate matter with an aerodynamic diameter 2.5 μ or less) concentrations are known to cause severe chronic cardiovascular and respiratory diseases. The present study assesses the dithiothreitol (DTT)-based oxidative potential (OP) measured on $PM_{2.5}$ filters extracted with a mixture of water and methanol. $PM_{2.5}$ samples were collected during paddy-residue burning that occurs every year in the northwest Indo-Gangetic Plain (IGP) during October-November. The entire study period was classified into four categories: pre-intense burning, Diwali, intense burning, and post-intense burning.

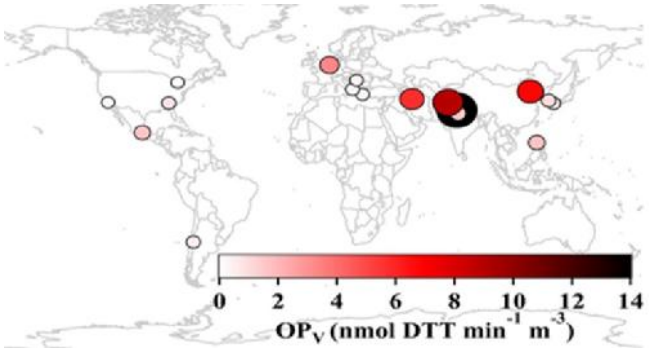

Figure 15: Worldwide comparison of volume-normalized OP

On average, $PM_{2.5}$ mass concentration were 154$\pm$59, 340$\pm$74, 271$\pm$122 and 156$\pm$19 μg m^{-3}; volume-normalized OP (OPV) were 7.6$\pm$2.8, 9.4 $\pm$ 1.1, 14 $\pm$ 5.1 and 12 $\pm$ 1.9 nmol DTT min^{-1} m^{-3}; and mass-normalized OP (OPM) were 51$\pm$18, 29$\pm$7, 55$\pm$12 and 78$\pm$9 pmol DTT min^{-1} μg^{-1} during pre-intense burning, Diwali, intense burning and post-intense burning periods, respectively. The intense burning period was associated with a relatively high mass fraction of organic aerosols compared to Diwali that was associated with relatively more fraction of inorganic aerosols. It likely caused higher OPV during the intense burning period compared to Diwali, which highlights the role of chemical composition in $PM_{2.5}$ OP. The observed OPV during the intense burning period is the globally highest reported value (average 14 nmol DTT min^1 m^3). Biomass burning markers, such as OC/EC and K^+/EC, correlated significantly with OP_V during the intense burning period, attesting the role of burning emissions on the observed OP. The relationship of OP_{OC} (ratio of OP^V and organic carbon (OC) mass concentration) with specific brown carbon chromophores during the post-intense burning period indicates the plausible link between atmospheric aging of redox-active organic aerosols and their optical properties. Development of mitigation strategy for such intrinsically high DTT-active $PM_{2.5}$ is important to avoid a wide array of possible health effects to the inhabitants of the study and downwind regions.

In this study, the aerosol sampling assistance was provided by Prof. Darshan Singh, and Dr. Atinderpal Singh, Punjabi University, Patiala.

doi : https://doi.org/10.1021/acsearthspacechem.1c00125

(A.Patel, R.Satish & N.Rastogi)

Signatures of natural to anthropogenic transition in a Himalayan lake sediments

Stable isotopic compositions of carbon (C) and nitrogen (N) in lake sediments have the potential to decipher natural and anthropogenic influences in a region, which has undergone significant cultural changes in the recent past. In this study, using carbon (δ^{13}C) and nitrogen (δ^{15}N) isotopic compositions of organic matter along with C isotopic ratio of black carbon ($\delta^{13}C_{BC}$) in sediments collected from a lake in the Lesser Himalaya, an attempt was made to decipher the biogeochemical changes in the lake under natural and anthropogenic stresses along with fire history of the region.The sediment core, dated using ^{210}Pb and ^{137}Cs, went back to 1949 AD, where isotopic compositions and elemental ratios (TOC/TN) suggested that the lake biogeochemistry was largely controlled by in-lake primary productivity. A noticeable change in isotopic compositions and elemental ratios was observed in the early 1970s, possibly due to increased input of soil organic matter from the catchment, which coincided with the urbanization and other human interventions in the region. At the same time, a consistent increase in differences between the measured and Suess effect corrected ^{13}C of organic matter from the early 1970s to 2016 AD indicated towards the increased utilization of fossil fuel-induced atmospheric CO_2 by the lake biota. Also, a sudden shift in $\delta^{13}C_{BC}$ in the early 1970s showed an increase in fossil fuel-induced black C in the region during that time. Overall, a comparison of the current study with other lakes in the region revealed the effect of land use change and population growth on the lake biogeochemistry, which was clearly recorded in elemental contents and stable isotopic composition of different components of lake sediments.

doi : https://doi.org/10.1016/j.apgeochem.2021.105095

(A.Rahman and S.Kumar)

Potential role of priming effect in the open ocean oxygen minimum zones

In contrast to earlier postulation that enhanced surface production is the sole source of organic carbon to heterotrophic respiration in open ocean as well as in oxygen minimum zones, recent studies provided evidences for the lateral transport of terrestrial organic carbon from continental margin to open ocean, supporting terrestrial organic carbon subsidized open ocean heterotrophy. However, actual sink mechanism of terrestrial organic carbon in the ocean remains to be resolved. “Priming effect” has been speculated to be possible sink mechanism of terrestrial organic carbon in ocean; however, realm in the ocean where the priming effect occurs is unknown. Since “elevated organic carbon re-mineralization” is one of the dominant causes of

sustenance and expansion of oxygen minimum zones, in this study, it was hypothesized that priming effect could be a significant contributor for the same. Based on the studies conducted so far, it appeared that nutrient scavenging could be the dominant mechanism of priming effect in oxygen minimum zones.

doi : https://doi.org/10.1007/s10750-021-04574-1

(P. Ragavan and S. Kumar)

Hydrological characteristics of the Bay of Bengal water column using oxygen isotopes

The Bay of Bengal, the eastern part of the northern Indian Ocean, experiences a reversal of monsoonal winds that control its surface and subsurface hydrological characteristics. Due to the limited number of studies, many aspects of the Bay of Bengal water column, particularly its deep hydrodynamic characteristics, are not thoroughly understood. For this purpose, oxygen isotopic compositions of water (δ^{18}O), a potential tracer of oceanographic study, were measured at twelve discrete depths at eight locations in the central Bay of Bengal during the summer monsoon. The water columns were sampled to include surface ($\leq$10 m), subsurface zone (25, depth of Deep Chlorophyll Maxima, 75, and 100 m), intermediate zone (150, 200, 300, and 500 m) and deep zone (1000, 1500, and 2000 m). Slopes of δ^{18}O-salinity relationships at the surface and subsurface zones were similar. The δ^{18}O and salinity showed an increasing southward trend at the surface, subsurface, and intermediate zones, which could be attributed to the influx of relatively saline and ^{18}O enriched water from the Arabian Sea through Southwest Monsoon Current. The TS characteristics along with the negative slope of δ^{18}O-salinity in the intermediate zone (-0.51 $\pm$ 0.14) indicated the presence of Indonesian Throughflow water in the Bay of Bengal. Temporal variation in δ^{18}O and slope of δ^{18}O-salinity relationship in the intermediate zone was also observed, possibly indicating variable contribution of Indonesian Throughflow water mass through time. The δ^{18}O of the deeper water showed the signature of existence of North Atlantic Deep Water in the Bay. Mesoscale eddies, a frequent phenomenon in the Bay of Bengal, also seem to modulate the δ^{18}O-salinity relationship in the basin.

doi : https://doi.org/10.1016/j.csr.2021.104491

(A. Rahman and S. Kumar)

Reassessing riverine carbon dioxide emissions from the Indian subcontinent

Anthropogenic perturbations are increasing uncertainties in estimating CO_2 emissions via air-water CO_2 flux (FCO_2) from large rivers of the Indian subcontinent. This study aimed to provide an improved estimate of the total FCO_2 from the subcontinental rivers by combining calculations of the partial pressure of CO_2 (pCO_2) in eight major rivers with new measurements in the Ganges and Godavari. The average CO_2 in the two newly surveyed rivers, including tributaries, wastewater drains, and impoundments, were 3-6 times greater than the previously reported values. In some highly polluted urban tributaries and middle reaches of the Ganges that drain metropolitan areas, the measured pCO_2 exceeded 20,000 μatm, $\sim$40 times the background levels of the headwaters originating in the carbonate-rich Himalayas. The high pCO_2 above 28,000 μatm in the lower reach of the Godavari was seven times the moderate levels of pCO_2 in the headwaters of the volcanic Deccan Traps, indicating enhanced CO_2 production in soils and anthropogenic sources under favourable conditions for organic matter degradation. Across the northern rivers, pCO_2 exhibited a significant negative relationship with dissolved oxygen, but a positive relationship with inorganic N or P concentrations. The strong influence of water pollution on riverine pCO_2 suggests that CO_2 emissions from hypoxic, eutrophic reaches can greatly exceed phytoplanktonic CO_2 uptake. Spatially resolved pCO_2 data, combined with three gas transfer velocity estimates, provided a higher range of FCO_2 from the subcontinental rivers (100.9-130.2 Tg CO_2.yr) than the previous estimates (7.5 - 61.2 Tg CO_2.yr). The revised estimates representing 25% of the global riverine FCO_2 illustrate the importance of the Indian subcontinental rivers under increasing anthropogenic pressures in constraining global inland waters FCO_2.

This is a collaborative study involving scientists from Korea, Bangladesh, India, and Germany.

doi : https://doi.org/10.1016/j.scitotenv.2021.151610

(S. Kumar)

Geochemistry of rodingites from the northeast India ophiolites: Petrogenetic significance and timing of rodingitization

The Indo-Myanmar Range is thought to represent a relict eastward-dipping subduction zone that runs from the eastern edge of the Himalayan Range. In the Indo-Myanmar Ophiolite (IMO) Belt rodingite is present as discontinuous lenses, dikes, and small- to medium-sized blocks in the serpentinized zones of ultramafic rocks. Petrological and geochronological studies of rodingite from the IMO Belt have been carried out to characterize and elucidate the timing and genesis of the rodingite. Petrography and mineral chemistry indicate that rodingites are composed of grossular garnet, vesuvianite, diopside, tremolite, actinolite, chlorite, albite, prehnite, apatite, and sphene (titanite). The investigated rodingite samples show variability in mineralogical assemblage and geochemical composition. Two mineral assemblages have been identified: (a) grossular, diopside, vesuvianite, apatite, and titanite, observed in veins and dikes; (b) chlorite, epidote, prehnite, diopside, apatite, anatase, and sphene.. Rodingites are classified into different categories based on their occurrence, and mineralogical and chemical composition. Subtype 1B rodingite is enriched in Al_2O_3 and incompatible trace elements, most likely formed during seawater infiltration as it contains minerals typically formed during ocean floor alteration. Subtypes 1A and Type 2 rodingite are highly enriched in CaO, Fe_2O_3T, MgO, and compatible trace elements. The formation of these types of rodingites probably followed serpentinization of the oceanic lithosphere as they contain minerals characteristic of high-Ca, low-Si fluid infiltration. These variations might have resulted due to infiltration of a metasomatic fluid that interacted with two different protoliths or infiltration of different fluids that may have interacted (at different times) with the same protolith. Complex variations in mineral assemblages and chemical compositions of Subtype 1 and Type 2 rodingites are the result of compositional variations in their protoliths and the degree of rodingitization. Our data indicate that the T of formation for the investigated rodingites varied from $\sim$435 to $\sim$200^{0}C, corresponding to greenschist facies. The T estimates deduced from the mineralogy of rodingites are consistent with the ambient T during cooling of an

oceanic lithospheric slab. Development of a low- to medium-T oceanic environment may be a result of exothermic reactions concurrent to serpentinization.

This work was carried out in collaboration with Dr. M. Bidyananda, Manipur University, Imphal

doi : https://doi.org/10.1002/gj.4301

(A.D. Shukla)

Sr-isotope stratigraphy of Phosphorite from the Zagros Fold-Thrust Belt, Iran

The Zagros phosphogenic horizon, hosted by the Eocene-Oligocene Pabdeh Formation, is located in the NW-SE-trending Zagros Fold-Thrust Belt (ZFTB), Iran. These phosphorites, which formed along the Tethyan Realm, are the most important and highest-grade phosphatic resources of Iran. Petrographic studies indicate that the main components of the ZFTB phosphatic horizons are pellet, ooid, intraclasts, and bone fragments and various microfossils, which are common in other Tethyan phosphorites. The trace elements and rare earth elements data in the majority of the studied samples suggest that these deposits are reflecting the original REE signature of the paleo-seawater. Based on petrographic evidences these phosphorite samples were selected for the analysis of Sr isotope in order to ascertain the stratigraphy of these deposit.The Sr-isotope stratigraphy is based on the premise of the pristine signature of the Seawater which could have been the source and responsible for the precipitation of Sr bearing carbonates or phosphates. By the analysis of Sr isotopes in unaltered mineral phases one can assign the age based on the evolution curve of through time on Earth. It is observed that the measured $^{87}Sr/^{86}Sr$ values with the Eocene secular seawater curve suggests a Lutetian age (47.8 and 41.2 m.y.) for the Sheykh-Habil deposit and a Priabonian age (37.8 and 33.9 m.y.) for the Kuh-e-Sefid and Kuh-Rish deposits. The Zagros and eastern Mediterranean phosphorites, which form part of the Tethyan Phosphogenic Province over a period of $\sim$50 m.y., developed in a long ($\sim$7000 km) and narrow ($<$800 km) east-west trending marine channel system. Apart from Sr isotope stratigraphy the $\delta^{18}O_{C_{arb}}$ values from the studied samples indicate minimal weathering, while the obtained $\delta^{13}C_{C_{arb}}$ values support an unaltered authigenic origin, as has been proposed for other eastern Mediterranean phosphorites.

The negative shifts evident in the $\delta^{13}C_{C_{arb}}$ data and presence of glauconite are consistent with precipitation of the Zagros phosphorites in a shallow marine environment, most likely a mid- to outer ramp setting at a depth of $\sim$150 m within which the Pabdeh Formation is believed to have been deposited.

This work was carried in collaboration Prof. Alireza, arasvandi, Shahid Chamran University of Ahvaz, Ahvaz, Iran

doi : https://doi.org/10.1016/j.oregeorev.2021.104563

(A.D. Shukla)

Temporal variations in the chemical composition of aerosols over the coastal Bay of Bengal

Variations in source, ionic composition and carbonaceous components of aerosols are expected in the atmosphere over the coastal Bay of Bengal due to reversing the direction of winds from winter to summer (BoB). To examine this monthly, samples were collected at the weekly interval between March 2016 and February 2017 in the coastal BoB. The air mass back trajectories suggested that the study region received aerosols from Indo-Gangetic Plain from October to February whereas from central India during June to September and south or southwest during March to May. A higher concentration of total suspended particulate matter (TSP) was observed from November to February (winter) compared to other months. The concentration of sulphate contributed more than half of water-soluble inorganic species followed by sodium, ammonium and nitrate. The dominant contribution of anthropogenic SO_4^{2} ($>$90%) to total SO_4^{2} was observed. The ambient elemental carbon loadings and organic carbon to EC ratios indicate the dominant contribution of biomass burning emissions in the study region. The significant contribution of non-sea salt sulphate and nss-K^{+} indicates a dominant contribution from the continental sources throughout the year. The mass ratio of NO^{3}/anthropogenic SO_4^{2} suggests stationary sources (i.e., coal burning in power plants) contribute significantly over vehicular emissions during the entire study period. The estimated secondary aerosols accounted for $\sim$50% of organic carbon and 7% of TSP in the study region. This study has implications for understanding the source, composition and nature of aerosols and possible impacts on coastal water upon its deposition.

This work was carried out in collaboration with Dr. V.V.S.S. Sarma, CSIR-NIO, RC Vishakhapatanam.

doi : https://doi.org/10.1016/j.apr.2021.101300

(A.K. Sudheer and M. Gaddam)

Carbonaceous aerosols and their light absorption properties over the Bay of Bengal during continental outflow

The marine atmosphere of the Bay of Bengal (BoB) is prone to get impacted by anthropogenic aerosols from the Indo-Gangetic Plain (IGP) and Southeast Asia (SEA), particularly during the northeast monsoon (NEM). We quantified and characterized carbonaceous aerosols and their absorption properties collected in two cruise campaigns onboard ORV Sindhu Sadhana during the continental outflow period over the BoB. Aerosol samples were classified based on the air mass back trajectory analyses, wherein samples were impacted by the continental air parcel (CAP), marine air parcel (MAP), and mix of both (CAP+MAP). Significant variability in the PM_{10} mass concentration (in μg m^3) is found with a maximum value for MAP samples (75.5$\pm$36.4) followed by CAP + MAP (58.5$\pm$27.3) and CAP (58.5$\pm$27.3). The OC/EC ratio ($>$2) and diagnostic tracers i.e. nss-K^{+}/EC (0.2–0.96) and nss-K^{+}/OC (0.11–1.32) along with the absorption angstrom exponent (AAE: 4.31–6.02) and MODIS (Moderate Resolution Imaging Spectroradiometer) derived fire counts suggest the dominance of biomass burning emission sources. A positive correlation between OC and EC (i.e. r = 0.86, 0.70, and 0.42 for CAP, MAP, and CAP + MAP, respectively) further confirmed the similar emission sources of carbonaceous species.

Similarly, a significant correlation between estimated secondary organic carbon (SOC) and water-soluble organic carbon (WSOC; r = 0.99, 0.96, and 0.97 for CAP, MAP, and CAP + MAP, respectively) indicate their similar chemical nature as well as dominant contribution of SOC to WSOC. The absorption coefficient ($b_{abs-365}$) and mass absorption efficiency ($MAEB_{rC-365}$) of the soluble fraction were estimated at 365 nm wherein, $b_{abs-365}$ showed a linear relationship with WSOC and nss-K^+, signifying the contribution of water soluble brown carbon from biomass burning emissions.

This work was carried out in collaboration with Dr. Ashwini Kumar, CSIR-NIO, Goa.

doi : https://doi.org/10.1039/D1EM00347J

(A.K. Sudheer)

Increase in summer monsoon rainfall over the northeast India during El Niño years since 1600

El-Niño Southern Oscillation (ENSO) affects Indian Summer Monsoon (ISM) at interseasonal to interannual time scales. Given the heterogeneity in rainfall patterns over India, we have revisited the linkages between El Niño and ISM for the period 1600-2016 in this study. Our analysis based on the instrumental, paleo-proxy, model and satellite data sets show significant spatiotemporal variation in the ISM in response to El Niño. We observed strengthening of ISM over the northeast India (NEI) in conjunction with El Niño events. We suggest that the decadal trends in ISM over the NEI and central India (CI) were controlled by the long term variation in strength of El Niño events. We observed spatial variation in isoGSM derived rainfall and its oxygen isotopic composition ($\delta^{18}O$) in response to El Niño events. We further verified our observations from isotope proxy palaeo-records. Two high resolution speleothem (cave deposits) records of reconstructed ISM during 1600-2008 confirmed the inverse relation of rainfall patterns over CI (negative) and NEI (positive) during moderate to strong El Niño periods. These speleothem records infer a long-term pause in the El Niño (or stronger La Niña) like conditions, which were persisted during 1625-1715 and favored the stronger (weaker) rainfall over the CI (NEI). Furthermore, speleothem records showed stronger El Niño events during 1715-1760 causing significant reduction and enhancement in rainfall amount over CI and NEI, respectively.

doi : https://doi.org/10.1007/s00382-021-05743-7

(P. Kiran Kumar and A. Singh)

Strengthening of basin-scale ocean currents in winter drives decadal salinity decline in the eastern Arabian Sea

Observations show a decreasing trend in sea surface salinity during the winter months in 1990-2010 in the southeastern Arabian Sea.

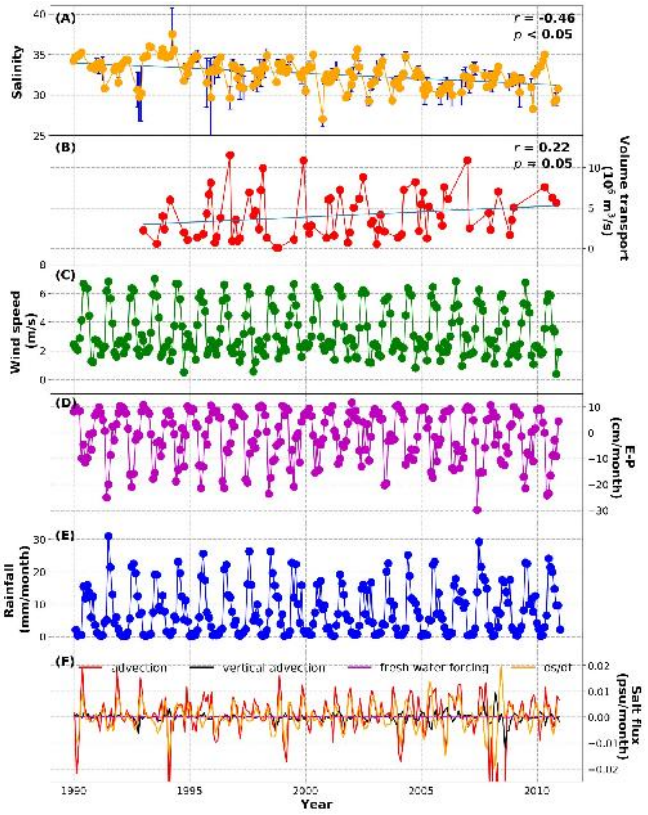

Figure 16: Monthly variation in (A) SSS at Mangalore coast, blue error bars represent standard deviation (1σ) of SSS measured at four stations in each month, (B) transport of water from the Bay to the Arabian Sea estimated at a region south of Sri Lanka as shown in Fig 16 (3.75^0N–5.87^0N, 80.5^0E–81.5^0E), (C) wind speed spatially averaged over the region between 6^0N–18^0N and 70^0E–78^0E, (D) Evaporation - Precipitation (E-P), (E) rainfall, and (F) mixed layer salt flux. Parameters presented in (D), (E) and (F) are spatially averaged over the region enclosing 10^0N–14^0N and 72^0E–76^0E.

To explain the observed salinity decline, we analyze changes in evaporation and precipitation, surface winds, sea level anomaly and the transport of low-salinity water from the Bay of Bengal to the eastern Arabian Sea via westward flow south of Sri Lanka and a northward coastal current. We find a 2-3 fold increase in the influx of low-salinity water to the eastern Arabian Sea in 1990-2010 associated with strengthening of the Northeast Monsoon Current and the West India Coastal Current. The observed decreasing trend of sea surface salinity in the southeastern Arabian Sea is due to the changes in basin-scale circulation of the northern Indian Ocean in winter (Fig. 16).

doi : https://doi.org/10.1029/2021GL094516

(M. Varna, D. Sahoo & A. Singh)

Role of eddies and N_2 fixation in regulating C:N:P proportions in the Bay of Bengal

Recent observations and numerical simulations have profoundly established that the C:N:P ratios in the ocean deviate from the canonical Redfield Ratio (106:16:1). Physical and biogeochemical processes have been hypothesized to be responsible for this deviation. However, a paucity of concurrent observations on biogeochemical and physical parameters have barred us to understand their exact role on the C:N:P ratios. For this purpose, we have sampled the Bay of Bengal for its C, N, and P contents in the organic and inorganic pools from 5 to 2000 m depth at eight stations (five coastal and three open ocean) during boreal spring 2019. Mesoscale anticyclonic eddies were identified at two of the sampling stations, where nutrient concentrations were lower in the top layer (5 m to the depth of chlorophyll maximum) compared to those at the non-eddy stations. Mean (NO_3 + NO_2):PO_4^{3} ratio was lower at the anticyclonic eddy stations compared to that at the non-eddy stations in the top layer. Yet C:N:P ratios in the particulate and dissolved organic matter in the top layer were the same at anticyclonic eddy and non-eddy stations. Overall the mean C:N:P ratios were 249:39:1 in particulate organic matter and 2338:146:1 in dissolved organic matter in the top layer. Biological N_2 fixation was not a driver in controlling the N:P ratio of the export flux and the subsurface water nutrient ratios during spring (Fig. 17). Although the Bay of Bengal receives large riverine influx, its influence in changing the C:N:P ratios was small during this study.

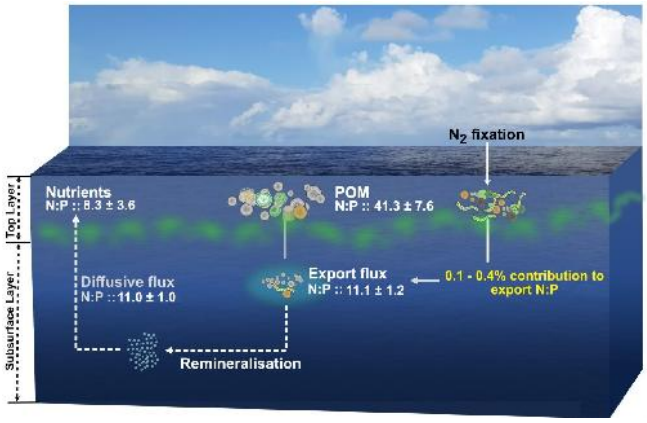

Figure 17: A schematic representing N:P ratio in the Bay of Bengal during spring 2019.

doi : https://doi.org/10.1007/s10533-021-00833-4

(D. Sahoo, H. Saxena, S. Nazirahmed, S. Kumar, A.K. Sudheer, R. Bhushan and A. Singh)

Impact of Indian Summer Monsoon Change on Ancient Indian Civilizations During the Holocene

Based on some marine and terrestrial climate data the role of Indian Summer Monsoon (ISM) on the cultural shifts in the Indian subcontinent for the last 10 kyr was assessed. The two major climate events at 8.2 kyr and 4.2 kyr BP are evident in most of the climate proxies. Though the 8.2 kyr event influenced the ISM significantly, but its role on the civilization is not obvious mainly due to lack of early Holocene archaeological data in the Indian subcontinent. The collapse of the Harappan Civilization was probably due to the weakening of the Indian Summer Monsoon after 4.2 kyr BP. However, the estimates of the variations of the monsoon strengths made in the study were qualitative. It is very important to quantitatively estimate the past variation of monsoon for assessing its possible impact in future human settlements. This can be achieved with some recently developed non-traditional isotope proxies.

This work was done in collaboration with Dr. A. Bohra, National Geophysical Research Institute, Hyderabad

doi : https://doi.org/10.3389/feart.2021.709455

(A.H. Laskar)

Impact of suboxic coastal water conditions on Mo isotopic composition (δ^{98}Mo) in northern Bay of Bengal

Molybdenum is the most abundant transition metal in the ocean and plays important role in regulating several biogeochemical processes (e.g., nitrogen fixation). Further, due to its linkage with the redox transformations, Mo isotopic composition (defined as δ^{98}Mo) can be used as an excellent tracer to understand past oceanic redox changes. The Mo isotopic composition of seawater at any point of time depends on its various sources and sink to/from the ocean. The dissolved riverine supply is the most dominant source of Mo in the ocean. Thus, changes in Mo isotopic composition of the riverine supply can influence the seawater Mo isotopic composition. Based on the analysis of few crustal materials (granites, clastic sediments), it has been estimated that average Mo isotopic composition of the Earth's crust is very close to 0. However, the present-day seawater δ^{98}Mo ($\sim$2.3) is significantly heavier than the average continental crustal value. This has been primarily attributed to the large isotopic fractionation of Mo during its adsorption onto Mn nodules and ferromanganese crusts. However, another point to consider that various processes operating in the rivers, estuaries and coastal zones can significantly influence the Mo isotopic composition of input to the ocean. Reductive dissolution of Fe/Mn^{-}(oxyhydr)oxide phases, and degradation of organic matter notably within high-Mo organic-rich muds in the costal zones can provide lighter than seawater Mo to the coastal waters. To understand all these processes, sediments and seawater samples were collected from the coastal Bay of Bengal region. These collected samples were subsequently analyzed for δ^{98}Mo at PRL. The obtained results showed, for the first time, lighter than seawater δ^{98}Mo in the water column of the northern coastal Bay of Bengal (average = 1.64 $\pm$ 0.42; 1σ). Based on the analyses of sediments, it was estimated that around 5-11% of Mo fraction is adsorbed on Fe-Mn oxyhydroxide phase, which can be easily released to the water column under suboxic to anoxic conditions. The lighter δ^{98}Mo in northern coastal Bay of Bengal waters could be due to in-situ reduction and dissolution of Fe-Mn oxyhydroxide phases adsorbed on suspended particulate matter. In addition, dissolution of Fe-Mn hydroxides in the bottom sediments followed by injection of pore water to the water column along the continental margins can also supply lighter Mo to the coastal waters. Repeated cycles of deposition and reductive dissolution of sedimentary Fe-Mn oxyhydroxide phases in the shelf/slope regions could supply lighter Mo to the porewaters. Further, subsequent diffusion/advection of these porewaters to the

water column and/or dissolution of Fe-Mn oxyhydroxide phases in the suboxic water column could supply lighter Mo to waters of the northern coastal Bay of Bengal.

doi : https://doi.org/10.1016/j.gca.2022.03.010

(V. Goswami)

Re-Os and Sr Isotopic analyses of Permian-Triassic (P-Tr) sediments from the Himalaya: Understanding the chronology and carbonate diagenesis

Sedimentary rocks from the Himalaya are well-preserved archives of the Neo-Tethys oceanic conditions during the late Permian mass extinction (LPME) event. These records, however, lack precise radiometric age information, which restricts their paleo-oceanographic application. In this contribution, Re-Os isotopic systematics of organic-rich shales from the Gunguri Formation, Spiti Valley (Atargu section) and siltstones from the Khunamu Formation, Guryul Ravine, Kashmir have been investigated to better constrain their depositional ages. Further, Sr isotopic ratios of lower Triassic (Induan) carbonates from the Spiti valley have also been analyzed and compared with the global $^{87}Sr/^{86}Sr$ stratigraphy. Average Re (3 ± 2 ng/g; n = 15) and Os (87 ± 14 pg/g; n = 15) concentrations of the samples from these two sections are higher than those of upper continental crust (200 pg/g and 31 pg/g, respectively). The $^{187}Os/^{188}Os$ ratios of the Gunguri shales vary significantly (1.67 - 2.35), but linearly with their corresponding $^{187}Re/^{188}Os$ ratios (257-416). The Re-Os isochron for these shales yielded a depositional age of 252 $\pm$ 33 Ma (2σ; n = 7; MSWD = 6.5), which is consistent with its biostratigraphic information (FAD of Hidendous parvus). The initial $^{187}Os/^{188}Os$ ratio (0.61 $\pm$ 0.19) for the Spiti samples is similar to that reported for the late Permian shales, indicating connection of the Neo-Theyas with global ocean. In contrast to the Spiti samples, the Re-Os systematic does not yield meaningful age information for the Guryul ravine section, which was a proximal site with strong influence of strong seismic/Tsunami events during this period. Global compilation of $^{187}Re/^{188}Os$ ratios in late Permian shales from this and other available studies show large spatial variation with lower ratios for the Neo-Theyas ocean. Bathymetric distribution of the Re/Os ratios and environmental conditions along the paleo-latitude point to strong role of Re/Os uptake by macro-algae, in addition to oceanic pH and redox state, in regulating the Re-Os systematic in organic-rich sediments. The $^{87}Sr/^{86}Sr$ ratios for the Induan carbonates (dolomites) from the Spiti shale show wide variation (0.71551 to 0.71837). These Sr isotopic ratios are highly radiogenic compared to that expected for lower Triassic ocean ($\sim$0.707). Co-variation of Sr and $^{87}Sr/^{86}Sr$ with Mn concentrations establish post-depositional diagenetic alteration of these dolomites, which in turn led to highly radiogenic $^{87}Sr/^{86}Sr$ ratios.

This work was done in collaboration with Dr. G.R. Tripathy, IISER, Pune and his team.

doi : https://doi.org/10.3390/min11040417

(V. Goswami)

Changing atmospheric acidity as a modulator of nutrient deposition and ocean biogeochemistry

The atmospheric supply of available nutrients to the ocean has changed in magnitude and distribution as a consequence of global industrialization and will continue to evolve over time with economic development and changes in regulatory emissions frameworks. These changes will occur in parallel with expected future changes in climate, for example, changing humidity, rainfall amounts, and distribution, which will also affect the atmospheric nutrient delivery to the oceans through altered atmospheric lifetimes and changes in deposition mode as well as dust generation and biomass burning emissions. This research work (with my participation as Co-chair of United Nations GESAMP-Working Group on “Atmospheric input of chemicals to the ocean”) examines the combined impacts of atmospheric pH changes, brought about by evolving anthropogenic emissions, on labile nutrient deposition to the oceans and their expected effects on marine biogeochemistry. These changes likely alter the manner in which the sea surface microlayer (SML) influences atmospheric nutrient transport to the ocean and the impacts of nutrient deposition on marine microbial ecology. Future changes in emissions will continue to alter atmospheric acidity and nutrient deposition in the coming decades. The analysis presented here indicates that the acidity and liquid water content of atmospheric aerosol are key state parameters that profoundly influence the patterns, fluxes, and impacts of atmospheric nutrient deposition to the oceans. What controls acidity in the atmosphere? Acidity for any atmospheric particle is directly related to the concentration of hydronium ion (H_3O^+, or H_{aq}^+ for simplicity) in the aqueous phase of aerosol particles or cloud droplets. H_{aq}^+ is controlled by the relative amounts and nature of dissolved ions present in the solution. Sulfuric acid (formed through oxidation of SO_2) is the primary strong acid in the atmosphere. Because of its extremely low volatility, it resides almost exclusively in aerosol and cloud particles. It is partially neutralized by the uptake of NH_3 from the gas phase to form NH_4^+ ions and by non-volatile cations (e.g., K^+, Na^+, Ca_2^+, Mg_2^+) found in sea salt and mineral dust. The latter cations can also react with acidic gases, including HCl and HNO_3, and affect the acidity of aerosol and droplets. Aerosol particles and cloud and rain droplets have very different acidities and responses to changes in acidity, largely because of their very different liquid water contents. Cloud and rain waters are relatively dilute solutions, with substantially lower acidity (as much as 4 pH units) than aerosols. Acidity also varies strongly depending on aerosol particle size, with smaller particles generally being more acidic. This causes acid processing that increases trace element solubility to be most efficient in the 1 μm to 2.5 μm particle diameter range. Emissions of NH_3, NO_x, SO_2 and dust influence atmospheric acidity, while dust, anthropogenic trace element emissions, and anthropogenic and biological sources of P, NH_3 and NO_x contribute to the atmospheric nutrient/trace element burden. Most sources are terrestrial, although ship-based emissions of Fe and NO_x are important, and marine emissions of DMS are a significant source of SO_2, particularly in the southern hemisphere. Acidity-driven atmospheric processing alters the labile nutrient flux to the ocean, either by affecting gasaerosol partitioning or by altering the labile fractions of Fe, P and trace metals. Organic N compounds (OrgN) are also generated during atmospheric processing. Overall, changes in nutrient supply will affect the microbial ecology and productivity of the ocean (one of the climate stressors). Not enough is known about the properties of the SML to predict the influence of decreasing atmospheric acidity (which will occur concurrently with ocean acidification) on the SML's impact on atmospheric nutrient

deposition. Rainfall can disrupt the SML, so acidity-induced changes in deposition mode can also affect the atmosphere-to-bulk seawater nutrient transfer process. Changes in nutrient supply ratios (N:P, N:Fe, P:Fe) from atmospheric deposition over the timescale may alter phytoplankton communities (affecting taxonomy and nutritional quality) and lead to wider ecological changes in the ocean. There are many uncertainties in the influences of changing atmospheric acidity on nutrient inputs to the ocean. Accurate atmospheric chemical transport models are required to assess the magnitude and impacts of these changes, because the large spatial and temporal scales involved cannot be studied by observational programs alone. However, the development and validation of these models relies on the availability of appropriate high-quality observations. Current deficiencies in this research area include high-frequency, long-term monitoring of atmospheric composition over representative regions of the remote ocean and observations of wet deposition (the dominant input across large areas of the global ocean but whose amounts and composition are very poorly sampled). Ocean acidification (OA) will also induce feedbacks on the acidity of the atmosphere, because OA will affect the air-sea exchange of ammonia, and is also expected to influence the production of gases such as dimethyl sulfide and volatile amines that alter the balance of acidity in the atmosphere.

doi : https://doi.org/10.1126/sciadv.abd8800

(M M Sarin)

Programmable Automated Field Deploy-able High Frequency Rainwater Sampler /noindent YUKTI-Sanchita 2021: YS/PD-IP/337

Collection of the rainwater samples at desire time interval or cumulative sample over a certain time duration is an essential perquisite for modern hydro meteorological and environmental applications. Due to non-availability of commercially available, automated and programmable sampler, many new scientific ideas are awaiting implementation. The prototype of High Frequency Rainwater Sampler has already been developed last year at PRL and successfully tested to collect rainwater samples. This project has been selected in ISRO program named YUKTI- Sanchita 2021. YUKTI-Sanchita is a compilation of all Product Development/ Innovative project proposals from all DOS/ISRO centers at a single place. The mentioned project has been suitable to be taken up by Space Technology Incubation Center (S-TIC) as the project outcome has good market potential and can lead to the initiation of Start-up in the line of theme "**Aatmanirbhar Bharat**". During this program, one of the STIC will be awarded to develop project under the guidance of mentors from proposal origin DOS centers. The project has been awarded to Maulana Azad National Institute of Technology, Bhopal in collaboration with S-TIC. The objective of the project is to a) collect rainwater sample accumulated over certain time duration b) measure amount of rainfall c) detect the isolated rain events d) be monitored and operated remotely with real time sampling programme through a computer. The final prototype of Programmable Automated Field Deploy-able High Frequency Rainwater Sampler delivers at the end of this project will be very useful for meteorological stations, aggro-meteorological stations, universities, colleges, research and academic institutions interested in amount and intensity of rainfall and its chemical and isotopic composition together with time and duration of various rain events. The project has already been initiated and completed the concept development and literature study.

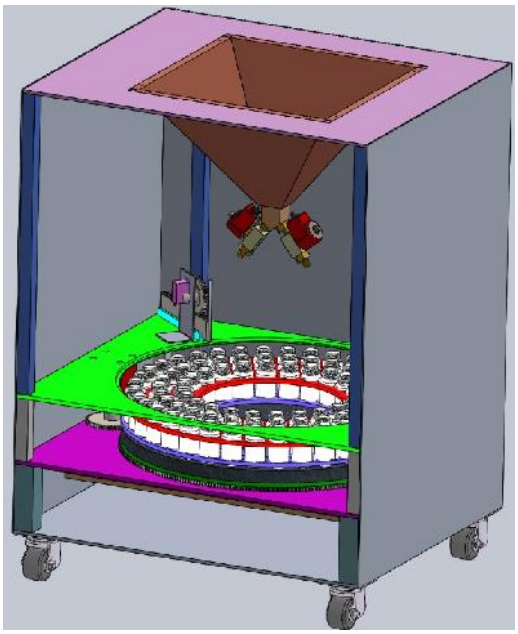

Figure 18: Rainwater Sampler developed at PRL (3D-image).

This work was carried out in collaboration with MANIT-Bhopal: Dr. Akhilesh Barwe and team members.

(M. Shah, H. Vaghela, R.D. Deshpande & L. Chavda)

Theoretical Physics

Thermodefect voltage in graphene nanoribbon junctions

Thermoelectric junctions are often made of components of different materials characterized by distinct transport properties. Single material junctions, with the same type of charge carriers, have also been considered to investigate various classical and quantum effects on the thermoelectric properties of nanostructured materials. We have introduced the concept of defect-induced thermoelectric voltage, namely, thermodefect voltage, in graphene nanoribbon (GNR) junctions under a temperature gradient. Our thermodefect junction is formed by two GNRs with identical properties except the existence of defects in one of the nanoribbons. We computationally demonstrate that the thermodefect voltage can be as high as 1.7 mV K^{-1} for 555777 defects in semiconducting armchair GNRs. Our study presents a new pathway to enhance the thermoelectric properties of nanomaterials.

This work was done in collaboration with Dr. Alhun Aydin [Harvard University, USA], Prof. Altug Sisman [Uppsala University, Sweden], Prof. Jonas Fransson [Uppsala University, Sweden], and Prof. Annica M. Black-Schaffer [Uppsala University, Sweden]

doi : https://doi.org/10.1088/1361-648X/ac553b

(Paramita Dutta)

Compact amplitudes for scalar mediated Higgs+2-jet production at the LHC

Concise and compact analytical expressions of one-loop Higgs$+4$-parton helicity amplitudes are derived when the circulating particle in the loop is a colour-triplet massive scalar instead of a massive quark. The utility of this study comes out to be twofold – (*i*) it reveals beautiful and fascinating relationship between the scattering amplitudes calculated in the scalar theory and fermion theory, (*ii*) compact analytic amplitudes, that are achieved in this case, make the numerical computation stable and faster facilitating the indirect search of Beyond Standard Model physics, for example Minimal Supersymmetric Standard Model, at the Large Hadron Collider (LHC). Many sophisticated methods such as on-shell recursion relation, momentum twistor *etc.* are employed to get these close-packed analytical results. Fortran readable format of these expressions are made public for better distribution and ready usage.

doi : https://doi.org/10.1088/1361-6471/abf7d6

(Satyajit Seth)

NNLO QCD corrections to the $\mathrm{W}(\to \ell\nu)+\gamma$ production at the LHC

Next-to-next-to-leading-order QCD corrected estimation of the $pp \to \mathrm{W}(\to \ell\nu)\gamma$ process at the LHC has been studied using N-jettiness slicing approach. This calculation is based entirely on the analytical amplitudes and therefore numerical evaluation of the code becomes at least four times faster than the Matrix code, which uses q_{T} subtraction method and employs OpenLoops to get one-loop amplitudes calculated numerically. Not only that, effect of non-diagonal CKM matrix is considered in this study and the impact of electroweak corrections is also investigated including, for the first time, the $\mathrm{O}(\alpha_s)$ quark-gluon initiated process which is numerically as important as the quark-antiquark initiated process. Results given in this paper are already used in the recent experimental analysis done by the CMS collaboration.

doi : https://doi.org/10.1007/JHEP07(2021)079

(Satyajit Seth)

$\frac{|\mathrm{V}_{ub}|}{|\mathrm{V}_{cb}|}$ and quest for new physics

Charged current semi-leptonic decays of B-meson are important for a precise determination of the Cabibbo Kobayashi Maskawa (CKM) elements. The twoelements, $|\mathrm{V}_{ub}|$ and $|\mathrm{V}_{cb}|$, show a discrepancy between the exclusive and inclusive determinations, and this is often taken as a hint of physics beyond the standard model. These determinations are however masked with hadronic and other uncertainties, and therefore can not be unambiguously taken as implying new physics. A new observable is proposed: the ratio of these two CKM elements, $\mathrm{R_V} \equiv \frac{|\mathrm{V}_{ub}|}{|\mathrm{V}_{cb}|}$. It is shown to receive negligible corrections due to hadronic as well as QED effects. Interestingly, there is an excellent agreement between $\mathrm{R_V}$ as constructed from exclusive determinations of $|\mathrm{V}_{ub}|$ and $|\mathrm{V}_{cb}|$ and that constructed from the inclusive determinations of these CKM elements. It can thus serve as an excellent tool for the test of the Standard Model.

doi : https://doi.org/10.1007/JHEP02(2022)130

(Anshika Bansal, Namit Mahajan, Dayanand Mishra)

Implications of the Dark-LMA solution for neutrino mass matrices

In this work we have re-investigated two different kinds of texture zero ansatz of the low energy neutrino mass matrix in view of the Dark-Large-Mixing-Angle (DLMA) solution of the solar neutrino

problem which can arise in the presence of non-standard interactions. In particular we revisit the cases of (i) one zero mass matrices when the lowest neutrino mass is zero and (ii) one zero texture with a vanishing minor. In our study we find that for most of the cases, the texture zero conditions which are allowed for the LMA solution, are also allowed for the DLMA solution. However, we found two textures belonging to the case of one zero texture with a vanishing minor where LMA solution does not give a viable solution whereas DLMA solution does. We analyze all the possible texture zero cases belonging to these two kinds of texture zero structures in detail and present correlations between different parameters. We also present the predictions for the effective neutrino mass governing neutrino-less double beta decay for the allowed textures.

doi : https://doi.org/10.1016/j.nuclphysb.2021.115460

(Srubabati Goswami, Ananya Mukherjee)

New Physics at nuSTORM

In this work we investigate the usefulness of the proposal nuSTORM, which is a facility that will use neutrinos from stored muons. We examined it's potential to probe of two scenarios beyond the Standard Model of particle physics. These are sterile neutrinos and non-unitarity of the neutrino mixing matrix. In this context we elucidate the role of nuSTORM, considering both charged current and neutral current events. The inclusion of the later can give rise to some improvements in the bounds on the new physics parameters. nuSTORM can provide stronger bounds on the parameters as compared to the other proposed experiments.

doi : https://doi.org/10.1103/PhysRevD.103.075009

(Srubabati Goswami, Kaustav Chakraborty)

Fermion mass hierarchies from supersymmetric gauged flavour symmetry in 5D

A mechanism to generate realistic fermion mass hierarchies based on supersymmetric gauged abelian symmetry in flat five-dimensional (5D) spacetime is proposed. The fifth dimension is compactified on S_1/Z_2 orbifold. The standard model fermions charged under the extra abelian symmetry along with their superpartners live in the 5D bulk. Bulk masses of fermions are generated by the vacuum expectation value of $N = 2$ superpartner of $U(1)_F$ gauge field, and they are proportional to $U(1)_F$ charges of respective fermions. This decides localization of fermions in the extra dimension, which in turn gives rise to exponentially suppressed Yukawa couplings in the effective 4D theory. Anomaly cancellation puts stringent constraints on the allowed $U(1)_F$ charges which leads to correlations between the masses of quarks and leptons. We perform an extensive numerical scan and obtain several solutions for anomaly-free $U(1)_F$, which describe the observed pattern of fermion masses and mixing with all the fundamental parameters of order unity. It is found that the possible existence of SM singlet neutrinos substantially improves the spectrum of solutions by offering more freedom in choosing $U(1)_F$ charges. The model predicts Z' boson mediating flavour violating interactions in both the quark and lepton sectors with the couplings which can be explicitly determined from the Yukawa couplings.

doi : https://doi.org/10.21468/SciPostPhys.10.6.154

(Ketan M. Patel)

Aspects of gravitational decoherence in neutrino lensing

Decoherence effects in neutrino flavour oscillations in curved spacetime are studied with particular emphasis on the lensing in a Schwarzschild geometry. Assuming Gaussian wave packets for neutrinos, it is argued that the decoherence length derived from the exponential suppression of the flavour transition amplitude depends on the proper time of the geodesic connecting the events of the production and detection in general gravitational setting. In the weak gravity limit, the proper time between two events of given proper distance is smaller than that in the flat spacetime. Therefore, in presence of a Schwarzschild object, the neutrino wave packets have to travel relatively more physical distance in space to lapse the same amount of proper time before they decoher. For non-radial propagation applicable to the lensing phenomena, it is shown that the decoherence, in general, is sensitive to the absolute values of neutrino masses as well as the classical trajectories taken by neutrinos between the source and detector along with the spatial widths of neutrino wave packets. At distances beyond the decoherence length, the probability of neutrino flavour transition due to lensing attains a value which depends only on the leptonic mixing parameters. Hence, the observability of neutrino lensing significantly depends on these parameters and in-turn the lensing can provide useful information about them.

doi : https://doi.org/10.1103/PhysRevD.104.095007

(Ketan M. Patel)

Weak scale right-handed neutrino as pseudo-Goldstone fermion of spontaneously broken $U(1)_{L_\mu - L_\tau}$

Possibility of a Right-Handed (RH) neutrino being a Goldstone fermion of a spontaneously broken global U(1) symmetry in a supersymmetric theory is considered. This fermion obtains mass from the supergravity effects leading to a RH neutrino at the electroweak scale with a mass similar to the gravitino mass. A prototype model realizing this scenario contains just three gauge singlet superfields needed for the type I seesaw mechanism. Masses of the other two neutrinos are determined by the U(1) breaking scale which too can be around the electroweak scale. Light neutrinos obtain their masses in this scenario through (a) mixing with the RH neutrinos (type I seesaw), (b) mixing with neutralinos (R-parity breaking), (c) indirectly through mixing of the RH neutrinos with neutralinos, and (d) radiative corrections. All these contributions are described by the same set of a small number of underlying parameters and provide a very constrained and predictive framework for the neutrino masses which is investigated in detail for various choices of U(1) symmetries. It is found that flavour

independent U(1) symmetries cannot describe neutrino masses if the soft supersymmetry breaking terms are flavour universal and one needs to consider flavour dependent symmetries. Considering a particular example of $L_\mu - L_\tau$ symmetry, it is shown that viable neutrino masses and mixing can be obtained without introducing any flavour violation in the soft sector. The leptonic couplings of Majoron are worked out in the model and shown to be consistent with various laboratory, astrophysical and cosmological constraints. The neutrino data allows sizeable couplings between the RH neutrinos and Higgsinos which can be used to probe the pseudo-Goldstone fermion at colliders through its displaced decay vertex.

doi : https://doi.org/10.1007/JHEP09(2021)115

(Anjan S. Joshipura and Ketan M. Patel)

Leptogenesis and fermion mass fit in a renormalizable SO(10) model

A non-supersymmetric renormalizable SO(10) model is investigated for its viability in explaining the observed fermion masses and mixing parameters along with the baryon asymmetry produced via thermal leptogenesis. The Yukawa sector of the model consists of complex 10_H and $\overline{126}_H$ scalars with a Peccei-Quinn like symmetry and it leads to strong correlations among the Yukawa couplings of all the standard model fermions including the couplings and masses of the right-handed (RH) neutrinos. The latter implies the necessity to include the second lightest RH neutrino and flavor effects for the precision computation of leptogenesis. We use the most general density matrix equations to calculate the temperature evolution of flavoured leptonic asymmetry. A simplified analytical solution of these equations, applicable to the RH neutrino spectrum predicted in the model, is also obtained which allows one to fit the observed baryon to photon ratio along with the other fermion mass observables in a numerically efficient way. The analytical and numerical solutions are found to be in agreement within a factor of order unity. We find that the successful leptogenesis in this model does not prefer any particular value for leptonic Dirac and Majorana CP phases and the entire range of values of these observables is found to be consistent. The model specifically predicts (a) the lightest neutrino mass between 2-8 meV, (b) the effective mass of neutrinoless double beta decay between 4-10 meV, and (c) a particular correlation between the Dirac and one of the Majorana CP phases.

doi : https://doi.org/10.1007/JHEP12(2021)042

(Ketan M. Patel)

Infra-red and collinear safe graph neural network algorithm

Hadronic signals of new-physics origin at the Large Hadron Collider can remain hidden within the copiously produced hadronic jets. Unveiling such signatures require highly performant deep-learning algorithms. We construct a class of Graph Neural Net- works (GNN) in the message-passing formalism that makes the network output infra-red and collinear (IRC) safe, an important criterion satisfied within perturbative QCD calculations. Including IRC safety of the network output as a requirement in the construction of the GNN improves its explainability and robustness against theoretical uncertainties in the data. We generalise Energy Flow Networks (EFN), an IRC safe deep-learning algorithm on a point cloud, defining energy weighted local and global readouts on GNNs. Applying the simplest of such networks to identify top quarks, W bosons and quark/gluon jets, we find that it outperforms state-of-the-art EFNs. Additionally, we obtain a general class of graph construction algorithms that give structurally invariant graphs in the IRC limit, a necessary criterion for the IRC safety of the GNN output.

doi : https://doi.org/10.1007/JHEP02(2022)060

(Partha Konar, Vishal S. Ngairangbam)

Freeze-in Dark Matter Through Forbidden Channel

We examine a scenario for freeze-in production of dark matter, which occurs due to the large thermal correction to the mass of a decaying mediator particle present in the thermal bath of the early Universe. We show that the decays, which are kinematically forbidden otherwise, can open up at very high temperatures and dominate the dark matter production. We explore such forbidden production of dark matter in the minimal $U(1)_{B?L}$ model, comparing dark matter phenomenology in the context of forbidden frozen-in with the standard picture.

doi : https://doi.org/10.1088/1475-7516/2022/03/021

(Partha Konar, Rishav Roshan and Sudipta Show)

Multiple pairing algebras in nuclei with isospin and F-spin

With nucleons occupying several shell model j orbits the isovector pair creation operator that creates a two particle state with angular momentum $J = 0$ and isospin $T = 1$ is no longer unique. The pair creation operator can be chosen to be a sum of single-j pair creation operators each with a phase. With this, there will be multiple pairing $SO(5)$ algebras and it is easy to see that there will be 2^{r-1} isovector pairing $SO(5)$ algebras for a system with r number of j orbits. Thus, with two j orbits there will be two $SO(5)$ algebras, with three j orbits there will be four $SO(5)$ algebras and so on. More importantly, corresponding to each $SO(5)$ there is a complementary $Sp(2\Omega)$ algebra $[2\Omega = \sum_j (2j+1)]$ that gives seniority and reduced isospin quantum numbers. These are all established using generators, quadratic Casimir invariants and the irreducible representations of the various algebras involved. These results along with three applications of multiple $SO(5)$ algebras are carried out by PRL group demonstrating the usefulness of considering $SO(5)$ pairing algebras with general sign factors. Results are also obtained for multiple pairing $SO(3,2)$ algebras with complementary $SO(\Omega)$ algebras in the proton-neutron interacting boson models with good F-spin symmetry.

doi : https://doi.org/10.1016/j.nuclphysa.2021.122313

(V.K.B. Kota)

Coherent elastic neutrino-nucleus scattering (CEνNS) event rates for Ge, Zn and Si detector materials

Realistic nuclear structure calculations are presented for the event rates due to coherent elastic neutrino-nucleus scattering (CEνNS), assuming neutrinos from pion-decay at-rest, from nuclear reactors and from Earth's interior. We focus on the currently interesting Germanium isotopes, ^{70,73,76}Ge, which constitute detector materials of the recently planned CEνNS experiments. We study in addition the potential use of ^{64,70}Zn and ^{28}Si isotopes as promising CEνNS detectors. From nuclear physics perspectives, calculations have been carried out within the framework of the deformed shell-model (DSM), based on realistic nuclear forces, and assessed on the reproducibility of spectroscopic nuclear properties. The high confidence level acquired by their agreement with experimental results and by their comparison with other mostly phenomenological calculations encouraged the use of DSM to extract predictions for the CEνNS event rates of the above isotopes. Our detailed estimation of the nuclear physics aspects of the recently observed neutral current coherent neutrino-nucleus scattering may shed light on unravelling the still remaining uncertainties for the CEνNS process within and beyond the Standard Model.

doi : https://doi.org/10.1103/PhysRevC.104.064618

(V.K.B. Kota)

Thermoelectric transport coefficients of hot and dense QCD matter

The presence of a nonvanishing thermal gradient and/or a chemical potential gradient in a conducting medium can lead to an electric fieldan effect known as thermoelectric effect or Seebeck effect. We discuss here the thermoelectric effects for hot and dense strongly interacting matter within the framework of relativistic Boltzmann equation in the relaxation time approximation. In the context of heavy-ion collisions, the Seebeck coefficients for the quark matter as well as for the hadronic matter are estimated within this approach. The quark matter is modeled by the two flavor NambuJonaLassinio (NJL) model and the hadronic medium is modeled by the hadron resonance gas (HRG) model with hadrons and their resonances up to a mass cutoff $\Lambda \sim 2.6$ GeV. For the estimation of thermoelectric transport coefficients, for the quark matter, we calculate the relaxation times for the quarks and antiquarks from the quarkquark and quarkantiquark scattering through meson exchange within the NJL model. On the other hand, for the hadronic medium, the relaxation times of hadrons and their resonances are estimated within a hard sphere scattering approximation. We also discuss the formalism of the thermoelectric effect in the presence of a nonvanishing external magnetic field. We give an estimation of the associated magneto-Seebeck coefficient and the Nernst coefficient for the hot and dense QCD matter.

doi : http://doi.org/10.1140/epjs/s11734-021-00022-2

(Aman Abhishek, Deepak Kumar and Hiranmaya Mishra)

Color Superconductivity in magnetised quark matter: an NJL model approach

We present the structure of the ground state in dense quark matter in strong magnetic fields at finite temperature and densities in a three-flavor Nambu Jona Lasinio (NJL) model using a variational method. The method uses an explicit structure for the ground state in terms of quarkantiquark condensates related to chiral symmetry breaking as well as diquark condensates related to color superconductivity. The mass gap equations and the superconducting gap equations are solved self-consistently and are used to compute the thermodynamic potential along with charge neutrality conditions. We also derive the equation of state for charge neutral strange quark matter in the presence of strong magnetic fields which could be relevant for neutron stars.

doi : http://doi.org/10.1140/epjs/s11734-022-00439-3

(Hiranmaya Mishra)

Critical exponents and transport properties near the QCD critical endpoint from the statistical bootstrap model

We present an estimate of the behavior of the shear and bulk viscosity coefficients when the QCD critical point is approached from the hadronic side, describing hadronic matter within the statistical bootstrap model of strong interactions. The bootstrap model shows critical behavior near the quark-hadron transition temperature if the parameter characterizing the degeneracy of Hagedorn states is properly chosen. We calculate the critical exponents and amplitudes of relevant thermodynamic quantities near the QCD critical point and combine them with an Ansatz for the shear and bulk viscosity coefficients to derive the behavior of these coefficients near the critical point. The shear viscosity to entropy density ratio is found to decrease when the temperature is increased, and to approach the KovtunSonStarinets bound $\frac{1}{4\pi}$ faster near the critical point, while the bulk viscosity coefficient is found to rise very rapidly.

doi : http://doi.org/10.1140/epjc/s10052-021-09596-6

(Hiranmaya Mishra)

Thermoelectric transport coefficients of quark matter

A thermal gradient and/or a chemical potential gradient in a conducting medium can lead to an electric field, an effect known as thermoelectric effect or Seebeck effect. In the context of heavy-ion collisions, we estimate the thermoelectric transport coefficients for quark matter within the ambit of the NambuJona Lasinio (NJL) model. We estimate the thermal conductivity, electrical conductivity, and the Seebeck coefficient of hot and dense quark matter. These coefficients are calculated using the relativistic Boltzmann transport equation within relaxation time approximation. The relaxation times for the quarks are estimated from the quarkquark and quarkantiquark scattering through meson exchange within the NJL model. As a comparison to the NJL model estimation of the Seebeck coefficient, we also estimate the Seebeck coefficient within a quasiparticle approach. doi : http://doi.org/10.1140/epjc/s10052-022-09999-z

(A. Abhishek, D. Kumar,and H. Mishra)

In medium properties of axion within a Polyakov loop enhanced Nambu-Jona-Lasinio model

We estimate in medium properties of axion i.e., its mass and self-coupling within a three flavor Polyakov loop extended NambuJona-Lasinio (PNJL) model with Kobayashi-Maskawa-tHooft determinant interaction. We also estimate the topological susceptibility of strong interaction within the same model. It is observed that (statistical) confinement effects simulated by Polyakov loop potential play an important role in the estimation of all these quantities, particularly, near the critical temperature. Both the mass and the self-coupling of the axion get correlated with the chiral and deconfinement transition. The results for all these quantities obtained within the PNJL model is compared with chiral perturbation theory, Nambu Jona-Lasinio (NJL) model and lattice QCD simulation results wherever available. The results for properties of axions at finite baryon densities are also presented

doi : http://doi.org/10.1103/PhysRevD.103.074015

(Aman Abhishek and Hiranmaya Mishra)

Statistical Nuclear Spectroscopy with q-normal and bivariate q-normal distributions and q-Hermite polynomials

Statical nuclear spectroscopy (also called spectral distribution method), introduced by J.B. French in late 60's and developed in detail in the later years by his group, PRL group and many other groups, is based on the Gaussian forms for the state (eigenvalue) and transition strength densities in shell model spaces with their extension to partial densities defined over shell model subspaces. The Gaussian forms have their basis in embedded random matrix ensembles with nuclear Hamiltonians consisting of a mean-field one-body part and a residual two-body part. However, following the recent random matrix results for the so called Sachdev-Ye-Kitaev model, embedded random matrix ensembles with k-body interactions are re-examined and it is shown that the density of states, transition strength densities and strength functions (partial densities) in fact follow more closely the q-normal distribution (the parameter q is related to the fourth moment of these distributions with $q = 1$ giving Gaussian and $q = 0$ giving semi-circle form). The q-normal has the important property that it is bounded for $0 \leq q < 1$. Following these, developed is statistical nuclear spectroscopy based on q-normal (univariate and bivariate) distributions and the associated q-Hermite polynomials. In particular, formulation is developed for nuclear level densities, shell model orbit occupancies, transition strengths (for electromagnetic and β and double β-decay type operators) and transition strength sums.

This work is done in collaboration with Manan Vyas of UNAM, Cuernavaca, Mexico.

doi : https://doi.org/10.48550/arXiv.2201.12509

(V.K.B. Kota)

Atomic, Molecular and Optical Physics

Experimental Side Channel Analysis of BB84 QKD Source

Quantum Cryptography (QC) will soon replace the conventional cryptosystems as it is more secure and future safe. Quantum Key Distribution (QKD) a form of QC, ensures the distribution of secret keys between two parties involved in communication and indicates if there is any presence of eavesdroppers between the communicating parties. One such QKD protocol is BB84. Since the devices used in the implementation are far from ideal, the actual key rate and security bound deviate from the theoretical value. The hacker will use this deviation to his/her advantage in estimating the key due to this weakness without being revealed. For secure key distribution one has to make QKD devices as close to ideal as possible. Proper calibration is needed while implementing the QKD systems in the field. Here we characterize the BB84 source for the possible leakages in the information due to side channel, and cover all the possible parameters.

A typical implementation of BB84 protocol for quantum communication uses four laser diodes for transmitting weak coherent pulses, which may not have the same characteristics. We have characterized these lasers for mismatch in various parameters such as spectral width, pulse width, spatial mode, peak wavelength, polarization and their arrival times at the receiver. This information is utilized to calculate possible information leakage through side channel by evaluating mutual information between source and eavesdropper. Based on our experimental observations of cross correlation between parameter values for different laser diodes, we suggest methods to reduce information leakage to the eavesdropper.

This work is done in collaboration with Rupesh Kumar from Quantum Communications Hub, University of York, York, U.K. doi : https://doi.org/10.1109/JQE.2021.3111332

(Biswas, A., Banerji, A., Chandravanshi, P., Kumar, R., and Singh, R. P.)

Quantum key distribution with multiphoton pulses: an advantage

Quantum key distribution is perhaps the most remarkable application of quantum theory. It exploits the principles of quantum mechanics to enable two distant parties to share a secret random key. Once the key has been established, the two can exchange encrypted messages using private key cryptographic methods.

We introduced a quantum key distribution protocol for the line-of-sight channels based on coincidence measurements. We presented a proof-of-concept implementation of our protocol. We showed that using coincidence measurements to monitor multi-photon pulses results in a higher secure key rate over longer distances for such channels. This key rate was higher than popular implementations of quantum key distribution protocol based on BB84, for example, the GLLP analysis. In the experiment, we could generate around 74% more key bits per signal pulse as compared to the GLLP analysis of BB84 protocol with similar parameters and equal value of mean photon number.

This work is done in collaboration with Rupesh Kumar from Quantum Communications Hub, University of York, York, U.K.

doi : https://doi.org/10.1364/OPTCON.445727

(Biswas, A., Banerji, A., Lal, N., Chandravanshi, P., Kumar, R., and Singh, R. P.)

Size-invariant twisted optical modes for the efficient generation of higher-dimensional quantum states

Optical vortex beams are profiled as helical wavefronts with a phase singularity carrying an orbital angular momentum (OAM) associated with their spatial distribution. The transverse intensity distribution of a conventional optical vortex has a strong dependence on the carried topological charge or the OAM. However, perfect optical vortex (POV) beams have their transverse intensity distribution independent of their charge. Such “size-invariant” POV beams have found exciting applications in optical manipulation, imaging, and communication. In this study, we investigate the use of POV modes in the efficient generation of high-dimensional quantum states of light. We generate heralded single photons carrying OAM using spontaneous parametric down conversion (SPDC) of POV beams. We show that the heralding efficiency of the SPDC single photons generated with a POV pump is greater than that with normal optical vortex beams. The dimensionality of the two-photon OAM states is increased with POV modes in the pump and projective measurements using BesselGaussian vortex modes that give POV, instead of LaguerreGaussian modes.

doi : https://doi.org/10.1364/JOSAB.436088

(Anwar, A., Prabhakar, S., and Singh, R. P.)

Correlations in scattered perfect optical vortices

We study correlations in the speckle patterns generated by the scattering of perfect optical vortex (POV) beams and use them to produce a new class of coherence functions, namely Bessel coherence functions. Higher (zeroth) order Bessel coherence functions have been realized in cross (auto)-correlation between the speckle patterns generated by the scattering of perfect vortex beams of different orders. We have also studied the propagation of produced Bessel coherence functions and characterized their divergence with

respect to the radius of their first ring for different orders starting from 0 to 4. We observe that the divergence varies linearly with the order of the coherence function. We provide the exact analytical expression for the auto-correlation, as well as cross-correlation functions for speckle patterns. Our experimental results are in good agreement with the analytical results.

(Nijil Lal, Anju Rani, R. P. Singh in collaboration with P. Vanitha, B.K. Das, S.G. Reddy from SRM University-AP, Amaravati.)

doi : https://doi.org/10.1088/2040-8986/ac094f

(Vanitha, P., Lal N., Rani, A., Das, B. K., Reddy S. G., and Singh, R. P.)

Nuclear charge radii of Na isotopes: Interplay of atomic and nuclear theory

The accuracy of atomic theory calculations limits the extraction of nuclear charge radii from isotope shift measurements of atomic systems. For the Na isotopes, calculations by different methods offer a wide range of values. We performed accurate atomic calculations to reliably extract the Na charge radii. By combining experimental matter radii with nuclear coupled-cluster calculations based on nucleon-nucleon and three-nucleon forces, we constrained the parameters obtained from the atomic calculations. Our study guided atomic theory and highlighted the importance of using accurate atomic and nuclear computations in the understanding of the size of light nuclei.

This work was carried out in collaboration with B. Ohayon of Institute for Particle Physics and Astrophysics, ETH Zrich, CH-8093 Zrich, Switzerland; R. F. Garcia Ruiz of Massachusetts Institute of Technology, Cambridge, Massachusetts 02139, USA; and Z. H. Sun, G. Hagen and T. Papenbrock of Physics Division, Oak Ridge National Laboratory, Oak Ridge, Tennessee 37831, USA.

doi : https://doi.org/10.1103/PhysRevC.105.L031305

(B. Ohayon, R. F. Garcia Ruiz, Z. H. Sun, G. Hagen, T. Papenbrockand, B. K. Sahoo)

Determination of quadrupole polarizabilities of the excited states of alkali-metal atoms

The scalar and tensor components of the electric quadrupole (E2) polarizabilities of the first two excited states of all the alkali-metal atoms were evaluated. We had also evaluated the ground state E2 polarizabilities of these atoms and compared them with the literature values. The dominant parts of these quantities were estimated by combining the precisely calculated E2 transition matrix elements of many low-lying transitions with the experimental energies, while the other contributions were estimated using lower-order methods. Our estimated values for the ground states of the above atoms were in good agreement with the literature values suggesting that our estimated E2 polarizabilities for the excited states of the alkali atoms, which were not known earlier except for the Li atom, were also quite accurate. These reported E2 polarizabilities will be useful in guiding many precision measurements in the alkali atom.

This work was carried out along with H. Kaur, S. Singh, and B. Arora of Department of Physics, Guru Nanak Dev University, Amritsar, Punjab 143005, India.

doi : https://doi.org/10.1103/PhysRevA.105.032819

(Harpreet Kaur, S. Singh, B. Arora and B. K. Sahoo)

Radiative properties of Cu-isoelectronic As, Se, and Br ions for astrophysical applications

We reported precise radiative data of line strengths, transition probabilities, and oscillator strengths for the allowed transitions among many low-lying states of the Cu-isoelectronic As, Se, and Br ions. Due to unavailability of precise observations of these spectroscopic data, their accurate estimations are of great interest and useful in analysing various astrophysical phenomena undergoing inside the heavenly bodies that contain As, Se, and Br elements. An all-order perturbative many-body method in the relativistic theory framework was employed to determine the atomic wave functions, which were further used to estimate the above quantities with the uncertainties. We found significant differences between some of our results and results that were available earlier.

This work was carried out along with Jyoti, H. Kaur, and B. Arora of Department of Physics, Guru Nanak Dev University, Amritsar, Punjab 143005, India.

doi : https://doi.org/10.1093/mnras/stac163

(Jyoti, Harpreet Kaur, B. Arora and B. K. Sahoo)

Towards CP-violation studies on superheavy molecules: Theoretical and experimental perspectives

Molecules containing superheavy atoms can be artificially created to serve as sensitive probes to study symmetry-violating phenomena. We provided detailed theoretical studies of quantities relevant to the electron electric dipole moment (eEDM) and nucleus-electron scalar-pseudoscalar interactions in diatomic molecules containing superheavy lawrencium nuclei. The sensitivity to parity and time reversal violating properties was studied for different neutral and ionic molecules. The effective electric fields in these systems were found to be about 3-4 times larger than other known molecules on which eEDM experiments were being performed. Similarly, these superheavy molecules exhibited an enhancement of more than 3 times for CP-violating scalar-pseudoscalar nucleus-electron interactions. Our preliminary analysis using the Woods-Saxon nuclear model also demonstrated that these results are sensitive to the diffuse surface interactions inside the Lr nucleus. We also briefly commented on some experimental aspects by discussing the production of these systems..

This work was carried out in collaboration with V. S. Prasannaa of Centre for Quantum Engineering, Research and Education, TCG CREST, Salt Lake, Kolkata 700091, India; R. F. Garcia

Ruiz of Department of Physics, Massachusetts Institute of Technology, Cambridge, Massachusetts 02139, USA; T. K. Sato of Advanced Science Research Center, Japan Atomic Energy Agency, Tokai, Ibaraki 319-1195, Japan; M. Abe of Department of Chemistry,Graduate School of Science, Hiroshima University, 1-3-2, Kagamiyama, HigashiHiroshima City, Hiroshima 739-8511, Japan; Y. Sakemi of Center for Nuclear Study, The University of Tokyo, Hongo, Bunkyo, Tokyo 113-0033, Japan; and B. P. Das of Department of Physics, Tokyo Institute of Technology, 2-12-1 Ookayama, Meguro-ku, Tokyo 152-8550, Japan.

doi : https://doi.org/10.1103/PhysRevA.104.062801

(R. Mitra, V. S. Prasannaa, R. F. Garcia Ruiz, T. K. Sato, M. Abe,Y. Sakemi, B. P. Das and B. K. Sahoo)

Relativistic-coupled-cluster-theory analysis of properties of Co-like ions

Ionization potentials, excitation energies, transition properties, and hyperfine structure constants of the low-lying atomic states of a number of Co-like highly charged ions were investigated. The singles and doubles approximated relativistic coupled-cluster theory in the framework of one electron removal Fock-space formalism was employed over the Dirac-Hartree-Fock calculations to account for the electron correlation effects for determining the aforementioned properties. Higher-order relativistic corrections due to the Breit interaction and quantum electrodynamics effects in the evaluation of energies were also quantified explicitly. Our estimated values were compared with the other available theoretical calculations and experimental results, which were found to be in good agreement with each other.

This work was done in collaboration with D. K. Nandy of Center for Theoretical Physics of Complex Systems, Institute for Basic Science (IBS), Daejeon 34126, Korea.

doi : https://doi.org/10.1103/PhysRevA.104.052812

(D. K. Nandy and B. K. Sahoo)

Quantum sensing of the electron electric dipole moment using ultracold entangled Fr atoms

We proposed a method to measure the electron electric dipole moment (eEDM) using ultracold entangled francium (Fr) atoms trapped in an optical lattice, yielding an uncertainty below the standard quantum limit. Among the alkali atoms, Fr offers the largest enhancement factor to the eEDM. With a Fr based experiment, quantum sensing using quantum entangled states could enable a search for the eEDM at a level below 10^{-30}e-cm. We estimated statistical and systematic errors attached to the proposed measurement scheme based on this quantum sensing technique. A successful quantum sensing of the eEDM could enable the exploration of new physics beyond the standard model of particle physics.

This work was carried out in collaboration with T. Aoki and collaborators from Japan; B. Arora of Department of Physics, Guru Nanak Dev University, Amritsar, Punjab-143005, India; and A. Kastberg of Institute de Physique de Nice, Universit Cte dAzur, CNRS, 06108 Nice, France.

doi : https://doi.org/10.1088/2058-9565/ac1b6a

(T. Aoki, R. Sreekantham, B. K. Sahoo, B. Arora, A. Kastberg, T.Sato, H. Ikeda, N. Okamoto, Y. Torii, T. Hayamizu, K. Nakamura, S. Nagase, M. Ohtsuka, H. Nagahama, N. Ozawa, M. Sato, T. Nakashita, K. Yamane, K. S. Tanaka, K. Harada, H. Kawamura, T. Inoue, A. Uchiyama, A. Hatakayama, A. Takamine, H. Ueno, Y. Ichikawa, Y. Matsuda, H. Haba, and Y. Sakemi)

Spectroscopic data of Rb-isoelectronic Zr and Nb ions for astrophysical applications

We presented high-accuracy spectroscopy data of line strengths, transition probabilities, and oscillator strengths for the allowed transitions among a large number of states of the Rb-isoelectronic Zr (Zr IV) and Nb (Nb V) ions. They can serve to analyse various astrophysical phenomena undergoing inside the heavenly bodies containing Zr and Nb elements. Since there was a lack of precise observational and calculated data for the spectroscopic properties in the above ions, their accurate determinations are of immense interest. The literature data, which were available only for a few selected lowlying transitions, have large discrepancies and they cannot be used reliably for the above purpose. After accounting for electron interactions through random phase approximation, Brueckner orbitals, structural radiations, and normalizations of wave functions in the relativistic many-body methods, we evaluated the electric dipole amplitudes precisely. Combining these values with the observed wavelengths, the above transition properties and lifetimes of a number of excited states of the Zr IV and Nb V ions were determined and compared with the literature data.

This work was carried out in collaboration with Jyoti, H. Kaur, and B. Arora of Department of Physics, Guru Nanak Dev University, Amritsar, Punjab 143005, India.

doi : https://doi.org/10.1093/mnras/stab2364

(Jyoti, M. Kaur, B. Arora and B. K. Sahoo)

New physics constraints from atomic parity violation in ^{133}Cs

Our improved calculation of the nuclear spin-independent parity violating electric dipole transition amplitude ($E1_{PV}$) for the $6s^2S_{1/2} \rightarrow 7s^2S_{1/2}$ transition in ^{133}Cs in combination with the most accurate (0.3%) measurement of this quantity yielded a new value for the nuclear weak charge Q_W = 73.71$(26)_{ex}(23)_{th}$ against the Standard Model (SM) prediction $Q^{SM}W$ = 73.23(1). The advances in our calculation of $E1_{PV}$ was achieved by using a variant of the perturbed relativistic coupled-cluster theory, which treated the contributions of the core, valence, and excited states to $E1_{PV}$ on the same footing unlike the previous high precision calculations. Furthermore, this approach resolved the controversy regarding the sign of the core correlation effects. We discussed the implications of the deviation of

our result for Q_W from the SM value by considering different scenarios of new physics.

This work was carried out in collaboration with B. P. Das of Department of Physics, School of Science, Tokyo Institute of Technology, 2-1-2-1H86 Ookayama Meguro-ku, Tokyo 152-8550, Japan; and H. Spiesberger of PRISMA+ Cluster of Excellence, Institut fr Physik, Johannes GutenbergUniversitt, D-55099 Mainz, Germany.

doi : https://doi.org/10.1103/PhysRevD.103.L111303

(B. K. Sahoo, B. P. Das and H. Spiesberger)

Relativistic Coupled-Cluster Calculations of Isotope Shifts for the Low-Lying States of Ca II in the Finite-Field Approach

We evaluated the isotope shift (IS) constants of the first five low-lying fine-structure states of the singly charged calcium ion (Ca II) by adopting a finite-field (FF) approach in the relativistic coupled-cluster (RCC), a method developed by us. A similar previous calculation using singles and doubles approximation RCC theory (RCCSD method), gives results for the individual states in the FF approach that deviate substantially, while the differential values (the shifts of the spectral lines) agreed reasonably well with other theoretical results and with experiments. However, we found a contrasting trend from the FF approach using our RCCSD method although calculations with the Dirac-Hartree-Fock (DHF) method showed good agreement. Our results also showed that inclusion of partial triple excitations in the perturbative approach (RCCSD(T) method) through energy derivation lessens accuracy, but these results can be improved when triple excitations are included in the wave function that determines the RCC equations. The differences between the RCCSD and RCCSD(T) results demonstrated the importance of triple excitations in evaluating energies and IS constants for Ca II.

This work was carried out in collaboration with A. Dorne and A. Kastberg of Institut de Physique de Nice, Universit Cte dAzur, CNRS, 06108 Nice, France.

doi : https://doi.org/10.3390/atoms9020026

(A. Dorne, B. K. Sahoo and Anders Kastberg)

Benchmarking many-body approaches for the determination of isotope-shift constants: Application to the Li, Be^+ and Ar^{15+} isoelectronic systems

We applied relativistic coupled-cluster (RCC) theory to determine the isotope-shift (IS) constants of the first eight low-lying states of the Li, Be^+, and Ar^{15+} isoelectronic systems. Though the RCC theory with singles, doubles, and triples approximation (RCCSDT method) is an exact method for these systems for a given set of basis functions, we noticed large differences in the results from this method when various procedures in the RCC theory framework were adopted to estimate the IS constants. This was demonstrated by presenting the IS constants of the aforementioned states from the finite-field, expectation value, and analytical response (AR) approaches of the RCCSDT method. Contributions from valence triple excitations, Breit interaction, and lower-order QED effects to the evaluation of these IS constants were also highlighted. Our results were compared with high-precision calculations reported using few-body methods wherever possible. We found that results from the AR procedure are more reliable than the other two approaches. This analysis was crucial for understanding the roles of electron correlation effects in the accurate determination of IS constants in the heavier atomic systems, where few-body methods cannot be applied.

This work was carried out in collaboration with B. Ohayon of Institute for Particle Physics and Astrophysics, ETH Zrich, CH-8093 Zrich, Switzerland.

doi : https://doi.org/10.1103/PhysRevA.103.052802

(B. K. Sahoo and B. Ohayon)

Tune-out and magic wavelengths, and electric quadrupole transition properties of the singly charged alkaline-earth metal ions

We presented the tune-out and magic wavelengths of the Mg, Ca, Sr and Ba alkaline earth-metal ions by determining dynamic electric dipole (E1) polarizabilities. Furthermore, we evaluated the electric quadrupole (E2) matrix elements of a large number of forbidden transitions using an all-order relativistic many body method and compared them with the previously reported values for a few selective transitions. Compilation of both the E1 and E2 transition matrix elements, will now provide a more complete knowledge about the transition properties of the considered singly charged alkaline earth-metal ions. Similarly, the listed precise values of tune-out and magic wavelengths due to the dominant E1 polarizabilities can be helpful to conduct experiments using the above ions with reduced systematics. Therefore, all these data will be immensely useful for various applications for carrying out the high-precision experiments and laboratory simulations in atomic physics, and interpreting transition lines in the astrophysical observations.

This work was carried out in collaboration with M. Kaur, S. Singh and B. Arora of Department of Physics, Guru Nanak Dev University, Amritsar, Punjab 143005, India.

doi : https://doi.org/10.1016/j.adt.2021.101422

(Mandeep Kaur, S. Singh, B. K. Sahoo and B. Arora)

Imaging inspired characterization of single photons carrying orbital angular momentum

We report on an imaging-inspired measurement of orbital angular momentum (OAM) using only a simple tilted lens and an intensified charged coupled device camera, allowing us to monitor the propagation of OAM structured photons over distance, which is crucial for free-space quantum communication networks. We demonstrate the measurement of OAM orders as high as ls = 14 in a heralded single-photon source and show, for the first time, the imaged

self-interference of photons carrying OAM in a modified MachZehnder interferometer. The described methods reveal both the charge and order of a photon's OAM and provide a proof of concept for the interference of a single OAM photon with itself. Using these tools, we are able to study the propagation characteristics of OAM photons over a distance, which is important for estimating transport in free-space quantum links. By translating these classical tools into the quantum domain, we offer a robust and direct approach for the complete characterization of a twisted single-photon source, an important building block of a quantum network.

This work was done in collaboration with Majid Ebrahim-Zadeh and his group from the Institute of Photonic Sciences, Barcelona and Andrew Forbes, University of the Witwatersrand, South Africa.

doi : https://doi.org/10.1116/5.0078870

(V.Kumar, V.Sharma, S.Singh, S. Chaitanya Kumar, Andrew Forbes, M. Ebrahim-Zadeh, and G. K. Samanta)

Tunable, high-power, high-order optical vortex beam generation in the mid-infrared

We report the generation of tunable high-order optical vortices in the mid-infrared (mid-IR) using a picosecond optical parametric oscillator (OPO). The OPO is based on MgO:PPLN as the nonlinear gain medium and synchronously pumped by a mode-locked Yb-fiber laser at 1064 nm. Using a singly-resonant oscillator configuration for the OPO, we have achieved direct transfer of pump optical vortices to the non-resonant idler beam, with the resonant signal in the Gaussian cavity mode. We demonstrate the successful transfer of pump optical vortices of order, 1p=1 to 5, to the idler beam of the same order across the mid-IR, with an output power of 630 mW to 130 mW across 2538 nm to 4035 nm for the highest idler vortex order, li=5. To the best of our knowledge, this is the first report of an OPO pumped by a vortex beam of order as high as lp=5 and generating idler vortices of high order in the mid-IR.

This work was done in collaboration with Majid Ebrahim-Zadeh and his group from the Institute of Photonic Sciences, Barcelona.

doi : https://doi.org/10.1364/OE.443345

(V.Sharma, S. Chaitanya Kumar, G. K. Samanta, and M. Ebrahim-Zadeh)

Tunable vortex beam generation using an optical parametric oscillator with an antiresonant-ring interferometer

We report a high-average-power picosecond optical vortex source tunable in the near-infrared, using an antiresonant-ring (ARR) interferometer internal to an optical parametric oscillator (OPO) in combination with an external cylindrical lens for astigmatic mode conversion. The ARR OPO is tunable in the signal across 14571647 nm with a vortex intensity profile and up to 1 W of average power at 1602 nm. The corresponding idler is tunable over 30063945 nm in a Gaussian intensity profile with as much as 1.6 W at 3168 nm. The vortex signal and the Gaussian idler exhibit passive power stability better than 1.7% rms and 1.3% rms, respectively, over $>$1h. The signal pulses have a Gaussian duration of $<$19 ps with a time-bandwidth product of $\Delta\tau\Delta\nu$ $<$3.6 across the tuning range.

doi : https://doi.org/10.1364/OL.426337

(V. Sharma, S. Chaitanya Kumar, G. K. Samanta, and M. Ebrahim-Zadeh)

Molecular emission dynamics from a femtosecond filament induced plasma plume

In this study, we have investigated the filament-induced plasma properties and the associated molecular emission features from three different non-metallic samples.

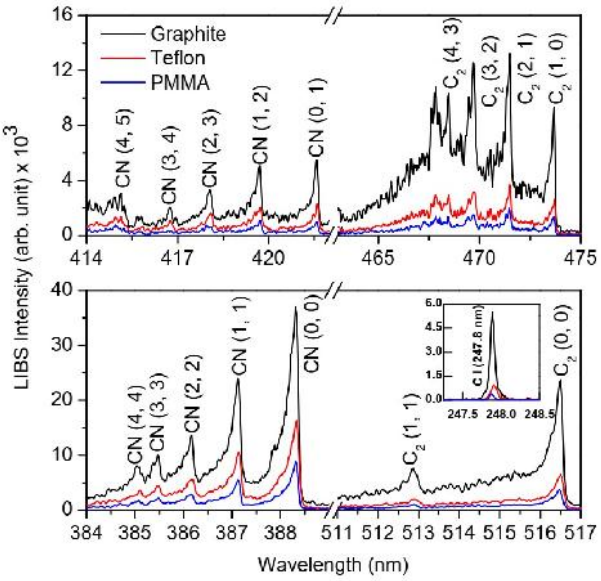

Figure 1: The LIBS emission spectra of graphite, PMMA, and Teflon in air when interacting with an 800 nm Ti: Sapphire laser pulses of duration 29 fs.

Teflon, Graphite, and polymethyl methacrylate (PMMA) samples were ablated using a tightly focused femtosecond laser-induced filament, and their emission spectra were analyzed using a time-integrated optical emission spectroscopy technique. The temporal responses and evolution dynamics of molecular species such as CN and C2 from these samples in ambient conditions are compared. The tightly focused filament was generated by focusing the Ti: Sapphire femtosecond pulses (29 fs) using a short focal length external focusing system. The influence of physical and chemical properties of the samples during filament ablation has also been studied by characterizing the optical emission spectra. We find that the molecular signal intensity strongly depends on the sample properties and the position of the sample in the filament. The increase in molecular emission intensity from a graphite sample as a function of incident laser intensity suggests that the tightly focused filament surpasses the intensity clamping value. A Laser-Induced Breakdown Spectroscopy (LIBS) spectrum of graphite, Teflon, and PMMA induced by 29 fs

is shown in figure to explain the sample-specific CN formation in plume-air interaction.

(Muhammed Shameem K M, Madhusudhan P, Rituparna Das, Pranav Bharadwaj, Nimma Vinitha, Swetapuspa Soumyashree and Rajesh Kumar Kushawaha)

doi : https://doi.org/10.1088/2040-8986/ac528a

(R. Das, D. K. Pandey, V. Nimma, P Madhusudhan, P. Bhardwaj, P. Chandravanshi, Muhammed Shameem KM, D. K. Singh, R. K. Kushawaha)

Three-dimensional complex architectures observed in shock processed amino acid mixtures

Asteroid and cometary impacts have been considered as one of the possible routes for exogenous delivery of organics to the early Earth. It is well established that amino acids can be synthesized due to impact-driven shock processing of simple molecules and that amino acids can survive the extreme conditions of impact events. In the present study, we simulate impact-induced shock conditions utilizing a shock tube that can maintain a reflected shock temperature of about 5,500 K for 2 ms time scale. We have performed shock processing of various combinations of amino acids with subsequent morphological analysis carried out using Scanning Electron Microscope (SEM), revealing that the shock processed amino acids demonstrate an extensive range of complex structures. These results provide evidence for the further evolution of amino acids in impact-induced shock environments leading to the formation of complex structures and thus providing a pathway for the origin of life.

(Surendra V. Singh, Jaya K. Meka, Mariyappan Muruganantham, Vijayan Sivaprahasam, Anil Bhardwaj and Bhalamurugan Sivaraman in collaboration with Indian Institute of Science, Bangalore, IIT Gandhinagar, Bhabha Atomic Research Center, Mumbai and University of Kent, UK)

doi : https://doi.org/10.1017/exp.2021.17

(Singh, S. V., Vishakantaiah, J., Meka, J. K., Muruganantham, M., Thiruvenkatam, V., Sivaprahasam, V., Rajasekhar, B. N., Bhardwaj, A., Mason, N. J. and Sivaraman, B.)

Vacuum ultraviolet photoabsorption spectra of icy isoprene and its oligomers

Isoprene and its oligomer (terpenes), the naturally occurring hydrocarbons which are responsible for the sweet aromas and beautiful colour of various plant including eucalyptus that fills the air of PRL campus, are also expected to be present along with other complex organic molecules in the diverse environments of the Interstellar Medium (ISM0 and in our solar system. Due to insufficient spectral information of these molecules at low temperature, detection and understanding the importance of these molecules have been rather elusive. For this purpose, we have carried out the vacuum ultraviolet (VUV) photoabsorption measurements on pure molecular ices of isoprene and a few of its oligomers: limonene, α-pinene and β-pinene by forming icy mantles on cold dust analogues. In this study, we report the first low temperature (10 K) VUV spectra of isoprene and its oligomers limonene, α-pinene and β-pinene. Isoprene absorption at the longer wavelength is found to be red shifted in comparison with the gas phase by nearly $\sim$20 nm which is unique as molecules are expected to be blue shifted with lowering temperatures. This unique property of isoprene along with distinctive absorption at longer wavelengths supports its candidature for detection on icy bodies.

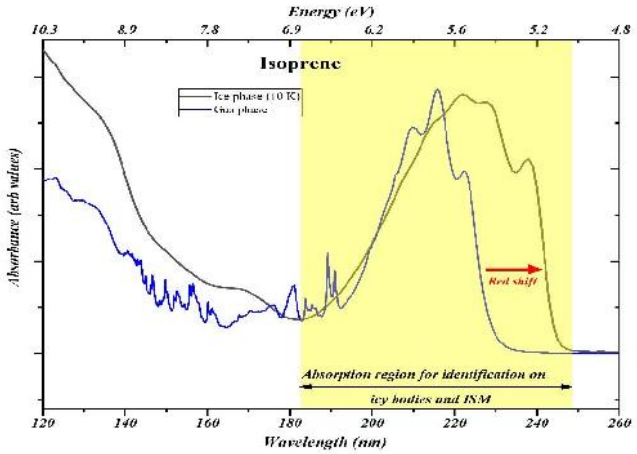

Figure 2: VUV spectra of Isoprene showing the red shift and the proposed region for identification of Isoprene

This work is done in collaboration with National Synchrotron Radiation Research Center, Taiwan, Bhabha Atomic Research Center, India, and University of Kent, UK.

doi : https://doi.org/10.1016/j.saa.2021.120586

(R Ramachandran, S Pavithraa, J K Meka, K K Rahul, J I Lo, S L Chou, B M Cheng, B N Rajasekhar, A Bhardwaj, N J Mason and B Sivaraman.)

New Signatures of Bio-Molecular Complexity in the Hypervelocity Impact Ejecta of Icy Moon Analogues

Impact delivery of prebiotic compounds to the early Earth from an impacting comet is considered to be one of the possible ways by which prebiotic molecules arrived on the Earth. Given the ubiquity of impact features observed on all planetary bodies, bolide impacts may be a common source of organics on other planetary bodies both in our own and other solar systems. Biomolecules such as amino acids have been detected on comets and are known to be synthesized due to impact-induced shock processing. Here we report the results of a set of hypervelocity impact experiments where we shocked icy mixtures of amino acids mimicking the icy surface of planetary bodies with high-speed projectiles using a two-stage light gas gun and analyzed the ejecta material after impact. Electron microscopic observations of the ejecta have shown the presence of macroscale structures with long polypeptide chains revealed from liquid chromatography mass spectrometry (LCMS) analysis. These results suggest a pathway in which impact on cometary ices containing building blocks of life can lead to the synthesis of material architectures that could have played a role in the emergence of life on the Earth and which may be applied

to other planetary bodies as well.

This work is done in collaboration with Indian Institute of Science, Bangalore, IIT Gandhinagar, Bhabha Atomic Research Center, Mumbai and University of Kent, UK.

doi : http://dx.doi.org/10.3390/life12040508

(Singh, S.V., Dilip, H., Meka, J.K., Thiruvenkatam, V., Jayaram, V., Muruganantham, M., Sivaprahasam, V., Rajasekhar, B.N., Bhardwaj, A., B Sivaraman, Mason, N.J. and Burchell, M.J.)

Distribution of natural beta dose in individual grains of sediments

In luminescence dating using single grains of quartz, statistical protocols are used to compute the most appropriate dose from the distribution of palaeodoses. The distribution of palaeodoses arises due to, (1) heterogeneity (at grain level) in bleaching at the time of deposition, (2) heterogeneous distribution of beta emitters present as randomly distributed feldspars (Mayya et al. in Radiat Meas 41:10321039, 2006) and, (3) heterogeneous distribution of grainsizes (Guérin et al. in Radiat Meas 47:778785, 2015). Mayya et al. (Radiat Meas 41:10321039, 2006) demonstrated that random distribution of feldspar grains(with up to 14% stoichiometric K) and shorter range of beta particles ($\sim$ 2.3 mm in quartz) lead to significant variation in dose received by individual grains of quartz. This study improves upon Mayya et al. (Radiat Meas 41:10321039, 2006) by, (1) using a more realistic energy deposition function that is estimated using Monte Carlo simulations and (2) computing the effects of porosity of the sediment and beta straggling on the dose distribution function. It additionally concludes that effects of beta straggling are small and can be ignored. Ages based on new calculations have led to improved concordance with control ages. The dose deposition function calculated using Monte- Carlo simulations suggests a higher value of the δ as compared to Mayya et al. (2006). The dose deposited at intermediate distances ($\sim$ 0.62 mm) is higher. Further it is found that soil porosity has considerable effect on the minimum dose (δ) values when K concentration is low, but at higher concentrations the δ values are almost the same. Thus in respect of heterogeneous distribution of beta dose, at lower concentrations of K, the porosity should be taken in consideration for computation of δ.

This work is done in collaboration with YS Mayya, T. P. Selvam and S. Anand, BARC, Mumbai and J.K. Feathers, university of Washington.

doi : https://doi.org/10.1007/s43538-021-00057-y

(Chauhan, N., Selvam, T. P., Anand, S., Shinde, D. P., Mayya, Y. S., Feathers, J. K., & Singhvi, A. K.)

Climatic history from early Weichselian (MIS 5D-C) valley-fill deposits and associated factors for basin sedimentation, mainland Kachchh, western India

Ephemeral fluvial systems in the dryland region of Kachchh are susceptible to climatic fluctuations. An increase in Indian Summer Monsoon Intensity (ISM) is responsible for the aggradation of sediments as valley-fill deposits in the river basins. In the present study sedimentological, chronometric, and geochemical analysis on the fluvial terrace sequences of Nirona and Bhukhi river basins are being used to interpret southwest summer monsoon variability from MIS 5D-5C along with the fluvial response to local tectonics. The sediment record indicates increased ISM precipitation from $\sim$110ka to $\sim$90ka, which corresponds to the MIS 5D to MIS 5C (Interstadial stage). The study indicates that ISM became progressively weaker during the MIS-5B (stadial stage), leading to present-day arid conditions. The climatic factors weakened along with an interplay of local tectonics, leading to present-day conditions of bedrock incision.

This work is done in collaboration with M. Dabhi, A. Chavan, A. Thakkar, G. Chauhan, R. Bhagora, S. Bhandari, Kachchh university.

doi : https://doi.org/10.1016/j.quaint.2021.10.019

(Dabhi, M., Chavan, A., Thakkar, A., Chauhan, G., Bhagora, R., Chauhan, N., Bhandari, S.)

Mid-late Holocene climatic reconstruction from coastal dunes of the western Kachchh

The study focuses on the mechanism, climate, and sea-level implications of the coastal dune building activity in the eastern coast of Kori Creek (Gulf of Kachchh). Around 10 m thick dune is investigated using sedimentology, geochemistry, and optical chronology. This study suggests that the dune sediment that overlies the Tertiary Oyster Bed is dated to $\sim$4 ka. The grain size analysis and correlation of textural parameters of the inland dunes and coastal dunes showed no stark difference, revealing they were deposited during the same time. Further, the geochemical data generated from the samples of the coastal dune site represent semi-arid to semi-humid climate with increasing chemical maturity and weakening monsoon during the time of deposition. Based on the current erosion dune face and optical ages of the samples, it can be related that the Kachchh coastline was exposed due to the lowering of the sea level at the time of the deposition of coastal dunes. The sea must be at a lower level to attain a preferable condition for the deposition of dunal landforms. The lowering of the sea exposed the beach with sandy material, which got blown away in strong wind, leading to dunes deposition. The cold phase at $\sim$4.2ka became the most conducive environment of coastal dune formation.

This work is done in collaboration with M. Dabhi, A. Chavan, A. Thakkar, G. Chauhan, R. Bhagora, S. Bhandari, Kachchh University.

doi : https://doi.org/10.1016/j.quaint.2021.09.011

(Dabhi, M., Thakkar, A., Chavan, A., Chauhan, G., Bhagora, R., Chauhan, N., Thakkar, M. G.)

Impact of Late Pleistocene climate variability on paleo-erosion rates in the western Himalaya

It has been proposed that at short timescales of 102105 yr, climatic variability can explain variations in sediment flux, but in orogens with pronounced climatic gradients rate changes caused by the oscillating efficiency in rainfall, runoff, and/or sediment transport and deposition are still not well-constrained. To explore landscape responses under variable climatic forcing, we evaluate time windows of prevailing sediment aggradation and related paleo-erosion rates

from the southern flanks of the Dhauladhar Range in the western Himalaya. We compare past and present ^{10}Be-derived erosion rates of well-dated Late Pleistocene fluvial landforms and modern river sediments and reconstruct the sediment aggradation and incision history based on new luminescence data. Our results document significant variations in erosion rates ranging from 0.1 to 3.4 mm/yr over the Late Pleistocene. We find that, during times of weak monsoon intensity, the moderately steep areas (hillslope angles of 27 $\pm 13^{\circ}$) erode at lower rates of 0.10.4 mm/yr compared to steeper ($> 40^{\circ}$) crestal regions of the Dhauladhar Range that erode at 0.81.3 mm/yr. In contrast, during several millennia of stronger monsoon intensity, both the moderately steep and high slope areas record higher erosion rates ($>$1-3.4 mm/yr). Lithological clast-count analysis shows that this increase of erosion is focused in the moderately steep areas, where Lesser Himalayan rocks are exposed. Our data thus highlight the highly non-linear response of climatic forcing on landscape evolution and suggest complex depositional processes and sedimentary signals in downstream areas.

This work is done in collaboration with S. Dey, V. Jain, IIT Gandhinagar; B. Bookhagen, M. R. Strecker, University of Potsdam; R.C. Thiede, University of Kiel; H. Wittmann, Deutsches Geoforschungszentrum Potsdam.

doi : https://doi.org/10.1016/j.epsl.2021.117326

(Dey, S., Bookhagen, B., Thiede, R. C., Wittmann, H., Chauhan, N., Jain, V., & Strecker, M. R.)

PleistoceneHolocene out-of-sequence faulting along the Medlicott-Wadia Thrust in the NW Himalaya

Understanding millennial-scale fault activity and related structural architecture from seismic gaps in active orogens is important for assessment of future seismic risks. Here, we present new Late PleistoceneHolocene shortening rates across a segment of the 600-km-long Medlicott-Wadia Thrust (MWT) system in the Sub-Himalaya (SH) from the far-western Himalayan sector of Jammu. OSL-dated offset and folded fluvial strath terraces provide a measure for the intra-wedge convergence and document strain partitioning within the SH, among which the MWT are the most active. Estimated differential uplift rates across the frontal and rear splay of the MWT is 3.2 $\pm$ 0.8 mm/a and 3.1 $\pm$ 0.4 which translate into a cumulative Late PleistoceneHolocene shortening rate of 5.5 $\pm$ 0.55.8 $\pm$ 0.5 mm/a on the MWT. Previously published balanced cross-sections proposed deformation pattern in range of $\sim$1 mm/a. Our study reaffirms deformation rates from neighbouring MWT fault segments; moreover, it provides independent constraints to the structural architecture of the frontal fold-and-thrust belt and implies changes in fault displacement rates on Quaternary time-scales

This work is done in collaboration with S. Dey, V. Jain, D. Nath IIT Gandhinagar; R.C. Thiede, Niklas W. Schaaf, University of Kiel.

doi : https://doi.org/10.1111/ter.12587

(Dey, S., Chauhan, N., Nath, D., Schaaf, N. W., Thiede, R. C., & Jain, V.)

Implications of the ongoing rock uplift in NW Himalayan interiors

The Lesser Himalaya exposed in the Kishtwar Window (KW) of the Kashmir Himalaya exhibits rapid rock uplift and exhumation ($\sim$ 3 mm/yr) at least since the late Miocene. However, it has remained unclear if it is still actively deforming. Here, we combine new field, morphometric and structural analyses with dating of geomorphic markers to discuss the spatial pattern of deformation across the window. We find two steep stream segments, one at the core and the other along the western margin of the KW, which strongly suggest ongoing differential uplift and may possibly be linked to either crustal ramps on the Main Himalayan Thrust (MHT) or active surface-breaking faults. High bedrock incision rates ($>$3 mm/yr) on HolocenePleistocene timescales are deduced from dated strath terraces along the deeply incised Chenab River valley. In contrast, further downstream on the hanging wall of the MCT, fluvial bedrock incision rates are lower ($<$0.8 mm/yr) and are in the range of long-term exhumation rates. Bedrock incision rates largely correlate with previously published thermochronologic data. In summary, our study highlights a structural and tectonic control on landscape evolution over millennial timescales in the Himalaya.

(This work is done in collaboration with S. Dey, V. Jain, P. Chakravarti IIT Gandhinagar; R. C. Thiede, University of Kiel; A. Biswas, IIT-ISM Dhanbad)

doi : https://doi.org/10.5194/esurf-9-463-2021

(Dey, S., Thiede, R. C., Biswas, A., Chauhan, N., Chakravarti, P., & Jain, V.)

Larger floods of Himalayan foothill rivers sustained flows in the GhaggarHakra channel during Harappan age

The humanlandform interaction in the region of the GhaggarHakra palaeochannel in the northwest Indo-Gangetic plains during the Bronze Age Indus/Harappan civilisation ($\sim$4.63.9 thousand years before the present, ka bp) remains an enigmatic case due to a paucity of evidence regarding the hydrology of the then existing river. Here, we estimated the palaeohydrology of the foothill Markanda River in the sub-Himalayan catchment of the GhaggarHakra (GH) palaeochannel. Our morphology and chronology results show aggradation of a fan (57.7 ka) during the Late Pleistocene and T1 to T5 fluvial terraces (13.1 to 6.0 ka) during the terminal Pleistocene to Holocene, and deposition of palaeoflood sediments (3.93.8 ka) over the T3 terraces during the Late Holocene. Considering the known uplift rates along the Himalayan frontal thrust, and our estimated aggradation rates, we have derived channel palaeogeometry and calculated peak discharge at the site of palaeoflood deposits. We conclude that the Markanda River's peak discharge was several orders of magnitude higher during the Late Holocene than the modern-day peak discharge of 100-year return period. The palaeoflood deposits represent larger flooding of the Foothill Rivers that sustained flows in the downstream reaches of the GhaggarHakra palaeochannel during the Late Harappan civilisation.

This work is done in collaboration with A. Singh, V. Jain, M. Danino, R. K. Kaushal, S. Guha, and V. N. Prabhakar IIT, Gandhinagar.

doi : https://doi.org/10.1002/jqs.3320

(Singh, A., Jain, V., Danino, M., Chauhan, N., Kaushal, R. K., Guha, S. and Prabhakar, V. N.)

High-accuracy longitudinal position measurement using self-accelerating light

Radially self-accelerating light exhibits an intensity pattern that describes a spiralling trajectory around the optical axis as the beam propagates. We demonstrate that generating such beams with simultaneously spirals with fast and slow rotation components enables a distance measurement with an accuracy of around 2 μm over a longitudinal range of more than 2 mm using a single beam and only two quadrant detectors. As our method relies on single-beam interference and only requires a static generation and simple intensity measurements, it is intrinsically stable, and could find applications in high-speed measurements of longitudinal position.

(Shashi Prabhakar in collaboration with Stephen Z. D. Plachta, Marco Ornigotti, and Robert Fickler from Tampere University, Finland)

doi : https://doi.org/10.1364/AO.420590

(Prabhakar, S., Plachta S. Z. D., Ornigotti M., and Fickler R.)

Publications in Journals

Astronomy and Astrophysics

1. Abraham, S., N. Mukund, A. Vibhute, V. Sharma, S. Iyyani, D. Bhattacharya,A. R. Rao, S. Vadawale, and V. Bhalerao, 2021, *"A machine learning approach for GRB detection in AstroSat CZTI data"*, Monthly Notices of the Royal Astronomical Society, v. 504, pp. 3084-3091, doi :https://doi.org/10.1093/mnras/stab1082.

2. Acciari, A., S. Ansoldi, L.A. Antonelli, A. Engels, M. Artero, K. Asano, et al., 2021, *"Investigation of the correlation patterns and the Compton dominance variability of Mrk 421 in 2017"*, Astronomy & Astrophysics, v. 655, pp. 36, doi :https://doi.org/10.1051/0004-6361/202141004.

3. Anusree, K. G., D. Bhattacharya, A. R. Rao, S. Vadawale, V. Bhalerao, and A. Vibhute, 2021, *"AstroSat-CZTI as a hard X-ray pulsar monitor"*, Journal of Astrophysics and Astronomy, v. 42, pp. 63, doi :https://doi.org/10.1007/s12036-021-09707-5.

4. Athulya, M. P., D. Radhika, V. K. Agrawal, B. T. Ravishankar, S. Naik, S. Mandal, A. Nandi, 2022, *"Unraveling the foretime of GRS 1915+105 using AstroSat observations: Wide-band spectral and temporal characteristics"*, Monthly Notices of the Royal Astronomical Society, v. 510, p 3019-3038, doi :https://doi.org/10.1093/mnras/stab3614.

5. Bhadari, N. K., L. K. Dewangan, P. M. Zemlyanukha, D. K. Ojha, I. I. Zinchenko, S. Sharma, 2021, *"Probing Gas Kinematics and PDR Structure around O-type Stars in the Sh 2-305 HII Region"*, The Astrophysical Journal, v. 922, pp.12, doi :https://doi.org/10.3847/1538-4357/ac2a44.

6. Bhowmick, R., D. Debnath, K. Chatterjee, S. Nagarkoti, S. K. Chakrabarti, R. Sarkar, D. Chatterjee, A. Jana, 2021, *"Relation between Quiescence and Outbursting Properties of GX 339-4"*, The Astrophysical Journal, v. 910, 138, p 1-8, doi :https://doi.org/10.3847/1538-4357/abe134.

7. Chandra, S., M. Boettcher, P. Goswami, K. P. Singh, M. Zacharias, N. Kaur, S. Bhattacharyya, S. Ganesh, D. Dornier, 2021, *"X-Ray Observations of 1ES 1959+650 in Its High-activity State in 2016-017 with AstroSat and Swift"*, The Astrophysical Journal, v. 918, p. 1-19, doi :https://doi.org/10.3847/1538-4357/ac01d1.

8. Chatterjee, D., A. Jana, K. Chatterjee, R. Bhowmick, S. K. Nath, S. K. Chakrabarti, A. Mangalam, D. Debnath, 2021, *"Properties of Faint X-ray Activity of XTE J1908+094 in 2019"*, Galaxy, v. 9, pp. 25, doi :https://doi.org/10.3390/galaxies9020025.

9. Chatterjee, K., D. Debnath, D. Chatterjee, A. Jana, S. K. Nath, R. Bhowmick, S. K. Chakrabarti, 2021, *"Accretion flow properties of GRS 1716-249 during its 2016–17 'failed' outburst"*, Astrophysics and Space Science, v. 366, pp. 18, doi :https://doi.org/10.1007/s10509-021-03967-x.

10. Chatterjee, R., S. Das, A. Khasnovis, R. Ghosh, N. Kumari, S. Naik, V. M. Larionov, T. S. Grishina, E. N. Kopatskaya, E. G. Larionova, A. A. Nikiforova, D. A. Morozov, S. S. Savchenko, Yu. V. Troitskaya, I. S. Troitsky, and A. A. Vasilyev, 2021, *"Short-Timescale Variability of the Blazar Mrk 421 from AstroSat and Simultaneous Multi-Wavelength Observations"*, Jour. of Astrophysics and Astronomy, v. 42, 80, p 1-7, doi :https://doi.org/10.1007/s12036-021-09709-3.

11. Chattopadhyay, T., S. Gupta, V. Sharma, S. Iyyani, A. Ratheesh, N. P. S. Mithun,E. Aarthy S. Palit, A. Kumar, S. V. Vadawale, A. R. Rao, V. Bhalerao, and D. Bhat- tacharya, 2021, *"Sub-MeV spectroscopy with AstroSat-CZT imager for gamma ray bursts"*, Journal of Astrophysics and Astronomy, v. 42, pp. 82, doi :https://doi.org/10.1007/s12036-021-09718-2.

12. Damian, B., J. Jose, M.R. Samal, E. Moraux, S.R. Das, S. Patra, 2021, *"Testing the role of environmental effects on the initial mass function of low-mass stars"*, Monthly Notices of the RoyalAstronomicalSociety, v.504, pp.2557-2576, doi :https://doi.org/10.1093/mnras/stab194.

13. Debnath, D., K. Chatterjee, D. Chatterjee, A. Jana, S. K. Chakraborty, 2021, *"Jet properties of XTE J1752-223 during its 2009-2010 outburst"*, MNRAS, v. 504, p 4242-4251, doi :https://doi.org/10.1093/mnras/stab1169.

14. Devaraj, R., D. P. Clemens, L. K. Dewangan, A. Luna, T. P. Ray, J. Mackey, 2021, *"Magnetic Fields and Star Formation around HII Regions: The S235 Complex"*, The Astrophysical Journal, v. 911, p. 19, doi :https://doi.org/10.3847/1538-4357/abe9b1.

15. Dewangan, L. K., 2021, *"Unraveling the inner substructure of new candidate hub-filament system in the HII region G25.4NW"*, Monthly Notices of the Royal Astronomical Society, v. 504, p. 1152-1161, doi :https://doi.org/10.1093/mnras/stab1008.

16. Dewangan, L. K., I. I. Zinchenko, P. M. Zemlyanukha, S. -Y. Liu, Y. -N. Su, , S. E. Kurtz, D. K. Ojha, A. G. Pazukhin, Y. D. Mayya, 2022, *"The Disk-Outflow System around the Rare Young O-type Protostar W42-MME"*, The Astrophysical Journal, v. 925, pp. 25, doi :https://doi.org/10.3847/1538-4357/ac36dd.

17. Dewangan, L. K., J. S. Dhanya, N. K. Bhadari, D. K. Ojha, T. Baug, 2021, *"Lynds Bright Nebulae: sites of possible twisted filaments and ongoing star formation"*, Monthly Notices of the Royal Astronomical Society, v. 506, p. 6081-6092, doi :https://doi.org/10.1093/mnras/stab2137.

18. Drake, J. J., J. Ness, K. L. Page, G. J. M. Luna, ... D. P. K. Banerjee,... K. P. Singh, 2021, *"The Remarkable Spin-down*

and Ultrafast Outflows of the Highly Pulsed Supersoft Source of Nova Herculis 2021", The Astrophysical Journal Letters, v. 922L, pp 9, doi :https://doi.org/10.3847/2041-8213/ac34fd.

19. Evans, A., D. P. K. Banerjee, T. R. Geballe,..., M. Shahbandeh, 2022, *"V4334 Sgr (Sakurai's Object): still churning out the dust"*, Monthly Notices of the Royal Astronomical Society, v. 511, pp.713-72, doi :https://doi.org/10.1093/mnras/stac095.
20. Guenther, E. W., D. Woeckel, P. Chaturvedi, V. Kumar, M. K. Srivastava, P. Muheki, 2021, *"The flare-activity of 2MASS J16111534-1757214 in the upper Scorpius association"*, Monthly Notices of the Royal Astronomical Society, v. 507, p. 2103-2114, doi :https://doi.org/10.1093/mnras/stab1973.
21. Gupta, R., S. Gupta, T. Chattopadhyay, V. Lipunov, ..., S. V. Vadawale, ..., V.V. Sokolov, 2022, *"Probing into emission mechanisms of GRB 190530A using time- resolved spectra and polarization studies: synchrotron origin?"*, Monthly Notices of the Royal Astronomical Society, v. 511, pp. 1694-1713, doi :https://doi.org/10.1093/mnras/stac015.
22. Gupta, S., J. Jose, S. More, S.R. Das, G. J. Herczeg, M.R. Samal, Z. Guo, P. Prakash, B. Damian, M. Takami, S Takahashi, K. Ogura, T, Terai, T Pyo, 2021, *"Subaru Hyper Suprime-Cam Survey of Cygnus OB2 Complex - I. Introduction, photometry, and source catalogue"*, Monthly Notices of the Royal Astronomical Society, v. 508, pp.3388-3407, doi :https://doi.org/10.1093/mnras/stab2751.
23. Jaisawal, G. K., S. Naik, P. Epili, B. Chhotaray, A. Jana, P. C. Agrawal, 2021, *"AstroSat observations of eclipsing high mass X-ray binary pulsar OAO 1657-415"*, Jour. of Astrophysics and Astronomy, v. 42, 72, p 1-11, doi :https://doi.org/10.1007/s12036-021-09701-x.
24. Jaisawal, G. K., S. Naik, S. Gupta, P. C. Agrawal, A. Jana, B. Chhotaray, P. Epili, 2021, *"Detection of X-ray pulsations at the lowest observed luminosity of Be/X-ray binary pulsar EXO 2030+375 with AstroSat"*, Jour. of Astrophysics and Astronomy, v. 42, 33, p 1-12, doi :https://doi.org/10.1007/s12036-021-09699-2.
25. Jana, A., G. K. Jaisawal, S. Naik, N. Kumari, B. Chhotaray, D. Altamirano, R. A. Remillard, K. C. Gendreau, 2021, *"NICER observations of the black hole candidate MAXI J0637430 during the 2019-2020 Outburst"*, Monthly Notices of the Royal Astronomical Society, v. 504, p 4793-4805, doi :https://doi.org/10.1093/mnras/stab1231.
26. Jana, A., G. K. Jaisawal, S. Naik, N. Kumari, D. Chatterjee, K. Chatterjee, R. Bhowmick, S. K. Chakrabarti, H. Chang and D. Debnath, 2021, *"Accretion Properties of MAXI J1813-095 during its Failed Outburst in 2018"*, Res. in Astronomy and Astrophysics, v. 21. 125, p 1-12, doi :https://doi.org/10.1088/1674-4527/21/5/125.
27. Jana, A., J. Shang, D. Debnath, S. K. Chakraborty D. Chatterjee, H-K Chang, 2021, *"Study of Accretion Flow Dynamics of V404 Cygni during Its 2015 Outburst"*, Galaxy, v. 9, 39, p 1-21, doi :https://doi.org/10.3390/galaxies9020039.
28. Jana, A., N. Kumari, P. Nandi, S. Naik, A. Chatterjee, G. K. Jaisawal, K. Hayasaki, C. Ricci, 2021, *"Broadband X-Ray Observations of the 2018 Outburst of the Changing-Look Active Galactic Nucleus NGC 1566"*, Monthly Notices of the Royal Astronomical Society, v. 507, p 687-703, doi :https://doi.org/10.1093/mnras/stab2155.
29. Jana, A., S. Naik, D. Chatterjee and G. K. Jaisawal, 2021, *"NuSTAR and Swift Observations of Extragalactic Black Hole X-ray Binaries"*, Monthly Notices of the Royal Astronomical Society, v. 507, p 4779-4787, doi :https://doi.org/10.1093/mnras/stab2448.
30. Jha, V. K., H. Chand, V. Ojha, A. Omar, S. Rastogi, 2021, *"A comparative study of the physical properties for a representative sample of Narrow and Broad-line Seyfert galaxies"*, Monthly Notices of the Royal Astronomical Society, v. 510, pp. 4379-4393, doi :https://doi.org/10.1093/mnras/stab3700.
31. Joshi, A., W. Wang, J. C. Pandey, K. P. Singh, S. Naik, A. Raj, G. C. Anupama, N. Rawat, 2022, *"X-ray Confirmation of the Intermediate Polar IGR J16547-1916"*, Astronomy and Astrophysics, v. 657A12, p 1-12, doi :https://doi.org/10.1051/0004-6361/202142193.
32. Kaminski, T., R. Tylenda, A. Kiljan, M. Schmidt, K. Lisiecki, C. Melis,A. Frankowski, V. Joshi, K. M. Menten, 2021, *"V838 Monocerotis as seen by ALMA: A remnant of a binary merger in a triple system"*, Astronomy & Astrophysics, v. 655, pp. 32, doi :https://doi.org/10.1051/0004-6361/202141526.
33. Karmakar, S., S. Naik, J. C. Pandey, I. S. Savanov, 2022, *"AstroSat observations of Long-duration X-ray superflares on active M-dwarf binary EQ Peg"*, Monthly Notices of the Royal Astronomical Society, v. 509, p 3247-3257, doi :https://doi.org/10.1093/mnras/stab3099.
34. Khandelwal, A., P. Chaturvedi, A. Chakraborty, R. Sharma, E. W. Guenther, C. M. Persson, M. Fridlund, A. P. Hatzes, N. J. S. S. V. Prasad, M. Esposito, S. Chamarthi, A. Nayak, Dishendra, S. B. Howell, 2021, *"Discovery of an inflated hot Jupiter around a slightly evolved star TOI-1789"*, Monthly Notices of the Royal Astronomical Society, v. 509, p. 3339-3354, doi :https://doi.org/10.1093/mnras/stab2970.
35. Kumar, A., T. Chattopadhyay, S. V. Vadawale, A. R. Rao, S. Gupta, N. P. S. Mithun, V. Bhalerao, and D. Bhattacharya, 2021, *"Exploring sub-MeV sensitivity of AstroSat-CZTI for ON-axis bright sources"*, Journal of Astrophysics and Astronomy, v. 42, pp. 67, doi :https://doi.org/10.1007/s12036-021-09711-9.
36. Kumar, V., M. K. Srivastava, D. P. K. Banerjee, C. E. Woodward, U. Munari, A. Evans, V. Joshi, S. Dallaporta, K. L. Page, 2022, *"Optical and near-infrared spectroscopy of Nova V2891 Cygni: evidence for shock-induced dust formation"*, Monthly Notices of the Royal Astronomical Society, v. 510, p. 4265-4283, doi :https://doi.org/10.1093/mnras/stab3772.
37. Kumari, N., M. Pal, S. Naik, A. Jana, G. K. Jaisawal, P. Kushwaha, 2021, *"Complex optical/UV and X-ray variability in Seyfert 1 galaxy Mrk 509"*, Astronomical Society of Australia, v. 38 E042, p 1-15, doi :https://doi.org/10.1017/pasa.2021.41.
38. Kushwaha, P., M. Pal, N. Kalita, N. Kumari, S. Naik, A. C. Gupta, E. M. de Gouveia Dal Pino, M. Gu, 2021, *"Blazar OJ 287 after First VHE Activity: Tracking the Reemergence of the HBL-like Component in 2020"*, The Astrophysical Journal, v. 921, 18, p 1-11, doi :https://doi.org/10.3847/1538-4357/ac19b8.

39. Liu, H., A. Tej, T. Liu, ..., L. K. Dewangan, ..., S. Dutta, 2022, *"ATOMS: ALMA Three-millimeter Observations of Massive Star-forming regions - V. Hierarchical fragmentation and gas dynamics in IRDC G034.43+00.24"*, Monthly Notices of the Royal Astronomical Society, v. 510, pp. 5009-5022, doi :https://doi.org/10.1093/mnras/stab2757.

40. Liu, H., T. Liu, N. J., II Evans, ..., L. K. Dewangan, ..., R. H. Ivarez-Gutirrez, 2022, *"Erratum: ATOMS: ALMA three-millimeter observations of massive star-forming regions - III. Catalogues of candidate hot molecular cores and hyper/ultra compact H II region"*, Monthly Notices of the Royal Astronomical Society, v. 511, pp. 501-505, doi :https://doi.org/10.1093/mnras/stac039.

41. Liu, H., T. Liu, N. J., II Evans, ..., L. K. Dewangan, ..., R. H. Ivarez-Gutirrez, 2021, *"ATOMS: ALMA three-millimeter observations of massive star-forming regions - III. Catalogues of candidate hot molecular cores and hyper/ultra compact H II regions"*, Monthly Notices of the Royal Astronomical Society, v. 505, pp. 2801-2818, doi :https://doi.org/10.1093/mnras/stab1352.

42. Mate, S., T. Chattopadhyay, V. Bhalerao, E. Aarthy, A. Balasubramanian, D. Bhat- tacharya, S. Gupta, K. Kutty, N. P. S. Mithun, S. Palit, A. R. Rao, D. Saraogi, S. Vadawale, and A. Vibhute, 2021, *"The AstroSat mass model: Imaging and flux studies of off-axis sources with CZTI"*, Journal of Astrophysics and Astronomy, v. 42, pp. 93, doi :https://doi.org/10.1007/s12036-021-09763-x.

43. Mondal, B., A. Sarkar, S. V. Vadawale, N. P. S. Mithun, P. Janardhan, G. Del Zanna,H. E. Mason, U. Mitra-Kraev, and S. Narendranath, 2021, *"Evolution of Elemental Abundances during B-Class Solar Flares: Soft X-Ray Spectral Measurements with Chandrayaan-2 XSM"*, The Astrophysical Journal, v. 920, pp. 4, doi :https://doi.org/10.3847/1538-4357/ac14c1.

44. Ojha, V., 2022, *"Intra-night optical variability study of a non-jetted narrow-line Seyfert 1 galaxy: SDSS J163401.94+480940.1"*, Journal of Astrophysics and Astronomy, v. 43, pp. 9, doi :https://doi.org/10.1007/s12036-022-09814-x.

45. Pal, M., N. Kumari, P. Kushwaha, K. P. Singh, A. C. Gupta, S. Naik, G. C. Dewangan, P. Tripathi, R. Adhikari, O. Adegoke, H. Nandan, 2021, *"Spectro-Timing Analysis of a highly variable narrow-line Seyfert 1 galaxy NGC 4748 with AstroSat and XMM-Newton"*, Jour. of Astrophysics and Astronomy, v. 42, 81, p 1-13, doi :https://doi.org/10.1007/s12036-021-09719-1.

46. Pandey, R., S. Sharma, L. K. Dewangan, D. K. Ojha, N. Panwar, S. Das, D. P. Bisen, A. Ghosh, T. Sinha, 2022, *"Sh 2-301: A Blistered HII Region Undergoing Star Formation"*, The Astrophysical Journal, v. 926, pp. 17, doi :https://doi.org/10.3847/1538-4357/ac41c3.

47. Paul, D. A. R. Rao, A. Ratheesh, N. P. S. Mithun, S. V. Vadawale, A. Vibhute,D. Bhattacharya, P. Pradeep, and S. Sreekumar, 2021, *"Characterisation of cosmic ray induced noise events in AstroSat-CZT imager"*, Journal of Astrophysics and Astronomy, v. 42, pp. 68, doi :https://doi.org/10.1007/s12036-021-09750-2.

48. Rajpurohit, K., F. Vazza, R. J., van Weeren, M. Hoeft, ..., A. S. Rajpurohit, ..., F. Andrade-Santos, 2021, *"Dissecting nonthermal emission in the complex multiple-merger galaxy cluster Abell 2744: Radio and X-ray analysis"*, Astronomy & Astrophysics, v. 654, pp. 24, doi :https://doi.org/10.1051/0004-6361/202141060.

49. Rajpurohit, K., M. Hoeft, D. Wittor, R. J. van Weeren, ..., A. S. Rajpurohit, ..., T. E. Clarke, 2022, *"Turbulent magnetic fields in the merging galaxy cluster MACS J0717.5+3745"*, Astronomy & Astrophysics, v. 657, pp. 22, doi :https://doi.org/10.1051/0004-6361/202142340.

50. Rajpurohit, K., R. J. van Weeren, M. Hoeft, F. Vazza, ..., A. S. Rajpurohit, ..., M. Rossetti, 2022, *"Deep Low-frequency Radio Observations of A2256. I. The Filamentary Radio Relic"*, The Astrophysical Journal, v. 927, pp. 21, doi :https://doi.org/10.3847/1538-4357/ac4708.

51. Ramesh, R., C. Kathiravan, N. P. S. Mithun, and S. V. Vadawale, 2021, *"Radio, X- Ray, and Extreme-ultraviolet Observations of Weak Energy Releases in the "Quiet" Sun"*, The Astrophysical Journal, v. 918, pp. L18, doi :https://doi.org/10.3847/2041-8213/ac1da3.

52. Ratheesh, A., A. R. Rao, N. P. S. Mithun, S. V. Vadawale, A. Vibhute, D. Bhat- tacharya, P. Pradeep, S. Sreekumar, and V. Bhalerao, 2021, *"A generalized event selection algorithm for AstroSat CZT imager data"*, Journal of Astrophysics and Astronomy, v. 42, pp. 37, doi :https://doi.org/10.1007/s12036-021-09716-4.

53. Rout, S. K., M. Méndez, T. M. Belloni, and S. Vadawale, 2021, *"Spectral and timing evolution of MAXI J1631-479 during the 2018-19 outburst with NICER"*, Monthly Notices of the Royal Astronomical Society, v. 505, pp. 1213-1222, doi :https://doi.org/10.1093/mnras/stab1341.

54. Rout, S. K., S. V. Vadawale, E. Aarthy, S. Ganesh, V. Joshi, J. Roy, R. Misra, and J.S. Yadav, 2021, *"Multi-wavelength view of the galactic black-hole binary GRS 1716- 249"*, Journal of Astrophysics and Astronomy, v. 42, pp. 39, doi :https://doi.org/10.1007/s12036-021-09696-5.

55. Sharma R., A. Chakraborty, 2021, *"Precision wavelength calibration for radial velocity measurements using uranium lines between 3800 and 6900 Å"*, Journal of Astronomical Telescopes, Instruments, and Systems, v. 7, pp. 038005, doi :https://doi.org/10.1117/1.JATIS.7.3.038005.

56. Sharma, Y., A. Marathe, V. Bhalerao, V. Shenoy, G. Waratkar, D. Nadella, P. Page,P. Hebbar, A. Vibhute, D. Bhattacharya, A. R. Rao, and S. Vadawale, 2021, *"The search for fast transients with CZTI"*, Journal of Astrophysics and Astronomy, v. 42, pp. 73, doi :https://doi.org/10.1007/s12036-021-09714-6.

57. Sicardy, B., N. M. Ashok, , ..., B. C. Bhatt, 2021, *"Pluto's Atmosphere in Plateau Phase Since 2015 from a Stellar Occultation at Devasthal"*, Astrophysical Journal Letters, v.923, pp. 5, doi :https://doi.org/10.3847/2041-8213/ac4249.

58. Singal, A. K., 2021, *"Our peculiar motion from Mid Infra Red AGNs and the discordance seen with the cosmological principle"*, Universe, v. 7, pp. 107, doi :https://doi.org/10.3390/universe7040107.

59. Singal, A. K., 2021, *"Solar system peculiar motion from mid infra red AGNs and its cosmological implications"*, Phys. Sci. Forum, v. 2, pp. 54, doi :https://doi.org/10.3390/ECU2021-09270.

60. Singal, A. K., 2021, *"Implications of a non-zero Poynting flux at infinity sans radiation reaction for a uniformly accelerated charge"*, Foundations of Physics, v. 51, pp. 81, doi :https://doi.org/10.1007/s10701-021-00486-1.

61. Singal, A. K., 2022, *"Solar system peculiar motion from the Hubble diagram of quasars and testing the Cosmological Principle"*, Monthly Notices of the Royal Astronomical Society, v. 511, pp. 1819, doi :https://doi.org/10.1093/mnras/stac144.

62. Singh V., S. Dutta, Y. Wadadekar, C. H. Ishwara-Chandra, 2021, *"Remnant radio galaxy candidates of small angular sizes, Galaxies"*, Galaxies, v. 9, pp. 121, doi :https://doi.org/10.3390/galaxies9040121.

63. Singhal, A., R. Srinivasan, V. Bhalerao, D. Bhattacharya, A. R. Rao, and S. Vadawale, 2021, *"Using collimated CZTI as all-sky X-ray detector based on Earth occultation technique"*, Journal of Astrophysics and Astronomy, v. 42, pp. 64, doi :https://doi.org/10.1007/s12036-021-09743-1.

64. Sow Mondal, S., A. Sarkar, B. Vaidya., A. Mignone, 2021, *"Acceleration of Solar Energetic Particles by the Shock of Interplanetary Coronal Mass Ejection"*, The Astrophysical Journal, v. 923, pp. 13, doi :https://doi.org/10.3847/1538-4357/ac2c7a.

65. Srivastava, M. K., V. Kumar, V. Dixit, A. Patel, M. Jangra, A. S. Rajpurohit, and S. N. Mathur, 2021, *"Design and development of Mt.Abu faint object spectrograph and camera Pathfinder (MFOSC-P) for PRL 1.2m Mt. Abu Telescope"*, Experimental Astronomy, v. 51, p. 345-382, doi :https://doi.org/10.1007/s10686-021-09753-5.

66. Vadawale, S. V., B. Mondal, N. P. S. Mithun, A. Sarkar, P. Janardhan, B. Joshi, A. Bhardwaj, M. Shanmugam, A. R. Patel, H. K. L. Adalja, S. K. Goyal, T. Ladiya, N.K. Tiwari, N. Singh, and S. Kumar, 2021, *"Observations of the Quiet Sun during the Deepest Solar Minimum of the Past Century with Chandrayaan-2 XSM: Elemental Abundances in the Quiescent Corona"*, The Astrophysical Journal, v. 912, pp. L12, doi :https://doi.org/10.3847/2041-8213/abf35d.

67. Vadawale, S. V., N. P. S. Mithun, B. Mondal, A. Sarkar, P. Janardhan, B. Joshi, A. Bhardwaj, M. Shanmugam, A. R. Patel, H. K. L. Adalja, S. K. Goyal, T. Ladiya, N.K. Tiwari, N. Singh, and S. Kumar, 2021, *"Observations of the Quiet Sun during the Deepest Solar Minimum of the Past Century with Chandrayaan-2 XSM: Sub-A-class Microflares outside Active Regions"*, The Astrophysical Journal, v. 912, pp. L13, doi :https://doi.org/10.3847/2041-8213/abf0b0.

68. Vagshette, N. D., S. Naik, N. Kumari, M. K. Patil, 2021, *"Imaging and photometric studies of NGC 1316 (Fornax A) using Astrosat/UVIT"*, Jour. of Astrophysics and Astronomy, v. 42, 34, p 1-8, doi :https://doi.org/10.1007/s12036-021-09708-4.

69. Vibhute, A., D. Bhattacharya, N. P. S. Mithun, V. Bhalerao, A. R. Rao, and S. V. Vadawale, 2021, *"Imaging calibration of AstroSat Cadmium Zinc Telluride Imager (CZTI)"*, Journal of Astrophysics and Astronomy, v. 42, pp. 76, doi :https://doi.org/10.1007/s12036-021-09762-y.

70. Woodward, C. E., A. Evans, D. P. K. Banerjee,R. M. Wagner, 2021, *"The Infrared Evolution of Dust in V838 Monocerotis"*, The Astronomical Journal, v. 162, pp. 9, doi :https://doi.org/10.3847/1538-3881/ac1f1e.

71. Woodward, C. E., D. P. K. Banerjee, ... R. M. Wagner, 2021, *"Near-infrared Studies of Nova V1674 Herculis: A Shocking Record Breaker"*, The Astrophysical Journal Letters, v. 922, pp. 7, doi :https://doi.org/10.3847/2041-8213/ac3518.

72. Yadav, R., M.R. Samal, E. Semenko, A. Zavagno, S. Vaddi, P. Prajapati, D.K. Ojha, A.K Pandey, M. Smith,J. Jose, S. Patra, S. Dutta, P. Irawati, S. Sharma, D.K Sahu, N. Panwar, 2022, *"A Comprehensive Study of the Young Cluster IRAS 05100+3723: Properties, Surrounding Interstellar Matter, and Associated Star Formation"*, The Astrophysical Journal, v. 926, pp. 20, doi :https://doi.org/10.3847/1538-4357/ac3a78.

73. Zhang, C., N. J., II Evans, T. Liu, ..., L. K. Dewangan, ..., D. Li, 2022, *"ATOMS: ALMA Three-millimeter Observations of Massive Star-forming regions - IV. Radio recombination lines and evolution of star formation efficiencies"*, Monthly Notices of the Royal Astronomical Society, v. 510, pp. 4998-5008, doi :https://doi.org/10.1093/mnras/stab2733.

74. Zhou, J., T. Liu, J. Li, ..., L. K. Dewangan, ..., I. Ristorcelli, 2021, *"ATOMS: ALMA Three-millimeter Observations of Massive Star-forming regions-VI. On the formation of the 'L' type filament in G286.21+0.17"*, Monthly Notices of the Royal Astronomical Society, v. 508, pp. 4639-4655, doi :https://doi.org/10.1093/mnras/stab2801.

75. Zinchenko, I. I., L. K. Dewangan, T. Baug, D. K. Ojha, N. K. Bhadari, 2021, *"ALMA discovery of a dual dense probably rotating outflow from a massive young stellar object G18.88MME"*, Monthly Notices of the Royal Astronomical Society, v. 506, p. L45-L49, doi :https://doi.org/10.1093/mnrasl/slab070.

Solar Physics

76. Bora, K., R. Bhattacharyya, A. Prasad, B. Joshi and Q. Hu, 2022, *"Comparison of the Hall Magnetohydrodynamics and Magnetohydrodynamics Evolution of a Flaring Solar Active Region"*, The Astrophysical Journal, v. 925, p. 197, doi :https://doi.org/10.3847/1538-4357/ac3bce.

77. Gupta, G. R. and S. S. Nayak, 2022, *"Spectroscopic and imaging observations of transient hot and cool loops by IRIS and SDO"*, Monthly Notices of the Royal Astronomical Society, v. 512, pp. 3149–3162, doi :https://doi.org/10.1093/mnras/stac657.

78. Ibrahim, M. S., W. Uddin, B. Joshi, R. Chandra and A. K. Awasthi, 2022, *"Investigation of two coronal mass ejections from circular ribbon source region: Origin, Sun-Earth propagation and Geo-effectiveness"*, Research in Astronomy and Astrophysics, v. 21, p. 318, doi :https://doi.org/10.1088/1674-4527/21/12/318.

79. Joshi, B., P. K. Mitra, R. Bhattacharyya, K. Upadhyay, D. Oberoi, K. Sasikumar Raja and C. Monstein, 2021, *"Two-Stage Evolution of an Extended C-Class Eruptive Flaring Activity from Sigmoid Active Region NOAA 12734: SDO and Udaipur-CALLISTO Observations"*, Solar Physics, v. 296, p. 85, doi :https://doi.org/10.1007/s11207-021-01820-6.

80. Kharayat, H., B. Joshi, P. K. Mitra, P. K. Manoharan, and C. Monstein, 2021, *"A Transient Coronal Sigmoid in Active Region NOAA 11909: Build-up Phase, M-class Eruptive Flare,*

and Associated Fast Coronal Mass Ejection", Solar Physics, v. 296, p. 99, doi :https://doi.org/10.1007/s11207-021-01830-4.

81. Louis, R. E., A. Prasad, C. Beck, D. P. Choudhary, and M. S. Yalim, 2021, *"Heating of the solar chromosphere in a sunspot light bridge by electric currents"*, Astronomy & Astrophysics, v. 652, p. L4, doi :https://doi.org/10.1051/0004-6361/202141456.
82. Mishra, W., K. Dave, N. Srivastava and L. Teriaca, 2021, *"Multipoint remote and in situ observations of interplanetary coronal mass ejection structures during 2011 and associated geomagnetic storms"*, Monthly Notices of the Royal Astronomical Society, v. 506, pp. 118-1197, doi :https://doi.org/10.1093/mnras/stab1721.
83. Mishra, W., U. Doshi and N. Srivastava, 2021, *"Radial Sizes and Expansion Behavior of ICMEs in Solar Cycles 23 and 24"*, Frontiers in Astronomy and Space Sciences, v. 8, p. 142, doi :https://doi.org/10.3389/fspas.2021.713999.
84. Mitra, P. K., B. Joshi, A. M. Veronig and T. Wiegelmann, 2022, *"Multiwavelength Signatures of Episodic Nullpoint Reconnection in a Quadrupolar Magnetic Configuration and the Cause of Failed Flux Rope Eruption"*, The Astrophysical Journal, v. 926, p. 143, doi :https://doi.org/10.3847/1538-4357/ac4756.
85. Nitta, N. V., T. Mulligan, E. K. J. Kilpua, B. J. Lynch, M. Mierla, J. OKane, P. Pagano, E. Palmerio, J. Pomoell, I. G. Richardson, L. Rodriguez, A. P. Rouillard, S. Sinha, N. Srivastava, D.-C. Talpeanu, S. L. Yardley and A. N. Zhukov, 2021, *"Understanding the Origins of Problem Geo-magnetic Storms Associated with "Stealth" Coronal Mass Ejections"*, Space Science Reviews, v. 217, p. 82, doi :https://doi.org/10.1007/s11214-021-00857-0.
86. Palmerio E., N. V. Nitta, T. Mulligan, M Mierla, J. OKane, I. G. Richardson, S. Sinha, N. Srivastava, et al., 2021, *"Investigating Remote-sensing Techniques to Reveal Stealth Coronal Mass Ejections"*, Frontiers in Astronomy and Space Sciences, v. 8, 695966, doi :https://doi.org/10.3389/fspas.2021.695966.
87. Patel, B. D., B. Joshi, K.-S. Cho and R.-S. Kim, 2021, *"DH Type II Radio Bursts During Solar Cycles 23 and 24: Frequency-Dependent Classification and Their Flare-CME Associations"*, Solar Physics, v. 296, p. 142, doi :https://doi.org/10.1007/s11207-021-01890-6.
88. Sharma, J., B. Kumar, A. K. Malik and H. O. Vats, 2021, *"Differential rotation of the solar transition region from STEREO/EUVI 30.4-nm image"*, Monthly Notices of the Royal Astronomical Society, v. 506, pp. 4952-4959, doi :https://doi.org/10.1093/mnras/stab1959.
89. Srivastava, N., M. Mierla and J. Zhang, 2021, *"Editorial: Space Weather Prediction: Challenges and Future prospects"*, Frontiers in Astronomy and Space Sciences, v. 8, p. 230, doi :https://doi.org/10.3389/fspas.2021.818878.

Planetary Sciences

90. Acharyya K., 2022, *"Understanding the impact of diffusion of CO in the astrochemical models"*, Publications of the Astronomical Society of Australia, v. 39, pp. e0009, doi :https://doi.org/10.1017/pasa.2022.7.
91. Ahmed S. and K. Acharyya, 2021, *"Gas-phase Modeling of the Cometary Coma of Interstellar Comet 2I/Borisov"*, Astrophysical Journal, v. 923, pp. 91, doi :https://doi.org/10.3847/1538-4357/ac2a42.
92. Almutawa, Shahd A., Tariq Majeed, Omar AlAryani, S. W. Bougher, P. Withers, S. A. Haider and A. A. Morschhauser, 2021, *"On the horizontal currents over the martian magnetic cusp"*, Advances in Space Research, v. 68, p. 3218-3224, doi :https://doi.org/10.1016/j.asr.2021.06.005.
93. Banerjee D., 2022, *"A New Quest for the Moon"*, Current Science, v. 122, p. 501, doi :https://www.currentscience.ac.in/show.issue.php?volume=122&issue=5.
94. Bharti R. R., Smith I. B., Mishra S. K., Srivastava N. and Shukla S. H., 2021, *"SHARAD detection of sedimentary infilling within an unnamed crater near Mangala Fossa region, Mars"*, Icarus, v. 371, pp. 114713, doi :https://doi.org/10.1016/j.icarus.2021.114713.
95. Chavan A., Sarkar S., Thakkar A., Solanki J., Jani C., Bhandari S., Bhattacharya S., Desai B., Ray D., Shukla A., Sajinkumar K. S., Mitra S., Gupta S., Chauhan G., Thakkar M. G., 2022, *"Terrestrial Martian Analog Heritage of Kachchh Basin, Western India"*, Geoheritage, v. 14, pp. 33, doi :https://doi.org/10.1007/s12371-022-00666-z.
96. Dhanya M. B., Smitha V Thampi, Tirtha Pratim Das, R. Satheesh Thampi, Neha Naik, J. K. Abhishek, P. Sreelatha, P. Pradeepkumar, G. Padma Padmanabhan, B. Sundar, Dinakar Prasad Vajja, Amarnath Nandi, Vipin K. Yadav, M. Mohammed Nazeer, P. T. Lali, Rosmy John, A. V. Aliyas, Vijay Kumar Sen, M. Ram Prabhu, A. Ajay Krishna, Tarun K Pant, and Anil Bhardwaj, 2021, *"Argon-40 in Lunar Exosphere: Observations from CHACE-2 on Chandrayaan-2 Orbiter"*, Geophysical Research Letters, v. 48, pp. e2021GL094970, doi :https://doi.org/10.1029/2021GL094970.
97. Dinesh Kumar V. R., J. P. Pabari, K. Acharyya, and C. T. Russell, 2021, *"Venus lightning: Estimation of charge and dimensions of charge regions for lightning initiation"*, Icarus, v. 365, pp. 114473, doi :https://doi.org/10.1016/j.icarus.2021.114473.
98. Dypvik H. Hellevang H., Krzesinska A., Satre C., Viennet C., Bultel B., Ray D., Poulet F., Loizeau D., Veneranda M., Rull F., Cousin A. and Werner S. C., 2021, *"The Planetary Terrestrial Analogues Library (PTAL)- An exclusive lithological selection of possible martian earth analogues"*, Planetary and Space Science, v. 208, pp. 105339, doi :https://doi.org/10.1016/j.pss.2021.105339.
99. Ghosh S., Tiwari K., Miyahara M., Rohrbach A., Vollmer C., Stagno V., Ohtani E. and Ray D., 2021, *"Natural Fe-bearing Aluminous Bridgmenite in the Katol Meteorite"*, Proceedings of the National Academy of Sciences, v. 118, p. e2108736118, doi :https://doi.org/10.1073/pnas.2108736118.
100. Haider, S. A., P. Thirupathaiah, I. S. Btista, M. A. Abdu, J. H. A. Sobral and D. Gobbi, 2022, *"Modeling and causative mechanism of OI630.0 nm nightglow emission over Cachoeira Paulista (22.7oS, 45oW)- Brazil: Seasonal and temporal variability"*, Advances in Space Research, v. 69, p. 889-904, doi :https://doi.org/10.1016/j.asr.2021.10.018.

101. Haider, S. A., Y. S. Siddhi, J. Masoom, Varun Sheel, and T. Kuroda, 2022, *"Impact of dust loading on ozone, winds and heating rates in the atmosphere of Mars: Seasonal variability, climatology and SPICAM observations"*, Planetary and Space Science, v. 212, pp. 105424, doi :https://doi.org/10.1016/j.pss.2022.105424.

102. Jain R. N., R. K. Choudhary, A. Bhardwaj, U. Parikh, B. K. Dai, and Roopa M. V, 2022, *"A study on the solar coronal dynamics during the post-maxima phase of the solar cycle 24 using S-band radio signals from the Indian Mars Orbiter Mission"*, Monthly Notices of the Royal Astronomical Society, v. 511, p. 1750-1756, doi :https://doi.org/10.1093/mnras/stac056.

103. Jaiswal B., G. Mahapatra, A. Nandi, M. Sudhakar, K. Sankarasubramanian, V. Sheel, 2021, *"Polarization signatures of Mars dust and clouds: Prospects for future spacecraft observations"*, Planetary and Space Science, v. 201, pp. 105193, doi :https://doi.org/10.1016/j.pss.2021.105193.

104. Jaiswal S., R. R. Mahajan and M. Ngangom, 2022, *"Neon in interior of the asteroid Vesta and comparison with the terrestrial planets"*, Journal of Asian Earth Sciences: X, v. 7, pp. 100084, doi :https://doi.org/10.1016/j.jaesx.2022.100084.

105. Krishnaprasad C., S. V. Thampi, A. Bhardwaj, T. K. Pant and R. S. Thampi, 2021, *"Ionospheric plasma energization at Mars during the September 2017 ICME event"*, Planetary and Space Science, v. 205, pp. 11, doi :https://doi.org/10.1016/j.pss.2021.105291.

106. Mahajan R. R., D. Raychaudhuri, A. Dutta and A. D. Shukla, 2022, *"Cosmogenic records and noble gases in Mukundpura CM2.0 carbonaceous chondrite"*, Planetary and Space Science, v. 215, pp. 105465, doi :https://doi.org/10.1016/j.pss.2022.105465.

107. Mahajan R. R., S. A., Ehgamberdiev and S. Naik, 2021, *"Noble gases and nitrogen in CV3 chondrite Bukhara"*, Planetary and Space Science, v. 207, pp. 105334, doi :https://doi.org/10.1016/j.pss.2021.105334.

108. Mishra S. K., 2021, *"Nonlinear dust acoustic perturbations within dusty plasma over sunlit lunar surface"*, Physics of Plasmas, v. 28, pp. 033702, doi :https://doi.org/10.1063/5.0043641.

109. Mishra S. K., 2021, *"On the possibility of dust-acoustic waves over sunlit lunar surface"*, Monthly Notices of the Royal Astronomical Society, v. 503, pp. 3965, doi :https://doi.org/10.1093/mnras/stab495.

110. Mishra S. K. and Trinesh Sana, 2021, *"Distribution of charge on floating dust particles over sunlit locations on Moon"*, Monthly Notices of the Royal Astronomical Society, v. 508, pp. 4332, doi :https://doi.org/10.1093/mnras/stab2862.

111. Mishra S. K., K. Durga Prasad, P. Nath, D. Agarwal, S. S. Kumar, and A. Bhardwaj, 2022, *"Effect of Lunar Landing on its surface and surrounding environment and hardware: A numerical perspective"*, Planetary and Space Sciences, v. 211, pp. 105398, doi :https://doi.org/10.1016/j.pss.2021.105398.

112. Mukundan V., S. V. Thampi, A. Bhardwaj and X. Fang, 2021, *"Impact of the 2018 Mars global dust storm on the ionospheric peak: A study using a photochemical model"*, Journal of Geophysical Research, v. 126, pp. e2021JE006823, doi :https://doi.org/10.1029/2021JE006823.

113. Pabari J. P. and T. Sana, 2021, *"Dependence of Martian Schumann resonance on the shape of dust devil and its implications"*, Current Science, v. 121, p. 769-774, doi :https://doi.org/10.18520/cs/v121/i6/769-774.

114. Pabari J. P., S. Nambiar, R. K. Singh, Anil Bhardwaj, K. A. Lad, K. Acharyya, J. M. Jakhariya, S. Jitarwal, Rashmi and V. Sheel, 2022, *"IDP detection in Earth environment: Prediction of plasma capture efficiency and detector response to high-energy particles"*, Planetary and Space Science, v. 215, pp. 105452, doi :https://doi.org/10.1016/j.pss.2022.105452.

115. Raghuram S., A. Bhardwaj, and M. Dharwan, 2022, *"Model for Nitric oxide and its dayglow emission in the Martian upper atmosphere using NGIMS/MAVEN measured neutral and ion densities"*, Icarus, v. 382, pp. 115010, doi :https://doi.org/10.1016/j.icarus.2022.115010.

116. Rani A., Basu Sarbadhikari A., Sinha R. K., Karunatillake S., Komatsu G. and Bates A., 2021, *"Evidence of Regionally Distributed TectonoVolcanism in a Floor Fractured Crater of NorthCentral Arabia Terra, Mars"*, Journal of Geophysical Research: Planets, v. 126, pp. 11, doi :https://doi.org/10.1029/2020JE006748.

117. Ray D., Baliyan S. and Nayak C., 2021, *"Progressive aqueous alteration and iron oxidation record in the matrix of Mukundpura CM2, a new fall"*, Advances in Space Research, v. 68, p. 3233-3241, doi :https://doi.org/10.1016/i.asr.2021.06.009.

118. Ray D., Panda D. K., Arora G., Ghosh S., Murty S. V. S., and Chakrabarty S., 2022, *"Petrochemistry and oxygen isotope of Karimati (L5) chondrite, a 2009 fall in Uttar Pradesh, India"*, Journal of the Geological Society of India, v. 98, p. 323-328, doi :https://doi.org/10.1007/s12594-022-1983-4.

119. Sanghani M. N., K. K. Marhas, S. S.-Y. Hsiao, Z. Peeters, H. Shang, D.-C. Lee, and M. Bizzarro, 2021, *"Presolar silicate and oxide grains found in lithic clasts from Isheyevo and fine grained matrices of NWA 801"*, The Astrophysical Journal Supplement Series, v. 253, pp. 41, doi :https://doi.org/10.3847/1538-4365/abdbab.

120. Sanghani M. N., L. Lajaunie, K. K. Marhas, W. D.A. Rickard, S. S.-Y. Hsiao, Z. Peeters, H. Shang, D.-C. Lee, J. J. Calvino and M. Bizzarro, 2022, *"Microstructural and Chemical Investigations of Presolar Silicates from Asymptotic Giant Branch Stars and Type-II Supernova Explosion"*, The Astrophysical Journal, v. 925, pp. 110, doi :https://doi.org/10.3847/1538-4357/ac3332.

121. Sheel V., Uttam S. and Mishra S. K., 2021, *"Numerical simulation of dust lifting within a steady state dust devil"*, Journal of Geophysical Research Planets, v. 126, pp. e2021JE006835, doi :https://doi.org/10.1029/2021JE006835.

122. Singh, T., N. Srivastava, M. Bhatt, and A. Bhardwaj, 2022, *"Geology of the Crger - Sirsalis Basin: Evidence for prolonged volcanism in the southwestern near side of the Moon"*, Icarus, v. 376, pp. 114875, doi :https://doi.org/10.1016/j.icarus.2021.114875.

123. Sinha, R. K., and Ray, D., 2021, *"Extensive glaciation in the Erebus Montes region of Mars"*, Icarus, v. 36, p. 1-21, doi :https://doi.org/10.1016/j.icarus.2021.114557.

124. Thirupathaiaha, P., S. A. Haider, and J. Masoom, 2022, *"Simulation of photoelectron flux, electron density, emission rate and limb intensity of CO($a^3\pi$) Cameron bands in the Martian thermosphere: Comparisons with (1) SPICAM and IUVS observations and (2) other model calculations"*, Journal of Earth System Science, v. 131, pp. 78, doi :https://doi.org/10.1007/s12040-022-01822-3.

125. Tiwari K., Ghosh S. Miyahara M. and Ray D., 2021, *"Shock-induced incongruent melting of olivine in Kamargaon L6 chondrite"*, Geophysical Research Letters, v. 48, p. e2021GL093592, doi :https://doi.org/10.1029/2021GL093592.

126. Vijayan S., Harish, K. B. Kimi, S. Tuhi, K. Vigneshwaran, R. K. Sinha, S. J. Conway, B. Sivaraman, and Anil Bharadwaj, 2022, *"Boulder Fall Ejecta: Present day activity on Mars"*, Geophysical Research Letters, v. 49, p. 1, doi :https://doi.org/10.1029/2021GL096808.

Space and Atmospheric Sciences

127. Ambade B., Kumar A., and Sahu, L. K., 2021, *"Characterization and health risk assessment of particulate bound polycyclic aromatic hydrocarbons (PAHs) in indoor and outdoor atmosphere of Central East India"*, Environmental Science and Pollution Research, v. 28, p. 56269-56280, doi :https://doi.org/10.1007/s11356-021-14606-x.

128. Ambade, B., Kumar, A., Kumar, A. and Sahu, L. K., 2021, *"Temporal variability of atmospheric particulate-bound polycyclic aromatic hydrocarbons (PAHs) over central east India: sources and carcinogenic risk assessment"*, Air Quality, Atmosphere & Health, 15, p. 115-130, doi :https://doi.org/10.1007/s11869-021-01089-5.

129. Andrioli, V. F., Xu, J., Batista, P. P., Resende, L. C. A., Da Silva, L. A., Marchezi, J. P., Li, H., Wang, C., Liu, Z., and Guharay, A., 2022, *"New findings relating tidal variability and solar activity in the low latitude MLT region"*, Journal of Geophysical Research: Space Physics, v. 127, e2021JA030239, doi :https://doi.org/10.1029/2021JA030239.

130. Chakraborty, P., Gadhavi, H., Prithiviraj, B., Mukhopadhyay, M., Khuman, S. N., Nakamura, M., and Spak, S. N., 2021, *"Passive Air Sampling of PCDD/Fs, PCBs, PAEs, DEHA, and PAHs from Informal Electronic Waste Recycling and Allied Sectors in Indian Megacities"*, Environmental Science and Technology, v. 55, p. 9469-9478, doi :https://doi.org/10.1021/acs.est.1c01460.

131. Choraghe, K., Raghav, A., Chakrabarty, D., Kasthurirangan, S., and Bijewar, N., 2021, *"Properties of the recovery phase of extreme storms"*, Journal of Geophysical Research: Space Physics, v. 126, e2020JA028685, doi :https://doi.org/10.1029/2020JA028685.

132. de Abreu, A. J., Correia, E., Denardini, C. M., de Jesus, R., Venkatesh, K., Roberto, M., Abalde, J. R., Fagundes, P. R., Bolan, M. J. A., and Gende, M., 2022, *"Ionospheric GPS-TEC responses from equatorial region to the EIA crest in the South American sector under intense space weather conditions"*, Journal of Atmospheric and Solar Terrestrial Physics, v. 227, 105801, doi :https://doi.org/10.1016/j.jastp.2021.105801.

133. Girach, I. A., Ojha, N., and Babu, S. S., 2021, *"Ozone chemistry and dynamics at a tropical coastal site impacted by the COVID-19 lockdown"*, Journal of Earth System Science, v. 130, 158, doi :https://doi.org/10.1007/s12040-021-01666-3.

134. Gopalan, K., Shukla, B. P., Sharma, S., Kumar, P., Shyam, A., Gaur, A., and Sunda, S., 2021, *"An observational study of GPS-derived integrated water vapor over India"*, Atmosphere, v. 12, 1303, doi :https://doi.org/10.3390/atmos12101303.

135. Guharay, A., Mondal, S., Sarkhel, S., Sivakandan, M., and Sunil Krishna., M. V., 2022, *"Signature of a mesospheric bore in 557.7 nm airglow emission using all-sky imager at Hanle (32.7° N, 78.9° E),"*, Advances in Space Research, v. 69, p. 2020-2030, doi :https://doi.org/10.1016/j.asr.2021.12.006.

136. Jain, M., Saxena, P., Sharma, S., and Sonwani, S., 2021, *"Investigation of forest fire activity changes over the central India domain using satellite observations during 2001-2020"*, GeoHealth (AGU), v. 5, e2021GH000528, doi :https://doi.org/10.1029/2021GH000528.

137. Kalita, B. R., Bhuyan, P. K., Nath, S. J., Choudhury, M. C., Chakrabarty, D., Wang, K., Hozumi, K., Supnithi, P., Komolmis, T., Yatini, C. Y., and Huy, M. L., 2022, *"The investigation on daytime conjugate hemispheric asymmetry along 100° E longitude using observations and model simulations: new insights"*, Advances in Space Research, v. 69, p. 3726-3740, doi :https://doi.org/10.1016/j.asr.2022.02.058.

138. Kumar, S., Pallamraju, D., Suryawanshi, P., Vijayalakshmi, T, Seemala, G. K., 2022, *"On the latitudinal variation in OI 630.0 nm dayglow emissions in response to the equatorial electrodynamic processes and neutral winds"*, Advances in Space Research, v. 69, p. 926-938, doi :https://doi.org/10.1016/j.asr.2021.10.034.

139. Lalchandani V., Srivastava, D., Dave, J., Mishra, S., Tripathi, N., Shukla, A. K., Sahu, R., Thamban, N. M., Gaddamidi, S., Dixit, K., Ganguly, D., Tiwari, S., Srivastava, A. K., Sahu, L., Rastogi, N., Gargava, P., and Tripathi, S. N., 2022, *"Effect of Biomass Burning on PM2.5 Composition and Secondary Aerosol Formation During Post-Monsoon and Winter Haze Episodes in Delhi"*, Journal of Geophysical Research: Atmospheres, v. 127, e2021JD035232, doi :https://doi.org/10.1029/2021JD035232.

140. Maji, S., Yadav, R., Beig, G., Gunthe, S., S., and Ojha, N., 2021, *"On the processes governing the variability of PTR-MS based VOCs and OVOCs in different seasons of a year over hillocky mega city of India"*, Atmospheric Research, v. 261, 105736, doi :https://doi.org/10.1016/j.atmosres.2021.105736.

141. Mallik, C., Gadhavi, H., Lal, S., Yadav, R. K., Boopathy, R., and Das, T., 2021, *"Effect of Lockdown on Pollutant Levels in the Delhi Megacity: Role of Local Emission Sources and Chemical Lifetimes"*, Frontiers in Environmental Science, v. 9, 743894, doi :https://doi.org/10.3389/fenvs.2021.743894.

142. Mitra, G., Guharay, A., Batista, P. P., and Buriti, R. A., 2022, *"Impact of the September 2019 minor sudden stratospheric warming on the low-latitude middle atmospheric planetary wave dynamics"*, Journal of Geophysical Research: Atmospheres, v. 127, e2021JD035538, doi :https://doi.org/10.1029/2021JD035538.

143. Mondal, A., Saharan, U. S., Arya, R., Yadav, L., Ahlawat, S., Jangirh, R., Kotnala, G., Choudhary, N., Banoo, R., Rai, A., Yadav, P., Rani, M., Lal, S., Stewart, G. J., Nelson, B. S., Acton, W. J. F., Vaughan, A. R.,Hamilton, J. F., Hopkins, J. R., Hewitt, C. N., Sahu, L. K., Tripathi, N., Sharma, S. K., and Mandal, T. K., 2021, *"Non-methane volatile organic compounds emitted from domestic fuels in Delhi: Emission factors and total city-wide emissions"*, Atmospheric Environment: X, v. 11, 100127, doi :https://doi.org/10.1016/j.aeaoa.2021.100127.

144. Mondal, A., Sharma, S. K., Mandal, T. K., Girach, I., and Ojha, N, 2021, *"Frequency distribution of pollutant concentrations over Indian megacities impacted by the COVID-19 lockdown"*, Environmental Science and Pollution Research, Published online, 21 Oct 2021, doi :https://doi.org/10.1007/s11356-021-16874-z.

145. Ojha, N., Girach, I., Sharma, K., Sharma, A., Singh, N., and Gunthe, S. S., 2021, *"Exploring the potential of machine learning for simulations of urban ozone variability"*, Scientific Reports, v. 11, 22513, doi :https://doi.org/10.1038/s41598-021-01824-z.

146. Panda, U., Boopathy, R., Gadhavi, H., Renuka, K., Gunthe, S., and Das, T., 2021, *"Metals in coarse ambient aerosol as markers for source apportionment and their health risk assessment over an eastern coastal urban atmosphere in India"*, Environmental Monitoring and Assessment, v. 193, 311, doi :https://doi.org/10.1007/s10661-021-09057-3.

147. Rajesh, T. A., Ramachandran, S., and Dhaker, V. K., 2021, *"Black carbon aerosols: Relative source strengths of vehicular emissions and residential/open wood burning over an urban and a semi-urban environment"*, Atmospheric Pollution Research, v. 12, 101060, doi :https://doi.org/10.1016/j.apr.2021.101060.

148. Ramachandran, S., and Priyadarshini, B., 2021, *"Biomass burning and impacts on aerosols: Optical properties and radiative effects"*, Biomass Burning in South and Southeast Asia, 2, pp. 193-207, doi :https://www.taylorfrancis.com/chapters/edit/10.1201/9780429022036-15/biomass-burning-impacts-aerosol.

149. Ramachandran, S., Rajesh, T. A., and Cherian, R., 2021, *"Black carbon aerosols over source vs. background region: Atmospheric boundary layer influence, potential source regions, and model comparison"*, Atmospheric Research, v. 256, 105573, doi :https://doi.org/10.1016/j.atmosres.2021.105573.

150. Ramachandran, S., Rupakheti, M., and Cherian, R., 2022, *"Insights into recent aerosol trends over Asia from observations and CMIP6 simulations"*, Science of the Total Environment, v. 807, 150756, doi :https://doi.org/10.1016/j.scitotenv.2021.150756.

151. Ramachandran, S., Rupakheti, M., Cherian, R. and Lawrence, M., 2022, *"Climate benefits of cleaner energy transitions in East and South Asia through black carbon reduction"*, Frontiers in Environmental Science, v. 10, 842319, doi :https://doi.org/10.3389/fenvs.2022.842319.

152. Saha, S., Pallamraju, D., Pant, T. K., and Chakrabarti, S., 2021, *"On the Cause of the Post-Sunset Nocturnal OI 630 nm Airglow Enhancement Over Low-Latitude Thermosphere"*, Journal of Geophysical Research: Space Physics, v. 126, e2021JA029146, doi :https://doi.org/10.1029/2021JA029146.

153. Saha, S., Sharma, S., Chhabra, A., Kondapalli, N. K., Kumar, P., Kamat, D., and Lal, S., 2022, *"Impact of dust storm on the atmospheric boundary layer: a case study from western India"*, Natural Hazards, 176 Accesses, 2 Altmetric, doi :https://doi.org/10.1007/s11069-022-05293-z.

154. Saha, S., Sharma, S., Kondapalli, N. K., Kumar, P., Joshi, V., Georgoussis, V., and Lal, S., 2021, *"A Case Study on the Vertical Distribution and Characteristics of Aerosols using Ground-based Raman Lidar, Satellite and Model over Western India"*, International Journal of Remote Sensing, v. 42, p. 6417-6432, doi :https://doi.org/10.1080/01431161.2021.1938737.

155. Saha, S., Sharma, S., Kondapalli, N. K., Kumar, P., Lal, S., and Kamat, D., 2021, *"Investigation of Atmospheric Boundary Layer characteristics using Ceilometer Lidar, COSMIC GPS RO satellite, Radiosonde and ERA-5 reanalysis dataset over Western Indian Region"*, Atmospheric Research, v. 268, 105999, doi :https://doi.org/10.1016/j.atmosres.2021.105999.

156. Sahu, L. K., Tripathi, N., Gupta, M., Singh, V., Yadav, R., and Patel, K., 2022, *"Impact of COVID-19 pandemic lockdown in ambient concentrations of aromatic volatile organic compounds in a metropolitan city of western India"*, Journal of Geophysical Research: Atmospheres, v. 127, e2022JD036628, doi :https://doi.org/10.1029/2022JD036628.

157. Sharma, S. and Kumar, P., 2021, *"Impact of Transmission of COVID-19 Epidemic: Scenario in the Tropical Environment"*, Pure & Applied Geophysics, v.178, p. 3169-3177, doi :https://doi.org/10.1007/s00024-021-02793-0.

158. Shiokawa, K., Dasso, S., Miteva, R., Pallamraju, D., and Zhang, Shung-Rong, 2021, *"Preface of the special issue: "Variability of the Sun and Its Terrestrial Impact (VarSITI) Completion Symposium 2019 and the SCOSTEP 14th Quadrennial Solar-Terrestrial Physics Symposium (STP14)""*, Journal of Atmospheric and Solar Terrestrial Physics, v. 215, 105593, doi :https://doi.org/10.1016/j.jastp.2021.105593.

159. Singh, A., Thakur, M., Geesupalli, P., Anandan, N. R., Lakshmi, T. V., Sharma, S., and Kumar, P., 2020, *"Scaling of heavy rainy days with upper air profiles over Chennai during Northeast monsoon"*, Indian Journal of Radio and Space Physics, v. 49, p.153-161, doi :http://nopr.niscair.res.in/handle/123456789/57665.

160. Singh, J., Singh, N., Ojha, N., Srivastava, A. K., Bisht, D. S., Rajeev, K., Kiran N. V. P. Kumar,Ravi S. Singh,Vivek Panwar, S. K. Dhaka,Vinay Kumar,Tomoki Nakayama,Yutaka Matsumi,Sachiko Hayashida,A. P. Dimri, 2022, *"Genesis of a severe dust storm over the Indian subcontinent: Dynamics and impacts"*, Earth and Space Science, v. 9, e2021EA001702, doi :https://doi.org/10.1029/2021EA001702.

161. Singh, V., Chandra, S., Thomas, S., Sharma, S., and Vats , H. O., 2021, *"A long-term multifrequency study of solar rotation using the solar radio flux and its relationship with solar cycles"*, Monthly Notices of the Royal Astronomical Society (MNRAS), v. 505, p. 5228-5237, doi :https://doi.org/10.1093/mnras/stab1574.

162. Singh, V., Chandra, S., Thomas, S., Sharma, S., and Vats , H. O., 2021, *"Radial differential rotation of solar corona using radio*

emissions", Monthly Notices of the Royal Astronomical Society (MNRAS), v. 505, pp. L16-L20, doi :https://doi.org/10.1093/mnrasl/slab042.

163. Sivakandan, M, Mondal, S., Sarkhel, S., Chakrabarty, D., Sunil Krishna, M. V., Upadhayaya, A. K., Shinbori, A., Sori, T., Kannaujiya, S., and Champati Ray, P. K., 2021, *"Evidence for the in-situ generation of plasma depletion structures over the transition region of geomagnetic low-mid latitude"*, Journal of Geophysical Research: Space Physics, v. 126, e2020JA028837, doi :https://doi.org/10.1029/2020JA028837.

164. Soni, A., Decesari, S., Gadhavi, H., Paglione, M., Orsini, D., Shridhar, V., Kumar, U., and Volpi, F., 2022, *"Chemical composition and radiative forcing of atmospheric aerosols over the high-altitude Western Himalayas of India"*, Environmental Science and Pollution Research, v. 29, p. 1961-1974, doi :https://doi.org/10.1007/s11356-021-15609-4.

165. Soni, M., Girach, I., Sahu, L. K., Ojha, N., 2022, *"Photochemical evolution of air in a tropical urban environment of India: A model-based study"*, Chemosphere, v.297, ., doi :https://doi.org/10.1016/j.chemosphere.2022.134070.

166. Stewart, G. J., Nelson, B. S., Acton, W. J. F., Vaughan, A. R., Hopkins, J. R., Yunus, S. S., Hewitt, C. N., Wild, O., Nemitz, E., Gadi, R. Sahu, L. K., Mandal T. K., Gurjar B. R., Rickard A. R., Lee, J. D., and Hamilton J. F., 2021, *"Emission estimates and inventories of non-methane volatile organic compounds from anthropogenic burning sources in India"*, Atmospheric Environment: X, v. 11, p.100115, doi :https://doi.org/10.1016/j.aeaoa.2021.100115.

167. Tripathi, N., Sahu, L. K., Patel, K., Kumar, A. and Yadav, R., 2021, *"Ambient air characteristics of biogenic volatile organic compounds at a tropical evergreen forest site in Central Western Ghats of India"*, Journal of Atmospheric Chemistry, v. 78, p. 139-159, doi :https://doi.org/10.1007/s10874-021-09415-y.

168. Venkatesh, K., and Patra, A. K., 2022, *"Formation of the evening time F3 layer investigated using Jicamarca incoherent scatter radar observations"*, Journal of Geophysical Research: Space Physics, v. 127, e2021JA029684, doi :https://doi.org/10.1029/2021JA029684.

169. Yadav, R., Vyas, P., Kumar, P., Sahu, L. K., Pandeya, U. K. V., Tripathi, N., Gupta, M., Singh, V., Dave, P. N., Rathode, D.S. and Beig, G., 2022, *"Particulate-matter pollution in urban cities of India during unusually restricted anthropogenic activities"*, Frontiers in Sustainable Cities, v. 4, 792507, pp-1-14, doi :https://doi.org/10.3389/frsc.2022.792507.

Geosciences

170. Ahmad, N., Singh, S.P., Lone, A.M., Qasim, A., Bhushan, R., Tripathy, G.R. and Shah, C., 2022, *"Historical variations in autochthonous and allochthonous sediment supplies to the largest freshwater lake in Central India"*, International Journal of Sediment Research, v. 37, p. 563-575, doi :https://doi.org/10.1016/j.ijsrc.2022.02.008.

171. Ali, S.N., and Shukla, A.D., 2021, *"An Exigency for Ice Core Studies to Determine Spatio-temporal Variability in Moisture Sources and Impact of Black CarbonMineral Aerosols on the Himalayan Glaciers"*, Journal of Atmospheric Science Research, v. 4, pp. 3556, doi :https://ojs.bilpublishing.com/index.php/jasr.

172. Baliyan, S., Moitra, H., Sarkar, S., Ray, D., Panda, D.K., Shukla, A.D., Bhattacharya, S.K., and Gupta, S., 2021, *"Mineralogy and Spectroscopy (Visible Near Infrared and Fourier Transform Infrared) of Mukundpura CM_2: Implications for asteroidal aqueous alteration"*, Geochemistry, v. 18, pp. 125729, doi :https://doi.org/10.1016/j.chemer.2020.125729.

173. Banerji, U.S., Goswami, V., and Joshi, J.B., 2022, *"Instrumental development and its application in Quaternary dating: An overview"*, Journal of Asian Earth Sciences, v. 7, pp. 100091, doi :https://doi.org/10.1016/j.jaesx.2022.100091.

174. Bharti, N., Bhushan, R., Skinner, L., Muruganantham, M., Jena, P.S., Dabhi, A., and Shivam, A., 2022, *"Evidence of poorly ventilated deep Central Indian Ocean during the last glaciation"*, Earth and Planetary Science Letters, v. 582, pp. 117438, doi :https://doi.org/10.1016/j.epsl.2022.117438.

175. Bhowmik, H.S., Shukla, A., Lalchandani, L., Dave, J., Rastogi, N., Kumar, M., Singh, V., and Tripathi, S.N., 2022, *"Inter-comparison of online and offline methods for measuring ambient heavy and trace elements and water-soluble inorganic ions (NO_3, $SO_4{}^2$, NH^{4+} and Cl) in $PM_{2.5}$ over a heavily polluted megacity, Delhi"*, Atmospheric Measurement Technique, v.15, p. 2667-2684, doi :https://doi.org/10.5194/amt-2021-191.

176. Gandhi, U., Khatri, N., Brahambhatt, V., Jha, A. K., Patel, A., and Rastogi, N., 2021, *"Health impact assessment from exposure to trace metals present in atmospheric PM_{10} at Ahmedabad, a big city in western India"*, Environmental Monitoring Assessment, v. 193, pp. 663, doi :https://doi.org/10.1007/s10661-021-09452-w.

177. George, B.G., Kumar, S.,and Ray, J.S., 2021, *"C-Sr isotope stratigraphy of carbonate formations of the late Neoproterozoic-Cambrian Marwar Supergroup, western India"*, Precambrian Research, v. 364, pp. 106378, doi :https://doi.org/10.1016/j.precamres.2021.106378.

178. Ghosh., A., Patel, A., Rastogi, N., Sharma, S.K., Mandal, T.K., and Chatterjee, A., 2021, *"Size-segregated aerosols over a high altitude Himalayan and a tropical urban metropolis in Eastern India: Chemical characterization, light absorption, role of meteorology and long range transport"*, Atmospheric Environment, v. 254, pp. 118398, doi :https://doi.org/10.1016/j.atmosenv.2021.118398.

179. Gopinath, G., Resmi, T.R., Pragath, M., Jesiya, N.P., Hameed, A. Shabul., and Deshpande, R.D., 2021, *"Isotopic differentiation of groundwater recharge processes in a semiarid region of southern India"*, Environmental Earth Sciences, v. 80, p. 522, doi :https://doi.org/10.1007/s12665-021-09816-y.

180. Goswami, V., Singh, S.K., Bhushan, R., and Rai, V.K., 2022, *"Spatial distribution of Mo and δ^{98}Mo in waters of the northern Indian Ocean: Role of suboxia and particle-water interactions on the lighter Mo in the Bay of Bengal"*, Geochimica et Cosmochimica Acta, v. 324, p. 174-193, doi :https://doi.org/10.3390/min11040417.

181. Jangirh, R., Ahlawat, S., Arya, R., Mondal, A., Yadav, L., Kotnala, G., Yadav, P., Choudhary, N., Rani, M., Banoo, R., Rai, A., Singh, U., Rastogi, N., Patel, A., Shivani, S., Gadi. R., Saxena, P., Vijayan, N., Sharma, C., Sharma, S.K., and, Mandal, T.K., 2022, *"Gridded distribution of total suspended particulates (TSP) and their chemical characterization over Delhi during winter"*, Environmental Science and Pollution Research, v. 29, p. 1789217918, doi :https://dx.doi.org/10.1007/s11356-021-16572-w.

182. Jeelani, Gh., Lone, S.A., Nisa, A.U., Deshpande, R.D., and, Padhya., V, 2021, *"Use of stable water isotopes to identify and estimate the sources of groundwater recharge in an alluvial aquifer of Upper Jhelum Basin (UJB), western Himalayas"*, Hydrological Sciences Journal, v. 66, p. 2330-2339, doi :https://doi.org/10.1080/02626667.2021.1985126.

183. Jeelani, Gh., Shah Rouf A., Deshpande, R.D., Dimri, A.P., Mal, S. and, Sharma, A., 2021, *"Isotopic analysis to quantify the role of the Indian monsoon on water resources of selected river basins in the Himalayas"*, Hydrological Processes, v. 35, e14406, doi :https://doi.org/10.1002/hyp.14406.

184. Jena P.S., Bhushan, R., Shivam, A., Bharti, N., and Sudheer, A.K., 2021, *"^{10}Be depositional flux variation in the central Indian Ocean during the last 43 ka"*, Science of the Total Environment, v. 802, p., doi :https://doi.org/10.1016/j.scitotenv.2021.149808.

185. Jena, P.S., Bhushan, R., Shivam, A., Nambiar, R., and Bharti, N., 2021, *"Production rate variation and changes in sedimentation rate of marine core dated with meteoric ^{10}Be and ^{14}C"*, Journal of Environmental Radioactivity, v. 237, pp. 106678, doi :https://doi.org/10.1016/j.jenvrad.2021.106678.

186. Joshi, K.B., Goswami, V., Banerji, U.S., and Shankar, R., 2021, *"Recent Developments in Instrumentation and its application in absolute dating: Historical perspective and Overview"*, Journal of Asian Earth Sciences, v. 211, pp. 104690, doi :https://doi.org/10.1016/j.jseaes.2021.

187. Kumar, A., Ray, J.S., Binusarma, P.E., Awasthi, N., George, B.G. Yadava, M.G., Bhutani, R., Balakrishnan, S., Pande, K., 2021, *"Origin of breccia in mud volcanoes of the Andaman accretionary prism: Implications for forearc processes"*, Chemical geology, v. 586, p. 120595, doi :https://doi.org/10.1016/j.chemgeo.2021.120595.

188. Kumar, A., Shukla, G., and Singh, A., 2022, *"Long Range Global Transport of Dust and Characterization of Dust, In Asian Atmospheric Pollution"*, Elsevier, v., p. 483-504, doi :https://doi.org/10.1016/B978-0-12-816693-2.00012-3.

189. Kumar, P.K., and Singh, A., 2021, *"Increase in summer monsoon rainfall over the northeast India during El Niño years since 1600"*, Climate Dynamics, v. 57, p. 851-863, doi :https://doi.org/10.1007/s00382-021-05743-7.

190. Kumari, V.R., Sarma, V., Mahesh, G., and Sudheer, A.K., 2022, *"Temporal variations in the chemical composition of aerosols over the coastal Bay of Bengal"*, Atmospheric Pollution Research, v. 13, pp. 101300, doi :https://doi.org/10.1016/j.apr.2021.101300.

191. Laskar, A.H.,and Bohra, A., 2021, *"Impact of Indian Summer Monsoon Change on Ancient Indian Civilizations During the Holocene"*, Frontiers in Earth Sciences, v. 9, pp. 709455, doi :https://doi.org/10.3389/feart.2021.709455.

192. Lone, A., Jeelani, Gh. Deshpande, R.D., and Padhya, V., 2021, *"Impact of Indian summer monsoon in westerly dominated water resources of western Himalayas"*, Isotopes in Environmental and Health Studies, v., pp. 1-26, doi :https://doi.org/10.1080/10256016.2021.2011725.

193. Lone, A., Jeelani, Gh., Deshpande, R.D.,and Padhya, V., 2021, *"Estimating the sources of stream water in snow dominated catchments of western Himalayas"*, Advances in Water Resources, v. 155, pp. 103995, doi :https://doi.org/10.1016/j.advwatres.2021.103995.

194. Lone, M., Sharma, S., Achyuthan, H., Shukla, A.D., Shah, R.A., Sangode, S.J., and Fousiya, A., 2021, *"Climatic implications of late Holocene loess and intervening paleosols, Southern Zanskar range, northwestern Himalaya"*, Physical Geography, v. 43, pp. 1938501, doi :https://doi.org/10.1080/02723646.2021.1938501.

195. Lone, S.A., Jeelani, Gh. Deshpande, R.D., Mukherjee, A., Jasechko, S., and Lone, A., 2021, *"Meltwaters dominate groundwater recharge in cold arid desert of Upper Indus River Basin (UIRB), western Himalayas"*, Science of The Total Environment, v.786, pp. 147514, doi :https://doi.org/10.1016/j.scitotenv.2021.147514.

196. Lone, S.A., Jeelani, Gh., Padhya, V., and Deshpande, R.D., 2022, *"Identifying and estimating the sources of river flow in the cold arid desert environment of Upper Indus River Basin (UIRB), western Himalaya"*, Science of The Total Environment, v. 832, pp. 154964, doi :https://doi.org/10.1016/j.scitotenv.2022.154964.

197. Maibam, B., Sharma, K.A., Shukla, A.D., Argyrios, A., and Elena, B., 2021, *"Geochemical and geochronological study of rodingites from the northeast India ophiolites: Petrogenetic significance and timing of rodingitisation"*, Geological Journal, v. 57, p. 768-781, doi :https://doi.org/10.1002/gj.4301.

198. Mandal, A., Tripathy, G.R., Goswami, V., Ackerman, L., Parcha, K., and Chandra, R., 2021, *"Re-Os and Sr isotopic study of Permian-Triassic sedimentary rocks from the Himalaya: Shale chronology and Carbonate diagenesis"*, Special issue "Timing, Duration, and Causes of Mass Extinctions", Minerals, v. 11, pp. 417, doi :https://doi.org/10.3390/min11040417.

199. Mandal, R., Das, A., Sudheer, A.K., Kumar, S., Verma, S., Gaddam, M., and Deshpande, R.D., 2021, *"Sources, controls, and probabilistic health risk assessment of fluoride contamination in groundwater from a semi-arid region in Gujarat, Western India: An isotopehydrogeochemical perspective"*, Environmental Geochemistry and Health, v. 43, p. 4043-4059, doi :https://doi.org/10.1007/s10653-021-00894-2.

200. Mehta, S., Singh, A., and Thirumalai, K., 2021, *"Uncertainty in palaeosalinity estimates from foraminiferal geochemical records in the northern Indian Ocean"*, Palaeogeography, Palaeoclimatology, Palaeoecology, v. 569, 110326, doi :https://doi.org/10.1016/j.palaeo.2021.110326.

201. Nambiar, R., Bhushan, R., and Raj, H., 2022, *"Paleoredox conditions of bottom water in the northern Indian Ocean since 39 ka"*, Palaeogeography, Palaeoclimatology, Palaeoecology, v. 586, 110766, doi :https://doi.org/10.1016/j.palaeo.2021.110766.

202. Naskar, M, Ghosh, R., Das, S., Paruya, D.K., Sardar, B., Yadava, M.G., and Bera, S., 2021, *"Grass phytoliths in surface sediments of the Sunderbans, India and their implications in reconstructing past deltaic environmental changes"*, The Holocene, v., p., doi :https://doi.org/10.1177/09596836211041736.

203. Nayak, G., Kumar, A., Bikkina, S., Tiwari, S., Sheteye, S.S., and Sudheer, A.K., 2022, *"Carbonaceous aerosols and their light absorption properties over the Bay of Bengal during continental outflow"*, Environmental Science: Processes & Impacts, v. 24, p. 72-88, doi :https://doi.org/10.1039/D1EM00347J.

204. Nayna, O.S., Begum, M.S., Sarma, V.V.S.S., Hartmann, J., Kumar, S., Tareq, S.M., and Hyung Park, J., 2021, *"Reassessing riverine carbon dioxide emissions from the Indian subcontinent"*, Science of the Total Environment, v. 816, pp. 151610, doi :https://doi.org/10.1016/j.scitotenv.2021.151610.

205. Oza, H., Padhya, V., Ganguly, A.K., and Deshpande, R.D., 2022, *"Investigating hydrometeorology of the Western Himalayas: Insights from stable isotopes of water and meteorological parameters"*, Atmospheric Research, v. 268, pp. 105997, doi :https://doi.org/10.1016/j.atmosres.2021.105997.

206. Patel, A., Satish, R., and Rastogi, N., 2021, *"Remarkably High Oxidative Potential of Atmospheric $PM_{2.5}$ coming from a Large-Scale Paddy-Residue Burning over the Northwestern Indo-Gangetic Plain"*, ACS Earth and Space Chemistry, v. 5, p. 2442-2452, doi :https://doi.org/10.1021/acsearthspacechem.1c00125.

207. Phillips, H.E., Tandon, A., Furue, R., Hood, R., Ummenhofer, C., Benthuysen, J., Menezes, V., Hu, S., Webber, B., Franks, A., Cherian, D., Shroyer, E., Feng, M., Wijeskera, H., Chatterjee, A., Yu, L., Hermes, J., Murtugudde, R., Tozuka, T., Su, D., Singh, A., Centurioni, L., Prakash, S., and Wiggert, J., 2021, *"Progress in understanding of Indian Ocean circulation, variability, airsea exchange, and impacts on biogeochemistry"*, Ocean Science, v.17, p. 1677-1751, doi :https://doi.org/10.5194/os-17-1677-2021.

208. Ragavan, P., and Kumar, S., 2021, *"Potential role of priming effect in open ocean oxygen minimum zones–an outlook"*, Hydrobiologia, v. 848, p. 2437-2448, doi :https://doi.org/10.1007/s10750-021-04574-1.

209. Ragavan, P., Kumar, S., Kathiresan, K., Mohan, P.M., Jayaraj, R.S.C., Ravichandaran, K., and Rana, T.S., 2021, *"Biomass and vegetation carbon stock in mangrove forests of the Andaman Islands, India"*, Hydrobiologia, v. 848, p. 4673-4693, doi :https://doi.org/10.1007/s10750-021-04651-5.

210. Rahman A., Rathi, A., Nambiar, R., Mishra, P.K., Ambili, A., Bhushan, R., and Kumar, S., 2021, *"Signatures of natural to anthropogenic transition in lake sediments from the Central Himalaya using stable isotopes"*, Applied Geochemistry, v. 134, 105095, doi :https://doi.org/10.1016/j.apgeochem.2021.105095.

211. Rahman, A., Atif Khan, M., Singh, S., and Kumar, S., 2021, *"Hydrological characteristics of the Bay of Bengal water column using $\delta^{18}O$ during the Indian summer monsoon"*, Continental Shelf Research, v. 226, pp., doi :https://doi.org/10.1016/j.csr.2021.104491.

212. Raj, H., and Bhushan, R., 2021, *"Spatial and temporal changes in bomb radiocarbon in the northern Indian Ocean"*, Journal of Environmental Radioactivity, v. 237, pp. 1066880, doi :https://doi.org/10.1016/j.jenvrad.2021.106680.

213. Raj, H., Bhushan, R., Banerji, U.S., Muruganantham, M., Shah, C., Nambiar, R., and Dabhi, A.J., 2022, *"Air-sea CO_2 exchange rate in the northern Indian Ocean based on coral radiocarbon records"*, Applied Geochemistry, v. 137, pp. 105208, doi :https://doi.org/10.1016/j.apgeochem.2022.105208.

214. Raj, H., Bhushan, R., Kumar, S., Banerji, U., Shah, C., and Verma, S., 2021, *"Monsoon signature in corals from the northern Indian Ocean"*, Journal of Marine Systems, v. 226, 103664, doi :https://doi.org/10.1016/j.jmarsys.2021.103664.

215. Rastogi, N., Satish, R., Singh, A., Kumar, V., Thamban, N., Lalchandani, V., Shukla, A., Vats, P., Tripathi, S.N., Ganguly, D., Slowik, J., and Prevot, A.S.H., 2021, *"Diurnal Variability in the Spectral Characteristics and Sources of Water-Soluble Brown Carbon Aerosols over Delhi"*, Science of the Total Environment, v. 794, pp. 148589, doi :https://doi.org/10.1016/j.scitotenv.2021.148589.

216. Sahoo, D., Saxena, H., Nazirahmed, S., Kumar, S., Sudheer, A.K., Bhushan, R., Sahay, A., and Singh, A., 2021, *"Role of eddies and N_2 fixation in regulating C:N:P proportions in the Bay of Benga"*, Biogeochemistry, v. 155, p. 413-429, doi :https://doi.org/10.1007/s10533-021-00833-4.

217. Samanta, A., Tripathy Ranjan, G., Nagender Nath, N., Bhushan, R., Rajani Panchang, R., Bharti, N., and Shrivastava, A., 2022, *"Holocene variability in chemical weathering and ocean redox state: A reconstruction using sediment geochemistry of the Arabian Sea"*, Journal of Asian Earth Sciences, v. 224, pp. 105029, doi :https://doi.org/10.1016/j.jseaes.2021.105029.

218. Sebastian, S., Bhutani, R., Balakrishnan, S., Tomson, J.K., and Shukla, A.D., 2021, *"Geochemical and isotopic studies of potassic granite from the western Dharwar craton, southern India: Implications for crustal reworking in the Neoarchean"*, Geological Journal, v. 56, p. 2930-2949, doi :https://doi.org/10.1002/gj.4085.

219. Shaji, J., Banerji, U., Maya, K., Joshi, K.J., Dabhi, A.J., Bharti, N., Bhushan, R., and Padmalal, D., 2022, *"Holocene monsoon and sea-level variability from coastal lowlands of Kerala, SW India"*, Quaternary International, v. 639, p., doi :https://doi.org/10.1016/j.quaint.2022.03.005.

220. Shirina Begum, M., Bogard, M., Butman, D., Eliyan, C., Kumar, S., Xi Xi Lu, Nayna, O.K., Ran, L., Richey, J.E., Tareq, S.M., Xuan, D.T., Yu, R.,and Park, J, 2021, *"Localized Pollution Impacts on Greenhouse Gas Dynamics in Three Anthropogenically Modified Asian River Systems"*, Journal of Geophysical Research: Biogeosciences, v. 126, p., doi :https://doi.org/10.1029/2020JG006124.

221. Shukla, A. K., Lalchandani, V., Bhattu, D., Dave, J. S., Rai, P., Thamban, N. M., Mishra, S., Gaddamidi, S., Tripathi, N., Vats, P., Rastogi, N., Sahu L. K., Ganguly, D., Kumar, M., Singh, V., Gargava, P., and Tripathi S.N., 2021, *"Real-time quantification and source apportionment of fine particulate matter including organics and elements in Delhi during summertime"*, Atmospheric Environment, v. 261, p.

118598, doi :https://doi.org/10.1016/j.atmosenv.2021.118598.

222. Singh, A., and Chaturvedi, P., 2021, *"Error Propagation"*, Resonance, v. 26, p. 853-861, doi :https://doi.org/10.1007/s12045-021-1185-1.

223. Singh, A., Bach, L., Löscher, C., Paul, A., Ojha, N., and Riebesell, U., 2021, *"Impact of increasing carbon dioxide on dinitrogen and carbon fixation rates under oligotrophic conditions and simulated upwelling"*, Limnology and Oceanography, v. 66, p. 2855-2867, doi :https://doi.org/10.1002/lno.11795.

224. Sivadas, S.K., Gupta, G.V.M., Kumar, S.,and Ingole, S., 2021, *"Trait-based and taxonomic macrofauna community patterns in the upwelling ecosystem of the southeastern Arabian Sea"*, Marine Environmental Research, v. 170, pp. 105431, doi :https://doi.org/10.1016/j.marenvres.2021.105431.

225. Talukdar, S., Tripathi S. N., Lalchandani, V., Rupakheti, M., Bhowmik, H. S., Shukla, A.K., Murari, V., Sahu, R., Jain, V., Tripathi, N., Dave. J., Rastogi, N., and Sahu, L., 2021, *"Air Pollution in New Delhi during Late Winter: An Overview of a Group of Campaign Studies Focusing on Composition and Sources"*, Atmosphere, v. 12, (11):1432, doi :https://doi.org/10.3390/atmos12111432.

226. Thamban, N., Lalchandani, V., Kumar, V., Mishra, S., Bhattu, D., Slowik, J., Prevot, A. S. H., Satish, R., Rastogi, N., and Tripathi, S.N., 2021, *"Evolution of size and composition of fine particulate matter in the Delhi megacity during later winter"*, Atmospheric Environment, v. 267, p. 118752, doi :https://doi.org/10.1016/j.atmosenv.2021.118752.

227. Varna, M., Singh, A., Sahoo, D., and Sengupta, D., 2021, *"Strengthening of basin-scale ocean currents in winter drives decadal salinity decline in the eastern Arabian Sea"*, Geophysical Research Letters, v. 48, pp. e2021GL094516, doi :https://doi.org/10.1029/2021GL094516.

228. Vinayachandran, P.N.M., Masumoto, Y., Roberts, M., Hugget, J., Halo, I., Chatterjee, P., Amol, P., Gupta, G.V.M., Singh, A., Mukherjee, A., Prakash, S., Beckley, L., Raes, E., and Hood, R., 2021, *"Reviews and syntheses: Physical and biogeochemical processes associated with upwelling in the Indian Ocean"*, Biogeosciences, v. 18, p. 5967-6029, doi :https://doi.org/10.5194/bg-18-5967-2021.

229. Zarasvandi, A., Fereydouni, Z., Alizadeh, B., Absar., N., Shukla, A.D., Raza, M. Q., and Ashok, M. Zentilli., 2021, *"Phosphogenesis in the Zagros Fold-Thrust Belt, Iran: The link between the Tethyan Paleoenvironment and Phosphate Ore Deposition"*, Ore Geology Reviews, v. 139, pp. 104563, doi :https://doi.org/10.1016/j.oregeorev.2021.104563.

Theoretical Physics

230. Abhishek, A., A.Das, D.Kumar,and H.Mishra, 2022, *"Thermoelectric transport coefficients of quark matter"*, The European Physics Journal C, 82, 71, doi :http://doi.org/10.1140/epjc/s10052-022-09999-z.

231. Abhishek,A., A.Das, H.Mishra and R.K. Mohapatra, 2021, *"In medium properties of axion within a Polyakov loop enhanced Nambu-Jona-Lasinio model"*, Physical Review D, 103, 074003, doi :https://doi.org/10.1103/PhysRevD.103.074003.

232. Atkinson, O., A. Bhardwaj, C. Englert, V. S. Ngairangbam, M. Spannowsky, 2022, *"Anomaly detection with convolutional Graph Neural Networks"*, Journal of High Energy Physics, 2021, 80, doi :https://doi.org/10.1007/JHEP08(2021)080.

233. Aydin A., A. Sisman, J. Fransson, A. M. Black-Schaffer, P. Dutta, 2022, *"Thermodefect voltage in graphene nanoribbon junctions"*, Journal of Physics: Condensed Matter, 34, 1-11, doi :https://doi.org/10.1088/1361-648X/ac553b.

234. Bansal, A., N. Mahajan, D. Mishra, 2022, *"$\frac{|V_{ub}|}{|V_{cb}|}$ and quest for new physics"*, JHEP, 02, 130-155, doi :https://doi.org/10.1007/JHEP02(2022)130.

235. Budge, L., J. M., Campbell, R. K. Ellis, S. Seth, 2021, *"Analytic results for scalar-mediated Higgs boson production in association with two jets"*, Journal of Physics G: Nuclear and Particle Physics, 48, 085006, doi :https://doi.org/10.1088/1361-6471/abf7d6.

236. Campbell, J. M., G. de Laurentis, R. K. Ellis, S. Seth, 2021, *"The $pp \to \mathrm{W}(\to \ell\nu) + \gamma$ process at next-to-next-to-leading order"*, Journal of High Energy Physics, 2107, 079, doi :https://doi.org/10.1007/JHEP07(2021)079.

237. Das Arpan and Hiranmaya Mishra, 2021, *"Thermoelectric transport coefficients of hot and dense QCD matter"*, European Physcs Journal: Special Topics, 230, 607-634, doi :http://doi.org/10.1140/epjs/s11734-021-00022-2.

238. Joshipura, A. S., K. M. Patel, 2021, *"Weak scale right-handed neutrino as pseudo-Goldstone fermion of spontaneously broken $\mathrm{U}(1)_{\mathrm{L}_\mu - \mathrm{L}_\tau}$"*, JHEP, 09 (2021), 115, doi :https://doi.org/10.1007/JHEP09(2021)115.

239. Kadam, G., H.Mishra and M.Panero, 2021, *"Critical exponents and transport properties near the QCD critical endpoint from the statistical bootstrap model"*, The European Physics Journal C, 81, 795, doi :http://doi.org/10.1140/epjc/s10052-021-09596-6.

240. Kaustav Chakraborty, Srubabati Goswami, Kenneth Long, 2021, *"New Physics at nuSTORM"*, Physical Review D, 107, I-12, doi :https://doi.org/10.1103/PhysRevD.103.075009.

241. Konar, P., B. Mukhopadhyaya, R. Rahaman, R. K. Singh, 2021, *"Probing non-standard hbb interactions at the LHC"*, Physics Letter B, 818, 136358, doi :https://doi.org/10.1016/j.physletb.2021.136358.

242. Konar, P., V. S. Ngairangbam, M. Spannowsky, 2022, *"Energy-weighted Message Passing: an infra-red and collinear safe graph neural network algorithm"*, Journal of High Energy Physics, 2022, 60, doi :https://doi.org/10.1007/JHEP02(2022)060.

243. Kosmas, T.S., V.K.B. Kota, D. Papoulias, R. Sahu, 2021, *"Coherent elastic neutrino-nucleus scattering (CEνNS) event rates for Ge, Zn and Si detector materials"*, Physical Review C, 104, 064618, doi :https://doi.org/10.1103/PhysRevC.104.064618.

244. Kota, V.K.B. and Manan Vyas, 2021, *"Wavefunction structure in quantum many-fermion systems with k-body interactions:*

conditional q-normal form of strength function", Journal of Statistical Mechanics: Theory and Experiment, 2021, 113103, doi :https://doi.org/10.1088/1742-5468/ac2df9.

245. Kota,V.K.B. and R. Sahu, 2021, *"Multiple SU(3) algebras in interacting boson model and shell model: Results for (β,γ) bands and scissors 1^+ band"*, Nuclear Phyics. A, 1016, 122313, doi :https://doi.org/10.1016/j.nuclphysa.2021.122313.

246. Lambiase, G., S.Mohanty, A.Nautiyal and S.Rao, 2021, *"Constraints on electromagnetic form factors of sub-GeV dark matter from the cosmic microwave background anisotropy"*, Phys. Rev. D, 104, 023519, doi :http://doi.org/10.1103/PhysRevD.104.023519.

247. Mishra, H., 2022, *"Color Superconductivity in magnetised quark matter: an NJL model approach"*, European Physics Journal: Special Topics, 231, 103-127, doi :http://doi.org/10.1140/epjs/s11734-022-00439-3.

248. Monojit Ghosh, Srubabati Goswami, Ananya Mukherjee, 2021, *"Implications of the Dark-LMA solution for neutrino mass matrices"*, Nuclear Physics B, 969, 1-18, doi :https://doi.org/10.1016/j.nuclphysb.2021.115460.

249. Mummidi, V. S., K. M. Patel, 2021, *"Leptogenesis and fermion mass fit in a renormalizable SO(10) model"*, JHEP, 12 (2021), 042, doi :https://doi.org/10.1007/JHEP12(2021)042.

250. Natwariya, P. K., 2021, *"Constraint on Primordial Magnetic Fields In the Light of ARCADE 2 and EDGES Observations"*, Eur. Phys. J. C, 81, 394, doi :https://doi.org/10.1140/epjc/s10052-021-09155-z.

251. Natwariya, P. K. and A. C. Nayak, 2022, *"Bounds on sterile neutrino lifetime and mixing angle with active neutrinos by global 21 cm signal"*, Physics Letters B, 827, 136955, doi :https://doi.org/10.1016/j.physletb.2022.136955.

252. Natwariya, P. K. and A. C. Nayak, 2022, *"Bounds on sterile neutrino lifetime and mixing angle with active neutrinos by global 21 cm signal"*, Physics Letters B, 827, 136955, doi :https://doi.org/10.1016/j.physletb.2022.136955.

253. Natwariya, P. K. and A. C. Nayak and T. Srivastava, 2022, *"Constraining spinning primordial black holes with global 21-cm signal"*, Mon Not R Astron Soc, 510, 4236–4241, doi :https://doi.org/10.1093/mnras/stab3754.

254. Patel, K. M., 2021, *"Fermion mass hierarchies from supersymmetric gauged flavour symmetry in 5D"*, SciPost Phys., 10 (2021) no.6, 154, doi :https://doi.org/10.21468/SciPostPhys.10.6.154.

255. Poddar, T. K, 2021, *"Constraints on axionic fuzzy dark matter from light bending and Shapiro time delay"*, JCAP, 09(2021), 041, doi :https://doi.org/10.1088/1475-7516/2021/09/041.

256. Poddar, T.K. , S.Mohanty and S.Jana, 2022, *"Gravitational radiation from binary systems in massive graviton theories"*, JCAP, 03, 019, doi :http://doi.org/10.1088/1475-7516/2022/03/019.

257. Poddar, T.K., S.Mohanty and S.Jana, 2021, *"Constraints on long range force from perihelion precession of planets in a gauged $\mathrm{L}_e - \mathrm{L}_{\mu,\tau}$ scenario"*, Eur. Phys. J. C, 81, 286, doi :http://doi.org/10.1140/epjc/s10052-021-09078-9.

258. Rao, K., S. Rindani, P. Sarmah, B. Singh, 2020, *"Use of Z polarization in $e^+e^- \to \mathrm{ZH}$ to measure the triple-Higgs coupling"*, Nuclear Physics B, 975, 1-13, doi :https://doi.org/10.1016/j.nuclphysb.2021.115649.

259. Sharma, A., 2021, *"On non-monotonic temperature dependence of linear contact probability in atomic chains"*, Physica Scripta, 96, 125723, doi :https://doi.org/10.1088/1402-4896/ac387a.

260. Swami, H., K. Lochan, K. Patel, 2021, *"Aspects of gravitational decoherence in neutrino lensing"*, Phys. Rev. D, 104 (2021) no.9, 095007, doi :https://doi.org/10.1103/PhysRevD.104.095007.

Atomic, Molecular and Optical Physics

261. A. Dorne, B. K. Sahoo and Anders Kastberg, 2021, *"Relativistic coupledcluster calculations of isotope shifts for the low-lying states of Ca II in the finite-field approach"*, ATOMS, v.9, p.26, doi :https://doi.org/10.3390/atoms9020026.

262. Anwar, A., Lal, N., Prabhakar, S., and Singh, R. P., 2021, *"Selective tuning of Hilbert spaces in states encoded with spatial modes of light"*, New Journal of Physics, v.22, p.113020, doi :https://doi.org/10.1088/1367-2630/abc783.

263. Anwar, A., Prabhakar, S., and Singh, R. P., 2021, *"Size-invariant twisted optical modes for the efficient generation of higher-dimensional quantum states"*, Journal of the Optical Society of America, v.38, p.2976-2983, doi :https://doi.org/10.1364/JOSAB.436088.

264. B. K. Sahoo and B. Ohayon, 2021, *"Benchmarking Many-body Approaches for the Determination of Isotope Shift Constants: Application to the Li, Be^+ and Ar^{15+} Isoelectronic Systems"*, Physical Review, v.103, p.052802, doi :https://doi.org/10.1103/PhysRevA.103.052802.

265. B. K. Sahoo, B. P. Das and H. Spiesberger, 2022, *"Comment on New Physics Constraints from Atomic Parity Violation in 133Cs'"*, Physical Review, v.105, p.018302, doi :https://doi.org/10.1103/PhysRevD.105.018302.

266. B. K. Sahoo, B. P. Das and H. Spiesberger, 2021, *"New Physics Constraints from Atomic Parity Violation in $^{133}\mathrm{Cs}$"*, Physical Review, v.103, p.L111303 (Letter), doi :https://doi.org/10.1103/PhysRevD.103.L111303.

267. B. Ohayon, R. F. Garcia Ruiz, Z. H. Sun, G. Hagen, T. Papenbrock and B. K. Sahoo, 2022, *"Nuclear charge radii of Na isotopes: A tale of atomic and nuclear theories"*, Physical Review, v.105, p.L031305, doi :https://doi.org/10.1103/PhysRevC.105.L031305.

268. Biswas, A., Banerji, A., Chandravanshi, P., Kumar, R., and Singh, R. P., 2021, *"Experimental Side Channel Analysis of BB84 QKD Source"*, IEEE Journal of Quantum Electronics, v. 57, p.8000207, doi :https://doi.org/10.1109/JQE.2021.3111332.

269. Biswas, A., Banerji, A., Lal, N., Chandravanshi, P., Kumar, R., and Singh, R. P., 2022, *"Quantum key distribution with multiphoton pulses: an advantage"*, Optics Continuum, v.1, p.68-79, doi :https://doi.org/10.1364/OPTCON.445727.

270. Chauhan, N., Selvam, T. P., Anand, S., Shinde, D. P., Mayya, Y. S., Feathers, J. K., & Singhvi, A. K., 2021, *"Distribution of natural beta dose to individual grains in sediments"*, Proceedings of the Indian National Science Academy, v.87, p.613627, doi :https://doi.org/10.1007/s43538-021-00057-y.

271. D. K. Nandy and B. K. Sahoo, 2021, *"Relativistic Coupled-cluster Theory Analysis of Properties of Co-like Ions"*, Physical Review, v.104, p.052812, doi :https://doi.org/10.1103/PhysRevA.104.052812.

272. Dabhi, M., Chavan, A., Thakkar, A., Chauhan, G., Bhagora, R., Chauhan, N.,Bhandari, S., 2021, *"Climatic history from early Weichselian (MIS 5D-C) valley-fill deposits and associated factors for basin sedimentation, mainland Kachchh, western India"*, Quaternary International, N/A, N/A, doi :https://doi.org/10.1016/j.quaint.2021.10.019.

273. Dabhi, M., Thakkar, A., Chavan, A., Chauhan, G., Bhagora, R., Chauhan, N.,Thakkar, M. G., 2021, *"Mid-late Holocene climatic reconstruction from coastal dunes of the western Kachchh, India"*, Quaternary International, N/A, N/A, doi :https://doi.org/10.1016/j.quaint.2021.09.011.

274. Dey, S., Bookhagen, B., Thiede, R. C., Wittmann, H., Chauhan, N., Jain, V., & Strecker, M. R., 2022, *"Impact of Late Pleistocene climate variability on paleo-erosion rates in the western Himalaya"*, Earth and Planetary Science Letters, v.578, p.117326, doi :https://doi.org/10.1016/j.epsl.2021.117326.

275. Dey, S., Chauhan, N., Nath, D., Schaaf, N. W., Thiede, R. C., & Jain, V., 2022, *"PleistoceneHolocene out-of-sequence faulting along the Medlicott-Wadia Thrust in the NW Himalaya"*, Terra Nova, N/A, N/A, doi :https://doi.org/10.1111/ter.12587.

276. Dey, S., Thiede, R. C., Biswas, A., Chauhan, N., Chakravarti, P., & Jain, V., 2021, *"Implications of the ongoing rock uplift in NW Himalayan interiors"*, Earth Surface Dynamics, v.9, p.463-485, doi :https://doi.org/10.5194/esurf-9-463-2021.

277. Harpreet Kaur, Sukhjit Singh, B. Arora and B. K. Sahoo, 2022, *"Accurate determination of quadrupole polarizabilities of the excited states of alkalimetal atoms"*, Physical Review, v.105, p.032819, doi :https://doi.org/10.1103/PhysRevA.105.032819.

278. Jyoti, Harpreet Kaur, B. Arora and B. K. Sahoo, 2022, *"Radiative properties of Cu-isoelectronic As, Se and Br ions for astrophysical applications"*, Monthly Notices of the Royal Astronomical Society, v.511, p.1999, doi :https://doi.org/10.1093/mnras/stac163.

279. Jyoti, M. Kaur, B. Arora and B. K. Sahoo, 2021, *"Spectroscopic data of Rbisoelectronic Zr and Nb ions for astrophysical applications"*, Monthly Notices of the Royal Astronomical Society, v.507, p.4030, doi :https://doi.org/10.1093/mnras/stab2364.

280. Mandeep Kaur, Sukhjit Singh, B. K. Sahoo and Bindiya Arora, 2021, *"Tuneout and magic wavelengths, and electric quadrupole transition properties of the singly charged alkaline-earth metal ions"*, Atomic Data and Nuclear Data Tables, v.140, p.101422, doi :https://doi.org/10.1016/j.adt.2021.101422.

281. Prabhakar, S., Plachta, S. Z. D., Ornigotti, M., and Fickler, R., 2021, *"High-accuracy longitudinal position measurement using self-accelerating light"*, Applied Optics, v.60, p.3203, doi :https://doi.org/10.1364/AO.420590.

282. R Ramachandran, S Pavithraa, J K Meka, K K Rahul, J I Lo, S L Chou, B M Cheng, B N Rajasekhar, A Bhardwaj, N J Mason and B Sivaraman., 2021, *"Vacuum ultraviolet photoabsorption spectra of icy isoprene and its oligomers, Spectrochimica Acta Part A: Molecular and Biomolecular Spectroscopy"*, Spectrochimica Acta Part A: Molecular and Biomolecular Spectroscopy, v.268, p.120586, doi :https://doi.org/10.1016/j.saa.2021.120586.

283. R. Mitra, V. S. Prasannaa, R. F. Garcia Ruiz, T. K. Sato, M. Abe,Y. Sakemi, B. P. Das, and B. K. Sahoo, 2021, *"Towards CP Violation Studies on Superheavy Molecules: Theoretical and Experimental Perspectives"*, Physical Review, v.104, p.062801, doi :https://doi.org/10.1103/PhysRevA.104.062801.

284. R. Thombre, D. Gupta, S. Pavithraa, J.-I. Lo, S.-L. Chou, Y.-J. Wu, R. Ramachandran, K. K. Rahul, B.-M. Cheng, H. Hill, Anil Bhardwaj, B. N. Rajasekhar, N. J. Mason and B. Sivaraman, 2022, *"Vacuum ultraviolet photoabsorption spectra of an in-situ synthesized peptide precursor: hydroxylamine on a cold astrochemical dust analogue"*, The European Physical Journal, v.76, p.53, doi :https://doi.org/10.1140/epjd/s10053-022-00365-y.

285. Rituparna Das, D.K.Pandey, V. Nimma, P Madhusudhan, P. Bhardwaj, P. Chandravanshi, Muhammed Shameem KM, D.K. Singh, R.K. Kushawaha, 2022, *"Molecular emission dynamics from a femtosecond filament induced plasma plume"*, Journal of Optics, v.24, p.044015, doi :https://doi.org/10.1088/2040-8986/ac528a.

286. Singh, A., Jain, V., Danino, M., Chauhan, N., Kaushal, R. K., Guha, S., & Prabhakar, V. N., 2021, *"Larger floods of Himalayan foothill rivers sustained flows in the GhaggarHakra channel during Harappan age"*, Journal of Quaternary Science, v.36, p.611-627, doi :https://doi.org/10.1002/jqs.3320.

287. Singh, S. V., Vishakantaiah, J., Meka, J. K., Muruganantham, M., Thiruvenkatam, V., Sivaprahasam, V., Rajasekhar, B. N., Bhardwaj, A., Mason, N. J. and Sivaraman, B., 2022, *"Three-dimensional complex architectures observed in shock processed amino acid mixtures"*, Experimental Results,Cambridge University Press, v.3, p.e8, doi :https://doi.org/10.1017/exp.2021.17.

288. Singh, S.V., Dilip, H., Meka, J.K., Thiruvenkatam, V., Jayaram, V., Muruganantham, M., Sivaprahasam, V., Rajasekhar, B.N., Bhardwaj, A., Mason, N.J. and Burchell, M.J., 2022, *"New signatures of bio-molecular complexity in the hypervelocity impact ejecta of icy moon analogues"*, Life, v.12, p.508, doi :http://dx.doi.org/10.3390/life12040508.

289. Surendra, V. S., Jayaram, V., Muruganantham, M., Vijay, T., Vijayan, S., Samarth, P., Hill, H., Bhardwaj, A., Mason, N. J. and Sivaraman, B., 2021, *"Complex structures synthesized in shock processing of nucleobases implications to the origins of life"*, International Journal of Astrobiology,Cambridge University Press, v.20, p.285-293, doi :https://doi.org/10.1017/S1473550421000136.

290. T. Aoki, R. Sreekantham, B. K. Sahoo, Bindiya Arora, A. Kastberg, T.Sato, H. Ikeda, N. Okamoto, Y. Torii, T. Hayamizu,

K. Nakamura, S. Nagase, M. Ohtsuka, H. Nagahama, N. Ozawa, M. Sato, T. Nakashita, K. Yamane, K. S. Tanaka, K. Harada, H. Kawamura, T. Inoue, A. Uchiyama, A. Hatakayama, A. Takamine, H. Ueno, Y. Ichikawa, Y. Matsuda, H. Haba, and Y. Sakemi, 2021, *"Quantum sensing of the electron electric dipole moment using ultracold entangled Fr atoms"*, Quantum Science and Technology, v.6, p.044008, doi :https://doi.org/10.1088/2058-9565/ac1b6a.

291. V. Sharma, S. Chaitanya Kumar, G. K. Samanta, and M. Ebrahim-Zadeh, 2022, *"Tunable, high-power, high-order optical vortex beam generation in the mid-infrared"*, Optics Express, v.30, p.1195-1204, doi :https://doi.org/10.1364/OE.443345.

292. V. Sharma, S. Chaitanya Kumar, G. K. Samanta, and M. Ebrahim-Zadeh, 2021, *"Tunable vortex beam generation using an optical parametric oscillator with an antiresonant-ring interferometer"*, Optics Letters, v.46, p.3235-3238, doi :https://doi.org/10.1364/OL.426337.

293. Vanitha, P., Lal N., Rani, A., Das, B. K., Reddy S. G., and Singh, R. P., 2021, *"Correlations in scattered perfect optical vortices"*, Journal of Optics, v.23, p.095601, doi :https://doi.org/10.1088/2040-8986/ac094f.

294. Vimlesh Kumar, V. Sharma, S. Singh, S. Chaitanya Kumar, Andrew Forbes, M. Ebrahim-Zadeh and G. K. Samanta, 2022, *"Imaging inspired characterization of single photons carrying orbital angular momentum"*, AVS Quantum Science, v.4, p.015001, doi :https://doi.org/10.1116/5.0078870.

Publications in Proceedings of Conference/ Symposia/ Workshops

Astronomy and Astrophysics

1. Karmakar, S., S. Naik, J. C. Pandey, I. S. Savanov, and B. Weaver, 2021, *"AstroSat detection of long-duration X-ray superflares on EQ Peg"*, The 20.5th Cambridge Workshop on Cool Stars, Stellar System, and the Sun, p. 1-4.

Planetary Sciences

2. Gupta N., Y. Srivastava, S. Narendranath, N. S. Pillai, A. Basu Sarbadhikari and M. Bhatt, 2022, *"Compositional Similarity of Sittampundi Anorthositic Complex Rocks to Lunar Highlands"*, 53^{rd} Lunar and Planetary Science Conference, Houston, USA. 07-11 March 2022, Abstract no. 1931.
3. Jaiswal S., R. R. Mahajan and M. Ngangom, 2021, *"What is the Noble gas composition and inventory in Venus interior?"*, 19th VEXAG Meeting 2021, LPI Contribution no. 2628, Abstract no. 8011.
4. Kimi K. B., Harish, and Vijayan S., 2022, *"Infilled Craters: Lava Modified Impact Craters"*, 53^{rd} Lunar and Planetary Science Conference, Houston, USA. 07-11 March 2022, pp. 01.
5. Kimi K. B., Harish, and Vijayan S., 2022, *"Geological Evolution Of Posidonius Crater, Moon"*, 53^{rd} Lunar and Planetary Science Conference, Houston, USA. 07-11 March 2022, pp. 01.
6. Lajaunie L., M. Sanghani, W. Rickard, S. S.-Y. Hsiao, Z. Peeters, H. Shang, D. C. Lee, J. Calvino, K. K. Marhas and M. Bizzarro, 2021, *"Isotopic, Structural and Chemical Analyses of Pre-Solar Silicates from Asymptotic Giant Branch Stars and Type-II Supernova Explosions"*, Microscopy and Microanalysis, v. 27, p. 2782-2784.
7. M. Bhatt, D Dhingra, S Purohit, K Bhuva, P Patadiya, H Julasana, U Mall, 2022, *"Machine Learning Enabled Global Mapping of Mg-Spinel Lithology Using Chandrayaan-1 Moon Mineralogy Mapper (M3) Data"*, 53^{rd} Lunar and Planetary Science Conference, Houston, USA. 07-11 March 2022, LPI Contribution no. 2267.
8. M. Bhatt, S Narendranath, C Whler, NS Pillai, N Srivastava, A Bhardwaj, 2022, *"First Global Lunar Magnesium and Aluminum Abundance Maps Derived Using Chandrayaan-1 and Chandrayaan-2 Data"*, 53^{rd} Lunar and Planetary Science Conference, Houston, USA. 07-11 March 2022, LPI Contribution No. 2267.
9. Mishra R. K., K. K. Marhas and M. Chaussidon, 2021, *"Multiple Episodes of Superflares from our Nascent Sun: evidences from Canonical CAI in Vigarano"*, 53^{rd} Lunar and Planetary Science Conference, Houston, USA. 07-11 March 2022, LPI contribution no. 2548, Abstract no. 1834.
10. S. Jitarwal, J. P. Pabari, V. R. Dinesh Kumar, S. Nambiar, Rashmi, T. Upadhyaya, K. Acharyya and V. Sheel, 2021, *"Sensitivity analysis and testing of electrically short dipole antenna for Lightning Instrument for VEnus (LIVE)"*, 193^{th} VEXAG Meeting, 8-9 November 2021, LPI Contribution no. 2628, Abstract no. 8042.
11. S. Nambiar and J. P. Pabari, 2021, *"Meteoric Ablation in Venus atmosphere: Mass, Speed and Temperature Variation"*, 19^{th} VEXAG Meeting, 8-9 November 2021, LPI Contribution no. 2628, Abstract no. 8020.
12. S. Tuhi, Kimi K. B., Harish, K. Vigneshwaran, K. S. Sharini, R. K. S. Priya and Vijayan S., 2022, *"Ma'adim vallis, mars: insights into late-stage water activity in an impact crater through fluvial deposits"*, 53^{rd} Lunar and Planetary Science Conference, Houston, USA. 07-11 March 2022, Abstract no. 1142.
13. Srivastava Y., A. Basu Sarbadhikari, A. Yamaguchi, A. Takenouchi and J. M. D. Day, 2022, *"Petrogenesis of Lunar Ferroan Gabbro Meteorite Asuka 881757"*, 53^{rd} Lunar and Planetary Science Conference, Houston, USA. 07-11 March 2022, Abstract no. 1903.
14. Srivastava, N, T. Singhal, A. Verma, V. Aasik, N. K. Upadhyay, R. R. Mahajan, M. V. Unnithan, K. D. Prasad, V. Sheel, U. A. Subramanian, A. Bhardwaj, 2021, *"Planetary Rock Sampling Technology"*, In proceedings of the DTDI technology conclave-2021, ISRO HQ, 22-26 Nov. 2021, Session SE-1: Solar System Exploration & Astronomy.
15. Uttam S., V. Sheel and S. K. Mishra, 2022, *"Electric Field Development Within a Dust Devil on Mars"*, 53^{rd} Lunar and Planetary Science Conference, Houston, USA. 07-11 March 2022, LPI Contribution no. 2678, Abstract no. 1782.
16. Vigneshwaran K., M. B. Al-Handawi, D. Atri, P. Naumov ,V. Thirukumaran, S. Vijayan and B. Sivaraman, 2022, *"Exploring The Impact Of Geological And Geomorphological Processes In Sedimentary Deposits In Abu Dhabi: A Potential Mars Analogue"*, 53^{rd} Lunar and Planetary Science Conference, Houston, USA. 07-11 March 2022, Abstract no. 2058.
17. Vijayan S., Kimi K. B., P. Achintya, Harish, S. Tuhi, V. J. Rajesh, B. Sivaraman, and Anil Bharadwaj, 2022, *"Amundsen Crater, South Pole Moon: Potential Landing Site To Explore Possible Floor Intrusion And Multiple PSR"*, 53^{rd} Lunar and Planetary Science Conference, Houston, USA. 07-11 March 2022, Abstract no. 1869.
18. Wagner J. D., S. Tuhi, Kimi K. B., Harish, and Vijayan S., 2022, *"Fluvial features at peridier crater, syrtis major, mars: evidence for hesperian warm ejecta induced shallow ice melting"*, 53^{rd} Lunar and Planetary Science Conference, Houston, USA. 07-11 March 2022, Abstract no. 1927.

Theoretical Physics

19. Abhishek, Aman and H. Mishra, 2021, *"Chiral Symmetry Breaking, Color Superconductivity, and Equation of State for Magnetized Strange Quark Matter"*, Springer Proc. Phys, 261 (2021), 593-598.
20. Bansal, A., N. Mahajan, 2021, *"LCSR application to radiative tau decay, Proceedings of Science"*, The Ninth Annual Conference on Large Hadron Collider Physics - LHCP2021 (PoS, LHCP2021), 193 197.
21. Bhatt, J.R., A. Das and H. Mishra, 2021, *"Thermoelectric Effect and Seebeck Coefficient of Hot and Dense Hadronic Matter in the Hadron Resonance Gas Model"*, Springer Proc. Phys, 261 (2021), 1103-1106.
22. Chakraborty, Kaustav and Goswami, Srubabati and Long, Kenneth R, 2022, *"Exploring Sterile Neutrino and Non-Unitary Neutrino Mixing at nuSTORM"*, Proceedings of NuFact, p. 178.
23. Deepthi, K. N. and Chakraborty, K, Goswami, S, Joshipura, A. S. and Nath, N, 2021, *"Exploring Partial $\mu - \tau$ Reflection Symmetry in DUNE and Hyper-Kamiokande"*, Proceedings of the 23rd DAE symposium in High Energy Physics 2018, ,Springer Proc. Phys, v-261 ,467473.
24. Jaiswal, A., N. Haque, A. Abhishek, R. Abir, A. Bandyopadhyay, K. Banu, S. Bhadury, S. Bhattacharyya, T. Bhattacharyya and D. Biswas, 2021, *"Dynamics of QCD matter current status"*, International Journal of Modern Physics E, 30 (2021) no.02, 2130001.
25. Lakshmi, S. M., Choubey, S and Goswami, S, 2021, *"Sensitivity of INO ICAL to Neutrino Mass Hierarchy and 23 Octant in Presence of Invisible Neutrino Decay in Matter"*, Springer Proc. Phys, 261, pp. (981986).
26. Poddar, T. K., 2021, *"Ultralight dark matter: constraints from gravitational waves and other astrophysical observations"*, 17^{th} International Conference on Topics in Astroparticle and Underground Physics (TAUP2021), J.Phys.Conf.Ser., 2156 (2021) 1, 012052..
27. Poddar, T. K., 2021, *"Probing light dark matter particles with astrophysical experiment"*, European Physical Society Conference on High Energy Physics 2021 (EPS-HEP2021), PoS EPS-HEP2021 (2022), 057.
28. Sarmah, P., K. Rao, S. Rindani, 2021, *"Constraining anomalous ZH couplings using Z polarization parameters"*, Proceedings of the 40th International Conference on High Energy Physics, PoS(ICHEP2020), v. 390, pp. 1-6.
29. Selvaganapathy, J., P. Konar, 2021, *"Inferring the Covariant Θ-Exact Noncommutative Coupling at Linear Colliders"*, Springer Proceedings in Physics, volume 261 P. 881-885.
30. Sharma, A, 2021, *"12 Temperature dependence of reciprocal susceptibility in linear Mn chains of Ti4MnBi2"*, 65th DAE Solid State Physics Symposium, DAE SSSP Conf. Proc., Vol. 55, ISBN No: 81-8372-085-4, 803-804..

Atomic, Molecular and Optical Physics

31. Hiekkamaki, M., Prabhakar, S., and Fickler, R., 2021, *"High-dimensional quantum operations using structured photons"*, Conference on Lasers and Electro-Optics Europe & European Quantum Electronics Conference (CLEO/Europe-EQEC)), 21-25 June 2021, N/A.
32. Mongia, V., Patil, S., Mishra, S., Biswas, A., and Singh, R. P., 2021, *"Towards a relationship between single photon nature and randomness"*, 11th International Conference on Quantum Cryptography held online, organized from Amsterdam, The Netherlands, 23-27 August 2021., p. 223.
33. Prabhakar, S., Plachta, S. Z. D., Ornigotti, M., and Fickler, R., 2021, *"Single-beam high-accuracy longitudinal position measurement using spiralling beams"*, Conference on Lasers and Electro-Optics Europe & European Quantum Electronics Conference (CLEO/Europe-EQEC), 21-25 June 2021, N/A.
34. S. Singh, V. Sharma, V. Kumar, G. K. Samanta, 2021, *"Variation of the Hong-Ou-Mandel interference dip with crystal length"*, Conference on Lasers and Electro-Optics Europe & European Quantum Electronics Conference (CLEO/Europe-EQEC), N/A.
35. V. Kumar, V. Sharma, S. Singh, and G. K Samanta, 2021, *"Divergence of single photons with different orbital angular momentum"*, European Quantum Electronics Conference, eb_p_27, N/A.

Books Edited / Review Articles / Other Publications

Books Edited

1. Srivastava, N., M. Mierla and J. Zhang, 2022, *"Space Weather Prediction: Challenges and Prospects"*, Frontiers in Astrophysics and Space Science, Lausanne: Frontiers Media SA.ISBN 978-2-88974-280-6
2. Y. Srivastava and A. B. Sarbadhikari, 2021, *"Silica, Silicate"*, In: Cudnik B. (eds) Encyclopedia of Lunar Science.p. 1-8, Springer, Cham. https://doi.org/10.1007/978-3-319-05546-6_215-1
3. Shekh, N. A., Dviwedi, V. and Pabari, J. P., 2021, *"Effect of Sandstorm on Radio Propagation Model of Mars"*, Springer, Cham, SwitzerlandIn: Raj, J. S. (eds) International Conference on Mobile Computing and Sustainable Informatics (ICMCSI), EAI/Springer Innovations in Communication and Computing, p. 441-447. https://doi.org/10.1007/978-3-030-49795-8_43
4. Sheel V., 2022, *"The Lower Ionosphere of Mars: Modeling and Effect of Dust"*, Oxford Research Encyclopedia of Planetary Sciencehttps://doi.org/10.1093/acrefore/9780190647926.013.57
5. Singh, A. and Rastogi, N., 2022, *"Airborne particles in indoor and outdoor environments"*, Chapter in the book 'Airborne Particulate MatterSpringer. ISBN: 978-981-16-5386-5, https://doi.org/10.1007/978-981-16-5387-2 (Book Chapter)
6. Banerji, U., Dubey, C.P., Goswami, V., and Joshi, K.B., 2021, *"Geochemical indicators in provenance estimation"*, book: Geochemical Treasures and Petrogenetic Processesin Armstrong-Altrin, J.S., Pandarinath, K., Verma, S.K. (eds.) Springer Nature
7. Jena, P.S., Bhushan, R., Shivam A., Bharti, N., and Sudheer, A. K., 2021, *"^{10}Be depositional flux variation in the Central Indian Ocean during the last 43 kyrs"*, Article published in PRL newsletter The SpectrumIssue 33
8. Ojha, N., Girach, I., Soni, M., and Singh, N., 2022, *"Chapter:"Distribution of reactive trace gases over South Asia: Observations and modelling", Book: "Asian Atmospheric Pollution: Sources, Characteristics and Impacts""*, ElsevierEditor: R. P. Singh, Elsevier, https://doi.org/10.1016/B978-0-12-816693-2.00022-6
9. L.K.Sahu, P.R.Sinha, 2022, *"Chapter 16: "Vertical profiles of trace gases in the troposphere over South Asia", Book: "Asian Atmospheric Pollution: Sources, Characteristics and Impacts""*, ElsevierEditor: R. P. Singh, Elsevier, https://doi.org/10.1016/B978-0-12-816693-2.00009-3

Review Articles

1. Mazumdar, A,S. Mohanty and P. Parashari, 2021, *"Evidence of dark energy in different cosmological observations"*, Eur. Phys. J. ST, v.9, 2055-2066
2. Singh, D., Sinha, R. K., Singh, P., Roy, N. and Mukherjee, S., 2022, *"Astrobiological potential of Fe/Mg smectites with special emphasis on Jezero crater, Mars 2020 landing site"*, Astrobiology, v.v. 22(5), p. 579-597, https://doi.org/10.1089/ast.2021.0013
3. Changela, H. G., Chatzitheodoridis, E., Antunes, A., Beaty, D., Bouw, K., Bridges, J. C., ..., Sinha, R. K., and Hallsworth, J. E., 2021, *"Mars: new insights and unresolved questions"*, International Journal of Astrobiology, v.v. 20(6), pp. 394-426, https://doi.org/10.1017/S1473550421000276
4. Mishra S. K. and S. Misra, 2021, *"Photo-induced thermionic emission from CNT cluster array: Edge effects"*, Asian Journal of Physics, v.v. 30, pp. 163, ISSN: 0971 - 3093
5. A.Bhardwaj and B.Sivaraman, 2021, *"Book: 'Life on Mars: What to Know Before We Go'"*, Current Science, v.121(8), p.1120-1121
6. Ward, W., Seppl, A., Yiit, E., Nakamura, T., Stolle, C., Latovika, J., Woods, T. N., Tomikawa, Y., Lbken, Franz-Josef, Solomon, S. C., Marsh, D. R., Funke, B., and Pallamraju, D., 2021, *"Role Of the Sun and the Middle atmosphere/thermosphere/ionosphere In Climate (ROSMIC): a retrospective and prospective view"*, Progress in Earth and Planetary Science, v.8, Article number: 47

Technical Notes and Other Publications

1. P. Malaidevan, Y. Shah, V. Goyal , M. N. Sanghani and K. K. Marhas, 2022, *"Microcontroller based Automated Freeze Thaw Instrument"*, PRL-TN-2022-115
2. Mathew, S. K., B. Ramya, B., A. Raja Bayanna, 2022, *"Liquid Crystal Variable Retarder (LCVR) driver electronics for studying Transient Nematic Effect"*, PRL-TN-2022-114
3. Bireddy Ramya, Shibu K. Mathew, Ankala Raja Bayanna, 2022, *"Automated pointing data acquisition for Multi Application Solar Telescope (MAST)"*, PRL-TN-2022-117
4. Ankita Patel, Vaibhav Dixit, Mohan Lal, Vipin Kumar, Mudit K. Srivastava, 2022, *"Development of an Instrument Control System: Automation of MFOSC-P Instrument to Facilitate Remote Operation at Mt. Abu"*, PRL-TN-2022-116
5. Ananthanarayan, B. and Subhendra Mohanty, 2021, *"The accelerating universe: evidence and theories"*, Eur. Phys. J. ST, v.9, 2051-2053
6. A Kumar, MB. Dhanya, G. Manju, P. Konar, 2021, *"AI-based Model for Prediction of Solar Flare Events, Fifteen Break-through AI solutions for Space Exploration & Applications - AI Models for Disruptive Technology"*, ISRO Report: DTDI-AI-REP-2021-01 (2021), v.0, 283-290
7. V. S. Ng, P. B Domadiya, P. K Mitra, B. Joshi, R. Bhattacharyya, Aveek Sarkar, A Kumar, MB. Dhanya, G. Manju, P. Konar, 2021, *"Deep learning towards Solar flare prediction, A Compendium of Disruptive & Futuristic Technologies for Space Sector"*, SRO Report: Proceedings of the DTDI Technology Conclave - 2021, v.0, 0
8. Pabari J. P. and F. M. Joshi, 2021, *"Dust in Our Solar System"*, Pragami Tarang, v.v. XIII, pp. 28-32, ISSN: 2347 2782

Papers Presented in National/ International Conferences

National (137)

1. Ankur Dabhi, Ravi Bhushan, Nisha Bharti, A.Shivam, "Performance of PRL-AURiS for Radiocarbon measurements", Frontiers and Geosciences Research Conference (FGRC-2021), Sept 27, 2021
2. Devaprasad, M.,Neeraj Rastogi, R. V. Satish, Ankur Dabi, Ravi Bhushan, "Radiocarbon-based source characteristics of paddy-residue burning derived aerosols", National Space Science Symposium - 2022, Jan 31 - 4 Feb, 2022
3. Satyam Agarwal and Ramit Bhattacharyya, "Data-constrained simulation of solar coronal transients", National Science Space Symposium-2022, 31 January - 04 February, 2022
4. Bhuwan Joshi, "CME production by the magnetic-arcade-blowout triggered by a compact B-class solar flare: SDO and XSM/Chandrayaan-2 observations", National Science Space Symposium-2022, 31 January - 04 February, 2022
5. Binal D Patel, Bhuwan Joshi, K.-S. Cho and R.-S. Kim, "CMEs associated with DH type II bursts and their Sun-Earth propagation", National Science Space Symposium-2022, 31 January - 04 February, 2022
6. Satyam Agarwal and Ramit Bhattacharyya, "Effects of initial conditions on magnetic reconnection in solar transients", 40^{th} Astronomical Society of India Meeting (ASI-2022), 25 - 29 March, 2022
7. Bhuwan Joshi, "On the formation and eruption of a magnetic flux rope and the flare-CME association: SDO and Udaipur-CALLISTO observations", 40^{th} Astronomical Society of India Meeting (ASI-2022), 25 - 29 March, 2022
8. Prabir K. Mitra and Bhuwan Joshi, "Storage of Excessive Magnetic Free Energy and Evolution of Photospheric Current in Solar Active Regions Leading to Extreme Solar Eruptive Phenomena", 36^{th} meeting of Plasma Science Society of India (PSSI), 13–15 Dec, 2021
9. Prabir K. Mitra, Bhuwan Joshi, Astrid M. Veronig and T. Wiegelmann, "What causes a failed solar eruption during an energetic HXR flare?: A multi-wavelength case study", First Indian Space Weather Conference (ISWC-2022), 11–12 January, 2022
10. Kamlesh Bora, "Comparison of the Hall MHD and MHD evolution of a flaring solar active region", First Indian Space Weather Conference (ISWC-2022), 11–12 January, 2022
11. Bhuwan Joshi, "Cause of extreme eruptive events from solar active region NOAA 12673 - the source region of many powerful outbursts including the largest flare of solar cycle 24", First Indian Space Weather Conference (ISWC-2022), 11–12 January, 2022
12. Binal D. Patel, Bhuwan Joshi, K.-S. Cho and R.-S. Kim, "DH Type II Radio Bursts During Solar Cycles 23 and 24: Frequency-dependent Classifica-tion and their Flare-CME Associations", First Indian Space Weather Conference (ISWC-2022), 11–12 January, 2022
13. Hirdesh Kumar and Brajesh Kumar, "Propagation of acoustic-gravity waves in magnetized regions in the lower solar atmosphere", National Science Space Symposium-2022, 31 January - 04 February, 2022
14. Kamlesh Bora, "Comparison of the Hall MHD and MHD evolution of a flaring solar active region", 40^{th} Astronomical Society of India Meeting (ASI-2022), 25 - 29 March, 2022
15. Anshika Bansal and Namit Mahajan, "$p \to e^+\gamma$ using LCSR", Anomalies 2021, 10-12 November, 2021
16. Dayanand Mishra and Namit Mahajan, "Soft photon QED corrections to $\mathrm{B} \to \mathrm{K}\ell^+\ell^-$", Anomalies 2021, 10-12 November, 2021
17. Anshika Bansal and Namit Mahajan, "$\tau^- \to \pi^-\nu_\tau\gamma$ Decay and LCSR", Virtual School on flavour structure of the Standard Model, 31 August-12 September, 2021
18. Dayanand Mishra and Namit Mahajan, "Impact of soft photons on $\mathrm{B} \to \mathrm{K}\ell\ell$", Virtual School on flavour structure of the Standard Model, 31 August-12 September, 2021
19. Vipin Kumar, "Exploring the short term H-alpha variability in a sample of M Dwarfs", 40th meeting of the Astronomical Society of India (ASI), 25-29 March, 2022
20. Neeraj Kumari, "Investigation of a small flare in NGC 4051", 21st National Space Science Symposium, IISER Kolkata, 31 January - 04 February, 2022
21. Mudit K. Srivastava, "Stars with Starlight: The Applications of Optical Technologies in Astronomy", 6th Student's Conference on Optics and Photonics (SCOP-2021), 24-26 November, 2021
22. Sushant Dutta, "Remnant radio galaxies detected in deep low-frequency surveys", 40th annual meeting of Astronomical Society of India, 25-29 March, 2021
23. Vineet Ojha, "Multiwavelength study of narrow-line Seyfert 1 galaxies", 40th annual meeting of Astronomical Society of India, 25-29 March, 2021
24. Abhay Kumar, "AstroSat CZTI as a sub-MeV spectrometer: hard X-ray spectral states in Cygnus X-1", 40th Annual Meeting of the Astronomical Society of India, 25-29 March, 2022
25. N. P. S. Mithun, "Soft X-ray Spectral Diagnostics of Multi-thermal Plasma in Solar Flares with Chandrayaan-2 XSM", 21st National Space Science Symposium, IISER Kolkata, 31 January - 04 February, 2022
26. N. P. S. Mithun, "Development of Position Sensitive Sub-MeV Detectors for Daksha Mission", 21st National Space Science Symposium, IISER Kolkata, 31 January - 04 February, 2022
27. Ekta Sharma, "Investigation of the evolution of dark clouds", 40th Annual Meeting of the Astronomical Society of India, 25-29 March, 2022

28. Abhjit Patil and Manash Samal, “Understanding the origin of extended structure in open cluster Theia 613”, 40th Annual Meeting of the Astronomical Society of India, 25 - 29 March, 2022
29. Vineet Rawat and Manash Samal, “Understanding the cluster formation potency of massive dark clouds”, 40th Annual Meeting of the Astronomical Society of India, 25-29 March, 2022
30. Naval Kishor Bhadari, L. K. Dewangan, and D. K. Ojha, “Simultaneous evidence of edge collapse and hub-filament configurations: A rare case study of a Giant Molecular Filament G45.3+0.1”, 40th Annual Meeting of the Astronomical Society of India, 25-29 March, 2022
31. Arup Kumar Maity, Lokesh Kumar Dewangan, and Naval Kishor Bhadari, “Shedding light on the formation process of O-type stars in W31: cloud-cloud collision”, 40th Annual Meeting of the Astronomical Society of India, 25-29 March, 2022
32. N. P. S. Mithun, Santosh V. Vadawale, D. Bhattacharya, Ajay Vibhute, A. R. Rao,V. B. Bhalerao, and T. Chattopadhyay, “Updates on Hard X-ray Spectroscopy with AstroSat CZT-Imager”, 40th Annual Meeting of the Astronomical Society of India, 25-29 March, 2022
33. C. S. Vaishnava, N.P.S. Mithun, S. V. Vadawale, V. Bhalerao, S. Tendulkar, and Daksha team, “Daksha - Prospects of classical GRB prompt emission studies”, 40th Annual Meeting of the Astronomical Society of India, 25-29 March, 2022
34. B. Mondal, S. V. Vadawale, A. Sarkar, N. P. S. Mithun, P. Janardhan, A. Bhardwaj,G. Del Zanna, and H. E. Mason, “Role of small-scale impulsive events in heating the X-ray bright points of the Sun insights from Ch-2/XSM observations”, 40th Annual Meeting of the Astronomical Society of India (ASI), 25-29 March, 2022
35. B. Mondal, S. V. Vadawale, A. Sarkar, N. P. S. Mithun, P. Janardhan, A. Bhardwaj,P.S. Athiray, G. Del Zanna, H. and E. Mason, “Investigating the coronal heating of quiet Sun: A DEM analysis using AIA and XSM observations”, 21st National Space Science Symposium, IISER Kolkata, 31 January - 04 February, 2022
36. Aravind, K., P. Halder, N. Uppal, P. Prajapati, and S. Ganesh, “Optical polarimetric study of cometary dust”, 40th Annual Meeting of the Astronomical Society of India, 25-29 March, 2021
37. Ganesh, S. and the INSIST Science Team, “Science with INdian Spectroscopic and Imaging Space Telescope (INSIST)”, 40th meeting of the Astronomical Society of India (ASI 2022), 25-29 March, 2021
38. Namita, U., S. Ganesh, and D. Bisht, “Optical linear polarization towards Czernik3: a distant open cluster in Galactic plane”, 40th Annual Meeting of the Astronomical Society of India, 25-29 March, 2022
39. Prachi Prajapati, A. Rawat, S. Ganesh, V. Joshi, N. Kumari, and S. Naik, “Near Infrared night sky at Mount Abu Observatory”, 40th Annual Meeting of the Astronomical Society of India, 25-29 March, 2022
40. A. Kayal, “Hard X-ray view of AGN with associated HI 21-cm absorption”, 40th Annual Meeting of the Astronomical Society of India, 25-29 March, 2021
41. Basu Sarbadhikari A., Y. Srivastava, and A. Rani, “Geochemistry of Silicic Highlands and Basaltic Plains of Venus”, Venus Science Conference (Venus-SC-2021), PRL, Ahmedabad, 23-24 September, 2021
42. Basu Sarbadhikari A., A. Rani, and Y. Srivastava, “Compositional Constraints on the Origin of Volcanism on Mars”, Meteoroids, Meteors and Meteorites: Messengers from Space Symposium (MetMeSS-2021). PRL, Ahmedabad, 29-30 November, 2021
43. Srivastava Y. and A. Basu Sarbadhikari, “Petrogenesis of A-881757: A non-KREEP low-Ti lunar meteorite basalt. Meteoroids”, Meteoroids, Meteors and Meteorites: Messengers from Space Symposium (MetMeSS-2021). PRL, Ahmedabad, 29-30 November, 2021
44. Gupta R. D., A. Basu Sarbadhikari and K. K. Marhas, “Formation of carbonate-sulfide association in the martian meteorite ALH84001 and implications for the nature of water-rock interactions on the martian surface in the Noachian Era”, Meteoroids, Meteors and Meteorites: Messengers from Space Symposium (MetMeSS-2021). PRL, Ahmedabad, 29-30 November, 2021
45. A. Basu Sarbhadikari, “Geochemistry of Silicic Highlands and Basaltic Plains of Venus”, Venus Science Conference (Venus-SC-2021), PRL, Ahmedabad, 23-24 September, 2021
46. A. Basu Sarbhadikari, “Compositional Constraints on the Origin of Volcanism on Mars”, Meteoroids, Meteors and Meteorites: Messengers from Space Symposium (MetMeSS-2021). PRL, Ahmedabad, 29-30 November, 2021
47. A. Basu Sarbhadikari, “Non-mare perspective of mare basalt generation”, 3^{rd} Indian Planetary Science Conference (IPSC-2022), PRL, Ahmedabad, 14-16 March, 2022
48. Goyal S. K., R. R. Mahajan, N. Upadhyay, A. Auknoor, P. Sharma, J. Kaur, M. Shanmugam, Varun Sheel, and Team, “Design of Neutral & Ion mass spectrometer (NIMS) for future planetary missions”, Venus Science Conference (Venus-SC-2021), PRL, Ahmedabad, 23-24 September, 2021
49. M. Bhatt, C. Whler, K. Aravind, J. Rogall, S. Ganesh and A. Bhardwaj, “Unique regolith characteristics of the Reiner Gamma swirl”, 21^{st} National Space Science Symposium, 31 January - 04 February, 2022
50. M. Bhatt, S. Narendranath, Netra S Pillai, C. Whler, N. Srivastava, and A. Bhardwaj, “Global lunar elemental abundances: A systematic study of CLASS and M3 data”, 21^{st} National Space Science Symposium, 31 January - 04 February, 2022
51. S. Purohit, M. Bhatt, P. Patadiya, K. Bhuva, H. Julasana, D. Dhingra, and U. Mall, “A machine learning framework for global Mg-Spinel detection based on Chandrayaan-1 data”, 21^{st} National Space Science Symposium, 31 January - 04 February, 2022
52. M. Bhatt, S. Purohit, K. Bhuva, P. Patadiya, H. Julasana, D. Dhingra, and U. Mall, “Global mapping of Mg-spinel lithology using Chandrayaan-1 data”, 3^{rd} Indian Planetary Science Conference (IPSC-2022), PRL, Ahmedabad, 14-16 March, 2022
53. Jaiswal S., R. R. Mahajan and M. Ngangom, “Neon in Terrestrial planets”, 21^{st} National Space Science Symposium, 31 January - 04 February, 2022

54. Kumar Avadh, R. R. Mahajan, “Constraint to formation history and regolith evolution in ordinary chondrites”, 21st National Space Science Symposium, 31 January - 04 February, 2022
55. Mahajan R. R., “Nitrogen isotopes in CV3 chondrites”, 21st National Space Science Symposium, 31 January - 04 February, 2022
56. Kumar Avadh and R. R. Mahajan, “Meteorite-Asteroid relation using Cosmic ray exposure ages in Ordinary Chondrites”, Meteoroids, Meteors and Meteorites: Messengers from Space Symposium (MetMeSS-2021). PRL, Ahmedabad, 29-30 November, 2021
57. Kumar Avadh and R. R. Mahajan, “Noble gases are the bridge to link Meteorites and Asteroids”, 3rd Indian Planetary Science Conference (IPSC-2022), PRL, Ahmedabad, 14-16 March, 2022
58. Mahajan R. R., “Down the memory lane: PRL meteorite studies”, Meteoroids, Meteors and Meteorites: Messengers from Space Symposium (MetMeSS-2021). PRL, Ahmedabad, 29-30 November, 2021
59. Srivastava N., A. J. Verma, M. Bhatt, Avadh Kumar, R. R. Mahajan, A. Bhardwaj, “Reflectance spectroscopy of selected Indian Meteorites”, 3rd Indian Planetary Science Conference (IPSC-2022), PRL, Ahmedabad, 14-16 March, 2022
60. Mishra S. K., “Few Particulars about Electrostatics Over Moon”, 3rd Indian Planetary Science Conference (IPSC-2022), PRL, Ahmedabad, 14-16 March, 2022
61. Sana T. and S. K. Mishra, “Lunar Photoelectron Sheath and Possibility of Dust Levitation”, 3rd Indian Planetary Science Conference (IPSC-2022), PRL, Ahmedabad, 14-16 March, 2022
62. Goyal S. K., Patel A. R., Tiwari N. K., Sharma P., Auknoor A., Sarada A., Shanmugham M., Vadawale S. V., Ladiya T., Kumar S., Singh N., Painkra D., Dalal B., Sebastian J., Chakrabarty D., Sarkar A., Bhardwaj A., Jananrdhan P., Lal A. K., Kumar P., Adhyaru P. R., Shah M. S., Adalja H., Yogesh and Bapat B., “Supra Thermal & Energetic Particle Spectrometer (STEPS) A subsystem of Aditya Solar wind & Particle Experiment (ASPEX), onboard Aditya-L1 mission”, 3rd Indian Planetary Science Conference (IPSC-2022), PRL, Ahmedabad, 14-16 March, 2022
63. S. Nambiar, J. P. Pabari, R. K. Singh, S. Jitarwal, Rashmi and K. Acharyya, “Characterization of a Dust Sensor using Pulse Laser”, 21st National Space Science Symposium, 31 January - 04 February, 2022
64. J. P. Pabari and Z. P. Patel, “Study of Meteor Showers during LADEE Observation Time”, 21st National Space Science Symposium, 31 January - 04 February, 2022
65. S. Jitarwal, J. P. Pabari, S. Nambiar, Rashmi, D. Kumar, T. Upadhaya, K. Acharyya, and V. Sheel, “Comparison of Solid and Hollow Cylindrical Antennas for Planetary Lightning Detection”, 21st National Space Science Symposium, 31 January - 04 February, 2022
66. S. Nambiar, J. P. Pabari, Rashmi and Sonam, “Dust Particle Dynamics in Solar System”, 3rd Indian Planetary Science Conference (IPSC-2022), PRL, Ahmedabad, 14-16 March, 2022
67. S. Jitarwal, J. P. Pabari, S. Nambiar, Rashmi, T. Upadhyaya, K. Acharyya and V. Sheel, “Spectral Comparison of Natural lightning vs Artificial source of lightning”, 3rd Indian Planetary Science Conference (IPSC-2022), PRL, Ahmedabad, 14-16 March, 2022
68. Jayesh Pabari, S. Nambiar, Rashmi, and S. Jitarwal, “Interplanetary Dust Variability between Earth and Venus from Latest Solar Orbiter Observations”, 3rd Indian Planetary Science Conference (IPSC-2022), PRL, Ahmedabad, 14-16 March, 2022
69. C. P. Pabari, S. Nambiar and J. P. Pabari, “Interplanetary Dust Distribution Derived from Galileo DDS Measurements”, 3rd Indian Planetary Science Conference (IPSC-2022), PRL, Ahmedabad, 14-16 March, 2022
70. J. P. Pabari, “Interplanetary Dust at Mars in Light of MAVEN Observations”, Meteoroids, Meteors and Meteorites: Messengers from Space Symposium (MetMeSS-2021). PRL, Ahmedabad, 29-30 November, 2021
71. S. Yadav and J. P. Pabari, “Venusian Lightning Phenomenon”, Venus Science Conference (Venus-SC-2021), PRL, Ahmedabad, 23-24 September, 2021
72. S. Iyer and J. Pabari, “Interplanetary dust around Venus”, Venus Science Conference (Venus-SC-2021), PRL, Ahmedabad, 23-24 September, 2021
73. V. R. Dinesh Kumar, J. P. Pabari, K. Acharyya, S. Nambiar, S. Jitarwal, and Rashmi, “Modeling of charged regions in Venus atmosphere to initiate Venusian Lightning”, Venus Science Conference (Venus-SC-2021), PRL, Ahmedabad, 23-24 September, 2021
74. S. Nambiar, J. P. Pabari, S. Jitarwal, Rashmi, and K. Acharyya, “Expected IDP Impact Rate in Venusian Orbit”, Venus Science Conference (Venus-SC-2021), PRL, Ahmedabad, 23-24 September, 2021
75. S. Jitarwal, J. P. Pabari, V. R. Dinesh Kumar, S. Nambiar, Rashmi, K. Acharyya, V. Sheel and T. Upadhyay, “Characterization of electric field using discharge pulse parameters of artificial lightning source”, Venus Science Conference (Venus-SC-2021), PRL, Ahmedabad, 23-24 September, 2021
76. A. Bhattacharya and J. P. Pabari, “Electrically active clouds near the landing sites of Venera 13 and 14”, Venus Science Conference (Venus-SC-2021), PRL, Ahmedabad, 23-24 September, 2021
77. Bharti R., I. B. Smith, S. K. Mishra, N. Srivastava, S. H. Shukla, “SHARAD detection of extensive sedimentary deposition in unnamed crater near Mangala Fossa, Mars”, 21st National Space Science Symposium, 31 January - 04 February, 2022
78. Bharti R., I. B. Smith, S. H. Shukla, “SHARAD study of the Martian graben system”, 3rd Indian Planetary Science Conference (IPSC-2022), PRL, Ahmedabad, 14-16 March, 2022
79. Chandan Kumar, K. Durga Prasad, Sanjeev K. Mishra, P. Kalyan Reddy, and Janmejay Kumar, “An efficient DDS-based signal generator for permittivity experiments for space missions”, 3rd Indian Planetary Science Conference (IPSC-2022), PRL, Ahmedabad, 14-16 March, 2022
80. K. Durga Prasad et al., “Mimicking the Moon in the Laboratory A Paradigm Shift in In-situ Exploration”, 3rd Indian Planetary Science Conference (IPSC-2022), PRL, Ahmedabad, 14-16 March, 2022

81. P. Kalyan Reddy, Janmejay Kumar and K. Durga Prasad, "Gas-Mixing System for PETC Start-up Chamber", 3^{rd} Indian Planetary Science Conference (IPSC-2022), PRL, Ahmedabad, 14-16 March, 2022
82. S. A. Haider, Y. S. Siddhi, and K. Durga Prasad, "Characteristics of Venus and Mars Ionopauses: Modelling and Observations", 3^{rd} Indian Planetary Science Conference (IPSC-2022), PRL, Ahmedabad, 14-16 March, 2022
83. Basu Sarbadhikari A. and Y. Srivastava, "Non-mare perspective of mare basalt generation", 3^{rd} Indian Planetary Science Conference (IPSC-2022), PRL, Ahmedabad, 14-16 March, 2022
84. Surendra V Singh, Haritha D, V Jayaram, J K Meka, T Vijay, S Vijayan, A Bhardwaj, N J Mason, B Sivaraman, "Amino acids in astrochemical impact induced shock conditions: implications to the origins of life", 21^{st} National Space Science Symposium (NSSS-2022), 31 January - 04 February, 2022
85. Surendra V Singh, H Dilip, Johnson Delna J K George, J K Meka, S Vijayan, T Vijay, B N Rajasekhar, Anil Bhardwaj, Mark J Burchell, Nigel J Mason, and B Sivaraman, "Hypervelocity impact induced formation of crystalline biomolecular dust - Implications to the impacts on icy moons", 3^{rd} Indian Planetary Science Conference (IPSC-2022), 14-16 March 2022
86. S Pavithraa, R Ramachandran, J K Meka, J I Lo, S L Chou, B M Cheng, B N Rajasekhar, A Bhardwaj, N J Mason, B Sivaraman, "VUV Photoabsorption of Thermally Processed Carbon disulphide and Ammonia Ice mixtures - Implications to icy objects in the solar system", 21^{st} National Space Science Symposium (NSSS-2022), 31 January - 04 February, 2022
87. S Pavithraa, R Ramachandran, S Gupta, W Khan, J K Meka, A Das, B N Rajasekhar, A Bhardwaj, N J Mason and B Sivaraman, "Astrochemical Ices Beyond their Sublimation Limit - Momentary Molecular Ices", 3^{rd} Indian Planetary Science Conference (IPSC-2022), 14-16 March 2022
88. W Khan, R Ramachandran, P Sundararajan, J K Meka, B N Rajashekar, A Bhardwaj, N Mason, B Sivaraman, "Effect of ethylene glycol on cometary water", 3^{rd} Indian Planetary Science Conference (IPSC-2022), 14-16 March 2022
89. Arijit Roy, V S Surendra, J K Meka, R Ramachandran, D Atri, B N Rajasekhar, P Janardhan, A Bhardwaj, H Hill, N J Mason, B Sivaraman, "Minerals in the ISM are Made in an Instant", 21^{st} National Space Science Symposium (NSSS-2022), 31 January - 04 February, 2022
90. Arijit Roy, V S Surendra, J K Meka, R Ramachandran, D Sahu, A Goutam, T Vijay, V Jayaram, P Janardhan, B N Rajasekhar, Anil Bhardwaj, N J Mason, B Sivaraman, "Shock Processing of Organometallic Dust - Ferrocene", 3^{rd} Indian Planetary Science Conference (IPSC-2022), 14-16 March 2022
91. Sandeep Kumar and Nandita Srivastava, "A parametric study of performance of solar wind forecasting models during 2006 to 2011", First Indian Space Weather Conference (ISWC-2022), 11–12 Jan, 2022
92. Sandeep Kumar and Nandita Srivastava, "A parametric study of performance of solar wind forecasting models during 2006 to 2011", 40^{th} Astronomical Society of India Meeting (ASI-2022), 25−29 March, 2022
93. Neeraj Rastogi, "Studies on Brown Carbon Aerosols in India: Current Status and Way Forward", National Space Science Symposium-2022, 31 Jan - 4 Feb, 2022
94. Partha Sarathi Jena and Ravi Bhushan, "Role of In-situ and Meteoric ^{10}Be in Quaternary Glaciation, Marine Chronology, and Paleomagnetic Reconstruction", Seventh National Conference of the Ocean Society of India (OSICON-2021), 14 Aug, 2021
95. Partha Sarathi Jena, Ravi Bhushan, Shivam Ajay, and A.K Sudheer, "Spatial variability and residence time of beryllium isotopes in the Indian Ocean: Role of oceanic processes", Frontiers and Geosciences Research Conference (FGRC-2021), 28 Sept, 2021
96. Puneet Kumar Verma, Dinesh Sah, R.V. Satish, Neeraj Rastogi, K. Maharaj Kumari, and Anita Lakhani, "Spatio-temporal variation and gas-particle partitioning of PAHs and Nitro-PAHs in the atmosphere", National Space Science Symposium-2022, 31 Jan - 4 Feb, 2022
97. Rohit Meena, Jay Dave, Atinderpal Singh, and Neeraj Rastogi, "Real-time measurements of NR-$PM_{2.5}$ during Covid-19 lockdown in Ahmedabad", National Space Science Symposium-2022, 31 Jan - 4 Feb, 2022
98. Shivam Ajay, Partha Sarathi Jena, Ankur Dabhi and Ravi Bhushan, "First resuts of Beryllium isotope measureents from PRL-AURIS", Frontiers and Geosciences Research Conference (FGRC-2021), 27 Sept, 2021
99. Kumar, S., Mandal, S., and Pallamraju, D., "3-D characterization of daytime gravity waves obtained using optical and radio measurements", 21^{st} National Space Science Symposium, 31 Jan-4 Feb, 2022
100. Kumar, S., Pallamraju, D., Suryawanshi, P., Vijayalakshmi, T., and Seemala, G. K., "Variation in OI 630 nm dayglow emission due to the equatorial electrodynamics and meridional winds", 21^{st} National Space Science Symposium, 31 Jan-4 Feb, 2022
101. Saha, S., Pallamraju, D., and Pant, T. K., "OI 630 nm nightglow variability during post-sunset time over low-latitude thermosphere", 21^{st} National Space Science Symposium, 31 Jan-4 Feb, 2022
102. Mandal, S., and D. Pallamraju, "Effects of geomagnetic storms on the gravity wave activity over low-latitudes", First Indian Space Weather Conference (ISWC-2022) held in virtual mode, 11-12 Jan, 2022
103. Mandal, S., D. Pallamraju, and T. K. Pant, "Daytime thermospheric wave dynamics and day-to-day variability in the occurrence of ESF", 21^{st} National Space Science Symposium held in virtual mode, 31 Jan-4 Feb, 2022
104. Upadhyay, Kshitiz and Duggirala Pallamraju, "Investigations of mid-latitude upper atmosphere", 21^{st} National Space Science Symposium, IISER, Kolkata held in virtual mode, 31 Jan-4 Feb, 2022
105. Yogesh, Dibyendu Chakrabarty, and Nandita Srivastava, "Investigation on variation in solar wind Helium abundance during the last four solar cycles", First Indian Space Weather Conference - 2022 (ISWC-2022) hosted by PRL, 11-12 Jan, 2022
106. Yogesh, Dibyendu Chakrabarty, and Nandita Srivastava, "On the variation of Helium abundance over solar cycles and ICMEs", 21^{st} National Space Science Symposium (NSSS-2022) held at IISER Kolkata, India, 31 Jan-4 Feb, 2022
107. Yogesh, Dibyendu Chakrabarty, and Nandita Srivastava, "Helium abundance variation in Interplanetary Coronal Mass

Ejections spanning over solar cycle 23 and 24", 40^{th} Annual Meeting of the Astronomical Society of India (ASI) held at IIT Roorkee, India, 25-29 Mar, 2022

108. Bijoy Dalal, Dibyendu Chakrabarty, and Nandita Srivastava, "Investigation on solar cycle dependence of interplanetary suprathermal populations", First Indian Space Weather Conference - 2022 (ISWC-2022) hosted by PRL, 11-12 Jan, 2022

109. Bijoy Dalal, Dibyendu Chakrabarty, and Nandita Srivastava, "Comparison of suprathermal particles between the last two solar cycles: Insights", 21^{st} National Space Science Symposium (NSSS-2022) held at IISER Kolkata, India, 31 Jan-4 Feb, 2022

110. R. Pathak, D. Chakrabarty, A. Sarda, S. Urmalia, D. Pallamraju, P. Kushwaha, M. Soni, A. Yadav, A. Ashruf, C. Raghavan, P. Suryawanshi, and M. Bhavsar, "NAVA Experiment: Recent developments on front-end and processing electronics using CMOS C650 and SCMOS CAPELLA-CIS120 chip", Venus Science Conference 2021 (Venus-SC-2021) held at PRL, 23-24-Sept, 2021

111. R. Pathak, A. Sarda, S. Urmalia, D. Chakrabarty, D. Pallamraju, P. Kushwaha, M. Soni, A. Yadav, C. Raghavan, J. Sebastian, P. Suryawanshi, and M. Bhavsar, "Developments on proof of concept prototype using CMOS C650 chip for Airglow Photometer payload onboard future Venus mission", Indian Planetary Science Conference 2022 (IPSC 2022) held at PRL, 14-16 Mar, 2022

112. Dibyendu Chakrabarty, "Space weather and probing the solar wind plasma from the first Lagrangian point of the Sun-Earth system", Plasma Science and Applications (PSA-2021), organized by the Department of Physics, Sardar Vallabhbhai National Institute of Technology, Surat, 20-21 Dec, 2021

113. Dibyendu Chakrabarty, "Air and Space", Ananth National University, Ahmedabad, 20 Nov, 2021

114. Dibyendu Chakrabarty, "Potential of atomic oxygen airglow diagnostics to probe Venusian upper atmosphere", Venus Science Conference, 2021 (Venus-SC-2021), PRL, 23-24 Sept, 2021

115. D. Chakrabarty, "Long term variation of solar wind helium and suprathermal population", 40^{th} Annual Meeting of the Astronomical Society of India (ASI) held at IIT Roorkee, India, 25-29 Mar, 2022

116. Guharay, A., Mondal, S., Sarkhel, S., Sivakandan, M., and Sunil Krishna, M. V., "Signature of a mesospheric bore in 557.7 nm airglow emission at a Himalayan location", 15^{th} Quadrennial Solar-Terrestrial Physics Symposium (STP-15), IIG Mumbai (India), 21-25 Feb, 2022

117. Mitra, G., Guharay, A., Batista, P. P., and Buriti, R. A., "Variability of low latitude planetary wave dynamics during September 2019 minor sudden stratospheric warming", 15^{th} Quadrennial Solar-Terrestrial Physics Symposium (STP-15), IIG Mumbai (India), 21-25 Feb, 2022

118. Guharay, A., Batista P. P., and Clemesha, B. R., "Intraseasonal oscillations in the equatorial middle atmosphere", 21^{st} National Space Science Symposium (NSSS-2022) held at IISER Kolkata, India, 31 Jan-4 Feb, 2022

119. Mitra, G., Guharay, A., Batista, P. P., and Buriti, R. A., "Planetary wave dynamical variability at low latitude middle atmosphere during September 2019 SSW", 21^{st} National Space Science Symposium (NSSS-2022) held at IISER Kolkata, India, 31 Jan-4 Feb, 2022

120. Venkatesh, K., "Super-fountain effect linked with 17 March 2015 geomagnetic storm manifesting distinct multi-layer stratification", First Indian Space Weather Conference - 2022 (ISWC-2022) hosted by PRL, 11-12 Jan, 2022

121. Venkatesh, K., "Formation of the evening time F3 layer investigated using Jicamarca incoherent scatter radar observations", 21^{st} National Space Science Symposium (NSSS-2022) held at IISER Kolkata, India, 31 Jan-4 Feb, 2022

122. S. Sharma, S. Saha, P. Kumar and M. Parmar, "Spread of COVID-19 Infection: Impact of Atmospheric Parameters", International Conference on Space Science and Technology (ICSST), Ahmedabad, 5-7 April, 2021

123. S. Saha and S. Sharma, "Evaluation of Atmospheric Boundary Layer over Western Indian region using Ground based Lidar", International Conference on Space Science and Technology (ICSST) 2021, Ahmedabad, 5-7 April 2021

124. S. Saha, and S. Sharma, "Study of atmospheric boundary layer using lidars", ANSH-2021, CSIR-NAL Bengaluru, 12-13 Aug, 2021

125. S. Sharma, S. Saha, D. Kamat, P. Kumar, "Atmospheric Investigations During COVID19 Pandemic", 21^{st} National Space Science Symposium (NSSS-2022) held at IISER Kolkata, India, 31 Jan-4 Feb, 2022

126. S. Saha, S. Sharma, N. K. Kondapalli, and D. Kamat, "Unravelling the characteristics of Atmospheric Boundary Layer over Ahmedabad", 21^{st} National Space Science Symposium (NSSS-2022) held at IISER Kolkata, India, 31 Jan-4 Feb, 2022

127. D. Kamat, S. Saha, S. Sharma, N. K. Kondapalli, and P. Kumar, "Finding the Missing Link for 2021 Rainfall: Atlantic Nino", 21^{st} National Space Science Symposium (NSSS-2022) held at IISER Kolkata, India, 31 Jan-4 Feb, 2022

128. H. Sreedevan, D. Kamat, S. Sharma, and S. Saha, "Analysis of Multi-Layer Atmospheric Clouds over Ahmedabad", 21^{st} National Space Science Symposium (NSSS-2022) held at IISER Kolkata, India, 31 Jan-4 Feb, 2022

129. A. Kundu, S. S. Kundu, S. Sharma, R. Mahanta, T. Banik, M. Gogoi, and A. Borgohain, "Understanding the vertical structure of clouds observed over a high-altitude station of North East India", 21^{st} National Space Science Symposium (NSSS-2022) held at IISER Kolkata, India, 31 Jan-4 Feb, 2022

130. R. Shah, R. Srivastava, and S. Sharma, "Study of spatio-temporal variations in aerosol-cloud properties over Western India and Arabian Sea", 21^{st} National Space Science Symposium (NSSS-2022) held at IISER Kolkata, India, 31 Jan-4 Feb, 2022

131. M. Gogoi, A. Borgohain, S. S. Kundu, S. Sharma, P. K. Bhuyan, A. Kundu, N. Barman, and P. L. N. Raju, "Characterization of Atmospheric Boundary Layer over High Altitude Station, Umiam", 21^{st} National Space Science Symposium (NSSS-2022) held at IISER Kolkata, India, 31 Jan-4 Feb, 2022

132. T. G. Malik, and L. K. Sahu, "Emissions of biogenic VOC from Achanakmar Amarkantak Biosphere Reserve (AABR) Forest in Central India", 21^{st} National Space Science Symposium (NSSS-2022) held at IISER Kolkata, India, 31 Jan-4 Feb, 2022

133. Mansi Gupta, Nidhi Tripathi, Arvind Singh, and L. K. Sahu, "Variability in atmospheric DMS over the Bay of Bengal during the post-monsoon season", 21^{st} National Space Science Symposium (NSSS-2022) held at IISER Kolkata, India, 31 Jan-4 Feb, 2022
134. Ravindra Pratap Singh, Duggirala Pallamraju, Pradip Suryawanshi, and Shashank Urmalia, "Terdiurnal and gravity wave influences on OH(3-1) brightness and its rotational temperatures measured by PRL Airglow InfraRed Spectrograph (PAIRS)", 21^{st} National Space Science Symposium (NSSS-2022) held at IISER Kolkata, India, 31 Jan-4 Feb, 2022
135. Ojha, N., Soni, M., Tripathi, N., Girach, I., and Sahu, L. K., "Photochemical evolution of air in tropical urban environments of India: A model-based study", 21^{st} National Space Science Symposium (NSSS-2022) held at IISER Kolkata, India, 31 Jan-4 Feb, 2022
136. Girach, I. A., Ojha, N., Ponmalar, M., Murugan, S., Rahman, P. A., Babu, S. S., and Ramachandran, R., "Demonstrating the capability of machine learning to simulate atmospheric trace gases", 21^{st} National Space Science Symposium (NSSS-2022) held at IISER Kolkata, India, 31 Jan-4 Feb, 2022
137. Soni, M., and Ojha, N., "Air chemistry in a tropical urban environment of India: a modeling perspective", Frontiers in Geosciences Research Conference (FGRC) - 2021, PRL Ahmedabad, India, 27-28 Sept, 2021

International (66)

1. Hema Kharayat, L. Prasad, R. Mathpal, S. Garia and B. Bhatt, "Study of Cosmic Ray Intensity in Association with Interplanetary Magnetic Field and Geomagnetic Storms", International Conference on Space Science and Technology (ICSST-2021), 5–7 April, 2021
2. Kamlesh Bora, "Impact of the Hall MHD on the evolution of three-dimensional complex magnetic structures", 16^{th} European Solar Physics Meeting (ESPM-16), 6–10 September, 2021
3. Hema Kharayat and Bhuwan Joshi, "Blowout expansion of a coronal mass ejection and subsequent filament eruption", 16^{th} European Solar Physics Meeting (ESPM-16), 6–10 September, 2021
4. Binal D patel, Bhuwan Joshi, K.-S. Cho and R.-S. Kim, "DH Type II Radio Bursts During Solar Cycles 23 and 24: Frequency-dependent Classifica-tion and their Flare-CME Associations", 15^{th} Quadrennial Solar-Terrestrial Physics Symposium (STP-15), 21–25 February, 2022
5. Kota, V.K.B. and R. Sahu, "Multiple $\mathrm{SO}(5)$ isovector pairing and seniority $Sp(2\Omega)$ multi-j algebras with isospin", International Workshop on Shapes and Dynamics of Atomic Nuclei: Contemporary Aspects (SDANCA-21), 2021
6. Anshika Bansal and Namit Mahajan, "LCSR application to $p \to e^+\gamma$", Light Cone 2021: Physics of Hadrons on the Light Front, 28 November-4 December, 2021
7. Anshika Bansal and Namit Mahajan, "LCSR application to radiative tau decay", 9^{th} Edition of the Large Hadron Collider Physics Conference, LHCP2021 ($7^{th} - 12^{th}$, June, 2021
8. Dayanand Mishra and Namit Mahajan, "Impact of soft photons on $\mathrm{B} \to \mathrm{K}\ell^+\ell^-$", 9^{th} Edition of the Large Hadron Collider Physics Conference, LHCP2021 ($7^{th} - 12^{th}$, June, 2021
9. Anshika Bansal and Namit Mahajan, "Application of LCSR to $\tau^- \to \pi^- \nu_\tau \gamma$", Weak Interactions and Neutrinos 2021, WIN-2021 ($7^{th} - 12^{th}$, June, 2021
10. N. P. S. Mithun, S. V. Vadawale, B. Mondal, A. Sarkar, B. Joshi and A. Bhardwaj, "Soft X-ray Spectral Diagnostics of Multi-thermal Plasma in Solar Flares with Chandrayaan-2 XSM", Virtual Workshop on Particle Acceleration in Solar Flares and the Plasma Universe Deciphering its features under magnetic reconnection, 15-19 November, 2021
11. B. Mondal, A. Sarkar, S. V. Vadawale, N.P.S. Mithun ,P. Janardhan ,G. Del Zanna, H.E. Mason , U. Mitra-Kreav and S. Narendranath, "Soft X-ray spectroscopy of the Sun during the minima of Solar cycle 24 with the Solar X-ray Monitor (XSM)", Hinode-14 / IRIS-11 Joint Science Meeting, 25-28 October, 2021
12. B. Mondal , A. Sarkar, S. V. Vadawale, N.P.S. Mithun , P. Janardhan , G. Del Zanna, H.E. Mason , U. Mitra-Kreav and S. Narendranath, "Soft X-ray spectroscopy of the Solar corona during the deepest solar minimum of the past hundred years with the Solar X-ray Monitor (XSM) on-board the Chandrayaan-2 orbiter.", 16th European Solar Physics Meeting, 6-10 Septmber, 2021
13. Rani A. and A. Basu Sarbadhikari, "Noachian Volcanism and its Implication to the Thermal Evolution of Mars", AGU Fall Meeting, 13-17 December, 2021
14. Tan X., S. Karunatillake, H. Haviland, P. Moitra, L. Ojha and A. Basu Sarbadhikari, "Characterizing the Magmatic Evolution of the Elysium Volcanic Province on Mars", AGU Fall Meeting, 13-17 December, 2021
15. K. Bhuva, P. Patadiya, H. Julasana, S. Purohit, M. Bhatt, D. Dhingra, and U. Mall, "A machine learning framework for data filtering: a case study on chandrayaan-1 SIR-2 data", IEEE International Geoscience and Remote Sensing Symposium (IGARSS), 11 - 16 July, 2021
16. Kumar Avadh and R. R. Mahajan, "Meteoroidal ejection events and trapped neon gas abundance of LL chondrites", DINGUE VII, Developments in noble gas understanding and expertise, 30 June - 01 July, 2021
17. A. Bhattacharya, C. Li, and J. P. Pabari, "Dusty plasma in Venus ionosphere and comparative study with ionospheric dusty plasma medium on Earth and Mars", AGU Fall Meeting, 13-17 December, 2021
18. A. K. Singhvi, "How robust are SAR single grain paleodoses: the role of sensitivity changes ?", Luminescence and ESR Dating Conference, 13-17 September 2021
19. Monika Parmar, "TL and OSL trap correlation studies to understand the luminescence mechanism in feldspar", Luminescence and ESR Dating conference, 13-17 September 2021
20. Naveen Chauhan, "A Revised Optimized Protocol for Violet Stimulated Luminescence (VSL) Dating to Extend the Dating Range using Quartz", Luminescence and ESR Dating conference, 13-17 September 2021
21. Santunu Panda, "Spatial variations in luminescence sensitivity of quartz extracted from source rocks and fluvial sediments

of the Sabarmati River basin, Western India: Implications for provenance studies", in Luminescence and ESR Dating conference, 13-17 September 2021

22. Surendra V Singh, Johnson Delna J K George, M J Burchell, A Bhardwaj, N J Mason, S Vijayan, T Vijay, B Sivaraman, "Hypervelocity impact-induced formation of crystalline biomolecular dust - Implications to the impacts on icy moons", European Astrobiology Network Association (EANA -2021), 7-10 September 2021
23. Surendra V Singh, Haritha D, J K Meka, T Vijay, V Jayaram, M Muruganantham, S Vijayan, A Bhardwaj, N J Mason, M J Burchell, B Sivaraman, "Hypervelocity impact on amino acids embedded in water ice", European Planetary Science Congress (EPSC 2021), 13-24 September 2021
24. Surendra V Singh, J K Meka, R Ramachandran, V Jayaram, T Vijay, S Vijayan, B N Rajasekhar, A Bhardwaj, N J Mason, B Sivaraman, "A possible explanation for the microstructures observed in meteorites, online symposium on Meteoroids, Meteors, Meteorites: Messenger from space (MetMeSS 2021)", Meteoroids, Meteors, Meteorites: Messenger from space (MetMeSS 2021), 29-30 November, 2021
25. W Khan, R Ramachandran, P Sundararajan, J K Meka, B N Rajasekhar, S Ganesh, A Bhardwaj, N J Mason, B Sivaraman, "Understanding the effect of ethylene glycol on cometary water", 53^{rd} Lunar and Planetary Science Conference (LPSC-2022), 7-11 March 2022
26. Arijit Roy, Venkataraman Veeman, and B Sivaraman, "Spectroscopic investigation of Comet 46P Wirtanen at UV wavelengths", European Planetary Science Congress (EPSC 2021), 13-24 September 2021
27. Arijit Roy, V S Surendra, J K Meka, R Ramachandran, D Atri, B N Rajasekhar, P Janardhan, A Bhardwaj, H Hill, N J Mason, B Sivaraman, "Minerals in the ISM are Made in an Instant", Meteoroids, Meteors, Meteorites: Messenger from space (MetMeSS 2021), 29-30 November, 2021
28. Nisha Bharti, Ravi Bhushan, Partha Sarathi Jena, Ankur Dabhi, A. Shivam and M. Muruganantham, "First Radiocarbon Evidence of Poorly Ventilated Deep Central Indian Ocean during the Last Glaciation: Implication to Glacial Carbon Sequestration and Atmospheric CO^2", American Geophysical Union (AGU) fall meeting - 2021, 14 Dec, 2021
29. Partha Sarathi Jena, Ravi Bhushan, Ajay Shivam, Nisha Bharti,and A.K. Sudheer, "$^{10}Be/^{9}Be$ Ratio Variation in the Central Indian Ocean during the Last 43 ka; Implication to Past Geomagnetic Field Intensity Changes", American Geophysical Union (AGU) fall meeting - 2021, 16 Dec, 2021
30. Anil Patel, Neeraj Rastogi, Arup Borgohain, Shyam S Kundu, and Rangu Satish, "Oxidative Potential of Atmospheric Aerosols and in situ Generation of Reactive Oxygen Species over a High Altitude Site in North-eastern India", European Aerosol Conference - EAC 2021, 30 Aug - 3 Sept, 2021
31. H. Vernier, N. Rastogi, H. Liu, T.D. Fairlie, A. K. Pandit, K.M. Bedka, A. Patel, M. Venkat Ratnam, B. Suneel Kumar, H. Gadhavi, F.G. Weinhold, Gwenael Berthet, and J.P. Vernier., "Exploring the ionic composition of the Asian Tropopause Aerosol Layer using medium duration balloon flights", EGU General Assembly 2021, 19 - 30 April, 2021
32. Joseph V. Puthussery, Ashutosh Shukla, Jay Dave, Sreenivas Gaddamidi, Atinderpal Singh, Dilip Ganguly, Neeraj Rastogi, Sachchida Nand Tripathi, and Vishal Verma, "Seasonal Trends and Influence of Episodic Events on the Oxidative Potential of Ambient Particulate Matter in Delhi, India", European Aerosol Conference - EAC 2021, 30 Aug - 3 Sep, 2021
33. Devaprasad, M., Neeraj Rastogi, Rangu Satish, Ankur Dabi, A. Shivam, and R. Bhushan, "Sources and characteristics of paddy-residue burning derived carbonaceous aerosols using dual carbon isotopes", 16^{th} IGAC Scientific Conference, 12 - 20 Sept, 2021
34. Sophie Haslett, Varun Kumar, Andre Prevot, Jay G. Slowik, David M. Bell, Sachchida Tripathi, Suneeti Mishra, Atinderpal Singh, Neeraj Rastogi, Dilip Ganguly, Joel Thornton, Kaspar Daellenbach, Markku Kulmala, Chao Yan, and Claudia Mohr., "Night-time NO emissions suppress large amounts of chlorine radical formation in Delhi", European Aerosol Conference - EAC 2021, 30 Aug - 3 Sept, 2021
35. Sophie L. Haslett, Varun Kumar, Andre S. H. Prevot, Jay G. Slowik, David M. Bell, Sachinda N. Tripathi, Suneeti Mishra, Atinderpal Singh, Neeraj Rastogi, Dilip Ganguly, Joel Thornton, Kaspar Dällenbach, Chao Yan, and Claudia Mohr., "Night-time NO emissions suppress large amounts of chlorine radical formation in Delhi", EGU General Assembly - 2021, 19-30 April, 2021
36. V. Goswami and S.K. Singh, "Impact of water mass circulation and dust deposition on spatial distribution of Nd concentrations and σNd in equatorial and southern Indian Ocean", International Indian Ocean Science Conference (IIOSC), March, 2022
37. R. Pathak, A. Sarda, S. Urmalia, D. Chakrabarty, D. Pallamraju, P. Kushwaha, M. Soni, A. Yadav, A. Ashruf, C. Raghavan, P. Suryawanshi, and M. Bhavsar, "NAVA payload: Identification of the array detector and recent developments on front-end and processing electronics", 2^{nd} Indian Planetary Science Congress, PRL, 25-26 Feb, 2021
38. Kumar, S., and Pallamraju, D., "Investigations of oxygen dayglow emission variability over low latitudes under the influence of equatorial electrodynamic processes", CEDAR workshop, 20-25 June, 2021
39. Kumar, S., Pallamraju, D., Suryawanshi, P., Vijayalakshmi, T., and Seemala, G. K., "Effect of equatorial electrodynamic processes and meridional winds on the OI 630.0 nm dayglow emission variability over low latitudes", 15^{th} Solar Terrestrial Symposium (STP-15), 21-25 Feb, 2022
40. Pallamraju, D. F. I. Laskar, M. Codrescu, R. Eastes, J. S. Evans, W. Wang, B. McClintock, S. Aryal, and X. Cai, "Themospheric Variability During Quiet and Active Geomagnetic Conditions Using GOLD Disk Observations", American Geophysical Union Fall Meeting 2021, 13-17 Dec, 2021
41. R. Pathak, D. Chakrabarty, A. Sarda, S. Urmalia, D. Pallamraju, P. Kushwaha, M. Soni, A. Yadav, A. Ashruf, C. Raghavan, P. Suryawanshi, and M. Bhavsar, "NAVA Experiment: Recent developments on front-end and processing electronics using CMOS C650 and SCMOS CAPELLA-CIS120 chip", Venus Science Conference 2021, 23 - 24 Sept, 2021
42. Saha, S., Pallamraju, D., and Ghodpage, R. N., "Dynamics and Structure of Plasma bubble observed in the OI 630 nm nightglow emissions over low and off-equatorial latitudes", 15^{th} Quadrennial Solar-Terrestrial Physics (STP-15) symposium, 21-25 Feb, 2022

43. Saha, S., and Pallamraju, D., "Latitudinal movement of the EIA crest as seen in OI 630 nm nightglow emissions over low-latitudinal region of Indian longitude", 15^{th} Quadrennial Solar-Terrestrial Physics (STP-15) symposium, 21-25 Feb, 2022
44. Saha, S., Pallamraju, D., Pant, T. K., and Chakrabarti, S., "On the Cause of Post-sunset Enhancement in OI 630 nm Airglow Emission over Low-latitude Thermosphere", Joint Scientific Assembly IAGA-IASPEI-2021, 21-27 Aug, 2021
45. Saha, S., and Pallamraju, D., "Influence of Seasonal and Solar Flux Variations on the Low-latitude OI 630 nm Thermospheric Nightglow", Joint Scientific Assembly IAGA-IASPEI-2021, 21-27 Aug, 2021
46. Saha, S., Pallamraju, D., and Ghodpage, R. N., "Coupling of the Ionospheric Plasma as investigated using OI 630 nm Emissions from Low- and Off-equatorial Latitude locations in Indian Longitudes", Joint Scientific Assembly IAGA-IASPEI-2021, 21-27 Aug, 2021
47. Saha, S., and Pallamraju, D., "Investigation of the Variability in OI 630 nm Nightglow Emission over Low-latitude Thermosphere", CEDAR workshop-2021, 20-25 June, 2021
48. Mandal, S., and D. Pallamraju, "Understanding the neutral wave characteristics in the daytime thermosphere using radio technique", CEDAR workshop-2021, 20-25 June, 2021
49. Mandal, S., and D. Pallamraju, "Investigation of daytime thermospheric wave dynamics using radio technique", 15^{th} Quadrennial Solar-Terrestrial Physics (STP-15) symposium, 21-25 Feb, 2022
50. Mandal, S., and D. Pallamraju, "An innovative approach to derive daytime gravity wave characteristics using digisonde", 15^{th} Quadrennial Solar-Terrestrial Physics (STP-15) symposium, 21-25 Feb, 2022
51. Singh, Dupinder and D. Pallamraju, "Longitudinal differences in the equatorial electrodynamics processes as deduced from the SWARM satellite constellation", 15^{th} Quadrennial Solar-Terrestrial Physics (STP-15) symposium, 21-25 Feb, 2022
52. Singh, R. P., D. Pallamraju, Pradip Suryawanshi, and Shashank Urmalia, "Short periodic gravity waves and tidal influences using OH(3-1) brightness and its rotational temperatures measured by PRL Airglow InfraRed Spectrograph (PAIRS)", 15^{th} Quadrennial Solar-Terrestrial Physics Symposium (STP-15), hosted by Indian Institute of Geomagnetism, India, 21-25 Feb, 2022
53. Upadhyay, Kshitiz, and Duggirala Pallamraju, "The O (^{1}D) 630.0 nm dayglow emission variability over Mid-latitudes", 15^{th} Quadrennial Solar-Terrestrial Physics Symposium (STP-15), IIG Mumbai (India), 21-25 Feb, 2022
54. L. K. Sahu, Nidhi Tripathi, Arvind Singh, Ravi Yadav, and Meenu, "Elevated levels of isoprene in the MBL of Arabian Sea during spring intermonsoon Season", International Indian Ocean Science Conference (IIOSC), 14-18 Mar, 2022 [Virtual]
55. Mansi Gupta, Nidhi Tripathi, Arvind Singh, and L. K. Sahu, "Spatio-temporal variation of atmospheric DMS over the Bay of Bengal during the post-monsoon season and the role of biological productivity", International Indian Ocean Science Conference (IIOSC), 14-18 Mar, 2022 [Virtual]
56. Nidhi Tripathi, L. K. Sahu, Purushottam Kumar and S. N. Tripathi, "Investigation of major emission sources and photochemical processes of Volatile Organic Compounds (VOCs) at a suburban site of New Delhi, India in the winter", 16^{th} IGAC Scientific Conference, 12-17 Sept, 2021 [Virtual]
57. Ankit Kumar, Dibyendu Chakrabarty, Diptiranjan Rout, Bela G. Fejer, Geoff D. Reeves, S. Sripathi, Gopi K. Seemala, Surendra Sunda, and Anil K. Yadav, "A case study on anomalous electric field variations in the F region equatorial ionosphere during post-sunset hours: insights", 15^{th} Quadrennial Solar-Terrestrial Physics Symposium (STP-15) held at IIG Alibag, India, 21-25 Feb, 2022
58. Yogesh, Dibyendu Chakrabarty, and Nandita Srivastava, "Helium abundance in solar wind and coronal mass ejections", 15^{th} Quadrennial Solar-Terrestrial Physics Symposium (STP-15) held at IIG Alibag, India, 21-25 Feb, 2022
59. Bijoy Dalal, Dibyendu Chakrabarty, and Nandita Srivastava, "Variations in the suprathermal populations in the solar wind during solar cycles 23 and 24", 15^{th} Quadrennial Solar-Terrestrial Physics Symposium (STP-15) held at IIG Alibag, India, 21-25 Feb, 2022
60. Dibyendu Chakrabarty, "Understanding the prompt electric field disturbances over low-equatorial latitude ionosphere A paradigm shift", S3 PRESTO Pillar 2: Space weather and Earth's atmosphere, STP-15, 21-25 Feb, 2022
61. Dibyendu Chakrabarty, "Penetration Electric Fields: Meaning, Nature, Importance and Complexities", International Space Weather Initiative (ISWI-2021) Workshop on Space Weather: Science and Applications jointly organized by the United Nations Office for Outer Space Affairs (UNOOSA) and the Vikram Sarabhai Space Centre (VSSC) of the Indian Space Research, 2 - 3 Nov, 2021
62. Dibyendu Chakrabarty, "Aditya Solar wind Particle EXperiment (ASPEX) on-board Aditya-L1 Mission of India", Joint Scientific Assembly of IAGA-IASPEI-2021, 21-27 Aug, 2021
63. Mitra, G., Guharay, A., Batista, P. P., and Buriti, R. A., "Impact of the September 2019 minor sudden stratospheric warming on the lowlatitude middle atmospheric planetary wave dynamics", AGU Fall meeting, USA, 13-17 Dec, 2021
64. Ravindra Pratap Singh, Duggirala Pallamraju, Pradip Suryawanshi, and Shashank Urmalia, "Short periodic gravity waves and tidal influences using OH(3-1) brightness and its rotational temperatures measured by PRL Airglow InfraRed Spectrograph (PAIRS)", 15^{th} quadrennial Solar-Terrestrial Physics symposium (STP-15), IIG Mumbai, 21 - 25 Feb, 2022
65. Soni, M., Girach, I., and Ojha, N., "Photochemistry over an urban environment of India: Integration of measurements with box model", International Global Atmospheric Chemistry (IGAC)-2021, 12-17 Sept, 2021
66. Girach I., Ojha N., Tripathi N., Sahu L., and Nair P. R., "Ozone and carbon monoxide over the northern Indian Ocean during winter and monsoon: Influence of chemistry and dynamics", International Global Atmospheric Chemistry (IGAC)-2021, 12-17 Sept, 2021

Events, and Outreach Activities at PRL

Azadi ka Amrut Mahotsav (AKAM)

Azadi Ka Amrit Mahotsav is an initiative of the Government of India to celebrate and commemorate 75 years of independence and the glorious history of its people, culture and achievements. This Mahotsav is dedicated to the people of India who have not only been instrumental in bringing India, thus far in its evolutionary journey, but also hold within them the power and potential to enable Prime Minister's vision of activating India 2.0, fuelled by the spirit of Aatmanirbhar Bharat.

The official journey of Azadi ka Amrit Mahotsav commenced on 12^{th} March 2021 which started a 75-week countdown to our 75^{th} anniversary of independence and will end post a year on 15 August 2023. This also coincides with the 75^{th} year of the foundation of the Physical Research Laboratory (PRL). Various events have been planned and organized to celebrate Indias 75^{th} independence and PRL's platinum jubilee. Activities at PRL includes but not limited to Science Popularization, Outreach Activities, Lectures, Webinars, Cultural Events, Sports Events, and Public Awareness Programs, ensuring public participation as well. A specific committee for Azadi ka Amrit Mahotsav (CAKAM) is taking care of all these activities. Following are list of activities held at PRL during April 2021 March 2022 to commemorate Azadi ka Amrut Mahotsav as well as celebrations of PRL's platinum jubilee. Some of these are regular events at PRL which are linked under AKAM:

1. 102^{nd} Vikram Sarabhai Jayanti on 12/08/2021
2. Independence Day Celebration 15/08/2021
3. An Evening in PRL 15/08/2021
4. Fire Safety & Security Training 23/08/2021
5. 150^{th} Birth Anniversary of Mahatma Gandhi 02/10/2021
6. National Unity Day 31.10.2021
7. Republic Day @ PRL 26/01/2022
8. Scientific Tour to Statue of Unity on 26/03/2022
9. Volleyball Tournament February-March 2022
10. Inter-Area PRL Football Tournament February-March 2022

PRL ka Amrut Vyakhyaan

As part of the AKAM celebrations, PRL is organizing "PRL Ka Amrut Vyakhyaan," a series of weekly vyakhyaan (colloquia) delivered online by eminent speakers from academia, arts, literature, business, and law. This series of vyakhyaan was inaugurated on August 4, 2021, by Dr. K Radhakrishnan, former Secretary, Department of Space, Government of India and former Chairman, ISRO. Each Vyakhyaan is of one-hour duration, followed by discussions and interactions at the end. This event is streamed live on PRL's YouTube channel.

National Science Day 2022

National Science Day (NSD) in India is celebrated on February 28 each year to mark the discovery of the Raman Effect. The primary focus of the NSD celebration is to widely spread the message about the importance of science in people's daily lives. As a result, this event is celebrated all over the country in schools, colleges, universities, and other academic, scientific, technical, medical, and research institutions. This year, due to the continued constraints posed by the COVID-19 pandemic, the NSD -2022 events Scholarship and Aruna Lal Scholarship examination and interviews were conducted online. The event and efforts were unconventional this time, but due to the efforts, the vision, concept, foresight, and execution with the support of the NSD committee and other PRL colleagues, the NSD 2022 event was conducted seamlessly. PRL celebrated NSD on February 26, 2022, by conducting various ONLINE events among the students selected through a screening test held on January 18, 2022. Five students were awarded the Aruna Lal scholarship selected through the personal interview held in ONLINE mode. In NSD-2022, around 569 students appeared in the ONLINE screening test. In total, 154 students were selected to participate in various events organized by PRL. Invitations to other students who gave the ONLINE screening test were sent to join the event, and also the NSD 2022 celebrations were live streamed on PRL's YouTube channel, which more than 500 viewers viewed. Twelve prizes for poster/model competition were given to the students. The winners presented their models/posters on "Indian Science @75 and way beyond" on February 26, 2022, via ONLINE mode.

Vikram Sarabhai Jayanti in PRL Campuses

Garlanding of the Dr. Vikram Sarabhai's statue by his family.

To celebrate the 102nd birth anniversary of Prof. Vikram Sarabhai, father of the Indian space Programme and founder of PRL, a function was organized in his remembrance at all campuses of PRL. Garlanding and tree plantation in the presence of family members

of Sarabhai and other dignitaries from Ahmedabad and Gandhinagar was done on Thursday, August 12, 2021.

The function started with garlanding by Sarabhai family members along with the dignitaries invited and other members of PRL. Owing to Covid-19 restrictions and keeping all the prevailing Covid guidelines, PRL staff were invited to attend the function in the open area. Live streaming of the function was arranged. Anecdotes were shared related to Prof. Vikram Sarabhai and his passion for the development of society through space science. Thereafter, a tree plantation drive at all PRL campuses was organised. The retirees, new joinees including students participated in the function with great zeal. PRLs moto this time in conjunction with Prof. Vikram Sarabhais birth anniversary celebration was to plant double the number of trees which were destroyed during the Tauktae cyclone.

Independence Day Celebration in PRL

The 75^{th} Independence Day of India, which coincides with the 75th anniversary of the establishment of the Physical Research Laboratory, was celebrated with great zeal and enthusiasm. The flag hoisting was done by Dr. Anil Bhardwaj, Director, PRL. The ceremony courtyard echoed with festive fervor, with the National Anthem recitation by one and all present. The Director PRL inspected the parade by the Central Industrial Security Force appointed in PRL. On this auspicious day of celebration of Independence Day, the Director, PRL, in his address to the audience, remembered the sacrifices of brave martyrs, paid tribute to them and discussed the institute's activities in the scientific field and related subjects. To attract the interest of the young minds in Science and Scientific Research, the Director PRL launched a welfare scheme named "Vikram A. Sarabhai Protsahan Yojana Vikas." This is a scholarship for class 9 and 10 students of Gujarat state. In this scheme, the scholarship will be given to 10 students, out of which fifty percent will be especially for girl students. A distinctive Logo marking India's Independence and PRL's institution was launched as a series of the Platinum Jubilee celebration year.

Independence Day-15 August 2021: celebrations at PRL campuses.

This was followed by merit and service awards to CISF Cadets and PRL Employees who have completed 25 years of services in PRL, respectively.

On Independence Day, every mind present in the ceremony arises and communicates a feeling of patriotism. PRL Staff member, on this occasion, conducted a cultural program. The Director, PRL, gave away merit awards to the children of staff members for securing the highest marks in Hindi in classes X and XII. Other prizes related to Official Language were also announced and distributed.

Trees and plants are the fundamental life support of living beings. To make this a sustainable resource, a tree plantation program was also organized on our office premises. Small children and their parents and guardians participated in this campaign. After this, as per tradition in PRL, every year, tricolor balloons were released by the small children to mark this day of Independence. This signifies peace for the country and the Earth, the prosperity and greenness of our Department and Institute.

An Evening in PRL

To celebrate Independence Day and 75^{th} year of PRL, a unique program, 'an evening in PRL,' was organized on August 15, 2021. PRL Main campus was beautifully illuminated with lights. On this evening, family members of PRL employees were allowed to visit the otherwise restricted Campus. The families were encouraged to take a card ride inside the Campus on a designated path. They were also allowed to take a walk if they preferred. During the trip, they were fervently welcomed by the PRL Director. He interacted with almost all the families and employees with great zeal and inquired about their experiences and views. The whole program lasted for almost 5 hours. For the families and colleagues who could not attend the program in person, the program was also telecasted live on YouTube. Special care was taken to follow the Covid appropriate behavior during the program.

Independence Day-15 August 2021: Glimpses of "An Evening in PRL".

Vibrant Gujarat Summit 2022

Dr Amzad H Laskar actively participated in ICAI, Vibrant Gujarat summit exhibition held during 5-6 January, 2022 at Science City Ahmedabad. PRLs scientific achievements, research activities were

presented and various opportunities for students and researcher was advertised in the summit.

GSDN Poster presented by Mr. A. Shivam in PRL's stall at ICAI exhibition on 5-6 January, 2022 at Science City Ground, Ahmedabad.

Dr. K. Venkatesh participated in the summit held at Science city, Ahmedabad, 5-6 Jan, 2022

29th National Children's Science Congress (NCSC-2021)

Mr. A. Shivam participated in the Virtual stall of PRL in (NCSC-2021) organised by GUJCOST during 15th-18th February, 2022.

PRL AMS Laboratory visit

Students of Astronomy Club, IIT- Gandhinagar visited PRL AMS Laboratory on 21st March 2022.

Gujarat Council on Science & Technology (GUJCOST)

Dr. Arvind Singh, was invited as a panellist on the special outreach program on Nobel Prize 2021 on 10 December 2021 by GUJCOST at Gandhingar.

SADBHAVANA DIWAS

As per the Government of India Department of Space directive, August 20 the birth anniversary of Late Shri Rajiv Gandhi is observed as 'SADBHAVANA DIWAS' to promote national integration and communal harmony among people of all religions, languages, and regions. In PRL, Staff members observed the Sadbhavana Diwas at one's workplace on Friday, August 19, 2021, following the COVID appropriate behaviour.

Fire Safety & Security

Fire safety awareness is essential to fire safety risks in any workspace/organization. Fire prevention planning & training for all staff members/ students/human resources available at various Campuses of PRL thus is an important aspect and should be periodically taken care of. In this connection, the following activities were conducted by PRL in coordination with CISF in August 2021:

(i) Special PRL@75 Lecture on Fire Safety through ONLINE MODE

(ii) PRL@75 Live Demo on Fire Safety in at both PRL campuses in Ahmedabad.

Two hundred forty participants attended an online lecture on Fire Safety, including 40 contractual staff (at all campuses, i.e., PRL Main & Thaltej Campus, MIRO and USOOB) who attended a live telecast, at a common place, at respective campuses. Close to 300 participants attended the demo comprising all PRL campuses. The cooperation and coordination of the CISF team are acknowledged on records. The Fire Safety demonstration was conducted in an interactive and well-participated manner by PRL staff members.

Vigilance Awareness week 2021

Based on the Circular of Central Vigilance Commission (CVC) dated 01.09.2021and endorsement of DOS thereon dated 16.09.2021, the Vigilance Awareness Week (VAW) 2021 was observed in PRL from 26$_{th}$ October 2021 to 01$_{st}$ November 2021. All the staff Members of PRL took Integrity Pledge at their respective work places on 26.10.2021. Apart from Integrity Pledge, all staff members were encouraged to take Integrity E-pledge in CVC portal (https://pledge.cvc.nic.in). A total of 86 PRL Staff have taken E-pledge for which online Certificates are downloadable from CVC portal. The theme of the VAW-2021 was "Independent India@75: Self Reliance with Integrity". An online lecture was also conducted on the subject "Independent India@75: Self Reliance with Integrity". The invited speaker was Shri Pawan Srivastava, IPS and Director, Central Academy of Police Training, Bhopal. This lecture, elaborated the evolution of Indian economy from pre-independence era to till date, how corruption is impacting our economy and remedial measures to combat corruption.

An online quiz on the occasion of VAW-2021 was also conducted on 29.10.2021 in which 36 PRLites had participated. The winners of this quiz were felicitated with a certificate and cash prize during the Republic Day celebration on 26.01.2022.

150TH BIRTH ANIVERSARY OF MAHATMA GANDHI

The 150th Birth Anniversary of India's Father of the nation, Mahatma Gandhi, was celebrated amidst Covid-19 Pandemic restrictions in PRL. On this auspicious occasion, by following all COVID-19 prevention guidelines at the workplace, the Director, PRL, Registrar PRL, Chair, PPEG, Heads of various Divisions, and other staff members have offered their remembrance and paid floral tribute to Mahatma by offering prayers and a minute silence. Further, to commemorate his 150th birth anniversary, a specific area in the Auditorium foyer was dedicated to the Mahatma, where a photograph and his autobiography in English/Hindi and Charaka were kept as a permanent display. Mahatma Gandhi's principles of truth, non-violence, and love pave the way for the welfare of society and the world at large by bringing equality and harmony. In commemoration, an online Quiz Competition was organized on Monday, 05 October 2021.

National Unity Day

The National Unity Day was observed in PRL on October 31, 2021, and PRL members undertook the National Unity Day Pledge at their workplace on this day.

Constitution Day

November 26, 2021, was observed as Constitution Day in PRL. On this occasion, staff members read the "Preamble" to the Constitution at their respective workplaces.

Republic Day @ PRL

The 73rd Republic Day was celebrated on January 26, 2022, at the PRL Thaltej campus with great zeal, following COVID-19 protocols. The PRL director hoisted the national flag, followed by the national anthem. Further, the Director briefed about the activities, achievements, honors, etc., acquired by PRL and appraised the work done by the PRL members for weeding out old records. The merit awards were given to the CISF Cadets, and Service awards were presented to the PRL Employees who have completed 25 years

of service in PRL. Rajbhasha Shikshan Yojna-related prizes were announced. The winners of the Online Quiz organized on Vishwa Hindi Diwas were also awarded.

Republic Day-26 January 2022: Glimpses of celebrations at PRL."

Swachhta Pakhwada @ PRL

As mandated by the Department of Space/GoI, Swachhta Pakhwada was celebrated during February 01-18, 2022 (extended by a week) at all the campuses and the Residential Colonies of PRL. The theme for Pakhwada was Health and Sanitisation. PRL urged all members to give particular focus and demonstrate real work on weeding out old records and eradicating plastic uses. The Pakhwada activity started with Mass Pledge duly following Covid -19 protocols. Swachhta Pakhwada Committee (SwPC) organized various activities and events in which PRL members enthusiastically participated. Weeding out of Record and Cleanliness Drives were organized on various schedules at all four campuses, focusing mainly on picking up the plastic materials. To attract public participation, awareness rallies and cleanliness drives were conducted outside the PRL office campus at Ahmedabad. PRL had arranged awareness lectures and cleanliness drives at the campuses, including residential colonies. To make Pakhwada Activity more participative for the staff members, an online quiz, essay competition (extended to family members), and skit competitions were announced. The Closing Ceremony was arranged at PRL Thaltej Campus, at an open venue. The Closing ceremony started with National Song sung by Cultural activity team member.

Volleyball Tournament

After a gap of two years, PRL resumed its sports activities with the annual volleyball tournament. The tournament was organized under the banner of Azadi Ka Amrit Mahotsav.

Scientific Tour to Statue of Unity

Due to the Covid-19 pandemic, welfare activities were almost suspended due to safety aspects. As a part of staff welfare measures, a Scientific Tour to the Statue of Unity was conducted under the Staff Welfare Committee of PRL. PRL Staff Members, Students, Post Doctoral Fellows, other Scientific personnel, and Trainees have joined a one-day tour to the Statue of Unity and Sardar Sarovar Dam. About 196 members have participated in the tour.

Inter-Area PRL Football Tournament for the year 2021-22

An Inter-area Football tournament was organised as a part of Azadi ka Amrit Mahotsav (AKAM) celebrations. There was a total of 6 teams divided into two groups. Group A had 1) AMOPH, 2) Theory Admin Services (TAS), and 3) PSDN; Group B had 1) Astronomy, 2) SPASC and 3) GSDN. Each team in a group played each other once, and the top two went to the semi-finals. The tournament was inaugurated by Director PRL on 24 March 2022.

Activities by the Internal Complaints Committee:

A Special PRL@75 online Lecture on "Sexual harassment of women at work place" by Ms. Sowmya Bhatt was organized by ICC and Women-cell on Tuesday, August 24 2021. More than 250 PRL staff and students attended it. The talk brought clarity to the many grey areas associated with sexual harassment at workplace. It was very well received and appreciated. To commemorate the 8th anniversary of notification of the landmark legislation of Sexual Harassment of Women at Workplace (Prevention, Prohibition & Redressal) Act, 2013, ICC-PRL organized an online talk on December 9 2021 on the topic' Workplace Sexual Harassment : The Present scenario' by Dr. Jharna Pathak, Secretary, AWAG, Ahmedabad. More than 100 PRL staff and students attended the talk. The speaker gave examples of various situations and case studies which brought clarity several aspects related with sexual harassment at workplace. It was well received especially by the new entrants Research Fellows and staff of PRL.

Celebration of Ambedkar Jayanti at PRL Due to increased number of COVID-19 cases in Gujarat, Dr. B. R. Ambedkar Jayanthi was not celebrated during April 2021 in PRL.

Capacity Building Programmes

Student Conference on Optics and Photonics (SCOP-2021)

The sixth edition of the Student Conference on Optics and Photonics (SCOP) was organized during 24-26 November, 2021 by the OPTICA (previously OSA) Student Chapter of PRL. The PRL-OPTICA student chapter has been organizing this annual conference since 2016. SCOP-2021 focussed on recent research and advancements in the numerous fields of optics, including Ultrafast Spectroscopy and Molecular Dynamics, Quantum optics and Quantum Information, Nonlinear Optics and Structured beams, Quantum Metrology, and Sensing. Furthermore, SCOP-2021 has included researchers from the interdisciplinary fields actively using light. This 3-day conference had thirty-three invited speakers, including nineteen faculty and fourteen students. Among the nineteen invited dignitaries, twelve speakers were from nine countries spanning three continents (Asia, Europe, and America) and seven from India. The conference had 129 registered participatnts, making SCOP-2021 a mega International student conference.

Venus Science Conference 2021

As a part of PRL's Platinum Jubilee celebration, the Planetary Science Division of PRL organised a two day online meeting "Venus Science Conference 2021" during 23-24 September 2021. It focused on modelling, observations, data analysis, and scientific experiments for Venus exploration. The major research areas covered in the conference were surface, atmosphere, clouds, GCM, lightning, airglow, habitability, chemistry, ionosphere, interplanetary dust, IMF, and solar wind interaction with the planet. Such gathering provided an opportunity to interact among the community over the globe and also, collaborate with people working in similar fields over a period of time. About 150 delegates from National and International Institutes attended the Conference. There were six sessions covering research areas like Global Geological Mapping, Surface Emissivity, VAMAN Project, Atmosphere Dynamics and Turbulence, Oxygen Airglow, Venusian Lightning, Sulphur Chemistry, Habitability of Clouds, Venus GCM, Results from Akatsuki Radio Science Experiment, Ionospheric Layers, Venusian Plasma Environment, Interplanetary Dust Towards Venus and BepiColombo flyby Results. There were about 60 talks including short presentations and the discussions covered a wide spectrum of topics. Participation for this conference was from eminent universities/institutes from India covering NISER, SAC, PRL, NARL, SPL, IISER, IIRS, IITB, IPR, IIST, BMSIS, MSU and IIGM. Also, there were several contributions from countries like the US, Germany, Australia, France, UK, Japan, Sweden, Norway, Taiwan and Russia.

Frontiers in Geosciences Research Conference (FGRC-2021)

Geosciences Division of PRL organized its first annual Frontiers in Geosciences Research Conference FGRC-2021 during 27- 28 September 2021 in online mode. The objectives of the conference were to highlight the recent advances in understanding various Earth System processes and their linkages through new studies and results. Besides, the other primary aim of this conference was to create a long-term platform for geoscientists of India to jointly address scientific and societal issues and increase collaborative research among researchers from various institutes/universities in India. The conference was divided into four broad scientific themes: (i) Solid Earth and Earth Surface Processes, (ii) Marine and Terrestrial Biogeochemistry, (iii) Paleoclimate and Isotope Hydrology and (iv) Aerosols, Air Quality and Ocean-Atmosphere Coupling. The penultimate session of the conference was a career guidance program. This session was primarily aimed at highlighting various challenges faced in research and opportunities available in India and abroad to MSc/MTech and PhD students, postdocs and early career researchers.

In total, 193 participants registered for the conference, and 100 scientific papers were presented as plenary/invited talks, contributory talks and poster/flash talks. With the success of the inaugural FGRC-2021, we look forward to the next version of the conference on a larger scale.

Meteoroids, Meteors and Meteorites - Messengers from Space (MetMeSS, 21)

As a part of PRL's Platinum Jubilee celebration, the Planetary Science Division of PRL organized a two-day online meeting "Meteoroids, Meteors and Meteorites - Messengers from Space" during 29-30th November 2021. The symposium was aimed at bringing prominent scientists to present their latest results that have advanced our understanding of the solar system formation and evolution. The scientific themes covered were Stardusts & Starbits, Chondrites & Micrometeorites: Events and Processes, Journey to Differentiated Worlds, Surface processing of planetary bodies, Atmosphere and Meteors, Impact Shocking and Shattering, Planetary Analogue: Similar Environment of Dissimilar World!

About 127 delegates from national and international institutes attended the conference. There were about 50 talks presented by scientists from universities/institutes within and out of India (PRL, St. Xavier's college, Tokyo institute of technology, Punjab University, IIT-Kharagpur, NIO-Goa, GSI, University of Bern Switzerland,, Florida State university, IISc, SSRI, IIT-Roorkee, SPPU-Pune, SPL, NIT-Calicut, University of Kerala, University of Allahabad, IIST, University of Lucknow, Presidency University, BMSIS Seattle, Washington).

PRL conference in Condensed Matter Physics 2021 (PRL CCMP-2021)

PRL conference in Condensed Matter Physics is biennial conference in current topics in Condensed Matter Physics and related areas. PRL CCMP-2021 was held online from 16-18 August, 2021. The topics included strongly correlated systems, topological Condensed Matter Physics, cold quantum gases, transport coefficient in QGP, color superconductivity, and magnetized quark matter. MSc. / Ph. D. students, Postdocs, and researchers participated in good numbers.

Twenty-One Invited talks and ten posters were presented in the conference.

Astrochemistry Early Career Talks at PRL

PRL has started the Astrochemistry Early Career Researchers Webinar series since April 2021. Early career researchers (PhD and PDF) working in research areas related to astrochemistry/astrobiology around the world present their work in this webinar. A total of 14 talks have been conducted till now.

First Indian Space Weather Conference (ISWC-2022)

The First Indian Space Weather Conference (ISWC-2022), was hosted by PRL during 11-12 January 2022 via online mode as a part of the Platinum Jubilee celebrations of PRL. The aim of this conference was to bring together the researchers of the nation who are working in different domains of solar, terrestrial, and planetary research. With several ISRO's space programs, like Aditya-L1, DISHA, and Venus missions being planned for scientific investigations of the atmospheres of the Sun, the Earth, and planets in the near future, this conference is intended to bring together the scientific community and garner momentum.

Highly encouraging response has been received with 62 abstracts submitted and over 180 registrations. More than 50% of abstracts and registrations are from universities and institutions other than DOS/ISRO. Also, more than 50% of the participants are below 35 years of age, which signifies the interest of young scientists in pursuing space weather research.

The scientific sessions were scheduled with three major topics which include, Space weather drivers and processes; Impact of space weather on the Earth's magnetosphere, ionosphere, and thermosphere; and Space and ground instruments for space weather research. Each session is divided into focused sub sub-sessions to convene dedicated discussion on individual themes. Various science themes deliberated on in the ISWC are: Solar cycle studies, Space weather forecasting models, Source regions of solar disturbances, Simulations of solar transients, Response of the magnetosphere to solar forcing, Space weather impact on the ionosphere-thermosphere system of planets, Space weather modeling studies, and instruments for space weather research.

At the end of day 2, a concluding session was conducted to summarize the scientific sessions, to get feedback and to deliberate on the way forward. All the SOC members and participants appreciated the initiative of conducting the ISWC, saying that a dedicated conference focusing on space weather science and applications is the need of the hour. Several important suggestions were given on the way forward. Early career scientist awards were given to two presenters who submitted their thesis and five presenters who are currently pursuing their thesis.

3rd Indian Planetary Science Conference (IPSC-2022) organised online by PRL

The 3rd Indian Planetary Science Conference (IPSC-2022) was organised by PRL during 14-16 March, 2022 in a fully virtual mode due to COVID restrictions, on the Webex platform. The conference included sessions under the following themes: Lunar science; the atmospheres, geology and surface processes of terrestrial planets; meteorites; small bodies; exoplanets; astrochemistry and astrobiology. Papers on modelling studies, remote sensing, instrumentation and in-situ observations using planetary missions, planetary analogues and laboratory studies were invited and presented.

The conference was inaugurated online by Shri. S. Somanath (Secretary, DOS & Chairman, ISRO). The opening address was delivered by Shri. A.S. Kiran Kumar (Chairman, Apex Science Board and Chairman, PRL Council of Management). Prof. Anil Bhardwaj, Director, PRL welcomed the delegates, while Prof. Varun Sheel, Convenor (IPSC-2022), provided an overview of the conference.

We had a very good response to the call for abstracts, with 280 registrations, out of which 50% of were from outside ISRO centers. In total, 116 presentations were made, out of which 92 were oral, spread over 2.5 days and over 6 sessions. In IPSC-2022, we accommodated large number of oral presentations for young researchers, divided into 10 minutes and 5 minutes categories. The highlights of each poster were given by the presenter, through a small 2-minute video, at the end of each session. Each technical session was supported by a team of moderators to oversee the smooth execution and transition of talks during that session. Early career research awards were presented, for the best oral presentation in each session, and for two best poster presentations.

The 12th CSSTEAP Post Graduate Course on Space and Atmospheric Science (01 October 2021 30 June 2022)

The 12th Post Graduate Course on Space and Atmospheric Science (SAS-12), organized by CSSTEAP (Centre for Space Science and Technology Education in Asia and the Pacific, affiliated to the United Nations) and hosted by Physical Research Laboratory, started online immediately after a combined Inaugural function of CSSTEAP courses was held at CSSTEAP Headquarters on 01 October 2021 through a virtual platform. There were 12 participants: 7 from India, and 1 each from Bangladesh, Ethiopia, Mongolia, Nepal and Uzbekistan. Given the Covid-19 pandemic, all lectures were presented in online mode only. The course was spread over two semesters. Faculty members included eminent Scientists/Engineers from PRL and other Institutions in India. A total of 360 lecture hours were devoted to explain various aspects of space and atmospheric science. Additionally, 19 practicals and several student seminars were conducted and graded. All exams were held online.

Visit of CSSTEAP participants to Udaipur Solar Observatory.

RESPOND Programme

Physical Research Laboratory (PRL) administers the Indian Space Research Organization (ISRO) RESPOND to provide funding to academia in India for conducting research and development activities related to Space Science, particularly in the fields of Astronomy and Astrophysics, the Physics of Earths atmosphere/ionosphere, Planetary Sciences, Solar Physics, Space Weather, Space Plasma Physics and Astrochemistry. The main aim of the RESPOND programme is to encourage quality research in areas of relevance to the Indian space programme. Through this programme, the proposers seek funding for research, augmenting computational facilities; occasionally the RESPOND grant is also utilised to set up a new laboratory facility for research at the University or Institute. The main deliverables of the RESPOND programme at PRL have been publication of research papers in international and national refereed journals, PhD theses of associated Research Fellows and training of scientists. In the year 2021, four RESPOND basket proposals were approved for funding from a total of 43 proposals received. The number of ongoing RESPOND projects is presently 15.

In March 2022, PRL brought out a RESPOND BASKET comprising of a good number of urgent and important research topics highlighting the major research programmes of PRL. The Basket proposal documents were released by Shri Somanath S., Chairman ISRO on March 15, 2022 on ISRO Academia Day and are available on link;

`https://www.isro.gov.in/sites/default/files/respond_basket_2022.pdf`

In total, 20 basket proposals have been offered by PRL scientists this year to the potential proposers to select and prepare detailed proposals under RESPOND BASKET programme.

In summary, the RESPOND programme of PRL has been very successful in training scientists in different parts of the country in various aspects and problems pertaining to Space Sciences and developing research infrastructure across the country.

Training, courses by PRL staff

DST sponsored training programme

D. Pallamraju: Managing Technology Value Chains for Directors & Division Heads, during October 25-29, 2021, conducted via online platform from Administrative Staff College of India (ASCI), Hyderabad.

ISRO-RESPOND projects

D. Chakrabarty: Focal point/Co-PI two ISRO-RESPOND projects

Centre for Space Science and Technology Education in Asia and the Pacific (CSSTEAP), 2021

D. Chakrabarty: As member, Board of Studies, contributed in formulating the Space and Atmospheric Science Course.

Administrative Staff College of India (ASCI) training programme

Lokesh Kumar Sahu: "Science Administration, Research Management for Scientists", (sponsored by Department of Science & Technology, Government of India, New Delhi) during 13-24 December, 2021.

The CSSTEAP Short Course on Use of Space Technology for Weather and Climate Studies

Lokesh Kumar Sahu: held at Space Applications Centre, ISRO Ahmedabad during 17-31 May 2021.

12^{th} course on Space and Atmospheric Science

Amitava Guharay: Delivered 2 lectures on "Dynamics of Earth's atmosphere", on 22nd and 23rd November 2021 conducted by PRL-Ahmedabad under the auspices of CSSTEAP, affiliated to the United Nations.

12^{th} course on Space and Atmospheric Science

Amitava Guharay: Instructed 2 practical sessions on 14-15, February 2022 conducted by PRL-Ahmedabad under the auspices of CSSTEAP, affiliated to the United Nations.

12^{th} PG course in space and atmospheric sciences, CSSTEAP

K. Venkatesh: Taught two practicals to the students.

Scientific and Technical Staff

1. Bhushit Vaishnav, Two-days workshop (online) "Best Practices & Procedures from Invention Disclosure to Patent Grant", organized by the Capacity Building Programme Office (CBPO), ISRO Headquarters, 29-30 July 2021.
2. Shibu K Mathew, First Science meeting on Solar Orbiter/Polarimetric and Helioseismic Imager (SO/PHI), Max-Planck institute of Solar System Research, Gottingen, Germany, 27 September - 02 August, 2021.
3. Aseem Jaini, Isro Induction Training Programme (IITP)-33, Online, 01-12 September, 2021.
4. Nimma Vinitha, Isro Induction Training Programme (IITP)-33, Online, 01-12 September, 2021.
5. Cherukuri Sree Vaishnava, Isro Induction Training Programme (IITP)-33, Online, 01-12 September, 2021.
6. Mohit Kumar Soni, Isro Induction Training Programme (IITP)-33, Online, 01-12 September, 2021.
7. Shreya Natrajan, Isro Induction Training Programme (IITP)-33, Online, 01-12 September, 2021.
8. Rashmi, Isro Induction Training Programme (IITP)-33, Online, 01-12 September, 2021.
9. Srishti Sharma, Two days training program on "Secure Coding", ISRO/DOS, 02-03 September, 2021.
10. Prashant Jangid, Two days training program on "Secure Coding", ISRO/DOS, 02-03 September, 2021.
11. Sonam Jiterwal, Internet of Things (IOT) for Women Scientists, Technologists, Engineers (Women Component), DST, 25-29 October, 2021.

12. Pratheeksha Nayak, Internet of Things (IOT) for Women Scientists, Technologists, Engineers (Women Component), DST, 25-29 October, 2021.
13. Bireddy Remya, Online Training Programme on General Management Programme for Women Scientists (Sponsored by Department of Science and Technology, Government of India, New Delhi), Administrative Staff College of India, Hyderabad, 06-17 December, 2021.
14. Shiv Kumar Goyal, Faculty Development Programme on Control and Automation, IIST, Thiruvananthapuram, 14-17 December, 2021.
15. Arpit Patel, Faculty Development Programme on Control and Automation, IIST, Thiruvananthapuram, 14-17 December, 2021.
16. Chandan Kumar, Faculty Development Programme on Control and Automation, IIST, Thiruvananthapuram, 14-17 December, 2021.
17. Aaditya Sarda, Faculty Development Programme on Control and Automation, IIST, Thiruvananthapuram, 14-17 December, 2021.
18. Pankaj Kumar Kushwaha, Faculty Development Programme on Control and Automation, IIST, Thiruvananthapuram, 14-17 December, 2021.
19. Swetapuspa Soumyashree, Community Resource Management (Women Components) sponsored by DST, Indian Institute of Forest Management, Bhopal, 21-25 February, 2022.
20. Pratheeksha Nayak, Community Resource Management (Women Components) sponsored by DST, Indian Institute of Forest Management, Bhopal, 21-25 February, 2022.
21. Nirbhay Kumar Upadhyay, Online Awareness Webinar series on “Aerospace Mateials and Applications” with special emphasis on Space Materials, Shiv Nadar University, Greater Noida, 25-27 February, 2022.
22. Neeraj Kumar Tiwari, Online Awareness Webinar series on “Aerospace Mateials and Applications” with special emphasis on Space Materials, Shiv Nadar University, Greater Noida, 25-27 February, 2022.
23. Peddireddy Kalyana Srinivasa Reddy, Online Awareness Webinar series on “Aerospace Mateials and Applications” with special emphasis on Space Materials, Shiv Nadar University, Greater Noida, 25-27 February, 2022.
24. Abhishek J Verma, Online Awareness Webinar series on “Aerospace Mateials and Applications” with special emphasis on Space Materials, Shiv Nadar University, Greater Noida, 25-27 February, 2022.
25. Ankita Patel, MDP on Environmental Leadership and Life Skills (Women Component) sponsored by DST, Indian Institute of Forest Management, Bhopal, 07-11 March, 2022.
26. Nimma Vinitha, MDP on Environmental Leadership and Life Skills (Women Component) sponsored by DST, Indian Institute of Forest Management, Bhopal, 07-11 March, 2022.
27. Amitava Guharay, DST sponsored “Training on Geospatial Technologies for Disaster Mitigation”, Motilal Nehru National Institute of Technology (MNNIT), Allahbad, 21-25 March, 2022.
28. Rishitosh K Sinha, DST sponsored “Training on InSAR: Theory, Processing and Application”, MNNIT, Allahabad, 27-31 March, 2022.
29. Rajiv Ranjan Bharti, DST sponsored “Training on InSAR: Theory, Processing and Application”, MNNIT, Allahbad, 27-31 March, 2022.

Administrative Staff

1. Hemal D Shah, Public Procurement (Advanced), Arun Jaitley National Institute of Financial Management (AJNIFM), Faridabad (Online), 10-12 May 2021.
2. Sunil D Hansrajani, Public Procurement (Advanced), Arun Jaitley National Institute of Financial Management (AJNIFM), Faridabad (Online), 10-12 May 2021.
3. Mantu Meher, Public Procurement (Advanced), Arun Jaitley National Institute of Financial Management (AJNIFM), Faridabad (Online), 10-12 May 2021.
4. Saba Abbasi, Public Procurement (Basic), Arun Jaitley National Institute of Financial Management (AJNIFM), Faridabad (Online), 17-20 May 2021.
5. Abhishke, Public Procurement (Basic), Arun Jaitley National Institute of Financial Management (AJNIFM), Faridabad (Online), 14-17 June 2021.
6. R K Jaroli, Public Procurement (Basic), Arun Jaitley National Institute of Financial Management (AJNIFM), Faridabad (Online), 14-17 June 2021.
7. Rashmi Ranjan, Public Procurement (Advanced), Arun Jaitley National Institute of Financial Management (AJNIFM), Faridabad (Online), 28-30 June 2021.
8. T S Neethu, Public Procurement (Advanced), Arun Jaitley National Institute of Financial Management (AJNIFM), Faridabad (Online), 28-30 June 2021.
9. Razaahmed Maniar M, Public Procurement (Advanced), Arun Jaitley National Institute of Financial Management (AJNIFM), Faridabad (Online), 28-30 June 2021.
10. Abhishek, RTI CPIO/Appellate Authorities, National Productivity Council, Jaipur (Online), 19-20 July, 2021.
11. Samir V Dani, Online Training for Doctors for Management of COVID-19 in Children, Directorate General of Health Services, Ministry of Family Welfare, 30 July, 2021.
12. Shital H Patel, Online Training for Doctors for Management of COVID-19 in Children, Directorate General of Health Services, Ministry of Family Welfare, 30 July, 2021.
13. Jyoti Limbat, Reservation in services for SC/ST/OBC, ISTM (Online), 02-05 August, 2021.
14. Megha Upendra Bhatt, Workshop on Prevention of Sexual Harassment of Women at Workplace, Institute of Secretariat Training And Management, 15-16 November, 2021.

Official Language promotion at PRL

Rajbhasha Activities in Physical Research Laboratory

Owing to Covid -19 situations, the world is getting accustomed to the new normal as evident in the ensuing time. Now that people have learnt to live with new normal, all are putting best efforts to transform the situation towards an era of new learning and new health etiquettes to fight the pandemic crisis. All categories of people have learnt to adapt the survival strategy and day-to-day work in a hybrid mode at being - online/offline. The off-and-on nature of the virus has compelled the work force to evolve and generate hybrid platforms so that the world and human existence does not come to a standstill once again. The Physical Research Laboratory (PRL), being one of the premier Research Institute, has maintained the outreach to different strata of work force and common people. This breeze of enthusiasm is maintained in the innovative ways of promotion Official Language activities too. Some of the illustrious points in this context are as follows:

Physical Research Laboratory (PRL) has received **"Second prize"** for best implementation of Official Language Policy of Government of India during 2020-21 at Town Official Language Implementation Committee (TOLIC) level. In the meeting of TOLIC, Dr. Anil Bhardwaj, Director, Physical Research Laboratory, was presented with a Trophy and citation by Dr. Ravindra Kumar, Chair, TOLIC, Ahmedabad.

Smt. Rumkee Dutta, Assistant Director (O.L.), PRL was also presented with a Trophy and a citation from Chair, TOLIC, Ahmedabad.

Dr. Anil Bhardwaj, Director, Physical Research Laboratory (PRL) receiving the Trophy and citation from the hands of Dr. Ravinder Kumar, Chair, TOLIC.

As per the Official Language Policies and Rules, to ensure smooth implementation and promotion of Official Language. The meetings of the Official Language Implementation Committee (OLIC) were held regularly in every quarter chaired by Director, PRL, Dr. Anil Bhardwaj, Chairman OLIC, PRL. A stock of progressive usage of Official language and its implementation were taken in these meetings. The decisions on policy related to implementation, promotion and progress in PRL, as a whole was reviewed. Keeping in view the safety protocols of the pandemic, all these meetings, were conducted through online mode.

The members of the various Scientific Divisions and Administrative Sections of PRL campuses were involved in organizing Hindi Pakhwada for promotion of Rajbhasha in all campuses of PRL viz. PRL Ahmedabad, Main campus, Thaltej Campus, Mount Abu Infrared Observatory and Udaipur Solar Observatory. This year Hindi Pakhwada was celebrated during 14-28 September 2021 and Hindi Pakhwada programs/competitions were mostly organized online. The theme of 75 years of India's independence was also included in the Hindi Pakhwada, programs/competitions. Before the commencement of Hindi Pakhwada, an appeal was put forth by Director, PRL to all staff members, to do maximum official work in Hindi. As per the directives of Ministry of Home affairs, Rajbhasha Pratigya was also administered.

Various programs were organized by the Hindi Pakhwada Committee and special emphasis was given to plan programs in such manner that irrespective of language barriers, PRL members could participate in these competitions at optimum. The Inaugural program of Hindi Pakhwada was done on 14 September,2021 via online mode. In this program, Prof. Devesh Kumar Sinha, Director, Delhi School of Climate Change and Sustainability (DSCCS), Delhi University was present as the Chief Guest. He delivered a very lucid and informative lecture in Hindi on the topic "Climate Change". In the Inaugural Program, Prof. D. Pallamraju, Dean, PRL addressed PRL fraternity. The entire program was streamed live on Youtube.

Events organized during Hindi Pakhwada:-

On 14^{th} September, 2021 Hindi Newspaper Reading Competition was organized for auxiliary staff members. All the 06 members enthusiastically participated in the competition.

Extempore competition was organized on 16^{th} September, 2021. In this competition, the participants were given various indicative pictures to select and on the basis of the picture, they had to speak in the given time, giving a suitable title to the speech. 23 members participated in this competition. The online speech competition was also telecast live and 53 viewers joined the telecast.

On Tuesday, 21^{st} September, 2021 - Hamara Prabhag- on the progress from foundation till now was organized with new flavour. It was program which presented splendid poster presentation of evolution of PRL in both Science & Administration. In this, various scientific/technical/administrative areas were to show case the development of their respective division in Hindi. One member from every Division/Section was nominated by the Head of the Division, to present the poster and to answer various question from the judges and the audiences during the Q&A session.

A total of 13 posters from different scientific/technical/administrative areas were presented. The competition was held offline at PRL Auditorium foyer duly following all Covid-19 safety guidelines. The enthusiasm for this competition was observed among the members and the posters were designed in a very informative, captivating manner.

Popular Word Quiz Competition was organized on 21st September, 2021. It included Hindi meaning of words and its usage in sentences, synonyms and antonyms and general knowledge. This competition was organized by forming groups of different Areas/Sections. 9 teams were formed this year and each team had five members. The competition was conducted offline with a limited number of spectators and participants. The contest was live streamed through Blue Jeans. There were 45 participants and 89 spectators who were encouraging the teams by joining online. An audience round was a quite lucrative addition and enjoyed by spectators with enthusiasm.

Hindi Poem Competition was organized on 28th September, 2021. This competition was organized for the members of PRL. In this, opportunity is given to recite/sing, self-created/written songs and poems written in Hindi. Poems/songs have to be given apriory to the Hindi Section for scrutiny. Only approved poetry/songs are allowed to be presented without use of any background visual/instrument music/visuals.

This year an innovative Skit competition was organized. The members of all the Division/Sections made video presentations of plays giving meaningful societal messages on various contemporary topics. All the participants and videos received in this competition were presented as a complete program in the presences of Senior Faculty members including Director, Dean, Chair, PPEG and other Senior officials. After a long time, people got an opportunity to get together and come out of the negative impact of Covid19 circumstances. This program received unprecedented appreciation. All the members displayed their excellent artistic talent. Prizes for first, Second and third place in each competition category was declared along with consolation and incentive prizes for Pakhwada competitions. The prize distribution ceremony was graced by Director, PRL and other senior authorities.

Glimpses of various programs of Hindi Pakhwada.

Winners of Hindi Incentive Scheme for doing Original Work in Hindi

Sr.No.	Name	Prize
1.	Shri Hemal D. Shah	First
2.	Shri Abhishek	Second
3.	Smt. Nandini Rao	Second
4.	Shri Shashikant	Second
5.	Sushri Jayashree Balan Iyer	Second
6.	Ms Jyoti Limbat	Third
7.	Shri Bhagirath K. Kuntar	Third
8.	Shri Ashish G. Sawadkar	Third
9.	Shri Suraj Kumar	Third
10.	Shri Kartik M. Patel	Third
11.	Smt. Richa P. Kumar	Third
12.	Smt. Harsha Parmar	Third
13.	Smt. Sneha Nair	Third
14.	Smt. Saba Abbasi	Third
15.	Shri Rajendra K. Patel	Consolation

Hindi workshops were organized in every quarter promoting implementation of Rajbhasha. In these Workshops members of different sections/divisions are nominated by turn. The focus of such training programme is to encourage to do official work in Hindi. A total of 5 workshops were organized in four quarters which are as follows:-

Smt. Rumkee Dutta, Assistant Director (OL) delivered talk in Workshop on 27 July 2021 and 20 December 2021. The topics were Official language Rules and day-to-day work, various check points to be monitored by higher authorities, Incentive Schemes related to Hindi, Compilation of Hindi quarterly progress report.

On 9thSeptember 2021, Shri Pradeep Kumar Sharma, Senior Administrative Officer, PRL delivered talk on the subject 'Hindi Noting and Drafting'.

Shri Abhishek, Administrative Officer, USO, spoke on the different administrative subjects on 23rdNovember 2021 and facilities available for doing work in Hindi during.

On 11thFebruary 2022, Smt. Neelu Seth, Deputy Director (OL), SAC, delivered talk in Workshop on the different Rules of Official Language and their monitoring criteria, various incentive programs etc.

The Departmental Inspection related to progressive use of Hindi of all campuses of PRL was conducted at different points of time. On 28thDecember 2021, PRL Main Campus, Ahmedabad inspection was conducted by Director, OMPR, ISRO Headquarters. The Departmental inspection of Mount Abu was conducted by the Controller, URSC on 31stDecember 2021. On 03rdMarch 2022 Udaipur Solar Observatory was inspected by Deputy Secretary, Department of Space.

According to the instructions of the Department of Space, the wards of PRL Staff members, who have secured the highest marks in Hindi subject in CBSE/ICSE and State board in class XII and X board examinations of the year 2021, were given Merit Awards.

In the field of scientific writing, meetings of the Original Book Writing in Hindi Committee was organized so that all the members of the Institute can be imparted guidance for writing original scientific book in Hindi.

Two e-versions of Hindi Patrika "Vikram" was released on 15th August 2021 and 31st March 2022 respectively. Dr. Anil Bhardwaj, Director, PRL, and Dr. Som Kumar Sharma, Patrika Editor, addressed about different topics covered in Patrika. The members of Editorial Board were present and it was a moment of immense pride for PRL Family.

Release of e-version of Hindi Patrika "Vikram".

A Hindi Competition (Online) "Chitra Varnan" was organized by PRL, Ahmedabad, on behalf of TOLIC on June 25, 2021. 37 nominations were received from the Central Government Offices of Ahmedabad. 35 members participated. Smt. Sneha Nair and Sushri Prachi Prajapati from PRL have received prizes in this competition.

In a Technical write-up competition organized in April 2021 by Hindustan Oil Corporation, Ahmedabad at Town Official Language Implementation Committee level, Shri Vaibhav Dixit won second prize and Shri Hitendra Mishra won consolation prizes.

Ms. Sourita Saha working as a Scientist/Engineer 'SC' at Physical Research Laboratory (PRL), Ahmedabad presented a technical paper for the Annual Seminar in Hindi: ANSH-2021, organized by CSIR-National Aerospace Laboratories, Bengaluru, during 20-21 May 2021.

In a competition "Apni Hindi Parkhein" organized by SAC, at Town Official language Implementation Committee level, on 30thNovember 2021, Smt. Harsha Parmar won Second prize.

Techincal/ Scientific talk given in Hindi

Jayesh P. Pabari "Shukra grah par antargrahiya dhul ka adhyayan", Inter Centre Technical Hindi Seminar, VSSC, Thiruvananthapuram, 10-02-2022

Facilities and Services

Computational Services Group

The Computational Services Group (CSG) is responsible for providing services/facilities like Networking (Internet, Local Area Network, Wifi, SPACENET), High performance Computing, E-mail, Web, DNS, Proxy, VPN, Centralized Printing, DHCP, Video Conference, EGPS, COWAA/COINS, software development and maintenance. Apart from this, Computational Services Group members have actively participated in ISRO/DOS level various Cyber Security Vulnerability Assessment & Penetration Testing (VAPT) activities. Following services/facilities are provided during the year 2021-2022.

[A] Participation in Hindi Language Promotion Activities:

Computer Services Group has enthusiastically participated in PRLs Hamara Prabhag Poster Pratiyogita of 2021-22. The main theme was to show case the Division activity in last 75 years of PRL. Computer Services Group won third prize in this competition for below poster.

Figure: Hamara Prabhag Poster Pratiyogita

[B] Implementation of New E-procurement System:

The CSG team has successfully implemented New EGPS system at PRL in coordination with VSSC team. The setup opened for users in August 2021.

[C] National Science Day (NSD) 2022:

In continuation of successful execution of NSD-2022 examination completely in online mode, there was again request to conduct NSD-2022 in online mode. To cater the need, the Computational Services Group Members have customized and fine tuned the open source software to conduct the NSD-2022 exam in completely online mode. Total 569 students from 137 schools had participated in the online examination. The examination went very well and without any technical glitch.

[D] Vulnerability Assessment & Penetration Testing:

Computational Services Group has actively participated & contributed in ISRO/DOS wide Vulnerability Assessment & Penetration Testing (VAPT) activities carried out during 2021-2022. Especially, the contribution of CSG team members was appreciated by Director, DISM, ISRO, for “Cyber Radar” VAPT activity.

[E] Cyber Security:

During the year 2021-2022, to protect PRL IT Infrastructure from cyber attacks/threats, the Computational Services Group members have taken suitable cyber security measures based on the advisory received from Computer Emergency Response Team (CERT-In), National Critical Information Infrastructure Protection Centre (NCIIPC) and ISRO. The Information Security Officer (ISO) and CSG team members also spreads cyber security awareness through online talk, allusers email.

[F] Data Networks and Services:

1. **PRL’s Main File Server to preparation in Virtual architecture** Migrated PRLs physical Central/Main File Server to virtual server environment using latest software packages of OpenSSL, Postfix and Dovecot and successfully migrated all users data and mail boxes to this new server without any data loss. This has increased overall availability and reliability of the Main file server.
2. **Live Streaming of PRL Events to Internet or LAN Network.** The CSG team members have successfully coordinated and managed live streaming of various events like Independence Day Celebrations, First Car-Ride Visit to PRL Main campus, Republic Day Celebrations, Fire Safety and PRL @75 event with USO campus.
3. **Local Area Network (LAN) expansion activities** PETC-Startup Laboratory and Free-space Quantum Communications Laboratory cabins in New building Terrace area of Thaltej campus are equipped with PRL structured LAN connectivity as per their scientific experiment requirements.

4. **ISRO/DOS Network SPACENET** SPACENET is a Close User Group (CUG) network of DOS/ISRO Centers/Units. This network is used for accessing Intranet of other DOS/ISRO Centers/Units. This secure SPACENET Network access connectivity has been extended to Thaltej new Building Payload Operation Centre (POC) area.
5. **Upgradation of PRLs VMware software suits** Upgraded PRLs VMware Replication software, Site Recovery manager (SRM) and core software components like VMware vSphere and vCentre Server to latest stable version in both PRLs primary (DC) Server Virtualization site and Disaster Recovery (DR) site by preserving all running services and virtual machines data.

[G] Software Development and Management:

The CSG members are also developing and managing various software like CoWAA/COINS, Sandesh, Intranet Web Services, CHSS software etc. During the year 2021-2022, newly developed software like Online CL/Addl. CL management, Online Canteen Booking, e-PPO etc. were made available for allusers.

[H] Vikram 100 High Performance Computing Cluster:

Vikram100 100TF High Performance Computing (HPC) facility is extensively used by PRL Scientific & Technical fraternity. During April 01, 2021 to March 31, 2022 period 28 Scientific Papers have been published in reputed Scientific Journals where Vikram100 facility has been acknowledged. In total, 132 Scientific Papers have been published since June 2015.

Library & Information Services

Library and Information Services play an important role in catering to the information needs of the PRL researchers and staff, these information services are being provided in all the campuses of PRL. To name a few important ones, documents (books, journals, CDs) lending services, Online Access (intranet and through remote access) to Institutional Repository, E-journals, Theses, E-books, Archives, Technical Reports, etc. Library also provides the Interlibrary loan facility, Plagiarism Check facility through the Ithenticate tool, Reprographic facility, Information display through Digital Notice Board, and Book procurement for research scholars using their academic allowance. The updates and additions to the library during the year 2021-22 are mentioned below:

Statistics

In the year 2021-22, there has been an addition of 93 Scientific, 15 General, and 49 Hindi books to the collections of three libraries in Main, Thaltej, and USO campuses. 978 visitors visited the library. 749 documents were issued, and the users returned 1045 documents to the library. The Library provides Inter Library Loan (ILL) service for its users and other Institutes. 50 ILL requests were fulfilled by PRL and 21 articles were sought from other institutes. The reprographic service of the library is high in demand where the library facilitated photocopies in-house along with 1507 photocopies from the outside agency. 552 e-books are available in the library, and 214 journals are accessible to the users.

Library Online Resources

PRL Library continues to have access to full-text databases like GSA Archive, PROLA, Science Archive, Proquest Dissertation and Theses (PQDT). The library has access to Nature.com, Springer Journals, Elsevier Journals and Wiley Journals in addition to SPIE and IEEE Digital Library through Antakriksh Gyaan which is an ISRO Library Consortium.

Plagiarism Check Facility

The library is responsible for carrying out the similarity check for students using the Ithenticate tool. They avail of this facility before submitting the thesis; users also get their manuscript checked for originality before submitting for publication in various journals

Digital Notice Board

The library maintains it to disseminate information about PRL activities like division seminars, colloquia, public talks, and images of events like Republic Day, Womens Day, etc. In addition, a list of recent publications of PRL scientists and new books added to the library collection is also displayed in 3 campuses simultaneously through the LAN. Mt. Abu campus will be linked soon

Institutional Repository

The Institutional repository maintained by the Library consists of journal articles published by the PRL authors from 1990 to the present and is also linked through the Library homepage. About 4300 articles by PRL authors are now part of this repository. All the PRL theses from 1952 onwards (449) are now available in full text for PRL users. All the Technical Notes since 1977, published by PRL, have been digitized (114) and are available in full text. Currently, Library is carrying out the digitization of the photographs archive. Giving the captions and metadata for each photograph for easy retrieval is in the process using the digital library software Greenstone Digital Library (GSDL).

Library homepage

Library's new website is functional and provides a seamless facility of online resources and information to the patrons of the library

Figure 1: Library Homepge.

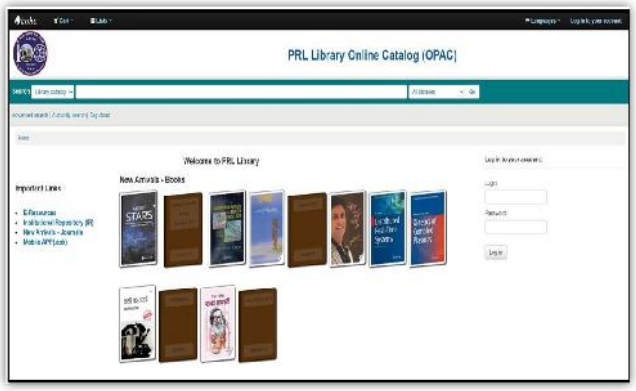

Figure no 2: Library OPAC.

Evolution of the Library Services at PRL

As a part of 75th foundation year of PRL, a poster competition was organized during the Hindi Pakhwada event and library and information services won the first prize. This poster showcases the journey of Library and Information Services in PRL for seven long decades. It is a documentation of how this division has supported the research at PRL since its inception.

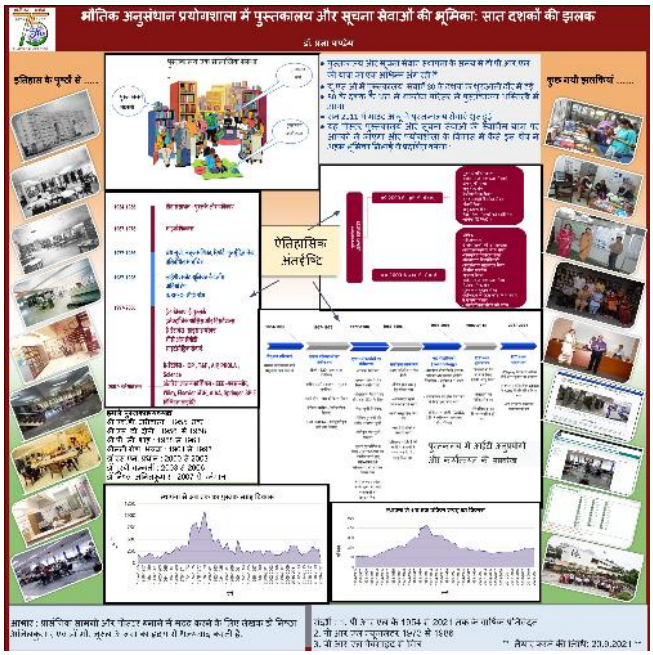

Figure 3: Library Poster

PRL-Workshop

PRL's mechanical workshop has been actively working with various groups in the PRL. The workshop is engaged in the design optimization, fabrication and testing of various mechanical subsystems of several ongoing developments projects in the laboratory. The PRL workshop facilities in Navrangpura and Thaltej campuses are with several state-of-the-art machines for the manufacturing of mechanical parts, e.g., Vertical Machining Centre (VMC850 & VMC 640), Wire Cut Electrical Discharge machine, Electrical Discharge Machine (EDM), CNC turning centre (DX 200), Turn Mill Center (nvu 200) etc. In the academic year 2021-2022, the workshop has made significant contributions in the development of back-end instruments of Mt. Abu observatory as well as development of various subsystems and setups for a number of scientific payloads for upcoming missions. In addition, the workshop continues to cater number of specific requirements of several R&D laboratories in PRL by closely working with the members of the different Projects/Groups to develop specialized experimental setups. The workshop also continue to support various operational activities of laboratories and facilities in PRL. Some of the major projects undertaken by the workshop during this year are briefly described below.

Activities related to the Mt. Abu observatory:

Back-end instruments for the 2.5 m telescope:

Fabrication work related to developing three backend instruments, namely, PARAS-2, Speckle imaging and CCD Imager for the 2.5m telescope, were undertaken at the workshop. More than 300 unique components have been fabricated for these backend instruments. Work has also been done on developing various experimental setups for these instruments.

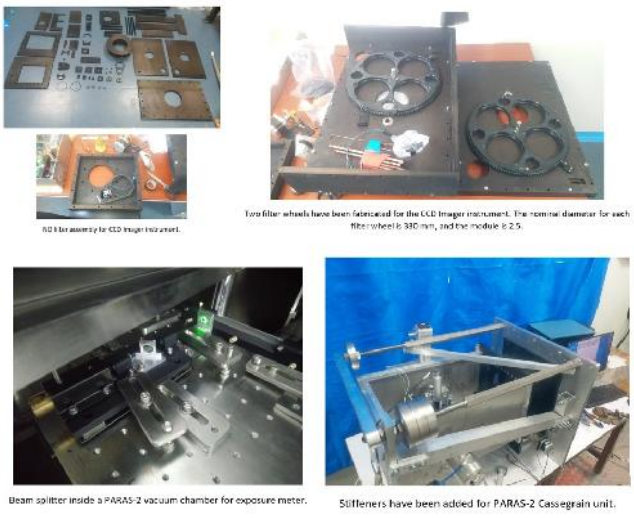

Figure 1: Few Components for CCD Imager, speckle imaging and PARAS2 instruments

CCD Imager will be the first light Instrument for the upcoming PRL 2.5m telescope. It comprises of a 4k X 4k CCD with a set of UGRIZ filters used for photometry in UGRIZ bands. The Instrument will be attached to the main port of the 2.5m telescope. The Instrument has 87 Opto-electro-mechanical components and all parts are machined on the VMC machine. The total weight of the Instrument is approximately 400 kg. Two filter wheels of about 360 mm diameter have been realized for mounting the filters. Each filter wheel is controlled by a separate gear assembly and stepper motor using Arduino base ccontroller. Provision has also been kept for carrying out photometry with neutral density filter, controlled by SG-90 servo motor. Few Components for CCD Imager, speckle imaging and PARAS2 instruments are shown in Figure 1.

PARAS-2 CCD Focal Unit with Spectrum Lamp assembly

Calibration lamps are the light source which are used in astronomical spectrographs for their wavelength calibration. Argon and krypton lamps are used for the calibration of the low resolution spectrograph in the visible wavelength range. Collimator lens is used to produce the beam of parallel rays. Assembly was fabricated to determine the characteristics of argon lamp and krypton lamp. Dedicated mount for the argon/krypton lamp has been fabricated. 30mm diameter lens has been used as a collimator. Holder assembly for collimator has also been fabricated, which was attached to the lamp mount. This assembly was used with PARAS-2 spectrograph for taking the spectra of the argon and krypton lamps. The fabrication was carried out at Thaltej workshop using the VMC-640, CNC turning centre and wire-cut EDM machine tools. A few components fabricated for the CCD Focal Unit with Spectrum Lamp assembly are shown in Figure 2.

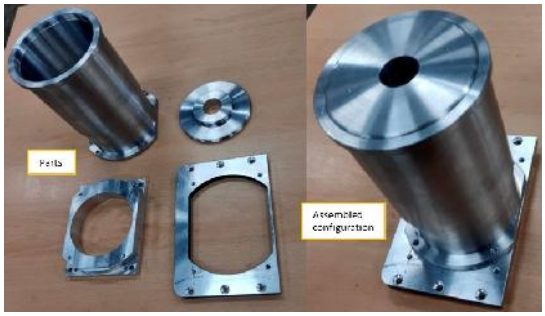

Figure 2 : Parts and Assembly configuration of CCD Focal Unit with Spectrum Lamp

Proto-Pol for 1.2/2.5 meter Telescope

This instrument is prototype version towards realization of M-FOCS-EP instrument for the 2.5 m telescope. The sub-assemblies of the instrument was fabricated at the Thaltej workshop, with high accuracy of linear and angular position. The fabrication of these subassembly components utilized the range of CNC turning, VMC-640, wire-cut EDM, conventional lathe and drill machine tools. The subassemblies like Echelle unit, camera and detector unit, parabolic mirror unit are shown in Figure 3.

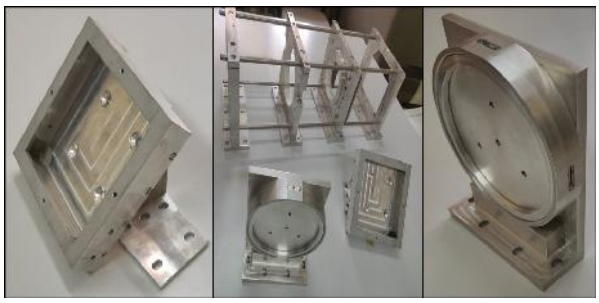

Figure3 :Subassemblies of Proto-Pol instrument for 1.2/2.5 metre telescope

Encoder wheel assembly for 1.2 meter Telescope instrumentation

The 1.2 metre telescope uses encoder for controlling the dome position for the given celestial target. The encoder is a part of the feedback system for this purpose. The encoder currently in use is more than 25 years old and hence a standby system was required to be tested and qualified. This necessitated the fabrication of the encoder wheel assembly for 1.2 metre Telescope. The components of this assembly, as shown in Figure 4, were fabricated at Thaltej workshop facility. The bigger wheel shown in the figure, is in contact with dome motion and provides feedback through encoder. The machine tools used were CNC turning centre DX-200, VMC-640 and EDM wire cut. The bearing mating surfaces were made with controlled tolerances and surface finish to end up in excellent bearing fitting. The positioning accuracy of the shafts location were maintained as per drawing specifications.

Figure 4: Encoder wheel assembly for 1.2 meter Telescope

Activities related to the development of payloads for future missions::

PRATHIMA Probe:

Permittivity and Thermophysical Instrument for Moons Aquatic scout (PRATHIMA) payload, for LUPEX mission of ISRO & JAXA, is a selected payload on-board rover.

Figure 5: PRATHIMA Probe Lab Models

The objective of this payload is to detect water-ice in the lunar surface using dielectric permittivity measurements. The probe has overall length of 150 mm and diameter of 25mm and is made using copper and Teflon material. The laboratory model was fabricated at the Thaltej

workshop. The copper transmitter and receiver were made in close fit with the cylindrical structure of the probe. The Teflon material base cylindrical structure were fabricated with precision turning while taking care of lateral deflection. The two assembled probes are shown in Figure 5.

PRATHIMA probe deployment set up

The PRATHIMA payload is one of the selecteds payload on-board rover for the LUPEX mission of ISRO & JAXA. In the proposal phase, it was envisaged to have a mechanism to lower down the probe to insert into the lunar regolith. For this purpose, a baseline configuration of vertical probe drilling mechanism for was designed. This mechanism is used for simulating the lowering of the PRATHIMA probe from LUPEX rover. Thaltej workshop fabricated the mechanism from aluminium and brass material using different machines like lathe, VMC, wire cut etc., which is shown in Figure 6. The mechanism was successfully demonstrated by the user team.

Figre 6: PRATHIMA probe deployment set up

Wien filter and Faraday cup for ASPEX payload of ADITYA L1 mission

Two sub-assemblies namely: Wien filter sub-assembly and faraday cup sub-assembly for the ASPEX payload testing were fabricated at Thaltej workshop. The fabrication of these subassembly components utilized the range of CNC turning, VMC-640, wire-cut EDM, conventional lathe and drill machine tools.

The Wien filter fabricated in-house is being used as a mass filter in the SWIS-ASPEX payload calibration set-up at Thermo-vac lab, Thaltej. It comprises of mutually orthogonal electrostatic and magnetic field allowing only a limited particle velocity to pass through. An electric field is applied on the two copper plates where Teflon spacers are used to provide necessary isolation. A pair of magnets is placed in orthogonal direction to the electric field. A fine aperture of 1mm at entrance and exit define the ion beam path. The Wien filter was tested independently with ion gun and the performance was satisfactory.

The Faraday Cup and mounting setup developed in-house is being used for flux measurement of Ion Gun in the SWIS-ASPEX payload calibration set-up at Thermo-vac lab, Thaltej. It comprises of 45 degree bend mounting arm made of aluminium to support and rotate Faraday Cup. Faraday Cup fabricated from copper, whereas Delrin spacers are used to provide necessary isolation between mounting arm and Faraday Cup. An enclosure of fine aperture of 1mm at entrance of Faraday cup was assembled to define entrance aperture to Faraday Cup. Complete setup was integrated with chamber, performance was evaluated and found satisfactory. It is now integrated with the calibration set-up for final tests of flight model packages.

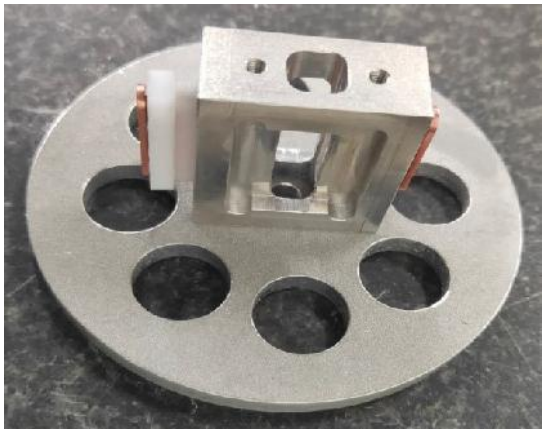

Figure 7 : Wien filter sub-assembly

Figure 8: Faraday cup sub-assembly

3. Other Developmental Activities for Various Divisions:

Scissor Table Jack for NIRIS Instrument

NIRIS (Deep Infrared Imaging Spectrograph) is a large FOV (80 degrees) grating spectrograph and provides spectra in the 823 - 894 nm wavelength range. It is commissioned in the Optical Aeronomy Observatory at Mt. Abu. The instrument weighing about 250 kg needs to be lifted to an appropriate position in the observatory dome, which is achieved by a lifting mechanism known as a Scissor Table. This table was designed and developed in the workshop and was transported to the observatory. It is assembled using a base frame, top frame, lead screw & nut and multiple link elements joined by screw joints. The table allows both horizontal and vertical movement as per requirement and can be locked any position. Figure 9 shows some images of the scissor table.

Fig:1 Minimum Position

Fig2:Maximum position

Fig3: Mechanism with NIRIS Mounted over it.

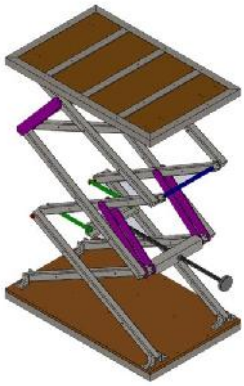

Fig: 4 Design of Scissor Table for NIRIS

Figure 9 : Different Images of Scissor Table for NIRIS

Design of Multiwavelength Imaging Spectrograph Using Echelle Grating (MISE)

MISE (Multiwavelength Imaging Spectrograph using Echelle Grating) is a high spectral resolution with a large field-of-view (FOV; 140 degrees) instrument that is capable of retrieving faint dayglow emissions at Multiwavelength (OI 557.7, 630.0, and 777.4 nm) that are buried in the strong solar scattered background continuum.

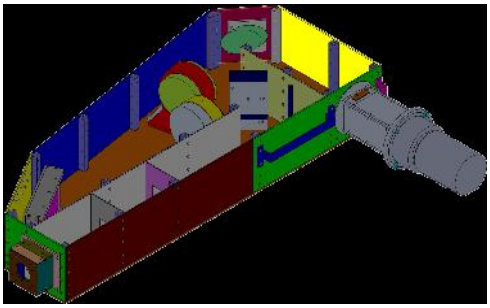

Figure10: Multiwavelength Imaging Spectrograph Using Echelle Grating (MISE)

The Design of MISE instrument having Lens of 1200 mm focal length is being completed in PRL-Workshop. The overall dimensions of the MISE instrument are 1180 mm x 500 mm x 500 mm. Total three such MISE assemblies are planned be deployed in different geographical locations across the country. The complete assembly involves total 124 parts, out of which 118 parts will be manufactured in PRL-Workshop, whereas 6 parts will be procured off the shelf. Machining of many of these parts is already completed on VMC machine. MISE hardware will be assembled with the optics for testing and operation in the near future.

Linear Actuator for SIMPEX lab and Photonics Lab.

Two type of linear stage assembly were developed and fabricated by Thaltej workshop for a) SIMPEX lab and b) Photonics lab instrumentation purposes, using precision components, for lab experiments which are show in fig. No-13 & 14 respectively. The Mars Environment Chamber (MEC) Facility of SIMPEX lab, PSDN consists of a vacuum chamber (height: 35cm diameter: 33cm) for simulation of Martian environment which is in development phase. The facility is currently utilized for reflectance spectroscopy. A manipulator (shown in fig. 11) is used in this facility for 2 axis motion of spectrometer probes. The screw used in this mechanism is having pitch of 1 mm which enables 2.78 micron movement for 1° of rotation.

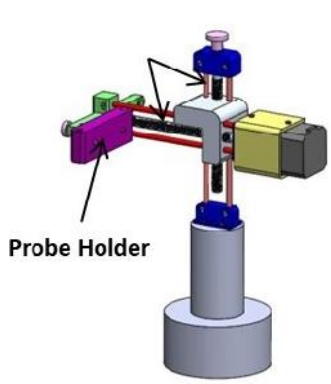

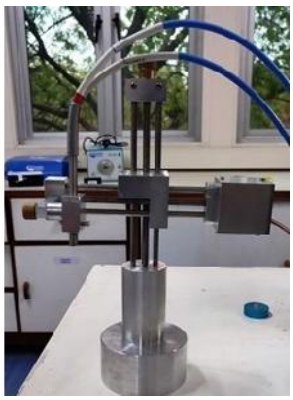

Figure 11: Assembled linear stage for Mars Environment Chamber (MEC) Facility

A 2-axis linear stage was designed and developed by Thaltej workshop, for the Photonics lab at Thaltej campus (shown in fig. No-14). This manipulator is used in the lab for 2 axis alignment of the optical elements mounted over it. The screw used in this mechanism is having pitch of 1 mm which enables 2.78 micron movement for 1° of rotation.

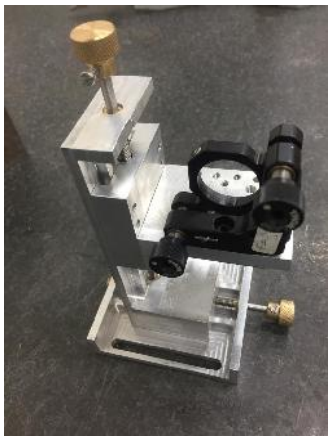

Figure 12: Assembled linear stage for optical elements

EPS (Entangled Photon Source)

The Entangled Photon Source (EPS) is used in the field of secure quantum communication for the quantum key distribution (QKD). Various source assemblies for accurate component placements were fabricated in the Teltej workshop for the EPS as shown in Figures 13, 14. The fabrication of these subassembly components utilized the range of CNC turning, VMC-640, wire-cut EDM, conventional lathe and drill machine tools.

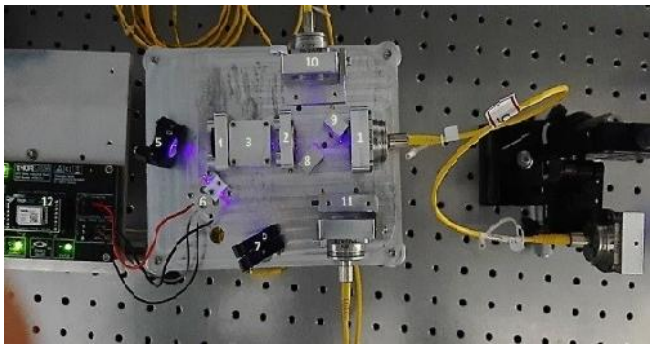

Figure 13 : Components for Entangled Photon Source in assembled condition

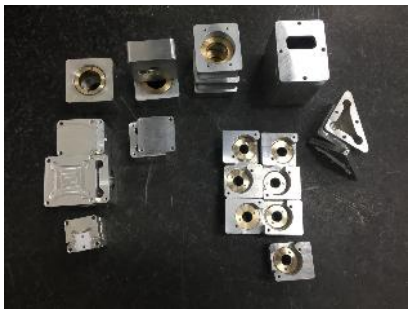

Figure 14: Components for Entangled Photon Source

In-House Development of Trophy for Sports Event at PRL

For the football tournament organized under AKAM (Azadi Ka Amrit Mahotsav), thaltej workshop team designed and realized the Football trophy. This trophy has provision of changing the winners name strip, so that same trophy may serve the similar requirement for years. The trophy design considers a combination of aesthetics and ergonomics. This trophy fabrication utilized the CNC machines available. The surfaces generated were polishing to mirror finish, so that the post anodising surface would-be of excellent surface finish. Anodizing and laser marking processes were outsourced. It is shown in Figure 15.

Figure 15: PRL Football championship trophy

Other Support Activities:

The PRL workshop also engaged in several support activities for various R & D laboratories of PRL, some which are mentioned below.

(a) Fabrication of M. S. Structure for the compressor of the Femto-Second Laser laboratory

(b) Fabrication of Porta Cabins for Ceilometer instruments for the ISRO-IBP project

(c) Design and replacement of a damaged source gun Tube HV cable shield for the AMS laboratory.

(d) Design and fabrication of customizable sample holder

(e) Design and fabrication of Aluminum casing for F.P. (Fabry Perot) and Filter Temperature controller

(f) Design & Fabrication of Gimbal Assembly for Sun photometer

Honorary Fellows & Faculty

Honorary Fellows

A. Hewish (Deceased September 2021)
K. Kasturirangan

Honorary Faculty

A. K. Singhvi
FNA, FASc, FNASc, FTWAS
DST Year of Science Chair Professor

DPK Banerjee
CSIR Emeritus Scientist

J. N. Goswami
FNA, FASc, FNASc, FTWAS
INSA Senior Scientist

S. A. Haider
FNA, FASc, FNASc, & J.C.Bose Fellow

M. M. Sarin
FNA, FASc, FNASc
DST-SERB-Distinguished Fellowship.

Shyam Lal
FNA, FASc, FNASc
INSA Senior Scientist

S.D. Rindani
FNASc & INSA Senior Scientist

P. Janardhan
FNA, INSA Senior Scientist

PRL Staff

Sr. No.	Name	Designation	Specialization	Division	Highest Degree Obtained
1	A B Shah	Sci./Eng.-SG	Automation, Robotics, Payload Development & FPGA	A&A	B.E. (1984)
2	A D Shukla	Asso. Professor	Geochemistry & Cosmochemistry	GSDN	PhD (2012)
3	A K Sudheer	Sci./Eng.-SF	Chemistry of Atmospheric Aerosol & Biogeochemistry	GSDN	PhD (2018)
4	A. Shivam	Sci./Eng.-SD	Electronics and Accelerator Mass Spectrometry	GSDN	M.Tech. (2018)
5	Aaditya Sarda	Sci./Eng.-SD	Design & Development of Space Based Instruments	SPASC	B.Tech. (2015)
6	Abhijit Chakraborty Chair, A&A	Professor	Astronomy, Exoplanets, Optical Instrumentation, Stellar High Resolution Spectroscopy	A&A	PhD (1999)
7	Abhishek	Admin. Officer	General Administration	USO	PGDIP (2009)
8	Abhishek J Verma	Sci./Eng.-SC	Mechanical design of payloads, Lab. reflectance spectroscopy, UHV Vacuum experimets	PSDN	B.E. (2016)
9	Abhishek Prasad	Assistant	Administration	ADMGN	B.Sc. (2013)
10	Adalja Hiteshkumar Lavjibhai	Sci./Eng.-SE	Mechanical and thermal design of space and ground based instruments	A&A	M.Tech. (2009)
11	Akash Ganguly	Sci./Eng.-SD	Machine Learning, Groundwater / Climate Change, Numerical Modelling and Instrumentation	GSDN	B.E. (2017)
12	Alka Singh	Sci./Eng.-SC	Hardware and Software Design and development, Embedded Systems	A&A	B.E. (2015)
13	Alok Shrivastava	Sci./Eng.-SD	Cyber Security, System Administration, Networking	COMSR	M.Sc. (1998)
14	Aman K Khatri	Sci./Eng.-SC	Civil Engineering	CMDV	B.E. (2017)
15	Amee K Patel	Sr. Proj. Assistant	Purchase and Accounts	ADMAC	M.B.A. (2011)
16	Amit Basu Sarbadhikari	Asso. Professor	Planetary Geochemistry	PSDN	PhD (2007)
17	Amitava Guharay	Asso. Professor	Atmospheric Waves, Middle Atmospheric Dynamics	SPASC	PhD (2010)
18	Amogh Auknoor	Sci./Eng.-SC	Structural Design of Space-based Payloads, Vacuum Setup & Experimentation	PSDN	B.Tech. (2017)
19	Amzad Hussain Laskar	Asst. Professor	Paleoclimate, Isotope Hydrology, Non-Traditional Stable Isotope Geochemistry, Geochronology	GSDN	PhD (2012)
20	Anand D Mehta	Head P & G A	Personnel and General Administration, Establishment	ADMGN	M.B.A. (2012)
21	Angom Dilipkumar Singh	Sr. Professor	Atomic Structure and Properties, Discrete Symmetry Violations, and Ultracold Atoms	THEPH	PhD (1998)
22	Anil Bhardwaj FNA, FASc, FNASc	Director	Planetary and Space Sciences, Solar System Exploration	ADMDIR	PhD (1992)
23	Anilkumar L Yadav	Sr. Sci. Assistant-A	Optical Instrumentation and GPS/GNSS/IRNSS For TEC Measurments	SPASC	M.Sc. (2014)
24	Anirban Ghosh	Sr. Sci. Assistant-A	Semiconductor Device, Photonics, Nonlinear Optics, Quantum Optics, Structured Optical Beams	AMOPH	M.Sc. (2016)
25	Anisha Kulhari	Sr. Sci. Assistant-A	Solar Observations	USO	M.Sc. (2016)
26	Ankala Raja Bayanna	Sci./Eng.-SF	Optical Instrumentation, Adaptive Optics, Solar Physics	USO	PhD (2015)
27	Ankita Patel	Sci./Eng.-SC	Electronics and Instrumentation	A&A	B.E. (2015)
28	Ankurkumar J Dabhi	Sr. Sci. Assistant-A	Graphitisation, Accelerator Mass Spectrometer, Radiocarbon Dating, Isotope-Ratio Mass Spectrometery	GSDN	M.Sc. (2016)
29	Arpit R Patel	Sci./Eng.-SE	FPGA based system, Hardware & Software for Space Missions	PSDN	M.E. (2010)
30	Arvind Singh	Asso. Professor	Ocean Biogeochemistry and Climate Change	GSDN	PhD (2011)
31	Arvind Singh Rajpurohit	Asst. Professor	Atmosphere of Very Low Mass Stars and Brown Dwarfs	A&A	PhD (2013)
32	Aseem Jaini	Sci./Eng.-SC	Civil Engineering	CMDV	B.Tech. (2016)
33	Ashirbad Nayak	Sci./Eng.-SC	Electronics	A&A	B.E. (2017)
34	Ashish G Sawadkar	Sr. Assistant	Hindi and Administration	ADMGN	B.A. (1999)
35	Ashish Kumar	Sci./Eng.-SC	Civil Engineering	USO	B.Tech. (2016)

Sr. No.	Name	Designation	Specialization	Division	Highest Degree Obtained
36	Atul A Manke	Sci./Eng.-SD	Software Development, Web-based application development	SPASC	M.Tech. (2013)
37	Avadh Kumar	Sci. Assistant	Noble Gase Mass spectrometery and Vacuum Setups	PSDN	M.Sc. (2018)
38	Aveek Sarkar	Asso. Professor	Magnetohydrodynamic Simulation	A&A	PhD (2005)
39	Ayisha M Ashruf	Sci./Eng.-SC	Astronomy and Astrophysics	SPASC	M.Tech. (2019)
40	B G Thakor	Sr. Proj. Attendent	Purchase attendent	ADMPR	NINTH (1991)
41	B. S. Bharath Saiguhan	Sci./Eng.-SC	Astronomy & Astrophysics	A&A	MS (Integrated) (2021)
42	B. Anne Matilda	Admin. Officer	General Administration and Accounts	ADMGN	M.Com. (1997)
43	Bankimchandra N Pandya	Technician-G	Scientific Glass Blowing	GSDN	I.T.I. (2003)
44	Bhalamurugan Sivaraman	Asso. Professor	Astrochemistry - Astrobiology	AMOPH	PhD (2009)
45	Bhupendra J Panchal	Sr.Tech.-A	Plumbing services	CMDV	M.A. (2002)
46	Bhushit G Vaishnav Head, Academic Services	Sci./Eng.-SE	Atomic & Molecular Physics, Academic Administration	ADMDN	PhD (2008)
47	Bhuwan Joshi	Asso. Professor	Solar Physics	USO	PhD (2007)
48	Bijaya Kumar Sahoo	Professor	Probing Sub-Atomic Physics, Relativistic Atomic and Molecular Many-Body Methods, Computational Physics	AMOPH	PhD (2006)
49	Binal P Umarwadia	Sr. Pharmacist-B	Pharmacy and PRL dispensary	DISSR	D.P. (1987)
50	Bireddy Ramya	Sci./Eng.-SD	Instrumentation, Programming and PCB Design	USO	M.Tech. (2019)
51	Brajesh Kumar	Asso. Professor	Solar Physics, Solar Oscillations, Solar Energetic Transients, Solar Adaptive Optics	USO	PhD (2007)
52	Chandan Kumar	Sci./Eng.-SD	Payload Development, & Space Mission Data Anlaysis	PSDN	B.Tech. (2015)
53	Chavali VRG Deekshitulu	Registrar	Accounts and General Administration	ADMRO	PGDIP (1997)
54	Cherukuri Sree Vaishnava	Sci./Eng.-SC	High Energy Astrophysics and Instrumentation	A&A	M.Sc. (2019)
55	Chithra Raghavan	Sci./Eng.-SC	Space-Based Instrumentation and Simulations For Ionospheric Studies	SPASC	M.Tech. (2019)
56	D L Kalal	Project Cook	Project Cook	ADMGN	NINTH (1986)
57	D. Pallam Raju Chair, SPASC	Dean & Sr. Professor	Space Weather, Magnetoshpere - Ionosphere -Thermosphere Coupling Processes	SPASC	PhD (1997)
58	Debabrata Banerjee	Professor	Planetary Science, Gamma Ray Spectroscopy and Luminescence Physics	PSDN	PhD (1997)
59	Debi Prasad Pradhan	Admin. Officer	General and CHSS administration	ADMGN	M.B.A. (2016)
60	Deekshya Roy Sarkar	Sci./Eng.-SD	Software and Ground Based Instrumentation	A&A	B.Tech. (2016)
61	Deepak Kumar Painkra	Sci./Eng.-SC	Electronics and Instrumentation	PSDN	B.Tech. (2018)
62	Deepak Kumar Prasad	Assistant	Accounts	ADMAC	B.Sc. (2014)
63	Dibyendu Chakrabarty	Professor	Space Weather, Ionosphere, Thermosphere, Magnetosphere, Solar Wind	SPASC	PhD (2008)
64	Dinesh Mehta	Sci./Eng.-SE	Web Development, Database and System Administration, Cyber Security, IT Security	ADMDN	M.Tech. (2013)
65	Dinesh Yadav	Sci. Assistant	Observations	A&A	M.Sc. (2018)
66	Dipak J Panchal	Sr. Assistant	Accounts	ADMAC	S.S.C (1982)
67	Dipak Kumar Panda	Sci./Eng.-SF	Nuclear Instrumentation, Planetary Science, Meteorites, Geochemistry, Isotope Geochemistry	PSDN	PhD (2019)
68	Dishendra	Sci. Assistant	Python, IoT, Blockhchains, Embedded Systems, Hardware Hacktivity	A&A	B.Sc. (2018)
69	Divyang G. Adyalkar	Sr. Nurse-B	PRL Dispensary	DISSR	D.N (2006)
70	Dwijesh Ray	Asso. Professor	Meteorites, Planetary Geology, Igneous Petrology, Geochemistry	PSDN	PhD (2009)
71	Femics George	Assistant	Accounts	ADMAC	B.Com. (2015)
72	G S Rajpurohit	Sr. Tech. Asst.-C	Mt. Abu Telescope Operations	A&A	B.Sc. (1986)
73	Garima Arora	Sr. Sci. Assistant-A	Laboratory analysis of Meteorite samples	PSDN	M.Sc. (2015)
74	Girjesh R Gupta	Asst. Professor	Solar Physics	USO	PhD (2011)

Sr. No.	Name	Designation	Specialization	Division	Highest Degree Obtained
75	Goutam K Samanta	Asso. Professor	Quantum Optics, Photonics, Nonlinear Optics, Quantum Sensing, Quantum Communication	AMOPH	PhD (2009)
76	H R Vaghela Head, Workshop	Sci./Eng.-SF	Workshop Management	WORSH	M.B.A. (2003)
77	Harish S Gadhavi	Asso. Professor	Atmospheric Aerosols, Black Carbon, Remote Sensing, Climate Change	SPASC	PhD (2006)
78	Harsh Chopra	Sr.Tech.-A	PCB preparation and USO Maintenance	USO	I.T.I. (1990)
79	Harshaben Parmar	Sr. Proj. Assistant	General Administration	ADMGN	M.B.A. (2011)
80	Hemal D Shah	Head, Pur. & Stores	Stores and Purchase administration	ADMPR	M.B.A. (2003)
81	Hiral D Modi	Sr. Assistant	Director's office administration	ADMDIR	B.Com. (2008)
82	Hiranmaya Mishra Chair, THEPH	Sr. Professor	Strong interaction under extreme conditions, Phase transitions, quark gluon plasma, relativistic hydrodynamics	THEPH	PhD (1994)
83	Hitendra Dutta Mishra	Sci./Eng.-SD	System Management, Networks and IT Security	COMSR	M.C.A (2003)
84	Hitesh C Panchal	Accounts Officer	Accounts	ADMAC	M.Com. (2012)
85	Ishita P Shah	Accounts Officer	Accounting related services and Taxation	ADMAC	CA (2011)
86	J K Jain	Sr. Tech. Assistant-C	Scientific Observations	A&A	M.Sc (2009)
87	Jayesh P Pabari	Sci./Eng.-SF	Interplanetary Dust, Planetary Lightning, Space Instrumentation and Signal/Image Processing	PSDN	PhD (2011)
88	Jacob Sebastian	Sci./Eng.-SF	Space & Atmospheric Sciences	SPASC	MTech (Integrated) (2021)
89	Jaldhi T Mehta	Sr. Assistant	General Administration of Geosciences Division	GSDN	PGDBM (2012)
90	Janmejay Kumar	Sci./Eng.-SC	Mechanical Engineering, Payload Design	PSDN	B.Tech. (2015)
91	Jappji Mehar	Sci./Eng.-SC	Simulation of Instrument Performance	PSDN	M.Tech. (2019)
92	Jayanth R.	Sci./Eng.-SC	Atomic Molecular and Optical Physics	AMOPH	MTech (Integrated) (2021)
93	Jaya Krishna Meka	Sci./Eng.-SD	CAD Design, Instrumentation and FPGA Programming	AMOPH	B.Tech. (2015)
94	Jayashree Balan Iyer	Sr. Proj. Assistant	Administration, CHSS and Visitor Management	ADMGN	B.HSc. (1993)
95	Jigar A Raval Head, Computer Centre	Sci./Eng.-SF	Cyber Security, Linux System and Network Administration, High Performance Computing	COMSR	B.E. (1999)
96	Jitender Kumar	Sr. Sci. Assistant-A	Mass spectrometric instruments	GSDN	M.Sc. (2015)
97	Jitendra Kumar Panchal	Technician-G	Electrical Maintenance	CMDV	I.T.I. (2007)
98	Jyoti Limbat	Assistant	Registrar's office Administration	ADMRO	M.Sc. (2015)
99	Jyotiranjan S. Ray	Sr. Professor	Isotope Geochemistry	GSDN	PhD (1998)
100	K J Bhavsar	Sci./Eng.-SE	Electrical Maintenance work	CMDV	B.E. (1995)
101	K R Nambiar	Sr. Pers. Secretary	Secretarial and Admin. Work	CMDV	P.U.C (1979)
102	K.K. Sasikumar	Sr. Admin. Officer	Administration, Transport, and Estate	ADMGN	M.B.A. (2014)
103	Kaila Bipinkumar	Technician-G	Operating & Programing on CNC/VMC and EDM Machines, CAD Modeling and CAM Programming	WORSH	TC (2007)
104	Kanhav Mulasi	Assistant	General Administration	ADMGN	B.Sc. (2017)
105	Kapil Kumar	Sci./Eng.-SD	Astronomical, Mechanical Structural Design	A&A	B.Tech. (2015)
106	Karanam Durga Prasad	Sci./Eng.-SE	Lunar and Planetary Surface Science, Instrumentation	PSDN	PhD (2018)
107	Kartik Patel	Admin. Officer	General Administration & Establishment	ADMGN	M.B.A. (2011)
108	Kasarla Prashanth Kumar	Sci./Eng.-SD	Opto-Mechanical System Design and Instrumentation	A&A	B.E. (2017)
109	Kavutarapu Venkatesh	Asst. Professor	Space and Atmospheric Sciences	SPASC	PhD(2013)
110	Keshav Prasad	Technical Assistant	Construction and Maintenance	CMG	B.Tech. (2018)
111	Ketan Patel	Asst. Professor	Theoretical High Energy Physics	THEPH	PhD (2012)
112	Keyur D Panchasara	Sr. Proj. Assistant	Accounts work	ADMAC	B.Com. (2003)
113	Kinsuk Acharyya	Asso. Professor	Astrochemistry and Astrobiology	PSDN	PhD (2008)
114	Kolencheri Jithendran Nikitha	Sci./Eng.-SC	Astronomy and Astrophysics	A&A	MS (Integrated) (2021)
115	Kuljeet Kaur Marhas	Professor	Isotope Cosmochemistry, Planetary Science	PSDN	PhD (2001)
116	Kuntar Bhagirathkumar K	Sr. Proj. Assistant	Admin. Work	ADMGN	M.B.A. (2010)

Sr. No.	Name	Designation	Specialization	Division	Highest Degree Obtained
117	Kushagra Upadhyay	Sci./Eng.-SC	Solar Radio Astronomy Instrumentation	USO	B.Tech. (2017)
118	Lad Kevikumar A	Sci./Eng.-SD	Instrumentation, CAD, Finite Element Analysis, Experimental and Computational Fluid Dynamics, Thin Film Coating Systems, Design and Optimization	A&A	B.E. (2017)
119	Lakhansinh G Chavda	Technician-G	Scientific Instruments, Soldering/Desoldering work	GSDN	I.T.I. (2006)
120	Lakum Yagnikkumar B	Technician-F	Electronics and IT assistance	COMSR	I.T.I. (2010)
121	Lokesh K Dewangan	Asst. Professor	Star Formation	A&A	PhD (2011)
122	Lokesh Kumar Sahu	Professor	Atmospheric Science, Trace Gases, Volatile Organic Compounds (VOCs)	SPASC	PhD (2005)
123	Lovjeet Meena	Tech. Assistant	Civil work	USO	D.C.E (2013)
124	M G Yadava	Professor	Radiocarbon Dating and Paleoclimatology	GSDN	PhD (2003)
125	Mahesh Chand Saini	Technical Assistant	Astronomy & Astrophysics	AST-AS	Dip. (2017)
126	Mahesh Gaddam	Sr. Sci. Assistant-A	Maintenance and Operation of Instruments	GSDN	M.Sc. (2013)
127	Mahesh A Raval	Sr. Lv Driver-B	Driver work	ADMGN	NINTH (1989)
128	Malaidevan P	Sci./Eng.-SD	Electronics simulation	SPASC	B.Tech. (2015)
129	Manan Shah	Sci./Eng.-SE	Development of Space and Ground Based Instruments	GSDN	M.Sc. (2016)
130	Manash Ranjan Samal	Asst. Professor	Star Formation, Star Clusters, Interstellar Medium, Young Stellar Objects	A&A	PhD (2011)
131	Maniar Razaahmed M.	Sr. Assistant	Purchase administration	ADMPR	PGDIP (2018)
132	Manisha D Patel	Sr. Nurse-B	Nursing work	DISSR	B.Sc. (2009)
133	Manisha Mishra	Sr. Proj. Assistant	Purchase and Procurement	ADMPR	M.Sc. (2011)
134	Mantu Meher	Assistant	Procurement and Purchase	ADMPR	B.Sc. (2015)
135	Md. Nurul Alam	Lib. Assistant-B	Lib. and Information Sciences	LIBSR	PhD (2017)
136	Megha U Bhatt	Reader	Planetary Remote Sensing, Visible - Infrared Spectroscopy	PSDN	PhD (2012)
137	Mistry Bhaveshkumar Vinodbhai	Technical Assistant	Astronomy & Astrophysics	AST-AS	B.E. (2021)
138	Mitesh B Bhavsar	Technician-G	Supporting Space Science Instrumentation	SPASC	I.T.I. (1998)
139	Mithun Neelakandan Ps	Sci./Eng.-SD	High Energy Astrophysics and Instrumentation	A&A	B.Tech. (2014)
140	Mohit Kumar Soni	Sci./Eng.-SC	Avionics Instrumentation (Hardware and Software), Ground Based Insturmentation, Image Processing and Deep Learning	SPASC	B.Tech. (2019)
141	Mudit Kumar Srivastava	Asso. Professor	Observational Astronomy, Development of Optical Imaging and Spectroscopy Instruments	A&A	PhD (2012)
142	Mukesh M. Saradava	Sr.Tech.-A	Mechanical components for solar instrument	USO	I.T.I. (1998)
143	N Jain	Sci./Eng.-SD	Design, Development and Coordinate Maintenance of Electrical Systems at USO	USO	AMIE (2002)
144	N S Rajput	Sr.Tech.-A	Assitance with Telescope operations	A&A	EIGHTH (1985)
145	Nafees Ahmad	Sci./Eng.-SC	Operations and Maintenance 1.2M Infrared Telescope	A&A	AMIE (2015)
146	Namit Mahajan	Professor	Theoretical High Energy Physics	THEPH	PhD (2004)
147	Nandini Ravi Rao	Pur. & Stores Officer	Purchase administration	ADMPR	B.Sc. (1991)
148	Nandita Srivastava Dy. Head (Admin)	Sr. Professor	Solar Physics, Space Weather	USO	PhD (1994)
149	Narendra Ojha	Reader	Atmospheric Chemistry, Earth System Modeling	SPASC	PhD (2014)
150	Naveen Chauhan	Asst. Professor	Luminescence Dating, Luminescence Physics, Dosimetry	AMOPH	PhD (2013)
151	Navinder Singh	Professor	Theoretical Condensed Matter Physics	THEPH	PhD (2006)
152	Neelam J S S V Prasad	Sci./Eng.-SD	Development of Telescope Back-end Instruments and Control System, Antenna Design	A&A	B.Tech. (2015)
153	Neeraj Kumar Tiwari	Sci./Eng.-SD	Mechanical and Thermal Design of Space Instruments	A&A	B.Tech. (2015)
154	Neeraj Rastogi	Asso. Professor	Atmospheric Science: Aerosol Chemistry	GSDN	PhD (2005)
155	Neeraj Srivastava	Asso. Professor	Planetary Remote Sensing, Laboratory Reflectance Spectroscopy	PSDN	PhD (2015)
156	Nileshkumar N Dodiya	Sr.Tech.-A	Carpentary Work	CMDV	S.S.C (2000)
157	Nimma Vinitha	Sci./Eng.-SC	Ultrafast Spectroscopy, Laser & Optical Instrumentation	AMOPH	M.Tech. (2019)
158	Nirbhay Upadhyay	Sci./Eng.-SE	System Engineering of Space Instrumentation	PSDN	M.Tech. (2008)
159	Nishant Singh	Sci./Eng.-SD	Design & Development of Space Based Instruments	PSDN	B.E. (2017)

Sr. No.	Name	Designation	Specialization	Division	Highest Degree Obtained
160	Nishtha Anilkumar Head, Lib.	Lib. Officer-F	Lib. & Information Services	LIBSR	PhD (2012)
161	P Narendra Babu	Sci./Eng.-SC	Electrical and Maintenance works	CMDV	B.Tech. (2013)
162	P S Patwal	Tech. Officer-C	Telescope Electrical Engineering	A&A	D.EL.E (1993)
163	P S Rajput	Sr.Tech.-A	Assistance with Telescope operations	A&A	NINTH (1983)
164	Padia Girishkumar D	Sci./Eng.-SD	Database Administration, Web Application Security Auditing, Applicationvirtualization, Linux Server Administration, Shell Scripting	COMSR	M.Tech. (2013)
165	Pankaj K Kushwaha	Sci./Eng.-SC	Electronics for Space-Borne and Ground Based Instruments	SPASC	B.Tech. (2016)
166	Paramita Dutta	Asst. Professor	Theoretical Physics	THEPH	PhD (2015)
167	Parmar Viral M	Sci./Eng.-SE	Electrical Engineering and Maintenance works	CMDV	B.E. (2002)
168	Partha Konar	Professor	Theoretical Particle Physics, High Energy Collider, Dark Matter, Neutrino, Supersymmetry, Deep Machine Learning	THEPH	PhD (2005)
169	Patel Anil S	Tech. Assistant	Electrical Maintenance	CMDV	B.E. (2015)
170	Peddireddy Kalyana Srinivasa R	Sci./Eng.-SC	Structural and Thermal Analysis of Payload Structures	PSDN	B.Tech. (2016)
171	Piyush Sharma	Sci./Eng.-SD	Electronics for Space Based Instruments	PSDN	M.Tech. (2017)
172	Pooja Chandravanshi	Sci./Eng.-SC	Quantum Communication, Data Acquisition and Automation	AMOPH	B.E. (2016)
173	Prabhaben T Chauhan	Sr. Assistant	Dispatch	ADMGN	B.A. (1999)
174	Prachi V Prajapati	Sci./Eng.-SC	NIR-Optical Instrumentation and Observations	A&A	M.S. (2019)
175	Pradeep Kumar Sharma	Sr. Admin. Officer	General Administration, CISF Matters	ADMGN	M.A. (2012)
176	Pradeep Singh Chauhan	Pur. & Stores Officer	Procurement, Contract Management	ADMPR	M.Com (2021)
177	Pradip S Suryawanshi	Sr. Sci. Assistant-A	Ground and Space Based Optical Instrumentation	SPASC	M.Sc. (2016)
178	Pragya Pandey	Library Officer-C	Information Services & Documentation	LIBSR	PhD (2019)
179	Pranav R Adhyaru	Sci./Eng.-SG	Design & Development of Electronics for Scientific Instruments	GSDN	B.E. (1991)
180	Prashant Jangid	Sci./Eng.-SD	Web Application Development, Website Development	COMSR	B.Tech. (2015)
181	Prashant Kumar	Sci./Eng.-SE	Laser Plasma Physics, Energetic Particle Mass Spectroscopy Development	AMOPH	PhD (2020)
182	Pratheeksha Nayak	Sci./Eng.-SD	Radiocarbon Dating Setups, Web Applications for Data Analysis	GSDN	B.Tech. (2017)
183	Priti K Poddar	Sr. Proj. Assistant	General Administration	ADMGN	PGDCA (1993)
184	R A Parmar	Sr. Proj. Attendent	Office attendant	ADMGN	NINTH (1988)
185	R D Deshpande Chair, GSDN	Professor	Isotope Hydrology, Hydrogeology	GSDN	PhD (2007)
186	R H Kalal	Canteen Boy-C	Canteen work	ADMGN	EIGHTH (1987)
187	R K Jaroli	Sr. Proj. Assistant	Assistance with office work at USO	USO	B.Com. (1987)
188	R P Singh Chair, AMOPH	Sr. Professor	Laser Physics, Singular Optics, Quantum Optics and Quantum	AMOPH	PhD (1994)
189	R R Mahajan	Sci./Eng.-SF	Meteorites, Noble Gas, Mass Spectrometry	PSDN	M.Tech. (1997)
190	R R Shah	Sci./Eng.-SG	Telescope Instrumentation & Control	A&A	M.B.A. (1997)
191	Rahul Pathak	Sci./Eng.-SC	Design & Development of Electronics for Ground-Based and Space-Borne Instruments	SPASC	B.Tech. (2013)
192	Rahul Sharma	Sci./Eng.-SD	Database Administration (EGPS, COWAA), Networking	COMSR	M.Sc. (2013)
193	Rajendra Kumar Patel	Sr. Lv Driver-B	Driver work	ADMGN	EIGHTH (1984)
194	Rajesh A Patel	Technician-F	Refridgeration and Air Conditioning Maintenance	CMDV	I.T.I. (2014)
195	Rajesh Kumar Kushawaha	Asst. Professor	Femtosecond/Attosecond Spectroscopy, Collision Physics, Extreme Photonics	AMOPH	PhD (2010)
196	Rajeshkumar G Kaila	Sr.Tech.-A	Operating & Programing VMC/ TMC Machine Using Mastercam Software, Lathe/ Milling Machines	WORSH	I.T.I. (1998)
197	Rajiv Ranjan Bharti	Sci./Eng.-SD	Planetary Remote Sensing	PSDN	M.Sc. (2003)
198	Rakeshkumar G Mahar	Sr.Tech.-A	Design and Fabrication of User Specific Scientific Jobs	CMDV	I.T.I. (1998)
199	Ram Lakhan Agrawal	Sci./Eng.-SD	Conventional Lathe and Milling Machines	CMDV	B.Tech. (2013)

Sr. No.	Name	Designation	Specialization	Division	Highest Degree Obtained
200	Ramitendranath Bhattacharyya	Professor	Solar Physics, Dynamics of The Solar Corona, Magnetic Reconnection, Numerical Simulation	USO	PhD (2006)
201	Rashmi	Sci./Eng.-SC	Design & Development of Space Based Instruments	PSDN	B.Tech. (2019)
202	Rashmi Ranjan	Sr. Pur. & Stores Officer	Stores Administration, Dgs&D Contract	ADMST	M.A. (2011)
203	Ravi Bhushan	Professor	Oceanography, Paleoclimate, Ocean Biogeochemistry, AMS Radiocarbon Dating	GSDN	PhD (2009)
204	Ravindra Pratap Singh	Sci./Eng.-SF	MLT Dynamics, Airglow, Atmospheric Waves, Optical/IR Instrumentation	SPASC	PhD (2018)
205	Richa Prashant Kumar	Catering Manager	Catering, Hospitality and Estate Management	ADMGN	B.Sc. (2009)
206	Rishikesh Sharma	Sr. Sci. Assistant-A	High-Resolution Spectroscopy & Photometric Data Analysis, Exoplanets, Astronomical Instrumentation	A&A	M.Sc. (2017)
207	Rishitosh Kumar Sinha	Sci./Eng.-SE	Planetary Remote Sensing of Mars and Moon	PSDN	M.Tech. (2011)
208	Rohan Eugene Louis	Asst. Professor	Solar Physics	USO	PhD (2011)
209	Rohit Meena	Sci. Assistant	Aerosol Chemistry	GSDN	M.Sc. (2018)
210	Rumkee Dutta	Asst. Director, Official Language	Hindi Cell Administration	ADMGN	M.A. (2004)
211	S Ramachandran	Sr. Professor	Aerosols, Radiation, and Chemistry-Climate Interactions	SPASC	PhD (1996)
212	S Venkataramani	Sci./Eng.-SG	Atmospheric Science, Trace Gases	SPASC	M.Sc. (1986)
213	S Vijayan	Asst. Professor	Planetary Remote Sensing	PSDN	PhD (2013)
214	Saba Abbasi	Assistant	Purchase services	ADMST	M.B.A. (2015)
215	Sachindranatha Naik	Professor	High Energy Astronomy and Astrophysics	A&A	PhD (2003)
216	Samir V Dani Head, Dispensary	Med. Officer-SF	Medical & CHSS Management	DISSR	MBBS (1993)
217	Sandeep B Manglani	Jr. Pers. Assistant	Stenography & Secretarial Work	ADMDIR	SHAND (2017)
218	Sandip H Doshi	Tech. Officer-D	Computer Maintenance	A&A	Dip. (1982)
219	Sandipkumar S Galthara	Sr.Tech.-A	Electrical Maintenance Work	CMDV	D.EL.E (2002)
220	Sangeeta Verma	Sr. Sci. Assistant-A	Geosciences, Stable Isotopes	GSDN	M.Phil. (2008)
221	Sanjay Kumar Mishra	Asst. Professor	Plasma Physics, Dusty Plasmas, Planetary Plasma Atmosphere	PSDN	PhD (2009)
222	Sanjay S Wairagade Head, CMG	Sci./Eng.-SF	Construction and Maintenance	CMDV	B.E. (1993)
223	Sanjeev Kumar	Professor	Biogeochemistry, Stable Isotopes, Climate and Environmental Change	GSDN	PhD (2006)
224	Sanjeev Kumar Mishra	Sci./Eng.-SD	Electronics Design & Development for Space-Based Applications	PSDN	B.Tech. (2016)
225	Sanket Patel	Sci. Assistant	Geosciences	GSDN	M.Sc. (2018)
226	Santosh V Vadawale	Professor	X-Ray Astronomy, Solar & Planetary X-Rays Astronomy & Instrumentation	A&A	PhD (2003)
227	Satyajit Seth	Asst. Professor	Theoretical High Energy Physics	THEPH	PhD (2014)
228	Satyendra Nath Gupta	Asst. Professor	Atomic Molecular and Optical Physics	AMOPH	PhD (2018)
229	Saurabh Suman	Jr. Pers. Assistant	Secretarial and Administrative Work	ADMDN	B.A Hons (2019)
230	Senthil Babu T.J.	Sr. Admin. Officer	Establishment & General Administration	ADMGN	B.Sc. (1995)
231	Shaileshgiri I Goswami	Technician-F	Electrical Maintenance	CMDV	I.T.I. (2013)
232	Shanmugam M	Sci./Eng.-SF	Design & Development of Space Instruments	PSDN	PhD (2017)
233	Shashank Urmalia	Sci./Eng.-SD	Mechanical Design for Ground Based and Space Instruments.	SPASC	B.E. (2014)
234	Shashi Kant	Assistant	CMG Office Assistance	CMDV	B.Sc. (2016)
235	Shashikiran Ganesh	Asso. Professor	Milky Way Galaxy, Comets, Astronomical Instrumentation, Polarimetry	A&A	PhD (2010)
236	Shashi Prabhakar	Asst. Professor	Atomic Molecular and Optical Physics	AMOPH	PhD (2015)
237	Shibu K Mathew Dy. Head (Tech)	Professor	Solar Physics, Solar Instrumentation	USO	PhD (1999)
238	Shital Hitesh Patel	Med. Officer-SF	Medical Management of Communicable and Non-Communicable Diseases	DISSR	M.D (1999)

Sr. No.	Name	Designation	Specialization	Division	Highest Degree Obtained
239	Shivansh Verma	Sci./Eng.-SC	Geosciences	GSDN	MS (Integrated) (2021)
240	Shivanshi Gupta	Sci./Eng.-SC	Atomic, Molecular and Optical Physics:	AMOPH	MS (Integrated) (2021)
241	Shiv Kumar Goyal	Sci./Eng.-SF	Planetary and Space Instrumentation for Radiation Measurements (Charged Particles, X-Rays, Gamma-Rays) and Mass Spectrometer	PSDN	M.Tech. (2019)
242	Shreeya Natrajan	Sci./Eng.-SC	Organic Studies In Meteorites, Isotope Cosmochemistry, Spectroscopic Studies	PSDN	M.Tech. (2019)
243	Shreya Mishra	Sci./Eng.-SC	Atomic Molecular and Optical Physics	AMOPH	B.Tech. (2021)
244	Shreya Pandey	Assistant	Project Accounting & Coins Compilation	ADMAC	M.Com. (2019)
245	Sneha Nair	Sr. Assistant	Administration & Office Work	SPASC	M.Sc. (2012)
246	Som Kumar Sharma	Asso. Professor	Atmospheric Dynamics, Weather and Climate, Lidar Probing of Atmosphere	SPASC	PhD (2010)
247	Somabhai N Koted	Sr. Proj. Attendent	Cleaner and assistance in Director's office	ADMDIR	FIFTH (1990)
248	Sonam Jitarwal	Sci./Eng.-SC	Design & Development of Space Based Instruments	PSDN	M.Tech. (2019)
249	Sourita Saha	Sci./Eng.-SC	Lower Atmosphere, Clouds, Boundary Layer, Ramanlidar, Ceilometer	SPASC	B.Tech. (2017)
250	Srirag Narayanan Nambiar	Sci./Eng.-SC	Planetary Science, Ablation Physics, Numerical Modelling, Space Instrumentation	PSDN	B.E. (2017)
251	Srishti Sharma	Sci./Eng.-SC	Web Application Development, Database Management	COMSR	B.Tech. (2012)
252	Srubabati Goswami FNA, FASc, FNASc, FTWAS	Sr. Professor	High Energy Physics	THEPH	PhD (1998)
253	Sujata Krishna	Sr. Proj. Attendent	Office assistance	ADMGN	S.S.C (1982)
254	Sunil D Hansrajani	Sr. Proj. Assistant	Stores Administration	ADMST	B.Com. (1991)
255	Sunil Kumar Singh FNA, FNASc	Professor	Isotope and Elemental Geochemistry	GSDN	PhD (1999)
256	Suraj Kumar	Assistant	General Administration	ADMGN	B.Com. (2015)
257	Surajit Mohanty	Sci./Eng.-SC	Astronomy & Astrophysics	A&A	B.Tech. (2018)
258	Suresh Babu A	Head, Accounts & IFA	Finance and Accounts	ADMAC	PGDIP (2005)
259	Sureshkumar K Patel	Accounts Officer	Accounts services	ADMAC	M.Com. (2014)
260	Sushil Kumar	Sci./Eng.-SC	Design & Development of Space Instruments	PSDN	B.Tech. (2014)
261	Suthar Pramodkumar	Technician-G	Workshop services	WORSH	D.M.E. (2016)
262	Swetapuspa Soumyashree	Sci./Eng.-SD	LIBS, Femtosecond Physics, Payload related Simulations	AMOPH	B.E. (2017)
263	T A Rajesh	Sci./Eng.-SF	Atmospheric Aerosols, Black Carbon	SPASC	PhD (2019)
264	T K Sunilkumar	Sr. Tech. Asst.-C	Maintenance of trace gas analyzers	SPASC	B.Pharm (1991)
265	T. S. Neethu	Sr. Proj. Assistant	Stores Administration	ADMST	M.Com. (2007)
266	Tejas N Sarvaiya	Sci./Eng.-SE	Cyber Security, Server Virtualization, Linux/Unix Sysadmin, Network Administration, Shell Scripting, Website/Server Auditing	COMSR	M.E. (2014)
267	Tinkal Ladiya	Sci./Eng.-SC	Electronics Design & Development for Space and Ground Based Instruments	PSDN	AMIE (2020)
268	V H Chavda	Technician-G	Masonary work	CMDV	NINTH (1980)
269	V R Patel	Sr.Tech.-A	Workshop services	WORSH	TWELVE (1985)
270	Vaibhav Dixit	Sci./Eng.-SD	Optical Astronomical Instrumentation, Adaptive Optics, AI, Deep Learning	A&A	M.Tech. (2017)
271	Vaibhav Varish Singh Rathore	Sci./Eng.-SC	Cyber Security, Linux and Unix System Admin, Network Management, Virtulization, Sever/Website Audit	COMSR	B.Tech. (2017)
272	Varun Sheel Chair, PSDN	Professor	Modeling of Planetary Atmospheres	PSDN	PhD (1996)
273	Veeresh Singh	Asst. Professor	Active Galactic Nuclei, Radio Astronomy	A&A	PhD (2012)
274	Vijaysinh M Rathod	Sr.Tech.-A	Electrical Repair and Maintance Work	CMDV	H.Sc. (1996)
275	Vikram Goyal	Sr. Sci. Assistant-A	Planetary Sciences, Isotope Cosmochemistry	PSDN	M.Sc. (2016)
276	Vimlesh Kumar	Sci./Eng.-SC	Mechanical, Photonics, Nonlinear Optics, Single Photons, Quantum Optics, Structured Optical Beams	AMOPH	B.Tech. (2016)

Sr. No.	Name	Designation	Specialization	Division	Highest Degree Obtained
277	Vinayak Kumar	Sci./Eng.-SD	Astrophysics, Programming	AMOPH	B.Tech. (2013)
278	Vineet Goswami	Asst. Professor	Isotope Geochemistry, Geochronology, Chemical Oceanography	GSDN	PhD (2012)
279	Virendra Kumar Padhya	Sci./Eng.-SD	Hydrology and IWIN Mass Spectrometery	GSDN	M.Tech. (2013)
280	Vishal Joshi	Asst. Professor	Astronomy & Astrophysics	A&A	PhD (2014)
281	Vishal M Shah	Tech. Officer-E	Scientific and Space Electronic Instrumention	A&A	D.E.E (1982)
282	Vishnu Kumar Dhaker	Sr. Sci. Assistant-A	Atmospheric Aerosols	SPASC	M.Sc. (2016)
283	Vishnubhai R Patel	Sci./Eng.-SC	CAD, CAM Programming, workshop services	WORSH	B.E. (2018)
284	Vivek Kumar Mishra	Sci./Eng.-SC	Mechanical Design,Telescope Mirror Coating & Cleaning, Mechanical Maintainance of Equipments	A&A	B.E. (2015)
285	Vudutala Naresh	Accounts Officer	Accounts services	ADMAC	CA (2012)
286	Yugal S Jain	Sr. Accounts Officer	Finance, Taxation, Accounts Budget and Audit	ADMAC	MBA(2009), CA (2013)







पीआरएल मे गतिविधियां
Events at PRL















पीआरएल मे गतिविधियां
Events at PRL















पीआरएल मे गतिविधियां
Events at PRL

"कुछ मूलभूत समस्याएं जो आज वैज्ञानिकों को उद्विग्न करती हैं, वे उन समस्याओं से भिन्न नहीं हैं जिन्होंने प्राचीन काल से मनुष्य की जिज्ञासा को उत्तेजित किया है। हम ब्रह्मांड, सौर मंडल, तारों और ग्रहों की संरचना, जीवन की उत्पत्ति और प्रतीयमान रहस्यमय प्रभावों को समझना चाहेंगे जिनके माध्यम से सूर्य, पृथ्वी पर मानव अस्तित्व के क्रम को प्रभावित करता है। अंतरिक्ष अनुसंधान इन सभी से संबंधित है।"

-डॉ. विक्रम ए. साराभाई

"Some of the fundamental problems which concern scientists today are no different from those that have excited man's curiosity from earliest times. We would like to understand the creation of the Universe, the solar system, the stars and the planets, the origin of life itself and the seemingly mysterious influences through which the sun affects the course of human existence on earth. Space research is related to all these."

-Dr. Vikram A. Sarabhai